Studies of Genetic Variants in Monogenic Renal Tubular Disorders



A thesis submitted to the University of Oxford in candidature for the degree of Doctor of Philosophy by

Charlotte Louise Philpott

Academic Endocrine Unit,
Radcliffe Department of Medicine,
University of Oxford

Lady Margaret Hall,
University of Oxford

Hilary 2019

Abstract

Studies of Genetic Variants in Monogenic Renal Tubular Disorders

Charlotte Louise Philpott, Lady Margaret Hall, Doctor of Philosophy

Hilary 2019

The renal tubules are the functional unit of the kidneys, responsible for: reabsorption of many substances including ions, solutes and water; and the secretion of waste products. The molecular mechanisms underlying these processes are tightly regulated by transporters, channels and receptors, which have different expression profiles within the renal tubular segments and their disruption can lead to disorders, with local and systemic phenotypes. Thus, monogenic renal tubular disorders affecting different segments are excellent tools for the study of specific pathways and mechanisms vital to reabsorption and secretion processes; as well as for gaining an insight into the biological and molecular differences between renal tubular segments. This thesis used next generation DNA sequencing (NGS) and Sanger DNA sequencing methods to identify novel candidate genes, and hence to study the genetic and molecular mechanisms underlying three monogenic renal tubular disorders: Dent's disease (DD), familial juvenile hyperuricaemic nephropathy (FJHN) and familial hypocalciuric hypercalcaemia (FHH), each affecting different renal segments. For each of these disorders a large proportion of patients (25-55%) lack mutations in any of the known associated genes. However, one of the main issues with NGS remains accurate variant interpretation and therefore, the first aim was to investigate the effectiveness of *in silico* analysis tools to identify pathogenic variants and to determine the optimum parameters, which were then applied to the 'gene-discovery' studies. This thesis identified novel candidate genes for DD (*CLCNKA),* FJHN *(CLDN3* and *DENND4C)* and FHH (*KLOTHO*) and revealed an approach for its potential successful application in the clinic for diagnosis.

Acknowledgements

I would like to acknowledge Professor Raj Thakker, Dr Sian Piret and Dr Caroline Gorvin for the opportunity to undertake my DPhil and for acting as my supervisors; as well as Kidney Research UK (KRUK) for funding my studies. Additionally, I would like to acknowledge all of the collaborators who have contributed to each of the projects and without whom they would not have been possible: Prof Friedhelm Hildebrandt and Dr Dervla Connaughton of Boston Children's Hospital; Dr Alistair Pagnamenta of the Wellcome Trust Centre for Human Genetics; Prim Prof Dr Kharl Lhotta of the Innere Medizin III (Nephrologie and Dialyse); and Dr Silvia Reichart and Prim Prof Dr Stefan Mennel of the Department of Ophthalmology, Akademisches Lehrkrankenhaus.

I would also like to thank my supervisors and KRUK for the expertise, teaching and support I have received. I would like to thank all of the members of the Academic Endocrine Unit, especially Dr Caroline Gorvin, Dr Kate Lines and Dr Kreepa Kooblall for all of their teaching, support and advice. I would also like to take this opportunity to thank Prof Leannne Hodson for everything she has done and for the support and encouragement she continues to provide me. Finally, I would like to acknowledge all the support and encouragement I have received from my friends and family, who have always been there to lend an ear and offer words of advice and encouragement. Especially, Tom for supporting me every step of the way, particularly through the more trying times and for sitting through endless practice talks. I will be forever grateful to everyone for all of their support and help they have provided me with throughout my DPhil.

Contents page

1 List of tables viii

2 List of figures xi

3 Abbreviations xvi

4 Introduction 1

4.1. The nephron 2

4.1.1 The proximal tubules (PTs) 3

4.1.1.1 Sodium (Na^+) and phosphate (Pi) reabsorption at the PT 4

4.1.1.2 Pi and parathyroid hormone (PTH) reabsorption at the PTs 5

4.1.1.3 Reabsorption of Ca^{2+}, potassium (K^+) and magnesium (Mg^{2+}) at the PT 8

4.1.1.4 Acid-base regulation by the PT 10

4.1.1.5 Reabsorption of low-molecular weight proteins (LMWPs), amino acids and glucose 11

4.1.2 Dent's disease (DD): A renal tubular disorder of the PT 16

4.1.3 Loop of Henle (LOH) 20

4.1.3.1 The thin descending limb (tDL) 21

4.1.3.2 The thin ascending limb (tAL) 21

4.1.3.3 The thick ascending limb (TAL) 22

4.1.4 FJHN: A renal tubular disorder of the TAL 25

4.1.5 Distal tubules (DTs) 27

4.1.5.1 Na^+ reabsorption at the DT 27

4.1.5.2 Cl^- reabsorption at the DT 28

4.1.5.3 K^+ secretion at the DTs 28

4.1.5.4 Mg^{2+} reabsorption at the DT 29

4.1.5.5 Ca^{2+} reabsorption at the DT 29

4.1.6 Collecting ducts (CDs) 31

4.1.7 Familial hypocalciuric hypercalcaemia (FHH): A renal tubular disorder of the TAL and DT 33

4.1.7.1 Role of the CaSR in the renal tubules 35

4.2. Identifying genetic causes of disorders of the renal tubules 36

4.3. Next-generation DNA sequencing (NGS) 37

5 Materials and Methods 42

5.1. Materials 43

5.1.1 Chemicals 43

5.1.2 Antibiotics 43

5.1.3 Oligonucleotides 43

5.1.4 Enzymes 43

5.1.5 Vectors 44

5.1.6 Buffers and stock solutions 44

5.1.6.1 Nucleic acid handling ... *44*
5.1.6.2 Transformation and culture of Escherichia coli (E.coli) ... *45*
5.1.6.3 Protein extraction and analysis ... *45*
5.1.6.4 Cell culture ... *48*
5.2. Ethics ... **49**
5.3. Patients ... **49**
5.4. Methods ... **49**
5.4.1 Nucleic acid analysis ... 49
5.4.1.1 Preparation of human genomic DNA from blood leukocytes ... *49*
5.4.1.2 Cloning of cDNA into mammalian expression vectors ... *50*
5.4.1.3 Manipulation of plasmid DNA by site-directed mutagenesis (SDM) ... *51*
5.4.1.4 Preparation of plasmid DNA from E.coli ... *52*
5.4.1.5 Nucleic acid quantification ... *53*
5.4.1.6 Amplification of DNA by PCR ... *53*
5.4.1.7 2-step reverse transcription PCR (RT-PCR) ... *54*
5.4.1.8 Restriction endonuclease (RE) digestion (RED) ... *55*
5.4.1.9 Amplification-refractory mutation system (ARMS) PCR ... *56*
5.4.1.10 Visualisation of nucleic acid samples ... *57*
5.4.1.11 Purification of DNA for Sanger DNA sequencing ... *57*
5.4.1.12 Sanger DNA sequencing and analysis ... *58*
5.4.1.13 WGS and WES ... *59*
5.4.1.14 Illumina TruSeq Custom Amplicon (TSCA) analysis ... *59*
5.4.2 Culture of *E. coli* ... 60
5.4.2.1 Transformation of competent E. coli cells ... *60*
5.4.2.2 Expanding mammalian expression vectors in E. coli ... *60*
5.4.3 Cell culture and manipulation of cell lines ... 61
5.4.3.1 Cryogenic preservation and re-derivation of frozen cells ... *61*
5.4.3.2 Transient transfection of HEK293 cells with Klotho ... *61*
5.4.3.3 Stable transfection of MDCK cells with claudin 3 ... *62*
5.4.3.3.1 Optimisation of Geneticin® concentration for the stable transfection of MDCK cells ... 62
5.4.3.3.2 Stable transfection of MDCK cells with claudin 3-tGFP ... 63
5.4.4 Expression studies ... 63
5.4.4.1 Protein extraction from cultured cells ... *63*
5.4.4.2 Quantification of protein concentration by coomassie assay ... *64*
5.4.4.3 Western blot analysis of protein lysates ... *64*
5.4.4.4 SRE luciferase dual reporter assay ... *65*
5.4.5 *In silico* variant analysis ... 66
5.4.5.1 Population genomics ... *67*
5.4.5.2 Prediction of functional effects ... *67*

5.4.5.3 Evolutionary conservation ... 69
5.4.5.4 miRNA-target site prediction ... 69
5.4.5.5 N-glycosylation site prediction ... 71
5.4.5.6 Structural analysis ... 71
5.4.6 Statistical analysis ... 72
6 Investigation of *in silico* methods for variant analysis ... 73
6.1. Declaration of contributions ... 77
6.2. Results ... 77
6.2.7 Data collection ... 77
6.2.8 Commonly used criteria for variant analysis ... 82
6.2.8.1 Population genomics: vAFs ... 82
6.2.8.2 Prediction of functional effects ... 84
6.2.8.3 Evolutionary conservation ... 89
6.2.8.4 Combined analysis ... 93
6.2.9 Improvement of the criteria for variant analysis ... 96
6.2.9.1 Population genomics: vAFs ... 96
6.2.9.2 Prediction of functional effects ... 101
6.2.9.3 Evolutionary conservation ... 104
6.2.9.4 Combined analysis ... 107
6.3. Discussion and future studies ... 111
7 Investigation of the *CLCNKA* gene in patients with Dent's disease ... 119
7.1. Declaration of contributions ... 120
7.2. Results ... 121
7.2.1 Patient characteristics ... 121
7.2.2 Identification of 13 non-synonymous exonic or UTR *CLCNKA* variants in patients with DD ... 121
7.2.2.1 Identification and in silico analysis of common variants in CLCNKA in patients with DD ... 122
7.2.2.1.1 Identification and *in silico* analysis of an Arg8His variant in ClC-Ka, in proband 15 ... 126
7.2.2.1.2 Identification and *in silico* analysis of an Arg83Gly variant in ClC-Ka in 14 probands ... 126
7.2.2.1.3 Identification and *in silico* analysis of a Tyr315Phe variant in ClC-Ka in seven probands ... 128
7.2.2.1.4 Identification and *in silico* analysis of a Leu334Val variant in ClC-Ka in probands 3 and 4 129
7.2.2.1.5 Identification and *in silico* analysis of an Ala447Thr variant in ClC-Ka in 14 probands ... 131
7.2.2.1.6 Identification and *in silico* analysis a Thr454Ala variant in ClC-Ka in three probands ... 132
7.2.2.1.7 Identification and *in silico* analysis of a Val457Ile variant in ClC-Ka in three probands ... 134
7.2.2.1.8 Identification and *in silico* analysis of an Arg534Trp variant in ClC-Ka in three probands 136
7.2.2.1.9 Identification and *in silico* analysis of a Pro683Leu variant in ClC-Ka in three probands ... 136
7.2.2.1.10 Identification and *in silico* analysis of a c.*126A>G variant in *CLCNKA* in three probands. 138
7.2.2.1.11 Identification and *in silico* analysis of a c.*163A>T variant in *CLCNKA* in 13 probands ... 140
7.2.2.1.12 *In silico* analysis of the effect of c.*126A>G and c.*163A>T on miRNA target sites ... 141
7.2.2.2 Identification and in silico analysis of rare variants in CLCNKA in patients with DD ... 144

7.2.2.2.1 Identification and *in silico* analysis of a Phe285del variant in ClC-Ka in proband 2 146
7.2.2.2.2 Identification and *in silico* analysis of a Thr562Met variant in ClC-Ka in proband 4 148
7.2.2.2.3 Structural analysis of the Phe285del and Thr562Met variants identified in ClC-Ka 150
7.2.3 Analysis of compound heterozygosity in *CLCNKA* in patients with DD 153
7.3. Discussion 156
8 Investigation of candidate variants in patients with familial juvenile hyperuricaemic nephropathy (FJHN) 163
8.1. Declaration of contributions 164
8.2. Results 165
8.2.1 Patient characteristics 165
8.2.2 Identification of 26 non-synonymous exonic candidate variants in patients diagnosed with FJHN 168
8.2.2.1 Co-segregation analysis of DNA variants in the eight FJHN families 169
8.2.2.1.1 Co-segregation analysis of a Val454Met variant in Ankyrin repeat domain 11 (ANKRD11) in a family 6 172
8.2.2.1.2 Co-segregation analysis of a Trp17Cys variant in claudin 3 variant in family 5 172
8.2.2.1.3 Co-segregation analysis of a Ser1251Phe variant in Denn domain containing 4C (Dennd4C) in family 6 173
8.2.2.1.4 Co-segregation analysis of an Arg1317Gln variant in Dennd4C in family 7 175
8.2.2.1.5 Co-segregation analysis of a Gly56Val variant in fibromodulin in family 7 176
8.2.2.1.6 Co-segregation analysis of a Pro338Ser variant in Myosin XVI in family 5 177
8.2.2.1.7 Co-segregation analysis of a Gly76Arg variant in Paired box 2 (Pax-2) in family 8 179
8.2.2.2 In silico analysis of seven variants identified in families with FJHN 180
8.2.2.2.1 *In silico* analysis of a Val454Met variant in ANKRD11 identified in proband I.2 from family 6 180
8.2.2.2.2 *In silico* analysis of a Trp17Cys variant in claudin 3 identified in proband II.1 from family 5 182
8.2.2.2.3 *In silico* analysis of a Ser1251Phe variant in Dennd4C identified in proband I.2 from family 6 183
8.2.2.2.4 *In silico* analysis of an Arg1317Gln variant in Dennd4C identified in proband II.1 from family 7 183
8.2.2.2.5 *In silico* analysis of a Gly56Val variant in fibromodulin identified in proband II.1 from family 7 184
8.2.2.2.6 *In silico* analysis of a Pro338Ser variant in myosin XVI identified in proband II.1 from family 5 185
8.2.2.2.7 *In silico* analysis of a Gly76Arg variant in Pax-2 identified in probands II.1 and II.2 from family 8 186
8.2.3 Prioritisation of candidate variants for functional analysis 187
8.2.3.1 Biological relevance 187
8.2.3.2 A case of revised diagnosis of RCS in family 8 due to a Gly76Arg Pax-2 variant 192
8.2.3.3 Expression analysis 193
8.2.3.4 Generation of WT and Trp17Cys claudin 3 stable cell-lines 194
8.2.3.5 Attempted generation of a full-length human WT Dennd4C expression vector 197

8.3. Discussion and future studies 199

9 Identification of rare *KLOTHO* variants in patients with familial hypocalciuric hypercalcaemia (FHH) 207

9.1. Declaration of contributions 208

9.2. Results 208

9.2.1 Patient characteristics 208

9.2.2 Identification of an Asn607Asp variant in Klotho in a patient with FHH 209

9.2.2.1 Confirmation and in silico analysis of the Asn607Asp variant in Klotho in a patient with FHH 214

9.2.3 Identification of three additional rare nonsynonymous Klotho variants in patients with FHH by Illumina TSCA analysis 219

9.2.3.1 Identification of a Met384Thr variant in Klotho patient 6 222

9.2.3.2 Identification of a Pro690Leu variant in Klotho in patient 7 222

9.2.3.3 Identification of a Tyr1003Cys Klotho variant in two FHH patients 223

9.2.3.4 Structural analysis of rare variants located in the extracellular Klotho domain 225

9.2.4 *In vitro* functional analysis of the four rare Klotho variants identified in patients with FHH by NGS 230

9.2.4.1 Expression analysis of co-receptors Klotho and FGFR1 230

9.2.4.2 Generation of WT and mutant Klotho-expressing constructs 231

9.2.4.3 Effect of rare Klotho variants on ERK1/2 signalling in response to FGF23 234

9.3. Discussion and future studies 238

10 Discussion 247

11 Appendix 257

11.1. Materials and methods 258

11.2. Results 263

12 Bibliography 340

1 List of tables

Table 1. Frequency of DD-associated characteristics in males with DD1 16
Table 2. Percentage of mutation types in *CLCN5* identified in patients with DD1 17
Table 3. Comparison of NGS techniques 38
Table 4. Components used in the preparation of separation gels for SDS-PAGE 48
Table 5. SDM thermal cycle steps 52
Table 6. PCR cycle steps for use with Blue MegaMix-Double. 54
Table 7. PCR cycle steps for use with Accumprime™ GC-rich DNA polymerase 54
Table 8. Cycling conditions used for the BigDye™ Terminator v3.1 Cycle Sequencing Kit 58
Table 9. Concentration of antibiotic required for selection of constructs 60
Table 10. The criteria proposed by the ACMG 2015 report for the classification of variants 75
Table 11. Evidence proposed by the ACMG 2015 report for the classification of variants 76
Table 12. Number of variants within each gene and cohort used in this analysis 79
Table 13. Prediction outcomes generated by PolyPhen-2, Proven Protein and MutationTaster 85
Table 14. Criteria for the conservation status (across four orthologs) for WT amino acid residues. 90
Table 15. Criteria used in the combined analysis of genetic variants. 93
Table 16. The revised categories and criteria used to determine the predicted functional effect of variants 101
Table 17. Criteria for the conservation status (across eight orthologs) for WT amino acid residues. 104
Table 18. Improved categories and criteria used in the combined analysis of genetic variants. 107
Table 19. Clinical phenotypes of DD patients, lacking mutations in *CLCN5* and *OCRL1* 123
Table 20. *In silico* analysis of *CLCNKA* common nonsynonymous coding and 3'UTR variants identified in DD patients 125
Table 21. Predicted impact of *CLCNKA* 3'UTR variants, identified in DD patients, on miRNA target sites 142
Table 22. *In silico* analysis of *CLCNKA* rare nonsynonymous coding variants identified in DD patients 145
Table 23. Clinical and biochemical details of FJHN probands and affected family members 166
Table 24. Co-segregation analysis of the prioritised variants identified in patients diagnosed with FJHN by WGS 171
Table 25. *In silico* analysis of the seven variants that co-segregated with FJHN 181
Table 26. Clinical characteristics reported in patients with RCS 191
Table 27. Clinical and biochemical details of the FHH probands for whom WES was performed 209
Table 28. Comparison of the phenotypes of FHH patient 4, tumoral calcinosis-3 and mice harbouring LOF *Klotho* mutations 213
Table 29. *In silico* analysis of an Asn607Asp variant in Klotho, identified in a patient with FHH 215
Table 30. *In silico* analysis of two common nonsynonymous *KLOTHO* variants identified in patients with FHH by TSCA sequencing 221
Table 31. *In silico* analysis of three rare nonsynonymous *KLOTHO* variants identified in patients with FHH by TSCA sequencing 221
Table 32. SDM primers 258

Table 33. cDNA/plasmid sequencing primers 258
Table 34. Genomic DNA sequencing and PCR primers and their corresponding annealing temperatures 259
Table 35. ARMS PCR primers and their corresponding annealing temperatures 260
Table 36. Reverse Transcription (RT)-PCR primers and their corresponding annealing temperatures 261
Table 37. REs and their corresponding buffers and incubation temperatures 261
Table 38. Antibodies used for Western blot analysis 262
Table 39. *In silico* analysis of *CASR* variants obtained from HGMD 263
Table 40. *In silico* analysis of *CLCN5* variants obtained from HGMD 278
Table 41. *In silico* analysis of *CLCNKB* variants obtained from HGMD 283
Table 42. *In silico* analysis of *OCRL1* variants obtained from HGMD 286
Table 43. *In silico* analysis of *UMOD* variants obtained from HGMD 293
Table 44. *In silico* analysis of *CASR* variants obtained from ExAC 297
Table 45. *In silico* analysis of *CLCN5* variants obtained from ExAC 305
Table 46. *In silico* analysis of *CLCNKB* variants obtained from ExAC 309
Table 47. *In silico* analysis of *OCRL1* variants obtained from ExAC 316
Table 48. *In silico* analysis of *UMOD* variants obtained from ExAC 319
Table 49. Clinical and biochemical details of the FHH probands for whom TSCA sequencing of *KLOTHO* was performed 338

2 List of figures

Figure 1. Reabsorption and secretion in the nephron 3
Figure 2. Na^+ and Pi transport in the PT 5
Figure 3. Regulation of Ca^{2+} by the parathyroids, kidney, bone and intestine 6
Figure 4. Regulation of NaPi-IIa and vitamin D metabolism in the PT by PTH 7
Figure 5. Paracellular transport in the PT 10
Figure 6. Acid-base transport in the PT 11
Figure 7. Reabsorption of LMWPs in the PT 13
Figure 8. Amino acid transport in the PT 14
Figure 9. Glucose transport in the PT 15
Figure 10. Reabsorption and secretion at the LOH 24
Figure 11. Ion transport in the DT 31
Figure 12. The role of the CaSR, $G\alpha_{11}$ and AP-2 proteins in CaSR trafficking and signaling 34
Figure 13. Schematic representation of primer binding during ARMS PCR 56
Figure 14. The proportion of variants in each gene in ExAC and HGMD cohorts 79
Figure 15. Correlation between variant number and gene size in the ExAC and HGMD cohorts. 81
Figure 16. The proportion of rare and common variants in the HGMD and ExAC cohorts 84
Figure 17. The proportion of variants predicted to have a functional effect in the HGMD and ExAC cohorts 88
Figure 18. The evolutionary conservation of WT amino acid residues affected by HGMD and ExAC variants across four orthologs. 92
Figure 19. Predicted pathogenicity of HGMD and ExAC variants using a commonly used combined analysis approach. 95
Figure 20. The range of vAFs observed in the ExAC and HGMD cohorts. 98
Figure 21. The proportion of variants observed in the ExAC and HGMD cohorts with vAFs <0.001% or ≥0.001% 100
Figure 22. The predicted functional effects of HGMD and ExAC variants using five categories 103
Figure 23. The evolutionary conservation of WT amino acid residues affected by HGMD and ExAC variants across eight orthologs. 106
Figure 24. Predicted pathogenicity of HGMD and ExAC variants using a new combined analysis approach. 110
Figure 25. Schematic representation of the genomic organisation of the human *CLCNKA* gene showing the location of common and rare variants identified in DD patients 124
Figure 26. Identification of an Arg8His variant in ClC-Ka in proband 15 127
Figure 27. Identification of an Arg83Gly variant in ClC-Ka in 14 probands 128
Figure 28. Identification of a Tyr315Phe variant in ClC-Ka in seven probands 130
Figure 29. Identification of a Leu334Val variant in ClC-Ka in proband 3 and 4 131
Figure 30. Identification of a Ala447Thr variant in ClC-Ka in 14 probands 133
Figure 31. Identification of a Thr454Ala variant in ClC-Ka in probands 9, 12 and 17 134
Figure 32. Identification of a Val457Ile variant in ClC-Ka in probands 9, 12 and 17 135
Figure 33. Identification of an Arg534Trp variant in ClC-Ka in probands 9, 12 and 17 137

Figure 34. Identification of a Pro683Leu variant in ClC-Ka in probands 9, 12 and 17 138
Figure 35. Identification of a c.*126A>G variant in *CLCNKA* in probands 9, 12 and 17 139
Figure 36. Identification of a c.*163A>T variant in *CLCNKA* in 13 probands 141
Figure 37. Identification of a Phe285del variant in ClC-Ka, in proband 2 147
Figure 38. Identification of a Thr562Met variant in ClC-Ka in proband 4 149
Figure 39. Structural characterisation displaying the location of rare ClC-Ka variants in the bovine ClC-K homodimer 151
Figure 40. Structural characterisation of the Phe285del ClC-Ka variant in the bovine ClC-K 152
Figure 41. Structural characterisation of the Thr562Met ClC-Ka variant in the human ClC-Ka cytoplasmic domain 153
Figure 42. Representation of the combination of rare and common nonsynonymous and 3'UTR variants identified in *CLCNKA* in 18 patients with DD 154
Figure 43. FJHN pedigrees 168
Figure 44. Flowchart to display the process of identification and analysis of a candidate gene for FJHN 170
Figure 45. Confirmation and co-segregation analysis of a Val454Met variant in ANKRD11 in family 6 173
Figure 46. Confirmation and co-segregation analysis of a Trp17Cys variant in claudin 3 in family 5 174
Figure 47. Confirmation and co-segregation analysis of a Ser1251Phe variant in Dennd4C in family 6 175
Figure 48. Confirmation and co-segregation analysis of an Arg1317Gln variant in Dennd4C in family 7 176
Figure 49. Confirmation and co-segregation analysis of a Gly56Val variant in fibromodulin in family 7 177
Figure 50. Confirmation and co-segregation analysis of a Pro338Ser variant in myosin XVI in family 5 178
Figure 51. Confirmation of a Gly76Arg variant, in Pax-2, in a family diagnosed with FJHN 179
Figure 52. Multiple sequence alignment of the residues surrounding the WT Val454 residue in ANKRD11 182
Figure 53. Multiple sequence alignment of the residues surrounding the WT Trp17 residue in claudin 3 182
Figure 54. Multiple sequence alignment of the residues surrounding the WT Ser1251 residue in Dennd4C 183
Figure 55. Multiple sequence alignment of the residues surrounding the WT Arg1317 residue in Dennd4C 184
Figure 56. Multiple sequence alignment of the residues surrounding the WT Gly56 residue in fibromodulin 185
Figure 57. Multiple sequence alignment of the residues surrounding the WT Pro338 residue in myosin XVI 186

Figure 58. Multiple sequence alignment of the residues surrounding the WT Gly76 residue in Pax-2 187
Figure 59. Identification of an optic pit in the left eye of proband II.1, family 8. 192
Figure 60. Qualitative RT-PCR expression analysis of prioritised genes across a control cDNA organ panel. 193
Figure 61. Confirmation and generation of WT and Cys17 claudin 3 expression vectors 194
Figure 62. Viability of MDCK cells in response to Geneticin® 196
Figure 63. Overexpression of claudin 3 in MDCK cells 197
Figure 64. Attempted generation of a full-length Dennd4C-tGFP expression vector 198
Figure 65. Attempted generation of a pcDNA™3.1(+)hDennd4C vector 199
Figure 66. Flowchart of the process of identification and analysis of a candidate gene for FHH 210
Figure 67. Schematic representation of the generation of multiple Klotho forms 214
Figure 68. Confirmation of an Asn607Asp variant, in Klotho in a patient diagnosed with FHH 217
Figure 69. The rare Klotho variant, Asn607Asp, is predicted to disrupt an N-glycosylation site 218
Figure 70. Schematic representation of the genomic organisation of the human *KLOTHO* gene showing the location of variants identified in patients with FHH, TC-3 and mouse models of ectopic calcification 220
Figure 71. Confirmation of a Met384Thr variant in Klotho in patient 6 223
Figure 72. Confirmation of a Pro690Leu variant in Klotho in patient 7 224
Figure 73. Confirmation of a Tyr1003Cys variant in Klotho in two patients diagnosed with FHH 225
Figure 74. Structural characterisation displaying the location of rare Klotho variants in the human Klotho:FGFR1c:FGF23 ternary complex 227
Figure 75. Structural characterisation of rare *KLOTHO* variants located in the extracellular domain 229
Figure 76. Expression of Klotho and FGFR1 in a panel of cell-lines 231
Figure 77. Generation and confirmation of the pcDNA™3.1(+)*hKLOTHO* vector 233
Figure 78. Confirmation of SDM in *KLOTHO* 234
Figure 79. Schematic representation of SRE-luciferase transcription induced by ERK1/2 signalling in response to FGF23 235
Figure 80. Dose-response of SRE-reporter activity to FGF23 237
Figure 81. SRE-reporter fold change in response to FGF23 in cells expressing WT or variant Klotho 238
Figure 82. Confirmation and segregration analysis of a His1842Arg variant in BSN in a family diagnosed with FJHN 325
Figure 83. Confirmation and segregration analysis of a Val2236Met variant in BSN in a family diagnosed with FJHN 326
Figure 84. Confirmation and segregration analysis of a Trp303Arg variant in ClC-6 in a family diagnosed with FJHN 326
Figure 85. Confirmation and segregration analysis of a Pro714Leu variant in Fat1 in a family diagnosed with FJHN 327

Figure 86. Confirmation and segregration analysis of an Asp1930His variant in Fat1 in a family diagnosed with FJHN....328
Figure 87. Confirmation and segregration analysis of a Gly147Asp variant in fibromodulin in a family diagnosed with FJHN....328
Figure 88. Confirmation and segregration analysis of an Arg236Gln variant in fibromodulin in a family diagnosed with FJHN....329
Figure 89. Confirmation and segregration analysis of a Phe48Leu variant in Igfn1 in a family diagnosed with FJHN....330
Figure 90. Confirmation and segregration analysis of a Ser2463Cys variant in Igfn1 in a family diagnosed with FJHN....330
Figure 91. Confirmation and segregration analysis of a Gln2789* variant in Igfn1 in a family diagnosed with FJHN....331
Figure 92. Confirmation and segregration analysis of a Val211Met variant in KDM4E in a family diagnosed with FJHN....332
Figure 93. Confirmation and segregration analysis of an Arg240Trp variant in KDM4E in a family diagnosed with FJHN....332
Figure 94. Confirmation and segregration analysis of a Gly570* variant in myosin XVI in a family diagnosed with FJHN....333
Figure 95. Confirmation and segregration analysis of an Arg83Trp variant in neuraminidase 2 in a family diagnosed with FJHN....334
Figure 96. Confirmation and segregration analysis of an Arg243His variant in PPRC1 in a family diagnosed with FJHN....334
Figure 97. Confirmation and segregration analysis of a Leu937Arg variant in PPRC1 in a family diagnosed with FJHN....335
Figure 98. Confirmation and segregration analysis of a Glu2013Lys variant in RP1 like 1 in a family diagnosed with FJHN....335
Figure 99. Confirmation and segregration analysis of a Pro68Ser variant in NACT in a family diagnosed with FJHN....336
Figure 100. Confirmation and segregration analysis of a Pro394His variant in NACT in a family diagnosed with FJHN....337

3 Abbreviations

$1,25(OH)_2D_3$	1,25-dihydroxyvitamin D3
$25(OH)D_3$	25-hydroxyvitamin D3
ACE	Angiotensin I-converting enzyme
ACMG	American college of medical genetics and genomics
ADAM	A disintegrin and metalloproteinase
ADH	Autosomal dominant hypocalcaemia
ADHR	Autosomal dominant hypophosphataemic rickets
ADP	Adenosine diphosphate
AE	Chloride/bicarbonate exchanger
AGT	Angiotensinogen
Amp^r	Ampicillin resistance
ANKRD11	Ankyrin repeat domain 11
ANKRD11	Ankyrin repeat domain 11
AP-2	Adapter protein-2
AP2S1	Adapter protein-2 sigma subunit
APS	Ammonium persulfate
AQP	Aquaporin
ARMS	Amplification-refractory mutation system
ATP	Adenosine triphosphate
$B^{0+}AT$	B(0,+)-type amino acid transporter 1
B^0AT1	Sodium-dependent neutral amino acid transporter
BK	Big potassium channel
BSA	Bovine serum albumin
BSN	Bassoon presynaptic cytomatrix protein
CA	Carbonic anhydrase
Ca^{2+}	Calcium
CAD	Occult atherosclerosis
cAMP	Cyclic adenosine monophosphate
CAPS	13-(cyclohexylamino)-1-propanesulfonic acid
CASR	Calcium sensing receptor
CaSR	Calcium sensing receptor
CBS	Cystathione-ß-synthase
CCD	Cortical collecting duct

CD	Collecting duct
cDNA	Complementary DNA
CFL1	Cofilin-1
CFTR	Cystic fibrosis transmembrane conductance regulator
CHO	Chinese hamster ovary
ciPTEC	Conditionally imortalised proximal tubule epithelial cells
Cl^-	Chloride
CLASH	Cross linking, ligation and sequencing of hybrids
CLC-5	Chloride/proton antiporter
ClC-K	Chloride channel protein K
CLCN4	Chloride voltage-gated channel 4
CLCN5	Chloride voltage-gated channel 5
CLCN6	Chloride voltage-gated channel 6
CLCNKA	Chloride voltage-gated channel Ka
CLCNKB	Chloride voltage-gated channel Kb
CLDN2	Claudin 2
CLDN3	Claudin 3
CNT	Connecting tubules
CO_2	Carbon dioxide
COL4A	Collagen type IV alpha
CYP24A1	Cytochrome P450 (CYP) family 24 subfamily A member 1
CYP27B1	Cytochrome P450 (CYP) family 27 subfamily B member 1
DAG	Diacylglycerol
DBP	Vitamin D binding protein
DCT	Distal convoluted tubule
DD	Dent's disease
Dennd4C	Denn domain containing 4C
DENND4C	Denn domain containing 4C
dH_2O	Distilled water
DMEM	Dulbecco's modified Eagle's medium
DMSO	Dimethyl sulfoxide
DNA	Deoxyribonucleic acid
dNTPs	Deoxyribonucleotide triphosphate

dsDNA	Double-stranded DNA
DT	Distal tubules
E. coli	*Escherichia coli*
EAAT3	Excitory amino acid transporter 3
ECACC	European collection of authenticated cell cultures
EDTA	Ethylenediaminetetraacetic acid
eGFR	Estimated glomerular filtration rate
EGR1	Early growth response 1
EMEM	Eagle's minimum essential medium
ENaC	Epithelial sodium channel
ER	Endoplasmic reticulum
ERK1/2	Extracellular signal-regulated kinase 1/2
EVS	Exome variant server
ExAC	Exome aggregation consortium
FAT1	FAT atypical cadherin 1
FBS	Fetal bovine serum
FGF23	Fibroblast growth factor 23
FGFR	Fibroblast growth factor receptor
FHH	Familial hypocalciuric hypercalcaemia
FHHNC	Familial hypomagnesaemia with hypercalciuria and nephrocalcinosis
FJHN	Familial juvenile hyperuricaemic nephropathy
FMOD	Fibromodulin
FSGS	Focal segmental glomerulosclerosis
Gα	G-protein alpha
GAPDH	Glyceraldehyde-3-phosphate dehydrogenase
gDNA	Genomic DNA
GDP	Guanine diphosphate
GEF	Guanine nucleotide exchange factor
GFP	Green fluorescent protein
GLUT	Glucose transporter
GNA11	G-protein subunit alpha 11
GPCR	G-protein coupled receptor
GTP	Guanine triphosphate

H^+	Hydrogen
H_2CO_3	Carbonic acid
H_2O	Water
H_2PO_4	Dihydrogen phosphate
HCO_3^-	Bicarbonate
HEK	Human embryonic kidney
HGMD	Human gene mutation database
HNF1B	Hepatocyte nuclear factor 1 beta
HPO_4	Hydrogen phosphate
IGFN1	Immunuglobulin-like and fibronectin type III domain containing 1
IMCD	Inner medullary collecting duct
indels	Insertions/deletions
IP_3	1,4,5-triphosphate
K^+	Potassium
KCC4	Chloride/potassium co-transporter
KDM4E	Lysine demethylase 4E
KL1	Glycosyl hydrolase 1 domain 1
KL2	Glycosyl hydrolase 1 domain 2
KnBC1	Sodium-bicarbonate co-transporter
Kv1.1	Voltage–gated potassium channel
LAT2-4F2hc	Large neutral amino acids transporter small subunit 2 associated with 4F2 cell-surface antigen heacy chain
LB	Luria bertani
LMWPs	Low-molecular-weight proteins
LOF	Loss of function
LOH	Loop of Henle
MAPK	Mitogen-activated protein kinase
MDCK	Madin-Darby canine kidney
Mg^{2+}	Magnesium
miRNA	MicroRNA
MODY	Maturity-onset diabetes of the young
MPGN	Mesongial proliferative gloemerulonephritis
mRIPA	Modified RIPA

MYO16	Mysoin XVI
Na^+	Sodium
Na^+/K^+ ATPase	Sodium/potassium-transporting ATPase
NaPi	Sodium-phosphate co-transporter
NCC	Sodium/chloride co-transporter
NEB	New England Biolabs
Neo^r	Neomycin resistance
NEU2	Neuraminidase 2
NGS	Next generation sequencing
NH_4^+	Ammonium
NHANES	National health and nutrition examination survey
NHE	Sodium/hydrogen exchanger
NHERF1	Sodium-hydrogen exchanger regulatory factor 1
NKCC2	The sodium/potassium/2 chloride co-transporter
NPXY	Asn-Pro-X-Tyr
NXC1	Sodium/calcium exchanger
OCRL1	Inositol polyphosphate 5-phosphatase
OK	Opossum kidney
OMCD	Outer medullary connecting duct
PAGE	Polyacrylamide gel electrophoresis
Pax-2	Paired box protein 2
PAX2	Paired box 2
PBS	Phosphate buffered saline
PCR	Polymerase chain reaction
PCT	Proximal convoluted tubule
PDB	Protein data bank
Pi	Inorganic phosphate
PI3K	Phosphoinositide 3-kinase
PiT-2	Sodium-dependent phosphate transporter 2
PK	Protein kinase
PKD	Polycystic kidney disease
pkd2	Polycystic kidney disease 2
pkhd1	Polycystic kidney and hepatic disease 1

PLC	Phospholipase C
PMCA4	Calcium-ATPase
PPRC1	Peroxisome proliferator-activated receptor gamma, co-activator-related 1
PST	Proximal straight tubule
PT	Proximal tubule
PTH	Parathyroid hormone
PTH1R	Parathyroid hormone type 1 receptor
PVDF	Polyvinylidene fluoride
qPCR	Quantitative real-time PCR
RCS	Renal coloboma syndrome
RE	Restriction endonuclease
RED	Restriction endonuclease digest
REN	Renin
RME	Receptor-mediated endocytosis
RNA	Ribonucleic acid
ROMK	Renal outer medullar potassium channel
RP1L1	RP1 like 1
RT	Room temperature
RT-PCR	Reverse transcription polymerase chain reaction
sdH_2O	Sterilised distilled water
SDM	Site-directed mutagenesis
SDS	Sodium dodecyl sulphate
SEM	Standard error of the mean
SFM	Serum-free media
SGLT	Sodium and glucose co-transporter
SHRSP	Spontaneously hypertensive stroke prone rat
SIFT	Sorting intolerant from tolerant
SLC13A5	Solute carrier family 13 member A5
SLC9A6	Solute carrier family 9 member A6
SNP	Single nucleotide polymorphism
SNV	Single nucleotide variant
SRE	Serum response element

SRF	Serum response factor
tAL	Thin ascending limb
TAL	Thick ascending limb
TAT1	T-type amino acid transporter 1
TBE	Tris-borate-EDTA
TBMD	Thin basement membrane disease
TBS	Tris-buffered saline
TBST	Tris-buffered saline-Tween®
TC	Tumoral calcinosis
TCFs	Ternary complex factors
tDL	Thin descending limb
TE	Tris-EDTA
TEMED	N,N,N',N'-tetramethylethylenediamine
TER	Transepithelial resistance
TGF-B	Transforming growth factor beta
tGFP	Turbo-GFP
TGS	Triglycine sulfate
TIM	Triosephosphate isomerase
TIRF	Total internal reflection fluorescence
TMEM27	Transmembrane protein 27
TRPM6	Transient receptor potential cation channel subfamily M member 6
TRPV	Transient receptor potential cation channel subfamily V
TSCA	Truseq custom amplicon
UCCR	Urinary calcium-creatinine ratio
UMOD	Uromodulin
UT	Urea transporter
UTR	Un-translated region
UUO	Unilateral ureteral obstruction
vAFs	Variant allele frequencies
WAVE	Wiskott-Aldrich syndrome protein family verprolin homologous protein
WES	Whole exome sequencing
WGS	Whole genome sequencing

WNK	With-no-lysine
WT	Wild-type
WTCHG	Wellcome Trust Centre for Human Genetics
y^+LAT1-4F2hc	Large neutral amino acids transporter small subunit 1 associated with 4F2 cell-surface antigen heavy chain

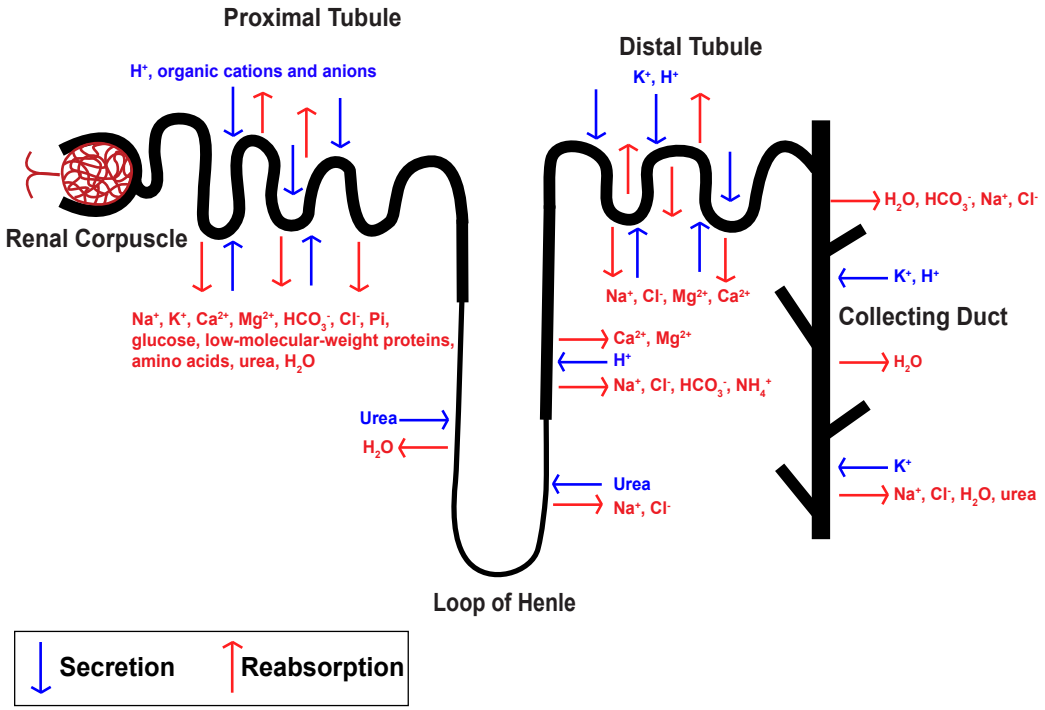
4 Introduction

4.1. The nephron

The nephrons are functional structures of the kidney, that filter blood; reabsorp filtered ions, solutes and fluids; and secrete waste products[1,2]. They are comprised of: the renal corpuscle and tubules, each of which have their own distinct roles (Figure 1). The renal corpuscle, comprised of a network of capillaries (glomerulus) encased by a double-walled capsule (Bowman's capsule) is the unit of the nephron responsible for blood filtration and the production of the ultrafiltrate or pre-urine[2,3]. Subsequently, the renal tubules are responsible for reabsorption of approximately 99% of the ultrafiltrate, as well as the secretion of waste products[1,2]. Thus, renal tubules are fundamental for maintaining the homeostasis of substances which, when impaired, can result in a range of disorders that can have systemic and local effects.

The renal tubules are comprised of different segments, including the proximal tubules (PT), loop of Henle (LOH), distal tubules (DT) and collecting duct (CD), each of which has their own specialised function (Figure 1). The specific role of each segment is orchestrated by the differential expression of transporters, channels and receptors between segments. Thus, mutations affecting a specific gene and protein typically result in a distinct phenotype depending on the segment affected. Furthermore, reabsorption and secretion in the renal tubules is also regulated by factors including hormones, fluid-flow, and the establishment and maintenance of membrane potentials. Thus, mutations affecting regulatory factors may also impact renal tubule function and result in a renal phenotype. The studies presented in this thesis focus on three disorders, each with a different renal presentation. The role of each kidney section will be described, followed by an introduction to a disorder affecting that segment.

Figure 1. Reabsorption and secretion in the nephron



Schematic representation of reabsorption and secretion in the nephron. The nephron is comprised of two functional units: the renal corpuscle and the renal tubules. The renal tubules, comprised of the proximal tubules (PTs), loop of Henle (LOH), distal tubules (DTs) and collecting duct (CD), are responsible for reabsorption of ions and solutes and secretion of waste products[1-3]. The majority of reabsorption occurs in the PTs, which reabsorb the widest range of ions and solutes[2,4-7]. Therefore, disorders affecting the PT tend to have broad and varied phenotypes, that fall under the umbrella term of renal Fanconi syndromes and are characterised by a generalised dysfunction of the PTs often resulting in: glycosuria, hypercalciuria, aminoaciduria, low-molecular-weight proteinuria and rickets[8,9]. The LOH is principally responsible for urine concentrating and the reabsorption of water (H_2O), salt and ions such a calcium (Ca^{2+}), magnesium (Mg^{2+}) and bicarbonate (HCO_3^-)[4,10-14]. Thus, disorders affecting this segment are associated with polyuria, salt wasting and impaired Ca^{2+} and Mg^{2+} reabsorption. The DTs are important for fine-tuning the final concentration of ions in the ultra-filtrate by reabsorbing sodium (Na^+), chloride (Cl^-), Mg^{2+}, Ca^{2+} and HCO_3^-[4,7,15-18]. The DTs are also involved in H_2O reabsorption, hydrogen (H^+) secretion and are the principle site of potassium (K^+) secretion[15,19]. Thus, disorders affecting the DTs often exhibit phenotypes such as hypo/hypermagnesaemia, hypo/hypercalciuria, metabolic acidosis/alkalosis and hypo/hyperkalaemia. The CDs are responsible for determining the final urinary concentration and are the final site for reabsorption of salt, H_2O and urea; and the secretion of K^+, H^+ and HCO_3^-[20-22]. Thus, disorders affecting the CDs are frequently characterised by hyper/hypokalaemia, metabolic alkalosis/acidosis, elevated renin and aldosterone, hypo/hypertension, hyponatraemia, polyuria and polydipsia. Adapted from Blaine, Chonchol and Levi[5].

4.1.1 The proximal tubules (PTs)

The PTs consist of three segments: S1, which comprises the beginning and middle proximal convoluted tubule (PCT); S2, comprising the late PCT and beginning of the

proximal straight tubule (PST); and S3, comprising the remaining PST[2]. Whilst ions are reabsorbed and/or secreted by multiple segments of the renal tubules, the majority of reabsorption (approximately 65%) occurs in the PTs, with distal segments providing the fine-tuning of urinary concentration[2,4-7,23.] This is largely due to the high ion and water (H_2O) permeability of the PT[23]. Additionally, the PT has metabolic functions, playing key roles in vitamin D metabolism and gluconeogenesis[6].

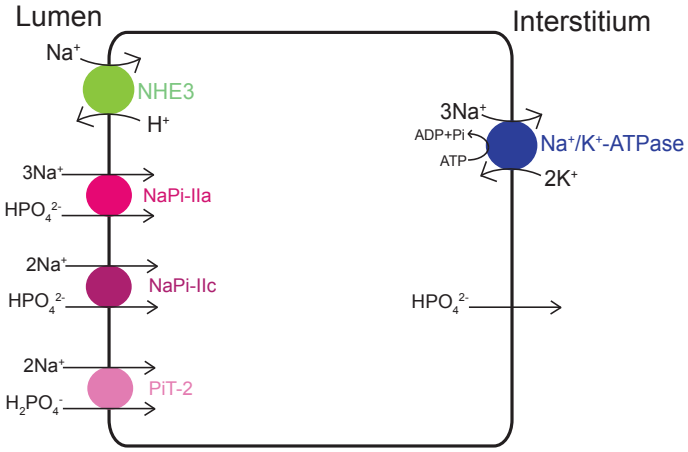
4.1.1.1 Sodium (Na^+) and phosphate (Pi) reabsorption at the PT

Almost all (>99%) filtered Na^+ is thought to be reabsorbed by the renal tubules, the majority of which (60-70%) takes place in the PT[23,24]. Transcellular reabsorption is the driving force of Na^+ reabsorption, establishing and maintaining transepithelial gradients required for the transport of filtered ions and solutes[6,23]. Whilst numerous antiporters, exchangers and co-transporters facilitate Na^+ reabsorption across the apical membrane, the sodium/hydrogen-exchanger 3 (NHE3) is the primary method by which Na^+ is reabsorbed in the PT[2,6,23] (Figure 2). Furthermore, NHE3 facilitates reabsorption of chloride (Cl^-) via both paracellular and transcellular mechanisms such as Cl^-/base exchange[23,25]. At the basolateral membrane the sodium/potassium-ATPase (Na^+/K^+-ATPase) is fundamental for Na^+ exit across the membrane and into the interstitial fluid[2,6,23] (Figure 2), thereby generating and maintaining an electrochemical gradient that drives the reabsorption of Na^+ and other solutes via transcellular and paracellular mechanisms[2,6].

Unlike many of the ions reabsorbed in the renal tubules, phosphate (Pi) reabsorption is completed almost entirely by the PT[5,6] and is driven by electrochemical gradients, primarily generated by the Na^+/K^+-ATPase. Pi reabsorption at the apical membrane

is carried out by the sodium-phosphate co-transporters NaPi-IIa, NaPi-IIc and PiT-2[5,6] (Figure 2). Studies in mice have suggested that NaPi-IIa is the principle mediator of Pi reabsorption, reabsorbing approximately 70% of filtered Pi[5]. In contrast, both NaPi-IIa and -IIc co-transporters likely contribute equally to Pi reabsorption in humans[5,26]. At present, the basolateral exit of Pi in humans remains unclear[5,6,26] (Figure 2).

Figure 2. Na^+ and Pi transport in the PT



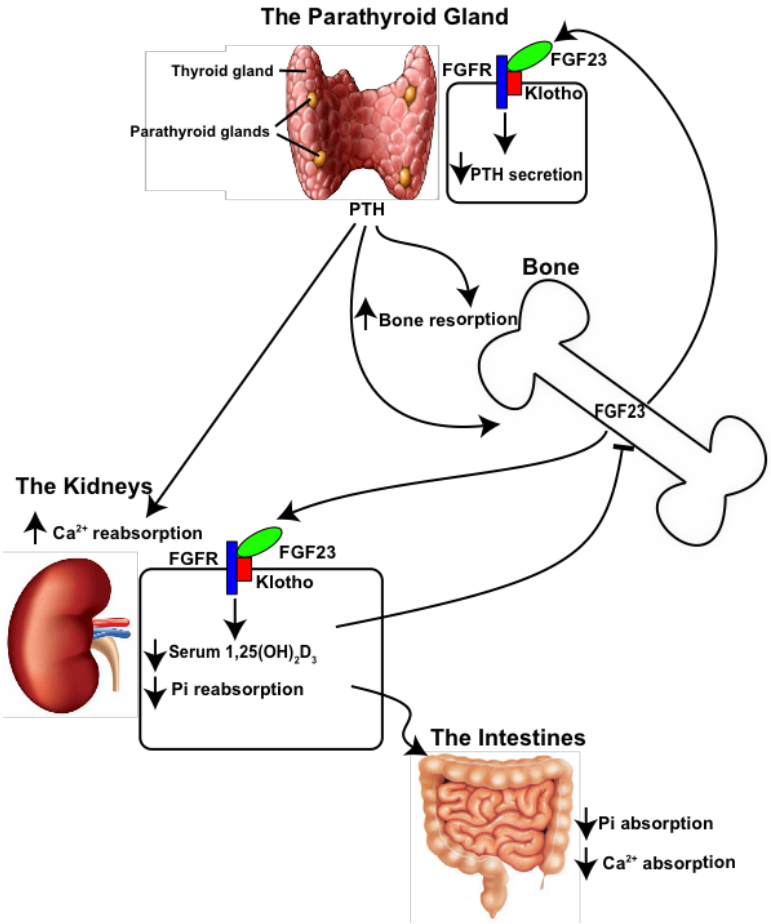
Schematic representation of Na^+ and Pi transport in the PT. Reabsorption of Na^+ from the lumen and into the interstitium occurs primarily via the apically expressed Na^+/H^+-exchanger 3 (NHE3) and the basolaterally expressed sodium/potassium-ATPase (Na^+/K^+-ATPase), respectively[2,6,23]. Driven by electrochemical gradients, Pi ($HPO_4^{2-}/H_2PO_4^-$) reabsorption from the lumen is performed by the Na^+-Pi co-transporters NaPi-IIa, NaPi-IIc and PiT-2[5,6]. However, the mechanisms underlying the basolateral exit of Pi into the interstitium are currently unknown[5,6,26]. Adapted from Curthoys and Moe[6].

4.1.1.2 Pi and parathyroid hormone (PTH) reabsorption at the PTs

Pi reabsorption is also regulated by external factors such as PTH, which is secreted into the blood stream by the chief cells of the parathyroid glands and acts directly on the bone and kidney as a key regulator of calcium (Ca^{2+}), Pi and vitamin D homeostasis[6,27] (Figure 3). Within the kidney, the luminal concentration of PTH is regulated locally at the PT[28]. PTH is internalised by receptor-mediated endocytosis (RME) involving the multiligand receptor megalin, which reduces the concentration

of luminal PTH[28]. This results in reduced signalling via the PTH type 1 receptor (PTH1R)[28-33].

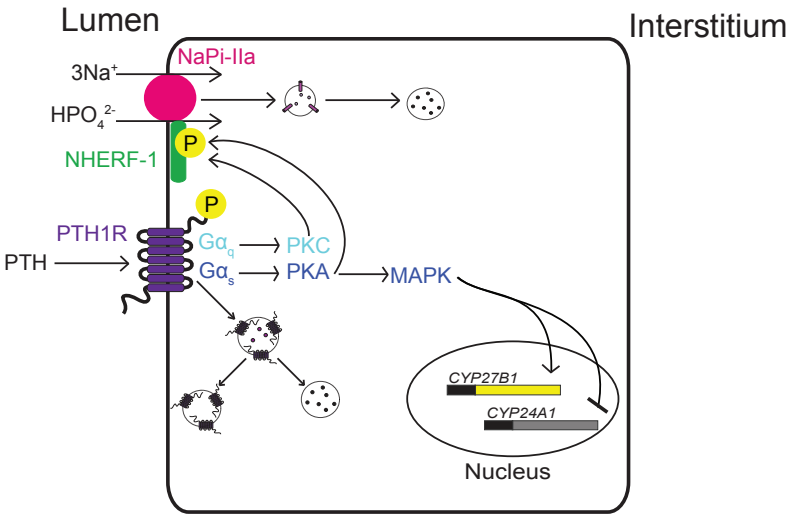
Figure 3. Regulation of Ca^{2+} by the parathyroids, kidney, bone and intestine



Schematic overview of PTH and Fibroblast Growth Factor (FGF) 23 (FGF23) regulation of ions, involving the Klotho-FGF receptor (FGFR) complex[34,35], in target organs. FGF23 is transcribed and expressed in osteoblasts[36] and osteocytes[37]; however it acts as an endocrine factor on multiple target organs, including the parathyroid gland and kidney via FGFRs. In the parathyroid gland, FGF23 binding to its receptors triggers the ERK1/2 signalling pathway which down-regulates the expression and secretion of PTH[38,39]. PTH acts on the kidneys to increase Ca^{2+} reabsorption and $1,25(OH)_2D_3$ levels[33] and to decrease Pi reabsorption via NaPi-IIa[31,40]. Additionally, PTH acts on the bone to increase resorption[41]. Thus, increasing serum Ca^{2+} and $1,25(OH)_2D_3$ and decreasing serum Pi. Furthermore, PTH increases FGF23 mRNA and protein levels, therefore PTH and FGF23 may regulate each other in a negative feedback loop[42,43]. Binding of FGF23 to Klotho-FGFR in the renal tubules stimulates ERK1/2 signalling and regulation of target genes and proteins such as *CYP27B1,* encoding 1α-hydroxylase[44], *CYP24A1,* encoding 24-hydroxylase[45] and NaPi-IIa[40,46]. Ultimately, reducing the levels of serum $1,25(OH)_2D_3$ and Pi and consequently reducing Pi and Ca^{2+} absorption in the intestine[47,48]. Adapted from Komaba and Fukagawa[49].

PTH signalling via PTH1R, a G-protein coupled receptor (GPCR) located in the apical membrane of the PT, triggers the internalisation of NaPi-IIa from the apical membrane and its subsequent degradation in lysosomes[30,32] (Figure 4). Consequently, Pi reabsorption is inhibited. PTH signalling via the PTH1R receptor regulates the expression of components of vitamin D metabolism including: increasing the expression of cytochrome P450 (CYP) family 27 subfamily B member 1 (*CYP27B1*), encoding 1-α-hydroxylase; and inhibiting the expression of *CYP24A1* encoding 24-α-hydroxylase[29,33,50,51] (Figure 4), thereby stimulating the conversion of the inactive 25-hydroxyvitamin D_3 ($25[OH]D_3$) into its active form 1,25-dihydroxyvitamin D_3 ($1,25[OH]_2D_3$)[52-54].

Figure 4. Regulation of NaPi-IIa and vitamin D metabolism in the PT by PTH



Schematic representation of the effect of PTH signalling via the PTH type 1 receptor (PTH1R) on Pi and vitamin D metabolism in the PTs. Activation of the PTH1R by PTH triggers signalling via the protein kinase A/C (PKA/C) pathways[50,51,55,56]. The PTH1R is a class B G-protein-coupled receptor (GPCR) that signals via the G-protein alpha (Gα) q ($G\alpha_q$)/phospholipase C (PLC)/PKC and $G\alpha_s$/cyclic adenosine monophosphate (cAMP)/PKA pathways to phosphorylate the Na^+/H^+ exchanger regulatory factor 1 (NHERF1)[55-57]. Thus, destabilising NaPi-IIa from the plasma membrane, results in the internalisation and degradation of NaPi-IIa and inhibition of phosphate (HPO_4^{2-}) reabsorption[30,32,55-57]. Additionally, signalling via the cAMP/PKA/mitogen-activated protein kinase (MAPK) pathway serves to regulate vitamin D metabolism by inducing the expression of *CYP27B1*, encoding 1-α-hydroxylase and inhibiting expression of *CYP24A1*, encoding the 24-α-hydroxylase[50,51]. Finally, upon agonist stimulation phosphorylation of PTH1R by a GPCR kinase induces rapid desensitisation of the receptor, followed by receptor internalisation, ligand dissociation and receptor recycling[58-61]. Adapted from Bastepe, Turan and He[62].

Another endocrine factor, fibroblast growth factor (FGF) 23 (FGF23), can regulate Pi reabsorption at the PT. FGF23 acts by binding to FGF receptors (FGFRs) and the co-receptor Klotho, a single span transmembrane protein, which increases the affinity of FGF23 for its receptor[35]. Binding of FGF23 to the FGFR-Klotho complex at the plasma membrane induces extracellular signal-regulated kinase 1/2 (ERK1/2) phosphorylation, thereby ultimately regulating the expression of downstream target genes such as parathyroid hormone (*PTH*), early growth response 1 (*EGR1*), *CYP27B1* and *CYP24A1*[34,35]. FGF23 has been reported to act on the parathyroid gland to suppress PTH expression[38,39], consequently increasing Ca^{2+} excretion and Pi reabsorption and decreasing $1,25(OH)_2D_3$ in the renal tubules[63] (Figure 3). Furthermore, FGF23 is thought to act directly on the renal tubules to inhibit NaPi activity[46,64-66], resulting in reduced Pi reabsorption; and to suppress $1,25(OH)_2D_3$[67], resulting in decreased Pi and Ca^{2+} absorption in the intestines[64] (Figure 3).

Additionally, Klotho has been shown to have roles in Ca^{2+} reabsorption in the DTs through its interactions with Ca^{2+}-selective transient receptor potential cation channel subfamily V member 5 (TRPV5)[68-70]. *In vitro* studies have shown that Klotho increased the expression of TRPV5 at the plasma membrane[69] by two mechanisms: modifying the N-glycan structure of TRPV5, impairing dynamin II-dependent endocytosis; and enhancing trafficking of TRPV5 to the plasma membrane[68,70].

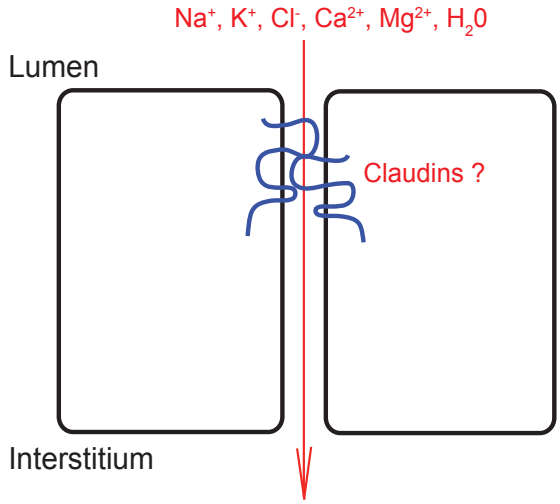
4.1.1.3 Reabsorption of Ca^{2+}, potassium (K^+) and magnesium (Mg^{2+}) at the PT

Given that Ca^{2+} is highly reactive and has a natural tendency to form microcrystals in fluids and tissues, Ca^{2+} homeostasis is tightly regulated by numerous organs,

including the renal tubules, to prevent unwanted biomineralisation in tissues[4]. Approximately 98% of filtered Ca^{2+} is reabsorbed across the renal tubules, with an estimated 60-70% reabsorbed in the PT[4]. The majority of Ca^{2+} reabsorption in the PT is performed by paracellular transport and solvent drag, in which the claudin tight junction proteins have key roles[4,5] (Figure 5). Expression of a number of claudin proteins has been reported in the PT including claudin 2, 10a, 11 and 17[71-73], with the role of claudin 2 being the best characterised[71,74]. Claudin 2 is thought to be the main claudin responsible for Na^+ reabsorption and has also been shown to be permeable to both K^+ and Ca^{2+}[71,75,76] (Figure 5). Claudin 2 knock-out mice (*Cldn2*$^{-/-}$) have been shown to exhibit a net decrease in Na^+ and H_2O reabsorption and are hypercalciuric, suggesting claudin 2 may also mediate paracellular Ca^{2+} reabsorption[76]. However, whilst a reduction in K^+ permeability was reported in *Cldn2*$^{-/-}$ mice , no abnormalities in K^+ excretion were reported[76]. Additionally, an estimated 20% of Ca^{2+} reabsorption in the PT is believed to occur via active transport; however, the precise mechanisms are yet to be elucidated[2,4,5].

The PT is the principal site for reabsorption of K^+ by paracellular mechanisms[77,78] (Figure 5), although additional K^+ reabsorption takes place in the LOH and CD[77,78]. Whilst the precise mechanisms remain to be elucidated, as previously stated, claudin 2 likely plays a key role due to its permeability to K^+[75,76] (Figure 5). Approximately 70-80% of Mg^{2+} is thought to be filtered by the glomerulus and is present in the ultrafiltrate and of this, 10-30% is estimated to be reabsorbed by the PT[5,16]. Similarly to K^+, reabsorption of Mg^{2+} in the PT is accomplished by paracellular pathways (Figure 5), driven by the reabsorption of Na^+ and H_20, creating a transepithelial Mg^{2+} gradient[5,16].

Figure 5. Paracellular transport in the PT



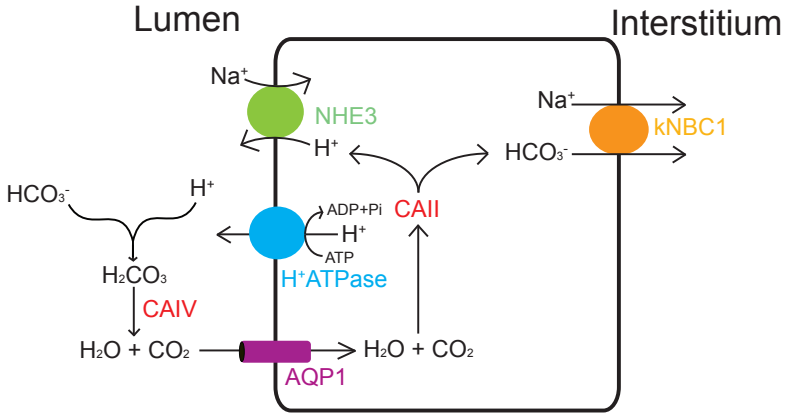
Schematic representation of the paracellular reabsorption of H_2O and ions in the PTs. Claudins are the most apical of the tight junction proteins and play fundamental roles in paracellular permeability[79]. A number of different claudin proteins have been reported to be expressed in the PT including claudins 2, 10a, 11 and 17[71-73], although the role of claudin 2 in the PT is the best characterised[71,74]. Claudin 2 is permeable to H_2O and a range of different ions including Na^+, K^+ and Ca^{2+}[71,75,76]. Additionally, claudin 10a and claudin 17 have been shown to be permeable to Cl^-[4,73,80]. Reabsorption of Mg^{2+} in the PT is also accomplished by paracellular pathways, however, the underlying mechanisms are yet to be characterised[5,16]. Adapted from Yu[71].

4.1.1.4 Acid-base regulation by the PT

The PTs are responsible for the reabsorption of approximately 80% of filtered bicarbonate (HCO_3^-)[2,7] contributing to the regulation of acid-base balance. HCO_3^- reabsorption in the PT is mediated by hydrogen (H^+) secretion into the lumen, largely by the apically expressed NHE3[2,4,7] (Figure 6). The H^+-ATPase also contributes, but to a much lesser degree[6,7] (Figure 6). In the lumen, secreted H^+ ions combine with filtered HCO_3^- forming carbonic acid (H_2CO_3), which is subsequently dehydrated by the membrane-tethered carbonic anhydrase (CA) CAIV[6,7,81] (Figure 6), thereby generating carbon dioxide (CO_2) and H_2O, both of which can be reabsorbed by the water channel aquaporin 1 (AQP1)[6,7] (Figure 6). In the cytoplasm and at the basolateral membrane CAII catalyses the hydration of diffused CO_2 and H_2O, reforming H^+ and HCO_3^-[81] (Figure 6). The HCO_3- can then be reabsorbed across the

basolateral membrane by the kidney Na^+-HCO_3^- co-transporter kNBC1[6,7,81] (Figure 6). Mutations in kNBC1 and CAII result in dysregulation of HCO_3^- reabsorption and renal tubular acidosis[82,83].

Figure 6. Acid-base transport in the PT



Schematic representation of acid-base transport in the PT. H^+ secreted by the apically expressed NHE3 and H^+-ATPase combine with filtered HCO_3^- in the lumen to form carbonic acid (H_2CO_3)[2,4,6,716]. Dehydration of H_2CO_3 by the membrane-tethered carbonic anhydrase (CA) CAIV results in the generation of CO_2 and H_2O, which are reabsorbed from the lumen across the apical membrane by aquaporin 1 (AQP1)[6,7,81]. CAII subsequently catalyses the hydration of CO_2 and H_2O, reforming H^+, which can be recycled across the apical membrane into the lumen and HCO_3^-, which can be reabsorbed across the basolateral membrane into the interstitium, by the kidney Na^+-HCO_3^- co-transporter kNBC1[6,7,81]. Adapted from Boron[7].

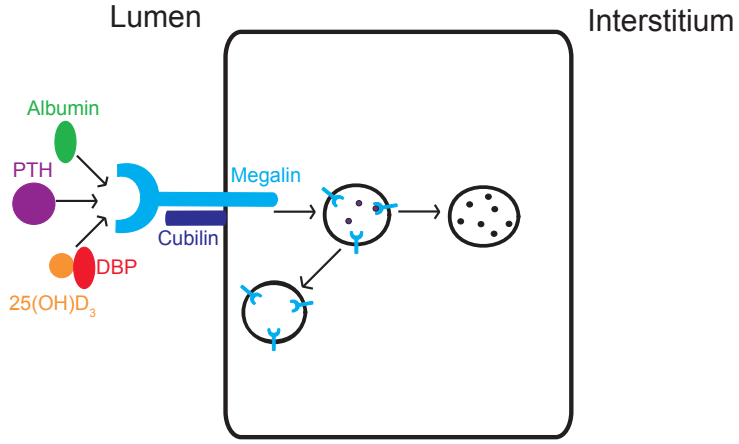
4.1.1.5 Reabsorption of low-molecular weight proteins (LMWPs), amino acids and glucose

In addition to the reabsorption of ions, the PT is the main site of reabsorption of filtered solutes such as LMWPs (<69KDa)[84] glucose, amino acids and urea[2,6]. Megalin and cubilin are fundamental multiligand, endocytic receptors required for the reabsorption of LMWPs including: hormones such as PTH and growth factors, vitamin and mineral-binding proteins and albumin, in the PT[85-87] (Figure 7). Although structurally dissimilar, megalin is a large transmembrane protein, whilst cubilin is a peripherally attached glycoprotein with no transmembrane domain; in the PT megalin and cubilin act as co-receptors expressed at the apical plasma membrane and

endocytic apparatus[87] (Figure 7). Both megalin and cubilin can each bind several ligands with different affinities and as co-receptors they can interact to form a dual-receptor complex[87]. As cubilin has no obvious signal for endocytosis, it is thought that megalin may mediate the co-internalisation of the receptor-ligand complex[87]. Two Asn-Pro-X-Tyr (NPXY) motifs, which are recognised by clathrin and adapter proteins, are located in the cytoplasmic tail of megalin and mediate internalisation of the receptor into clathrin-coated pits[88,89]. Internalised vesicles then fuse with early endosomes, entering the endosomal-lysosomal pathway for ligand-receptor dissociation, ligand processing and receptor recycling or degradation[87,90] (Figure 7). Impairment of this process, results in the low-molecular-weight proteinuria observed in many Fanconi syndrome patients, as is the case in Dent's disease (DD), which will be discussed in detail in Section 4.1.2.

Many of the LMWPs reabsorbed by megalin and cubilin are carrier proteins, enabling the reabsorption of vitamins and minerals such as retinol, vitamin D, cobalamin and iron[87]. Reabsorption of 25(OH)D_3 complexed to the vitamin D binding protein (DBP) (Figure 7) is important for preventing urinary loss and the subsequent conversion of 25(OH)D_3 to its active form, 1,25-$(OH)_2D_3$[87]. Megalin and cubilin also play an important role in the reabsorption of albumin in the PT (Figure 7). Approximately 71% of filtered albumin is estimated to be reabsorbed by the PT, a further 23% by the LOH and DTs and the remaining 3% by the CDs[91]. Reabsorption of albumin by megalin and cubilin ultimately results in albumin entering the RME pathway, where albumin is degraded into amino acids at lysosomes[91].

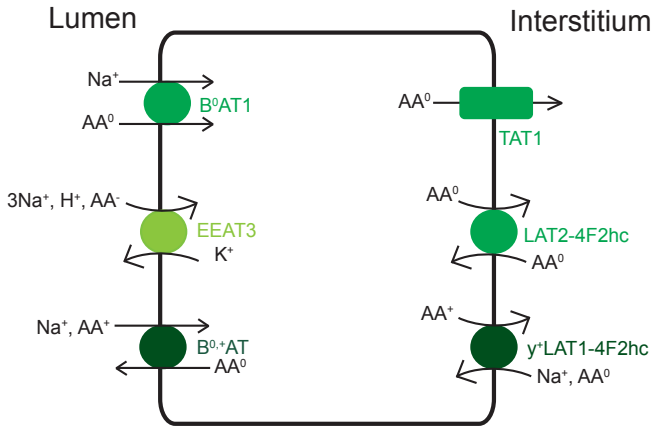
Figure 7. Reabsorption of LMWPs in the PT



Schematic representation of LMWP reabsorption in the PT via the multi-ligand co-receptors, megalin and cubilin. As co-receptors megalin and cubilin can interact forming a dual-receptor complex, reabsorbing a wide-range of LMWPs including hormones such as PTH, vitamin and mineral binding proteins such as 25(OH)D_3 complexed to the vitamin D binding protein (DBP) and albumin in the PT[85-87]. Asn-Pro-X-Tyr (NPXY) motifs in the cytoplasmic tail of megalin are recognised by clathrin and adapter proteins that mediate the internalisation of the receptor into clathrin-coated pits[87,88]. The internalised vesicle containing the ligand-receptor complex then fuses with early endosomes and enters the endosomal-lysosomal pathway responsible for ligand-receptor dissociation, ligand processing and receptor recycling or degradation[90]. Adapted from Christensen and Birn[87].

Reabsorption of amino acids in the PT is complicated by their diverse range of structures and ionic properties, but is largely accomplished as a result of Na^+-co-transport[6,92] (Figure 8). Three solute carriers: the Na^+-dependent neutral amino acid transporter (B^0AT1), the Na^+ and H^+-dependent excitory amino acid transporter 3 (EAAT3) and the b(0,+)-type amino acid transporter 1 ($B^{0+}AT$) mediate the reabsorption of neutral, acidic and basic amino acids, respectively across the apical membrane[6] (Figure 8). However, the mechanisms underlying basolateral transport of amino acids are not as well characterised[6] (Figure 8).

Figure 8. Amino acid transport in the PT

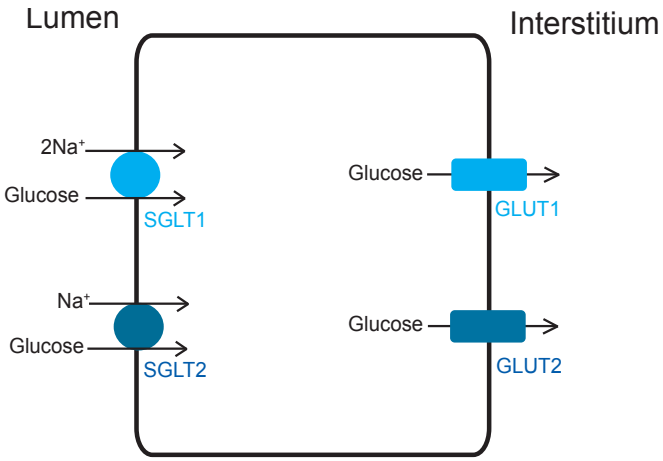


Schematic representation of amino acid transport in the PT. Three apically expressed Na^+-dependent transporters, neutral amino acid transporter (B^0AT1), excitory amino acid transporter 3 (EEAT3) and the b(0,+)-type amino acid transporter 1 ($B^{0,+}AT$), are responsible for the transport of neutral (AA^0), anionic (AA^-) and cationic (AA^+) amino acids, respectively, from the lumen into the cell[6,93]. Whilst the transporters responsible for the basolateral reabsorption of neutral and cationic amino acids from the cell into the interstitium have been revealed (the T-type amino acid transporter 1 [TAT], the large neutral amino acids transporter small subunit [LAT] 2 associated with 4F2 cell-surface antigen heavy chain [4F2hc[[LAT2-4F2hc)] and y^+LAT1-4F2hc), much less is known about the basolateral reabsorption of anionic amino acids[93]. Adapted from Verrey et al.,[93].

The renal tubules also play an important role in maintaining glucose homeostasis, through reabsorption of glucose and gluconeogenesis[94]. Under normal physiological conditions, almost all glucose is reabsorbed by the PT[94]. Approximately 90% of glucose reabsorption takes place in the S1 segment of the PT by the apically expressed high-flux, low-affinity Na^+ and glucose co-transporter (SGLT) 2 (SGLT2)[2,6,94] (Figure 9). Any remaining glucose is then reabsorbed from the ultrafiltrate in the S3 segment by the low-flux, high-affinity apically expressed SGLT1[2,6,94] (Figure 9). Thus, reabsorption of glucose across the apical membrane requires a Na^+ gradient[94]. A low concentration of intracellular Na^+ is generated and maintained by the Na^+/K^+-ATPase located on the basolateral membrane[94]. Diffusion of glucose across the basolateral membrane is carried out by specific facilitative glucose transporters (GLUTs) and is conditional on the generation of a glucose gradient, whereby the intracellular concentration of glucose exceeds the interstitial levels[94]. Much like the differential

expression of SGLT1 and 2 across the PT, GLUT2 is a high-capacity, low-affinity transporter expressed in the S1 segment and GLUT1 is a low-capacity, high-affinity transporter expressed in the S3 segment of the PT[6,94] (Figure 9). Mutations in SGLT2 and GLUT2 have both been associated with renal glycosuria and Fanconi-Bickel syndrome, respectively, both of which are characterised by glycosuria[95,96]. In addition to glycosuria, Fanconi-Bickel syndrome is also associated with aminoaciduria, HCO_3^--wasting, hypophosphataemic rickets, phosphaturia and hypophosphataemia[94,96].

Figure 9. Glucose transport in the PT



Schematic representation of glucose reabsorption in the PT. Reabsorption of glucose from the lumen, across the apical membrane is mediated by two Na^+ and glucose co-transporters (SGLTs), SGLT2 in the S1 segment and SGLT1 in the S3 segment[2,6,94]. Transport of glucose by the glucose transporters (GLUTs) across the basolateral membrane exhibits similar segmental differences. In the S1 segment diffusion of glucose across the basolateral membrane, into the interstitium, is mediated by GLUT2, whilst in the S3 segment it is mediated by GLUT1[6,94]. Adapted from Bakris et al.,[97].

Additionally, it has been suggested that the kidney may be responsible for approximately 40% of gluconeogenesis, ultimately producing approximately 20% of all glucose[94]. Whilst four substrates (lactate, glutamine, glycerol and alanine) are thought to be jointly responsible for approximately 90% of gluconeogenesis in the kidney, lactate has been suggested to be the principal precursor[94].

4.1.2 Dent's disease (DD): A renal tubular disorder of the PT

DD is a heterogeneous group of X-linked disorders of PT dysfunction, with characteristics consistent with a renal Fanconi syndrome[98]. Comprised of two subtypes: DD1, due to mutations in the chloride/proton antiporter CLC-5, which is encoded by the chloride voltage-gated channel 5 gene (*CLCN5*)[99] and DD2, due to mutations in the inositol polyphosphate 5-phosphatase gene (*OCRL1*)[100]. Patients with DD exhibit both inter and intra-familial variability (Table 1). In common all DD1 and DD2 patients have low-molecular-weight proteinuria, the majority have hypercalciuria (95% and 70-86%, respectively), while aminoaciduria, nephrocalcinosis, hypophosphataemia, glycosuria, hypokalaemia, rickets and renal failure are more common in DD1 than in DD2 (Table 1).

Table 1. Frequency of DD-associated characteristics in males with DD1

Clinical characteristics	Frequency	
	Dent's disease 1	Dent's disease 2
Low-molecular-weight proteinuria	100%	100%
Hypercalciuria	≤95%	70-86%
Haematuria	94%	Not known
Concentrating defect	82%	Not known
Aminoaciduria	≤76%	52%
Nephrocalcinosis	≤76%	≤39%
Renal Failure	≤64%	≤32%
Hypophosphataemia	≤60%	24%
Glycosuria	≤54%	11%
Nephrolithiasis	≤49%	Not known
Hypokalaemia	≤44%	6%
Rickets/ osteomalacia	≤30%	9%
Renal tubular acidosis	≤15%	4%

As a renal Fanconi syndrome DD is associated with an array of characteristics of PT dysfunction that are reported at varying frequencies in patients with DD[98,101-103]. This table provides an overview of the clinical characteristics reported in patients with DD1[101-103] and DD2[103] and the frequencies at which they are reported.

DD1 is the most prevalent of the two subtypes, accounting for approximately 60% of DD cases[98,104]. Analysis of reported and novel *CLCN5* mutations in 234 patients with DD1, revealed that DD1 mutations were located along all exons and protein domains of CLC-5, and comprised missense, nonsense, splicing, large deletions and in-frame deletions (Table 2). However, the majority comprise missense (33.33%) and frameshift (29%) mutations[101] (Table 2).

Table 2. Percentage of mutation types in *CLCN5* identified in patients with DD1

Mutation type	Percentage
Missense	33.33%
Frameshift	29.05%
Nonsense	17.52%
Splicing	12.39%
Large deletion	4.70%
Inframe	2.56%
Other (Alu insertion)	0.42%

Percentage of mutation types identified in *CLCN5,* in patients with DD1 in 234 patients[101].

CLC-5 is predominantly expressed in the PT where it facilitates reabsorption of LMWPs such as PTH and DBP, by playing a critical role in the acidification of early endosomes that is required for RME[87,98,105]. Endosomal acidification occurs as a result of the active transport of H^+ into endosomes by the electrogenic vacuolar H^+-ATPase (V-ATPase), coupled with the countercurrent for electoneutrality provided by CLC-5 ($2CL^-$:$1H^+$), which has been shown to co-localise with V-ATPase in renal endosomes[106-109]. RME in the PT occurs via megalin and cubilin, located at the apical brush border of PT cells[87]. Ligand-binding triggers internalisation of the receptor-ligand complex into clathrin-coated vesicles, that then enter the endocytic

pathway[87,110]. Endocytosis is characterised by a gradual acidification from the plasma membrane (almost neutral pH) to the early endosomes, followed by the late endosomes and lysosomes, which are the most acidic[111,112]. Acidification is required for progression along the RME pathway leading to the dissociation of the ligand from the receptors, activation of enzymes within endocytic compartments that are necessary for ligand processing or degradation and receptor recycling or degradation[113]. Furthermore, defects in both RME and endosomal acidification have been reported in conditionally immortalised proximal tubule epithelial cells (ciPTECs) from patients with DD1, as a result of mutations in CLC-5[109].

When this endocytic pathway is defective, as is the case in DD1 patients[114], LMWPs such as PTH and DBP-25(OH)D_3 are not reabsorbed effectively, and proteinuria occurs.[87]. Consequently, there is an elevation in these proteins within the lumen, which may enhance PTH stimulation of PTH1Rs located more distally within the tubule, triggering increased endocytosis of NaPi-IIa and consequently phosphaturia[115]. Whilst the PTs are responsible for the majority of Ca^{2+} reabsorption in the renal tubules, the precise mechanisms underlying this are yet to be fully characterised[2,4,5]. Therefore, at present, the Ca^{2+}-related phenotypes observed in patients with DD are thought to be secondary to hypophosphataemia and increased 1,25$(OH)_2D_3$. 1,25$(OH)_2D_3$, is an important regulator of Ca^{2+} absorption in the intestines by stimulating the expression of the TRPV6 Ca^{2+} channel[116,117]. Thus, increased levels of 1,25$(OH)_2D_3$ are hypothesised to lead to increased Ca^{2+} absorption and hypercalciuria. Furthermore, hypercalciuria is one of the main risk factors for nephrolithiasis and nephrocalcinosis, thus providing an explanation for the higher prevalence of nephrolithiasis in DD patients[118,119]. Additionally, it is estimated that

rickets/osteomalacia are present in approximately 30% of male DD1 patients[101,102] (Table 1), which is likely secondary to the defects in Ca^{2+} and Pi homeostasis in these patients. The mechanisms underlying aminoaciduria in DD1 patients are yet to be fully elucidated; however, it has been hypothesised that it may be due to defective recycling of the relevant transporters. cDNA expression profiling has revealed altered expression of amino acid transporters in DD1 conditionally immortalised proximal tubule cells (ciPTECs) compared with wild-type (WT) ciPTECs[109].

DD2, due to mutations in *OCRL1*, accounts for a further 15% of DD patients and is clinically indistinguishable from DD1[98]. Additionally**,** mutations in *OCRL1* are also associated with the X-linked oculocerebrorenal syndrome of Lowe[120], which is characterised by: congenital cataracts, intellectual impairment and renal tubular dysfunction (including aminoaciduria, hypercalciuria, nephrocalcinosis, nephrolithiasis, phosphaturia, glycosuria and slowly progressive renal failure)[98]. *OCRL1* encodes an inositol polyphosphate 5-phosphatase (OCRL1), which plays key roles in intracellular trafficking in the PT[98,121]. Thus, impaired function of OCRL1 results in disrupted endosomal trafficking, much like that observed in DD1[98]. Notably, patients with DD2 lack the intellectual impairment and congenital cataracts observed in patients with Lowe syndrome[98]. The phenotypic differences associated with DD2 and Lowe syndrome are thought to be due to the differences observed in the location of mutations in *OCRL1* for each of the disorders[98,121]. *OCRL1* mutations associated with DD2 are mostly located within exons 1-7, whilst those associated with Lowe syndrome have been reported to be located in exons 8-23[121].

Notably, 25-35% of DD patients lack mutations in *CLCN5* and *OCRL1*, suggesting a role for additional genes in DD[98]. Whilst attempts have been made previously to identify such genes (e.g. chloride voltage-gated channel 4 [*CLCN4*], cofilin [*CFL1*], transmembrane protein 27 [*TMEM27*] and solute carrier family 9 member A6 [*SLC9A6*]), as yet there has been no success[100,122-124].

4.1.3 Loop of Henle (LOH)

There are two types of nephron, determined by the depth the bend of the LOH reaches: short-loop nephrons, where the bends are formed in the outer medulla, and long-loop nephrons where the bends are formed in the inner medulla[12]. In humans the ratio of short-loop to long-loop nephrons is estimated to be approximately 85:15[12]. The LOH, comprised of the thin descending limb (tDL), thin ascending limb (tAL) (short-loop nephrons only) and thick ascending limb (TAL), plays important roles in urea recycling, reabsorption and secretion of ions, reabsorption of HCO_3^- and ammonium (NH_4^+) and urinary concentration mechanisms[12-14]. The U-shaped arrangement of the LOH; the parallel and close arrangement of vessels and tubules (including the LOH and CD) in the medulla; and the varying permeability's of the descending and ascending limbs enables efficient urea recycling and the generation and maintenance of the renal countercurrent multiplication system[14,125]. This ultimately results in the accumulation of urea in the inner medulla, generating an osmotic force driving water reabsorption and the concentration of urine, including a relatively high urinary urea concentration, compared to the plasma[14,125].

4.1.3.1 The thin descending limb (tDL)

The tDL is highly permeable to H_2O and H_2O transport in these tubules is thought to be primarily mediated by AQP1; which has been shown to be abundantly expressed in both the apical and basolateral membranes of the tDLs of long-loop nephrons[12,126] (Figure 10). Conversely, the tDL has been shown to have low HCO_3^- permeability, with the concentration of HCO_3^- in the lumen increasing significantly at the bend of the LOH[14]. Additionally, expression of the urea transporter (UT) UT-A2 has been reported in the lower half of the tDL in short looped nephrons and in the initial inner medullary section of the tDL in long-looped nephrons[12,127] (Figure 10), suggesting a role in urea recycling, water reabsorption and urinary concentration[125,128].

4.1.3.2 The thin ascending limb (tAL)

Whilst, tALs are reported to have little or no transepithelial osmotic water permeability, they do have a relatively high permeability to urea, contributing to renal urea recycling and urinary concentration[12,129] (Figure 10). Additionally, the tAL plays a role in transepithelial Cl^- transport through the Cl^- channel ClC-Ka and its accessory protein barttin[12,130-132] (Figure 10). Expression of Cl^- channels ClC-Ka and ClC-Kb (expressed in the TAL and DT) with barttin has also been reported in the stria vascularis of the inner ear[131,133]. Thus, mutations in barttin or simultaneous mutations in ClC-Ka and ClC-KB, are associated with a severe form of Bartter syndrome (type 4a and 4b respectively), which are associated with renal salt wasting, polyuria and sensorineural deafness[131,134].

4.1.3.3 The thick ascending limb (TAL)

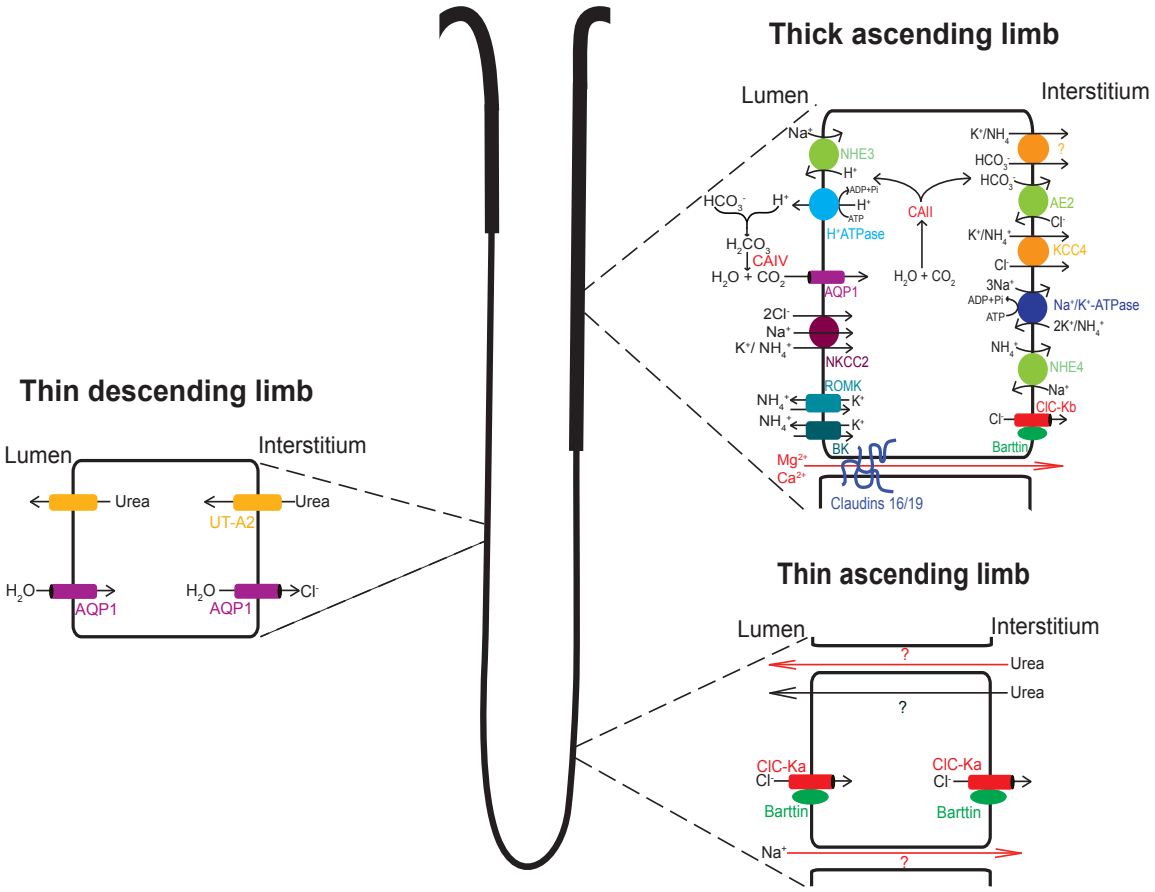
The TAL is the final segment of the LOH and whilst it is impermeable to water, it is responsible for the reabsorption and secretion of a variety of ions (Figure 10). Thus, it plays a vital role in generating and maintaining osmotic gradients and urinary concentrating mechanisms[13,14]. Reabsorption of approximately 30% of Na^+ and Cl^- from the ultrafiltate occurs in the TAL, predominantly via the $Na^+/K^+/2Cl^-$ co-transporter NKCC2 (apical membrane), the Na^+/K^+-ATPase (basolateral membrane) and ClC-Kb and it's accessory protein barttin (basolateral membrane)[13,14,135] (Figure 10). Conversely, approximately 90% of the K^+ reabsorbed from the lumen by NKCC2 is recycled back across the apical membrane into the lumen by the renal outer medullar K^+ channel (ROMK) and the 'big' K^+ channel BK[13,14] (Figure 10). Thus, the net K^+ reabsorption is minimal and the secretion of K^+ into the lumen acts to increase paracellular reabsorption of cations[13,14].

Paracellular transport in the TAL is important for the reabsorption of additional cations such as Ca^{2+} and Mg^{2+}, as well as for the additional reabsorption of Na^+[14] (Figure 10). Specifically, the TAL is thought to be responsible for the reabsorption of approximately 50-60% of filtered Mg^{2+} and approximately 20% of filtered Ca^{2+} via this route[4,10,11] (Figure 10). Reabsorption of Ca^{2+} and Mg^{2+} via the paracellular route is facilitated by the tight junction proteins claudins 16 and 19, mutations of which are associated with familial hypercalciuric hypomagnesaemia[136,137] (Figure 10). Inhibition of paracellular Ca^{2+} and Mg^{2+} reabsorption via claudins 16 and 19 is accomplished by claudin 14[4,138,139].

In addition to ion reabsorption and secretion, the TAL plays an important role in the reabsorption of HCO_3^- and NH_4^+[10] (Figure 10). The TAL is estimated to reabsorb approximately 15% of filtered HCO_3^-, mediated by NHE3, whereby the apical secretion of H^+ is accompanied by the basolateral absorption of HCO_3^- by a number of mechanisms including Cl^-/HCO_3^- exchange via the Cl^-/HCO_3^- exchanger 2 (AE2) and K^+/HCO_3^- co-transport via an uncharacterised transporter[13,14] (Figure 10). NH_4^+ generated in the PT is reabsorbed in the TAL by NKCC2 and other K^+ transporters in the apical membrane, NHE4 in the basolateral membrane and paracellular transport[13] (Figure 10). NH_4^+ can be reabsorbed by K^+ transporters as NH_4^+ has the same ionic radius as K^+ (Figure 10); however, increases in the luminal concentration of K^+ have been shown to inhibit active NH_4^+ reabsorption, likely due to the competitive inhibition of K^+ transporters[13].

Finally, the TAL is known to express uromodulin[13]. Proteolytic cleavage of the membrane-anchored protein releases it into the lumen where it is excreted as the most abundant protein in human urine[13]. Whilst the precise role and function of uromodulin is not known, studies have hypothesised a potential role in ion transport, including facilitating membrane trafficking and function of K^+ transporters NKCC2 and ROMK[13]. Mutations in uromodulin are associated with familial juvenile hyperuricaemic nephropathy (FJHN), which is characterised by hyperuricaemia, reduced fractional uric acid clearance, gout and progressive renal insufficiency associated with interstitial fibrosis[140].

Figure 10. Reabsorption and secretion at the LOH



Schematic representation of reabsorption and secretion in the LOH. The tDL reabsorbs water from and secretes urea into the lumen via the water channel aquaporin 1 (AQP1) and urea transporter UT-A2, respectively[12,126,141,142]. In the tAL, reabsorption of Cl^- from the lumen and into the interstitum occurs through ClC-Ka and barttin, located at both the apical and basolateral membranes[12,130,143]. Additionally, the precise mechanisms respsonsible for the secretion of urea into the lumen and the paracellular reabsorption of Na^+ from the lumen in the tAL remains unknown[12,129,144,145]. The TAL is responsible for the reabsorption and secretion of a wide variety of different ions including: Na^+, Cl^-, HCO_3^-, K^+ and NH_4^+[13,14]. Na^+ reabsorption from the lumen into the interstitium occurs via NKCC2, NHE3 and the Na^+/K^+-ATPase[13,14,135]. Additionally, NKCC2 is responsible for Cl^- reabsorption from the lumen, across the apical membrane[13,14,135]. ClC-Kb and barttin, and the Cl^-/K^+ co-transporter KCC4 are required for Cl^- reabsorption across the basolateral membrane into the interstitium[13,14,135]. Net K^+ reabsorption from the lumen to the interstitium by NKCC2, ROMK, BK and KCC4 is minimal in the TAL due to its secretion across the basolateral membrane from the intersitium by the Na^+/K^+-ATPase and across the apical membrane into the lumen by ROMK and BK[13,14]. As NH_4^+ has the same ionic radius as K^+, the K^+ transporters and channels also transport NH_4^+[13]. The TAL is also responsible for the reabsorption of HCO_3^-. H^+ secreted across the apical membrane by NHE3 and the H^+-ATPase combines with HCO_3^- in the lumen to form H_2CO_3[13,14]. The membrane-tethered CAIV dehydrates H_2CO_3 to generate CO_2 and H_2O, which are reabsorbed across the apical membrane, from the lumen, by AQP1[13,14]. In the cytoplasm, CAII catalyses the hydration of CO_2 and H_2O, reforming H^+, which can be recycled across the apical membrane, into the lumen, and HCO_3^-, which can be reabsorbed across the basolateral membrane, into the interstitium, by the Cl^-/HCO_3^- exchanger 2 (AE2) and an uncharacterised K^+/HCO_3^- co-transporter[13,14]. Paracellular transport in the TAL is also important for the reabsorption of additional ions such as Ca^{2+} and Mg^{2+} via claudins 16 and 19[4,10,11,14,136,137]. Adapted from Mount[13].

4.1.4 FJHN: A renal tubular disorder of the TAL

Principally affecting the TAL, FJHN is a genetically heterogeneous disorder characterised by hyperuricaemia, reduced fractional uric acid clearance, gout and progressive renal insufficiency associated with interstitial fibrosis[140]. To date four subtypes have been identified: FJHN1 due to mutations in uromodulin (*UMOD*)[140]; FJHN2 due to mutations in renin (*REN)*[146]*;* FJHN3 which has been mapped to chromosome 2p22.1-p.21.2[147]; and an atypical form of FJHN which is associated with mutations in hepatocyte nuclear factor 1ß *HNF1ß*[148]. However, mutations in *UMOD*, *REN* and *HNF-1ß* have only been identified in approximately 45% of patients, with mutations in *UMOD* alone being identified in 40% of patients[147], indicating a role for additional gene(s) in the pathogenesis of FJHN.

Uromodulin is expressed predominantly in the TAL and the early DCT and is the most abundant protein in human urine, where it is predominantly present as a polymer[149-151]. Mature uromodulin protein is generated by a series of post-translation modifications, including the formation of disulphide bonds in the endoplasmic reticulum (ER)[152,153]. Subsequently, mature uromodulin is targeted to the apical membrane where it is secreted into the lumen by proteolytic cleavage[150,152-154]. However, uromodulin mutations in FJHN patients are reported to result in impaired trafficking and secretion of the mature protein and consequently the aggregation and retention of mutant uromodulin in the ER, leading to ER stress[150,155,156]. It has been suggested that this may be a key stage in the pathogenesis of FJHN1 and interstitial fibrosis, although the precise mechanisms responsible remain to be determined[150,157].

Mutations in *REN*, encoding renin, are responsible for FJHN2[146]. Renin is a central enzyme in the renin-angiotensin system, reported to be central to the control and regulation of blood pressure and fluid-electrolyte homeostasis[158-161]. Renin is responsible for catalysing the first step of the activation pathway, cleaving angiotensinogen (AGT) to form angiotensin I, which is subsequently converted to angiotensin II by the angiotensin I-converting enzyme (ACE)[160,161]. Furthermore, as AGT levels are in excess in the human body and ACE is ubiquitously expressed in the endothelium and plasma, renin is thought to be the rate limiting step in this process[160]. Thus, whilst it has been established that renin levels are key regulators of blood pressure and electrolyte balance, the molecular mechanisms underlying how mutations in renin result in the phenotypes observed in FJHN2 remain to be elucidated.

Atypical FJHN, caused by mutations in *HNF1ß,* is associated with hyperuricaemia, gout, renal cysts and diabetes[148]. *HNF1ß* encodes the hepatocyte nuclear factor-1ß transcription factor (HNF-1ß*)*, which is associated with both renal and extra-renal disorders and phenotypes. First associated with maturity-onset diabetes of the young (MODY) type 5[162], the presence of renal cystic disease in many of these patients resulted in the disease being renamed renal cysts and diabetes syndrome[162,163]. More recently, a more varied spectrum of clinical phenotypes has been observed in patients with *HNF1ß* mutations, with or without renal cysts and diabetes[162,163]. Significantly, hyperuricaemia and gout had been reported in patients with mutations in *HNF1ß*, thus some patients fulfil the diagnostic criteria for atypical FJHN[148]. As a transcription factor, HNF-1ß expression has been reported in a range of different tissues including: the pancreas, liver, kidneys and gastrointestinal tract[162,163], which may explain the

multisystem phenotypes observed in individuals harbouring *HNF1ß* mutations. Interestingly, reduced expression of *Umod* has been reported in mice with renal-specific inactivation of *HNF1ß*[164], suggesting that HNF-1ß may regulate the transcription of *UMOD*. Therefore, the hyperuricaemia and gout phenotypes observed in patients with atypical FJHN may be a result of the same mechanism as those in FJHN1. Furthermore, the mice were also reported to have reduced polycystic kidney disease 2 (*Pkd2*) and polycystic kidney and hepatic disease 1 (*Pkhd1*) expression[164], mutations in both of which are associated with polycystic kidney disease (PKD)[165-167], thereby providing an explanation for the formation of renal cysts in some patients with atypical FJHN.

4.1.5 Distal tubules (DTs)

The DT, comprised of the DCT and connecting tubules (CNT), encompass the region between the LOH and CD. The ultrafiltrate that reaches the DT is largely devoid of amino acids, glucose, HCO_3^- and other non-waste solutes, having been reabsorbed in the PT and LOH[168,169]. However, The DT and CD play important roles in the regulation of blood volume and therefore blood pressure by regulating the reabsorption of Na^+ and H_2O as well as the secretion of K^+[18].

4.1.5.1 Na^+ reabsorption at the DT

The DCT is responsible for the reabsorption of <10% of filtered Na^+ and is therefore responsible for the final fine-tuning of Na^+ reabsorption and ultimately the final concentration of Na^+ in the urine[15,18]. Na^+ reabsorption at the apical membrane is predominantly accomplished via the Na^+/Cl^- co-transporter NCC in the early DCT and the epithelial Na^+ channel ENaC in the late DCT[15,18,19,168-170] (Figure 11), both of which

are regulated by multiple factors including aldosterone and the with-no-lysine (WNK) serine/threonine kinases 1 and 4[18,19,78,171,172]. Whilst at the basolateral membrane Na^+/K^+-ATPase is responsible for transporting Na^+ out of the cell (Figure 11), establishing and maintaining a favourable electrochemical gradient for further reabsorption of Na^+[17,173]. The DT and CD are often referred to as the aldosterone-sensitive distal nephron due to the role aldosterone plays in the regulation of Na^+ reabsorption by increasing the cell-surface expression of ENaC and the Na^+/K^+-ATPase[18,19,78,171]. Conversely, WNK4 decreases the surface expression of NCC[19].

4.1.5.2 Cl^- reabsorption at the DT

Cl^- ions are transported alongside Na^+ by the NCC, but can also undergo transcellular uptake by ClC-Kb and its accessory subunit barttin at the basolateral membrane and the cystic fibrosis transmembrane conductance regulator CFTR at the apical membrane[18] (Figure 11). Cl^- is also reabsorbed in the DT by paracellular mechanisms (Figure 11), driven by the lumen-negative transepithelial potential established by Na^+ reabsorption via ENaC[15].

4.1.5.3 K^+ secretion at the DTs

Although the majority of K^+ is reabsorbed in the PT and TAL, the luminal concentration of K^+ has been shown to increase through the DT, indicating the DT and CD are responsible for net secretion of K^+[15,17]. Secretion of K^+ by the DT is regulated by a range of factors including WNK4 inhibition of ROMK[19]; depolarisation of the apical membrane by ENaC-mediated Na^+ reabsorption[15,19]; and the rate of urinary flow[15] (Figure 11). Whilst, ROMK is the primary mechanism by which K^+ is secreted across the apical membrane into the lumen[15,19], K^+ secretion is also accomplished in a

flow-dependent manner by BK channels[15] (Figure 11). At the basolateral membrane, in addition to mediating Na^+, the Na^+/K^+-ATPase mediates the import of K^+ in the cell, building a high intracellular K^+ concentration and ultimately driving K^+ secretion into the lumen[18] (Figure 11).

4.1.5.4 Mg^{2+} reabsorption at the DT

The DT is also involved in the fine-tuning of Mg^{2+} reabsorption. Whilst the majority of Mg^{2+} is reabsorbed in the TAL, the DT is estimated to reabsorb 5-10% of filtered Mg^{2+}[15,16]. In the DCT Mg^{2+} reabsorption is mediated by transcellular mechanisms[16] (Figure 11). At the apical membrane of the DCT the transient receptor potential cation channel subfamily M member 6 (TRPM6) mediates the reabsorption of Mg^{2+}[15,16] (Figure 11), mutations in which are associated with hypomagnesaemia with secondary hypocalcaemia[174,175]. TRPM6 also localises with multiple cofactors at the membrane including the voltage-gated potassium channel Kv1.1, parvalbumin in the early DCT and the Ca^{2+}-binding protein calbindin-D28k in the late DCT[16]. At the basolateral membrane, Mg^{2+} is transported out of the cell by active transport; however, the identity of these transporters is yet to be fully elucidated[16] (Figure 11).

4.1.5.5 Ca^{2+} reabsorption at the DT

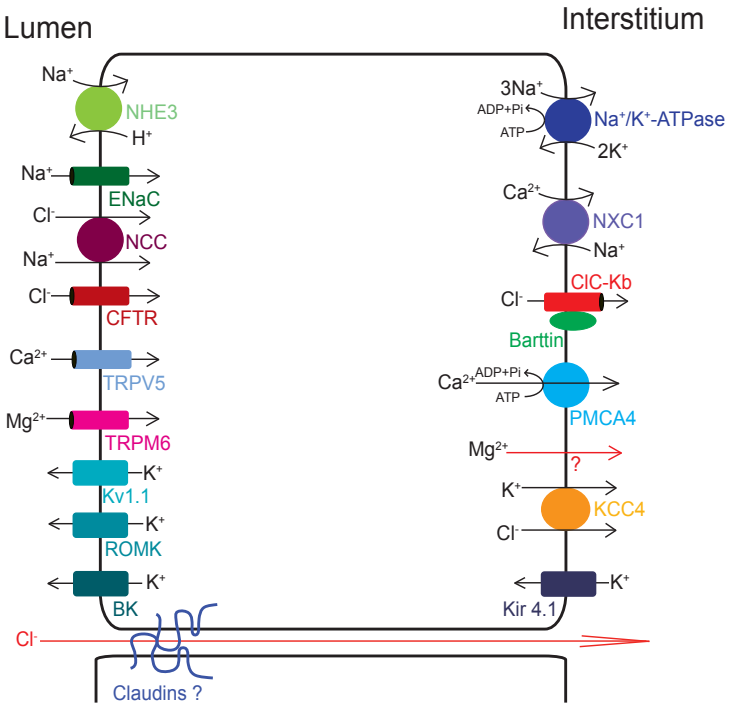
Similarly, to Na^+ and Mg^{2+} reabsorption, the majority of Ca^{2+} reabsorption is accomplished in more proximal segments, with the DT responsible for the final fine-tuning, reabsorbing approximately 8% of Ca^{2+} via transcellular mechanisms[4,15]. At the apical membrane Ca^{2+} is reabsorbed from the lumen by TRPV5[4,15] (Figure 11). Ca^{2+} that enters via TRPV5 then associates with calbindin-D28k, which shuttles Ca^{2+} to the

basolateral membrane[4,15]. At the basolateral membrane Ca^{2+} exits the DT cells via the Na^{+}/Ca^{2+} exchanger NXC1 or the Ca^{2+}-ATPase PMCA4[4] (Figure 11).

Regulation of Ca^{2+} reabsorption can occur via a number of different mechanisms including Na^{+} transepithelial gradients established by the NCC in the DCT and ENaC in the DCT and CNT, as well as by regulation of TRPV5 expression[4]. Expression of TRPV5 at the apical membrane has been suggested to be the rate-limiting step in the reabsorption of Ca^{2+} in the DT and has been shown to be regulated by $1,25(OH)_2D_3$, PTH, Klotho, uromodulin and cytosolic Ca^{2+}[4,15,68].

The importance of TRPV5 in the fine-tuning of Ca^{2+} reabsorption has been shown in models of TRPV5-deficiency, resulting in hypercalciuria in TRPV5-null mice (*TRPV5*$^{-/-}$)[176] and reduced Ca^{2+} transport (26% of control) in primary cell cultures of DT cells isolated from *TRPV5*$^{-/-}$ mice[177]. Despite *TRPV5*$^{-/-}$ mice exhibiting hypercalciuria, normal serum Ca^{2+} levels suggested the presence of compensatory mechanisms[176]. Further investigation revealed elevated serum $1,25(OH)_2D_3$ levels and the upregulation of the TRPV6 Ca^{2+} channel in the small intestines, consistent with increased Ca^{2+} absorption in *TRPV5*$^{-/-}$ mice[176].

Figure 11. Ion transport in the DT



Schematic representation of paracellular and transcellular transport of ions in the DTs. Reabsorption of Na^+ from the lumen, across the apical membrane is performed by NHE3, the Na^+/Cl^- co-transporter NCC and the epithelial sodium channel ENaC; and across the basolateral membrane into the interstitium by the Na^+/K^+-ATPase[15,17-19,168-170,173]. NCC also transports Cl^- from the lumen across the apical membrane, as does the cystic fibrosis transmembrane conductance regulator CFTR[18]. At the basolateral membrane ClC-Kb and KCC4 facilitate reabsorption of Cl^- into the interstitium[18]. Further Cl^- reabsorption is facilitated by paracellular mechanisms, however the claudin(s) that mediate this remain to be elucidated[15]. Reabsorption of Ca^{2+} from the lumen is performed by TRPV5[4,15]. In the cytoplasm Ca^{2+} associates with the Ca^{2+}-binding protein calbindin-D28k, which shuttles Ca^{2+} to the basolateral membrane where it exits the cell, entering the interstitium, via the Na^+/Ca^{2+} exchanger NXC1 or the Ca^{2+}-ATPase PMCA4[4,15]. Reabsorption of Mg^{2+} from the lumen is mediated by the transient receptor potential cation channel subfamily M member 6 (TRPM6)[15,16]. Additionally, reabsorption of Mg^{2+} across the basolateral membrane, into the interstitium, is reported to be mediated by active transport mechanisms, the identity of which is yet to be fully elucidated[16]. At the apical membrane ROMK, BK and the voltage-gated K^+ channel Kv1.1 are responsible for the secretion of K^+ into the lumen[15,19]; whilst the Na^+/K^+-ATPase and the inward rectifying K^+ channel Kir4.1 mediate the import of K^+ into the cell at the basolateral membrane from the interstitium[18]. Adapted from Subramanya and Ellison[15].

4.1.6 Collecting ducts (CDs)

The CD is the final component of the renal tubules and plays an important role in the concentration of urine[20]. It is made up of three segments: the cortical collecting duct (CCD), the outer medullary collecting duct (OMCD) and the inner medullary collecting

duct (IMCD)[20,178,179]. The most proximal is the CCD, responsible for increasing the concentration of urea in the lumen; which occurs largely as a result of salt and H_2O reabsorption[20]. Furthermore, the CCD is also responsible for K^+ secretion[20]. The OMCD is similarly impermeable to urea[20]; thus it also contributes to the high concentration of urea in the lumen[20]. Finally, the IMCD is the most terminal segment and is responsible for the generation of maximally concentrated urine and reabsorption of urea by UT-A1 and UT-A3[20,180].

The differences in the reabsorption and secretion capacities between the three segments is thought to be partly due to the varying ratios of principal and intercalated cells in each. Whilst principal cells make up the majority of cells in the DT and CD, intercalated cells are interspersed among them at varying, segment-specific ratios[22,170]. In the CCD, the ratio of principal:intercalated cells is approximately 2-3:1, in the OMCD this increases to approximately 5:1 and the IMCD is thought to be only principal cells[22].

Principal cells play a fundamental role in salt and water transport reabsorption via the apical ENaC, the basolateral Na^+/K^+-ATPase, AQP2 (apical), AQP3 and AQP4 (both basolateral)[168,170]. Principal cells also play an important role in the secretion of K^+ by the basolateral Na^+/K^+-ATPase and the apical ROMK[168,170,181]; and the reabsorption and secretion of Cl^- by the apical CFTR and the paracellular pathway[168].

Unlike, principal cells, the primary role of intercalated cells is to regulate acid-base homeostasis in the CD[21]. The secretion of H^+ into the lumen is mediated by the V-ATPase and the H^+/K^+-ATPase, whilst absorption of HCO_3^- is mediated by the

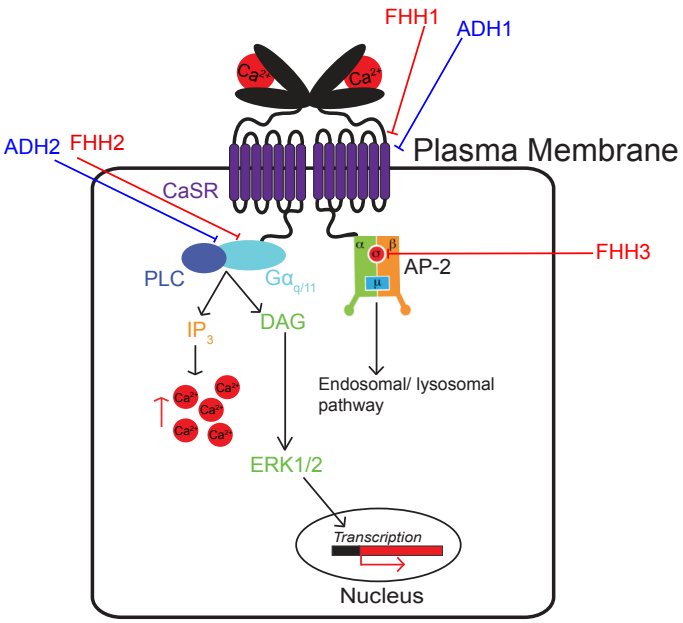
basolateral Cl^-/HCO_3^- exchanger AE1[21,22]. Finally, whilst reabsorption of K^+ is performed by the H^+/K^+-ATPase, Cl^- reabsorption is carried out by multiple transporters and exchangers, including the Cl^- transporter A11[21,22].

4.1.7 Familial hypocalciuric hypercalcaemia (FHH): A renal tubular disorder of the TAL and DT

Familial hypocalciuric hypercalcaemia (FHH) is a genetically heterogeneous disorder of Ca^{2+} homeostasis, characterised by elevated levels of serum Ca^{2+}, decreased urinary Ca^{2+} excretion and normal or increased PTH[182]. Three subtypes have been identified to date: FHH1 due to loss-of-function (LOF) mutations in the Ca^{2+}-sensing receptor (CaSR) (*CASR*)[183], a class C GPCR; FHH2 due to LOF mutations in $G\alpha_{11}$ (*GNA11*)[184], which is involved in G_α mediated signalling downstream of CaSR; and FHH3 due to LOF mutations in adaptor protein-2 (AP-2) sigma subunit (*AP2S1*)[185], which is involved in clathrin-mediated endocytosis of CaSR. Whilst FHH1 and 2 are typically asymptomatic, associated with normal circulating PTH and mild hypermagnesaemia, some cases of pancreatitis and gallstones, as well as an increased prevalence of chondrocalcinosis with advancing age have been reported FHH[186-188]. In contrast, FHH3 is characterised by increased PTH concentrations, hypophosphataemia and osteomalacia[189]. Whilst, LOF mutations in *CASR* and *GNA11* causes FHH, gain-of-function mutations in *CASR* and *GNA11* result in autosomal dominant hypocalcaemia (ADH) 1 and 2 respectively, which is associated with the opposite phenotype to FHH of hypocalcaemia, normal or low serum PTH and hyperphosphataemia[184,190].

The CaSR plays a principal role in regulation of Ca^{2+} homeostasis by regulating PTH secretion from the parathyroid[182]. The principal ligand for CaSR is Ca^{2+} and binding to the CaSR extracellular domain mediates conformational changes within the receptor's seven transmembrane domain region, triggering activation of associated G-proteins[191] (Figure 12). For the CaSR, the principal G-protein pathway by which signalling is mediated is the $G_{q/11}$ family, which activates phospholipase C (PLC), mediating intracellular Ca^{2+} mobilisation from intracellular stores and mitogen-activated protein kinase (MAPK) pathways[182,192] (Figure 12).

Figure 12. The role of the CaSR, $G\alpha_{11}$ and AP-2 proteins in CaSR trafficking and signaling



Schematic representation of the role of the CaSR, $G\alpha_{11}$ and AP-2 proteins in CaSR trafficking and signalling. Binding of Ca^{2+} to the CaSR triggers $G\alpha_{11}$-dependent stimulation of PLC[182,192]. This catalyses the formation of 1,4,5-triphosphate (IP_3), the accumulation of which results in the release of Ca^{2+} from intracellular stores; and diacylglycerol (DAG), which activates the MAPK/ERK1/2 signalling cascade resulting in changes in gene transcription[182,192,193]. The expression of the CaSR at the plasma membrane is regulated by agonist-driven insertional signalling (not shown)[194] and trafficking of the CaSR to the endosomal/lysosomal pathway by the AP-2 complex, consisting of α, ß, σ and μ subunits[182,195,196]. Loss of function mutations in the CaSR, $G\alpha_{11}$ and AP-2-σ subunit result in FHH1, 2 and 3 respectively[183-185] (highlighted in red). Conversely, gain-of-function mutations result in the CaSR and $G\alpha_{11}$ result in ADH1 and 2 respectively[184,190] (highlighted in blue). Adapted from Hannan et al.,[182].

4.1.7.1 Role of the CaSR in the renal tubules

The CaSR is expressed across the entire nephron, but is reported to be most highly expressed in the TAL and DCT where it regulates the reabsorption and secretion of multiple ions including Ca^{2+}, although the underlying mechanisms are yet to be fully elucidated[197]. The CaSR is expressed at the apical membrane of the PT where activation of the receptor inhibits the phosphaturic action of PTH[198] and 1α-hydroxylase activity[199]. In the TAL, the basolaterally expressed CaSR regulates the transcellular and paracellular reabsorption and secretion of a range of ions[200,201]. Hypercalcaemia results in the inhibition of the apically expressed ROMK, thus reducing the luminal concentration of K^+ and the rate of $Na^+/K^+/2Cl^-$ transport by NKCC2[200,201]. Additionally, the CaSR is thought to regulate the paracellular reabsorption of Ca^{2+} by regulating the transcription of the tight junction protein claudin 14. Studies showed that mice with a kidney-specific CaSR-deficiency had hypocalciuria, normal Ca^{2+} and PTH serum levels, and reduced claudin 14 expression[138]. CaSR regulation of claudin 14 is thought to be via two microRNAs (miRNAs): miR-9 and miR-374, that target the 3'-untranslated region (UTR) of *CLDN14*, suppressing its expression[139]. Claudin 14 has an inhibitory role in the reabsorption of divalent cations, such as Ca^{2+}, by abolishing the cation selectivity of the claudin 16-claudin 19 heteromeric channel, which is responsible for the reabsorption of divalent cations in the TAL[139]. Thus, LOF mutations in the CaSR or components of its signalling and trafficking pathways may be anticipated to suppress expression of claudin 14 and thus increase reabsorption of Ca^{2+} via the paracellular pathway, ultimately resulting in hypercalcaemia and hypocalciuria. In the human DT, the CaSR has been shown to be expressed both apically and in intracellular vesicles, where is regulates transcellular reabsorption of Ca^{2+} via TRPV5 and PMCA[200]. It has

been reported that the CaSR and TRPV5 co-localise at the apical membrane of DCT/CNT cells and that the elevated Ca^{2+} reabsorption in response to CaSR activation occurs via TRPV5[202]. However, it has been reported that in Madin-Darby canine kidney (MDCK) cells, stimulation of the basolaterally expressed CaSR results in a concentration-dependent inhibition of Ca^{2+} transport by inhibition of PMCA[203]. Thus, the overall effect of the CaSR on Ca^{2+} reabsorption in the DT is controversial.

Similarly, to both DD and FJHN, approximately 25% of FHH patients lack mutations in *CASR*, *GNA11* and *AP2S1.* Identification of novel genes in monogenic renal tubular disorders, such as these, is vital for improving the understanding of the molecular mechanisms underpinning such disorders; and to further elucidate the biological function and mechanisms of each segment. Furthermore, these findings can have direct applications in the clinic such as identification of novel therapeutic targets, improving familial genetic testing and reproductive counselling, providing a clearer diagnosis and prognosis, and improving disease management. Consequently, researchers and clinicians alike are more frequently turning to next-generation DNA sequencing (NGS) to identify mutations in novel and known causative genes in patients with monogenic disorders.

4.2. Identifying genetic causes of disorders of the renal tubules

The wide-ranging phenotypes observed in patients with monogenic renal tubular disorders can be attributed to the specialised function of each segment. Each segment is responsible for performing different reabsorption and secretion roles, orchestrated by the differential expression of channels, transporters and receptors between segments. However, some proteins that are mutated in renal tubular disorders are

expressed in multiple segments. Such is the case with the DTs and CDs where many proteins are expressed in both segments including ENaC (mutated in Liddle syndrome and pseudohypoaldosteronism type I)[204-207], AQP2 (mutated in hereditary nephrogenic diabetes insipidus)[208] and ROMK (mutated in Bartter syndrome type 2)[209]. Thus, the shared phenotypes between some renal tubular disorders can make clinical diagnoses difficult. Furthermore, the precise mechanisms underlying the phenotypes attributed to a particular disorder remain to be fully elucidated, such is the case for FJHN. Therefore, an unbiased approach to the identification of genetic causes of renal tubular disorders may be beneficial in cases of complex phenotypes. The identification of novel candidate genes and pathways in this way may improve the understanding of fundamental renal tubular processes. Additionally, improved understanding of renal tubular processes in health and disease and identification of novel candidate genes may identify novel therapeutic targets and improve clinical management of patients. Therefore, this thesis aimed to identify novel candidate genes in three monogenic renal tubular disorders (DD, FJHN and FHH) affecting different segments of the nephron using NGS technologies.

4.3. Next-generation DNA sequencing (NGS)

Traditionally, clinical genetic diagnosis and 'gene-discovery' studies relied on direct sequencing of single genes by Sanger DNA sequencing[110,210]. Whilst Sanger DNA sequencing remains the 'gold-standard', with accuracies up-to 99.99%[110,211,212], it is increasingly being replaced by NGS approaches for 'gene-discovery' studies[110,210,213,214]. Whilst the principles behind Sanger DNA sequencing and NGS do not markedly differ, the key difference is the ability of NGS to simultaneously sequence millions of DNA fragments compared to the individual fragments in Sanger

DNA sequencing[210]. Furthermore, the ever-decreasing cost and increasing availability of NGS make it the preferred method for 'gene-discovery' studies and genetic diagnosis for patients with heterogeneous disorders[110,210,213,214].

NGS is an umbrella term used to describe non-Sanger-based high-throughput DNA sequencing of the whole genome or a specified part of it. Specifically, NGS can be used to analyse the entire genome (whole-genome sequencing [WGS]), the protein-coding regions (whole-exome sequencing [WES]) or a specified selection of genes (targeted panel sequencing) each of which have their own advantages and disadvantages[213] (Table 3).

Table 3. Comparison of NGS techniques

NGS techniques	Coverage	Cost	*Identified variants
Whole-genome sequencing	Whole genome	£££	4 million
Whole-exome sequencing	Exome	££	20,000
Targeted gene panel	Selected genes	^£	^Variable

Overview of the coverage, cost and number of variants identified by whole-genome, whole-exome and targeted panel sequencing. Cost (£) represents the comparable costs of the NGS techniques, from least (£) to most (£££) expensive[210,214,215]. *Approximate number of variants identified by each technique, compared to the reference genome. ^Unknown and variable cost and number of variants as this is dependent on the number of genes included in the panel.

WGS is the most comprehensive and unbiased of the three, covering almost the entire genome, including both coding and non-coding regions[110,213,216], thus allowing the identification of variants in coding, regulatory and intronic regions[210,213]. This is significant as whilst the majority of diagnostic variants identified in clinical WGS investigations were exonic variants, non-coding pathogenic variants have been identified in various renal disorders, including intronic variants in patients with

Gitelman syndrome[213,217]. However, with this, comes a greater cost and complexity[210,216]. The assembly of the genome and interpretation of the vast amount of generated data (approximately 4 million variants) is laborious and requires bioinformatics expertise[110,210].

WES, as the name suggests, covers just the protein-coding portion of the genome (the exome), which accounts for approximately 1% of the human genome (approximately 20,000 genes)[110,216,218], thereby representing a more comprehensive and unbiased method than targeted panel sequencing[210,213,216]. Due to the reduced coverage, in comparison to WGS, the quantity of data generated is substantially lessened (approximately 20,000 variants compared to 4 million)[210,216] (Table 3). Consequently, data analysis is simpler, although as with all of these NGS approaches challenges in variant interpretation remain[210]. Furthermore, as the majority of known pathogenic variants have been identified in protein-coding regions, WES is thought to represent a time- and cost-efficient method in comparison to WGS[210,213,216]. However, WES does not detect variations in non-coding regions and therefore some clinically relevant variants may be missed[213,218].

NGS gene panels, represent a targeted approach for the sequencing of a select number of genes[213]. This is beneficial in the clinic when more than one gene may be associated with the clinical presentation of the patient[110,210,213]. As the sequencing is selective, the number of variants identified is significantly reduced when compared to WES and WGS and the potential of incidental findings is reduced[210,213]. Thus, simplifying the data analysis although, as previously stated, challenges with variant interpretation remain. Furthermore, the reduced cost, and relatively rapid pace at which targeted

panels can be completed in comparison to sequential Sanger DNA sequencing, often makes NGS targeted panels the favoured NGS method in the clinic[210]. However, like all of the NGS techniques, targeted panels do have their disadvantages including the prerequisite to know the candidate genes[210]. Consequently, whilst targeted panels may be useful in the clinic to provide a genetic diagnosis for patients with heterogenic disorders, they are not suitable for the initial stages of 'gene-discovery' studies[210].

These techniques have been rapidly changing the landscape of clinical genetics and genetic research[110,216]. However, one of the similarities of all of these techniques is the accurate interpretation of variants. In fact, this is largely thought to be the rate-limiting step[219]. Whilst *in vitro or in vivo* functional analysis of potentially pathogenic variants is thought to be the 'gold-standard' of variant interpretation[220], it would be too time-, cost- and labour-intensive to perform such studies on all the variants identified through NGS studies[220], as whilst they provide a great insight in the genetic variation within an individual, such studies identify vast numbers of variants[210,216] (Table 3). Furthermore, there are a number of additional difficulties facing the accurate interpretation of NGS data, including: the frequency of common variants, or those not related to the disorder being investigated[213]; detection of false-positive LOF variants[221]; and the presence of supposedly LOF variants in healthy individuals[221]. Thus, identification of the causative variant in a particular disorder remains challenging[213].

In an attempt to overcome the challenges faced by researchers and clinicians a number of strategies are used to validate and interpret variants identified through sequencing studies. NGS techniques may give rise to LOF false-positives arising from

base mis-calls and read mis-mapping[221]; therefore, confirmation of potential pathogenic variants using Sanger DNA sequencing and a secondary method such as restriction endonuclease digest (RED) or amplification-refractory mutation system (ARMS) PCR is required. Additionally, NGS techniques have revealed the presence of supposedly LOF variants in asymptomatic, apparently healthy individuals[221]. Thus, further complicating the process of accurate variant interpretation and highlighting the value of large-scale population datasets such as the Exome Aggregation Consortium (ExAC), which aim to map the genetic variation within a population; the inclusion of healthy 'normal' controls in confirmatory approaches; and co-segregation analysis to confirm the absence of the variant in healthy family members. However, as with validation by functional analysis, many of these approaches are time- and labour-intensive for the researcher and therefore are unsuitable for the large quantity of variants identified by NGS studies[220]. Thus, highlighting the importance of using *in-silico* analysis tools (such as allele frequencies in population databases, pathogenicity prediction algorithms and conservation analysis of amino acids) for the prioritisation of candidate pathogenic variants for confirmation and validation through *in vitro* and *in vivo* analysis. Therefore, the first part of this thesis aimed to investigate the effectiveness of *in silico* analysis tools at identifying and prioritising pathogenic variants, ultimately determining the optimal parameters to do so.

5 Materials and Methods

5.1. Materials

5.1.1 Chemicals

All chemicals were of analytical grade and purchased from Sigma-Aldrich®, VWR Chemicals, Promega, Gibco™, BDH Chemicals, Bio-Rad and AMRESCO®.

5.1.2 Antibiotics

Antibiotics were purchased from Gibco™ and Sigma-Aldrich®.

5.1.3 Oligonucleotides

Primers used for polymerase chain reaction (PCR), DNA sequencing analysis and site-directed mutagenesis (SDM) were synthesised by Sigma-Aldrich®. Quantitect primers for quantitative real-time PCR (qPCR) were purchased from Qiagen. A full list of all primers used can be found within the appendix (Table 32 to Table 36).

5.1.4 Enzymes

AccuPrime™ GC-rich DNA polymerase was obtained from ThermoFisher Scientific (Invitrogen™) and Blue MegaMix-Double (containing a proprietary formula of non-hot-start Taq DNA polymerases, 5mM Magnesium, $[NH_4]_2SO_4$ and a blue agarose loading dye) was obtained from Microzone. RNAse A was purchased from Qiagen; and the restriction endonucleases (REs), as well as their recommended buffers, were purchased from New England Biolabs® Inc. (NEB). A full list of REs and the conditions used for each can be found within the appendix (Table 37).

5.1.5 Vectors

Plasmid expression vectors encoding the protein of interest and a selectable marker, conferring resistance to selective antibiotics were used for *in vitro* functional studies. The pCMV6-AC-tGFP vectors encoding human Klotho (RG224132), human claudin 3 (RG204882) or human Denn Domain Containing 4C (Dennd4C) (RG219039) were purchased from Origene™ Technologies. The pcDNA™3.1(+) mammalian expression vector used for cloning studies was obtained from Invitrogen™.

5.1.6 Buffers and stock solutions

Autoclaving was undertaken at 121°C, 15lbs/square inch, for 15 minutes and the resulting product was labelled with the prefix 's' to indicate that it had been sterilised e.g. sd$H_2$0.

5.1.6.1 Nucleic acid handling

Nucleic acid loading buffer:

5x DNA Loading Buffer Blue (premixed with bromophenol blue) was obtained from Bioline.

Molecular weight markers:

Hyperladder™ 100bp and Hyperladder™ 1kb were obtained from Bioline.

10x Tris Borate-EDTA (TBE) buffer:

10x TBE buffer (containing 89mM Trizma® and 2mM EDTA, adjusted to pH 8.3 with

boric acid) was purchased from Sigma-Aldrich®.

Agarose gels for DNA electrophoresis:

1x TBE with 0.75%, 1.5% or 2% (w/v) UltraPure™ Agarose (ThermoFisher Scientific).

5.1.6.2 Transformation and culture of Escherichia coli (E.coli)

Luria Bertani (LB) Broth:

1% (w/v) Bacto™ Tryptone (Becton, Dickinson and Company [BD]), 0.5% (w/v) Select yeast extract (Sigma-Aldrich®), 0.5% (w/v) NaCl in distilled H_2O (dH_20), autoclaved and stored at room temperature (RT).

LB-Agar:

LB Broth with 1.5% (w/v) Select Agar™ (Invitrogen™), autoclaved and stored at RT.

NZY$^+$ broth:

1% (w/v) casenin hydrolysate, 0.5% (w/v) Select yeast extract (Sigma-Aldrich®), 0.5%, (w/v) NaCl, pH adjusted to 7.5 with NaOH, (plus 12.5mM $MgCl_2$), 12.5mM $MgSO_4$, 20mM glucose, autoclaved and stored at -20^{o}C.

5.1.6.3 Protein extraction and analysis

Modified RIPA (mRIPA):

150mM NaCl, 50mM Tris (pH 7.4), 1mM EDTA, 1% (v/v) Triton® X-100, 0.05% (v/v) Sodium dodecyl sulphate (SDS), made up to desired volume with dH_20. 1 cOmplete™

Mini EDTA-free Protease inhibitor cocktail tablet (Roche) was added to 10ml of the mRIPA buffer for cell lysis.

1x Tris/Glycine/SDS (TGS):

10x TGS solution (containing: 25mM Tris, 192mM glycine, 0.1% [w/v] SDS, pH 8.3) purchased from Bio Rad was diluted 1:10 with dH_20 for use as 1x TGS.

Phosphate buffered saline (PBS):

PBS tablets (containing 140mM NaCl, 10mM phosphate and 2.68mM KCL) purchased from Gibco™ were added 1 per 500ml dH_2O.

1x 3-(Cyclohexylamino)-1-propanesulfonic acid (CAPS) buffer:

10mM CAPS in 1L dH_20, titrated with approximately 0.25% (v/v) NaOH to pH11, was diluted 1:10 with dH_20 for use as 1x CAPS buffer.

1x Tris buffered saline (TBS):

8.8% (w/v) NaCl, 1.2% (w/v) Trizma® Base and 6.4% (w/v) Trizma® HCl in 500ml dH_20, was diluted 1:10 with dH_20 for use as 1x TBS.

1x TBS-Tween (TBS-T):

1x TBS plus 0.1% (v/v) Tween® 20.

Blocking buffer (1x TBS-T-Marvel):

1x TBS-T plus 5% (w/v) Marvel dried skimmed milk powder.

Protein loading buffers:

Protein loading buffers were made up as 2x stocks and added 1:1 to the sample. Buffers contained 2x Laemmli sample buffer (Bio-Rad) plus 2.5% (v/v) β-mercaptoethanol to make a final concentration of 1.25% β-mercaptoethanol when combined with the protein lysate samples.

Molecular weight estimation marker:

Precision Plus Protein™ Dual Colour Standard (Bio-Rad).

Stripping buffer:

Restore™ Western blot Stripping Buffer was obtained from ThermoFisher Scientific.

SDS polyacrylamide gel electrophoresis (SDS-PAGE):

Stacking gel (5%):

In a total volume of 3ml, 2.1ml dH_20, 500µl 30% acrylamide/Bis Solution (Bio-Rad), 250µl 0.5M Tris (pH6.8), 0.1% (w/v) SDS, 0.1% (w/v) ammonium persulfate (APS), 3µl N,N,N',N'-tetramethylethylenediamine (TEMED)[222].

Separation gels (6-12%):

Separation gels of varying percentages (6-12%) were used to provide the optimum resolution for the size range of interest for each protein. Each was made up to a total volume of 5ml and contained varying volumes of the same standard components (Table 4)[222].

Table 4. Components used in the preparation of separation gels for SDS-PAGE

Components	6% gel	8% gel	12% gel
dH_20	2.6ml	2.3ml	1.6ml
30% acrylamide/Bis solution	1ml	1.3ml	2ml
1.5M Tris (pH 8.8)	1.3ml	1.3ml	1.3ml
10% SDS	50µl	50µl	50µl
10% APS	50µl	50µl	50µl
TEMED	4µl	3µl	2µl

Separation gels of varying percentages (6%, 8% or 12%) were used for Western blot analysis and were each made up to total volumes of 5ml. Each gel contained the same standard components (dH_20, 30% acrylamide/Bis solution, 1.5M Tris, SDS, APS and TEMED) in varying quantities.

5.1.6.4 Cell culture

MDCK growth media:

MDCK cells, purchased from the European Collection of Authenticated Cell Cultures (ECACC), were maintained in Eagle's Minimum Essential Medium (EMEM) (ATCC® 30-2003™) supplemented with 10% (v/v) fetal bovine serum (FBS) (Gibco™) according to manufacturer's instructions.

MDCK selection media:

Cells were maintained in MDCK growth media supplemented with 400µg/ml Geneticin® (Gibco™).

HEK293 (Human Embryonic Kidney 293) growth media:

HEK293 cells re-derived from liquid nitrogen storage were maintained in Dulbecco's modified eagle's medium (DMEM) 1x GlutaMAX™ (Gibco™) supplemented with 10% (v/v) FBS (Gibco™) as previously described[185].

Cell dissociation:

Trypsin-EDTA (0.05%) phenol red (Gibco™) was used for cell dissociation.

Freezing media:

Serum-free growth media (SFM) supplemented with 10% Dimethyl sulfoxide (DMSO) was used for the preservation of cells to be stored at -80^{o}C or in liquid nitrogen.

5.2. Ethics

Informed consent was obtained from patients and where appropriate the parents and guardians of children using protocols approved by local and national ethics committees (approval number MREC/02/2/93).

5.3. Patients

The patients whose DNA was analysed in these studies had either been referred directly to Prof R.V. Thakker, collaborating clinicians or the Oxford Clinical Genetics Department.

5.4. Methods

5.4.1 Nucleic acid analysis

5.4.1.1 Preparation of human genomic DNA from blood leukocytes

Genomic DNA from blood leukocytes, collected in tubes containing EDTA to prevent coagulation and stored at -80^{o}C, was extracted using the Gentra Puregene Blood Kit (Qiagen)[223] as detailed in the manufacturer's protocol and summarised here. Blood samples were thawed and 3ml of the blood samples were used for DNA extraction. RBC lysis solution and Cell lysis solution were used to lyse the red and white blood cells in the presence of a DNA stabiliser to limit the activity of DNases. RNA was

removed by incubating with RNAse A solution for 15 minutes at 37°C and the remaining contaminants were removed using the Protein Precipitation Solution and centrifugation. The DNA in the supernatant was recovered by precipitation with isopropanol and centrifugation, followed by washing with 70% ethanol. The purified DNA pellet was dissolved in sdH_20 and incubated at 65°C for 1 hour followed by gentle shaking at RT overnight. DNA samples were quantified using the NanoDrop® 1000 Spectrophotometer (ThermoFisher Scientific).

5.4.1.2 Cloning of cDNA into mammalian expression vectors

Human, WT *KLOTHO* and *DENND4C* cDNA was sub-cloned out of the pCMV6-AC-tGFP vector, encoding the Klotho-turbo-GFP (tGFP) (RG224132) and Dennd4C-tGFP (RG219039) fusion proteins (Origene™ Technologies), into the more efficient pcDNA™3.1(+) vector (Invitrogen™). *KLOTHO* cDNA was cleaved out of the pCMV6-AC-tGFP vector using the REs *BamHI* and *XhoI,* which cut at recognition sites identified 5' and 3' of *KLOTHO*, respectively[222]. *DENND4C* cDNA was cleaved out of the pCMV6-AC-tGFP vector using the REs *KpnI* and *XhoI,* which cleave at recognition sites identified 5' and 3' of *DENND4C* respectively[222]. The same REs were then used to cleave and linearise the pcDNA™3.1(+) vector at the multiple cloning site (as described in Section 5.4.1.8), thus leaving compatible ends[222].

The restriction products from each reaction were visualised on a 0.75% agarose gel and subsequently excised and purified using the GENECLEAN® III kit as detailed in the manufacturer's protocol[224]. In brief, bands containing the digested *KLOTHO* and *DENND4C* cDNA and the digested pcDNA™3.1(+) vectors were cut from the agarose gel and incubated with NaI solution at 55°C for up-to 5 minutes to melt the agarose.

GLASSMILK® was then added to the NaI/DNA solution and incubated at RT for 5 minutes, mixing every 1-2 minutes. The GLASSMILK® was pelleted with the bound DNA by centrifugation at 14,000xg for 5 seconds and the supernatant discarded. The pelleted GLASSMILK®/DNA was washed in 500ul of NEW Wash solution two times. Following pelleting, 30ul of TE buffer was used to resuspend the pellet, incubated at 37°C for 5 minutes and then pelleted for a final time. The supernatants, each containing either the eluted *KLOTHO* cDNA, *DENND4C* cDNA, or pcDNA™3.1(+) vectors were removed and used in the ligation reaction. Ligation reactions contained the cut cDNA, cut vector (in 3 different ratios: 1:1µl, 1:3µl and 3:1µl), T4 DNA ligase and T4 DNA ligase buffer (10x) (NEB). sdH_2O was then added to make the final reaction volume 20µl and the reaction incubated at 4°C overnight. The ligated products were then used to transform XL10-Gold ultracompetent cells (Agilant). Confirmation of successful cloning was performed by RED and Sanger DNA sequencing of purified plasmid DNA.

5.4.1.3 Manipulation of plasmid DNA by site-directed mutagenesis (SDM)

Point mutations were introduced into the cDNA of human *KLOTHO,* contained within a pcDNA™3.1(+) (Invitrogen™) construct, and human *CLDN3,* contained within a pCMV6-AV-GFP construct (Origene™ Technologies), for *in vitro* functional studies[185]. SDM was carried out using the QuikChange Lightning SDM Kit (Agilent) in accordance with the manufacturer's protocol[185] and primers were designed using the QuikChange Primer Design website (http://www.genomics.agilent.com/primerDesignProgram.jsp) (appendix Table 32). SDM reactions contained: 100ng of template plasmid, forward and reverse 10µM SDM primers, dNTP mix, QuikSolution reagent, 10x QuikChange Lightning buffer, sdH_2O

and QuikChange Lightening Enzyme. Reactions were performed in thin-walled PCR tubes in a PTC-225 Peltie thermal cycler (MJ Research) using a heated lid to prevent sample condensation in the cap of the tube. cDNA was amplified over a series of 18 cycles of denaturation of the double stranded template, annealing of the SDM primers and extension of the product (Table 5)[222]. Digestion of the methylated template strand was carried out by incubating with *Dpn I* enzyme at 37°C for 5 minutes and the resultant products were then used to transform XL10-Gold ultracompetent cells (Agilent).

Table 5. SDM thermal cycle steps

Cycle step	Temperature	Duration	Number of cycles
1. Initial denaturation	95°C	2 Minutes	1
2. Denaturation	95°C	20 Seconds	(Steps 2-4) 18
3. Annealing	60°C	10 Seconds	
4. Extension	68°C	*30 Seconds/kb	
5. Final extension	68°C	5 Minutes	1

The extension time used varied depending on the size of the construct (30 seconds/kb of construct). Extension times for the constructs used were as follows: 3 minutes 30 seconds for the 7.2kb construct containing human claudin 3 cDNA (RG204882) (Origene™ Technologies) and 4 minutes 15 seconds for the 8.5kb construct containing human Klotho cDNA (generated by cloning human Klotho cDNA into the pcDNA™3.1[+] vector [Invitrogen™]).

5.4.1.4 Preparation of plasmid DNA from E.coli

Extraction of plasmid DNA from overnight suspension cultures was carried out using the Wizard® Plus SV Miniprep Kit (Promega) in accordance with the manufacturer's protocol[222]. Cells from the overnight cultures were pelleted by centrifugation[222], the supernatant was discarded and the pellet re-suspended in Cell Resuspension Solution. The re-suspended cells were lysed by the addition of Cell Lysis Solution and incubated with Alkaline Protease Solution at RT for 5 minutes. Following cell lysis, Neutralisation Solution was added and the reaction was centrifuged at RT for 10 minutes[222]. The resulting lysate was transferred into Wizard® SV Minicolumns, where

a series of centrifugations and washes with Column Wash Solution was carried out. Plasmid DNA was eluted in 30µl of dH_2O and quantified using the NanoDrop® 1000 Spectrophotometer (ThermoFisher Scientific).

5.4.1.5 Nucleic acid quantification

Nucleic acid samples were dissolved in dH_2O and quantification of nucleic acids was carried out using the NanoDrop® 1000 Spectrophotometer (ThermoFisher Scientific), which is able to accurately measure double-stranded DNA (dsDNA) samples up to 3700ng/µl[225]. The standard nucleic acid setting was used on the NanoDrop® 1000 Spectrophotometer, measuring absorbance at 230nm, 260nm and 280nm, which in turn was used to generate 260/280 and 260/230 ratios used to assess the purity of nucleic acids[222,225]. A 260/280 ratio of approximately 1.8 is generally accepted as 'pure' for DNA and approximately 2.0 for RNA (appreciably lower ratios may indicate the presence of contaminants such as protein)[225]. A 260/230 ratio of approximately 1.8-2.2 is generally accepted as 'pure' nucleic acids, as before, an appreciably lower ratio may indicate the presence of contaminants.[225] The results were measured relative to a blank control sample of sdH_20.

5.4.1.6 Amplification of DNA by PCR

The majority of PCR reactions contained: 50% (v/v) Blue MegaMix-Double (Micro-Zone), 10µM forward and reverse primers, sdH_20 and 20-50ng DNA. However, where DNA sequences for amplification were GC-rich, Accuprime™ GC-rich DNA polymerase (Invitrogen™) was used, in this case each reaction contained: 10uM forward and reverse primers, 2% (v/v) GC-rich Taq DNA polymerase (Invitrogen™), 5x Buffer A

(Invitrogen™), 20-50ng DNA and sdH_20. For each reaction a negative 'blank' control was also carried out to identify potential contaminations by substituting the added DNA with sdH_20. Reactions were performed in thin walled PCR tubes in a PTC-225 Peltie thermal cycler (MJ Research) using a heated lid to prevent sample condensation in the cap of the tube. DNA samples were amplified over a series of 35 cycles of denaturation of the double stranded template, annealing of specific primers and extension of the PCR product[222] (Table 6 and Table 7). Details of the primers and annealing temperatures used for each can be found within the appendix (Table 34).

Table 6. PCR cycle steps for use with Blue MegaMix-Double.

Cycle step	Temperature	Duration	Number of cycles
1. Initial denaturation	96°C	3 Minutes	1
2. Denaturation	92°C	30 Seconds	(Steps 2-4) 35
3. Annealing	*50-70°C	30 Seconds	
4. Extension	72°C	1 Minute	
5. Final extension	72°C	5 Minutes	1

*The annealing temperature varied depending on the primers used, annealing temperatures for specific primer sets can be found within the appendix (Table 34).

Table 7. PCR cycle steps for use with Accumprime™ GC-rich DNA polymerase

Cycle step	Temperature	Duration	Number of cycles
1. Initial denaturation	95°C	3 Minutes	1
2. Denaturation	95°C	30 Seconds	(Steps 2-4) 30
3. Annealing	*50-65°C	30 Seconds	
4. Extension	72°C	1 Minute	
5. Final extension	72°C	10 Minutes	1

*The annealing temperature varied depending on the primers used, annealing temperatures for specific primer sets can be found within the appendix (Table 34).

5.4.1.7 2-step reverse transcription PCR (RT-PCR)

Reverse transcription of human control RNA samples, obtained from Ambion™ (Invitrogen™) and Agilent, was performed using the Quantitect Reverse Transcriptase kit (Qiagen) and in accordance with the manufacturer's protocol[114].

Genomic DNA was first removed from the purified RNA samples though incubation with gDNA Wipeout Buffer at 42°C for 2 minutes. Quantiscript RT buffer, RT primer mix and Quantiscript Reverse Transcriptase were subsequently added to the reaction and incubated at 42°C for a further 15 minutes for reverse transcription, followed by inactivation at 95°C for 3 minutes. The resulting cDNA was used at a 1-in-10 dilution for PCR reactions with gene specific primers, which are detailed within the appendix (Table 36) using the previously described PCR protocol (Section 5.4.1.6) and the products were visualised by agarose gel electrophoresis.

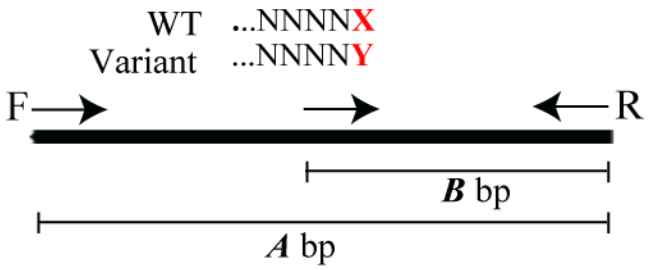
5.4.1.8 Restriction endonuclease (RE) digestion (RED)

REs are enzymes that recognise and cleave specific sequences in dsDNA and were therefore used as a second method to confirm variants in DNA samples that either resulted in a gain- or loss- of a RE cleavage site[185]. Furthermore, RED was also used to digest plasmid sequences for cloning[222] (Section 5.4.1.2) and for confirmation of the desired purified production. NEBcutter V2.0 (http://nc2.neb.com/NEBcutter2/) was used to identify RE cleavage sites within the DNA sequence of interest. RED reactions of PCR products contained: 15µl PCR product, 1.5-2µl sdH_2O, 0.5-1µl enzyme and 2.5µl buffer (enzyme and buffer both obtained from NEB) for a total reaction volume of 25µl in accordance with the manufactuer's protocol. For RED of plasmids, reactions were incubated for >4 hours at the temperature recommended by the manufacturer and products were analysed by agarose gel electrophoresis. The combination of enzymes, buffers and incubation temperatures used are detailed within the appendix (Table 37).

5.4.1.9 Amplification-refractory mutation system (ARMS) PCR

ARMS PCR is a PCR reaction whereby an internal forward or reverse primer, that either matches the WT or variant sequence is incorporated into the PCR reaction, thus producing two bands when the internal primer matches the sequence of interest, or a single band when the internal primer does not match the sequence of interest[226]. Thus, ARMS PCR was used as a second method to confirm variants in DNA samples that did not result in a gain- or loss- of a RE cleavage site. Internal ARMS PCR primers were designed such that the nucleotide of interest was the terminal nucleotide in the primer sequence and would match either the WT or variant sequence (Figure 13)[226,227].

Figure 13. Schematic representation of primer binding during ARMS PCR



WT and variant internal primers were designed so that each matched the WT or variant sequence respectively. Primers were approximately 20-30 nucleotides in length (represented by …NNNN), with the 3' nucleotide (X or Y) matching the WT (X) or variant (Y) nucleotide of interest. Reactions also contain a forward (F) and reverse (R) primer as in a typical PCR reaction, thus in an ARMS PCR reaction there is a possibility, of 1 or 2 products being generated. In all cases a full-length fragment of ***A*** bp was generated and if the 3' nucleotide of the primer in each reaction matches the template sequence a second small fragment of ***B*** bp was generated. Thus, If the template sequence contained the WT nucleotide of interest, in the WT reaction 2 fragments will be generated, however in the variant reaction only 1 fragment will be generated and *vice versa* for variant sequence templates.

In cases of poor specificity primers were optimised to include an additional nucleotide change at the penultimate nucleotide, thus reducing nonspecific binding[226,227]. For each DNA sample both a WT (containing the WT internal primer) and a variant (containing the variant internal primer) PCR reaction was carried out with the

addition of a 10μM internal ARMS primer. Products were visualised by agarose gel electrophoresis. A full list of primers, cycling conditions and Taq reagents can be found in the appendix (Table 35).

5.4.1.10 Visualisation of nucleic acid samples

Agarose gel electrophoresis was used to visualise nucleic acid samples. Agarose gels of varying percentages (0.75-2%) were used depending on the size of the fragments to be resolved[222]. For each, agarose was disolved in 1x TBE by heating in a microwave and ethidium bromide was added to a final concentration of 0.5μg/ml[222]. Where required, loading buffer was added to samples prior to loading onto the gel and the samples were run alongside an appropriate marker (Hyperladder 100bp or 1kb+, both obtained from Bioline)[222]. Agarose gels were electrophoresed at a constant voltage of approximately 10V/cm in 1x TBE. The standard settings for ethidium bromide gel analysis were used on the ChemiDoc™ XRS+ System (BioRad Laboratories) to visualise and photograph the DNA bands.

5.4.1.11 Purification of DNA for Sanger DNA sequencing

PCR products to be sequenced were purified using SureClean Plus reagent (Bioline)[228]. PCR products were incubated at RT with an equivalent volume of the SureClean reagent (1:1) before being pelleted by centrifugation for 45 minutes at 2750rcf. The supernatant was then discarded, and the remaining pellet washed with 70% ethanol before being pelleted again and re-suspended in 15-30μl of sdH_20 depending on the intensity of the band visualised via agarose gel electrophoresis, as an indicator of the concentration of the PCR product.

5.4.1.12 Sanger DNA sequencing and analysis

Sanger DNA sequencing was carried out using the BigDye™ Terminator v3.1 Cycle Sequencing Kit (ThermoFisher Scientific) and an ABI 3730 automated capillary sequencer (Applied Biosystems)[228]. Each sequencing reaction contained: 5x Sequencing Buffer, BigDye Terminator, sdH_20, 0.7μM primer and purified DNA. Reactions were carried out in 96-well plates in a PTC-225 Peltie thermal cycler (MJ Research) using a heated lid to prevent sample condensation in the cap of the tube. Purified DNA samples were amplified and the fluorescently labelled dideoxy terminator nucleotides incorporated over a series of 30 cycles of denaturation, primer annealing and extension of the DNA (Table 8)[222]. A list of the primers used can be found in the appendix (Table 33 and Table 34).

Table 8. Cycling conditions used for the BigDye™ Terminator v3.1 Cycle Sequencing Kit

Cycle step	Temperature	Duration	Number of cycles
1. Denaturation	96°C	10 Seconds	
2. Annealing	50 °C	5 Seconds	(Steps 1-3) 30
3. Extension	60°C	2 Minutes	

Cycling conditions of the PTC-225 Peltie thermal cycler (MJ Research) used in accordance with the BigDye™ Terminator v3.1 Cycle Sequencing Kit. Over a series of 30 cycles of denaturation (96°C), annealing (50°C) and extension (60°C) DNA samples were amplified and the fluorescently labelled dideoxy terminator nucleotides were incorporated.

The resulting fragments were purified by incubating at RT with a mixture of 96% (v/v) ethanol and 4% (v/v) sodium acetate for 30 minutes before being pelleted by centrifugation for 45 minutes at 2750rcf. The supernatant was then discarded, and the remaining pellet washed with 70% ethanol before being pelleted again. The dried DNA pellets were sent to the sequencing facility at the Department of Zoology, University of Oxford, which uses an ABI 3730 automated capillary sequencer (Applied

Biosystems), and the returned data was analysed using DNADynamo (Blue Tractor Software Ltd).

5.4.1.13 WGS and WES

WGS was performed using DNA samples from seven unrelated patients and two brothers with FJHN, lacking mutations in *UMOD*, *REN* and *HNF1β*, by the Wellcome Trust Centre for Human Genetics, University of Oxford (WTCHG). WES was performed on DNA samples from five unrelated patients with FHH, lacking mutations in *CASR*, *GNA11* and *AP2S1* at the WTCHG, Oxford. Bioinformatic analysis of the sequencing data was performed by Dr Alistair Pagnamenta at the WTCHG, Oxford. Additional, subsequent *in silico* analysis was performed by Dr Sian Piret or myself, Academic Endocrine Unit, University of Oxford.

5.4.1.14 Illumina TruSeq Custom Amplicon (TSCA) analysis

TSCA analysis is a form of gene-targeted NGS, whereby custom amplicons are designed and generated to target specific genes or regions of interest. TSCA analysis of *KLOTHO* was carried out in 75 DNA samples from patients with FHH, lacking mutations in *CASR*, *GNA11* and *AP2S1.* DNA samples were prepared to a concentration of 50ng/µl in 10mM Tris-Cl pH8.5 and primers with 99% coverage were designed using the Custom Amplicon software from Illumina®. Custom Amplicon kits were also obtained from Illumina®. TSCA sequencing was performed by Dr Jérôme Nicod at the WTCHG, Oxford and the returned data was visualised using the Integrative Genomics Viewer IGV 2.3 (Broad Institute)[229].

5.4.2 Culture of *E. coli*

5.4.2.1 Transformation of competent E. coli cells

Transformation of XL10-Gold ultracompetent cells (Agilant) with plasmid DNA was carried out in accordance with the manufacturer's protocol. Plasmids were amplified in ultracompetent XL10-Gold® cells (Agilant). In brief, 1µl of XL10-Gold β-mercaptoethanol (Agilant) was added to 20µl of XL10-Gold ultracompetent cells in pre-chilled 14ml BD falcon polypropylene round-bottom tubes then plasmid DNA added (either 100ng WT plasmid DNA or 2ul of *Dpn I*-treated SDM product). The reaction was incubated on ice for a further 30 minutes, before heat-pulsing at 42°C in a water bath for 30 seconds[222]. The cells were cooled on ice for 2 minutes before the addition of 500µl of NZY+ broth (preheated in the 42°C water bath) and incubated at 37°C in a shaking incubator (225-250rpm), prior to plating onto LB-Agar plates supplemented with the relevant selection antibiotic (Table 9)[222].

Table 9. Concentration of antibiotic required for selection of constructs

Vector	Selection antibiotic
pcDNA™3.1(+)	50µg/ml Ampicillin
pCMV6-AC-tGFP	100µg/ml Ampicillin

Both the pcDNA™3.1(+) and pCMV6-AC-tGFP vectors express the gene conferring resistance to the antibiotic Ampicillin, to be used as a selection marker. This table details the concentration required to select for cells that have been transformed with the vector encoding the gene of interest.

5.4.2.2 Expanding mammalian expression vectors in E. coli

Transformed E.coli culture or a streak of glycerol stock culture was applied to LB-Agar plates containing the relevant selection antibiotics (Table 9)[222]. Plates were then incubated inverted at 37°C overnight, and the following day individual colonies were picked for overnight suspension culturing in LB broth supplemented with the

relevant antibiotic (Table 9)[222]. The following day, 1ml of suspension culture was pelleted and re-suspended in 750µl of 50% (v/v) glycerol and 50% (v/v) LB broth for preservation and stored at -80°C[222]. Plasmid extraction and purification (Section 5.4.1.4) was carried out using the remaining culture.

5.4.3 Cell culture and manipulation of cell lines

5.4.3.1 Cryogenic preservation and re-derivation of frozen cells

Cells to be preserved and stored at -80°C or in liquid nitrogen were firstly washed with sPBS before incubation with Trypsin-EDTA (0.05%) (GibcoTM) at 37°C, 5% CO_2[230]. The dissociated cells were pelleted by centrifugation and the supernatant removed[230]. The remaining cell pellet was re-suspended in 1ml freezing media and transferred to CryoTubes®, which were then cooled to -80°C[230]. Cells were re-derived from storage in liquid nitrogen by quickly warming the cells in a water bath heated to 37°C[230]. Thawed cells were then transferred to a 15ml falcon tube and 10ml growth media added. The cells were then pelleted by centrifugation, re-suspended in growth media and transferred to an appropriate culture vessel.

5.4.3.2 Transient transfection of HEK293 cells with Klotho

HEK293 cells were transiently co-transfected with the human WT or variant Klotho construct alongside the pGL4.33-Serum Response Element (SRE) reporter gene plasmid and the pRL (renilla) control plasmid for studies of ERK1/2/MAPK signalling in response to FGF23. Cells were transfected using the transfection reagent Lipofectamine® 2000 (Invitrogen™)[185], a cationic lipid that interacts with the phosphate backbone of the nucleic acid, facilitating DNA condensation and the formation of a DNA cationic lipid reagent complex[231,232], in accordance with the

manufacturer's protocol. The positive surface charge of the complex mediates the interaction of the nucleic acid and the cell membrane, resulting in the internalisation of the transfection complex via endocytosis[232]. HEK293 cells were seeded in 48 well plates and once at 70% confluency were transfected with 0.25µl Lipofectamine® 2000, 50ng of the *KLOTHO* and pGL4.33-SRE reporter gene construct (Promega) and 5ng of the pRL (renilla) control vector[233]. The constructs and Lipofectamine® 2000 were diluted in SFM to a volume of 12.5µl each. The diluted DNA was then added to the diluted Lipofectamine® 2000 Reagent, for a total volume of 25µl, and incubated at RT for 5 minutes prior to adding the DNA-lipid complex drop-wise to the cells.

5.4.3.3 Stable transfection of MDCK cells with claudin 3

5.4.3.3.1 Optimisation of Geneticin® concentration for the stable transfection of MDCK cells

MDCK cells were incubated with varying concentrations (0-600µg/ml) of Geneticin® (Gibco™) for 0-10 days at the end of which cell viability was measured using the CellTiter-Blue® Cell Viability Assay (Promega)[234] to determine the optimum concentration of Geneticin® to use in the establishment of stable cell-lines expressing claudin 3-tGFP (RG204882) (Origene™ Technologies). Cultured MDCK cells were counted using a haemocytometer and seeded at a concentration of $1x10^4$ cells per well in 11x 96-well plates, each containing 6 technical replicates. Cells were incubated in 200µl of varying concentrations of selection media (growth media containing 0, 10, 50, 100, 200, 400 or 600µg/ml Geneticin®), at 37°C, 5% CO_2 for 0-10 days, with the selection media being replenished every 2 days. The CellTiter-Blue® Cell Viability Assay (Promega) was performed at the end of each designated time period for each plate i.e every 24 hours for 10 days. 100µl of media was removed from each well and

replaced with 20µl of CellTiter-Blue® Reagent per well, cells were then incubated at 37°C for 2 hours prior to analysis using the PHERAstar FS plate reader (BMG LABTECH)[234].

5.4.3.3.2 Stable transfection of MDCK cells with claudin 3-tGFP

MDCK cells were seeded into T25 flasks and at 70% confluency they were transfected with 25µl of Lipofectamine® 2000 transfection reagent (Invitrogen™) and 9µg of either WT or variant (Trp17Cys) constructs encoding claudin 3-tGFP (RG204882) (OrigeneTM Technologies). The construct and Lipofectamine® 2000 Transfection Reagent were each diluted in 300µl SFM and incubated at RT for 5 minutes prior to adding the DNA-lipid complex to the cells[185]. The transfected cells were incubated at 37°C, 5% CO_2 for 24 hours prior to replacement of MDCK Growth media with MDCK selection media (Section 5.1.6.4). The cells were incubated at 37°C, 5% CO_2 for approximately 7-10 days, with the selection media being replenished every 2-3 days. Polyclonal cell-lines were then established by thinly seeding the surviving cells into additional T25 flasks.

5.4.4 Expression studies

5.4.4.1 Protein extraction from cultured cells

Growth media was removed and cells were washed twice with sPBS prior to incubation with mRIPA buffer supplemented with protease inhibitors on a rocker at 4°C for 10 minutes[228]. If cells had not lifted in the 10 minutes, they were mechanically lifted with a cell scraper and collected in 1.5ml eppendorfs on ice. Cells then underwent two rounds of sonication using the Soniprep 150 (MSE). Tubes were then

continuously rotated using a tube rotator at 4°C for 1 hour prior to pelleting of the insoluble lysate by centrifugation at 14,000rpm for 10 minutes. The soluble fraction was then removed and stored at -80°C.

5.4.4.2 Quantification of protein concentration by coomassie assay

The Pierce™ Coomassie (Bradford) Protein Assay Kit (Thermo Scientific) was used to quantify the total protein concentration of lysates extracted from cultured cells. The coomassie G-250 dye binds protein in an acidic environment resulting in a spectral shift of the dye from red/brown (absorbance maximum at 465nm) to blue (absorbance maximum at 610nm)[222]. Bovine Serum Albumin (BSA) serial dilutions of 0-2mg/ml prepared in mRIPA buffer were used as protein standards. 5µl per well of standards/sample were added in triplicate to a 96-well plate, followed by 250µl of Coomassie Reagent. After mixing, the absorbance was read using the PHERAstar FS plate reader (BMG LABTECH). Generation of a standard curve from the protein standards enabled the determination of protein lysate concentrations.

5.4.4.3 Western blot analysis of protein lysates

Equivalent quantities of protein lysates were used for Western blot analysis, in most incidences this was 1µg. The lysates were firstly incubated with the loading buffer containing the thiol reducing agent β-mercaptoethanol (Section 5.1.6.3) at 80°C for 5 minutes prior to being cooled on ice and subsequently loaded onto SDS-PAGE gels (Section 5.1.6.3)[222,228] alongside a size marker (Section 5.1.6.3) for electrophoresis at a constant voltage of 100V in 1x TGS buffer. Proteins were then transferred onto a polyvinylidene fluoride (PVDF) membrane (PerkinElmer®) by electrophoresis transfer in cold 1x CAPS buffer at 100V for 1 hour[222,228]. The membrane was then

blocked in blocking solution (Section 5.1.6.3) at 4°C overnight and on the following morning was probed with the relevant primary antibody at RT for 1 hour, following which the membrane was washed 4x for 5 minutes with 1x TBS-T[222,228]. The membrane was subsequently incubated with the relevant Horseradish Peroxidase-conjugated secondary antibody (primary and secondary antibody combinations are detailed in the appendix in Table 38) for 1 hour prior to undergoing 4x 5 minute washes with 1x TBS-T[222]. Visualisation of antibodies bound to the protein of interest was enabled by incubating membranes with Clarity™ Western ECL substrate system (Bio-Rad) for 3 minutes and exposing the images using the ChemiDoc™ XRS+ system (Bio-Rad)[228]. The membrane was then incubated in stripping buffer for 10-15 minutes at 37°C to remove bound antibodies and re-blocked in blocking solution for 30 minutes at RT prior to incubating with a loading control primary antibody (Calnexin).

5.4.4.4 SRE luciferase dual reporter assay

SRE luciferase dual reporter assays generate a quantifiable intracellular luminescent response as a result of signalling via ERK1/2 and can therefore be used to measure ERK1/2 signalling. Thus, SRE reporter assays were used to investigate the effect of Klotho variants on the ERK1/2/MAPK pathway in response to FGF23. Recombinant human FGF23, with the Arg179Gln mutation ($FGF23^{Arg179Gln)}$, which is known to be resistant to proteolytic cleavage, whilst remaining active and able to induce FGFR1c/Klotho signalling[65], was obtained from R&D Systems and was reconstituted in DMSO. Cells were transiently co-transfected with Klotho cDNA and the experimental pGL4.10-SRE vector (Promega) that contains a firefly luciferase cassette, and the pRL renilla luciferase construct (Promega), which acts as a loading control. Cells were subsequently treated with $FGF23^{Arg179Gln}$ to induce signalling. After

48 hours cells were lysed and a Veritas automated luminometer (Promega) used to inject the Dual-Glo® Luciferase Reagent, which also acts as a substrate for firefly luciferase[233], followed by the Dual-Glo® Stop & Glo® Reagent, which quenches the luminescence from the firefly reaction and provides the substrate for Renilla luciferase[233]. Quantified firefly luciferase reporter activity was normalised to the control Renilla luciferase activity[233]. Luciferase activities were determined in quadruplicates and expressed as fold increase, relative to basal activities measured in cells treated with 0ng/ml FGF23^{Arg179Gln} in SFM. For each Klotho construct four biological replicates were performed, averaged normalised luciferase activities were expressed as fold increase relative to cells transfected with the WT Klotho vector[233].

5.4.5 *In silico* variant analysis

Variants identified by WGS, WES, TSCA and Sanger DNA sequencing were prioritised and characterised using a variety of *in silico* variant analysis tools including: population genomics, prediction of functional effects, evolutionary conservation, N-glycosylation site prediction, miRNA target site prediction and three-dimensional structural modelling. The effectiveness of 3 of these tools (population genomics, prediction of functional effects and evolutionary conservation) at predicting potential pathogenicity were investigated in Chapter 6 by analysing likely pathogenic and benign nonsynonymous, exonic, single nucleotide variants obtained from the Human Gene Mutation Database (HGMD) (http://www.hgmd.cf.ac.uk/ac/index.php)[235] ExAC (http://exac.broadinstitute.org/) (both accessed September 2017) which holds the genetic data of 60,706 unrelated individuals[236], respectively.

5.4.5.1 Population genomics

Population genomics, such as allele and genotype frequencies were used to provide an indication of potential pathogenicity by studying the reported and observed variant allele and genotype frequencies. Reported variant allele frequencies (vAFs) were used to distinguish between rare and common variants, with rare variants classified as those with a vAF <1%, and common variants as those with a vAF ≥1%[237]. Reported allele and genotype frequencies were obtained from the following population databases: ExAC (http://exac.broadinstitute.org) which holds the genetic data of 60,706 individuals[236] (accessed September 2015 [Chapter 9], July 2016 [Chapter 8], March-April 2017 [Chapters 7 and 9] and September 2017 [Chapter 6]), the 1000 Genomes database (http://phase3browser.1000genomes.org/index.html) which holds the genetic data of 2504 individuals[238] (accessed prior to October 2014 [Chapter 9] and March-April 2017 [Chapter 7]); and the Exome Variant Server (EVS) (http://evs.gs.washington.edu/EVS/) which holds the genetic data of 6503 individuals[239] (accessed prior to October 2014 [Chapters 8 and 9]). Observed variant allele and genotype frequencies were also calculated for some of the cohorts studied to determine whether a cohort was enriched for a particular variant or genotype when compared to a representative population database. Reported and observed frequencies were expressed as a percentage of the population studied and include all ethnic groups combined.

5.4.5.2 Prediction of functional effects

Various publically available web servers and software are available for the prediction of the functional effects of variants and these generally include determination of the effect of the variant at the nucleotide and/or amino acid level, although the algorithms

used by each may differ[225,237,240-242]. Using a combination of multiple prediction tools is recommended to mitigate for any differences and weaknesses between programmes[237]. Therefore, multiple publically accessible online functional prediction tools were used to indicate the potential pathogenicity of variants and to predict the functional impact of each variant. Provean Protein (http://provean.jcvi.org/index.php) predicts the effects of amino acid substitutions and insertions/deletions (indels) based on the alignment and measurement of similarity between the variant sequence and protein sequence homolog[225,241] (accessed September 2015 [Chapter 9], July 2016 [Chapter 8], March-April 2017 [Chapter 7] and September-December 2017 [Chapter 6]); PolyPhen-2 (http://genetics.bwh.harvard.edu/pph2/) predicts the effects of amino acid substitutions based on sequence homology, protein databank structure and phylogenetic information[242] (accessed September 2015 [Chapter 9], July 2016 [Chapter 8], March-April 2017 [Chapter 7] and September-December 2017 [Chapter 6]); MutationTaster (http://www.mutationtaster.org) predicts the effects of nucleotide alterations based on protein structure-functional and evolutionary conservation[240] (accessed September 2015 [Chapter 9], July 2016 [Chapter 8], March-April 2017 [Chapter 7] and September-December 2017 [Chapter 6]); and Sorting Intolerant From Tolerant (SIFT) (http://sift.bii.a-star.edu.sg) which predicts the effects of amino acid substitutions based on sequence homology and the physical properties of amino acids[243-245] (accessed prior to October 2014 by Dr Sian Piret [Chapter 8]).

5.4.5.3 Evolutionary conservation

The degree of conservation of a WT amino acid residue across a number of orthologs is often used as an indicator of the functional importance of that residue[210,219]. Therefore, the conservation of the WT residue affected by the variant of interest can be used as an indicator of variant pathogenicity. This is based on the assumption that the observed amino acid sequences are those that have not been removed by natural selection and therefore deleterious mutations would be removed[219,246]. WT amino acid sequences for each ortholog were obtained from Ensembl (http://www.ensembl.org/index.html) and were subsequently aligned using the Clustal Omega multiple sequence alignment programme (https://www.ebi.ac.uk/Tools/msa/clustalo/)[247] (both accessed March-November 2015 [Chapter 8], September 2016 [Chapter 9], March-November 2017 [Chapter 7 and 9], September–December 2017 [Chapter 6] and May-July 2018 [Chapter 8 and 9]). For the most part, eight orthologous sequences were used, except in Chapter 6, where four orthologs were used in Section 6.2.8.3 and eight in Section 6.2.9.3. Each variant was then allocated a conservation score out of four or eight depending on the number of orthologs used, this was then used to indicate the conservation status of the affected residue: conserved, partially conserved and not conserved as detailed in Chapter 6. The specific orthologs used are detailed in each chapter.

5.4.5.4 miRNA-target site prediction

Located within the 3'UTR of genes are conserved miRNA recognition and binding sites, variations within which have been shown to be associated with disease risk and changes in gene expression[248,249]. Therefore, online prediction platforms were used

to determine whether 3'UTR variants might result in the gain or loss of miRNA target sites. Four publically available miRNA-target site prediction tools were used to analyse the effect of 3'UTR *CLCNKA* variants in Chapter 7 (all accessed March-November 2017): miRDB (http://mirdb.org/custom.html), PolymiRTS (http://compbio.uthsc.edu/miRSNP/), TargetScan (http://www.targetscan.org/vert_71/) and microSNiPer (http://epicenter.ie-freiburg.mpg.de/services/microsniper/). miRDB uses MirTarget to predict targets within WT and variant sequences[250,251]. MirTarget was developed analysing thousands of miRNA-target interactions to identify common features associated with miRNA target binding[250,251]. PolymiRTS is a database of 3'UTR variants, collected from dbSNP, that uses CLASH (cross linking, ligation and sequencing of hybrids) data and TargetScan criteria to predict whether the two alleles lead to different miRNA target sites[252]. TargetScan predicts targets within the WT sequence by searching for conserved sites that match the seed region of each putative miRNA[253]. miRNAs are categorised based on their family and target site conservation[253]. microSNiPer predicts targets within the WT and variant sequence based on seed region binding and applying the FASTA alignment program to determine if a SNP would shift the miRNA along the 3'UTR indicating a creation/disruption event[254]. miRNA target sites were predicted to be gained if a new target site was predicted by ≥2/4 platforms and was also predicted to be absent from the WT sequence by all platforms. Conversely, a target site was predicted to be lost if it was predicted to be present in the WT sequence by ≥2/4 platforms and was also predicted to be absent in the variant sequence by all platforms.

5.4.5.5 N-glycosylation site prediction

N-glycosylation is an important post translational modification that has been shown to be important for processes such as protein folding and stability, ER-Golgi trafficking, apical sorting and quality control[255]. Thus, the presence of a variant that is predicted to disrupt an N-glycosylation site may indicate the pathogenicity of the variant. The site of N-glycosylation sites can be predicted based on the presence of the following consensus sequence: Asn-Xaa-Ser/Thr, where X is any amino acid except proline[255]. The NetNGlyc 1.0 server (http://www.cbs.dtu.dk/services/NetNGlyc/)[256] (accessed September 2015) was used to predict potential N-glycosylation sites in *KLOTHO* (Chapter 9). NetNGlyc uses nine artificial neural networks that examine the sequence context of consensus sequences, generating averaged N-glycosylation potentials. Only sites with potentials >0.5 are predicted to be N-glycosylated.

5.4.5.6 Structural analysis

Three-dimensional modelling using previously determined crystal structures was performed to indicate whether variants may be likely to impact the structure of the encoded protein. Crystal structures were obtained from the Protein Data Bank (PDB) and three-dimensional modelling was performed using the PyMOL molecular graphics system software[257]. The bovine model of a CLC-K chloride channel (PDB ID:5TQQ) was used to model all rare variants identified in *CLCNKA*, as this model had an 84% amino acid sequence identity with the human ClC-K channel and covered the full-length protein[258]. The human model of the cytoplasmic domain of ClC-Ka (PDB ID:2PFI) was also used to study rare *CLCNKA* variants within this domain[259]. Additionally, the crystal structure of the human Klotho-FGFR1c-FGF23 ternary complex was used to model variants identified in *KLOTHO* (PDB ID:5W21)[260].

5.4.6 Statistical analysis

All analyses were performed using the GraphPad Prism software and were presented as mean ± standard error of the mean (SEM)[261]. A value of $p<0.05$ was considered significant for all analyses[261]. Analyses were corrected for multiple comparisons using the Bonferroni method as appropriate and where indicated[262].

The correlation and linear regression comparing the number of variants with the size of the corresponding gene's coding region (Chapter 6) was calculated using the Pearson correlation coefficient and linear regression, respectively[261,263]. Differences in the distribution of results between the HGMD and ExAC cohort in Chapter 6 were calculated using Fishers exact test or chi-square test depending on the number of categories being studied[261]. Fishers exact and chi-square tests was also used to compare differences in the distribution of variant allele and genotype frequencies between those observed in the patient cohort and those reported on the population database ExAC[261] and the proportion of total HGMD[235] and ExAC variants for all genes combined in each category (Chapter 6) was calculated using multiple t-tests. A two-way ANOVA was performed to compare the percentage of viable MDCK cells after treatment with varying concentrations of Geneticin® and compared to untreated MDCK cells[261]. One-way ANOVAs were used to analyse differences in SRE reporter fold change, in response to different concentrations of FGF23 and in HEK293 cells transfected with mutant or WT *KLOTHO* constructs[234].

6 Investigation of *in silico* methods for variant analysis

Large proportions of patients diagnosed with rare monogenic renal tubule disorders do not have mutations in known associated genes[98,147,182,184-186]. In recent decades NGS has become more widespread in both the clinic and laboratory[110,264] and is often used in genetic studies, such as the ones described within this thesis, to try to identify novel candidate genes for disorders. However, due to the large output of variants identified by NGS, it poses the question as to how best to interpret each variant's clinical significance[210,219,265,266]. The most effective way to provide evidential support of a variant's suspected pathogenicity remains *in vitro* and *in vivo* studies such as co-occurrence in multiple families, segregation and functional analysis[220]. However, performing these analyses on all variants identified by NGS is not viable and would be cost-, time- and labour-intensive[220]. Therefore, effective *in silico* analysis for the prioritisation of genetic variants for further study is required.

Current variant analysis often utilises three methods: population genomics, prediction of functional effects and evolutionary conservation of affected amino acids[210,219,237]. Traditionally, laboratories have had their own criteria and classification systems for this, and often these are not included in published findings[237]. The American College of Medical Genetics and Genomics (ACMG) and Association for Molecular Pathology published a set of recommended standards, guidelines and criteria developed for the interpretation of genetic variants[237] (Table 10 and Table 11). The report suggests a five-tier classification system (Table 10), which they also found was preferred and already used in most laboratories in North America[237]. However, variants of uncertain significance may represent a problem in the interpretation process as there are few guidelines on how to interpret these further[267]. Furthermore, the ACMG report includes evidence such as segregation analysis and functional studies (Table 11) which

is often not practical in the initial variant interpretation stages of NGS data[220]. Therefore, the aim of this chapter was to investigate the effectiveness of current methods used for *in silico* analysis and the criteria frequently applied. Furthermore, I aimed to determine whether by modifying the criteria, the effectiveness of these methods at prioritising and separating pathogenic from benign variants could be improved. This chapter describes this investigation using genes associated with rare monogenic renal tubule disorders and outlines the criteria found to be the most effective at separating pathogenic variants from benign variants in this cohort.

Table 10. The criteria proposed by the ACMG 2015 report for the classification of variants

Classification	Criteria
Pathogenic	Either: 1. 1 pathogenic very strong ***AND:*** a) ≥1 pathogenic strong ***OR*** b) ≥2 pathogenic moderate ***OR*** c) 1 pathogenic moderate ***AND*** 1 pathogenic supporting ***OR*** d) ≥2 pathogenic supporting ***OR*** 2. ≥2 pathogenic strong ***OR*** 3. 1 pathogenic strong ***AND***: a) ≥3 pathogenic moderate ***OR*** b) 2 pathogenic moderate ***AND*** ≥2 pathogenic supporting ***OR*** c) 1 pathogenic moderate *AND* ≥4 pathogenic supporting
Likely pathogenic	Either: 1. 1 pathogenic very strong ***AND*** 1 pathogenic moderate ***OR*** 2. 1 pathogenic strong ***AND*** a. 1-2 pathogenic moderate ***OR*** b. ≥2 pathogenic supporting ***OR*** 3. ≥3 pathogenic moderate ***OR*** 4. 2 pathogenic moderate ***AND*** ≥2 pathogenic supporting ***OR*** 5. 1 pathogenic moderate ***AND*** ≥4 pathogenic supporting
Uncertain significance	Criteria for benign and pathogenic are contradictory or criteria are not met.
Likely benign	Either: 1. 1 Benign strong ***AND*** 1 benign supporting ***OR*** 2. ≥2 benign supporting
Benign	Either: 1. 1 benign stand-alone ***OR*** 2. ≥2 benign strong

The criteria proposed by the ACMG 2015 report[237] for the classification of variants using the five-tier system. The criteria refers to the strength of the evidence as described in Table 11.

Table 11. Evidence proposed by the ACMG 2015 report for the classification of variants

Strength of evidence	Pathogenic	Benign
Stand-alone	N/A	1. vAF>5% in population databases
Very strong	1. Null variant in a gene where LOF is a known mechanism of disease	N/A
Strong	1. Same amino acid change as a previously established pathogenic variant, regardless of nucleotide change. 2. *De novo* in a patient with the disease and no family history. 3. Well-established *in vitro*/*in vivo* functional studies supportive of a damaging effect. 4. Prevalence of the variant in affected individuals is significantly increased compared to controls.	1. vAF> than expected for the disorder. 2. Observed in a healthy adult for a disorder with full penetrance expected at an early age. 3. Well-established *in vitro* or *in vivo* functional studies shows no damaging effect. 4. Lack of segregation in affected family members.
Moderate	1. Located in a mutational hotspot and/or critical and well-established functional domain without benign variation. 2. Absent from controls (or at a very low frequency if recessive). 3. For recessive disorders, detected in *trans* with a pathogenic variant. 4. Protein length changes due to in-frame deletions/insertions in a non-repeat region or stop-loss variants. 5. Novel missense change at an amino acid residue where a different missense change determined to be pathogenic has been seen before. 6. Assumed *de novo*, but without confirmation of paternity and maternity.	N/A
Supporting	1. Co-segregation with disease in multiple affected family members in a gene known to cause the disease. 2. Missense variant in a gene that has a low rate of benign missense variation and where missense variants are a common mechanism of disease. 3. Multiple lines of computational evidence support a deleterious effect. 4. Patients phenotype or family history is highly specific for a disease with a single genetic aetiology. 5. Reputable source recently reports variant as pathogenic but the evidence is not available to the laboratory to perform an independent evaluation.	1. Missense variant in a gene in which primarily truncating variants are known to cause disease. 2. Observed in *trans* with a pathogenic variant for a fully penetrant dominant gene/disorder or observed in *cis* with a pathogenic variant in any inheritance pattern. 3. In-frame deletions/insertions in a repetitive region without a known function. 4. Multiple lines of computational evidence suggest no impact. 5. Variant found in a case with an alternate molecular basis for disease. 6. Reputable source recently reports variant as benign but the evidence is not available to the laboratory to perform an independent evaluation. 7. A synonymous variant for which splicing prediction algorithms predict no impact to the splice consensus sequence nor the creation of a new splice-site AND the nucleotide is not highly conserved.

Overview of the type and strength of the evidence for classifying variants proposed by the ACMG report 2015[237]. The evidence is then used to determine the classification of the variant using the criteria outlined in Table 10. N/A, not applicable.

6.1. Declaration of contributions

The work in this chapter is my own, unless otherwise stated.

6.2. Results

6.2.7 Data collection

All data was collected from publically accessible online databases and analysis programmes. Nonsynonymous, exonic, single nucleotide variant (SNV) data was acquired for five genes associated with rare monogenic renal tubule disorders: *CASR*, associated with FHH1[183], ADH1[190] and Bartter's syndrome type 5[268,269]; *UMOD*, associated with FJHN1[140]; *CLCN5* and *OCRL1*, associated with DD1 and 2, respectively[99,100]; and *CLCNKB*, associated with Bartter's syndrome type 3[270] and when found in combination with mutations in *CLCNKA*, Bartter syndrome type 4B[271]. For most of these disorders, varying proportions (25-55%) of diagnosed patients are known to lack mutations in associated genes[98,147,182,184-186]; however, no details were available regarding Bartter's syndrome patients. Additionally, these disorders are associated with different segments of the renal tubules and were therefore selected as a representative population of rare monogenic renal tubule disorders for this analysis[140,272-275]. Variants were acquired from the population database, ExAC and the mutation repository, HGMD to generate two distinct cohorts representing likely benign and pathogenic variants, respectively. The population database ExAC was chosen to source the SNVs that made up the cohort of likely benign variants in this study, as it is the largest aggregation of publically available population exome sequencing data, consisting of sequencing data from 60,706 unrelated individuals[236]. Whilst population databases such as ExAC, can't be assumed to include only healthy individuals, ExAC state that they "have made every effort to exclude individuals with

severe paediatric diseases" (http://exac.broadinstitute.org/faq). Furthermore, none of the cohorts represented in the ExAC dataset are knowingly enriched for renal monogenic disorders such as those associated with the genes in this analysis[236]. However, it remains possible that this cohort may contain individuals with such variants, who may be asymptomatic or as yet were not diagnosed with these diseases, or that such variants may contribute to polygenic or common diseases. For example, patients with FHH are typically asymptomatic[182,186-188]. Conversely, HGMD is a mutation repository which aims to act as a reference source for human disease-causing genetic variants as it "represents an attempt to collate all known (published) gene lesions responsible for human inherited disease"[235]. Thus, SNVs obtained from HGMD constituted the pathogenic cohort in this study.

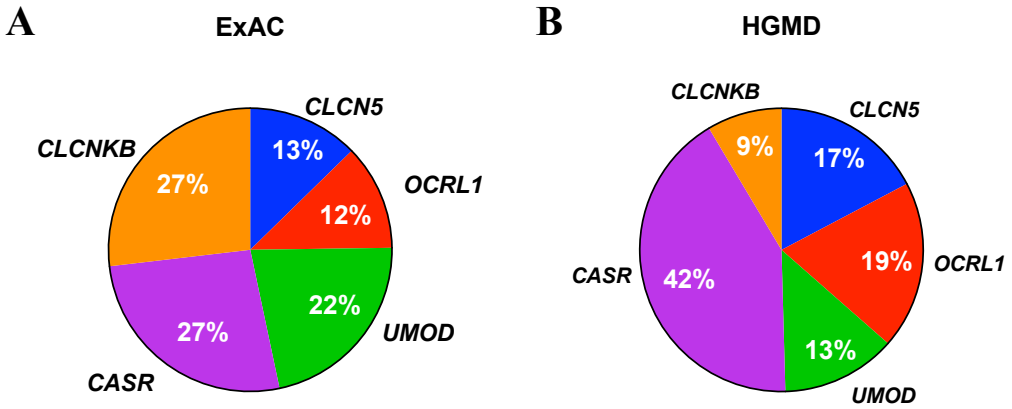
Variants were excluded or included based on variant type, i.e. synonymous and non-coding variants were excluded and nonsynonymous variants prioritised. *In silico* tools and methods for the analysis of coding variants are relatively abundant, frequently used and attempts have previously been made to characterise the effectiveness of such methods. Furthermore, the majority of known pathogenic variants have been identified in protein-coding regions[210,213,216]. Therefore, for this study nonsynonymous, exonic, SNVs were used. Table 12 displays the total number of variants within each cohort and Figure 14 shows the proportion of variants acquired for each gene as a fraction of the whole. The full list of variants and individual analyses are detailed in the appendix (Table 39 to Table 48).

Table 12. Number of variants within each gene and cohort used in this analysis

Gene	Size of coding region (bp)	ExAC cohort	HGMD cohort
CASR	3237	267	240
UMOD	2022	221	75
CLCN5	2241	128	99
OCRL1	2706	122	110
CLCNKB	2064	271	49
Total	**N/A**	**1009**	**573**

The number of nonsynonymous, exonic single nucleotide variants (SNVs) acquired for each gene and cohort, the total number of variants used for each cohort, and the size of the coding region of each gene (bp). Coding region gene sizes were obtained from Ensembl: *CASR* ENST00000639785.1 is 3237bp, *CLCN5* ENST00000376108.7 is 2241bp, *CLCNKB* ENST00000375679.8 is 2064bp, *OCRL1* ENST00000371113.8 is 2706bp and *UMOD* ENST00000396134.6 is 2022bp. Variants in the pathogenic cohort were acquired from HGMD. Variants in the benign cohort were acquired from ExAC. N/A, not applicable.

Figure 14. The proportion of variants in each gene in ExAC and HGMD cohorts.



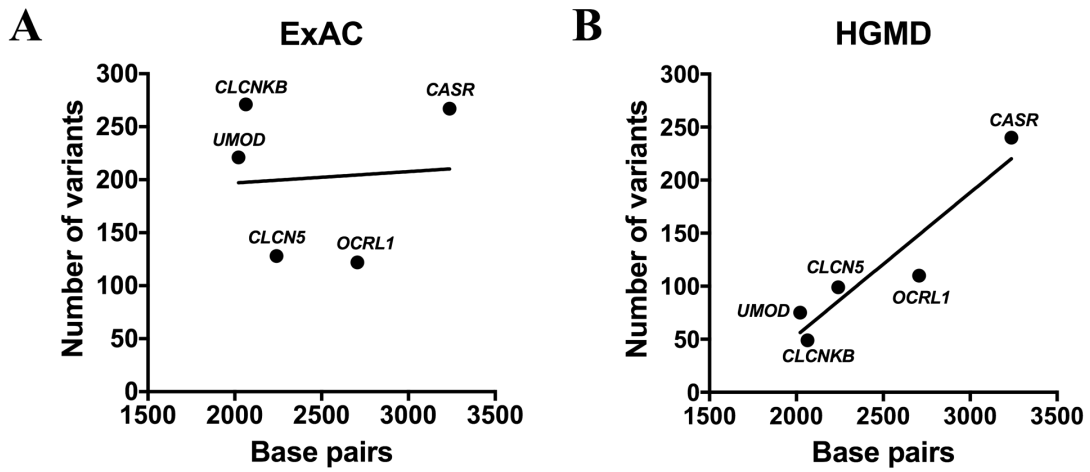
Pie charts to display the proportion of variants in each of the five genes that make up the two cohorts, displayed as a fraction of the whole. (A) The proportion of variants for each gene in the benign cohort, whereby variants were acquired from ExAC (total number of variants studied:1009). (B) The proportion of variants for each gene in the pathogenic cohort, whereby variants were acquired from HGMD (total number of variants studied:573).

The largest number of nonsynonymous, exonic, single nucleotide, ExAC variants was reported in *CLCNKB* (271), accounting for approximately 27% of the ExAC cohort (Table 12 and Figure 14). Similarly, *CASR* was shown to harbour the second largest number of ExAC variants (267), which also accounted for approximately 27% of the ExAC cohort (Table 12 and Figure 14). Equally, *CASR* variants accounted for the largest proportion (42%) of the HGMD cohort with 240 variants reported (Table 12 and Figure 14). Conversely, *CLCNKB* HGMD variants accounted for just 9% of the

HGMD cohort, contributing the smallest number of HGMD variants (49) (Table 12 and Figure 14). *CLCN5* and *OCRL1* ExAC variants accounted for similar proportions of the ExAC cohort (13% and 12%, respectively), with 128 and 122 variants reported, respectively (Table 12 and Figure 14). Likewise, the proportion of HGMD *CLCN5* and *OCRL1* variants was highly similar (17% and 19%, respectively), with 99 and 110 variants reported, respectively (Table 12 and Figure 14). Finally, the third largest number (221) and proportion (22%) of ExAC variants was reported in *UMOD*, whilst a smaller proportion of *UMOD* variants (13%) was observed in the HGMD cohort with just 75 variants reported (Table 12 and Figure 14).

It was initially hypothesised that the diversity in the number of variants identified in each gene may be due, in part, to the size of the genes. Investigation into the number of nonsynonymous, exonic, SNVs identified in each gene (Table 12) and the size of the coding region of each respective gene revealed a significant positive correlation in the HGMD cohort ($p=0.018$, $r=0.94$, $r^2=0.88$; Pearson correlation coefficient and linear regression analysis) (Figure 15B). However, this was shown not to be the case in the ExAC cohort, with no correlation observed between the number of variants and the coding-region size ($p=0.904$, $r=0.078$ $r^2=0.0058$ Pearson correlation coefficient and linear regression analysis) (Figure 15A).

Figure 15. Correlation between variant number and gene size in the ExAC and HGMD cohorts.



For each of the genes studied the number of nonsynonymous, exonic, SNVs identified in each gene was plotted against the size of the coding region. Coding region gene sizes were obtained from Ensembl and the number of variants obtained for each gene from ExAC and HGMD are detailed in Table 12. A) No correlation was observed between the coding region size and number of variants obtained from ExAC ($p=0.904$, $r=0.078$, $r^2= 0.0058$). B) Statistical analysis revealed a significant positive correlation between the number of variants obtained from HGMD and the size of the coding region ($p=0.018$, $r=0.94$, $r^2=0.88$). Statistical analysis was performed using linear regression and Pearson correlation coefficient.

The largest of the five genes studied, by coding region, was *CASR* (3237bp), which also harboured the greatest number of variants in the HGMD cohort (240) (Figure 15 and Table 12). This is to be expected as variants in *CASR* are associated with a larger number of disorders than any of the other genes studied, including FHH1[183], ADH1[190] and Bartter's syndrome type 5[268,269]. The largest number of variants in the ExAC cohort in a single gene was identified in *CLCNKB* (271), with the second largest number of ExAC variants observed in *CASR* (267) (Figure 15 and Table 12). Conversely, whilst *CLCNKB* harboured the largest number of ExAC variants it was shown to harbour the smallest number of HGMD variants (49) and was also shown to be the gene with one of the smallest coding regions (2064bp) (Figure 15 and Table 12). The gene shown to have the smallest coding region (2022bp) was *UMOD* and similarly had one of the lowest number of HGMD variants (75) (Figure 15 and Table 12). However, 221 ExAC variants were reported in *UMOD*, accounting for 22% of the

cohort (Figure 15 and Table 12). The smallest number of ExAC variants was reported in *OCRL1* (122), which conversely, had the second largest coding region reported (2706bp) (Figure 15 and Table 12). In contrast, the second highest number of HGMD variants was reported in *OCRL1* (110), accounting for 19% of the HGMD variants (Figure 15 and Table 12). Finally, *CLCN5* had the one but smallest number of ExAC variants reported (128), accounting for 13% of ExAC variants, whilst an intermediary number of HGMD variants (99) were reported (Figure 15 and Table 12). Similarly, the coding region of *CLCN5* was also shown to be intermediate (2241bp) (Figure 15 and Table 12). Therefore, to minimise the effect of the observed differences in variant number for each gene, the results included in this study display the proportion of variants for each gene and cohort, rather than the exact number of variants.

6.2.8 Commonly used criteria for variant analysis

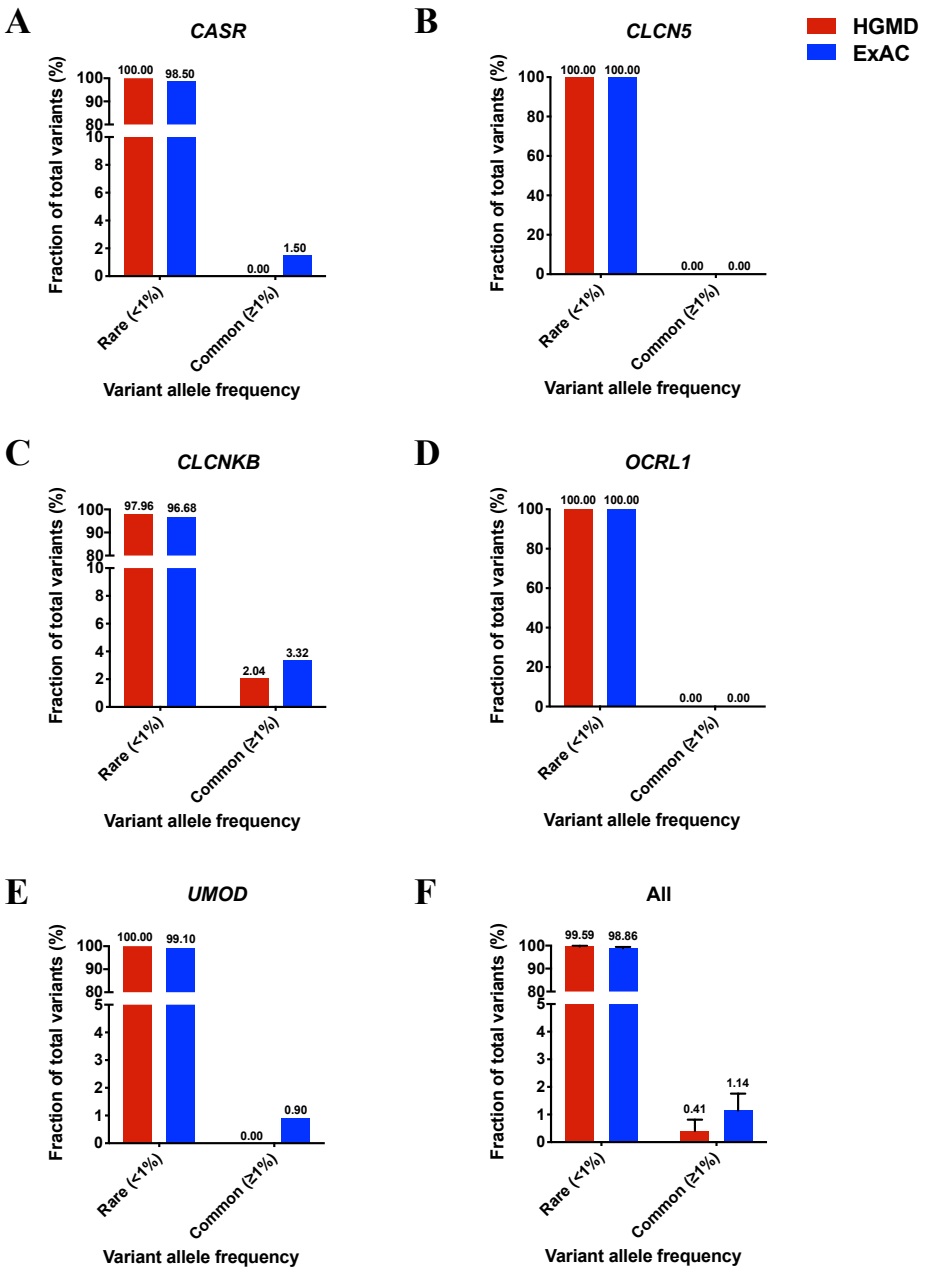
Population genomics, prediction of functional effects and evolutionary conservation are often used as indicators of pathogenicity and therefore to prioritise candidate variants identified in genetic studies[237,267]. This section investigates the effectiveness of commonly used criteria for each of these analysis methods, independently and in combination with one another. The full list of variants and individual analysis for each variant is detailed in appendix Table 39 to Table 48.

6.2.8.1 Population genomics: vAFs

vAFs are used to distinguish between rare (vAF <1%) and common (vAF ≥1%) variants[237]. Rare variants are prioritised in genetic studies of rare monogenic disorders due to the low frequency of occurrence of the disorder[210,237,276]. The

proportion of rare and common HGMD and ExAC variants were first analysed for each gene individually (Figure 16A-E). The majority (≥96%) of HGMD and ExAC variants were classified as rare variants (Figure 16A-E). All *CASR*, *CLCN5, OCRL1* and *UMOD* HGMD variants had vAFs <1%, as did 97.96% of *CLCNKB* HGMD variants. Additionally, all *CLCN5* and *OCRL1*, 98.50% of *CASR*, 96.68% of *CLCNKB* and 99.10% of *UMOD* ExAC variants had vAFs <1%. Similarly, combined analyses of all genes showed the majority of HGMD (99.59%) and ExAC (98.86%) variants had vAFs <1%. These findings are consistent with previous reports, in which 99% of high-quality variants in the ExAC database were shown to have vAFs <1%[236]. Whilst these findings suggest this criteria is effective at prioritising pathogenic variants, as represented by the HGMD cohort, they also show this criteria is not effective at distinguishing between pathogenic and benign variants, represented by the ExAC cohort, thereby highlighting the need for improved criteria for the analysis of population genomics in the context of rare monogenic renal tubule disorders.

Figure 16. The proportion of rare and common variants in the HGMD and ExAC cohorts.



Graphs A-E display the results for each gene individually (A) *CASR*, (B) *CLCN5*, (C) *CLCNKB*, (D) *OCRL1*, (E) *UMOD*, and (F) the combined analysis. The majority of HGMD and ExAC variants (>96%) had a vAF <1%, when analysed individually or combined. Statistical analyses were carried out using Fisher's exact test for the data shown in graphs A-E and multiple t-tests, which were corrected for multiple comparisons using the Sidak-Bonferroni method for the data shown in graph F. No significant differences were observed between the HGMD and ExAC variants.

6.2.8.2 Prediction of functional effects

Various web servers and software exist for the prediction of functional effects of variants. Whilst the algorithms of these tools may differ they generally include

determination of the effect of the variant at the nucleotide and/or amino acid level[225,237,240-242,276]. The impact of a variant may depend on one or a combination of criteria included within these algorithms such as: evolutionary conservation; the location and context within the protein sequence and the biochemical consequence of the amino acid substitution; as well as whether it is reported on mutation databases such as HGMD[225,237,240-242]. Several studies have previously assessed the accuracy of these programmes, finding that most algorithms tested were 65-80% accurate when examining known disease variants[237,277]. The ACMG report highlighted that whilst many of the tools used to predict functional effects have similarities in their underlying basis, using a combination of multiple prediction tools is recommended[237], thus mitigating any differences or weaknesses between programmes[237]. Therefore, the prediction of functional effects was performed using three *in silico* pathogenicity prediction tools, PolyPhen-2, Provean Protein and MutationTaster, the possible outcomes of each are detailed in Table 13.

Table 13. Prediction outcomes generated by PolyPhen-2, Proven Protein and MutationTaster

Prediction tools	Possible outcomes
PolyPhen-2	Probably damaging
	Possibly damaging
	Benign
Provean Protein	Deleterious
	Neutral
MutationTaster	Disease causing
	Polymorphism

Overview of the possible qualitative outcomes generated by the three online tools used to predict the functional effect of variants in this analysis: PolyPhen-2[242], Provean Protein[225,241], and MutationTaster[240].

In this analysis, for a variant to be predicted as probably damaging or benign ≥2/3 prediction tools must predict the variant to be probably damaging or benign, respectively (or equivalent). In cases where the results were in disagreement i.e.

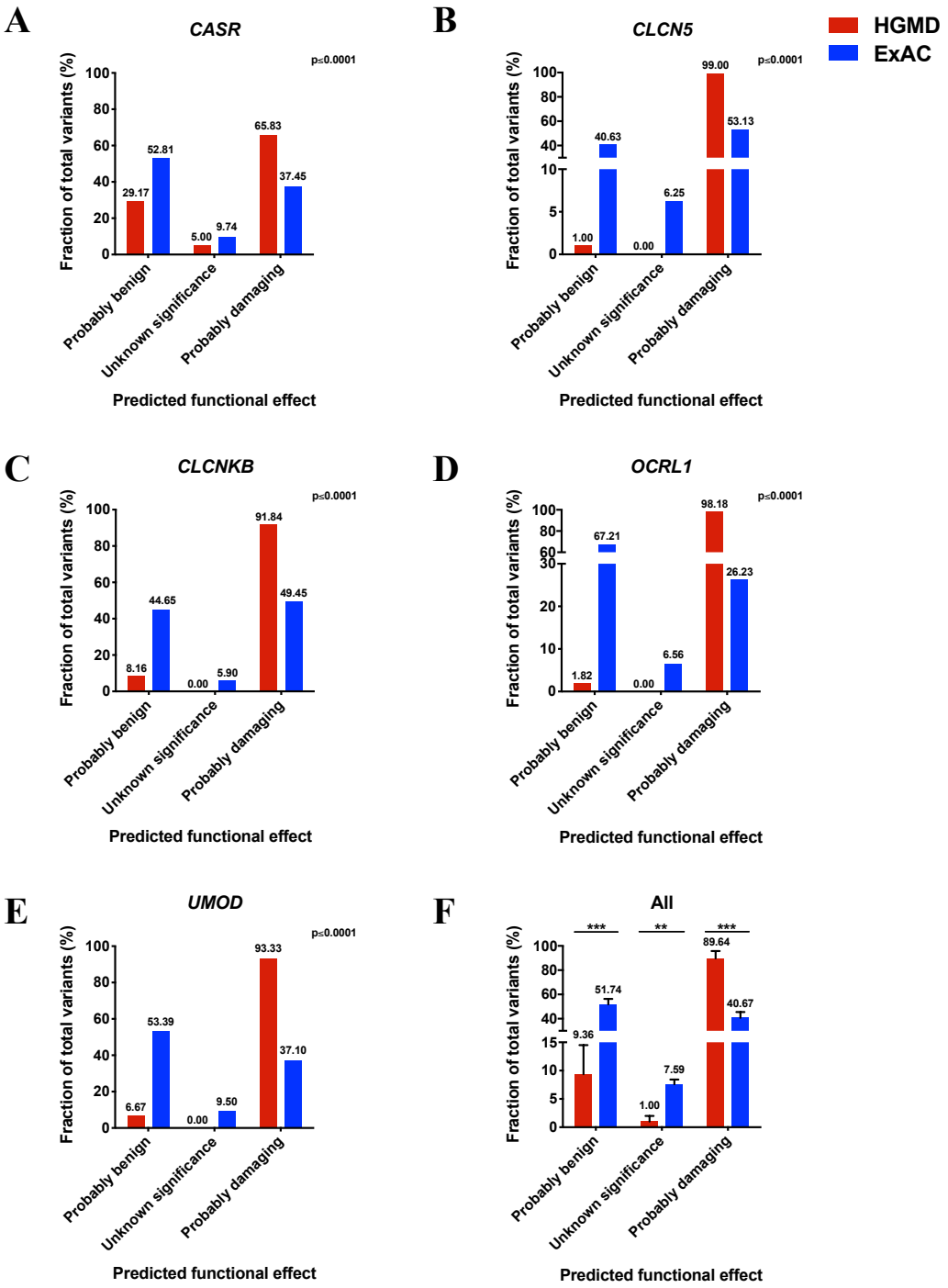
when the outcomes of MutationTaster and Provean Protein were in disagreement and PolyPhen-2 predicted the variant to be possibly damaging, the variant was classified as being of unknown significance, to take into account this degree of uncertainty. In the case of nonsense variants only one of the prediction tools could be used (MutationTaster).

Variants in the two cohorts were first analysed for each gene individually, (Figure 17A-E). The differences observed between the distribution of HGMD and ExAC variants were shown to be statistically significant ($p \leq 0.0001$, chi-square test) for each of the five individual genes studied (Figure 17A-E). For all genes, the majority of HGMD variants were predicted to be probably damaging; however, the proportion of variants in this category differed for each gene (Figure 17A-E). The lowest proportion of HGMD variants predicted to be probably damaging was observed for *CASR* (65.83%) (Figure 17A), compared to >90% of HGMD variants for *CLCN5* (99%), *CLCNKB* (91.84%), *OCRL1* (98.18%) and *UMOD* (93.33%) (Figure 17B-E). The smallest proportion of variants in the HGMD cohort were characterised as probably benign (29.17% for *CASR*, 1% for *CLCN5*, 8.16% for *CLCNKB*, 1.82% for *OCRL1* and 6.47% for *UMOD*) (Figure 17A-E). The distribution of ExAC variants for all of the genes was roughly equally spread between the probably benign and the probably damaging categories (Figure 17A-E).

The results of the individual gene analyses were then combined to compare the two cohorts (Figure 17F). There was a statistically significant difference between the proportion of HGMD and ExAC variants in each of the three categories ($p \leq 0.01$, multiple t-tests corrected for multiple comparisons). The majority of HGMD variants

(89.64%) were predicted to be probably damaging, compared to ExAC variants (40.67%) ($p \leq 0.001$) (Figure 17F). Conversely, a higher proportion of ExAC variants (51.74%) were predicted to be probably benign compared to HGMD variants (9.36%) ($p \leq 0.001$) (Figure 17F). Overall, whilst this criteria was effective at correctly predicting the majority of HGMD variants (89.64%) as being probably damaging and therefore is effective at prioritising pathogenic variants, a large proportion (40.67%) of the ExAC variants, representing the benign cohort, were also predicted to be probably damaging (Figure 17F). This is consistent with previous reports regarding the effectiveness of prediction software[277]. Furthermore, a small proportion (9.36%) of HGMD variants, representing the pathogenic cohort, were incorrectly predicted to be probably benign (Figure 17F), thereby indicating that these criteria, whilst effective at prioritising pathogenic variants, would be only partially effective at separating pathogenic from benign variants in genetic studies of rare monogenic renal tubule disorders.

Figure 17. The proportion of variants predicted to have a functional effect in the HGMD and ExAC cohorts.



Prediction of functional effects was performed using a combination of three *in silico* pathogenicity prediction tools: Provean Protein, PolyPhen-2 and MutationTaster. Graphs A-E display the results for each gene individually, (A) *CASR*, (B) *CLCN5*, (C) *CLCNKB*, (D) *OCRL1*, (E) *UMOD*, and (F) the combined analysis. The majority of HGMD variants were predicted to be probably damaging, while the ExAC variants were distributed largely between the probably benign and probably damaging categories. Statistical analyses were carried out using the chi-square test for the data shown in graphs A-E and multiple t-tests, corrected for multiple comparisons using the Sidak-Bonferroni method for graph F. **p≤0.01, ***p≤0.001.

6.2.8.3 Evolutionary conservation

The extent to which the affected WT amino acid residue is conserved across orthologs is frequently used as an indicator of functional importance and thus of variant pathogenicity[210,219,276]; particularly in circumstances where limited protein data, such as known functional domains and structural information is available. In cases where this data is available additional *in silico* methods such as structural modelling by PyMOL can also be used to indicate functional importance. Generally, the more highly conserved the residue the more functionally important that residue is suggested to be, and the more pathogenic any change to that residue may be. This is based on the assumption that the amino acid sequences observed are those that have not been removed by natural selection and that mutations that proved deleterious would be selected against; however, this is not always the case[219,246]. In this group, four orthologs are commonly used to study the evolutionary conservation of residues of interest. The following orthologs were used for this analysis: chimpanzee, mouse, chicken and xenopus for *CASR*, *CLCN5*, *CLCNKB* and *OCRL1*. However, due to the lack of chimpanzee and chicken orthologs for *UMOD*, orangutan and cow were used instead. Each variant was given a conservation score from 0-4 to represent the number of orthologs the affected WT residue was conserved in. This score was then used to indicate the conservation status of the affected residue using the criteria outlined in Table 14.

Table 14. Criteria for the conservation status (across four orthologs) for WT amino acid residues.

Conservation status	Number of orthologs
Conserved	≥3/4
Partially conserved	2/4
Not conserved	≤1/4

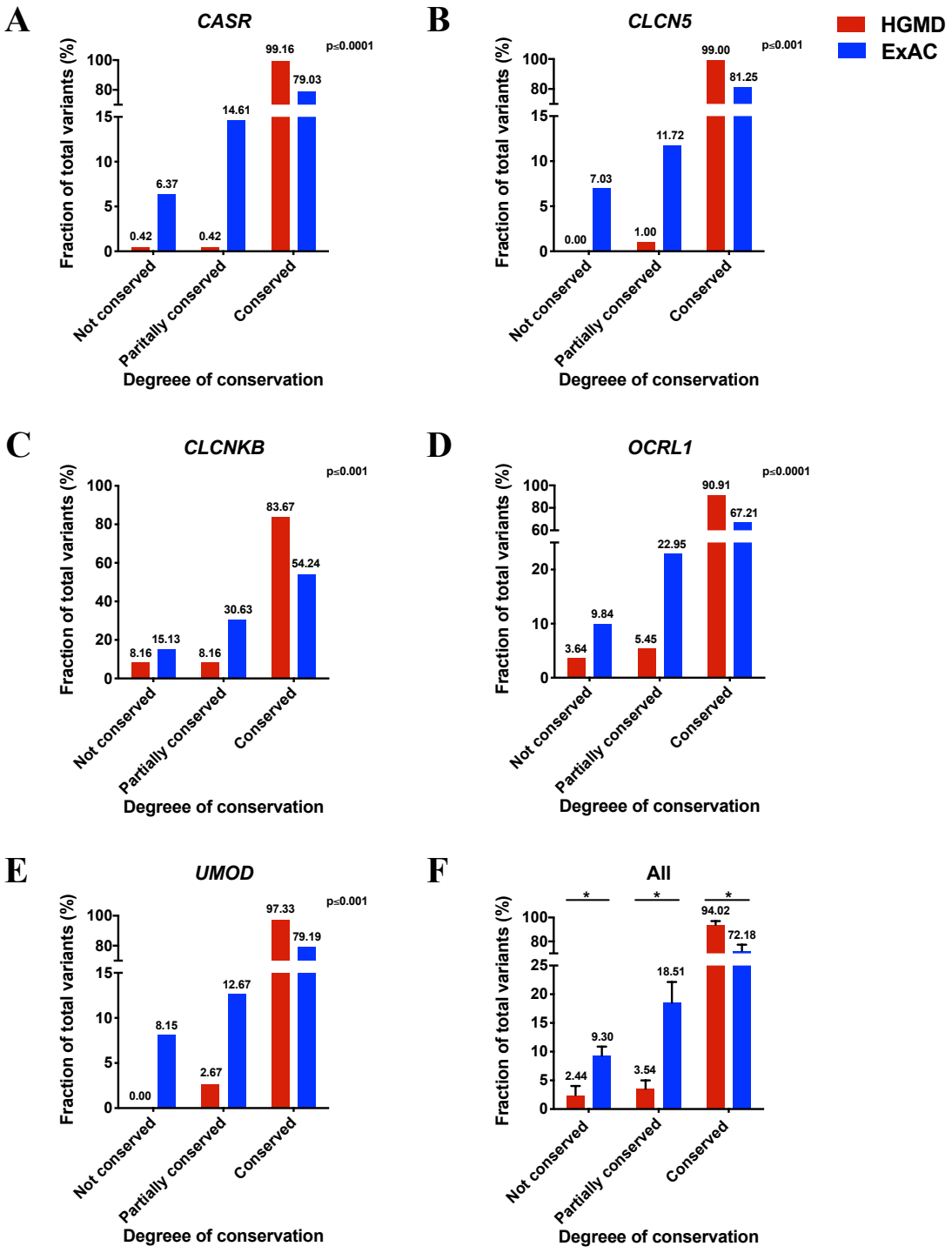
The categories used to indicate the conservation status of the WT amino acid residues affected by each variant. The conservation status was determined by studying the conservation of each WT residue across four orthologs: chimpanzee, mouse, chicken and xenopus for *CASR*, *CLCN5*, *CLCNKB* and *OCRL1;* and orangutan, mouse, cow and xenopus for *UMOD*.

The proportion of likely benign (ExAC) and pathogenic (HGMD) variants within each conservation category was firstly calculated for each gene separately, before being pooled (Figure 18). The distribution of HGMD and ExAC variants across the three categories was found to be significantly different (*CASR*, *CLCN5* and *OCRL1* [p≤0.0001, chi-square test]; and *CLCNKB* and *UMOD* [p≤0.001, chi-square test]) (Figure 18A-E). For each gene, the majority of HGMD variants were found to affect conserved residues (Figure 18A-E), varying from 83.67% of *CLCNKB* variants (Figure 18C) to 99.16% of *CASR* variants (Figure 18A). However, the majority of ExAC variants were also shown to affect conserved residues (Figure 18A-E). Just 0.42% of *CASR* HGMD variants were shown to affect partially conserved residues and residues conserved in ≤1/4 orthologs (Figure 18A), similarly just 1% and 0% of *CLCN5* HGMD variants affected partially conserved residues and residues conserved in ≤1/4 orthologs, respectively (Figure 18B). A larger proportion of ExAC variants in *CASR* and *CLCN5* were shown to affect partially conserved residues (14.61% and 11.72%, respectively) and residues conserved in ≤1/4 orthologs (6.37% and 7.03% respectively) residues (Figure 18A and B). *CLCNKB* had the lowest proportion of HGMD and ExAC variants affecting conserved residues (83.67% and 54.24%, respectively) (Figure 18C). The gene with the second highest proportion of ExAC variants affecting conserved residues was

UMOD, with 79.19% of ExAC variants shown to affect residues conserved in ≥3/4 of the orthologs studied (Figure 18E). Similarly, a very high proportion of *UMOD* HGMD variants (97.33%) were shown to affect conserved residues (Figure 18E), comparable to the results observed for both *CASR* and *CLCN5*. The majority of *OCRL1* HGMD and ExAC variants were shown to affect conserved residues (90.91% and 67.21%, respectively), with just 5.45% and 22.95%, respectively shown to affect partially conserved residues and 3.64% and 9.84%, respectively shown to affect residues conserved in ≤1/4 orthologs (Figure 18D).

The combined analysis revealed that whilst there was a statistically significant difference between the proportion of HGMD and ExAC variants in all three categories ($p \leq 0.05$, multiple t-tests corrected for multiple comparisons), the degree of overlap in each of the categories, particularly the conserved category, was very high (Figure 18F). These results suggest that these criteria are only partially effective at being able to separate pathogenic variants from benign variants, with 72.18% of ExAC variants also found to affect conserved residues (Figure 18F), thereby highlighting the need for an improvement in the analysis and application of evolutionary conservation as an indicator for pathogenicity.

Figure 18. The evolutionary conservation of WT amino acid residues affected by HGMD and ExAC variants across four orthologs.



The degree of evolutionary conservation of the WT amino acid residues affected by each of the HGMD and ExAC variants across four orthologs (chimpanzee/orangutan, mouse, chicken/cow and xenopus). Graphs A-E display the results for each of the individual genes studied, (A) *CASR*, (B) *CLCN5*, (C) *CLCNKB*, (D) *OCRL1*, (E) *UMOD*, and (F) the combined analysis. The majority of all variants in HGMD and ExAC were conserved. However, a larger proportion of variants in the ExAC cohort were not conserved or partially conserved. Statistical analysis was performed using chi-square test for graphs A-E and multiple t-tests which were corrected for multiple comparisons using the Sidak-Bonferroni method for the grouped analysis displayed in graph F. * p≤0.05.

6.2.8.4 Combined analysis

The results of the population genomics (Section 6.2.8.1), prediction of functional effects (Section 6.2.8.2) and evolutionary conservation (Section 6.2.8.3) analyses showed that whilst these criteria were effective at prioritising HGMD variants, none of these methods were highly effective at distinguishing between the two cohorts. As recommended in the ACMG report, the results of the individual analyses were combined to provide an overall pathogenicity prediction[237] (Table 15).

Table 15. Criteria used in the combined analysis of genetic variants.

Category	Criteria
Pathogenic	≥2/3 of the following: Population genetics: Rare variant (vAF <1%) Predicted functional effects: Probably damaging (by ≥2/3 tools) Evolutionary conservation: Conserved (≥3/4 orthologs)
Unknown significance	3 methods in disagreement
Benign	≥2/3 of the following: Population genetics: Common variant (vAF ≥1%) Predicted functional effects: Probably benign (by ≥2/3 tools) Evolutionary conservation: Not conserved (≤1/4 orthologs)

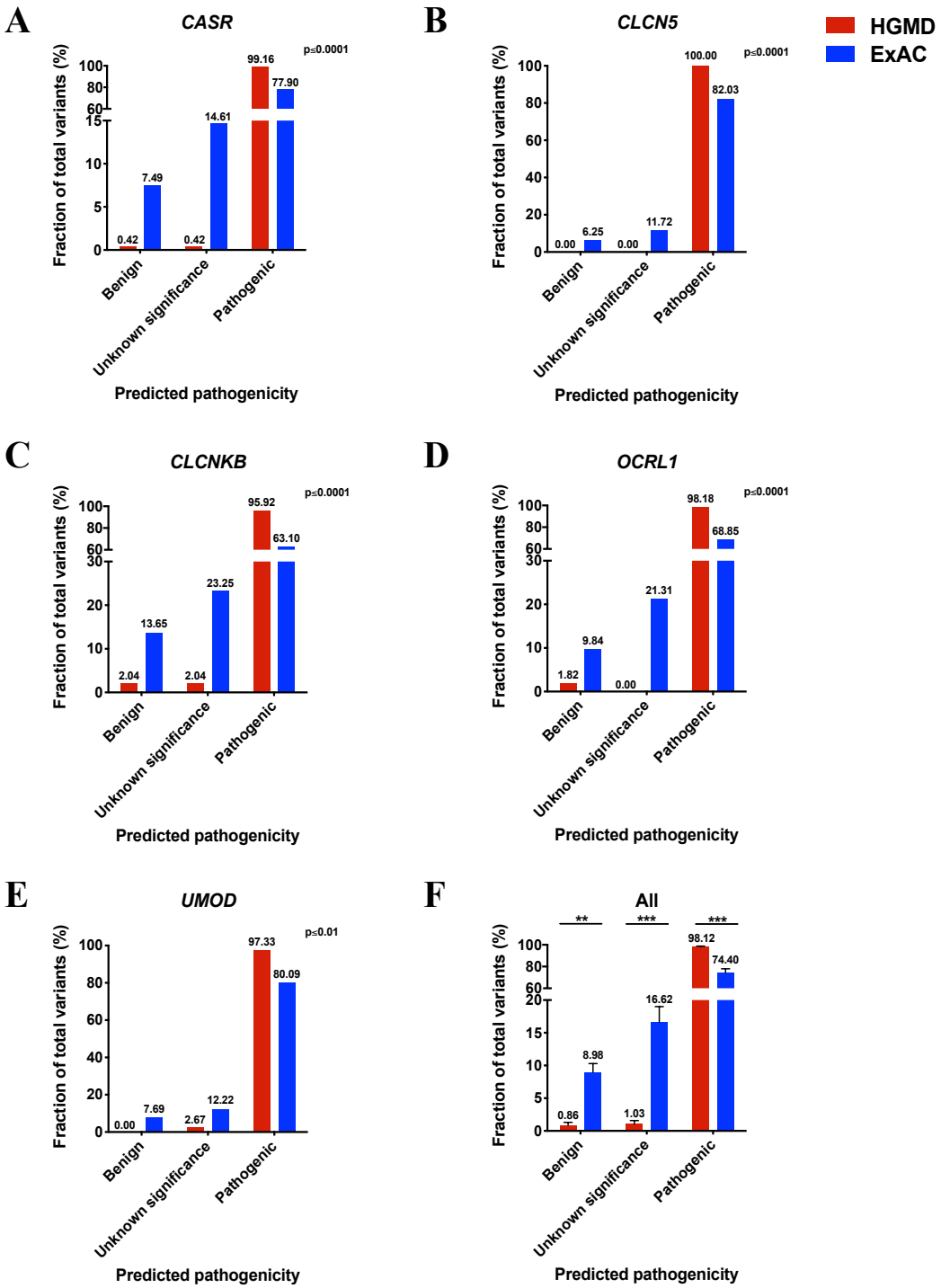
The categories and criteria used to predict the pathogenicity of each variant. Variants are classed as pathogenic or benign if they meet ≥2/3 criteria in that section. Variants are classed as being of unknown significance if the three methods are in disagreement and the variant does not fit into either the probably damaging or probably benign category.

Analyses were first performed for each gene individually (Figure 19A-E). For each of the genes, the distribution of HGMD and ExAC variants was significantly different ($p \leq 0.0001$ for *CASR*, *CLCN5*, *CLCNKB* and *OCRL1*; $p \leq 0.01$ for *UMOD,* chi-square test) (Figure 19A-E). Additionally, the criteria used successfully predicted 100% of *CLCN5* HGMD variants as pathogenic (Figure 19B). For the remaining four genes, the majority were successfully predicted to be pathogenic, (99.16% for *CASR,* 95.92% for *CLCNKB*, 98.18% for *OCRL1* and 97.33% for *UMOD* variants, Figure 19). Although the majority of ExAC variants were also predicted to be pathogenic for each gene, the

proportions of ExAC variants in this category were smaller than the proportion of HGMD variants (Figure 19A-E). The largest proportion of ExAC variants predicted to be pathogenic was observed for *CLCN5* (82.03%) (Figure 19B). The results from the analysis of *CASR* and *UMOD* ExAC variants revealed similar results to those observed for *CLCN5*. In both cases the majority of ExAC variants were predicted to be pathogenic (77.90% of *CASR* and 80.09% of *UMOD* variants), with just 7.49% of *CASR* and 7.69% of *UMOD* ExAC variants predicted to be benign (Figure 19A and E, respectively). The lowest proportions of ExAC variants predicted to be pathogenic were in *CLCNKB* (63.10%) and *OCRL1* (68.85%) (Figure 19C and D, respectively).

Combined analysis revealed a significant difference between the proportion of HGMD and ExAC variants in all three categories (benign, $p \leq 0.01$; unknown significance, $p \leq 0.001$; and pathogenic, $p \leq 0.001$, multiple t-tests corrected for multiple comparisons) (Figure 19F). Over 98% of HGMD variants were predicted to be pathogenic (Figure 19F) showing that these criteria are highly effective at correctly predicting pathogenic (HGMD) variants. However, the majority of ExAC variants (74.40%) were also predicted to be pathogenic, and a relatively small proportion of ExAC variants were predicted to be benign (8.98%) (Figure 19F). These results suggest that whilst these criteria may be effective at prioritising pathogenic variants in genetic studies of rare monogenic renal tubule disorders, they would also prioritise the majority of benign variants. These findings highlight the need for an improvement in the criteria used for the analysis of genetic variants in such studies, that would enable researchers to more effectively differentiate between pathogenic and benign variants; thereby ultimately reducing the time and cost to the researcher.

Figure 19. Predicted pathogenicity of HGMD and ExAC variants using a commonly used combined analysis approach.



The pathogenicity of each variant was predicted using vAFs, prediction of functional effects and evolutionary conservation (Table 15). Graphs A-E display the results for each gene individually, (A) *CASR*, (B) *CLCN5*, (C) *CLCNKB*, (D) *OCRL1*, (E) *UMOD*, and (F) the combined analysis. The majority of variants in the HGMD and ExAC cohorts were predicted to be pathogenic. However, there were more HGMD variants in the pathogenic category than ExAC variants. Statistical analysis was carried out using chi-square test for the data shown in graphs A-E and multiple t-tests, corrected for multiple comparisons using the Sidak-Bonferroni method for the data shown in graph F. **p≤0.01, ***p≤0.001.

6.2.9 Improvement of the criteria for variant analysis

This study has shown that the criteria used for variant analysis are effective for the prioritisation of pathogenic variants but only partially effective at separating benign and pathogenic variants. Therefore, I investigated whether modifying the criteria would increase the efficacy of the three methods at distinguishing between the two cohorts and for the prioritisation of pathogenic (HGMD) variants.

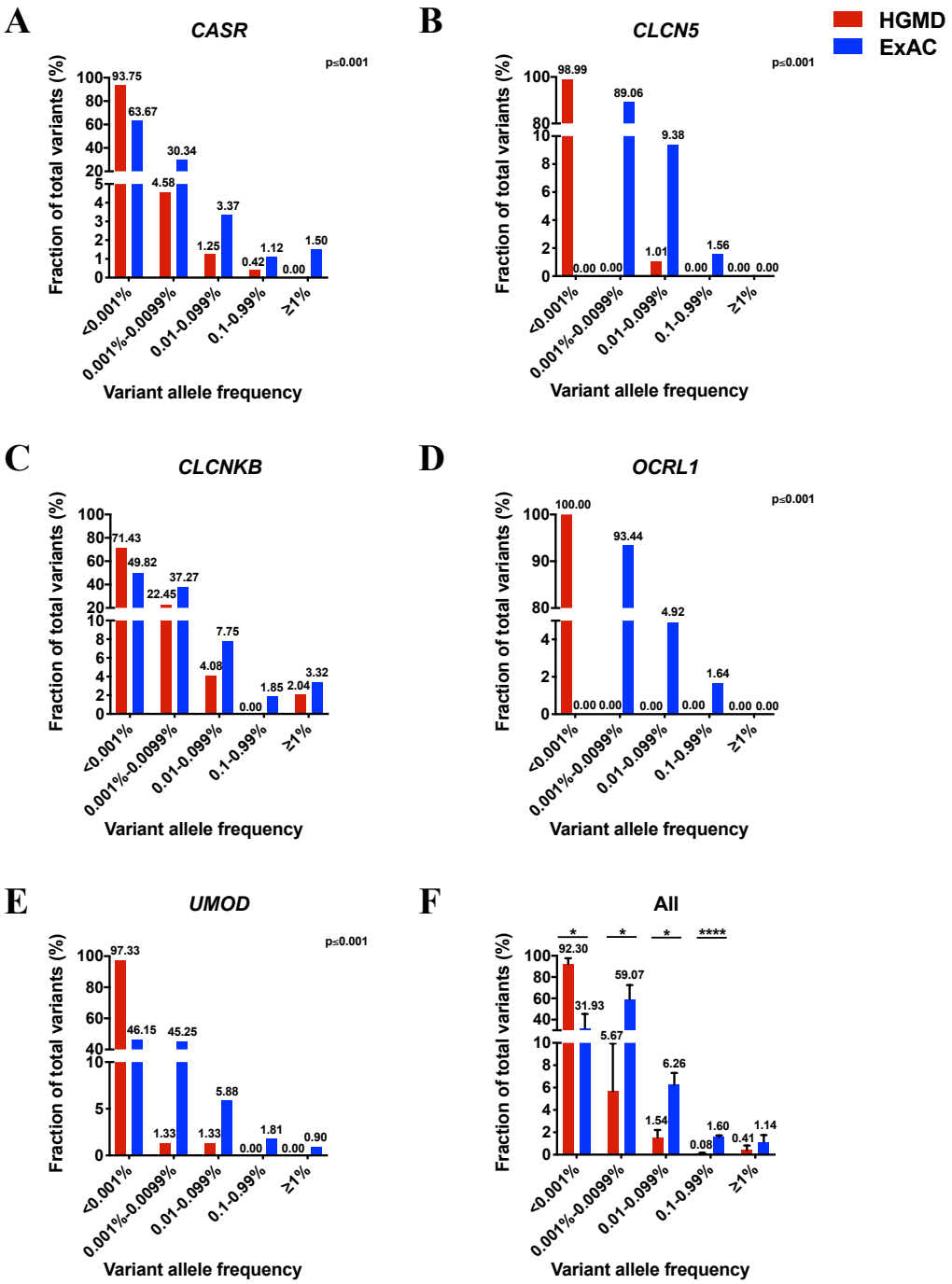
6.2.9.1 Population genomics: vAFs

As shown in Section 6.2.8.1, a cut-off of <1% vAF to distinguish between pathogenic (HGMD) and likely benign (ExAC) variants is not effective for this cohort of genes. Therefore, I investigated whether there is a more effective cut-off that could be used for rare monogenic renal tubule disorders. The variants were sorted into one of five intervals (<0.001%, 0.001-0.0099%, 0.01-0.099%, 0.1-0.99%, ≥1%) depending on their vAFs (Figure 20A-E). The majority of HGMD variants had vAFs <0.001% for all five genes studied (Figure 20A-E). However, the interval with the largest proportion of ExAC variants varied between the five genes (<0.001% for *CASR* [63.67%] and *CLCNKB* [49.82%], 0.001-0.0099% for *CLCN5* [89.06%] and *OCRL1* [93.44%]) (Figure 20A-D). There was very little difference in the proportion of *UMOD* ExAC variants in both of those categories (46.15% and 45.25%, respectively) (Figure 20E). Whilst very high proportions of HGMD variants were observed in the <0.001% interval for four of the five genes (93.75% *CAS*R, 98.99% *CLCN5*, 71.43% *CLCNKB*; and 97.33% *UMOD*), in *OCRL1* all HGMD variants had vAFs <0.001% (Figure 20). The remaining *CASR* HGMD variants were spread across the 0.001-0.0099%, 0.01-0.099% and 0.1-0.99% intervals, with 4.58%, 1.25% and 0.42% of variants in each, respectively (Figure 20A). Whereas, the vAFs of the remaining 1.01% of *CLCN5* HGMD variants fit into the 0.01-

0.99% category (Figure 20B). Similarly to *CASR*, the vAFs of *CLCNKB* HGMD variants were spread across three of the remaining four intervals with 22.45% in the 0.001-0.0099% interval, 4.08% in the 0.01-0.099% interval and 2.04% in the ≥1% interval (Figure 20C). Finally, whilst the majority of *UMOD* HGMD variants (97.33%) had vAFs <0.001%, 1.33% of variants had vAFs of 0.001-0.0099% and a further 1.33% of variants had vAFs of 0.01-0.099% (Figure 20E). A much greater spread of variants was observed in the ExAC cohort for each gene ($p \leq 0.01$, chi-square test, for *CASR*, *CLCN5*, *OCRL1* and *UMOD*) (Figure 20). The exception being *CLCNKB* where there was no significant difference in the distribution of HGMD and ExAC variants ($p=0.086$, chi-square test) (Figure 20C). For the *CASR, CLCNKB* and *UMOD* ExAC variants the vAFs were distributed across all five groups (Figure 20). The *CLCN5* and *OCRL1* variants were distributed across three categories (0.001-0.0099%, 0.01-0.099% and 0.1-0.99%) (Figure 20).

The results for each gene were then combined and showed that the majority of HGMD variants (92.30%) had vAFs <0.001%, compared to 31.93% of ExAC variants ($p \leq 0.05$, multiple t-tests corrected for multiple comparisons) (Figure 20F). The majority (59.07%) of ExAC variants had vAFs of 0.001-0.0099%, compared to 5.67% of HGMD variants (Figure 20F). Furthermore, there was a significant difference between the proportion of HGMD and ExAC variants in every category except ≥1% (<0.001%, 0.001-0.099% and 0.01-0.099, all $p \leq 0.05$; 0.1-0.99%, $p \leq 0.0001$) (Figure 20F). The only category that had a higher proportion of HGMD variants compared to ExAC variants was <0.001% (Figure 20F). These results suggest that a new cut-off of <0.001% for the prioritisation of pathogenic variants in monogenic renal tubule disorders would be more effective than the 1% cut-off used to define rare variants.

Figure 20. The range of vAFs observed in the ExAC and HGMD cohorts.



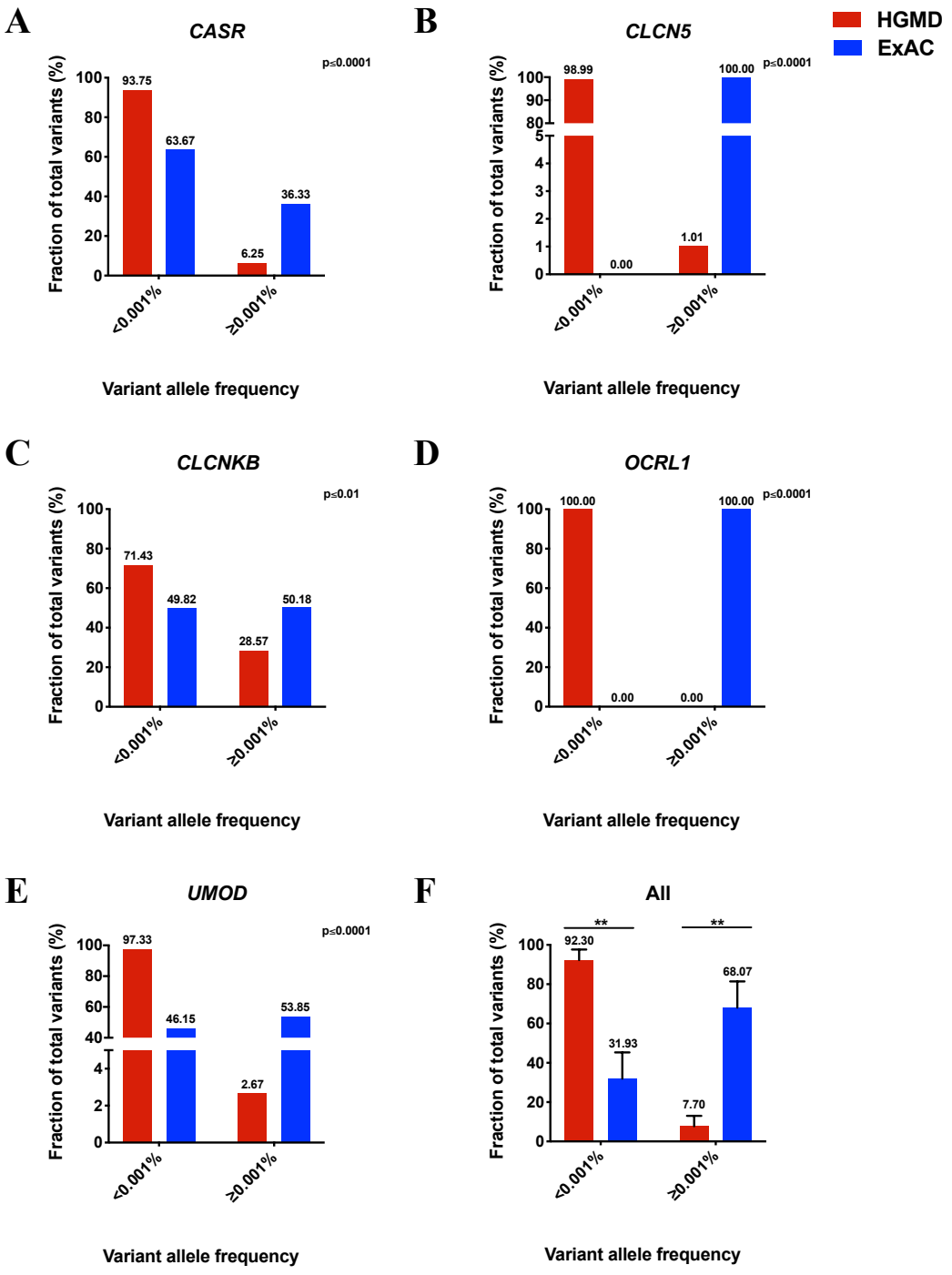
Graphs A-E display the results for each gene individually, (A) *CASR*, (B) *CLCN5*, (C) *CLCNKB*, (D) *OCRL1*, (E) *UMOD*, and (F) the combined analysis. The majority of HGMD variants had vAFs <0.001%, the interval with the largest proportion of ExAC variants varied between the five genes. Statistical analysis was carried out using chi-square tests for the data shown in graphs A-E and multiple t-tests, which were corrected for multiple comparisons using the Sidak-Bonferroni method for the data shown in graph F. * p≤0.05, ****p≤0.0001.

Therefore, to demonstrate the effectiveness of the <0.001% vAF cut-off, variants were classified into two intervals, those with a vAF <0.001% and those with a vAF ≥0.001%

(Figure 21). These results showed a larger proportion of HGMD variants had vAFs <0.001% compared to ≥0.001% for all genes studied (*CLCNKB* p≤0.01; *CASR, CLCN5, OCRL1* and *UMOD* p≤0.001, Fishers exact test) (Figure 21A-E). Furthermore, there was a complete separation of *OCRL1* HGMD and ExAC variants using this criteria (Figure 21D). Additionally, an almost entire separation of *CLCN5* HGMD and ExAC variants was observed, with 98.99% of HGMD variants having vAFs <0.001% and 1.01% having vAFs ≥0.001%, compared to 100% of ExAC variants with vAFs ≥0.001% (Figure 21B). For the remaining three genes, a large proportion of ExAC variants were also shown to have vAFs <0.001%. Whilst the majority (93.75%) of *CASR* HGMD variants were found to have vAFs <0.001%, 63.67% of ExAC variants also had vAFs <0.001% (Figure 21A). A similar result was observed for *CLCNKB* variants, 71.43% of HGMD variants had vAFs <0.001% compared to 49.82% of ExAC variants (Figure 21C); and *UMOD* variants, 97.33% of HGMD variants had vAFs <0.001% compared to 46.15% of ExAC variants (Figure 21E).

The results of the individual gene analyses were combined and showed a significantly larger proportion of HGMD variants (92.30%) had vAFs <0.001% compared to ExAC variants (31.93%) (p≤0.01, multiple t-tests corrected for multiple comparisons) (Figure 21F). These results show that this new criteria is much more effective at distinguishing between these variants than using the 1% cut off used to classify rare variants, thereby suggesting that this criteria may be better to use in the prioritisation of pathogenic variants in genetic studies of rare monogenic renal tubule disorders. However, a degree of overlap between both cohorts remained for three of the genes. Thus, highlighting the need for a combined analysis with additional *in silico* methods.

Figure 21. The proportion of variants observed in the ExAC and HGMD cohorts with vAFs <0.001% or ≥0.001%.



Graphs A-E display the results for each gene individually, (A) *CASR*, (B) *CLCN5*, (C) *CLCNKB*, (D) *OCRL1*, (E) *UMOD*, and (F) the combined analysis. These results showed that for every gene studied a larger proportion of HGMD variants had vAFs <0.001% compared to ≥0.001%. In contrast, the majority of ExAC variants had vAFs ≥0.001%. Statistical analysis was carried out using Fishers exact test for the data shown in graphs A-E and multiple t-tests, which were corrected for multiple comparisons using the Sidak-Bonferroni method for the data shown in graph F. **p≤0.01.

6.2.9.2 Prediction of functional effects

Whilst the criteria used for the analysis of predicted functional effects in Section 6.2.8.2 did result in a statistically significant difference between the proportion of HGMD and ExAC variants in all three categories, with a significantly larger proportion of HGMD variants classified as probably damaging compared to ExAC variants in the grouped analysis, a degree of overlap within this category was also observed (Figure 17). This indicates that whilst these criteria are effective at prioritising and separating pathogenic (HGMD) variants from likely benign (ExAC) variants in monogenic renal tubule disorders, there may be room for improvement. Therefore, the variants were next classified using new criteria, with five categories rather than 3 (Table 16), with the aim to reduce the level of overlap in each of the categories.

Table 16. The revised categories and criteria used to determine the predicted functional effect of variants

Predicted functional effect	Criteria
Probably benign	3/3 Predicted probably benign (or equivalent)
Possibly benign	2/3 Predicted probably benign (or equivalent)
Unknown significance	Tools in disagreement
Possibly damaging	2/3 Predicted probably damaging (or equivalent)
Probably damaging	3/3 Predicted probably damaging (or equivalent) or 2/3 predicted probably damaging (or equivalent) and PolyPhen-2 predicted possibly damaging

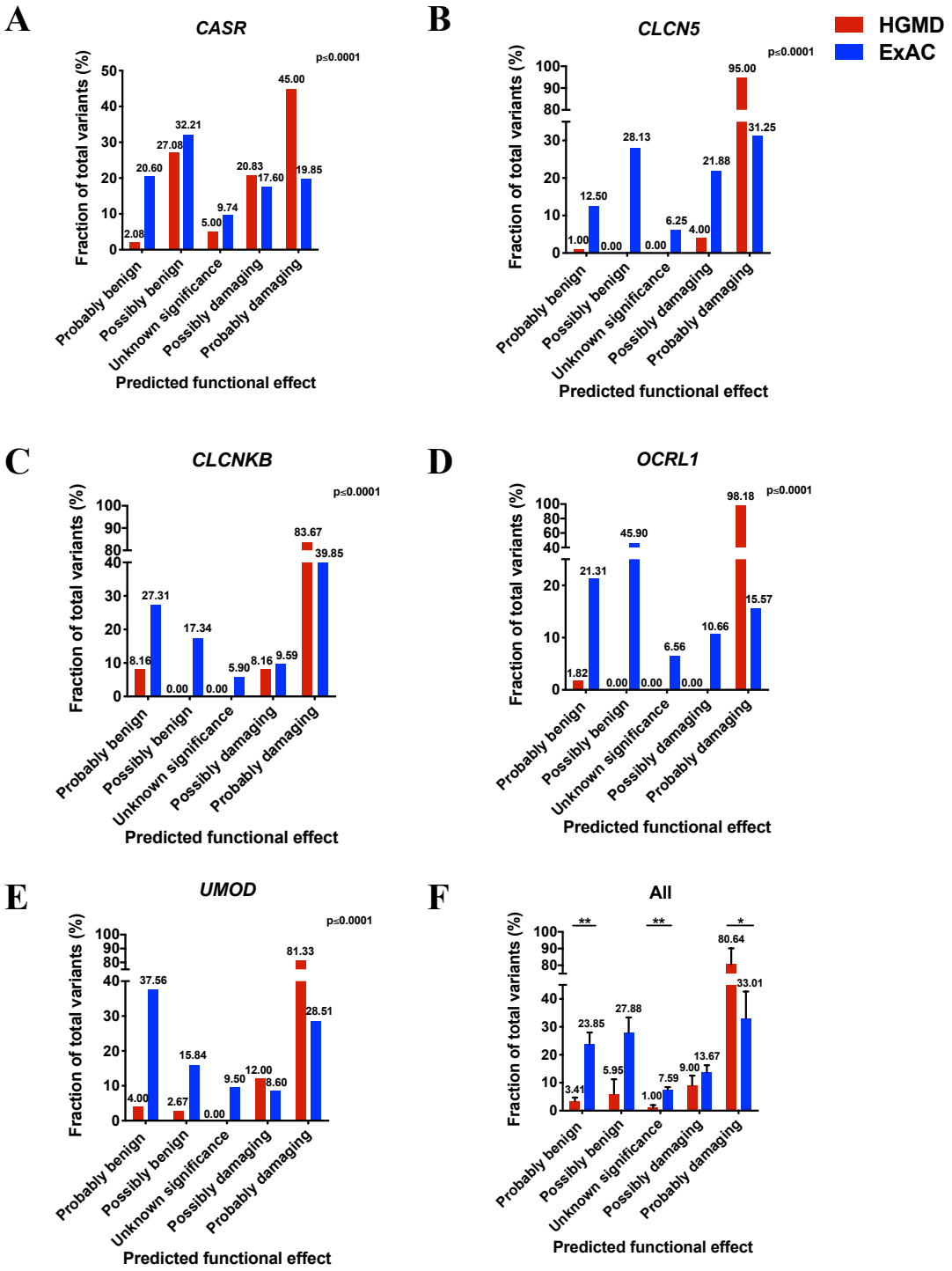
Overview of the criteria used to indicate the predicted functional effect of HGMD and ExAC variants. Criteria are based on the outcomes generated by the three online tools used to predict the functional effect of variants in this analysis: Provean Protein, PolyPhen-2 and MutationTaster.

For all of the genes studied, the difference in the distribution of HGMD and ExAC variants across the five categories was statistically significant ($p \leq 0.0001$, chi-square test) (Figure 22A-E). Furthermore, for each gene, the highest proportion of HGMD variants was found within the probably damaging category (Figure 22A-E); however, it is worth noting that in the case of *CASR* variants this accounted for <50% of the

HGMD variants (Figure 22A). The vast majority of *CLCN5* (95%), *CLCNKB* (83.67%), *OCRL1* (98.18%) and *UMOD* (81.33%) HGMD variants were correctly predicted to be probably damaging (Figure 22). In contrast, the ExAC variants were distributed across all five categories for all genes (Figure 22). In particular, for *CASR*, while 20% of ExAC variants were categorised as probably benign, and 32.21% possibly benign, 17.60% and 19.95% of ExAC variants were predicted to be possibly damaging or probably damaging, respectively (Figure 22A). Therefore, these revised categories are poor at predicting pathogenicity of *CASR* ExAC variants. Similarly, a high proportion of ExAC variants were still predicted to be probably damaging for *CLCN5* (31.25%), *CLCNKB* (39.85%), *OCRL1* (15.57%) and *UMOD* (28.51%) (Figure 22A-E).

Similarly, when all five genes were combined, while the new analyses were useful for predicting HGMD variants as pathogenic (>80%), the ExAC variants were distributed across all five categories, with similar proportions of variants classified as probably benign (23.85%) and probably damaging (33.01%) (Figure 22F). Therefore, these findings suggest that this criteria, using five categories, is not more effective at predicting the functional effects of variants, in these rare monogenic renal tubule disorders, compared to the criteria analysed in Section 6.2.8.2, consisting of three categories. These findings also highlight that similarly to population genomics, prediction of functional effects alone is not sufficient for the prioritisation and separation of pathogenic variants from benign variants for these disorders and genes; and therefore should be used in combination with other methods to increase the efficacy.

Figure 22. The predicted functional effects of HGMD and ExAC variants using five categories



Prediction of functional effects using Provean Protein, PolyPhen-2 and MutationTaster. Graphs A-E display the results for each gene individually, (A) *CASR*, (B) *CLCN5*, (C) *CLCNKB*, (D) *OCRL1*, (E) *UMOD*, and (F) the combined analysis. Statistical analysis was carried out using chi-square test for the data shown in graphs A-E and multiple t-tests, corrected for multiple comparisons using the Sidak-Bonferroni method for graph F. *p≤0.05, **p≤0.01.

6.2.9.3 Evolutionary conservation

Section 6.2.8.3 showed that whilst using four orthologs for the analysis of evolutionary conservation resulted in a significant difference between the proportion of HGMD and ExAC variants in all three categories, the degree of overlap in each of the categories remained high. Therefore, this section outlines a new analysis using eight orthologs (chimpanzee, mouse, cow, chicken, elephant, anole lizard, xenopus and zebrafish for *CASR*, *CLCN5*, *CLCNKB* and *OCRL1*; and orangutan, mouse, cow, elephant, opossum, anole lizard, xenopus and zebrafish for *UMOD*) to indicate the degree of conservation of affected WT residues, with the aim of reducing the degree of overlap. Variants were then categorised based on the indicated degree of conservation (Table 17).

Table 17. Criteria for the conservation status (across eight orthologs) for WT amino acid residues.

Category	Degree of conservation
Not conserved	≤2/8
Partially conserved	3-5/8
Conserved	≥6/8

The categories used to indicate the conservation status of the WT amino acid residues affected by each variant across eight orthologs: chimpanzee, mouse, cow, chicken, elephant, anole lizard, xenopus and zebrafish for *CASR*, *CLCN5*, *CLCNKB* and *OCRL1*; and orangutan, mouse, cow, elephant, opossum, anole lizard, xenopus and zebrafish for *UMOD.*

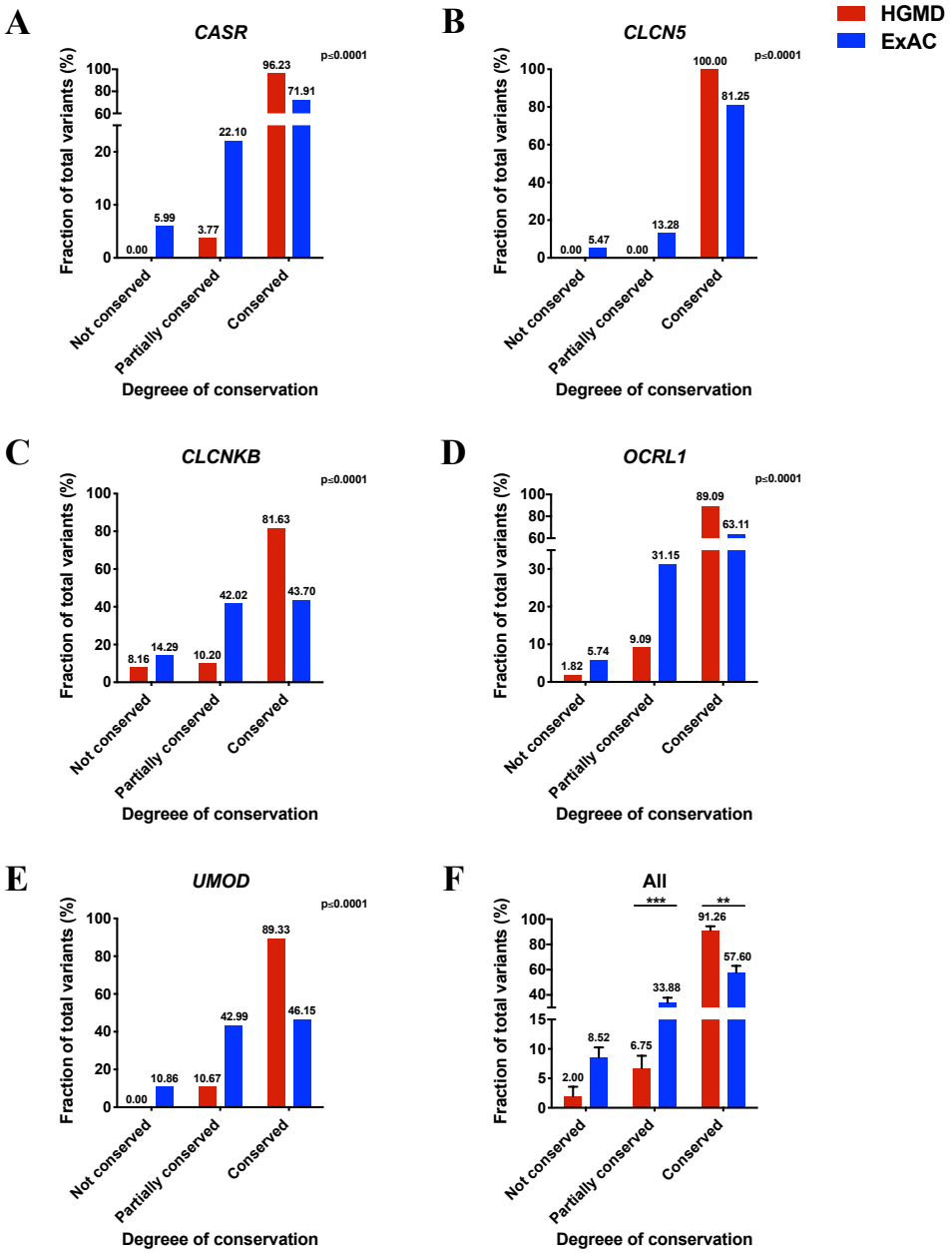
For all of the genes the differences in the distribution of HGMD and ExAC variants across the three categories was statistically significant ($p \leq 0.0001$, chi-square test) (Figure 23A-E). Almost all (96.23%) the *CASR* HGMD variants were found to affect residues conserved across ≥6/8 orthologs (Figure 23). The majority (71.91%) of *CASR* ExAC variants, although lower than the proportion of HGMD variants, were also found to affect conserved residues (Figure 23). A further 22.1% *CASR* ExAC variants were found to affect partially conserved residues (Figure 23A). All of the *CLCN5* HGMD variants affected residues conserved in ≥6/8 of the orthologs, compared to

81.25% of ExAC variants (Figure 23B). A further 13.28% of ExAC variants were found to affect partially conserved residues (Figure 23B). A greater difference in the proportion of *CLCNKB* HGMD and ExAC variants in the conserved category was seen, 81.63% and 43.7% respectively (Figure 23C). A similar proportion of ExAC variants (42.02%) were found to affect partially conserved residues, compared to 10.20% of HGMD variants (Figure 23C). The highest proportion of *OCRL1* HGMD (89.09%) and ExAC (63.11%) variants were both found to affect conserved residues (Figure 23D). A further 9.09% of HGMD and 31.15% ExAC variants were shown to affect partially conserved residues (Figure 23D). Finally, 89.33% of HGMD and 46.15% of ExAC *UMOD* variants were found to affect conserved residues, with a further 10.67% of HGMD and 42.99% of ExAC variants affecting partially conserved residues (Figure 23E).

The results of the individual analyses were then combined and showed that similarly to Section 6.2.8.3, the highest proportion of HGMD (91.26%) and ExAC (57.6%) variants were found to affect conserved residues (Figure 23F). However, there was a statistically significant difference in the proportion of HGMD and ExAC variants in both the conserved ($p \leq 0.01$, multiple t-tests corrected for multiple comparisons) and partially conserved categories ($p \leq 0.001$), with 33.88% of ExAC variants affecting partially conserved residues compared to 6.75% of HGMD variants (Figure 23F). No difference was observed between the proportion of HGMD and ExAC variants affecting residues conserved in ≤2/8 orthologs (Figure 23F). Therefore, these results suggest that using eight orthologs to study the evolutionary conservation of variants in genes associated with rare monogenic renal tubule disorders is more effective than using four; but that this method alone, is not sufficient for the prioritisation and

separation of pathogenic from benign variants and may be more effective in combination with other methods.

Figure 23. The evolutionary conservation of WT amino acid residues affected by HGMD and ExAC variants across eight orthologs.



The evolutionary conservation of WT amino acid residues affected by HGMD and ExAC variants across 8 orthologs (chimpanzee, mouse, cow, chicken, elephant, anole lizard, xenopus and zebrafish for *CASR*, *CLCN5*, *CLCNKB* and *OCRL1*; and orangutan, mouse, cow, elephant, opossum, anole lizard, xenopus and zebrafish for *UMOD*). Graphs A-E display the results for each of the genes studied, (A) *CASR*, (B) *CLCN5*, (C) *CLCNKB*, (D) *OCRL1*, (E) *UMOD*, and (F) the combined analysis. Statistical analysis was performed using chi-square test for graphs A-E and multiple t-tests, corrected for multiple comparisons using the Sidak-Bonferroni method for graph F. **p≤0.01, ***p≤0.001.

6.2.9.4 Combined analysis

Results of the initial (Section 6.2.8) and improved (Section 6.2.9) analysis of each of the three *in silico* methods showed that on their own, none were highly effective at separating the two cohorts. Therefore, the most effective criteria for each of the *in silico* methods at prioritising and separating pathogenic from benign variants were used for a new combined analysis and are outlined in Table 18.

Table 18. Improved categories and criteria used in the combined analysis of genetic variants.

Category	Criteria
Pathogenic	All of the following: Population genetics: vAF <0.001% Predicted functional effects: Probably damaging (by ≥2/3 tools) Evolutionary conservation: Conserved (≥6/8 orthologs)
Likely pathogenic	2/3 of the Probably damaging criteria
Unknown significance	3 methods in disagreement
Likely benign	2/3 of the Probably benign criteria
Benign	All of the following: Population genetics: vAF ≥0.001% Predicted functional effects: Probably benign (by ≥2/3 tools) Evolutionary conservation: Not conserved (<6/8 orthologs)

The categories and criteria used to indicate the predicted degree of pathogenicity of each variant. Variants were classified as pathogenic or benign if they met all of the criteria in that section.

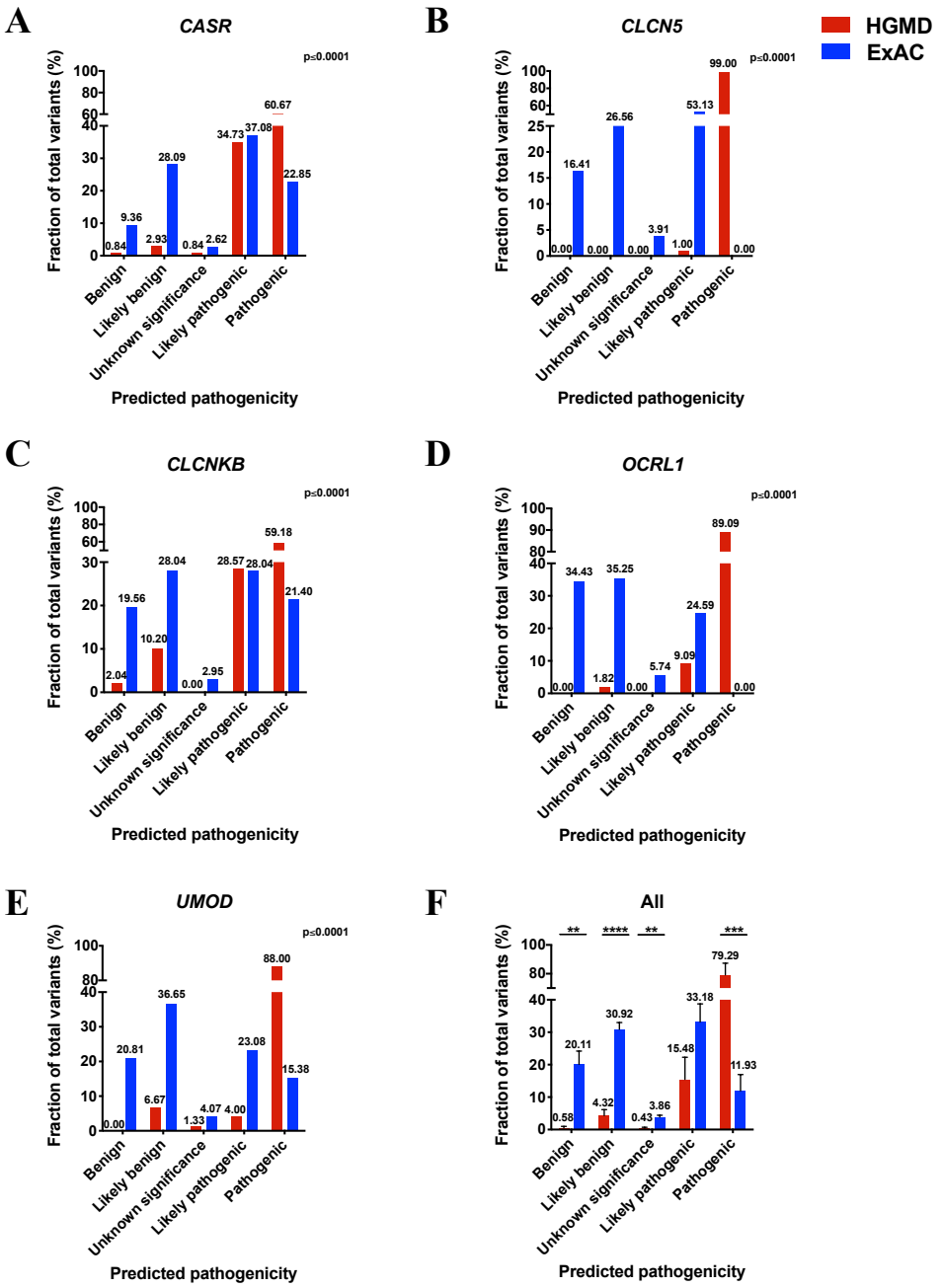
Similarly, to the previous combined analysis (Section 6.2.8.4), the distribution of HGMD and ExAC variants were significantly different for all of the five genes studied ($p \leq 0.0001$, chi-square test) (Figure 24A-E). The lowest proportions of HGMD variants predicted to be pathogenic were in *CASR* and *CLCNKB* for which 60.67% and 59.18%, respectively, were correctly predicted to be pathogenic (Figure 24A and C). Notably, this is still the majority of HGMD variants for each gene and a markedly lower proportion of ExAC variants were predicted to be pathogenic for each gene, with 22.85% of *CASR* and 21.40% of *CLCNKB* ExAC variants predicted to be pathogenic

(Figure 24A and C). However, a further 37.08% of *CASR* and 28.04% of *CLCNKB* ExAC variants were predicted to be likely pathogenic, which was also a marginally larger proportion than for the HGMD cohort (34.73% and 28.57%, respectively) (Figure 24A and C). Smaller proportions of HGMD and ExAC variants in both genes were predicted to be benign and likely benign with 0.84% of *CASR* HGMD variants and 9.36% of *CASR* ExAC variants predicted to be benign; 2.04% of *CLCNKB* HGMD and 19.56% of *CLCNKB* ExAC variants predicted to be benign; 2.93% of *CASR* HGMD and 28.09% *CASR* ExAC variants predicted to be likely benign; and 10.20% *CLCNKB* HGMD and 28.04% *CLCNKB* ExAC variants predicted to be likely benign (Figure 24A and C). Almost all *CLCN5* (99%) HGMD variants were correctly predicted to be pathogenic compared to 0% of ExAC variants, therefore showing this criteria was successful at almost completely separating HGMD and ExAC variants in this gene (Figure 24B). The largest proportion of *CLCN5* ExAC variants were predicted to be likely pathogenic (52.34%), as were the remaining 1% of *CLCN5* HGMD variants; compared to 15.63% predicted to be benign, 27.34% predicted to be likely benign and 4.69% predicted to be of unknown significance (Figure 24B). Similarly, the majority of *OCRL1* HGMD variants were also predicted to be pathogenic (89.09%) and again, none of the ExAC variants in this gene were predicted to be pathogenic (Figure 24D). Instead, the majority of ExAC variants were predicted to be either benign or likely benign (34.43% and 35.25%, respectively) (Figure 24D). Furthermore, just 1.82% of *OCRL1* HGMD variants were predicted to be likely benign and none were predicted to be benign (Figure 24D). The remaining *OCRL1* HGMD and ExAC variants were predicted to be either likely pathogenic (9.09% and 24.59%, respectively) or of unknown significance (0% and 5.74%, respectively) (Figure 24D). Finally, the majority of *UMOD* HGMD variants were predicted to be pathogenic (88%) compared to just 15.38% of ExAC

variants (Figure 24E). Conversely, the majority of ExAC variants were predicted to be either benign (20.81%) or likely benign (36.65%), with just 4.07% predicted to be of unknown significance and 23.08% predicted to be likely pathogenic (Figure 24E). The remaining 12% of *UMOD* HGMD variants were either predicted to be likely pathogenic (4%), of unknown significance (1.33%) or likely benign (6.67%) (Figure 24E).

The results of the individual gene analyses were then combined (Figure 24F) and showed that the majority of HGMD (79.29%) variants were correctly predicted to be pathogenic (Figure 24F). However, a higher proportion of HGMD variants (20.71%) fell into other categories (15.48% were predicted to be likely pathogenic, 0.43% to be of unknown significance, 4.32% to be likely benign and the remaining 0.58% to be benign) (Figure 24F) compared to the initial combined analysis (1.88%) (Figure 19F). Nevertheless, a significant difference between the proportion of HGMD and ExAC variants in all of the categories, apart from likely pathogenic, was observed in the combined analysis (benign and unknown significance $p \leq 0.01$; pathogenic $p \leq 0.001$; and likely benign $p \leq 0.0001$, multiple t-tests corrected for multiple comparisons) (Figure 24F). Furthermore, a lower proportion of ExAC variants (11.93%) were predicted to be pathogenic in this combined analysis (Figure 24F) compared to the first analysis (74.40%) (Figure 19F). Instead, the category with the largest proportion of ExAC variants was likely pathogenic (33.18%), closely followed by likely benign (30.92%) (Figure 24F). Thus, the degree of overlap in the pathogenic category was considerably lower than in the initial combined analysis (Figure 19F). These results suggest that the improved criteria are effective at prioritising pathogenic variants in genetic studies of monogenic renal tubule disorders, and more effective at separating pathogenic and benign variants.

Figure 24. Predicted pathogenicity of HGMD and ExAC variants using a new combined analysis approach.



The predicted pathogenicity of each variant was generated using vAFs, prediction of functional effects and evolutionary conservation (Table 18). Graphs A-E display the results for each gene individually, (A) *CASR*, (B) *CLCN5*, (C) *CLCNKB*, (D) *OCRL1*, (E) *UMOD*, and (F) the combined analysis. The majority of HGMD variants were correctly predicted as pathogenic or likely pathogenic. Statistical analysis was carried out using chi-square test for the data shown in graphs A-E and multiple t-tests, corrected for multiple comparisons using the Sidak-Bonferroni method for graph F. **p≤0.01, ***p≤0.001, ****p≤0.0001.

6.3. Discussion and future studies

With the vast improvements and reduction in costs of DNA sequencing technology in recent decades, NGS techniques are being used more frequently and widely in both the laboratory and clinic[110,210,212,278]. Whilst Sanger DNA sequencing remains the 'gold-standard' for DNA sequencing [210-212], this technique is most useful for the sequencing of one, or a small number of, known-disease causing or candidate gene(s)[210]. For the sequencing of a large number of genes, or in cases where the gene(s) of interest are unknown, NGS methods such as WES and WGS may be more appropriate. Thus, for studies such as those detailed in this thesis, where candidate gene(s) for the disorder(s) of interest are unknown, WES and WGS have been used. These methods present a problem: How to interpret the vast quantities of genetic data generated? In fact, variant interpretation is widely considered the rate-limiting step in NGS studies[210,219,265,266]. *In vitro* functional analysis of variants is common place and remains one of the 'gold-standard' methods, along with segregation studies and co-occurrence in multiple families, to provide evidence of pathogenicity[220]. However, NGS methods such as WES and WGS result in the identification of vast quantities of variants (approximately tens of thousands[218] and 4 million, respectively[210]) for which *in vitro* analysis is not viable for all variants due to the cost, time and labour required[220]. Therefore, to overcome these issues, *in silico* methods are used to prioritise candidate variants for *in vitro* analysis[220]. However, there is limited data available regarding best practice for *in silico* analysis and interpretation of genetic variants, and many publications do not disclose the criteria and methods used to identify pathogenic variants. The ACMG have published reports with suggested methods and guidelines for the effective interpretation of variants, including: vAFs, literature searches for biological relevance, functional prediction

software, segregation studies and *in vitro* or *in vivo* studies[237]; which have been updated and adapted over the years in line with changes and developments in NGS and *in silico* methods[237,276,279]. However, some of the suggested analyses, such as segregation and functional studies, are not appropriate for the initial stages of genetic variant analysis, which are neither time- nor cost-effective at this stage[220]. Therefore, this study aimed to investigate the effectiveness of commonly used *in silico* methods for the interpretation of genetic variants and to investigate the most effective criteria for the identification and separation of pathogenic variants from benign variants.

Since the sequencing of the human genome and the subsequent development of population databases, population genomics is one of the most commonly used *in silico* methods for the genetic analysis of potentially pathogenic variants[210,236-238]. The ACMG report recommend using the known or estimated frequency of occurrence of a disorder as a vAF cut-off[237]; however, this figure is not always known or reliable[276]. Therefore, for this study I began by investigating how effective using vAF <1%, which is used to classify rare variants from common variants, was at identifying pathogenic variants and separating them from benign variants. These results showed that whilst 99.59% of HGMD variants were rare (vAF <1%), so were 98.86% of ExAC variants, which is consistent with previous reports[236]. Furthermore, the difference in the proportion of HGMD and ExAC variants classified as rare and common was not statistically significant. Therefore, this criteria was ineffective at separating pathogenic and benign variants, and new methods are required. Each variant's allele frequency was next analysed and sorted into 1 of 5 intervals ranging from <0.001% to ≥1%. The results of which showed the majority of HGMD variants (92.30%) had vAFs <0.001% compared to 31.93% of ExAC variants. Conversely, the majority of

ExAC variants (59.07%) had vAFs of 0.001-0.0099% compared to just 5.67% of HGMD variants. Therefore, suggesting a more effective cut-off vAF for the separation of HGMD and ExAC variants for these five genes is <0.001%. Combining the results of the individual gene analysis revealed that 91.50% of all HGMD variants were found to have vAFs <0.001%, compared to 41.16% of all ExAC variants. Therefore, suggesting that on its own this method and criteria whilst effective at prioritising pathogenic variants from benign variants, is not entirely effective at separating the two cohorts, thus highlighting the need for a combined analysis with additional *in silico* methods.

Multiple publically accessible online tools for the prediction of functional effects of protein-altering variants are available. Each programme uses one or a combination of criteria that may include evolutionary conservation, location and context with the protein sequence and the biochemical consequence of the amino acid substitution to predict the impact of a variant[225,237,240-242,276]. However, numerous studies investigating the effectiveness of such programmes have shown they may only be 65-80% accurate in predicting pathogenicity of known disease-causing variants[277]. To mitigate any variation and weaknesses the programmes may have, the ACMG report suggests the use of multiple programmes for the prediction of functional effects[237]. Therefore, three commonly used programmes were used for this analysis: PolyPhen-2, Provean Protein and MutationTaster. In the initial analysis variants were analysed by each of the three programmes to give an overall predicted functional effect of probably benign, unknown significance or probably damaging. Using this criteria, a higher proportion of HGMD variants were correctly predicted to be probably damaging (89.64%), compared to ExAC variants (40.67%). Conversely, a higher

proportion of ExAC variants (51.74%) were correctly predicted to be probably benign compared to HGMD variants (9.36%), thus suggesting that these criteria and tools are effective at prioritising pathogenic variants, but are only partially effective at separating pathogenic from benign variants. To investigate whether these criteria could be improved further, reducing the degree of overlap in the probably damaging category, the analysed variants were instead sorted into one of five categories: probably damaging and benign, possibly damaging and benign and unknown significance. Whilst the majority of HGMD variants (80.64%) were correctly predicted to be probably damaging compared to 33.01% of ExAC variants, as with the first analysis there remained a degree of overlap. Furthermore, 9% less HGMD variants were correctly predicted to be probably damaging in the new analysis using five categories compared to the initial analysis using three categories. These findings suggest that the initial criteria using three categories was the most effective criteria for prioritising and separating pathogenic from benign variants of rare monogenic renal tubule disorders. However, due to the degree of overlap in the probably damaging category, similarly to the results of the population genomic analysis, these findings highlight the requirement for a combination analysis approach using multiple *in silico* methods.

The degree of conservation of a WT amino acid residue across a range of orthologs is often used as an indicator of the functional importance of that residue and thus the potential pathogenicity of a variant affecting that residue[210,219]. This is based on the assumption that amino acids with a deleterious effect have been removed due to natural selection and thus those that remain and are observed in reference ortholog sequences are neutral; however, this is not always the case[219,246]. Conservation

analysis is a particularly useful tool in circumstances where additional protein data is limited e.g. when functional domains and three-dimensional structures are not known or available. For the initial analysis, four orthologs were used to indicate the degree of conservation of each of the affected residues across the animal kingdom. The results from this analysis show that this method and criteria is effective at prioritising pathogenic variants in the conserved category (94.02% of HGMD variants) with a higher proportion of HGMD variants in this category compared to ExAC variants. However, there was a high degree of overlap within the conserved category with the majority of ExAC variants (72.18%) also being considered as affecting a conserved residue, thereby showing that these criteria are not effective at separating pathogenic from benign variants associated with rare monogenic renal tubule disorders. Consequently, the number of orthologs studied was increased from four to eight to determine if this would increase the efficacy of this method. The results showed that this reduced the degree of overlap between the HGMD and ExAC variants in the conserved category. The increased number of orthologs studied had very little effect on the proportion of HGMD variants prioritised. However, by increasing the number of orthologs studied, the proportion of ExAC variants affecting conserved residues was reduced from 72.18% in the initial analysis to 57.60% in the second analysis. These findings suggest that using eight orthologs instead of four for evolutionary conservation analysis is effective at prioritising pathogenic variants and is more effective at separating pathogenic and benign variants. However, similarly to the results observed in the population genomics and prediction of functional effects analyses, these findings show that alone, this method is not sufficient for the prioritisation and separation of pathogenic and benign variants, highlighting the need for a combined approach to variant analysis.

Results of the independent analyses for each of the three commonly used methods showed that whilst these methods and criteria are effective at prioritising pathogenic (HGMD) variants, none of the methods alone were highly effective at separating pathogenic from benign variants. Consequently, as suggested in the ACMG report, a combined analysis approach was taken[237]. The initial combined analysis utilised the results from the initial independent analyses: vAF cut-off of 1%, prediction of functional affects using three categories and conservation in four orthologs. The results from this analysis show that combined, these methods were effective at correctly identifying pathogenic variants with 98.12% of HGMD variants in this category. However, whilst there was a significant difference in the proportion of HGMD and ExAC variants predicted to be pathogenic, the degree of overlap was higher in this combined analysis than in the individual analysis for predicted functional effect. In fact, the majority of ExAC variants (74.40%) were also predicted to be pathogenic. Therefore, a second combined analysis was performed using the most effective criteria for each of the three methods from the independent analyses: vAF cut off of <0.001%, prediction of functional effects using three categories and evolutionary conservation across eight orthologs. These results showed a higher proportion of HGMD variants (79.29%) were correctly predicted to be pathogenic compared to ExAC variants (11.93%). Importantly, in the improved combined analysis one of the smallest proportions of ExAC variants (11.93%) were predicted to be pathogenic, compared to 74.40% in the initial analysis, thereby showing a vast improvement in the effectiveness of the criteria at prioritising and separating pathogenic variants from benign variants associated with rare monogenic renal tubule disorders.

Several large studies have assessed the effectiveness of WES to provide a molecular diagnosis, reporting success rates ranging from 22-46%[110,280-283], although estimates of the success of NGS methods are inherently difficult to determine as often negative results are not published. It is thought that a number of factors may contribute to these low success rates in WES such as the interpretation of variants, incomplete coverage of the exome, mutations elusive to WES and incorrect variant annotations[110,284]. Furthermore, whilst some NGS variant annotation systems are available to use in large-scale genetic studies, they are not always available for all studies. Therefore, the criteria identified in this study can be applied to these annotation systems and can also be performed independently by the researcher, for variants identified by Sanger DNA sequencing or for single and multi-gene panel sequencing. Therefore, it is hoped that the improvements in the criteria used for the *in silico* analysis of genetic variants achieved by this study will increase the effectiveness of these methods at identifying and prioritising pathogenic variants, whilst simultaneously excluding benign variants, for *in vitro* analysis. This will help to reduce the time and cost to the researcher or clinician, and improve the success rate of NGS methods in genetic studies of rare monogenic renal tubule disorders. The results of this study will now be applied to the NGS and Sanger DNA sequencing studies detailed within this thesis.

Whilst these findings could putatively be applied to other rare monogenic disorders, it is important to note that these findings are based on a small study of rare monogenic renal tubule disorders and that even within this cohort there was distinct variation in the effectiveness of different methods and criteria between genes. Therefore, further study of genes associated with other rare monogenic disorders

would be required to confirm or alter the criteria identified in this study. Additionally, these findings would not be appropriate for studies of common disorders; for example, the optimum vAF cut-off of <0.001% determined by this study may not be appropriate as the prevalence of such disorders would be higher than those associated with the genes in this study. Therefore, a new study using variants associated with common disorders would be required to determine the optimum criteria. Finally, this study focussed on coding variants and, as such, many of the methods and tools used here such as evolutionary conservation of amino acid residues and prediction of functional effects using PolyPhen-2 and Provean Protein would not be applicable for the interpretation of non-coding variants. Population genomics and MutationTaster, for the prediction of functional effects, would on the other hand, still be useful tools as unlike Provean Protein and PolyPhen-2, MutationTaster is able to analyse non-coding genomic variants providing information regarding regulatory features, splice-sites and nucleotide conservation[240]. Therefore, other methods such as miRNA-target site, splice-site and nucleotide conservation analysis and prediction would be required for studies of non-coding variants. Further study of the effectiveness of these methods and the criteria applied to them is required for each method independently, and in combination, to provide a robust methodology and criteria for the interpretation of non-coding variants.

7 Investigation of the *CLCNKA* gene in patients with Dent's disease

Between 25-35% of DD patients lack mutations in *CLCN5* and *OCRL1*, indicating a role for additional genes in DD[98]. Recently, collaborators at Harvard performed WES on a male patient with DD, lacking a mutation in *CLCN5* or *OCRL1,* identifying a homozygous variant in *CLCNKA* (unpublished data), located on chromosome 1p36.13[285], whereas *CLCN5* and *OCRL1* are both located on Xp11.23 and Xq26.1 respectively[99,100]. Compound heterozygous and homozygous mutations in *CLCNKA* and *CLCNKB* together, have previously been associated with Bartter syndrome type 4B[134,271]. Therefore, it was hypothesised that homozygous variants in *CLCNKA* alone are associated with DD. This chapter describes the subsequent search for variants in *CLCNKA* in a further 18 unrelated patients with DD, previously screened for mutations in *CLCN5* and *OCRL1*.

7.1. Declaration of contributions

The work in this chapter is my own, unless otherwise stated. Collaborators Prof Friedhelm Hildebrandt and Dr Dervla Connaughton of Boston Children's Hospital, Harvard Medical School carried out WES on a patient with DD, lacking mutations in *CLCN5* and *OCRL1*, and identified a homozygous variant in *CLCNKA*. *CLCNKA* primers for Sanger DNA sequencing were designed by Dr Caroline Gorvin and sequencing of prepared DNA pellets was performed at the Department of Zoology, University of Oxford.

7.2. Results

7.2.1 Patient characteristics

Sanger DNA sequencing of *CLCNKA* was performed using DNA samples from 18 unrelated patients with DD, previously screened for mutations in *CLCN5* and *OCRL1,* as well as one unaffected control. All of these patients had low-molecular-weight proteinuria and some were known to have additional features such as hypercalciuria, nephrocalcinosis and nephrolithiasis (Table 19). Sequencing was performed on the 2064bp coding region of *CLCNKA* which has 39 exon-intron boundaries, the 5'UTR and approximately half (excluding the last 180bp) of the 3'UTR. This encodes the 75kDa ClC-Ka protein which consists of ten transmembrane domains encoded by the mid-portion of exon 3 to exon 15; as well as the cytoplasmic domain encoded by the 3' portion of exon 15 to exon 20, within which are cystathione-ß-synthase (CBS) domains 1 and 2 (Figure 25).

7.2.2 Identification of 13 non-synonymous exonic or UTR *CLCNKA* variants in patients with DD

Non-synonymous exonic, splice-site (of which there were none) and UTR variants that were not observed in the unaffected control were selected for *in silico* analysis. In total 13 variants fit this criteria. Of the 13 variants, 11 were located in coding regions spanning exon 2-20 and two were located within the 3'UTR, with the highest frequency (46%) of variants observed in exons 14 and 20 (Figure 25). With the exception of Arg8His, all of the coding variants were localised to transmembrane domain regions or the cytoplasmic domain (Figure 25). Specifically, the majority of coding variants (63.6%) were localised to transmembrane domain regions, whilst

27% of coding variants were located within the cytoplasmic domain (Figure 25). *In silico* analysis of vAFs identified two distinct populations of variants: rare variants (vAF <1% on population databases), of which there were two, Phe285del and Thr562Met, (highlighted in red in Figure 25); and common variants (vAF oF ≥1% on population databases), of which there were 11 (Arg8His, Arg83Gly, Tyr315Phe, Ala447Thr, Leu334Val, Thr454Ala, Val457Ile, Arg534Trp, Pro683Leu, c.*126A>G and c.*163A>T) (highlighted in black in Figure 25). No unreported variants were identified.

7.2.2.1 Identification and in silico analysis of common variants in CLCNKA in patients with DD

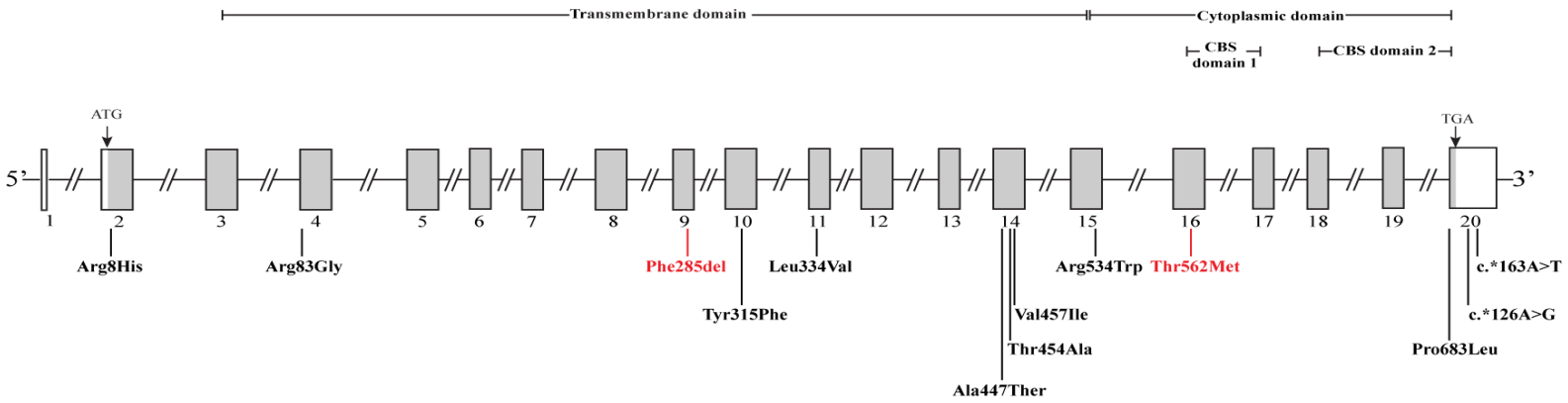
Eleven common variants were identified by Sanger DNA sequencing (Figure 25 and Table 20). *In silico* analysis was performed for each of the common variants, as described in Section 6.2.9.4 and included population genomics (ExAC and 1000 genomes), prediction of functional effects using three online tools (PolyPhen-2, MutationTaster and Provean Protein) and evolutionary conservation. The results are summarised in Table 20. Additionally, miRNA target site prediction was performed to investigate the predicted effects of the two non-coding variants on miRNA target sites, the results of which are described in Section 7.2.2.1.12

Table 19. Clinical phenotypes of DD patients, lacking mutations in *CLCN5* and *OCRL1*

Patient ID	Sex	Low-molecular-weight proteinuria	Hypercalciuria	Nephrocalcinosis	Nephrolithiasis	Other
1	Male	+	+	+	Not known	Hypokalaemia and acidosis.
2	Male	+	Not known	Not known	Not known	Not known
3	Male	+	+	+	Not known	Unidentified dysmorphic syndrome with slight mental retardation and severe nystagmus.
4	Male	+	+	+	+	Not known
5	Male	+	Not known	Not known	Not known	Not known
6	Female	+	+	+	Not known	Turner syndrome, complete congenital heart disease
7	Male	+	Not known	Not known	Not known	Not known
8	Male	+	-	-	Not known	Not known
9	Male	+	Not known	Not known	Not known	Not known
10	Female	+	Not known	Not known	Not known	Not known
11	Female	+	+	+	Not known	Born small for date, has slight microcephaly and oedema on the dorsum pedis. Turner syndrome was excluded. Also has aminoaciduria and glycosuria.
12	Not known	+	Not known	Not known	Not known	Not known
13	Male	+	Not known	Not known	Not known	Not known
14	Male	+	Not known	Not known	Not known	Not known
15	Male	+	Not known	Not known	Not known	Not known
16	Male	+	Not known	Not known	Not known	Not known
17	Female	+	-	+	Not known	Mild renal insufficiency, hypocitraturia and recurrent urolithiasis.
18	Female	+	+	Not known	+	Not known

Clinical phenotypes of the 18 Dent's disease patients studied. +, present, -, absent. No patients were described to have rickets or renal failure.

Figure 25. Schematic representation of the genomic organisation of the human *CLCNKA* gene showing the location of common and rare variants identified in DD patients



Common and rare variants are those with a reported vAF of ≥1% and <1% respectively. The *CLCNKA* gene consists of 20 exons with the start (ATG) and stop (TGA) codons located in exons 2 and 20, respectively. The transmembrane domains (encoded by the mid portion of exon 3 to exon 15) are followed by the cytoplasmic domain (encoded by the 3'portion of exon 15 to exon 20). Within the cytoplasmic domain are 2 cystathione-ß-synthase (CBS): CBS domain 1 (encoded by the 3' portion of exon 16 and the 5' portion of exon 17) and CBS domain 2 (encoded by the 3' portion of exon 18 to the 5' portion of exon 20). The ^rare variants Phe285del and Thr562Met (highlighted in red) are located within exon 9, encoding a transmembrane domain, and exon 16, encoding CBS domain 1 within the cytoplasmic domain, respectively. The common variants (highlighted in black) span exons 2-20: Arg8His is located within the coding region of exon 2; Arg83Gly, located within exon 4, Tyr315Phe, located within exon 10, and Ala447Thr, located within exon 14, encode transmembrane domain regions; Leu334Val, located within exon 11, Thr454Ala and Val457Ile, both located within exon 14, encode transmembrane domains; Arg534Trp, located within exon 15, and Pro683Leu, located within exon 20, encode the cytoplasmic domain, with Pro683Leu also encoding CBS domain 2; and the 3'UTR variants c.*126A>G and c.*163A>T are located within the 3'UTR region within exon 20. Coding regions are shaded grey and untranslated regions are shaded white.

Table 20. *In silico* analysis of *CLCNKA* common nonsynonymous coding and 3'UTR variants identified in DD patients

Nucleotide Change	Amino Acid Change	Patients with the variant	Patient cohort vAF	Patient cohort genotype frequencies	^Reported vAF	^Reported genotype frequencies	PolyPhen-2	MutationTaster	Provean Protein	Evolutionary conservation	Combined *in silico* prediction
c.23G>A	p.Arg8His	1/18 (5.56%)	2.78% (A)	Heterozygotes (GA): 1(5.56%) Homozygotes (AA): 0 (0%)	3.8% (A)	Heterozygotes (GA): 7.53% Homozygotes (AA): 0.068%	Benign (score:0.062)	Polymorphism	Deleterious (score:-2.555)	Partially conserved (5/8)	Benign
c.247A>G	*p.Arg83Gly	14/18 (77.78%)	55.56% (G)	Heterozygotes (AG): 8 (44.44%) Homozygotes (GG): 6 (33.33%)	56.36% (G)	Heterozygotes (AG): 47.29% Homozygotes (GG): 32.7%	Benign (score:0.00)	Polymorphism	Neutral (score: -0.165)	Not conserved (2/8)	Benign
c.944A>T	*p.Tyr315Phe	7/18 (38.89%)	22.22% (T)	Heterozygotes (AT): 6 (33.33%) Homozygous (TT) : 1 (5.56%)	20.70% (T)	Heterozygotes (AT): 31.95% Homozygotes (TT): 4.73%	Benign (score: 0.00)	Polymorphism	Neutral (score: 0.369)	Not conserved (1/8)	Benign
c.1000C>G	p.Leu334Val	2/18 (11.11%)	5.56% (G)	Heterozygotes (CG): 2 (11.11%) Homozygotes (GG): 0 (0%)	2.24% (G)	Heterozygotes (CG): 4.28% Homozygotes (GG): 0.10%	Benign (score: 0.015)	Polymorphism	Neutral (score: -0.473)	Partially conserved (5/8)	Benign
c.1339G>A	*p.Ala447Thr	14/18 (77.78%)	55.56% (A)	Heterozygotes (GA): 8 (44.44%) Homozygotes (AA): 6 (33.33%)	56.12% (A)	Heterozygotes (GA): 47.29% Homozygotes (AA): 32.48%	Benign (score: 0.008)	Polymorphism	Neutral (score: -0.100)	Partially conserved (4/8)	Benign
c.1360A>G	*p.Thr454Ala	3/18 (16.67%)	11.11% (G)	Heterozygotes (AG): 2 (11.11%) Homozygotes (GG): 1 (5.56%)	7.78% (G)	Heterozygotes (AG): 14.14% Homozygotes (GG): 0.71%	Benign (score: 0.00)	Polymorphism	Neutral (score: 0.067)	Not conserved (0/8)	Benign
c.1369G>A	p.Val457Ile	3/18 (16.67%)	11.11% (A)	Heterozygotes (GA): 2 (11.11%) Homozygotes (AA): 1 (5.56%)	7.74% (A)	Heterozygotes (GA): 14.13% Homozygotes (AA): 1.35%	Benign (score:0.003)	Polymorphism	Neutral (score: -0.171)	Partially conserved (3/8)	Benign
c. 1600C>T	*p.Arg534Trp	3/18 (16.67%)	11.11% (T)	Heterozygotes (CT): 2 (11.11%) Homozygotes (TT): 1 (5.56%)	7.88% (T)	Heterozygotes (CT): 14.2% Homozygotes (TT): 0.77%	Benign (score: 0.01)	Polymorphism	Neutral (score: -1.695)	Partially conserved (3/8)	Benign
c.2048C>T	p.Pro683Leu	3/18 (16.67%)	11.11% (T)	Heterozygotes (CT): 2 (11.11%) Homozygotes (CT): 1 (5.56%)	7.96% (T)	Heterozygotes (CT): 14.66% Homozygotes (TT): 0.63%	Possibly damaging (score:0.866)	Polymorphism	Deleterious (score: -2.567)	Partially conserved (5/8)	Likely benign
c.*126A>G	N/A	3/18 (16.67%)	11.11% (G)	Heterozygotes (AG): 2 (11.11%) Homozygotes (GG): 1 (5.56%)	5.73% (G)	Heterozygotes (AG): 10.74% Homozygotes (GG): 0.36%	N/A	Polymorphism	N/A	N/A	Benign
c.*163A>T	N/A	13/18 (72.22%)	44.44% (T)	Heterozygotes (AT): 10 (55.56%) Homozygotes (TT): 3 (16.67%)	58.9% (T)	Heterozygotes (AT): 44.69% Homozygotes (TT): 36.58%	N/A	Polymorphism	N/A	N/A	[+]Benign

Common variants are those with a ^reported vAF ≥1%. ^Reported vAFs and genotype frequencies are from ExAC or the 1000 Genomes database. Eight orthologous protein sequences were used to assess the degree of evolutionary conservation of the affected amino acid residue: human, chimpanzee, mouse, cow, chicken, elephant, anole lizard, zebrafish and fugu. Variants were classified as conserved (≥6/8), partially conserved (3-5/8) or not conserved (≤2/8) in accordance with Section 6.2.9.4. A prediction of pathogenicity was made using a combined *in silico* analysis approach as described in Section 6.2.9.4 using the data generated from population genomics, prediction of functional effects and conservation analysis where possible. N/A, not applicable. *Indicates a possible major amino acid change e.g. substitution of an uncharged amino acid for a charged amino acid, a positively charged amino acid for a negatively charged amino acid, a hydrophilic for a hydrophobic amino acid or one that is likely to break a helix.

7.2.2.1.1 Identification and *in silico* analysis of an Arg8His variant in ClC-Ka, in proband 15

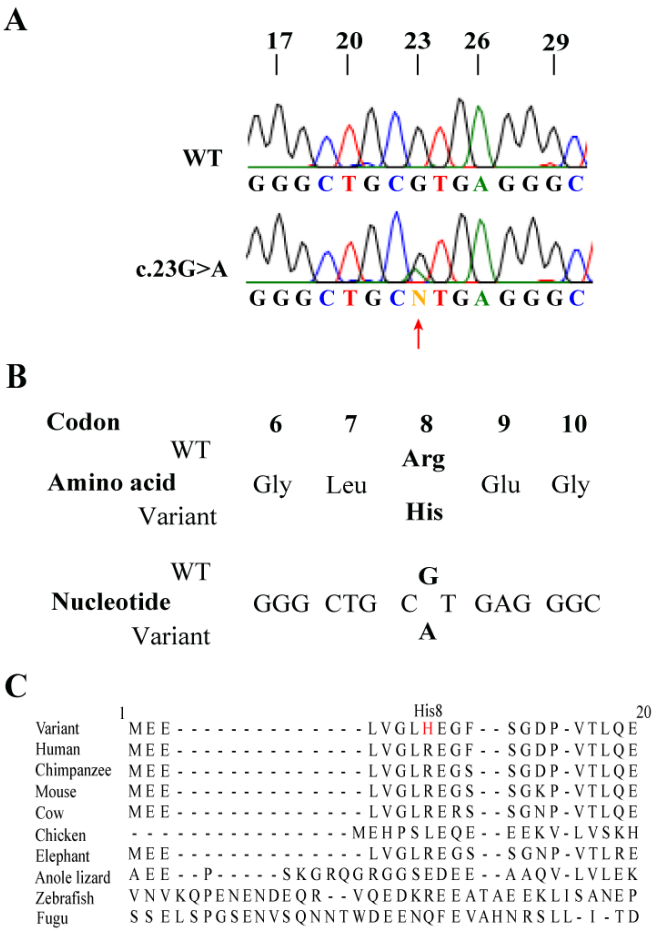
With the exception of Arg8His, all the common variants were identified in multiple patients in the DD cohort. A heterozygous G-to-A transition at nucleotide c.23 was identified in proband 15 and is predicted to result in the substitution of an arginine for a histidine at codon 8 (Figure 26). *In silico* analyses revealed that the Arg8His variant had a reported vAF of 2.78%. Additionally, the variant allele and genotype frequencies observed in the DD cohort for the heterozygous Arg8His variant are not significantly different to those reported on ExAC (p=0.7484 and p=0.9448 respectively, chi-square test) (Table 20). The functional effect of the Arg8His variant was predicted to be benign by two of the three prediction tools and deleterious by Provean Protein (Table 20). Furthermore, the WT Arg8 residue was only partially conserved across five of the eight species studied (Table 20 and Figure 26). A combined *in silico* approach therefore predicted the Arg8His variant to be benign.

7.2.2.1.2 Identification and *in silico* analysis of an Arg83Gly variant in ClC-Ka in 14 probands

The Arg83Gly variant, resulting from an A-to-G transition at nucleotide 247 (Figure 27), was one of the most commonly observed variants within the DD cohort. The Arg83Gly variant was identified in 14 of the 18 DD patients as either heterozygous (probands 4, 6, 7, 10, 11 and 13-15 [8/14, 44.44%]) or homozygous (probands 1,2 8, 9, 12 and 17 [6/14, 33.33%]) (Table 20). The genotype frequencies observed in this cohort were not found to be significantly different from those reported on ExAC (Table 20) (p=0.9622, chi-square test). Additionally, the vAF observed in the DD

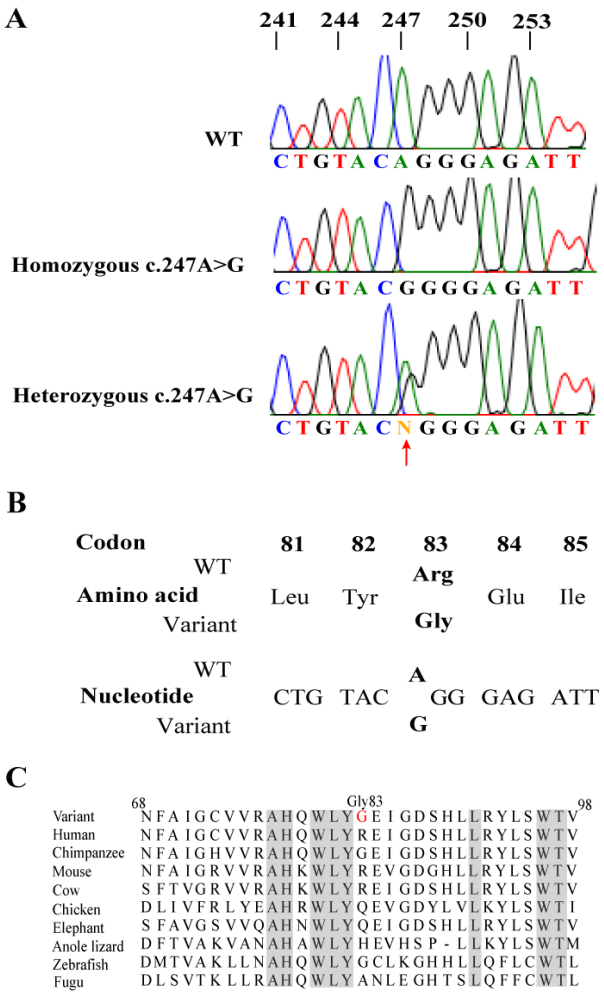
cohort (55.56%) is consistent with that reported by ExAC (56.30%) (p=0.9225, chi-square test); and is much higher than the <0.001% cut-off suggested in Section 6.2.9.1 (Table 20). Furthermore, the pathogenicity prediction programmes predicted Arg83Gly to be benign; and evolutionary conservation analysis of the WT Arg83 residue revealed it was not conserved (2/8) (Figure 27 and Table 20). Equally, the variant Gly83 residue was present in two species (Figure 27 and Table 20). Thus, combined *in silico* analysis predicted the Arg83Gly variant to be benign.

Figure 26. Identification of an Arg8His variant in ClC-Ka in proband 15



(A) A heterozygous G-to-A transition at nucleotide c.23 was identified in proband 15. (B) This G-to-A transition (CGT to CAT) is predicted to result in a missense amino acid change from arginine (Arg) to histidine (His) at codon 8 of the ClC-Ka protein. (C) Multiple sequence alignment of residues surrounding the human Arg8 residue of the ClC-Ka protein sequence in eight species. The His8 residue identified in DD patients is shown in red. The Arg8 residue is only partially conserved across the eight species. Codon numbers are displayed for the human sequence.

Figure 27. Identification of an Arg83Gly variant in ClC-Ka in 14 probands



A homozygous and heterozygous A-to-G transition at nucleotide c.247 was identified in 6 and 8 probands respectively. (B) This A-to-G transition (AGG to GGG) is predicted to result in a missense amino acid change from arginine (Arg) to glycine (Gly) at codon 83 within the transmembrane region of the ClC-Ka protein. (C) Multiple sequence alignment of residues surrounding the human Arg83 residue of the ClC-Ka protein sequence in eight species. The Gly83 residue identified in DD patients is shown in red. Entirely conserved residues are highlighted in grey, the Arg83 residue is not conserved across the eight species. Codon numbers are displayed for the human sequence.

7.2.2.1.3 Identification and *in silico* analysis of a Tyr315Phe variant in ClC-Ka in seven probands

An A-to-T transversion at nucleotide 944, predicted to result in a tyrosine-to-phenylalanine substitution at codon 315 (Figure 28), was identified in seven of the eighteen DD patients. The Tyr315Phe variant was observed in the heterozygous state in six probands (3, 4, 9, 13, 17 and 18 [6/18, 33.33%]) and homozygous state in one

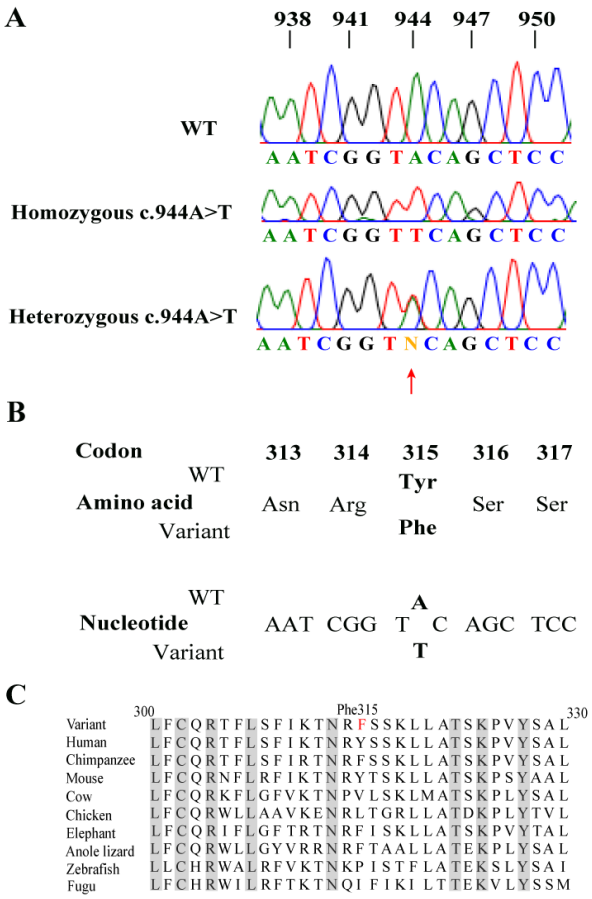
proband (12 [1/18, 5.56%]) (Table 20); neither of which is significantly different to the genotype frequencies reported in ExAC (31.95% and 4.73% respectively) (p=0.9750, chi-square test) (Table 20). Additionally, the reported vAF (ExAC) (20.7%) is higher than the <0.001% cut-off optimised in Section 6.2.9.1; and was shown not to be significantly different to the vAF observed in the DD cohort (38.89%) (p=0.8216, chi-square test) (Table 20). The Tyr315Phe variant was predicted to be benign by all of the prediction programmes used (Table 20); and the WT Tyr315 residue was conserved in just one of the eight species (Figure 28 and Table 20) and was therefore classified as not conserved. Furthermore, the Phe315 variant was present in three of the eight species studied (Figure 28). Overall the combined *in silico* analysis predicted the Tyr315Phe variant to be benign.

7.2.2.1.4 Identification and *in silico* analysis of a Leu334Val variant in ClC-Ka in probands 3 and 4

A C-to-G transversion at nucleotide 1000 was identified in probands 3 and 4 by Sanger DNA sequencing and is predicted to result in the substitution of a leucine with a valine at codon 334 (Figure 29). The Leu334Val variant is just one of two common variants that was observed in the heterozygous state only (Figure 29 and Table 20); furthermore, there was no significant difference in the genotype frequency observed within the DD cohort (11.11% heterozygous) compared to those reported on ExAC (4.28% heterozygous) (p=0.3560, chi-square test) (Table 20). *In silico* analysis of the vAFs also revealed no significant difference between the vAF observed in the DD cohort (5.56%) and that reported on ExAC (2.24%) (p=0.1788, chi-square test) (Table 20). Furthermore, the reported vAF is higher than the <0.001% cut-off suggested by the study in Section 6.2.9.1. The Leu334Val variant was also predicted to be benign by

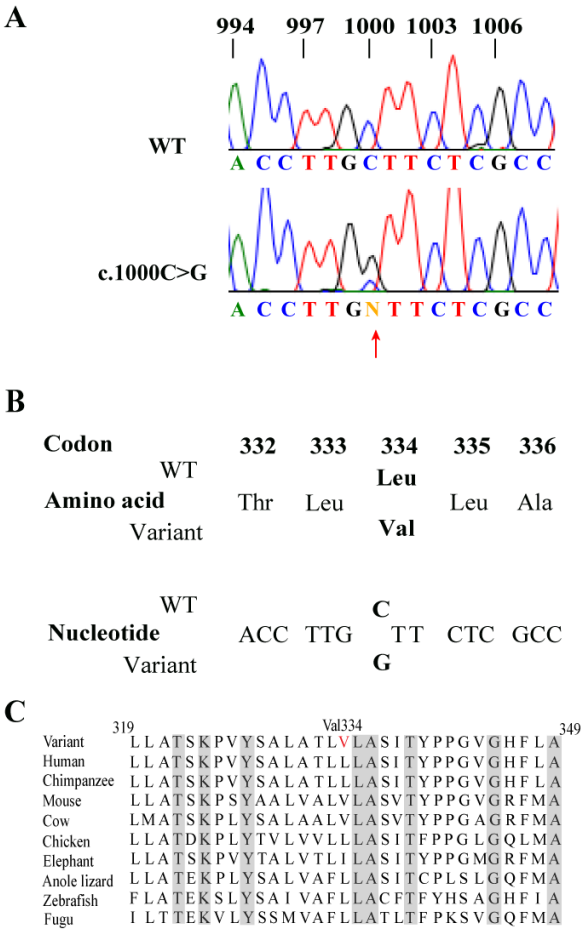
all three of the pathogenicity prediction programmes (Table 20); and evolutionary conservation analysis showed that the WT Leu334 residue was partially conserved, with the residue present in five of the eight species studied (Figure 29 and Table 20). Additionally, the variant Val334 residue was present in two species (Figure 29). Thus, the combined *in silico* analysis indicated the variant is benign.

Figure 28. Identification of a Tyr315Phe variant in ClC-Ka in seven probands



(A) A homozygous and heterozygous A-to-T transversion at nucleotide c.944 was identified in one and six probands respectively. (B) This A-to-T transversion (TAC to TTC) is predicted to result in a missense amino acid change from tyrosine (Tyr) to phenylalanine (Phe) at codon 315 within the transmembrane region of the ClC-Ka protein. (C) Multiple sequence alignment of residues surrounding the human Tyr315 residue of the ClC-Ka protein sequence in eight species. The Phe315 residue identified in DD patients is shown in red. Residues conserved across all of the orthologs studied are highlighted in grey, the Tyr315 residue is not conserved across the eight species. Codon numbers are displayed for the human sequence.

Figure 29. Identification of a Leu334Val variant in ClC-Ka in proband 3 and 4



(A) A heterozygous C-to-G transversion at nucleotide c.1000 was identified in two probands (3 and 4). (B) This C-to-G transversion (CTT to GTT) is predicted to result in a missense amino acid change from leucine (Leu) to valine (Val) at codon 334 within a transmembrane domain of the ClC-Ka protein. (C) Multiple sequence alignment of residues surrounding the human Leu334 residue of the ClC-Ka protein sequence in eight species. The Val334 residue identified in DD patients is shown in red. Residues conserved across all of the orthologs studied are highlighted in grey, the Leu334 residue is partially conserved across the eight species. Codon numbers are displayed for the human sequence.

7.2.2.1.5 Identification and *in silico* analysis of an Ala447Thr variant in ClC-Ka in 14 probands

The other most commonly identified variant, was a G-to-A transition at nucleotide 1339, predicted to result in the substitution of an alanine for a threonine at codon 447 (Figure 30 and Table 20). The Ala447Thr variant was also observed as heterozygous or homozygous in the same probands (6,7,10,11 and 13-15 and 1, 2, 8, 9, 12 and 17 respectively) as Arg83Gly (Table 20). Additionally, analysis of the genotype

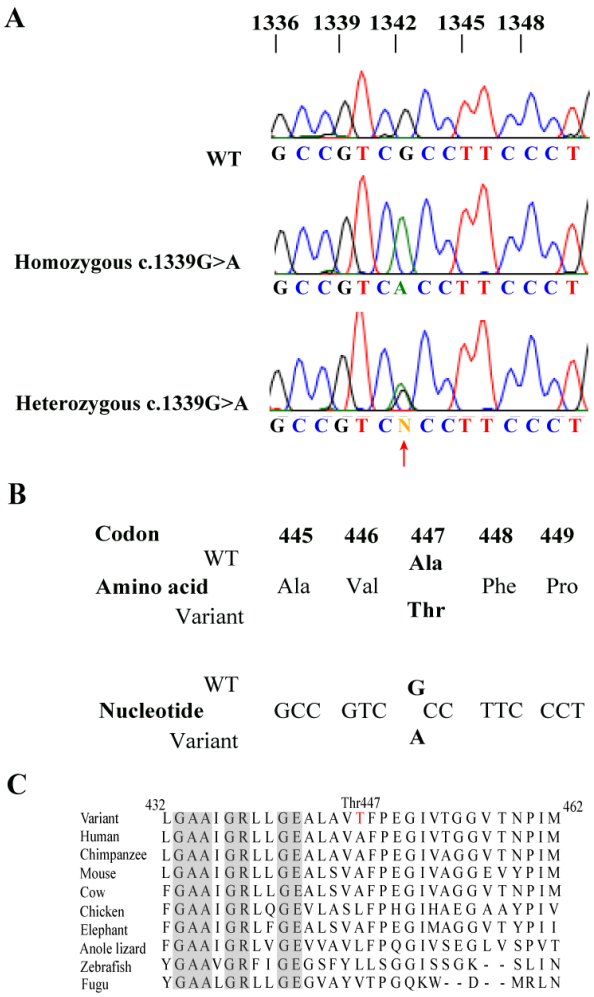
frequencies showed there was no significant difference between those observed in the DD cohort (AA: 33.33%, AG: 44.44% and GG: 22.23%) and those reported on ExAC (AA: 32.48%, AG: 47.29%, GG: 20.23%) (p=0.9655, chi-square test) (Table 20). *In silico* analysis of the vAFs also found no significant difference between the DD cohort (55.56%) and ExAC (56.12%) (p=0.9456,chi-square test) (Table 20). All three of the pathogenicity prediction programmes used predicted the Ala447Thr variant to be benign (Table 20). Evolutionary conservation analysis showed that the WT Ala447 residue was partially conserved due to its presence in four of the eight species studied (Figure 30 and Table 20). Thus the combined *in silico* analysis predicted the Ala447Thr variant to be benign.

7.2.2.1.6 Identification and *in silico* analysis a Thr454Ala variant in ClC-Ka in three probands

Similarly, to Arg83Gly and Ala447Thr, five other variants (Thr454Ala, Val457Ile, Arg534Trp, Pro683Leu and c.*126A>G) were identified as either heterozygous or homozygous in the same individuals (probands 9 and 17; and proband 12 respectively) (Table 20). An A-to-G transition at nucleotide 1360 was predicted to result in the substitution of a threonine with an alanine at codon 454 (Figure 31). *In silico* analysis of genotype frequencies showed a statistically significant (p≤0.05, chi-square test) difference between those observed in the DD cohort (GG:5.56% AG:11.11% GG:83.33%) and those reported on ExAC (GG:0.71%, AG14.14% and AA:85.15%) (Table 20). However, no significant difference (p=0.4556, chi-square test) was observed between the vAFs observed in the DD cohort (11.11%) and that reported on ExAC (7.78%) (Table 20). Additionally, the vAF is greater than <0.001%, all three pathogenicity prediction programmes predicted the Thr454Ala to be benign,

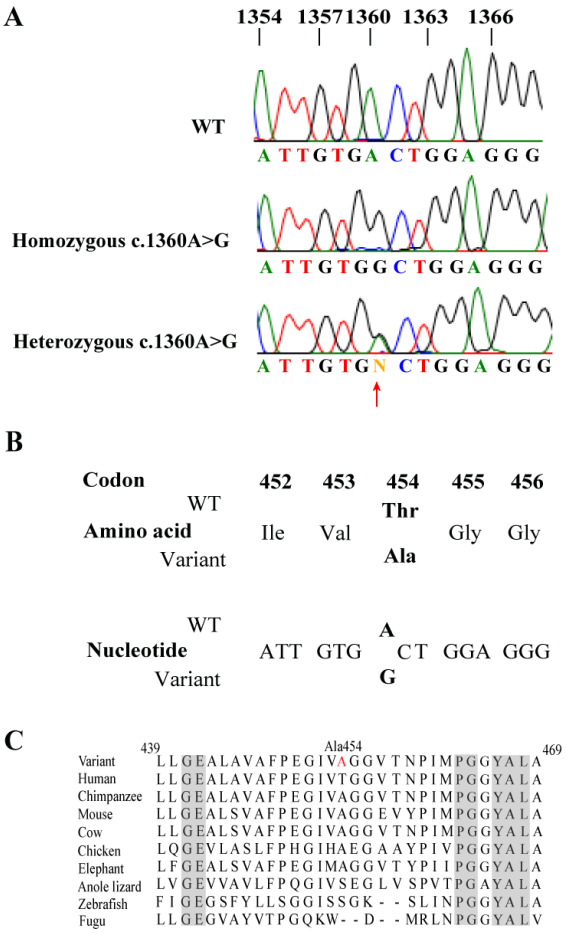
and evolutionary conservation analysis revealed that the the WT Thr454 residue was not conserved across any of the species studied (Figure 31 and Table 20). Conversely, the variant Ala454 residue was present in five species (Figure 31). Overall the combined *in silico* analysis predicted the Thr454Ala residue to be benign.

Figure 30. Identification of a Ala447Thr variant in ClC-Ka in 14 probands



A homozygous and heterozygous G-to-A transition at nucleotide c.1339 was identified in 6 and 8 probands respectively. (B) This G-to-A transition (GCC to ACC) is predicted to result in a missense amino acid change from alanine (Ala) to threonine (Thr) at codon 447 within the transmembrane region of the ClC-Ka protein. (C) Multiple sequence alignment of residues surrounding the human Ala447 residue of the ClC-Ka protein sequence in 8 species. The Thr447 residue identified in DD patients is shown in red. Residues conserved across all of the orthologs studied are highlighted in grey, the Ala447 residue is partially conserved across the 8 species. Codon numbers are displayed for the human sequence.

Figure 31. Identification of a Thr454Ala variant in ClC-Ka in probands 9, 12 and 17



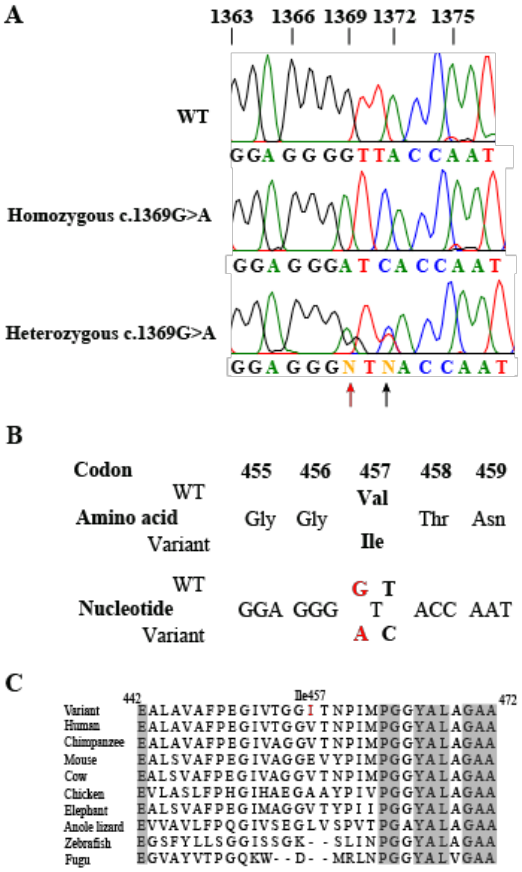
(A) A homozygous and heterozygous A-to-G transition at nucleotide c.1360 was identified in 1 and 2 in probands respectively. (B) This A-to-G transition (ACT to GCT) is predicted to result in a missense amino acid change from threonine (Thr) to alanine (Ala) at codon 454 within a transmembrane domain of the ClC-Ka protein. (C) Multiple sequence alignment of residues surrounding the human Thr454 residue of the ClC-Ka protein sequence in 8 species. The Ala454 residue identified in DD patients is shown in red. Residues conserved across all of the orthologs studied residues are highlighted in grey, the Ala454 residue is not conserved across the 8 species. Codon numbers are displayed for the human sequence.

7.2.2.1.7 Identification and *in silico* analysis of a Val457Ile variant in ClC-Ka in three probands

A G-to-A transition at nucleotide 1369 predicted to result in the substitution of a valine for isoleucine at codon 457 was identified in probands 9 and 17 as a heterozygous variant and in proband 12 as a homozygous variant (Figure 32). The Val457Ile genotype frequencies and vAFs observed in the DD cohort were not

significantly different from those reported in ExAC (p=0.2898 and p=0.4491 respectively, chi-square test) (Table 20). Additionally, the Val457Ile variant was predicted to be benign by all of the online pathogenicity prediction tools; and the WT Val457 residue was found to be just partially conserved due to its presence in three of the eight species studied (Figure 32 and Table 20). Therefore, the combined *in silico* analysis predicted the Val457Ile variant to be benign.

Figure 32. Identification of a Val457Ile variant in ClC-Ka in probands 9, 12 and 17



(A) The red arrow indicates nonsynonymous homozygous and heterozygous G-to-A transitions at nucleotide c.1369 identified in one and two probands, respectively. The black arrow indicates synonymous homozygous and heterozygous T-to-C transitions at nucleotide c.1371 identified in one and two probands, respectively. (B) The nonsynonymous G-to-A transition (highlighted in red) (GTT to ATT) is predicted to result in a missense amino acid change from valine (Val) to isoleucine (Ile) at codon 457 within a transmembrane domain of the ClC-Ka protein. The synonymous T-to-C transition is highlighted in black. (C) Multiple sequence alignment of residues surrounding the human Val457 residue of the ClC-Ka protein sequence in eight species.The Ile457 residue identified in DD patients is shown in red. Residues conserved across all of the orthologs studied are highlighted in grey, the Val457

residue is partially conserved across the eight species. Codon numbers are displayed for the human sequence.

7.2.2.1.8 Identification and *in silico* analysis of an Arg534Trp variant in ClC-Ka in three probands

A C-to-T transition at nucleotide 1600, predicted to result in the substitution of an arginine for tryptophan at codon 534, was identified as a heterozygous in probands 9 and 17 and as a homozygous in proband 12 (Figure 33). The observed vAF and genotype frequencies for the Arg534Trp variant in the DD cohort were not significantly different to those reported in ExAC (p=0.4718 and p=0.0645 respectively, chi-square test) (Table 20). Furthermore, the vAF was higher than the <0.001% cut-off determined in Section 6.2.9.1, the functional effect of the Arg534Trp variant was predicted to be benign (Table 20), and evolutionary conservation analysis revealed the WT Arg534 residue was partially conserved (3/8 orthologs) (Figure 33 and Table 20). However, the variant Trp534 residue was also present in three of the species (Figure 33). Overall, the combined *in silico* analysis predicted the Arg534Trp variant to be benign.

7.2.2.1.9 Identification and *in silico* analysis of a Pro683Leu variant in ClC-Ka in three probands

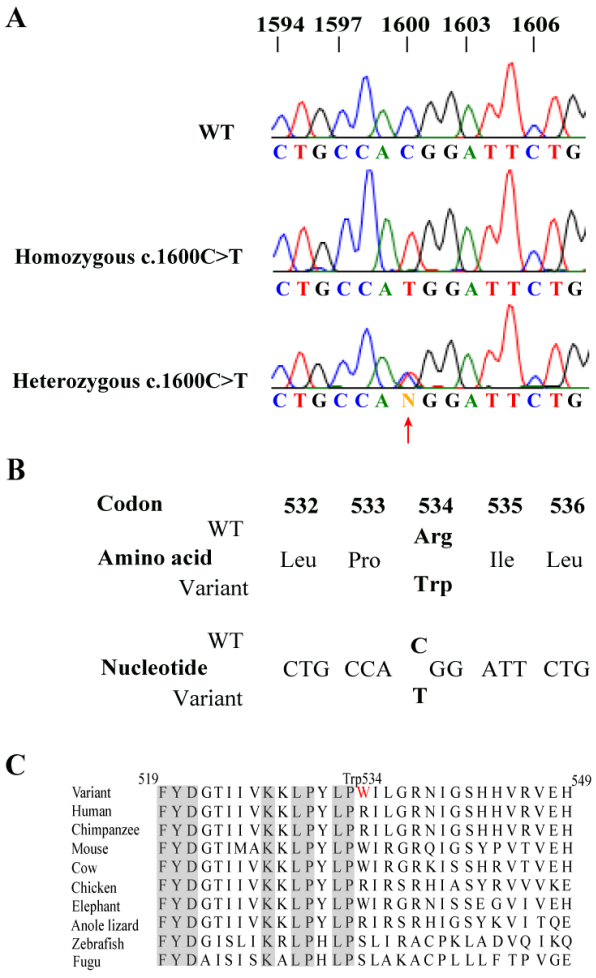
A C-to-T transition at nucleotide 2048 predicted to result in the substitution of a proline for leucine at codon 683 was identified in probands 9 and 17 as heterozygous and in proband 12 as homozygous (

Figure **34**). Similarly, to the results detailed in Section 7.2.2.1.6 for the Thr454Ala variant, whilst there was no significant difference between the vAF observed for the Pro683Leu variant in the DD cohort (11.11%) and that reported on ExAC (7.96%)

(p=0.4849, chi-square test); there was a significant difference (p≤0.05, chi-square test) in the genotype frequencies observed in the DD cohort compared to those reported on ExAC (Table 20). However, the vAF reported on ExAC is higher than the cut-off determined in Section 6.2.9.1. The Pro683Leu variant was predicted to be of unknown significance and evolutionary conservation analysis revealed the WT Pro683 residue was partially conserved due to its presence in five of the eight species studied (

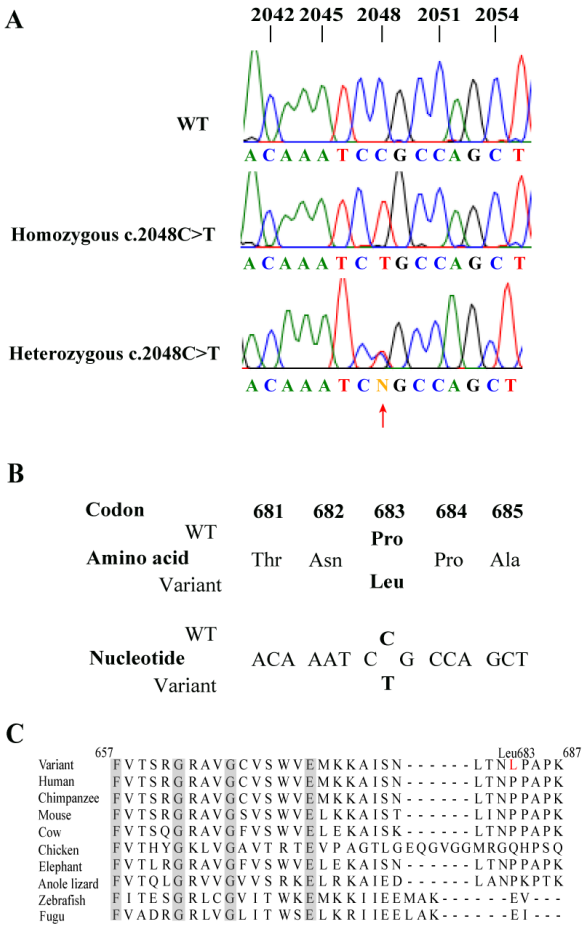
Figure **34** and Table 20). Thus, the combined *in silico* analysis predicted the Pro683Leu variant to be likely benign.

Figure 33. Identification of an Arg534Trp variant in ClC-Ka in probands 9, 12 and 17



(A) A homozygous and heterozygous C-to-T transition at nucleotide c.1600 was identified in one and two probands respectively. (B) This C-to-T transition (CGG to TGG) is predicted to result in a missense amino acid change from arginine (Arg) to tryptophan (Trp) at codon 534 within the cytoplasmic domain of the ClC-Ka protein. (C) Multiple sequence alignment of residues surrounding the human Arg534 residue of the ClC-Ka protein sequence in eight species. The Trp534 residue identified in DD patients is shown in red. Residues conserved across all of the orthologs studied are highlighted in grey, the Arg534 residue is partially conserved across the eight species. Codon numbers are displayed for the human sequence.

Figure 34. Identification of a Pro683Leu variant in ClC-Ka in probands 9, 12 and 17

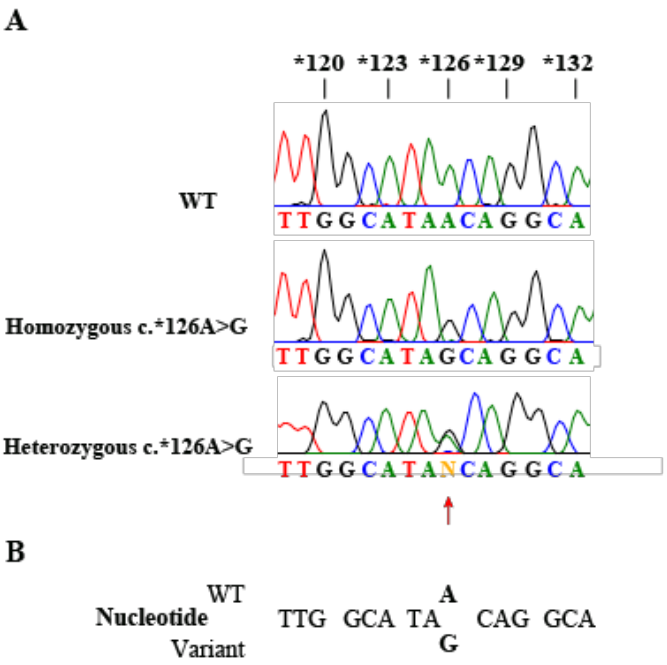


(A) A homozygous and heterozygous C-to-T transition at nucleotide c.2048 was identified in one and two probands respectively. (B) This C-to-T transition (CCG to CTG) is predicted to result in a missense amino acid change from proline (Pro) to leucine (Leu) at codon 683 within CBS domain 2 of the cytoplasmic domain of the ClC-Ka protein. (C) Multiple sequence alignment of residues surrounding the human Pro683 residue of the ClC-Ka protein sequence in eight species. The Leu683 residue identified in DD patients is shown in red. Residues conserved across all of the orthologs studied are highlighted in grey, the Pro683 residue is partially conserved across the eight species. Codon numbers are displayed for the human sequence.

7.2.2.1.10 Identification and *in silico* analysis of a c.*126A>G variant in *CLCNKA* in three probands

The c.*126A>G variant, due to an A-to-G transition 126 nucleotides past the stop codon, is non-coding and therefore does not affect the amino acid sequence (Figure 35). Identified in probands 9 and 17 as a heterozygous variant and in proband 12 as a homozygous variant, the genotype frequencies observed in the DD cohort were found to be significantly different to those reported on ExAC (Table 20) ($p \leq 0.005$, chi-square test). Conversely, there was no significant difference between the vAF observed in the DD cohort (11.11%) and the vAF reported on ExAC (5.73%) ($p = 0.1648$, chi-square test) (Table 20); and the vAF is higher than the <0.001% cut-off optimised in Section 6.2.9.1. MutationTaster was the only programme of the three (PolyPhen2, Provean Protein and MutationTaster) that is able to predict the functional effect of non-coding variants and predicted the c.*126A>G variant to be a polymorphism (Table 20). Thus, combined *in silico* analysis using the data available predicted the c.*126A>G variant to be benign (Table 20).

Figure 35. Identification of a c.*126A>G variant in *CLCNKA* in probands 9, 12 and 17

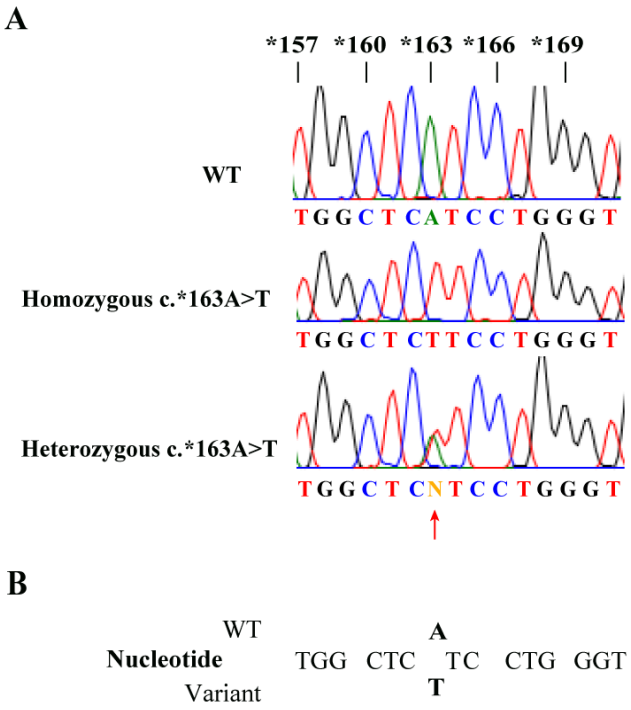


(A) A homozygous and heterozygous A-to-G transition at nucleotide c.*126 was identified in one and two probands respectively. (B) This A-to-G transition is a 3'UTR variant and therefore predicted not to result in an amino acid change.

7.2.2.1.11 Identification and *in silico* analysis of a c.*163A>T variant in *CLCNKA* in 13 probands

A second 3'UTR variant, an A-to-T transversion 163 nucleotides past the stop codon, was identified in 13/18 (72.22%) probands as either a heterozygous (ten probands: 4, 6, 7, 9-11, 13-15 and 17) or homozygous (three probands: 1, 2 and 8) variant (Figure 36 and Table 20). *In silico* analysis revealed no significant difference in the genotype frequencies observed in the DD cohort (AA:27.77%, AT:55.56%, TT:16.67%) and those reported in 1000 Genomes (AA:18.73%, AT:44.69%, TT:36.58%) (p=0.1991, chi-square test) or in the vAF observed in the DD cohort (44.44%) and that reported in 1000 Genomes (58.9%) (p=0.0779, chi-square test) (Table 20). MutationTaster predicted this variant to be a polymorphism (Table 20); and as with the c.*126A>G variant, evolutionary conservation analysis was not performed as the c.*163A>T variant is non-coding and therefore does not affect the amino acid sequence. Thus, combined *in silico* analysis predicted the c.*163A>T variant to be benign.

Figure 36. Identification of a c.*163A>T variant in *CLCNKA* in 13 probands



(A) A homozygous and heterozygous A-to-T transversion at nucleotide c.*163 was identified in three and 10 probands respectively, within the DD cohort (N=18). (B) This A-to-T transversion is a 3'UTR variant and therefore predicted not to result in an amino acid change.

7.2.2.1.12 *In silico* analysis of the effect of c.*126A>G and c.*163A>T on miRNA target sites

Located within the 3'UTR of genes are conserved miRNA recognition and binding sites, variations within which have been shown to be associated with disease risk and changes in gene expression[248,249]. Therefore, *in silico* analysis of the two 3'UTR variants (c.*126A>G and c.*163A>T) included analysing the predicted gain and/or loss of potential miRNA target sites, using four platforms: miRDB[250,251], PolymiRTS[252], TargetScan[253] and microSNiPer[254] (Table 21), as detailed in Section 5.4.5.4.

Table 21. Predicted impact of *CLCNKA* 3'UTR variants, identified in DD patients, on miRNA target sites

Variant	miRNAs predicted to lose target sites	miRNAs predicted to gain target sites
c.*126A>G	hsa-miR-214-5p hsa-miR-4633-5p hsa-miR-6811-3p	hsa-miR-31-3p
c.*163A>T	hsa-miR-1255a hsa-miR-1255b-5p hsa-miR-6807-5p	hsa-miR-6077

Nucleotide number is according to transcript ENST00000331433.4. Four platforms were used to analyse putative miRNA target sites in the WT and variant sequences: miRDB[250,251], PolymiRTS[252], TargetScan[253] and microSNiPer[254]. Predictions of a loss of a miRNA target site were made based on the prediction of a miRNA target site in the WT sequence by ≥2 platforms and a lack of prediction of this site in the variant sequence by all platforms. Predictions of a gain of a miRNA target site were made based on the prediction of a miRNA target site in the variant sequence by ≥2 platforms and a lack of prediction of this site in the WT sequence by all platforms.

In silico miRNA target site analysis of the c.*126A>G variant revealed it was predicted to result in the potential loss of three (hsa-miR-214-5p, hsa-miR-4633-5p and hsa-miR-6811-3p) and gain of one (hsa-miR-31-3p) miRNA target sites (Table 21). There have been a number of reports regarding the potential functional roles of miR-214-5p and miR-31-3p. Whilst there are no reports regarding the role of either of these miRNAs in DD or with *CLCNKA*, both miRNAs have been linked to a range of different genes, processes and disorders including *HNF1B* and type 2 diabetes mellitus[286], angiogenesis[287] and most frequently, cancer biology[288-290].

miR-31-3p is predominantly linked to various tumours and tumour processes and has been suggested as being one of the most frequency altered miRNAs in human cancers[290]. As DD is not a disorder associated with an increased risk of tumour development, miR-31-3p is unlikely to be of functional significance in relation to DD. Additionally, whilst reduced expression of miR-31 has been reported in a mouse model of PKD[291], indicating a role for miR-31 in the kidneys; cyst formation is not a

feature of DD[98,101-103,292,293], further suggesting miR-31 is unlikely to be functionally relevant in DD. In contrast, whilst miR-214 has also been associated with cancer, specifically ovarian carcinomas[294], miR-214 has more commonly been shown to be up-regulated in models of renal disease, including models of mesangial proliferative glomerulonephritis (MPGN), unilateral ureteral obstruction (UUO) and spontaneously hypertensive stroke prone rat (SHRSP)[295-297]. However, little is known about the precise role of miR-214 within this context, with most data associating the changes in miR-214 expression with regulation by transforming growth factor beta (TGF-ß)[295]. Furthermore, miR-214 expression in SHRSP rats was increased under salt loading[295]. These findings, suggest that whilst miR-214 may play a role in the kidneys and renal disease, most data suggests the reported changes in miR-214 expression are secondary to changes in TGF-ß and hypertension[295]; neither of which have reported associations with DD. The roles of miR-4633-5p and miR6811-3p have not been determined in detail in the literature and therefore their significance in the context of DD is unknown. Thus, the functional significance of these findings in regards to the potential pathogenicity of the c.*126A>G variant in DD is uncertain.

In silico miRNA target site analysis of the c.*163A>T variant revealed the potential loss of three (hsa-miR-1255a, hsa-miR-1255b-5p and hsa-miR-6807-5p) and gain of one (hsa-miR-6077) miRNA target sites (Table 21). Unfortunately, little is known about the miRNAs highlighted in this analysis, therefore the significance of these findings are uncertain in regards to the potential pathogenicity of this variant in DD.

Secondary confirmation and co-segregation analysis was not performed for any of the 11 common variants due to the relatively high vAFs (>2%) reported in control

populations such as ExAC and 1000 Genomes database (Table 20) compared to the approximate prevalence of DD (approximately 250 families reported worldwide[98]) and the 0.001% cut-off suggested in Section 6.2.9.1. Furthermore, no family history, and in most cases, no DNA samples from additional family members were available to aid co-segregation studies.

7.2.2.2 Identification and in silico analysis of rare variants in CLCNKA in patients with DD

Two rare variants were identified by Sanger DNA sequencing: Phe285del and Thr562Met (Figure 25 and Table 22). *In silico* analysis was performed for each of the rare variants, as described in Section 6.2.9.4 and included population genomics (ExAC), prediction of functional effects using three online tools (PolyPhen-2, MutationTaster and Provean Protein) and evolutionary conservation (Table 22).

Table 22. *In silico* analysis of *CLCNKA* rare nonsynonymous coding variants identified in DD patients

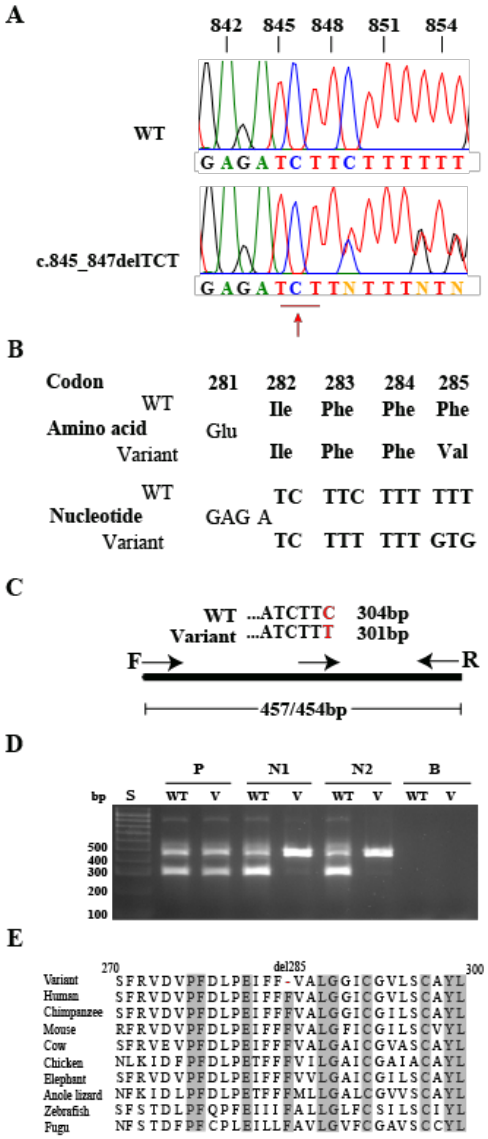
Nucleotide Change	Amino Acid Change	Patient cohort: Individuals with the variant	Patient cohort: vAF	Patient cohort: genotype frequencies	^Reported vAF	^Reported genotype frequencies	PolyPhen-2	MutationTaster	Provean Protein	Evolutionary conservation	Combined *in silico* prediction
c.845_847delTCT	p.Phe285del	1/18 (5.56%)	2.78% (del)	Heterozygotes (TCTdel): 1 (5.56%) Homozygotes (deldel): 0 (0%)	0.0026% (del)	Heterozygotes (TCTdel): 0.005% Homozygotes (deldel): 0%	N/A	Disease causing	Deleterious (score: -8.229)	Conserved (8/8)	Likely pathogenic
c.1685C>T	*p.Thr562Met	1/18 (5.56%)	2.78% (T)	Heterozygotes (CT): 1 (5.56%) Homozygotes (TT): 0 (0%)	0.0083% (T)	Heterozygotes (CT): 0.017% Homozygotes (TT): 0%	Benign (score:0.032)	Polymorphism	Neutral (score: -0.606)	Partially conserved (3/8)	Benign

Rare variants are those with a ^reported vAF <1%. ^Reported vAFs and genotype frequencies on ExAC. Eight orthologous protein sequences were used to assess the degree of evolutionary conservation of the affected amino acid residue: human, chimpanzee, mouse, cow, chicken, elephant, anole lizard, zebrafish and fugu. A prediction of pathogenicity was made using a combined *in silico* analysis approach as described in Section 6.2.9.4, using the data generated from population genomics, prediction of functional effects and conservation analysis where possible. *Indicates a possible major amino acid change e.g. substitution of a hydrophilic for a hydrophobic amino acid. N/A, not applicable.

7.2.2.2.1 Identification and *in silico* analysis of a Phe285del variant in ClC-Ka in proband 2

A heterozygous deletion of three nucleotides (TCT) from nucleotide 845 to 847, identified in proband 2, was predicted to result in the in-frame deletion of a phenylalanine at codon 285 and a shorter 686 amino acid protein (Figure 37). This in-frame deletion is not predicted to result in the gain or loss of a RE recognition site, and ARMS PCR was therefore used to confirm the presence of this variant in the proband and absence in two unaffected controls (Figure 37). *In silico* analysis of the Phe285del genotype frequencies showed a significant difference ($p \leq 0.0001$, chi-square test) between those observed in the DD cohort and those reported on ExAC (Table 22). Additionally, whilst the vAF of the del285 variant reported on ExAC (0.0026%) was significantly lower than that observed in the DD cohort (2.78%) ($p \leq 0.0001$, chi-square test), it was higher than the <0.001% cut-off optimised in Section 6.2.9.1 (Table 22). To predict the functional effect of the Phe285del variant two of the three tools were used; PolyPhen-2 was not used to analyse this variant as it is only able to analyse amino acid substitutions and not indels. MutationTaster and Provean Protein both predicted the Phe285del variant to be probably damaging (Table 22). Evolutionary conservation analysis revealed the WT Phe285 residue was fully conserved across all of the eight species studied and was the only variant identified to be so (Figure 37 and Table 22). Thus, the combined *in silico* analysis predicted the Phe285del variant to be likely pathogenic.

Figure 37. Identification of a Phe285del variant in ClC-Ka, in proband 2

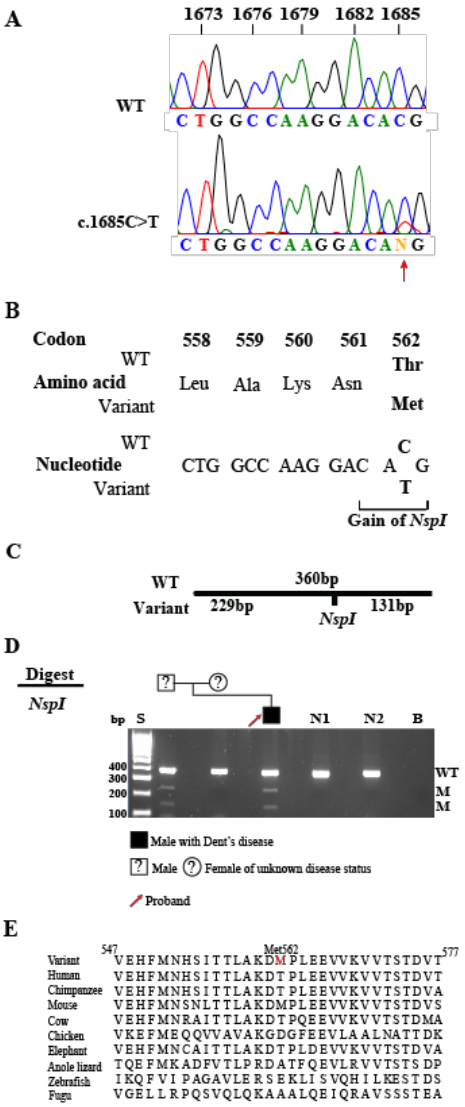


(A) A heterozygous TCT deletion from nucleotide c.845 to c.847 was identified in one proband. (B) This TCT deletion is predicted to result in the in-frame deletion of a phenylalanine (Phe) at codon 285 within a transmembrane domain of the ClC-Ka protein, which is predicted to result in a 686 amino acid protein instead of the full-length 687 amino acid protein. (C) ARMS PCR map showing the last 6 base pairs (bp) of the WT and variant 5' (F) ARMS primers that would result in two products of 457bp and 304bp for the WT and two products of 454bp and 301bp for the variant. The nucleotide highlighted in red is the terminal nucleotide for the primers and corresponds to the first nucleotide affected by the TCT deletion. Each ARMS reaction is specific for the WT or variant sequences, if the highlighted nucleotide differs from the sample sequence only one product of 457bp (or 454bp) will result. (D) ARMS PCR of *CLCNKA* exons 9-10 demonstrating the heterozygous TCT deletion in the proband (P) by the presence of two bands in both the WT and variant (V) reactions; and the lack of the TCT deletion in the two normal controls (N1 and N2) shown by the presence of two bands in the WT reaction and one in the V reaction. S= size marker, B= water blank. (E) Multiple sequence alignment of residues surrounding the human Phe285 residue of the ClC-Ka protein sequence in eight species. The del285 residue identified in a DD patient is shown in red. Residues conserved across all of the orthologs studied are highlighted in grey, the Phe285 residue is fully conserved across the eight species. Codon numbers are displayed for the human sequence.

7.2.2.2.2 Identification and *in silico* analysis of a Thr562Met variant in ClC-Ka in proband 4

A C-to-T transition at nucleotide 1685 predicted to result in the substitution of a threonine for a methionine at codon 562 was identified in proband 4 (Figure 38). This substitution was also predicted to result in the gain of a *NspI* RE recognition site and therefore restriction digest was used as the secondary method to confirm the variant in the proband; and for co-segregation analysis which revealed the presence of the Met562 variant in the father and its absence in two unaffected controls and the mother (Figure 38). However, clinical details for the parents were unavailable. Similarly, to the Phe285del variant, *in silico* analysis of the Thr562Met variant revealed significantly different ($p \leq 0.0001$, chi-square test) genotype frequencies for this variant between the DD cohort and ExAC (Table 22). Furthermore, the vAF observed in the DD cohort (2.78%) was significantly different to that reported on ExAC (0.0083%) ($p \leq 0.0001$, chi-square test) (Table 22). Similarly to the Phe285del variant, the vAF of the Thr562Met variant is higher than the <0.001% cut-off determined in Section 6.2.9.1. The predicted functional effect of the Thr562Met variant was probably benign, as predicted by all three of the pathogenicity prediction programmes (Table 22). Evolutionary conservation analysis revealed the WT Thr562 residue is only partially conserved across the eight species studied due to its presence in three of the eight species (Figure 38 and Table 22). Additionally, the Met562 variant residue was shown to be present in one of the species (mouse) (Figure 38). Thus, combined *in silico* analysis predicted the Thr562Met variant to be benign.

Figure 38. Identification of a Thr562Met variant in ClC-Ka in proband 4



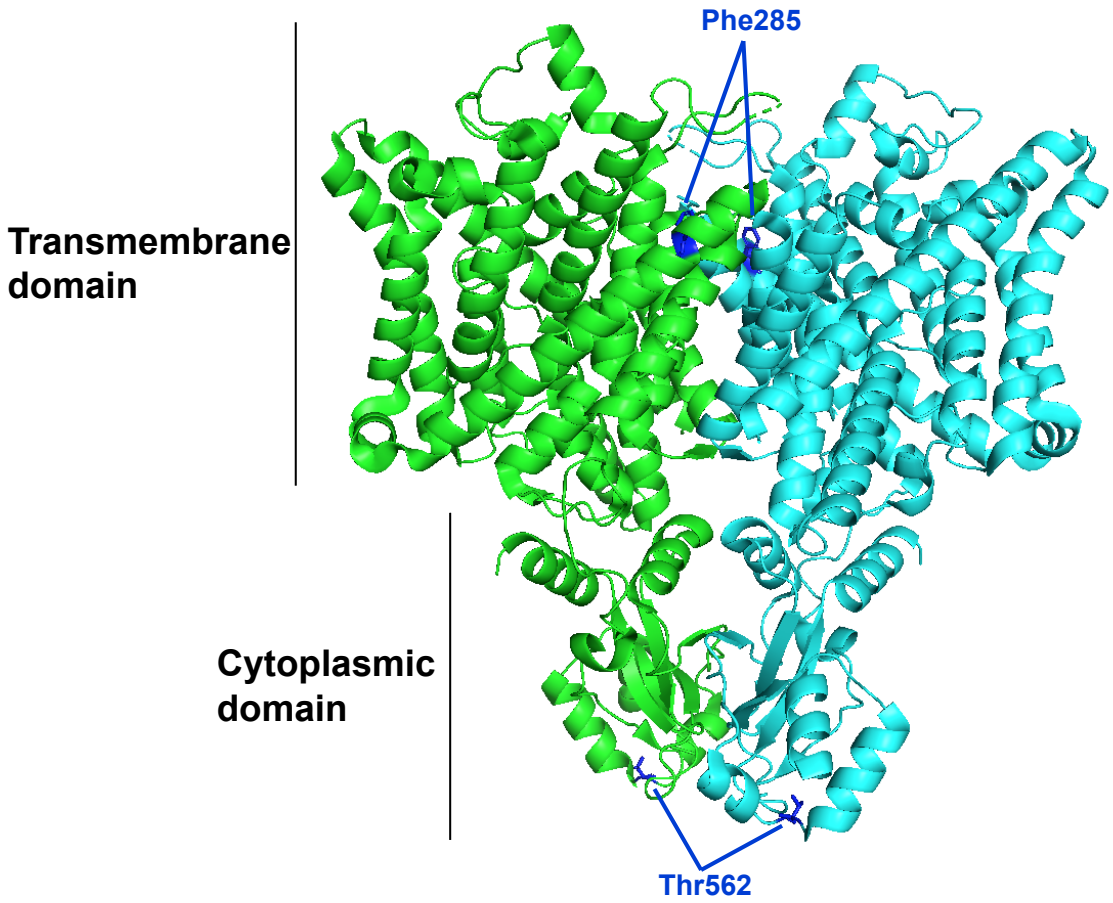
(A) A heterozygous C-to-T transition at nucleotide c.1685 was identified in 1 proband. (B) This C-to-T transition (ACG to ATG) is predicted to result in a missense amino acid change from threonine (Thr) to methionine (Met) at codon 562 within CBS domain 1 of the cytoplasmic domain of the ClC-Ka protein, which would also result in the gain of a *NspI* RE site. (C) Restriction map showing that *NspI* digestion would result in one product of 360bp for the WT and two products of 229bp and 131bp for the variant. (D) RED of *CLCNKA* exon 16 PCR products demonstrating the C-to-T transition in the proband and the father of the proband as well as the absence of the C-to-T transition in the mother and two normal controls (N1 and N2). S= size marker, B= water blank (E) Multiple sequence alignment of residues surrounding the human Thr562 residue of the ClC-Ka protein sequence in eight species. The Met562 residue identified in the DD patients is shown in red. The Thr562 residue is partially conserved across the eight species. Codon numbers are displayed for the human.

7.2.2.2.3 Structural analysis of the Phe285del and Thr562Met variants identified in ClC-Ka

Investigation of a protein's three-dimensional structure can provide insights into the interactions between amino acid residues within the protein and between proteins, which are important for a protein's structure, stability and function. Thus, the loss-or-gain of contacts between amino acid residues, as a result of mutation, may predict the impact of variants on the structure or stability of ClC-Ka. Three-dimensional modelling to determine the location of the two rare variants, Phe285del and Thr562Met, was performed using the previously described bovine ClC-K crystal structure (PDB ID:5TQQ)[258] (Figure 39). The bovine ClC-K shares 84% amino acid sequence identity with the human ClC-K channel orthologs (ClC-Ka and ClC-Kb) and, like ClC-Ka and Kb, it also requires barttin for cell surface expression and Cl- transport activity[258], therefore making it a good structure to model the two human variants. Furthermore, whilst a human ClC-K crystal structure exists it only consists of the cytoplasmic domain and therefore cannot be used to look at the overall location of the two variants or to model the Phe285del variant, which is located in the transmembrane domain.

Structural analyses confirmed the WT Phe285 is located within the transmembrane domain and within an alpha-helix close to the binding interface of the homodimer (Figure 39); and the WT Thr562 residue is located within the cytoplasmic domain, further away from the dimer interface (Figure 39).

Figure 39. Structural characterisation displaying the location of rare ClC-Ka variants in the bovine ClC-K homodimer

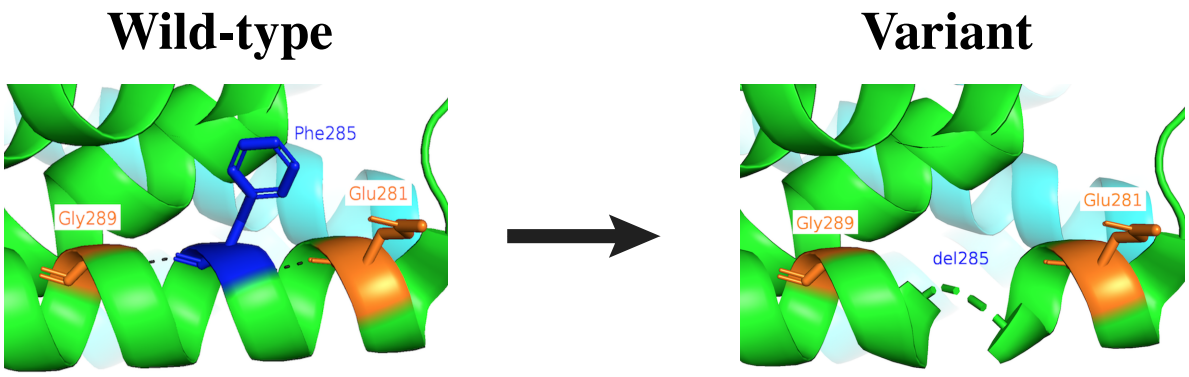


Overview of the position of WT residues affected by rare variants, Phe284del and Thr562Met, located in the transmembrane and cytoplasmic domains of ClC-Ka respectively, using the bovine ClC-K crystal structure (PDB ID:5TQQ)[258]. The WT Phe285 and Thr562 residues are highlighted in blue in both of the bovine ClC-K subunits (green and cyan).

The impact of the Phe285del variant on the tertiary structure of ClC-Ka was also analysed using the bovine ClC-K homodimer structure (PDB ID:5TQQ). Three-dimensional modelling indicated that the WT Phe285 residue is situated within an alpha-helix and; whilst it is predicted to form contacts with two neighbouring residues (Gly289 and Glu281) within the same subunit, it is not predicted to form contacts between the two subunits (Figure 40). However, deletion of the Phe285 residue is predicted to disrupt these polar contacts and may lead to the loss of part of

the alpha-helix (Figure 40). Thus, it is suggested this variant may have an impact on the structure of the protein and as a result may also impact dimerisation.

Figure 40. Structural characterisation of the Phe285del ClC-Ka variant in the bovine ClC-K

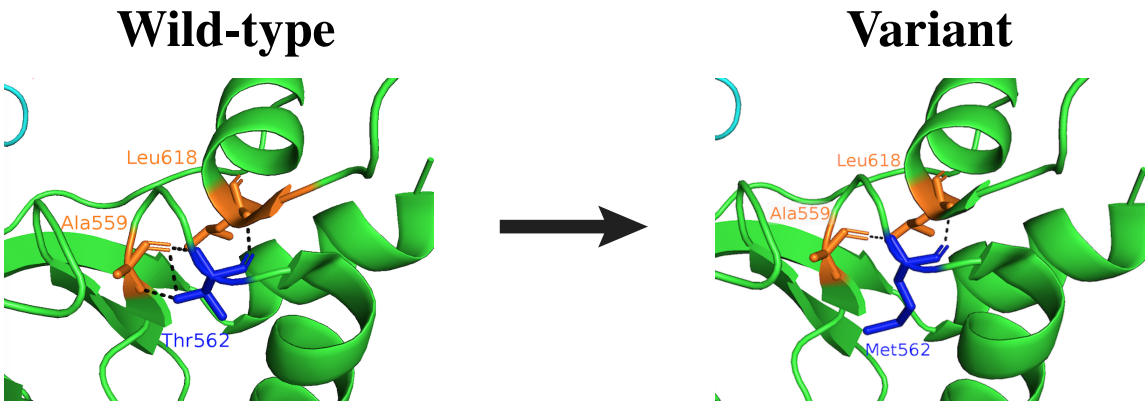


Structural characterisation of the rare Phe285del variant, located in the transmembrane domain of ClC-Ka, using the bovine ClC-K crystal structure (PDB ID:5TQQ)[258]. The WT Phe285 residue (blue), located within an alpha helix, is predicted to form polar contacts with two neighbouring residues (Gly289 and Glu281, both highlighted in orange) also located within the same alpha-helix. Deletion of this residue (del285), is predicted to disrupt the predicted contacts with Gly289 and Glu281 and is also predicted to result in the loss of part of the alpha-helix. Polar contacts are displayed using black dashed lines. Deletion of the Phe285 residue is displayed using a green dashed line.

The three-dimensional crystal structure of the cytoplasmic domain of the human chloride channel ClC-Ka (PDB ID:2PFI)[259] was used to study the Thr562Met variant, instead of the bovine model previously used, to provide the most accurate prediction of the impact of this variant on the tertiary structure of ClC-Ka. As with the Phe285 residue, the WT Thr562 residue is also not predicted to form contacts between the two ClC-Ka subunits; and instead forms polar contacts with two neighbouring residues (Ala559 and Leu618) within the same subunit (Figure 41). Substitution of this residue for the variant Met562 residue is not predicted to affect the contact formed with Leu618; however, it is predicted to disrupt formation of two of the three

polar contacts formed with Ala559 (Figure 41). Therefore, this variant may have in impact on the tertiary structure of the ClC-Ka protein.

Figure 41. Structural characterisation of the Thr562Met ClC-Ka variant in the human ClC-Ka cytoplasmic domain

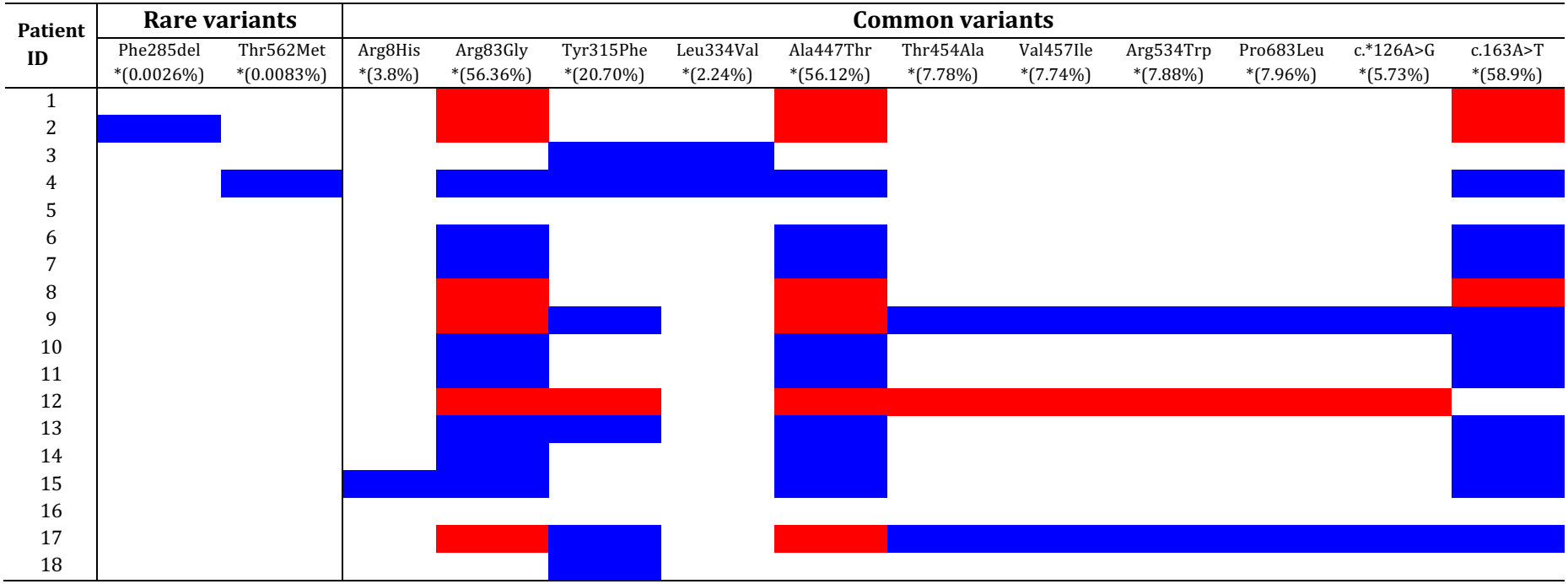


Structural characterisation of the rare Thr562Met variant, using the human ClC-Ka cytoplasmic domain crystal structure (PDB ID:2PFI)[259]. The WT Thr562 residue (blue), is predicted to form polar contacts with two neighbouring residues (Ala559 and Leu618, both highlighted in orange). Substitution of this residue to a methionine (Met562) is predicted to disrupt the two of the three predicted contacts with Ala559 and to not disrupt the contact formed with Leu618. Polar contacts are displayed using black dashed lines.

7.2.3 Analysis of compound heterozygosity in *CLCNKA* in patients with DD

Whilst the heterozygous Phe285del variant was predicted to be likely pathogenic by the combined *in silico* analysis, neither of the rare variants were identified as homozygous. Furthermore, none of the 13 variants were present only as homozygous variants within the cohort. As the *CLCNKA* variant originally identified by Prof Friedhelm Hildebrandt and Dr Dervla Connaughton, Boston Children's Hospital, Harvard Medical School, was a homozygous variant it was hypothesised that homozygous or compound heterozygous variants in *CLCNKA* may cause DD. To investigate this, the common and rare variants identified in each patient, were plotted on a graph as displayed in Figure 42.

Figure 42. Representation of the combination of rare and common nonsynonymous and 3'UTR variants identified in *CLCNKA* in 18 patients with DD



*Reported vAFs as reported on ExAC[298] or the 1000 Genomes browser[238]. Homozygote variants are highlighted in red and heterozygote variants are highlighted in blue.

Compound heterozygosity was immediately excluded in: proband 1 as all three variants identified (Arg83Gly, Ala447Thr and c.*163A>T) in this proband were homozygous (Figure 42); proband 5 as no variants were identified in this proband (Figure 42); and proband 18 as just one heterozygous variant (Tyr315Phe) was identified in this proband (Figure 42). Additionally, despite the most promising candidate from the *in silico* analysis (Phe285del) being identified in proband 2, compound heterozygote analysis revealed this proband carried no other heterozygote variants (Figure 42), thus excluding the possibility of compound heterozygosity in proband 2. Conversely, proband 4, in which the Thr562Met variant was identified, was found to carry five other heterozygote variants (Arg83Gly, Tyr315Phe, Leu334Val, Ala447Thr and c.*126A>T) (Figure 42), making compound heterozygosity a possibility in this proband. However, most of these five variants had reported vAFs ≥20% on ExAC or 1000 Genomes, with the exception being Leu334Val (2.24%) (Table 20). Although it should be noted that Leu334Val, like Thr562Met, was also predicted to be benign by the combined *in silico* analysis (Table 20) and the reported vAF (2.24%) is greater than the 0.001% cut-off determined by Section 6.2.9.1 and the estimated prevalence of DD[98], thus suggesting that compound heterozygosity is not likely in proband 4. The Leu334Val variant was also identified in proband 3 as a heterozygote (Figure 42). This proband was found to carry only one other variant, Tyr315Phe, which had a reported vAF of 20.70%, and was predicted benign by combined *in silico* analysis and was identified as a heterozygous variant in a further five probands (4, 9 13, 17 and 18) (Figure 42) (Table 20). The relatively high vAFs and benign combined *in silico* prediction suggest compound heterozygosity is also unlikely to cause DD in proband 3. Most of the other probands (6, 7, 9-11, 13-15 and 17) were found to carry multiple common variants (Figure 42), which were

reported to be frequently observed in population databases (vAFs >2% in ExAC or 1000 Genomes) and were predicted to be benign or likely benign by the combined *in silico* analysis (Table 20). Thus, similarly to proband 3 and 4, whilst possible, compound heterozygosity is unlikely in probands 6, 7, 9-11, 13-15 and 17.

7.3. Discussion

It is estimated that approximately 25-35% of DD patients lack mutations in *CLCN5* and *OCRL1*, suggesting a role for an additional gene(s) in DD[98]. Although previous attempts to identify such genes (e.g *CLCN4*, *CFL1*, *TMEM27* and *SCL9A6*) have not been successful[100,122-124]; recently a homozygous variant in *CLCNKA* in a patient with DD, lacking mutations in *CLCN5* or *OCRL1*, was identified by WES. As compound heterozygote or homozygote mutations in *CLCNKA* and *CLCNKB* together are associated with Bartter syndrome type 4b[134,271]; it was hypothesised that homozygous variants in *CLCNKA* alone may be associated with DD.

Sanger DNA sequencing of an additional 18 probands with DD, previously screened for mutations in *CLCN5* and *OCRL1*, identified 13 nonsynonymous exonic or 3'UTR variants. As DD is a rare disorder with an estimated 250 families reported worldwide[98], reported vAFs were used to classify variants into two distinct categories: rare variants, with a reported vAF <1%, and common variants, with a reported vAF oF ≥1%, on population databases ExAC and 1000 Genomes. Of the 13 variants, 2 were classified as rare and 11 as common. Combined *in silico* analysis, comprising of population genomics, prediction of functional effects, and where applicable evolutionary conservation predicted all of the common variants to be benign (Arg8His, Arg83Gly, Tyr315Phe, Leu334Val, Ala447Thr, Thr454Ala, Val457Ile,

Arg534Trp, c.*126A>G and c.*163A>T) or likely benign (Pro683Leu). However, two of the common variants, Arg83Gly and Ala447Thr, are listed on HGMD suggesting they may be pathogenic[299-301].

The Ala447Thr variant is listed on HGMD due to a reported association with an increase in mean blood pressure in response to Na-load in a cohort of patients with essential hypertension[300]. However, hypertension is not known to be associated with DD, further suggesting the Ala447Thr variant may be unlikely to be involved in the pathogenesis of DD. Arg83Gly is present on HGMD and is reported to be associated with heart failure and estimated glomerular filtration rate (eGFR)[299,300]. The Gly83 variant has been associated with an increased risk of heart failure, independent of age, sex and prior hypertension in Caucasian populations (odds ratio= 1.27)[299]; which may be a result of reduced chloride currents detected by whole cell patch clamp recordings in cells expressing the Gly83 variant ClC-Ka compared to those expressing the WT ClC-Ka[299]. However, heart failure is not known to be characteristic of DD, suggesting that Arg83Gly may also be unlikely to be involved in the pathogenesis of DD. Additionally, the homozygous copies of the Gly83 variant have been associated with a reduced eGFR (RENASTUR cohort of 569 Caucasian individuals, aged 55-85, 42% male, from the region of Asturias in Northern Spain)[301], thereby indicating a role in renal disease. Taken together these findings suggest that whilst the homozygous Arg83Gly variant may play a role in the kidneys and its disease, it is unlikely to cause DD in this cohort, which is consistent with the *in silico* analysis.

miRNA target site analysis was also performed for the two non-coding variants: c.*126A>G and c.*163A>T, to investigate whether the loss of gain of miRNA target sites in *CLCNKA* may cause DD. miRNA target sites are located within the 3'UTR of genes and have been shown to be associated with a range of different diseases and changes in gene expression[248,249]. Furthermore, disrupted miRNA biogenesis, due to inactivation of Dicer, has been shown to be associated with glomerular function[302,303], thus implicating miRNAs in renal disease. miRNA target site analysis of the two 3'UTR variants, c.*126A>G and c.*163A>T predicted a gain of a single miRNA target site (miR-31-3p and miR-6077 respectively) and loss of three miRNA target sites (miR-214-5p, miR-4633-5p and miR-6811-3p; and miR-1255a, miR-1255b-5p and miR-6807-5p respectively) in each variant. However, none of the miRNAs identified in this study had been previously associated with DD or *CLCNKA*. Furthermore, for the majority of the miRNAs very little is known in regards to their reported function. Thus, it is uncertain whether these findings are of any significance in regards to the pathogenicity of DD in these patients. Conversely, changes in the expression of miR-31 and miR-214 have been associated with both cancer biology[290,294] and models of renal disease including PKD (miR-31)[291], MPGN[295-297], UUO[295-297] and SHRSP[295-297]. Whilst these findings suggest a role for these miRNAs in the kidneys and renal disease, most of the data pertaining to the changes in miR-31 and miR-214 expression in these disorders are associated with changes in TGFß expression[291,295], thus suggesting that in some cases the reported changes in miR-31 and miR-214 expression may be secondary to other factors[295]. Furthermore, the characteristics associated with PKD, MPGN, UUO and SHRSP are not known to be associated with patients with DD, suggesting miR-31 and miR-214 are unlikely to be functionally relevant in DD[98]. Therefore, the results of the *in silico* analysis of the common variants, particularly the

relatively high reported vAFs (ExAC and 1000 Genomes) compared to the rarity of the disorder, suggested that none of the common variants play a role in the aetiology of DD.

In silico analysis comprised of population genomics, prediction of functional effects and evolutionary conservation analysis using the criteria determined in Section 6.2.9.4. Interestingly, *in silico* analysis revealed that the frequency of heterozygotes and the vAFs observed for both Phe285del and Thr562Met in the DD cohort were significantly higher than those reported on ExAC; which would suggest pathogenicity using the criteria outlined in the ACMG 2015 report[237]. However, the ACMG report also suggests that variants with vAFs greater than the estimated frequency of the disorder are unlikely to be pathogenic[237]. The reported vAFs of 0.0026% and 0.0083% for Phe285del and Thr562Met, respectively are likely to be greater than the possible incidence of DD based on the estimated number of reported families affected[98]; and are greater than the 0.001% cut-off determined in Section 6.2.9.1, thus suggesting that the variants are unlikely to be involved in the pathogenicity of DD. Whilst the prediction of functional effects and evolutionary conservation analysis performed for the Thr562Met variant was in agreement with these findings, resulting in a combined *in silico* prediction of benign; the converse was found for the Phe285del variant with both predicting the variant to be pathogenic. Therefore, the Phe285del variant was predicted to be likely pathogenic.

Whilst most *in silico* analysis was performed for all variants where appropriate, due to the rarity of the disorder, rare variants (Phe285del and Thr562Met) were additionally prioritised for confirmation by a secondary method (either ARMS PCR or

restriction digest), co-segregation analysis, and three-dimensional structural modelling. Confirmation and co-segregation analysis of the Phe285del and Thr562Met variants confirmed the presence of the variant in proband 2 and 4, respectively, and revealed the absence of variant in two unaffected controls, thus showing that both variants co-segregate with DD. Three-dimensional modelling revealed that whilst the Phe285del was predicted to have a larger impact on the ClC-Ka protein, both variants were likely to disrupt the polar contacts formed between the WT and neighboring residues, thereby suggesting that they may disrupt the tertiary structure of ClC-Ka and impact on its dimerisation.

It is important to note that the *CLCNKA* variant identified by WES was a homozygous variant, whilst both DD1 and DD2, due to mutations in *CLCN5* and *ORCL1* respectively, are X-linked disorders that predominantly affect males, who are hemizygous[98]. Female patients are often associated with a milder phenotype, although there are reports of some female patients with more severe manifestations such as nephrolithiasis and end-stage renal failure[98]. Therefore, it was predicted that homozygous or compound heterozygous variants in *CLCNKA* would be of greater interest for the aetiology of an autosomal form of DD and therefore for *in vitro* functional studies. However, neither of the rare variants identified in this study were homozygous variants and none of the 13 variants were present as only homozygous variants within the cohort. Moreover, compound heterozygosity was excluded in probands 1 (carrying three homozygous variants: Arg83Gly, Ala447Thr and c.*163AT>), 2 (carrying just one heterozygous variant: Phe285del), 5 (no *CLCNKA* variants identified) and 18 (carrying only one heterozygous variant: Tyr315Phe). Additionally, compound heterozygosity in *CLCNKA* was also shown to be an unlikely

cause of DD in the remaining probands, due to the high vAFs of many of the heterozygous variants compared to the estimated incidence of DD[98]. Consequently, whilst the *in silico* and co-segregation analysis suggest the Phe285del variant could be a promising candidate, initial functional studies would help to identify the pathogenic (if any) role of the homozygous *CLCNKA* variant identified by collaborators at Harvard.

Finally, as previously discussed in Chapter 6, *in silico* prediction tools can be misleading and whilst they provide a tool by which to prioritise candidate variants, they shouldn't be solely relied upon for pathogenicity determination. Therefore, *in vitro* functional studies are required to determine whether any of the candidate variants identified here may impact the function of the ClC-Ka protein and consequently play a role in the pathogenesis of DD. *CLCNKA* encodes the chloride voltage-gated channel Ka (ClC-Ka), that like CLC-5, belongs to the CLC family of chloride channels that are predominantly expressed in the kidney[304,305]. However, unlike ClC-5 which is expressed intracellularly, ClC-Ka has been reported to be expressed at both apical and basolateral membranes[304] and is responsible for mediating Cl^- reabsorption from the lumen[130,131]. As ClC-Ka has been shown to require the co-expression of barttin for proper function[131,306], future *in vitro* functional studies will need to be performed in cells co-expressing barttin and ClC-Ka. *In vitro* whole cell patch clamp analysis has commonly been performed to study the function of ClC-Ka, ClC-Kb (and their rat orthologs ClC-K1 and 2 respectively) and barttin[131,132,307,308]; therefore, similar analyses could be used in future studies to determine whether the variants affect the function of the ClC-Ka. Additionally, as ClC channels form homodimers and barttin is required for ClC-Ka and ClC-Kb

function[131,306,309,310], co-immunoprecipitation experiments could also be performed to determine if the ClC-Ka variant(s) affect its ability to interact with barttin and form homodimers. However, DD is characterised by proximal tubular dysfunction and ClC-Ka is predominantly expressed in the tAL[143,304,306], with just one study reporting expression of the rat homolog ClC-K1 in the S3 segment of the PT[273]. Therefore, further *in vitro* and *in vivo* studies to determine the effect, if any, the homozygous *CLCNKA* variant identified by collaborators has on ClC-Ka function, may also help to confirm a role for ClC-Ka in the PT or reveal mechanisms of segmental cross-talk in the renal tubules.

Based on the results discussed in this chapter, the original homozygous *CLCNKA* variant identified by WES by collaborators at Harvard should be prioritised for functional analysis to further determine whether this variant may play a role in the pathogenicity of DD. However, as mutations in *CLCNKA* in combination with mutations in *CLCNKB* are associated with Bartter syndrome type 4B[134,271]; and as there has been a report of a male DD patient with mutations in both *CLCN5* and *OCRL1*[311], it could be postulated that some of the heterozygous variants identified within this cohort may occur in combination with another variant in an additional gene. Therefore, sequencing of *CLCNKB* and other candidate genes, that may have been highlighted in the WES performed at Harvard, in these patients may be of future interest. Finally due to the high amino acid sequence homology (>90%) between ClC-Ka and ClC-Kb[273], sequencing of *CLCNKB* would also be required to minimise the effect and risk of potential chimera formation.

8 Investigation of candidate variants in patients with familial juvenile hyperuricaemic nephropathy (FJHN)

FJHN, which is principally due to TAL dysfunction, is a genetically heterogeneous disorder and is characterised by hyperuricaemia, reduced fractional uric acid clearance, gout and progressive renal insufficiency associated with interstitial fibrosis[140]. Four subtypes are identified to date: FJHN1 due to mutations in *UMOD*[140] which encodes the uromodulin protein; FJHN2 due to mutations in *REN*[146] which encodes renin; FJHN3 which has been mapped to chromosome 2p22.1-p21.2[147]; and an atypical form, characterised by renal cysts and diabetes associated with mutations in *HNF-1ß*[148], which encodes the transcription factor HNF-1*ß*. Mutations in *UMOD*, *REN* and *HNF-1ß* have been identified in approximately 45% of patients, with mutations in *UMOD* alone being identified in 40% of patients[147], indicating a role for additional gene(s) in the pathogenesis of FJHN. Therefore, this study aimed to identify novel candidate genes in FJHN. This chapter describes the search for candidate variants in patients with FJHN, lacking mutations in *UMOD*, *REN* and *HNF-1ß.*

8.1. Declaration of contributions

The work in this chapter is my own, unless otherwise stated. WGS was performed at the WTCHG, Oxford. Initial bioinformatic analysis of WGS data was performed by Dr Alistair Pagnamenta at the WTCHG, Oxford and Dr Sian Piret at the Academic Endocrine Unit, University of Oxford. Additional *in silico* analysis; primer design for Sanger DNA sequencing; preparation of DNA pellets for Sanger DNA sequencing; and segregation analysis was performed by Dr Sian Piret or me. Sanger DNA sequencing of prepared DNA pellets was performed at the Department of Zoology, University of Oxford. Ophthalmological examinations were co-ordinated by Prim Prof Dr Kharl Lhotta of the Innere Medizin III (Nephrologie and Dialyse) and performed by Dr Silvia

Reichart and Prim Prof Dr Stefan Mennel of the Department of Ophthalmology, both of the Akademisches Lehrkrankenhaus, Feldkirch, Austria.

8.2. Results

8.2.1 Patient characteristics

WGS was performed using DNA samples, from seven unrelated patients (families 1-7) and two brothers (family 8) diagnosed with FJHN and lacking mutations in *UMOD*, *REN* or *HNF-1ß*. The clinical and biochemical details, where available, are summarised in Table 23, including: serum and urinary creatinine (S.Cr and U.Cr, respectively) and uric acid (S.UA and U.UA, respectively) concentrations; fractional excretion of uric acid (FEUA); additional clinical details; and genes sequenced. Furthermore, DNA samples were also obtained from an additional 35 individuals in seven of the eight families for co-segregation analysis (16 affected, 15 unaffected and four whose disease status was unknown). DNA samples were not available at the time of analysis from proband I.I or additional individuals from family 8. The clinical and biochemical details, where available, for these individuals are also summarised in Table 23. Affected family members of family 8 were diagnosed with FJHN and were all described as having hyperuricaemia, however, limited biochemical details were available (Table 23). The pedigrees for each of the families are shown in Figure 43.

Table 23. Clinical and biochemical details of FJHN probands and affected family members

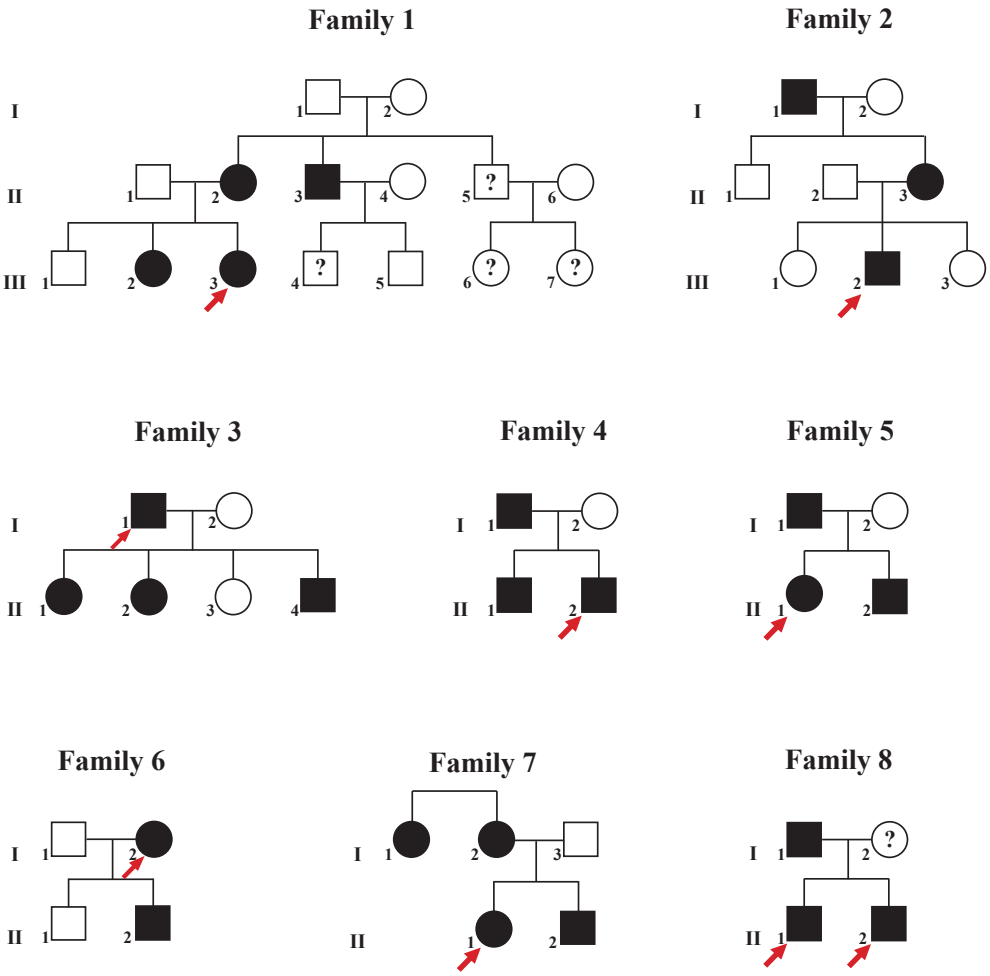
Family	ID	^Age at diagnosis	Sex	S.Cr (mg/dL) *<1.5	$S.UA (mg/dL)	U.Cr (mg/dL) *25-400	U.UA (mg/dL) *25-75	$FEUA	Clinical symptoms	Candidate genes sequenced
1	II.2	51	Female	High	High	Not known	Not known	ᵛ5.2%	Not known	Not known
	II.3	22	Male	High	High	Not known	Not known	ᵛLow	Not known	Not known
	III.2	Not known	Female	High	High	Not known	Not known	ᵛLow	Not known	Not known
	III.3	**27**	**Female**	**^2.2**	**High**	**Not known**	**Not known**	**ᵛ4.4%**	**Not known**	***UMOD, REN* and *HNF1ß.***
2	I.1	65	Male	1.35	^10.54	193.9	52.67	ᵛ3.5%	Gout	Linkage to chromosome 2p22.1-p21.2
	II.3	39	Female	^2.98	4.67	26.1	^6.36	ᵛ7%	Small kidneys, no cysts, gout.	Linkage to chromosome 2p22.1-p21.2
	III.2	**8**	**Male**	**0.65**	**^6.36**	**91.5**	**49.2**	**ᵛ5.5%**	**Not known**	*UMOD, REN* and *HNF1ß.* Linkage to chromosome 2p22.1-p21.2
3	**I.1**	**47**	**Male**	**0.9**	**ᵛ4.9**	**Not known**	**Not known**	**ᵛ3.6%**	**Not known**	**Linkage to chromosome 2p22.1-p21.2**
	II.1	17	Female	^1.5	^7.8	Not known	Not known	ᵛ2.6%	Small kidneys	*UMOD, REN* and *HNF1ß.* Linkage to chromosome 2p22.1-p21.2
	II.2	15	Female	1.1	^7.8	Not known	Not known	ᵛ1.8%	Not known	Linkage to chromosome 2p22.1-p21.2
	II.4	13	Male	0.8	4.9	Not known	Not known	ᵛ5.9%	Not known	Linkage to chromosome 2p22.1-p21.2
4	I.1	28	Male	Not known	High	Not known	Not known	10%	Renal failure	Not known
	II.1	21	Male	^1.5	High	Not known	Not known	6%	Renal failure	Not known
	II.2	**23**	**Male**	**^2.6**	**^8.6**	**Not known**	**Not known**	**9%**	**Renal failure**	***UMOD, REN* and *HNF1ß.***
5	I.1	50	Male	^10.5	^7.6	Not known	Not known	Not known	Atrophic kidneys, no cysts and gout.	*UMOD, REN* and *HNF1ß.* Linkage to chromosome 2p22.1-p21.2
	II.1	**23**	**Female**	**^2.3**	**^8.2**	**84.6**	**33.9**	**11.2%**	**Not known**	**Linkage to chromosome 2p22.1-p21.2**
	II.2	21	Male	^2.6	^7.7	Not known	Not known	Not known	Small kidneys and no cysts.	Linkage to chromosome 2p22.1-p21.2

Table 23. Clinical and biochemical details of FJHN probands and affected family members continued

Family	ID	^Age at diagnosis	Sex	S.Cr (mg/dL) *<1.5	$S.UA (mg/dL)	U.Cr (mg/dL) *25-400	U.UA (mg/dL) *25-75	$FEUA	Clinical symptoms	Candidate genes sequenced
6	**I.2**	**47**	**Female**	**Not known**	**4.7**	**Not known**	**#Low**	**Not known**	**Not known**	**Linkage to chromosome 2p22.1-p21.2**
	II.2	13	Male	^2.2	^12.9	100	ᵛ21.8	ᵛ2.9%	Gout	*UMOD, REN* and *HNF1ß*. Linkage to chromosome 2p22.1-p21.2
7	I.I	48	Female	0.76	^7.18	79.7	32.6	ᵛ4.2%	Not known	Linkage to chromosome 2p22.1-p21.2
	I.2	Not known	Female	Not known	Not known	Not known	Not known	Not known	Not known	Linkage to chromosome 2p22.1-p21.2
	II.1	**21**	**Female**	**0.64**	**4.47**	**56**	**ᵛ21.9**	**ᵛ5.5%**	**Not known**	**Linkage to chromosome 2p22.1-p21.2**
	II.2	15	Male	0.7	5.6	65.2	ᵛ17.5	ᵛ3.3%	Not known	*UMOD, REN* and *HNF1ß*. Linkage to chromosome 2p22.1-p21.2
8	I.1	Not known	Male	Not known	Hyperuricaemia	Not known	Not known	ᵛ1.5%	Gouty attacks, renal biopsy showed unclear tubulointerstitial nephropathy with mild and focal tubular atrophy and vacuolisation of tubular cells.	None
	II.1	Not known	**Male**	**^4.2**	Hyperuricaemia	Not known	Not known	**ᵛ4.5%**	**Kidney biopsy was inconclusive (only one glomerulum), stage IV chronic kidney disease, secondary hyperparathyroidism and proteinuria (2.5g/24hrs)**	***UMOD* and *REN***
	II.2	Not known	**Male**	**^1.8**	Hyperuricaemia	Not known	Not known	**ᵛ4.7%**	**Recurrent gouty attacks and proteinuria (0.3g/day)**	***UMOD* and *REN***

Biochemical and clinical phenotypes of the FJHN probands whose DNA was used for WGS and their affected family members. Abbreviations: S.Cr, serum creatinine; S.UA, serum uric acid; U.Cr urinary creatinine; U.UA, urinary uric acid; and FEUA, fractional excretion of uric acid. *denotes normal range and #based on 24hr uric acid excretion. $Normal range serum uric acid and FEUA values vary with sex and age[312,313]. $Normal range serum uric acid values <5 years old: 3.6mg/dL; 5-10 years old: 4.1mg/dL; Males: 10-12 years old: 4.4±0.7mg/dL; 12-15 years old: 5.6±1.1mg/dL; >15 years old: 6.2±0.8mg/dL; Females: 10-15 years old: 4.5±0.9mg/dL; >15 years old: 4.0±0.7mg/dL[312]. $Normal range FEUA values: Children: 18.4±5.1%; Adults: Females: 12.8±2.9%; Males: 8.1±3.2%[313]. ^denotes biochemical measurement above the normal range and ᵛdenotes biochemical measurements below the normal range. 'Candidate genes sequenced' details which of the three FJHN candidate genes (*UMOD*, *REN* and *HNF1ß*) were sequenced and in which proband; as well as which probands (and families [2,3,5-7]) were previously shown to exhibit linkage between SNPs in chromosome 2p22.1-p21.2 and FJHN in a previous study[147]. Probands whose DNA samples were used for WGS are highlighted in bold. Affected family members of family 8 were diagnosed with FJHN and were all described as having hyperuricaemia, however limited biochemical details were available.

Figure 43. FJHN pedigrees



Pedigrees of the eight families with FJHN included in this study. Squares indicate males and circles indicate females. Unfilled symbols indicate unaffected individuals and filled symbols indicate affected individuals. Individuals whose disease status is unknown are indicated by a '?'. Probands whose DNA was used for WGS are indicated by a red arrow.

8.2.2 Identification of 26 non-synonymous exonic candidate variants in patients diagnosed with FJHN

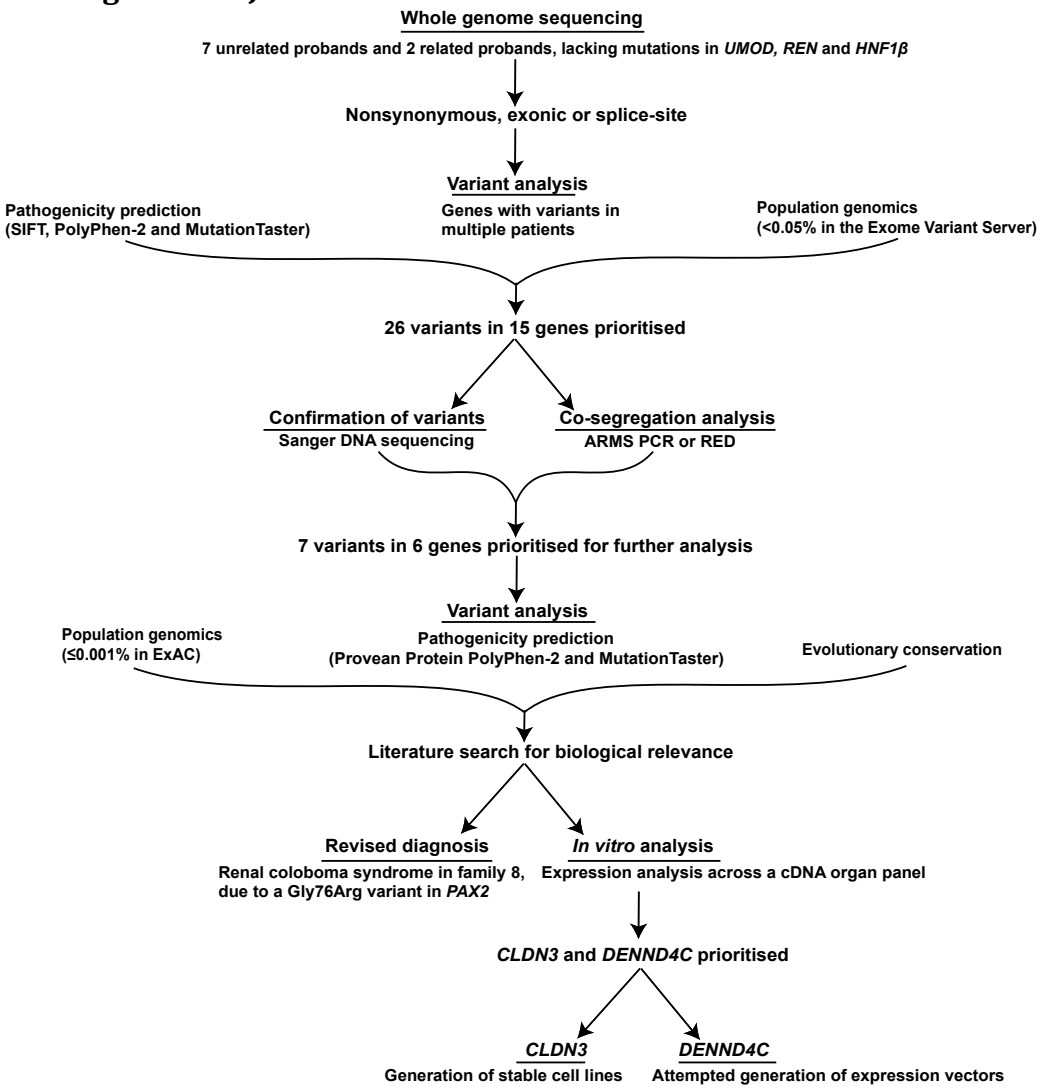
Initial bioinformatics analysis of WGS data of all families combined was performed to identify candidate genes. A series of bioinformatics analyses including: population genomics (variants were excluded that had vAFs >0.05% in the EVS); genes with variants in multiple families; and pathogenicity prediction resulted in 26 candidate variants in 15 genes (Table 24) being prioritised for confirmation and co- segregation

analysis (Figure 44). Notably, none of the prioritised genes were found to be located within the FJHN3 interval, previously mapped to chromosome 2p22.1-p21.2, in a study that included five of the eight families (2,3,5-7) included in this study[147]. Analysis of population genomics was performed using the EVS in the initial bioinformatics analysis, as this was performed prior to the public release of the ExAC browser (October 2014). Therefore, secondary *in silico* analysis, performed in 2015 and 2017 also included population genomics using ExAC.

8.2.2.1 Co-segregation analysis of DNA variants in the eight FJHN families

Following identification of the 26 genetic variants in the eight FJHN families, a series of confirmatory analyses were performed to determine whether each variant could be verified by Sanger DNA sequencing, and whether the variant co-segregated in affected family members (Table 24). In total, seven variants in six genes (Val454Met in Ankyrin repeat domain 11 [*ANKRD11*], Trp17Cys in claudin 3 [*CLDN3*], Ser1251Phe and Arg1317Gln in DENN domain containing 4C [*DENND4C*], Gly56Val in fibromodulin [*FMOD*], Pro338Ser in myosins class XVI [*MYO16*] and Gly76Arg in paired box 2 [*PAX2*]) were revealed to co-segregate with FJHN (Table 24).

Figure 44. Flowchart to display the process of identification and analysis of a candidate gene for FJHN



Flowchart to show the process from WGS to the prioritisation of candidate genes for FJHN4. WGS was performed using the DNA of seven unrelated individuals and two related probands diagnosed with FJHN and lacking mutations in *UMOD, REN* and *HNF1ß.* Variants were filtered based on mutation type; population genomics (EVS)[239]; pathogenicity prediction (SIFT, PolyPhen-2 and MutationTaster); and the occurrence of genes with variants in multiple patients. A total of 26 variants in 15 genes were prioritised from this initial analysis. Each of the 26 variants were confirmed in the proband by Sanger DNA sequencing and subsequent co-segregation analysis was performed for each of the variants. Of the 26 variants, just seven variants in six genes were found to co-segregate with FJHN and were prioritised for further analysis. Additional *in silico* analysis was performed including: population genomics (ExAC), pathogenicity prediction (MutationTaster, PolyPhen-2 and Provean Protein) and evolutionary conservation (eight orthologs). Subsequent literature searches for biological relevance, revealed that mutations in one of the six genes (*PAX2*) are associated with renal coloboma syndrome (RCS). As RCS is characterised by both renal and ocular anomalies, ophthalmological examinations were performed on the probands, confirming a revised diagnosis of RCS in family 8 due to a Gly76Arg variant in *PAX2*. *In vitro* expression analysis of the remaining five genes across a cDNA organ panel was performed. The combined literature searches, *in silico* and *in vitro* analyses resulted in *CLDN3* and *DENND4C* being prioritised as good candidates for FJHN4.

Table 24. Co-segregation analysis of the prioritised variants identified in patients diagnosed with FJHN by WGS

Family	Proband ID	Gene name	Gene symbol	Nucleotide change	Amino acid change	Co-segregates?	Co-segregation method
6	I.2	Ankyrin repeat domain 11	*ANKRD11*	c.G1360A	p.Val454Met	Yes	ARMS
2	III.2	Bassoon presynaptic cytomatrix protein	*BSN*	c.A5525G	p.His1842Arg	No	ARMS
7	II.1	Bassoon presynaptic cytomatrix protein	*BSN*	c.G6706A	p.Val2236Met	No	ARMS
3	I.1	Chloride voltage-gated channel 6	*CLCN6*	c.T907C	*p.Trp303Arg	No	ARMS
5	II.1	Claudin 3	*CLDN3*	c.G51T	*p.Trp17Cys	Yes	ARMS
6	I.2	DENN domain containing 4C	*DENND4C*	c.C3752T	*p.Ser1251Phe	Yes	ARMS
7	II.1	DENN domain containing 4C	*DENND4C*	c.G3950A	*p.Arg1317Gln	Yes	ARMS
6	I.2	FAT atypical cadherin 1	*FAT1*	c.C2141T	p.Pro714Leu	No	RED
7	II.2	FAT atypical cadherin 1	*FAT1*	c.G5788C	*p.Asp1930His	No	ARMS
7	II.1	Fibromodulin	*FMOD*	c.G167T	*p.Gly56Val	Yes	ARMS
1	III.3	Fibromodulin	*FMOD*	c.G440A	*p.Gly147Asp	No	RED
5	II.1	Fibromodulin	*FMOD*	c.G707A	*p.Arg236Gln	No	RED
7	II.1	Immunoglobulin-like and fibronectin type III domain containing 1	*IGFN1*	c.T144A	p.Phe48Leu	No	ARMS
3	I.1	Immunoglobulin-like and fibronectin type III domain containing 1	*IGFN1*	c.C7388G	p.Ser2463Cys	No	RED
4	II.2	Immunoglobulin-like and fibronectin type III domain containing 1	*IGFN1*	c.C8365T	p.Gln2789X	No	ARMS
2	III.2	Lysine demethylase 4E	*KDM4E*	c.G631A	p.Val211Met	No	RED
3	I.1	Lysine demethylase 4E	*KDM4E*	c.C718T	*p.Arg240Trp	No	ARMS
5	II.1	Myosins, class XVI	*MYO16*	c.C1012T	*p.Pro338Ser	Yes	ARMS
6	I.2	Myosins, class XVI	*MYO16*	c.G1708T	p.Gly570X	No	RED
3	I.1	Neuraminidase 2	*NEU2*	c.C247T	*p.Arg83Trp	No	RED
8	II.1 and II.2	Paired box 2	*PAX2*	c.G226C	*p.Gly76Arg	Yes	ARMS
1	III.3	Peroxisome proliferator-activated receptor gamma, coactivator-related 1	*PPRC1*	c.G728A	p.Arg243His	No	RED
5	II.1	Peroxisome proliferator-activated receptor gamma, coactivator-related 1	*PPRC1*	c.T2810G	*p.Leu937Arg	No	RED
4	II.2	RP1 like 1	*RP1L1*	c.G6037A	*p.Glu2013Lys	No	RED
6	I.2	Solute carrier family 13 member 5	*SLC13A5*	c.C202T	*p.Pro68Ser	No	ARMS
5	II.1	Solute carrier family 13 member 5	*SLC13A5*	c.C1181A	*p.Pro394His	No	ARMS

Co-segregation analysis of 26 variants in 15 genes prioritised from WGS analysis of nine probands in eight families with FJHN. Co-segregation analysis was performed using RED or ARMS PCR on available DNA samples. Co-segregation occurred when the variant was shown to be present in all available samples with FJHN and absent from all available unaffected samples within each family. *Indicates a possible major amino acid change e.g. substitution of an uncharged amino acid for a charged amino acid, a positively charged amino acid for a negatively charged amino acid, a hydrophilic for a hydrophobic amino acid or one that is likely to break a helix.

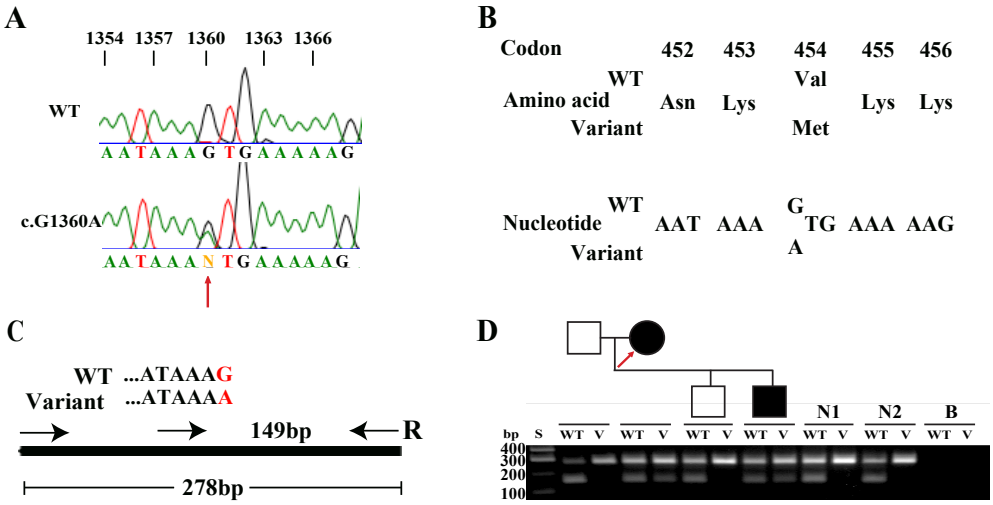
8.2.2.1.1 Co-segregation analysis of a Val454Met variant in Ankyrin repeat domain 11 (ANKRD11) in a family 6

A heterozygous G-to-A transition at nucleotide 1360 was identified in proband I.2 from family 6 and is predicted to result in the substitution of a valine with a methionine at codon 454 (Figure 45A-B). The variant was confirmed in the proband by Sanger DNA sequencing and co-segregation analysis by ARMS PCR was performed using DNA from the proband and additional family members (Figure 45C-D). The co-segregation analysis showed that the variant was present in all the affected family members tested (proband and affected son) and was absent from the unaffected husband and son, showing that the variant did co-segregate with FJHN in this family (Figure 45D).

8.2.2.1.2 Co-segregation analysis of a Trp17Cys variant in claudin 3 variant in family 5

A heterozygous G-to-T transversion at nucleotide 51 identified in proband II.1 from family 5 is predicted to result in the substitution of a tryptophan with a cysteine at codon 17 (Figure 46A-B). Confirmation of this variant by Sanger DNA sequencing and co-segregation analysis by ARMS PCR was performed using DNA from the proband and additional family members (Figure 46A-B). Co-segregation analysis, by ARMS PCR, showed that this variant was present in all the affected family members tested and was absent from the unaffected mother (Figure 46C-D), thus showing this variant does co-segregate with FJHN in this family.

Figure 45. Confirmation and co-segregation analysis of a Val454Met variant in ANKRD11 in family 6



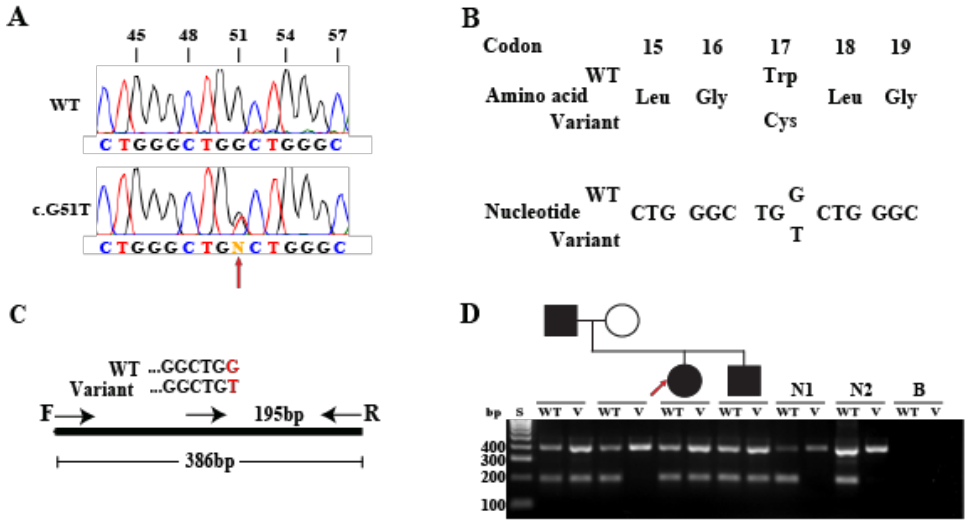
Nucleotide number is according to the *ANKRD11* transcript ENST00000301030.9 and amino acid number is according to the full-length 2663 amino acid protein (NCBI, NP_001243112; UniProt Q6UB99). (A) A heterozygous G-to-A transition at nucleotide c.1360 was identified in proband I.2 from family 6. (B) This G-to-A transition (GTG to ATG) is predicted to result in a missense amino acid change from valine (Val) to methionine (Met) at codon 454 of the ANKRD11 protein. (C) ARMS PCR map showing the last 6bp of the WT and variant internal ARMS primers that would result in two products of 278bp and 149bp. The nucleotide highlighted in red is the terminal nucleotide for the primers and corresponds to the first nucleotide affected by the G-to-A transition. Each ARMS reaction is specific for the WT or variant sequences, if the highlighted nucleotide differs from the sample sequence only one product of 278bp will result. (D) ARMS PCR of *ANKRD11* demonstrating the heterozygous G-to-A transition in the proband (highlighted by an arrow) and the affected son by the presence of two bands in both the WT and variant (V) reactions; and the lack of the G-to-A transition in the unaffected husband and son and two normal controls (N1 and N2), shown by the presence of two bands in the WT reaction and one in the variant reaction. S= size marker, B= water blank.

8.2.2.1.3 Co-segregation analysis of a Ser1251Phe variant in Denn domain containing 4C (Dennd4C) in family 6

A heterozygous C-to-T transition at nucleotide 3752 was identified in proband I.2 from family 6 by WGS and is predicted to result in the substitution of a serine with a phenylalanine at codon 1251 (Figure 47A-B). Confirmation of this variant was performed by Sanger DNA sequencing and co-segregation analysis was performed by ARMS PCR using DNA from the proband and additional family members (Figure 47C-D). Co-segregation analysis showed that this variant was present in all the affected

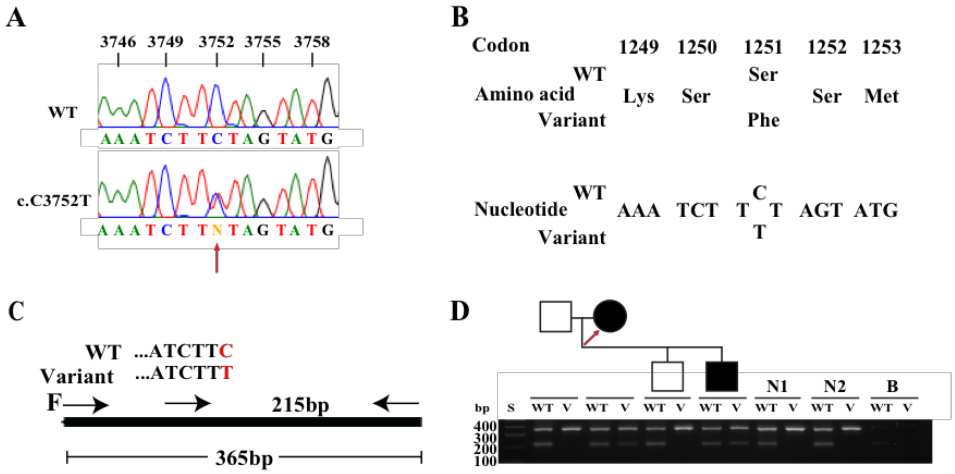
family members tested and was absent from the unaffected husband and son, thus showing this variant does co-segregate with FJHN in this family (Figure 47D).

Figure 46. Confirmation and co-segregation analysis of a Trp17Cys variant in claudin 3 in family 5



Nucleotide number is according to the *CLDN3* transcript ENST00000395145.3 and amino acid number is according to the full-length 220 amino acid protein (NCBI, NP_001297; UniProt O15551). (A) A heterozygous G-to-T transversion at nucleotide c.51 was identified in proband II.1 from family 5.(B) This G-to-T transversion (TGG to TGT) is predicted to result in a missense amino acid change from tryptophan (Trp) to cysteine (Cys) at codon 17 of the claudin 3 protein. (C) ARMS PCR map showing the last 6bp of the WT and variant internal ARMS primers that would result in two products of 386bp and 195bp. The nucleotide highlighted in red is the terminal nucleotide for the primers and corresponds to the first nucleotide affected by the G-to-T transversion. Each ARMS reaction is specific for the WT or variant sequences, if the highlighted nucleotide differs from the sample sequence only one product of 386bp will result. (D) ARMS PCR of *CLDN3* demonstrating the heterozygous G-to-T transversion in the proband (highlighted by an arrow) and affected family members by the presence of two bands in both the WT and variant (V) reactions; and the lack of the G-to-T transversion in the unaffected mother and two normal controls (N1 and N2), shown by the presence of two bands in the WT reaction and one in the variant reaction. S= size marker, B= water blank.

Figure 47. Confirmation and co-segregation analysis of a Ser1251Phe variant in Dennd4C in family 6

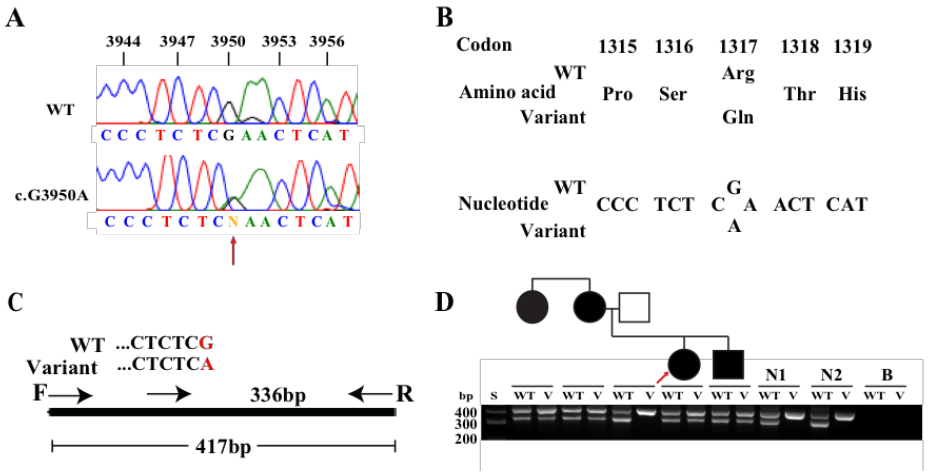


Nucleotide number is according to the *DENND4C* transcript ENST00000602925.5 and amino acid number is according to the full-length 1909 amino acid protein (NCBI, NP_060395; UniProt Q5VZ89). (A) A heterozygous C-to-T transition at nucleotide c.3752 was identified in proband I.2 from family 6. (B) This C-to-T transition (TCT to TTT) is predicted to result in a missense amino acid change from serine (Ser) to phenylalanine (Phe) at codon 1251 of the Dennd4C protein. (C) ARMS PCR map showing the last 6bp of the WT and variant internal ARMS primers that would result in two products of 365bp and 215bp. The nucleotide highlighted in red is the terminal nucleotide for the primers and corresponds to the first nucleotide affected by the C-to-T transition. Each ARMS reaction is specific for the WT or variant sequences, if the highlighted nucleotide differs from the sample sequence only one product of 365bp will result. (D) ARMS PCR of *DENND4C* demonstrating the heterozygous C-to-T transition in the proband (highlighted by an arrow) and affected son by the presence of two bands in both the WT and variant (V) reactions; and the lack of the C-to-T transition in the unaffected husband and unaffected son as well as the two normal controls (N1 and N2) shown by the presence of two bands in the WT reaction and one in the variant reaction. S= size marker, B= water blank.

8.2.2.1.4 Co-segregation analysis of an Arg1317Gln variant in Dennd4C in family 7

A heterozygous G-to-A transition at nucleotide 3950 was identified in proband II.1 from family 7 by WGS and is predicted to result in the substitution of an arginine with a glutamine at codon 1317 (Figure 48A-B). The variant was confirmed in the proband by Sanger DNA sequencing (Figure 48A), and co-segregation analysis was performed by ARMS PCR using DNA from the proband and additional family members (Figure 48C-D). The co-segregation analysis showed that this variant was present in all the affected family members tested and was absent from the unaffected father, thus showing this variant does co-segregate with FJHN in this family (Figure 48D).

Figure 48. Confirmation and co-segregation analysis of an Arg1317Gln variant in Dennd4C in family 7

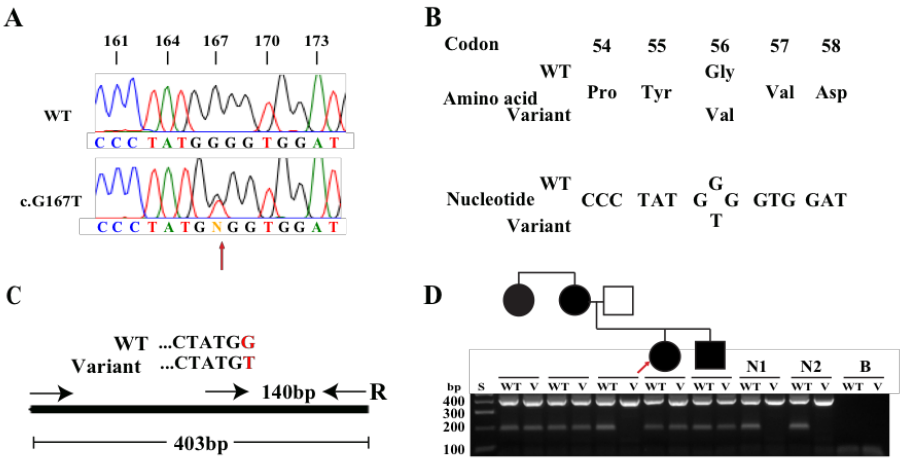


Nucleotide number is according to the *DENND4C* transcript ENST00000602925.5 and amino acid number is according to the full-length 1909 amino acid protein (NCBI, NP_060395; UniProt Q5VZ89). (A) A heterozygous G-to-A transition at nucleotide c.3950 was identified in proband II.1 from family 7. (B) This G-to-A transition (CGA to CAA) is predicted to result in a missense amino acid change from arginine (Arg) to glutamine (Gln) at codon 1317 of the Dennd4C protein. (C) ARMS PCR map showing the last 6bp of the WT and variant internal ARMS primers that would result in two products of 417bp and 336bp. The nucleotide highlighted in red is the terminal nucleotide for the primers and corresponds to the first nucleotide affected by the G-to-A transition. Each ARMS reaction is specific for the WT or variant sequences, if the highlighted nucleotide differs from the sample sequence only one product of 417bp will result. (D) ARMS PCR of *DENND4C* demonstrating the heterozygous G-to-A transition in the proband (highlighted by an arrow) and affected family members by the presence of two bands in both the WT and variant (V) reactions; and the lack of the G-to-A transition in the unaffected father and two normal controls (N1 and N2) shown by the presence of two bands in the WT reaction and one in the variant reaction. S= size marker, B= water blank.

8.2.2.1.5 Co-segregation analysis of a Gly56Val variant in fibromodulin in family 7

A heterozygous G-to-T transversion at nucleotide 167 identified in proband II.1 from family 7 is predicted to result in the substitution of a glycine with a valine at codon 56 (Figure 49A-B). Confirmation of this variant by Sanger DNA sequencing (Figure 49A) and co-segregation analysis by ARMS PCR was performed using DNA from the proband and additional family members (Figure 49C-D). Co-segregation analysis showed that this variant was present in all the affected family members tested and was absent from the unaffected father, thus showing this variant does co-segregate with FJHN in this family (Figure 49D).

Figure 49. Confirmation and co-segregation analysis of a Gly56Val variant in fibromodulin in family 7

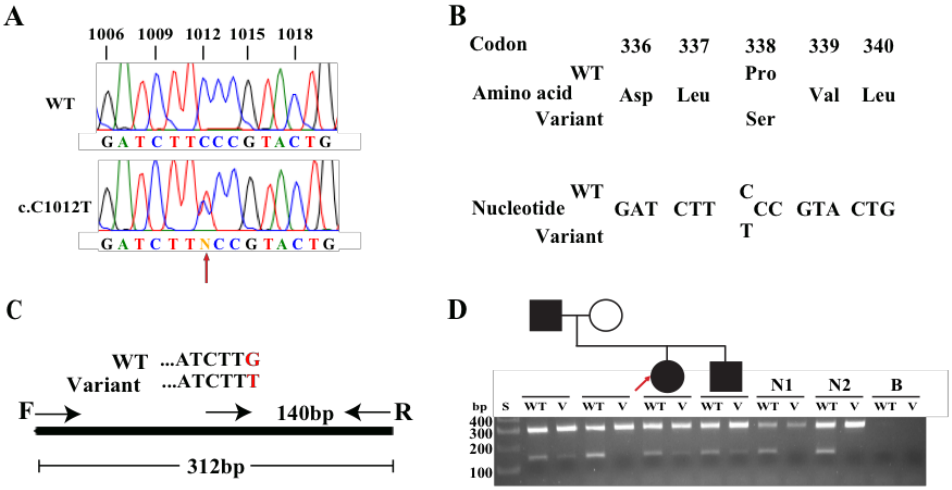


Nucleotide number is according to the *FMOD* transcript ENST00000354955.4 and amino acid number is according to the full-length 3310 amino acid protein (NCBI, NP_002014; UniProt Q06828). (A) A heterozygous G-to-T transversion at nucleotide c.167 was identified in proband II.1 from family 7. (B) This G-to-T transversion (GGG to GTG) is predicted to result in a missense amino acid change from glycine (Gly) to valine (Val) at codon 56 of the fibromodulin protein. (C) ARMS PCR map showing the last 6bp of the WT and variant internal ARMS primers that would result in two products of 403bp and 140bp. The nucleotide highlighted in red is the terminal nucleotide for the primers and corresponds to the first nucleotide affected by the G-to-T transversion. Each ARMS reaction is specific for the WT or variant sequences, if the highlighted nucleotide differs from the sample sequence only one product of 403bp will result. (D) ARMS PCR of *FMOD* demonstrating the heterozygous G-to-T transversion in the proband (highlighted by an arrow) and affected family members by the presence of two bands in both the WT and variant (V) reactions; and the lack of the G-to-T transversion in the unaffected father and two normal controls (N1 and N2) shown by the presence of two bands in the WT reaction and one in the variant reaction. S= size marker, B= water blank.

8.2.2.1.6 Co-segregation analysis of a Pro338Ser variant in Myosin XVI in family 5

A heterozygous C-to-T transition at nucleotide 1012, predicted to result in the substitution of a proline with a serine at codon 338, was identified in proband II.1 from family 5 in the FJHN cohort (Figure 50A-B). The variant was confirmed in the proband by Sanger DNA sequencing (Figure 50A) and co-segregation analysis by ARMS PCR was performed using DNA from the proband and additional family members (Figure 50C-D). The variant was found to be present in all the affected family members tested and absent from the unaffected mother, showing that it does co-segregate with FJHN in this family (Figure 50D).

Figure 50. Confirmation and co-segregation analysis of a Pro338Ser variant in myosin XVI in family 5

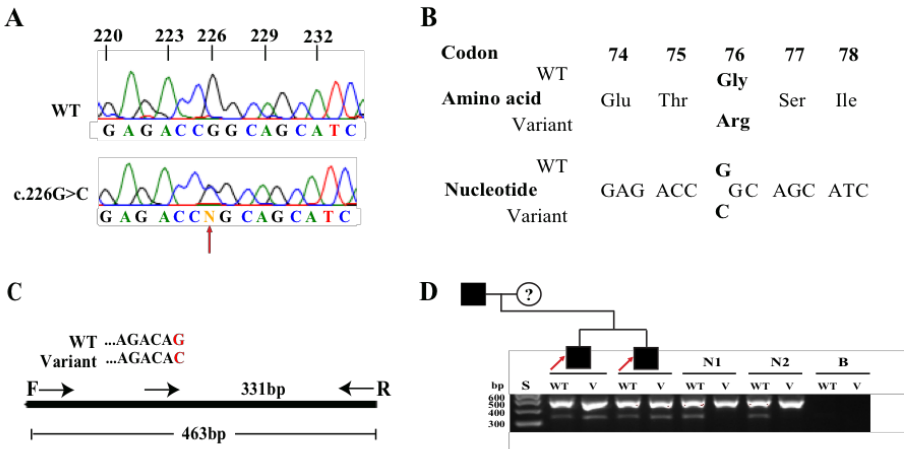


Nucleotide number is according to the *MYO16* transcript ENST00000356711.6 and amino acid number is according to the full-length 1858 amino acid protein (NCBI, NP_055826; UniProt Q9Y6X6). (A) A heterozygous C-to-T transition at nucleotide c.1012 was identified in proband II.1 from family 5. (B) This C-to-T transition (CCC to TCC) is predicted to result in a missense amino acid change from proline (Pro) to serine (Ser) at codon 338 of the myosin XVI protein. (C) ARMS PCR map showing the last 6bp of the WT and variant internal ARMS primers that would result in two products of 312bp and 140bp. The nucleotide highlighted in red is the terminal nucleotide for the primers and corresponds to the first nucleotide affected by the C-to-T transition. Each ARMS reaction is specific for the WT or variant sequences, if the highlighted nucleotide differs from the sample sequence only one product of 386bp will result. (D) ARMS PCR of *MYO16* demonstrating the heterozygous C-to-T transition in the proband (highlighted by an arrow) and affected family members by the presence of two bands in both the WT and variant (V) reactions; and the lack of the C-to-T transition in the unaffected mother and two normal controls (N1 and N2) shown by the presence of two bands in the WT reaction and one in the variant reaction. S= size marker, B= water blank.

8.2.2.1.7 Co-segregation analysis of a Gly76Arg variant in Paired box 2 (Pax-2) in family 8

A heterozygous G-to-C transversion at nucleotide 226 was identified in two brothers diagnosed with FJHN, probands II.1 and II.2 from family 8, and is predicted to result in the substitution of a glycine with an arginine at codon 76 (Figure 51A-B). Confirmation of this variant by Sanger DNA sequencing (Figure 51A) and co-segregation analysis by ARMS PCR was performed using DNA from the two brothers, DNA from additional family members was not available (Figure 51C-D). Co-segregation analysis shows this variant did co-segregate with FJHN (Figure 51D).

Figure 51. Confirmation of a Gly76Arg variant, in Pax-2, in a family diagnosed with FJHN



Nucleotide number is according to the *PAX2* transcript ENST00000370296.6 and amino acid number is according to the full-length 687 amino acid protein (NCBI, NP_003979; UniProt Q02962). (A) A heterozygous G-to-C transversion at nucleotide c.226 was identified in 2 related probands (II.1and II.2) from family 8. (B) This G-to-C transversion (GGC to CGC) is predicted to result in a missense amino acid change from glycine (Gly) to arginine (Arg) at codon 76 of the Pax-2 protein. (C) ARMS PCR map showing the last 6bp of the WT and variant internal ARMS primers that would result in two products of 463bp and 331bp. The nucleotide highlighted in red is the terminal nucleotide for the primers and corresponds to the first nucleotide affected by the G-to-C transversion. The penultimate nucleotide was also designed to differ from the WT sequence to increase the specificity of each primer sequence[226,227]. Each ARMS reaction is specific for the WT or variant sequences, if the highlighted nucleotide differs from the sample sequence only one product of 463bp will result. (D) ARMS PCR of *PAX2* exon 3 demonstrating the heterozygous G-to-C transversion in the probands (highlighted by arrows) by the presence of two bands in both the WT and variant (V) reactions; and the lack of the G-to-C transversion in the two normal controls (N1 and N2) shown by the presence of two bands in the WT reaction and one in the variant reaction. S= size marker, B= water blank.

8.2.2.2 In silico analysis of seven variants identified in families with FJHN

The seven variants that co-segregated with FJHN in each family were next assessed using *in silico* tools consisting of: vAFs in ExAC, prediction of functional effects using MutationTaster[240], PolyPhen-2[242] and Provean Protein[225,241], and evolutionary conservation to determine the possible effects of each variant on gene function (Table 25). The results of the *in silico* analyses were assessed using the criteria outlined in Section 6.2.9.4.

8.2.2.2.1 *In silico* analysis of a Val454Met variant in ANKRD11 identified in proband I.2 from family 6

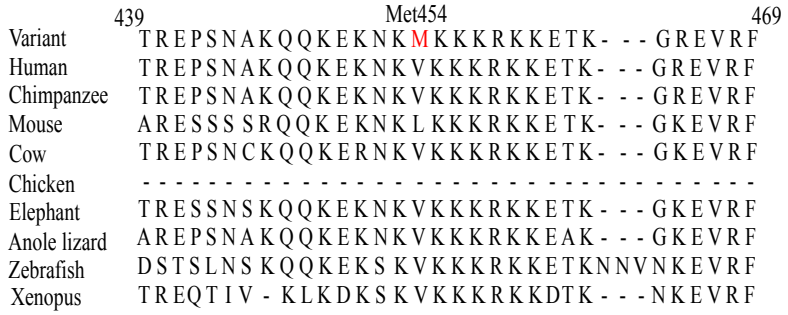
In silico analysis of the Val454Met variant identified in ANKRD11 in proband I.2 from family 6 revealed a reported vAF of 0.0093% in ExAC (Table 25). This is higher than the 0.001% cut off suggested by the *in silico* analysis study detailed in Section 6.2.9.1, therefore suggesting this variant may not be pathogenic in FJHN. Furthermore, the functional effect of this variant was predicted to be a polymorphism and neutral by two of the three of the pathogenicity prediction software used: MutationTaster and Provean Protein respectively; and possibly damaging by PolyPhen-2 (Table 25), overall indicating this variant is probably benign. Evolutionary conservation analysis of the WT valine residue showed that it is conserved across six of the eight orthologs studied, suggesting this variant may be pathogenic (Figure 52). Overall, combined *in silico* analysis predicted this variant to be likely benign (Table 25).

Table 25. *In silico* analysis of the seven variants that co-segregated with FJHN

Family	Proband ID	Gene symbol	Amino acid change	^Reported vAF	MutationTaster	PolyPhen-2	Provean Protein	Evolutionary conservation	Combined *in silico* prediction
6	I.2	*ANKRD11*	p.Val454Met	0.0093%	Polymorphism	Possibly damaging (score 0.868)	Neutral (score -1.750)	Conserved (6/8)	Likely benign
5	II.1	*CLDN3*	*p.Trp17Cys	0%	Disease causing	Probably damaging (score 0.999)	Deleterious (score -10.408)	Conserved (8/8)	Pathogenic
6	I.2	*DENND4C*	*p.Ser1251Phe	0%	Disease causing	Possibly damaging (score 0.659)	Neutral (score -2.461)	Partially conserved (4/8)	Unknown significance
7	II.1	*DENND4C*	*p.Arg1317Gln	0%	Polymorphism	Possibly damaging (score 0.524)	Neutral (score -1.614)	Conserved (7/8)	Likely pathogenic
7	II.1	*FMOD*	*p.Gly56Val	0.0058%	Disease causing	Benign (score 0.000)	Neutral (score -0.596)	Partially conserved (4/8)	Benign
5	II.1	*MYO16*	*p.Pro338Ser	0.0124%	Polymorphism	Probably damaging (score 0.967)	Deleterious (score -2.504)	Conserved (7/8)	Likely pathogenic
8	II.1 and II.2	*PAX2*	*p.Gly76Arg	0%	Disease causing	Probably damaging (score 1.000)	Deleterious (score -6.962)	Conserved (8/8)	Pathogenic

In silico analysis of seven variants in six genes that were found to co-segregate with FJHN. ^Reported on ExAC. Three publically available online software were used to predict the functional effect of variants: MutationTaster[240], PolyPhen-2[242], and Provean Protein[225,241]. Eight orthologous protein sequences were used to assess the degree of evolutionary conservation of each of the affected amino acid residues. The following orthologs were used for all genes except *CLDN3*, *IGFN1* and *MYO16,* for which some of these protein sequences were not available: chimpanzee, mouse, cow, chicken, elephant, anole lizard, zebrafish and xenopus. Variants were classified as conserved (≥6/8), partially conserved (3-5/8) or not conserved (≤2/8). A prediction of pathogenicity was made using a combined *in silico* analysis approach as described in Section 6.2.9.4. *Indicates a possible major amino acid change e.g. substitution of an uncharged amino acid for a charged amino acid, a positively charged amino acid for a negatively charged amino acid, a hydrophilic for a hydrophobic amino acid or one that is likely to break a helix.

Figure 52. Multiple sequence alignment of the residues surrounding the WT Val454 residue in ANKRD11

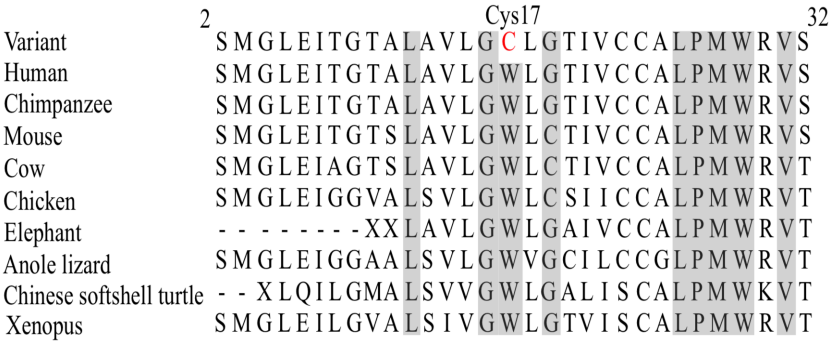


Multiple sequence alignment of residues surrounding the human Val454 residue of the ANKRD11 protein sequence in eight orthologs. The Met454 residue identified in proband I.2 from family 6 is shown in red. None of the residues were highly conserved across all the orthologs studied, the Val454 residue was conserved across six of the eight orthologs.

8.2.2.2.2 *In silico* analysis of a Trp17Cys variant in claudin 3 identified in proband II.1 from family 5

In silico analysis of the Trp17Cys variant in claudin 3 identified in proband II.1 from family 5 revealed that this variant was not reported on ExAC, was predicted to be probably damaging by all three of the pathogenicity prediction software and evolutionary conservation analysis found the WT tryptophan residue was conserved across all of the eight orthologs studied (Table 25 and Figure 53). Overall, combined *in silico* analysis predicted the Trp17Cys variant to be pathogenic (Table 25).

Figure 53. Multiple sequence alignment of the residues surrounding the WT Trp17 residue in claudin 3

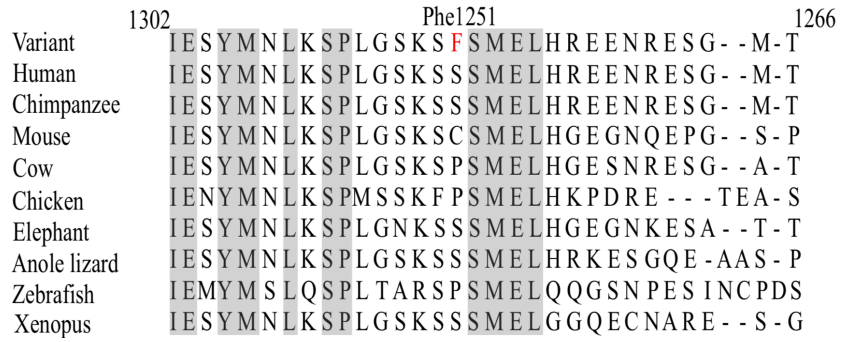


Multiple sequence alignment of the residues surrounding the human Trp17 residue of the claudin 3 protein sequence in eight orthologs. The Cys17 residue identified in proband II.1 from family 5 is shown in red. Residues conserved across all of the orthologs studied are highlighted in grey, the Trp17 residue was fully conserved across the eight.

8.2.2.2.3 *In silico* analysis of a Ser1251Phe variant in Dennd4C identified in proband I.2 from family 6

Analyses revealed that the Ser1251Phe variant in Dennd4C, identified in proband I.2 from family 6, was not present on ExAC, was predicted to be of unknown significance and evolutionary conservation analysis of the WT serine residue found it to be only partially conserved across the eight orthologs (4/8) (Table 25 and Figure 54). Overall, combined *in silico* analysis classified this variant as being of unknown significance (Table 25).

Figure 54. Multiple sequence alignment of the residues surrounding the WT Ser1251 residue in Dennd4C



Multiple sequence alignment of residues surrounding the human Ser1251 residue of the Dennd4C protein sequence in eight orthologs. The Phe1251 residue identified in proband I.2 from family 6 is shown in red. Residues conserved across all of the orthologs studied are highlighted in grey, the Ser1251 residue was partially conserved across the eight orthologs.

8.2.2.2.4 *In silico* analysis of an Arg1317Gln variant in Dennd4C identified in proband II.1 from family 7

In silico analysis of population genomics showed the Arg1317Gln variant in Dennd4C, identified in proband II.1 from family 7, was not present on ExAC (Table 25). Pathogenicity prediction software indicated this variant is probably benign in two of the three software used and evolutionary conservation analysis of the WT arginine residue found it to be conserved across seven of the eight orthologs studied (Table 25

and Figure 55), indicating the likely pathogenicity of this variant. Overall, combined *in silico* analysis classified this variant as likely pathogenic (Table 25).

Figure 55. Multiple sequence alignment of the residues surrounding the WT Arg1317 residue in Dennd4C

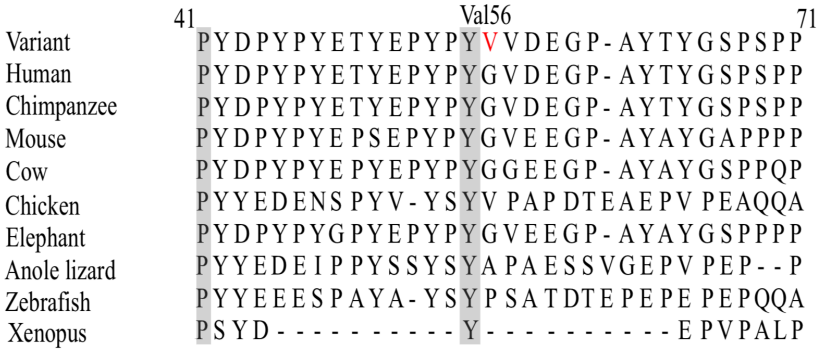


Multiple sequence alignment of residues surrounding the human Arg1317 residue of the Dennd4C protein sequence in eight orthologs. The Gln1317 residue identified in proband II.1 from family 7 is shown in red. Residues conserved across all of the orthologs studied are highlighted in grey, the Arg1317 residue was conserved across seven of the eight orthologs.

8.2.2.2.5 *In silico* analysis of a Gly56Val variant in fibromodulin identified in proband II.1 from family 7

In silico analysis revealed that the Gly56Val variant in fibromodulin, identified in proband II.1 from family 7, was reported in 0.0058% of alleles on ExAC (Table 25). This is greater than the 0.001% cut off suggested by the *in silico* analysis study detailed in Section 6.2.9.1. Furthermore, the functional effect of this variant was predicted to be probably benign (Table 25). Evolutionary conservation analysis showed the WT glycine residue was only partially conserved across the eight orthologs studied (Figure 56). Overall, the combined *in silico* analysis classified this variant as likely benign (Table 25).

Figure 56. Multiple sequence alignment of the residues surrounding the WT Gly56 residue in fibromodulin



Multiple sequence alignment of residues surrounding the human Gly56 residue of the fibromodulin protein sequence in eight orthologs. The Val56 residue identified in proband II.1 from family 7 is shown in red. Residues conserved across all of the orthologs studied are highlighted in grey. The Gly56 residue was partially conserved, with the Gly56 residue shown to be conserved across four of the eight orthologs.

8.2.2.2.6 *In silico* analysis of a Pro338Ser variant in myosin XVI identified in proband II.1 from family 5

Population genomic analysis revealed the Pro338Ser variant in myosin XVI, identified in proband II.1 from family 5, had a reported vAF of 0.0124% on ExAC (Table 25); which is higher than the 0.001% cut off suggested in Section 6.2.9.1, thereby indicating this variant may be benign. However, the functional effect of this variant was predicted to be probably damaging by two of the three pathogenicity prediction programmes used (PolyPhen-2 and Provean Protein) and a polymorphism by MutationTaster (Table 25). Evolutionary conservation analysis of the WT proline residue found it to be conserved across seven of the eight orthologs studied (Figure 57). Therefore, the combined *in silico* analysis predicted this variant to be likely pathogenic (Table 25).

Figure 57. Multiple sequence alignment of the residues surrounding the WT Pro338 residue in myosin XVI

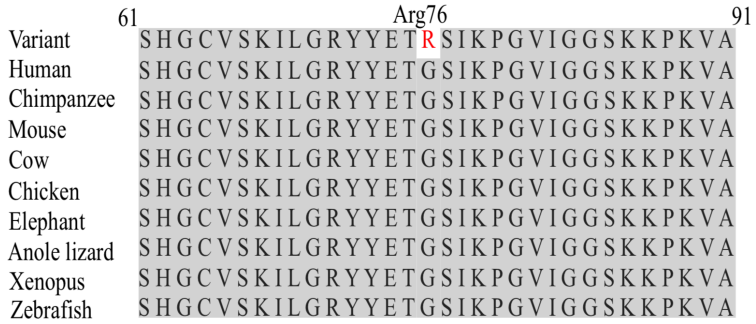


Multiple sequence alignment of residues surrounding the human Pro338 residue of the myosin XVI protein sequence in eight orthologs. The Ser338 residue identified in proband II.1 from family 5 is shown in red. Residues conserved across all of the orthologs studied are highlighted in grey, the Pro338 residue was conserved across the seven of the eight orthologs.

8.2.2.2.7 *In silico* analysis of a Gly76Arg variant in Pax-2 identified in probands II.1 and II.2 from family 8

In silico analysis revealed the Gly76Arg variant in Pax-2, identified in two probands (II.1 and II.2) from family 8, was not reported on ExAC, was predicted to be probably damaging by all three of the pathogenicity prediction software, and evolutionary conservation analysis of the WT glycine residue found this residue to be conserved across all of the eight orthologs studied (Table 25 and Figure 58). Overall, combined *in silico* analysis classified this variant as pathogenic (Table 25).

Figure 58. Multiple sequence alignment of the residues surrounding the WT Gly76 residue in Pax-2



Multiple sequence alignment of residues surrounding the human Gly76 residue of the Pax-2 protein sequence in eight orthologs. The Arg76 residue identified in probands II.1 and II.2 from family 8 is shown in red. Residues conserved across all of the orthologs studied are highlighted in grey, the Gly76 residue was fully conserved across the eight orthologs.

8.2.3 Prioritisation of candidate variants for functional analysis

Co-segregation analysis revealed that just seven of the 26 variants initially prioritised co-segregated with FJHN in their respective families (the segregation analysis of other genes that did not co-segregate can be found in the appendix [Figure 82 to Figure 100]). The subsequent *in silico* analysis, using the criteria optimised in Section 6.2.9.4, predicted two of the seven variants to be pathogenic (Trp17Cys in claudin 3 and Gly76Arg in Pax-2), two to be likely pathogenic (Arg1317Gln in Dennd4C and Pro338Ser in myosin XVI), one to be of unknown significance (Ser1251Phe in Dennd4C), one to be likely benign (Val454Met in ANKRD11) and one to be benign (Gly56Val in fibromodulin).

8.2.3.1 Biological relevance

ANKRD11

ANKRD11 encodes the ankyrin repeat domain-containing protein 11 (ANKRD11), a nuclear protein that is reported to play an important role in neural development, regulating gene expression by functioning as a transcriptional co-regulator that

interacts with histone deacetylases to regulate histone acetylation[314,315]. Mutations in *ANKRD11* have been reported to cause the autosomal dominant syndrome KBG, so named to represent the initials of the first families diagnosed. KBG syndrome is characterised by: intellectual disability, macrodonita, distinct craniofacial findings, short stature and skeletal anomalies[316]. Furthermore, the Yoda mouse model which harbours the heterozygous missense mutation, Glu2502Lys in *Ankrd11*, also exhibits craniofacial anomalies including deformed nasal bones, shortened snouts and wider skulls similar to the craniofacial features observed in KBG syndrome[316,317]. To date, no renal anomalies have been reported in KBG patients or Yoda mice[316,317]. However, epigenome-wide association studies of eGFR and chronic kidney disease showed that hypermethylation was associated with higher eGFR and a lower percentage of renal fibrosis at a CpG site identified in *ANKRD11* (cg27660627)[318]. With no evidence of a distinct role in the renal tubules and no reports of a renal phenotype in KBG patients (or Yoda mice), these findings would suggest *ANKRD11* is an unlikely candidate for FJHN.

CLDN3

CLDN3 encodes claudin 3, a transmembrane protein required for the formation of tight junctions between epithelial cells, which are major determinants of paracellular permeability[319]. Although most claudin proteins exhibit tissue-specific expression, claudin 3 has been suggested to be a key component of tight junctions due to its wide expression pattern, with expression reported in the epithelia of the kidney, liver, skin, lung, intestine and endothelia[320-323]. Additionally, expression in tubular structures such as the renal tubules and gastrointestinal tract is reported to be greater in distal segments[320,322,323]. Furthermore, mutations in *CLDN16* and *19* have previously been

reported in the rare renal tubule disorder, familial hypomagnesaemia with hypercalciuria and nephrocalcinosis (FHHNC)[136,137,324]. FHHNC is characterised by progressive renal wasting of Mg^{2+} and Ca^{2+} leading to impaired renal function and chronic renal disease[137,324]. Additionally, hyperuricaemia has also been observed in the majority of patients[136,137,324-326]. Together, this would support *CLDN3* being a likely candidate for FJHN.

DENND4C

Whilst very little is known about the specific role of the DENN/MADD Domain Containing 4C (Dennd4C) protein encoded by *DENND4C*, it has been implicated as a guanine nucleotide exchange factor (GEF) for Rab10[327]. GEFs play a key role in the activation and regulation of specific Rab GTPases by facilitating the exchange of GDP for GTP[328,329]. Rab10 has been reported to be involved in the regulation of trafficking in polarised cells and Glut4 translocation in adipocytes[330,331]. Significantly, impaired trafficking of uromodulin *in vitro* has been shown to be a consistent result of *UMOD* mutations identified in FJHN patients[155,156]. This results in aggregation of mutant uromodulin in the ER, which has been hypothesised to ultimately reduce uromodulin polymers in the lumen and cause ER stress[150,155,156]. Thus, it was hypothesised Dennd4C may have a role in trafficking of uromodulin and may therefore by a likely candidate for FJHN.

FMOD

The fibromodulin protein, encoded by *FMOD*, is a small leucine-rich proteoglycan suggested to have a role in the assembly of the extracellular matrix due to its role in the inhibition of fibrillogenesis *in vitro* and its ability to interact with type I and II

collagen fibrils[332-334]. Furthermore, fibromodulin-deficient mice exhibited altered tail tendon morphology with fewer and abnormal collagen fibre bundles[335]. More recently, *FMOD* has also been implemented in tumourigenesis, with roles in angiogenesis[336]; association with glioma cell migration and consequently glioblastoma multiforme prognosis[337]; and overexpression of *FMOD* was identified in patients with B-cell chronic lymphocytic leukemia and mantle cell lymphoma, but not in patients with other haematologic malignancies[338]. No reports of a specific role of fibromodulin in the renal tubules or a renal phenotype in fibromodulin-deficient mice have been reported, thereby suggesting that *FMOD* is an unlikely candidate for FJHN.

MYO16

MYO16 encodes the unconventional myosin protein, myosin XVI, principally expressed in the brain during development[339]. It is thought to play a role in neuronal morphogenesis and catalytic targeting of the protein phosphatase 1 (PP1) during brain development[339,340]. Myosin XVI has been shown to be associated with phosphoinositide 3-kinase (PI3K) activation and the recruitment of the Wiskott-Aldrich syndrome protein family verprolin homology protein (WAVE) complex to within close proximity of PI3K[339,341,342]; as well as co-precipitating with the PP1 catalytic subunits 1α and 1Υ[339]. In line, with the reported neuronal role of myosin XVI, copy number variations encompassing a number of genes, including *MYO16*, have been reported in patients with neurodevelopmental disorders[343]. Much of the current literature implicates myosin XVI in the brain and neuronal tissues rather than the kidneys; and neurodevelopmental phenotypes are not associated with FJHN, therefore, suggesting *MYO16* is an unlikely candidate for FJHN.

PAX2

PAX2 encodes the paired box 2 DNA binding protein (Pax-2), required for renal tubule development[344,345]. Whilst expressed in the renal tubules, *PAX2* is also expressed in the developing ear, central nervous system, eye and urogenital tract[344-346]. Mutations in *PAX2* are associated with renal coloboma syndrome (RCS), an autosomal dominant disorder which is characterised by renal and ocular anomalies[347,348]. RCS exhibits both inter-and intra-familial variability, some of the more common and rare characteristics are detailed in Table 26[349-352].

Table 26. Clinical characteristics reported in patients with RCS

Typical ocular anomalies	Typical renal anomalies	Additional anomalies
Optic disc pits	Renal hypodysplasia	High frequency hearing loss
Optic nerve or retinal coloboma	Multicystic dysplastic kidney	Hyperuricaemia and gout
Morning glory anomaly	Oligomeganephronia	Horse shoe kidneys
	Renal insufficiency progressing to end-stage renal disease	Nephrolithiasis
	Vesicoureteral reflux	Ligamentous laxity
	Renal cysts	Central nervous system and neurological anomalies
		Microphthalmia
		Non-renal genitourinary anomalies

RCS is a phenotypically heterogeneous disorder characterised by renal and ocular anomalies. The most commonly reported renal and ocular anomalies in patients with RCS are shown, as are the less frequently reported clinical findings[349-352].

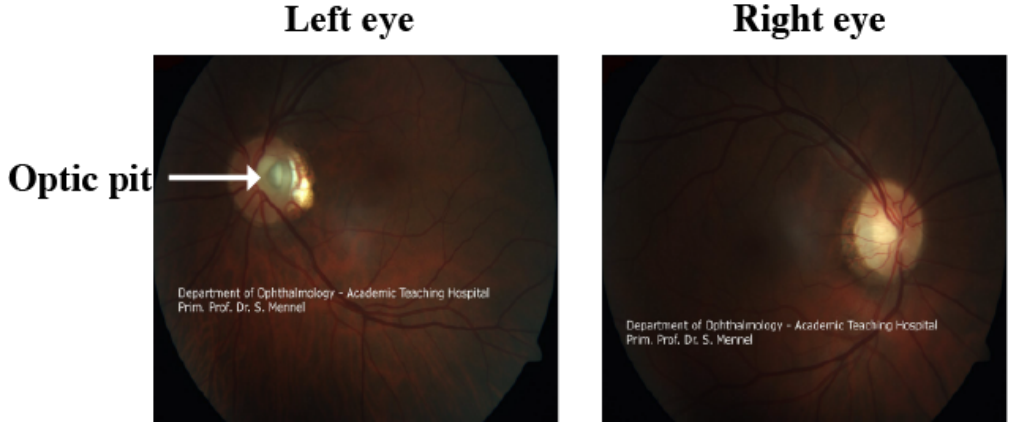
Hyperuricaemia and gout are not typical characteristics of RCS. However, there has been a reported case of a family with RCS due to a heterozygous c.567_569dup (Ile190ArgfsX85) mutation with ocular anomalies including dysplastic optic discs and renal anomalies such as hypoplastic kidneys, gout and ultimately kidney failure[351]. Furthermore, a variant affecting the Gly76 residue (also affected in the two probands) has previously been reported in a family with RCS (Gly76Ser), where optic disc dysplasia and renal failure caused by hypoplasia were reported in affected family members[353]. Consequently, this led us to hypothesise whether the probands with the

Gly76Arg Pax-2 variant in this study may have RCS with hyperuricaemia rather than FJHN.

8.2.3.2 A case of revised diagnosis of RCS in family 8 due to a Gly76Arg Pax-2 variant

As RCS is characterised by both renal and optic anomalies (Table 26), ophthalmological examinations of both brothers were performed by Dr Silvia Reichart and Prim Prof Dr Stefan Mennel of the Department of Ophthalmology, Akademisches Lehrkankenhaus, Feldkirch, Austria (Figure 59).

Figure 59. Identification of an optic pit in the left eye of proband II.1, family 8.



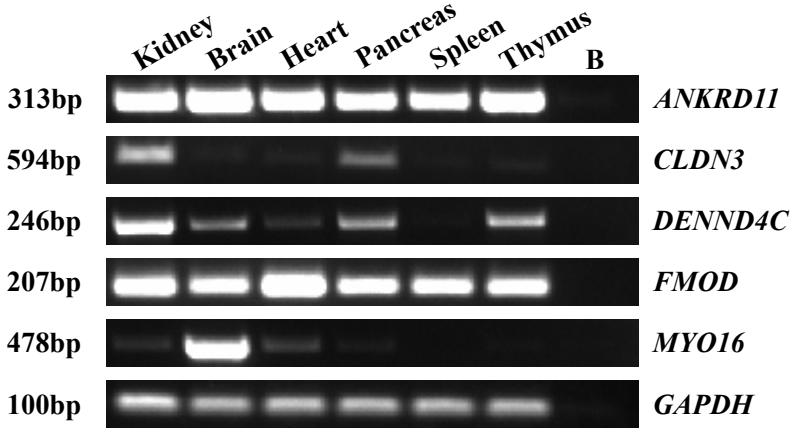
The presence of an optic pit in the left eye of proband II.1 from family 8 was identified by ophthalmological examination, highlighted by an arrow. Similarly, ophthalmologic examination of proband II.2 also revealed the presence of an optic pit (data not shown).

The presence of an optic pit was confirmed in the left eye of proband II.1 (Figure 59) and subsequently the presence of an optic pit was also identified in proband II.2 (data not shown). Examination of additional clinical details showed that proband II.1 had a renal biopsy performed in 1995, whereby a single glomerulus was observed, no further details were given; however, this could indicate oligomeganephronia in this patient. Additionally, whilst rare, hyperuricaemia and gout has also been reported in a family with RCS[351]. These findings resulted in the diagnosis being revised to RCS in this family.

8.2.3.3 Expression analysis

Qualitative RT-PCR analysis of each of the prioritised genes across a cDNA organ panel consisting of: kidney, brain, heart, pancreas, spleen and thymus, was performed to determine the expression of each gene within these tissues (Figure 60).

Figure 60. Qualitative RT-PCR expression analysis of prioritised genes across a control cDNA organ panel.



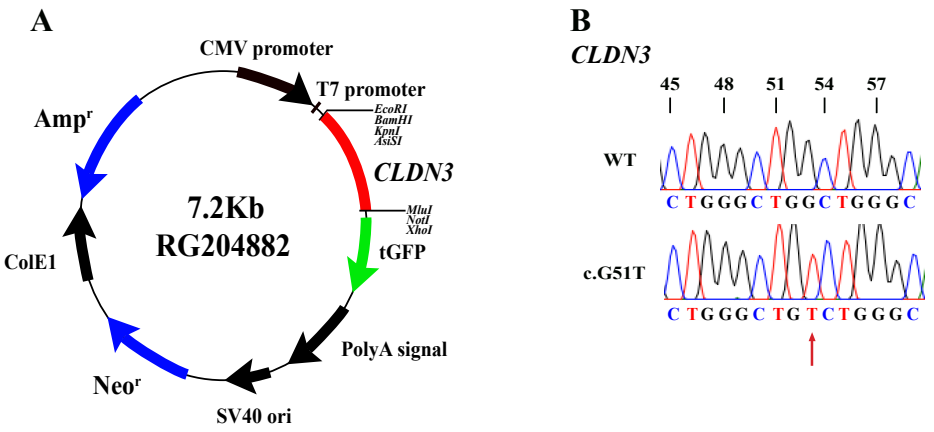
RT-PCR analysis of *ANKRD11, CLDN3, DENND4C, FMOD, MYO16* and the housekeeper *GAPDH* in cDNA from a panel of control human organ samples. The size of the PCR fragment is shown on the left. B, water blank.

RT-PCR analysis detected: *ANKRD11* expression in all of the organs tested, consistent with its role in the ubiquitous process of histone acetylation regulation[314,315]; *FMOD* expression was also detected in all of the organs tested, consistent with its ubiquitous role in the assembly of the extracellular matrix[332-334]; *CLDN3* expression in the kidney and pancreas and an absence of expression in the other organs tested; *DENND4C* expression in all organs tested except for the spleen; and *MYO16* was predominantly expressed in the brain, with relatively low levels of expression observed in the heart (Figure 60). All these findings are consistent with the data reported by the Human Protein Atlas[354-359]. From these combined analyses three genes (*CLDN3*, *DENND4C* and *PAX2*) were prioritised for further analysis.

8.2.3.4 Generation of WT and Trp17Cys claudin 3 stable cell-lines

To determine whether the Trp17Cys claudin 3 variant may be pathogenic, *in vitro* functional studies are required. *CLDN3* encodes the tight junction protein claudin 3 which is a major determinant of paracellular permeability[319]; therefore, studies of transepithelial resistance (TER), used to measure the integrity of tight junctions, can be performed to determine whether claudin variants impact paracellular permeability[360,361]. The MDCK cell line, an established kidney cell line for studying epithelia and TER due to their well characterised polarisation and cell junction formation, was used to generate cells stably expressing either WT (Trp17) or variant (Cys17) claudin 3[360,362] (Section 5.4.3.3). The vector encoding WT claudin 3 with a C-terminally tagged tGFP was obtained from Origene™ Technologies (RG204882) (Figure 61A) and SDM performed to generate a claudin 3 Cys17 variant construct. Sanger DNA sequencing was used to confirm the successful generation of the Cys17 claudin 3 construct (Figure 61B).

Figure 61. Confirmation and generation of WT and Cys17 claudin 3 expression vectors

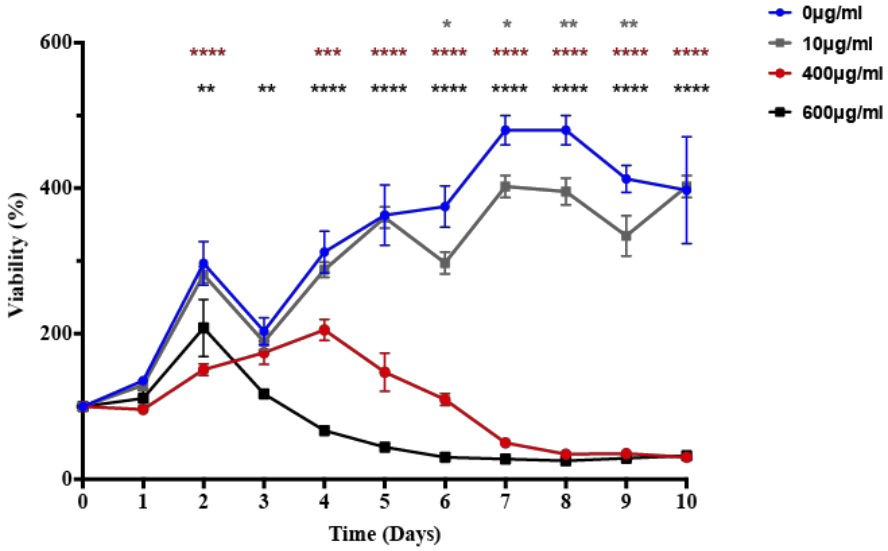


(A) Plasmid vector map of the 7.2Kb claudin 3 expression vector obtained from Origene™ Technologies (RG204882). *CLDN3* is located between the upstream CMV promoter and downstream tGFP tag. The plasmid also encodes two selective markers of antibiotic resistance: ampicillin for bacterial selection (amp^r) and neomycin for mammalian selection (neo^r). (B) Confirmation of the successful G-to-T site-directed mutagenesis at nucleotide c.51 was confirmed in the plasmid obtained from Origene™ Technologies (RG204882).

The RG204882 plasmid obtained from Origene™ Technologies also contains a neomycin cassette for selection in mammalian cells. This enables stable cell generation following transient transfection, by the addition of Geneticin®-selection media. Only those cells that express the neomycin cassette (and thus claudin 3) should survive in Geneticin®-selection media. To determine the optimal dose of Geneticin® (i.e. that which allows selection without killing the cells too rapidly), a kill curve was performed by incubating MDCK cells in different concentrations of Geneticin® (0-600μg/ml) (Figure 62). Untransfected MDCK cells were incubated with different concentrations of Geneticin® (0-600μg/ml) over a period of 10 days with the percentage of viable cells measured on each day using a CellTiter Blue cell viability assay. A dose of 10μg/ml Geneticin® did not reduce the viability, below 100%, of MDCK cells over 10 days, although it did result in a significant difference in the percentage of viable treated cells compared to untreated between days 6 and 9 (day 6 and 7 $p \leq 0.05$, day 8 and 9 $p \leq 0.01$, two-way ANOVA) (Figure 62). Incubation of cells with both 600 and 400μg/ml Geneticin® resulted in a decreased percentage of viable cells after 2 and 4 days respectively (Figure 62). Until this point the percentage of viable cells had been increasing in both cases, with the percentage of viable cells peaking at 208% on day 2 for cells incubated with 600 μg/ml Geneticin® and 205% on day 4 for cells incubated with 400μg/ml Geneticin® (Figure 62). The percentage of viable cells incubated with 600μg/ml Geneticin® was statistically significantly lower compared to untreated cells each day from day 2 (day 2 and 3 $p \leq 0.01$, days 4-10 $p \leq 0.0001$, two-way ANOVA) (Figure 62). Similarly, a statistically significant reduction in the percentage of viable cells treated with 400μg/ml Geneticin® was observed compared to untreated on day 2 and each day from day 4 onwards (day 2 and 5-10 $p \leq 0.0001$, day 4 $p \leq 0.001$, two-way ANOVA) (Figure 62). For cells treated with both

400 and 600µg/ml Geneticin® cell viability levels were reduced to their lowest point by day 10 and 8 respectively (30% and 25% respectively). Therefore, these results concluded that the optimum dose of Geneticin® for selection of transfected cells is 400µg/ml as this is the lowest dose at which cells are killed after 7-10 days incubation with the selection antibiotic (Geneticin®) (Figure 62).

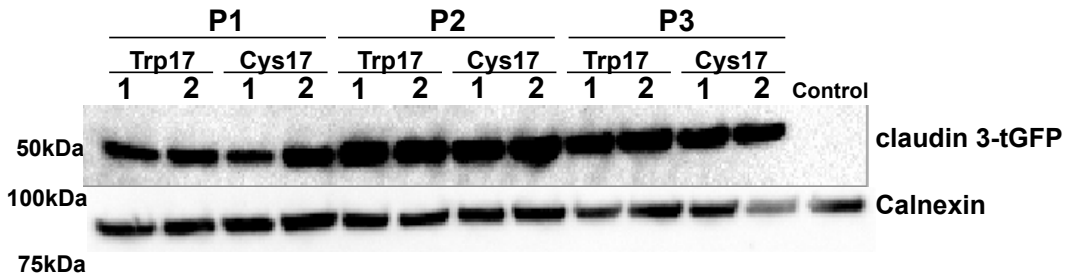
Figure 62. Viability of MDCK cells in response to Geneticin®



Dose response curve to measure the viability of MDCK cells to varying doses (0-600µg/ml) of Geneticin® over 10 days. The viability of MDCK cells was measured using the CellTitre-Blue® Cell Viability Assay (Promega). These studies demonstrated 400ug/mL was the optimal dose to treat MDCK cells with to select transfected cells. Statistical analysis was carried out using a two-way ANOVA. Untreated cells (0µg/ml) were used as a control for the statistical analyses. *p≤0.05, **p≤0.01, ***p≤0.001, ****p≤0.0001.

MDCK cells transfected with WT or Cys17 variant claudin 3 constructs were incubated with 400µg/ml of Geneticin® 24 hours post transfection, as described in Section 5.4.3.3, to generate stable cells. Clones were picked and re-plated in 6-well plates and expanded to larger volumes. This resulted in two clones of WT and two clones of the Cys17 variant claudin 3 MDCK stable cell-lines. To confirm the stable expression of claudin 3-tGFP, protein was extracted over three passages and Western blot analysis performed (Figure 63).

Figure 63. Overexpression of claudin 3 in MDCK cells



Western blot analysis of lysates from three passages (P1-3) of MDCK cells stably transfected with either WT (Trp17) or mutant (Cys17) tGFP-tagged claudin 3 and a control untransfected MDCK cell line. Two cell-lines were generated (1 and 2) for both the WT and variant Cys17 claudin 3 stable cell-lines. The housekeeper calnexin was used as a loading control.

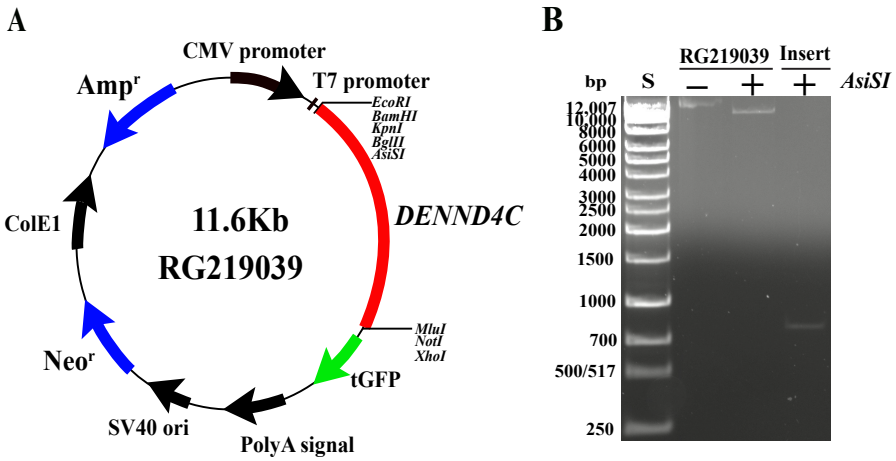
Western blot analysis confirmed stable overexpression of tGFP-tagged WT and mutant (17Cys) claudin 3 protein over multiple passages and absence in the control untransfected MDCK cells (Figure 63). Therefore, confirming that these cell-lines could be used for future functional studies to determine the potential pathogenicity of the claudin 3 Trp17Cys variant in FJHN.

8.2.3.5 Attempted generation of a full-length human WT Dennd4C expression vector

To determine the functional effect of the Ser1251Phe and Arg1317Gln Dennd4C variants *in vitro*, the generation of a vector encoding the full-length WT Dennd4C was attempted as described in Section 5.4.1.2. The RG219039 vector, made up of the pCMV6-AC-GFP vector encoding WT Dennd4C with a C-terminally tagged tGFP, was obtained from Origene™ Technologies (Figure 64A). However, sequencing analysis showed this vector did not encode the full-length Dennd4C protein (data not shown). Therefore, primers including an *AsiSI* restriction site were designed to amplify the absent region (708bp) using human kidney cDNA, resulting in a 740bp PCR product. The RG219039 vector and resulting PCR product were then digested with *AsiSI* (Figure 64B); and the products excised and ligated as described in Section 5.4.1.2. The

ligated products were subsequently used for the transformation of XL-10-Gold ultracompetent cells (Agilant) and confirmation performed by Sanger DNA sequencing (Section 5.4.1.12). However, this method was unsuccessful with none of the purified plasmids found to encode the full-length Dennd4C protein (data not shown). Therefore, a second method to generate a Dennd4C expression vector was used.

Figure 64. Attempted generation of a full-length Dennd4C-tGFP expression vector

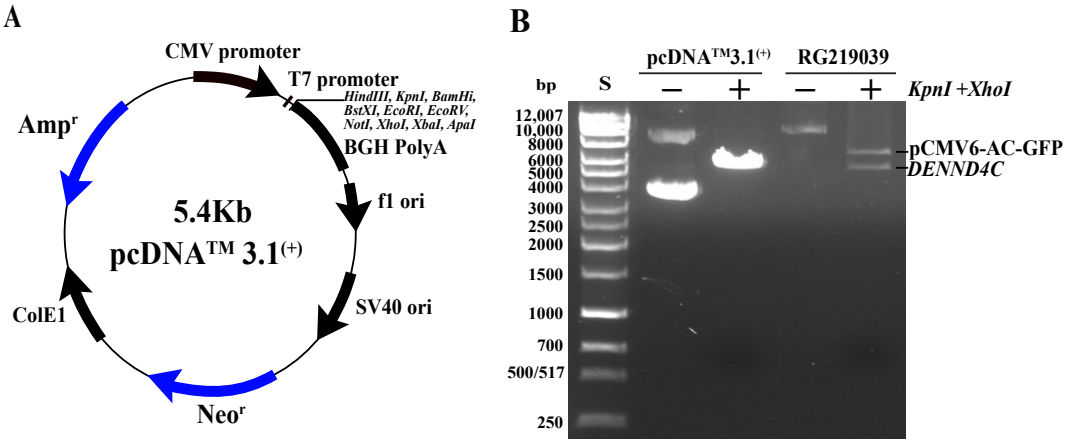


(A) Plasmid map of the pCMV6-AC-GFP mammalian expression vector, encoding the Dennd4C-tGFP fusion protein that was obtained from Origene™ and termed RG219039. The vector also encodes two selective markers: *Amp*^{r} and *Neo*^{r}, which confer resistance to the antibiotics ampicillin (for bacterial expression) and neomycin (for mammalian expression). Downstream of the CMV and T7 promoter is a multiple cloning site made up of a series of RE recognition sites, including *AsiSI*. (B) RED of the 11.6Kb RG219039 vector and 740bp *DENND4C* PCR product by *AsiSI* was performed to linearise the receiving vector and generate compatible ends prior to ligation. Digestion of the 11.6Kb RG219039 vector and 740bp PCR product resulted in single bands of 11.6kb and 715bp respectively.

As the transformation efficiency of the RG219039 vector was very low and protein tags such as GFP may interfere with the activity of the Dennd4C protein, sub-cloning of the incomplete *DENND4C* sequence (from RG219039) into the more efficient pcDNA™3.1$^{(+)}$ vector (Figure 65A), was attempted; with the aim that the absent 708bp of *DENND4C* cDNA would be subsequently inserted. Both the pcDNA™3.1$^{(+)}$

(Figure 65A) and RG219039 (Figure 64A) vectors were incubated with the REs *KpnI* and *XhoI*, linearising the pcDNA™3.1(+) vector and excising the *DENND4C* sequence from the pcMV6-AC-GFP vector (Figure 65B). The linearised pcDNA™3.1(+) vector and *DENND4C* sequence were then ligated and the products used to transform competent cells as previously described. However, this method also proved unsuccessful, with none of the purified plasmids found to encode the *DENND4C* sequence. Thus, *in vitro* functional analysis of the Dennd4C variants was not performed.

Figure 65. Attempted generation of a pcDNA™3.1(+)hDennd4C vector



(A) Plasmid map of the pcDNA™3.1(+) mammalian expression vector, encoding two selective markers: *Amp*^{r} and *Neo*^{r}, which confer resistance to the antibiotics ampicillin (for bacterial expression) and neomycin (for mammalian expression). Furthermore, downstream of the CMV and T7 promoter is a multiple cloning site made up of a series of RE recognition sites, including *KpnI* and *XhoI*. (B) RED digestion of the 5.4Kb pcDNA™3.1(+) and 11.6Kb RG219039 vector by *KpnI* and *XhoI* was performed to linearise the receiving vector (pcDNA™3.1(+)), resulting in a single band of 5.4Kb; to excise the human WT *DENND4C* cDNA from the pcMV6-AC-GFP vector (RG219039), resulting in two bands of 5061bp (*DENND4C*) and 6518bp (pCMV6-AC-GFP); and to generate compatible ends prior to ligation.

8.3. Discussion and future studies

FJHN is a genetically heterogeneous disorder, principally affecting the TAL, that is characterised by hyperuricaemia, reduced fractional uric acid clearance, gout and progressive renal insufficiency associated with interstitial fibrosis[140]. Four subtypes have been defined to date: *FJHN1* associated with mutations in *UMOD*[140]; FJHN2

associated with mutations in *REN*[146]; FJHN3 which has been mapped to chromosome 2p22.1-p.21.2[147]; and an atypical form of FJHN which is associated with mutations in *HNF1ß*[148]. *UMOD* mutations are the most common cause of FJHN reported to date, with approximately 40% patients reported to have FJHN1[147]. *UMOD*, encoding uromodulin, is expressed in the TAL and early DCT and is the most abundant protein in human urine, where it is predominantly present as a polymer[13,149-151]. Precursor uromodulin proteins undergo a series of post-translational modifications to generate the mature protein that is targeted to the apical membrane where it is subsequently secreted into the lumen by proteolytic cleavage[150,152-154]. The rate-limiting step in this process is the formation of disulphide bonds in the ER[152,153]. Commonly reported consequences of *UMOD* mutations include impaired trafficking and secretion of mature uromodulin, resulting in the aggregation and retention of mutant uromodulin in the ER, leading to ER stress[150,155,156]. Thus, indicating that ER stress due to retention of mutant uromodulin may be a key stage in the pathogenesis of FJHN1, although the precise mechanisms responsible remain to be determined[150,157]. Mutations in *UMOD, REN* and *HNF1ß* only account for 45% of mutations in patients[147] therefore, indicating a role for additional gene(s) in the pathogenicity of FJHN. This chapter covers the search for novel candidate genes for FJHN.

To identify novel candidate variants in FJHN, WGS was performed using nine probands (seven unrelated and two brothers) from eight families with FJHN, lacking mutations in *UMOD, REN* and *HNF1ß*. Despite FJHN3 being mapped to chromosome 2p22.1-p.21.2 in a previous study, which included families 2,3,5-7[147], initial bioinformatic analysis of WGS data prioritised 26 variants in 15 genes, none of which are located in the region identified. Subsequent analyses of the 26 variants identified

by WGS: including co-segregation studies, *in silico* analysis, literature searches for biological relevance and cDNA expression analysis, prioritised three genes (*PAX2, CLDN3* and *DENND4C*) for further study.

The *PAX2* gene was prioritised as the gene has previously been described to cause RCS, which is associated with similar phenotypes to FJHN. A Gly76Arg variant in *PAX2* was identified in probands II.1 and II.2 from family 8 and *in silico* analyses predicted the variant to be pathogenic. Pax-2, encoded by *PAX2*, has been shown to be important in the development of the renal tubules[339,341]. Furthermore, expression of *PAX2* has been reported in the developing ear, central nervous system, eye and urogenital tract[344-346]. This is analogous with the characteristics reported in RCS, which is associated with mutations in *PAX2*[347,348,350-352]. As renal and ocular anomalies such as optic disc pits and optic nerve colobomas are the hallmark features of RCS[349-352], ophthalmological examinations of both probands were performed and confirmed the presence of optic disc pits as shown in proband II.1, thus resulting in a revised diagnosis of RCS in this family (8). At the time of analysis, DNA samples were available for probands II.1 and II.2 only. However, more recently DNA samples were obtained for additional family members including the affected father, unaffected children of proband II.1 and an unaffected child from proband II.2. Co-segregation analysis, performed at the Academic Endocrine Unit, University of Oxford, by Dr Mark Stevenson, demonstrated that the *PAX2* Gly76Arg variant co-segregated with hyperuricaemia in the affected father and was absent from unaffected children (data not shown). These findings demonstrate the usefulness of NGS technologies, such as WGS, in establishing a definitive diagnosis in disorders with overlapping clinical characteristics, which significantly, may alter or impact the clinical management of

these patients. Unlike FJHN, ophthalmological management is recommended for RCS patients to prevent complications associated with retinal detachment[349,352]. Furthermore, whilst visual acuity in RCS patients may range from normal to significant visual impairment, it has been suggested that a reduction in visual acuity may be progressive over time[349,352], indicating a need for frequent ophthalmological examinations. As most *PAX2* mutations in RCS described to date affect DNA binding sites, future *in vitro* studies could examine DNA binding of this *PAX2* variant. This could include electropheric mobility shift assays to assess the ability of Pax-2 to bind the PRS4 oligonucleotide sequence, which has previously been shown to bind with Pax-2[363,364]. However, it has been previously reported that a G-to-A transition at nucleotide c.223, predicted to result in a missense amino acid substitution of a glycine for a serine at codon 75 (which corresponds to nucleotide c.226 and codon 76 in the human sequence), did not alter the DNA-binding properties of the murine Pax-2[365]. Instead they showed that this mutation resulted in a reduced ability of Pax-2 to transactivate a luciferase reporter gene (PRS4-luciferase), which may be as a result of reduced Pax-2 protein levels[365]. Therefore, the effect of the Gly76Arg variant on the protein levels and transactivation properties of Pax-2 could also be assessed using Western blot and luciferase reporter analysis, respectively.

A heterozygous Trp17Cys variant in *CLDN3* was identified in proband II.1 in family 5 by WGS. Co-segregation analysis showed that the variant co-segregated with FJHN in family 5 and combined *in silico* analysis predicted the variant to be pathogenic. Furthermore, the results of the literature search for biological relevance suggested *CLDN3* may be the most promising candidate for FJHN. Expression of *CLDN3* in the renal tubules is reported to be similar to that of *UMOD* and is localised to the distal

segments[13,149,151,322,323]. Expression of *CLDN3* and *UMOD* has been reported in the TAL and early DCT[13,149,151,323]; additionally, *CLDN3* has been shown to be expressed in the tAL, DTs and CD[322,323]. Whilst the precise function of uromodulin remains to be ascertained, one hypothesis is a role in water and electrolyte balance[13,149,150,366,367]. *CLDN3*, encoding the transmembrane protein claudin 3, plays a critical role in maintaining paracellular permeability as tight junctions of epithelial cells[319,323,368]. Furthermore, mutations in claudin family members *CLDN16* and *19* are associated with the progressive renal wasting of Mg^{2+} and Ca^{2+} leading to impaired renal function and chronic renal disease in FHHNC patients[137,324,325]. Of note, hyperuricaemia, a key characteristic of FJHN, has also been observed in the majority of FHHNC patients[136,137,324-326]. Thus, it was hypothesised that mutations in *CLDN3* may result in impaired paracellular transport in the renal tubules of FJHN patients.

The best methodology to investigate this would be TER assays. TER is an established method to study the integrity of tight junctions and the permeability across a cellular monolayer[361,369]. TER of MDCK cells stably expressing WT or Cys17 claudin 3 can be measured by culturing cells in a monolayer on permeable inserts (which are used to define a partition for apical and basolateral compartments) and taking electrical measurements using electrodes placed in the apical and basolateral compartments[361,369]. To do this, a voltohmmeter passes an alternating current between the two electrodes and measures the difference in voltage, allowing for the calculation of resistance across the monolayer[361,369]. By comparing the results generated for WT claudin 3–expressing cells with those generated for mutant Cys17 expressing cells one could determine the effect, of this variant on paracellular permeability, and thus use this data as an indicator of pathogenicity in FJHN.

TER studies would be best performed in cells in which the WT or variant claudin 3 protein was expressed in all cells and therefore it was decided that stable cell-lines would be required for these studies. MDCK cells were selected for the generation of cell-lines stably expressing claudin 3 proteins as these cells have previously been used to examine epithelial resistance as the cells polarise and form cell junctions[360,362]. A dose-response assay measuring the viability of untransfected MDCK cells incubated with increasing concentrations of Geneticin® revealed that 400µg/ml Geneticin® was the optimum dose for the selection of cells expressing the selective marker (and consequently claudin 3). Stable cell-lines were generated and overexpression of claudin 3-tGFP (WT and Cys17 variant) across a series of three passages was confirmed by Western blot analysis. Therefore, Section 8.2.3.4 describes the successful generation of the Cys17 claudin 3 expression vector and stable claudin 3 cell-lines that can be used for future functional studies of TER; and consequently, to determine whether the Trp17Cys *CLDN3* variant has a role in the pathogenicity of FJHN.

DENND4C was initially highlighted as a promising potential candidate due to two heterozygous variants, Ser1251Phe and Arg1317Gln, both located in exon 22, co-segregating with FJHN in family 6 and 7, respectively. However, the combined *in silico* analysis which predicted the Ser1251Phe variant to be of unknown significance and the Arg1317Gln to be likely pathogenic, was inconclusive. A literature search for biological relevance revealed that whilst little data is available regarding the precise function of Dennd4C in the renal tubules, it may have a role in trafficking via Rab10 [327,330,331,370]. Significantly, impaired maturation and secretion of uromodulin *in vitro* has been shown to be a consistent result of *UMOD* mutations identified in FJHN

patients[155,156]. This results in aggregation of mutant uromodulin in the ER, which has been hypothesised to ultimately reduce uromodulin polymers in the lumen and cause ER stress[150,155,156]. Few publications are available describing the specific role of Dennd4C, however, it has been reported to be a GEF for the GTPase Rab10[327,370]. Rab10, is a ubiquitously expressed Rab protein; which unlike most of the Rab family, appears to have diverse functions and subcellular localisations with roles in both endocytosis and exocytosis[371]. One of the earliest reported functions of Rab10 was its role in polarised transport in epithelial cells, where it has been reported to localise with the trans-Golgi network and endosomes, which are accessible to both the apical and basolateral recycling pathways[331,371]. More recently, Rab10 has also been suggested to play a role in the morphology and dynamics of the ER[371]. Mutations in *UMOD*, lead to ER stress[155,156]. Thus, *DENND4C* mutations could cause similar defects as *UMOD* mutations. Given these findings, it was hypothesised Dennd4C may have a role in trafficking of uromodulin by acting as a GEF for Rab10. Thus, future studies would use Western blot analysis of cultured cell media to detect the amount of mature (approximately 97kDa) and immature (approximately 84kDa) uromodulin secreted into the cell media, from cells expressing the Dennd4C mutations[155]. Furthermore, immunofluorescence studies and confocal microscopy[155] would be used to determine whether uromodulin was localised to the ER or plasma membrane respectively in cells expressing WT uromodulin and either WT or variant Dennd4C. A previous study used these methods to investigate the effect of a range of different *UMOD* mutations on trafficking, maturation and secretion of uromodulin[155], and one of these previously studied mutant *UMOD* constructs would be used as a positive control.

Attempts were made to generate full-length Dennd4C expression vectors for use in these studies; however, these were unsuccessful. Therefore, future studies could instead investigate whether knock-down of endogenous *DENND4C* expression, using shRNA, has any effect on the expression, maturation and secretion of uromodulin. Whilst, this may indicate whether Dennd4C has a role in the maturation, trafficking and secretion of uromodulin it does not determine the specific impact the Ser1251Phe and Arg1317Gln Dennd4C variants may have. Therefore, if the shRNA studies were to indicate a role for Dennd4C in FJHN, cell-lines expressing CRISPR-Cas9- or TALEN-induced Ser1251Phe or Arg1317Gln Dennd4C mutations could be generated for further analysis.

In conclusion, two novel candidate genes for FJHN (*CLDN3* and *DENND4C*) were identified for three of the families analysed in this study (families 5-7). MDCK cells stably expressing WT or Cys17 claudin 3 have been generated for future *in vitro* functional studies to confirm or reject a role for *CLDN3* in the pathogenicity of FJHN. Notably, for four of the families (families 1-4) included in this study no candidate gene was identified. None of the variants prioritised in the initial bioinformatic analysis were found to co-segregate in these families. Thus, further studies and a re-analysis of the data generated by WGS of these probands is required to identify new candidates for FJHN in these families. Finally, identification of the Gly76Arg *PAX2* variant in the two probands in family 8 resulted in the revised diagnosis of RCS in this family, highlighting the usefulness of NGS techniques such as WGS in the establishment of correct diagnoses in the clinic, especially for disorders with overlapping clinical characteristics. Ultimately, this aids with genetic testing of patient's families and the clinical management of patients.

9 Identification of rare *KLOTHO* variants in patients with familial hypocalciuric hypercalcaemia (FHH)

FHH is a genetically heterogeneous disorder of Ca^{2+} homeostasis, with three subtypes identified to date: FHH1, 2 and 3 due to heterozygous LOF mutations in the CaSR encoded by *CASR*[183], $G\alpha_{11}$ encoded by *GNA11*[184] and AP-2 sigma subunit encoded by *AP2S1*[185], respectively. However, mutations in *CASR*, *GNA11* and *AP2S1* have only been identified in a approximately f75% of FHH patients, with mutations in *CASR* alone being identified in 65% of patients[183-186,372], thus indicating a role for additional gene(s) in the pathogenesis of FHH. This chapter describes the search for candidate gene(s) in patients with FHH, lacking mutations in *CASR, GNA11* and *AP2S1.*

9.1. Declaration of contributions

The work in this chapter is my own, unless otherwise stated. WES and Illumina TSCA sequencing was performed at the WTCHG, Oxford. Bioinformatic analysis of WES data was performed by Dr Alistair Pagnamenta at the WTCHG, Oxford and Dr Sian Piret at the Academic Endocrine Unit, University of Oxford. Sanger DNA sequencing of prepared DNA pellets was performed at the Department of Zoology, University of Oxford.

9.2. Results

9.2.1 Patient characteristics

WES was performed using DNA samples, from five unrelated patients diagnosed with FHH, lacking mutations in *CASR, GNA11 and AP2S1*. The available clinical and biochemical details for these patients are summarised in Table 27, all patients were hypercalcaemic with inappropriately normal PTH. TSCA sequencing was performed using DNA samples from an additional 70 unrelated FHH patients lacking mutations in *CASR, GNA11 and AP2S1.* As limited clinical and biochemical details, aside from a

clinical diagnosis of FHH, were available, any additional clinical details for these patients are discussed in Section 9.2.3.

Table 27. Clinical and biochemical details of the FHH probands for whom WES was performed

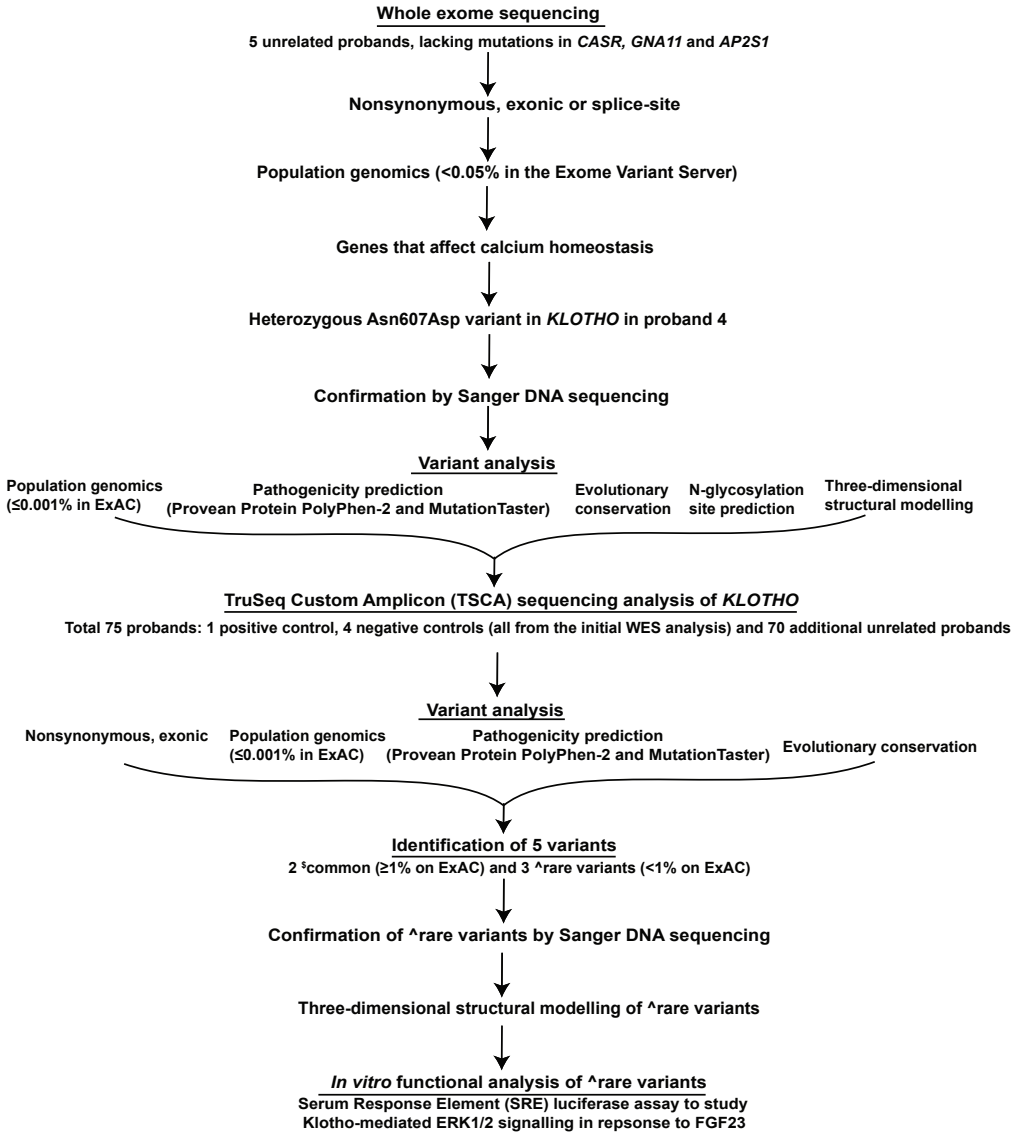
Patient ID	Serum					UCCR	Family history
	Adjusted Ca^{2+} (mmol/L) *2.2-2.6	Pi (mmol/L) *0.7-1.4	Creatinine (µmol/L) *40-130	ALP (U/L) *30-130	PTH (pmol/L) * 1-7	*>0.02	
1	2.75	0.65	88	141	4.4	0.008	Son diagnosed with hypercalcaemia/primary hyperparathyroidism aged 36
2	3.05	0.9	88	Not known	4	Not known	Son affected
3	2.82	Not known	98	Not known	<5	0.004	Yes, but not known which relatives are affected
4	2.99	0.7	79	105	6.7	0.013	Newborn son also hypercalcaemic
5	2.72	Not known	Not known	Not known	4.7	0.005	No

Clinical and biochemical details of the five FHH patients, whose DNA was used for WES. Abbreviations: ALP, alkaline phosphatase activity; PTH; UCCR, urinary Ca^{2+}:creatinine ratio. *Denotes normal ranges: adjusted Ca^{2+}2.2-2.6mmol/L[373]; Pi 0.7-1.4mmol/L[373]; creatinine 40-130µmol/L[373]; ALP 30-130U/L[373]; PTH 1-7pmol/L[373]; and UCCR >0.02[373].

9.2.2 Identification of an Asn607Asp variant in Klotho in a patient with FHH

Initial bioinformatic analysis of WES data was performed by Dr Alistair Pagnamenta at the WTCHG, Oxford and Dr Sian Piret at the Academic Endocrine Unit, University of Oxford and included: variant type, population genomics (vAF <0.05% in the EVS[239]) and biological relevance (genes that affect Ca^{2+} homeostasis) (Figure 66). Analysis of population genomics was performed using the EVS in the initial bioinformatics analysis, as this was performed prior to the public release of the ExAC browser (October 2014). This resulted in the identification of an Asn607Asp variant in *KLOTHO* in patient 4, which was not reported on the EVS or 1000 Genomes database and is known to play a role in the regulation of Ca^{2+} homeostasis. Secondary *in silico* analysis, performed in 2015 and 2017 also included population genomics using ExAC.

Figure 66. Flowchart of the process of identification and analysis of a candidate gene for FHH



Flowchart showing the process from WES to functional analysis for the candidate gene: *KLOTHO*, in FHH. WES was performed using the DNA of five unrelated individuals with FHH, lacking mutations in *CASR*, *GNA11* and *AP2S1*. Variants were filtered based on mutation type population genomics (EVS[239] and 1000 Genomes database[238]) and biological context. An Asn607Asp variant in *KLOTHO* was identified in one patient and further *in silico* analysis was performed including: population genomics (ExAC), prediction of functional effects (MutationTaster, PolyPhen-2 and Provean Protein), evolutionary conservation (eight orthologs) and prediction of N-glycosylation sites. The variant was confirmed in patient 4 by Sanger DNA sequencing. Illumina TSCA seuqencing of *KLOTHO* was performed using the DNA of 75 unrelated patients with FHH, lacking mutations in *CASR*, *GNA11* and *AP2S1*, including patient 4, to act as a positive control and patients 1-3 and 5, to act as negative controls. Variant analysis included: mutation type, population genomics (ExAC), prediction of functional effects (MutationTaster, PolyPhen-2 and Provean Protein) and evolutionary conservation (eight orthologs). An additional, five nonsynonymous exonic variants were identified in 32 patients. Two were $common, with vAFs ≥1% reported on ExAC and three were ^rare, with vAFs <1% reported on ExAC. ^Rare *KLOTHO* variants were prioritised for *in vitro* functional analysis using a SRE reporter assay to investigate the effect of *KLOTHO* variants on signalling in response to FGF23.

KLOTHO encodes the type I membrane bound protein, Klotho, which has been shown to be predominantly expressed in the DTs, the parathyroid and the choroid plexus of the brain[38,374,375]. However, Klotho expression has also been reported in a range of additional tissues such as the muscular artery, pituitary gland, PTs, testis, ovary and pancreas[374-376]. *KLOTHO* was originally named after the Greek Fate Clotho who spun the thread of life due to the aging-related phenotypes observed in *Klotho*-deficient mice[374] (Table 28); and the rescue of these phenotypes by overexpression of *Klotho*[374]. A homozygous His193Arg mutation in *KLOTHO* was identified in a patient with tumoral calcinosis (TC), designated TC-3, which is typically characterised by the development of often severe calcifications in soft tissues and hypherphosphataemia[377] (Table 28). The phenotypes of proband 4 (FHH), the TC-3 patient and four mouse models of Klotho deficiency, each due to different homozygous LOF mutations in *Klotho,* including a severe *Klotho* hypomorph due to the insertion of a transgene in the 5' upstream region of the *Klotho* gene (*kl/kl*)[374,378]; a *Klotho* null mutant ($kl^{-/-}$) due to a deletion in exon 1[379]; a partial deletion of Klotho in DT segments (*Ksp*-$kl^{-/-}$)[380]; and a point mutation resulting in a premature stop codon ($kl^{203*/203*}$)[381], are detailed in Table 28. The $kl^{604Asn/604Asn}$ mouse model reported in the same study as the $kl^{203*/203}$ mouse was not included as the study focused its phenotypic examination on the $kl^{203*/203}$ model[381]. Many of the phenotypes reported can be attributed to disturbances in Ca^{2+} and Pi homeostasis[374], hyperphosphataemia was observed in all four mouse models, as well as the TC-3 patient[374,377-380] and hypercalcaemia was also observed in the majority of cases, with the exception being mice harbouring a DT partial deletion of *Klotho* and $kl^{203*/203*}$ mice[381]. Elevated serum levels of $1,25(OH)_2D_3$, ectopic calcifications, skeletal anomalies and characteristics of premature ageing were reported in the TC-3 patient, both mouse models harbouring

system-wide Klotho deficiencies[374,377-379] and *kl*$^{203*/203*}$ mice[381]. These findings were not reported in the FHH proband 4 or mice harbouring a DT partial deletion of *Klotho* (Table 28)[380].

The multi-organ characteristics observed in Klotho-deficient mice and the TC-3 patient may be attributed to the ability of Klotho to act both locally and systemically through the generation of multiple forms of Klotho. In its full-length form, Klotho is a 135kDa type I membrane-bound protein consisting of an extracellular domain comprised of 2 glycosidase 1 domains (KL1 and 2), a transmembrane domain and a cytoplasmic domain[382] (Figure 67). Secreted and shed forms of Klotho have also been shown to be generated by alternative splicing in exon 3 (approximately 65-70kDa) and proteolytic cleavage of membrane-bound Klotho by A Disintegrin And Metalloproteinase (ADAM) 10 and 17 at two cleavage sites (α1 and α2), generating 130- and 68-kDa Klotho proteins, respectively[382-384] (Figure 67). However, the functional roles of each form of Klotho remain to be elucidated. In humans the secreted form is thought to predominate, whilst the opposite has been reported in mice[382,385], which may, in part, be responsible for the differences in phenotypes observed between mouse models of Klotho and the human TC-3 and FHH patients.

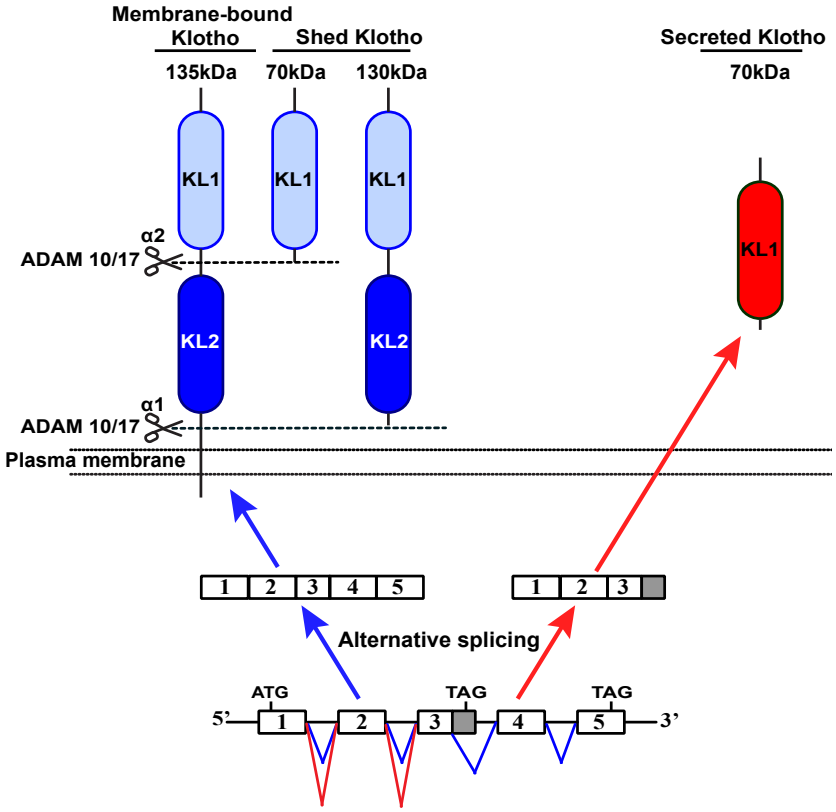
As well as roles in ageing, Klotho plays a role in the regulation of Ca^{2+}, Pi, PTH and $1,25(OH)_2D_3$[35,36]. Two main mechanisms have been identified to date: facilitating signalling of the endocrine FGF23 via FGFRs[35] (Section 4.1.1.2); and regulation of the levels of the Ca^{2+} channel TRPV5 at the apical membrane of DT cells[68] (Section 4.1.5.5).

Table 28. Comparison of the phenotypes of FHH patient 4, tumoral calcinosis-3 and mice harbouring LOF *Klotho* mutations

Parameter		Human disease		Mouse models			
		FHH (proband 4)	**Familial tumoral calcinosis-3[377]**	**Hypomorph (*kl/kl*)[374,378]**	**Null (*kl*$^{-/-}$)[379]**	**Distal-tubular partial deletion (*Ksp-kl*$^{-/-}$)[380]**	**Point mutation (*kl*$^{203*/203*}$)[381]**
***KL* mutation**		Heterozygous Asn607Asp (exon 4)	Homozygous His193Arg (exon 1)	Homozygous insertional mutation of a transgene	Homozygous knock-out (deletion in exon 1)	Homozygous exon 2 deletion	Homozygous Gln203* (exon 1)
Plasma/ serum	Pi	Normal	Hyperphosphataemia	Hyperphosphataemia	Hyperphosphataemia	Hyperphosphataemia	Hyperphosphataemia
	Ca^{2+}	Hypercalcaemia	*Hypercalcaemia	Hypercalcaemia	Hypercalcaemia	Normal	Normal
	PTH	Normal	*Elevated	Reduced	Not reported	Reduced	Not reported
	FGF23	Not reported	Elevated	Not reported	Not reported	Elevated	Elevated
	$1,25(OH)_2D_3$	Not reported	Elevated	Elevated	Elevated	Normal	Elevated
	ALP	Normal	Normal	Not reported	Not reported	Not reported	Elevated
	Creatinine	Normal	Normal	Normal	Not reported	Not reported	Not reported
Calcifications		Not reported	Severe vascular, cranial and soft tissue calcifications.	Vascular and soft-tissue calcifications.	Soft-tissue and epiphysis calcifications.	None	Extensive aortic calcification, leading to vessel occlusion; parenchymal renal calcification; pulmorary calcification; and calcification of the auditory ossicles.
Skeletal anomalies		Not reported	Diffuse osteopenia, patchy sclerosis in the hands, feet, long bones and calcariae.	Osteoporosis	Reduced bone density and malformation of bones.	Not reported	Reduced bone mineral content and density; osteopenia; shortened femora; kyphoscoliosis; and irregular widended ribs.
Additional characteristics of premature ageing		Not reported	None	Growth retardation, reduced lifespan, hypokinesis, gait disturbance, emphysema and atrophy of skin, genital organs and thymus.	Growth retardation, reduced life-span.	Not reported	Growth retardation, reduced life-span, skin atrophy; and a negative preyer reflex, indicating a hearing deficit.
Other		Not reported	Not reported	Abnormalities in the pituitary gland and hypoglycaemia.	Not reported	Not reported	Females had hypoglycaemia, whereas males were hypoalbuminaemic.

Overview of the phenotypes observed in the FHH proband 4, in whom WES identified a heterozygous Asn607Asp variant in *KLOTHO*; the patient with tumoral calcinosis-3 (TC-3), in whom a homozygous His193Arg variant was identified in *KLOTHO*; and four mouse models, each harbouring different homozygous LOF mutations in *Klotho*: a severe *Klotho* hypomorph due to the insertion of a transgene in the 5' upstream region of the *Klotho* gene (*kl/kl*)[374,378]; a *Klotho* null mutant (*kl*$^{-/-}$) due to a deletion in exon 1[379]; a partial deletion of Klotho in DT segments (*Ksp-kl*$^{-/-}$)[380]; and a homozygous point mutation in exon 1 (*kl*$^{203*/203*}$)[381]. ALP, alkaline phosphatase. *Ca^{2+} and PTH levels were normalised in the TC patient after a subtotal parathyroidectomy due to the identification of a 4-gland hyperplasia[377]. Hyperphosphataemia was observed in all mouse models and the TC-3 patient. Hypercalcaemia was observed in the majority of cases, the exceptions being *ksp-kl*$^{-/-}$ mice and *kl*$^{203*/203*}$ mice. Elevated $1,25(OH)_2D_3$ and ectopic calcifications were reported in the TC-3 patient, both mouse models harbouring system-wide klotho deficiencies and the *kl*$^{203*/203*}$ mouse model. Serum $1,25(OH)_2D_3$ levels were not measured in the FHH proband 4 and no calcifications were reported. Varying levels of skeletal anomalies and characteristics of premature aging were reported in the TC-3 patient, the two mouse models of system-wide Klotho deficiencies and the *kl*$^{203*/203*}$ mouse model. These findings were not reported in the FHH proband 4 or mice harbouring a DT partial deletion of *Klotho*.

Figure 67. Schematic representation of the generation of multiple Klotho forms



Multiple forms of Klotho exist due to alternative splicing in exon 3 of the *KLOTHO* transcript and protein ectodomain shedding by A Disintegrin And Metalloproteinase (ADAM) 10 and 17[382]. Studies have identified two *KLOTHO* transcripts arise from alternative splicing, one of which encodes a single-pass membrane-bound protein comprising an N-terminal signal sequence, a putative extracellular domain with two internal repeats (KL1 and KL2), a single membrane-spanning region and a short intracellular domain[382]. The second transcript was identical to the membrane-bound form, with the exception of a 50bp insertion at the end of exon 3, which was found to contain an in-frame premature stop codon[382]. This encodes a secreted truncated Klotho protein, which lacks the second internal repeat of the extracellular domain (KL2), the transmembrane domain and the intracellular domain[382]. Additionally, shed forms of Klotho, generated by proteolytic cleavage of membrane-bound Klotho by ADAM10 and 17 have been described[383,384]. Two cleavage sites in Klotho have been identified (α1 and 2), α1 is located close to the juxtamembrane region and α2 is located between the KL1 and 2 domains[383]. Adapted from Chen et al.,[383].

9.2.2.1 Confirmation and in silico analysis of the Asn607Asp variant in Klotho in a patient with FHH

As Klotho plays an important role in Ca^{2+} and Pi homeostasis, the Asn607Asp variant in Klotho was prioritised for further analysis by Sanger DNA sequencing (Figure 68). The variant was first confirmed by Sanger DNA sequencing.

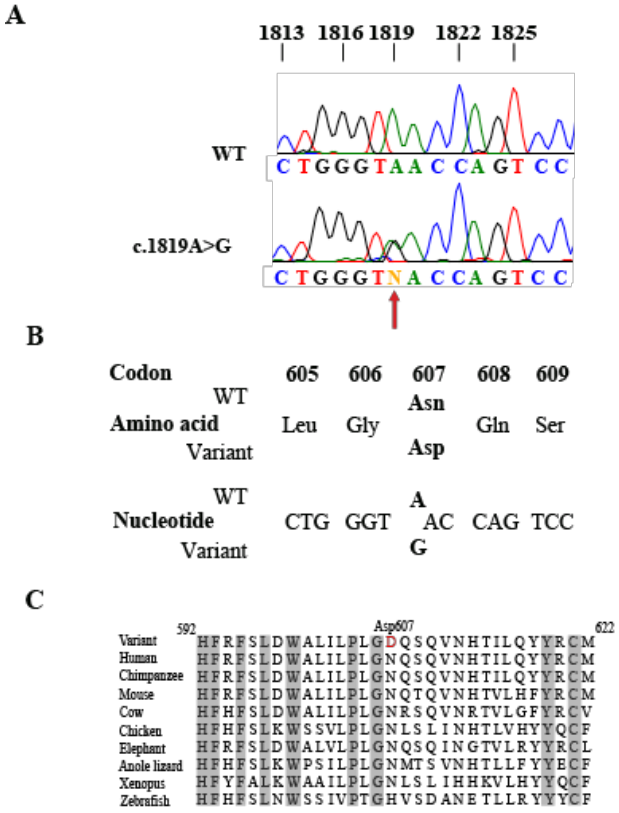
Table 29. *In silico* analysis of an Asn607Asp variant in Klotho, identified in a patient with FHH

Nucleotide change	Amino acid change	Patient ID	^Reported vAF	MutationTaster	PolyPhen-2	Provean Protein	Evolutionary conservation	Combined *in silico* prediction
c.1819A>G	*p.Asn607Asp	4	0.00082%	Disease causing	Benign (score 0.019)	Neutral (score -1.085)	Conserved (7/8)	Likely pathogenic

In silico analysis of the Asn607Asp variant in Klotho identified in patient 4 by WES. *^Reported on ExAC[236]. The ^reported vAF 0.00082% represents an allele count of 1/121278 and therefore one heterozygous individual. Three publically available online software, accessed September 2015, were used to predict the functional effect of variants: MutationTaster[240], PolyPhen-2[242], and Provean Protein[225,241]. Eight orthologous protein sequences were used to assess the degree of evolutionary conservation of the affected amino acid residue: chimpanzee, mouse, cow, chicken, elephant, anole lizard, xenopus and zebrafish. Multiple sequence alignment of residues surrounding the human residue of interest was performed using Clustal Omega[247], accessed September 2015 and May-July 2018. Variants were classified as conserved (≥6/8), partially conserved (3-5/8) or not conserved (≤2/8). A prediction of pathogenicity was made using a combined *in silico* analysis approach as described in Section 6.2.9.4 using the data generated from population genomics, prediction of functional effects and conservation analysis. *Indicates a possible major amino acid change e.g. substitution of an uncharged amino acid for a charged amino acid.

Sanger DNA sequencing confirmed the presence of a heterozygous A-to-G transition at nucleotide 1819 in patient 4 with FHH. This A-to-G transition (AAC to GAC) is predicted to result in a missense amino acid change from asparagine to aspartic acid at codon 607 of the Klotho protein. No samples were available from relatives to assess the inheritance of the variants. *In silico* analysis was performed as detailed in Section 6.2.9.4. Analysis of population genomics revealed the Asn607Asp variant had a reported vAF of 0.00082% on ExAC (which represents just one heterozygous individual in the ExAC cohort) (Table 29); and is lower than the 0.001% cut-off suggested in Section 6.2.9.1, therefore suggesting this variant may be pathogenic in FHH. Furthermore, this is lower than the estimated prevalence of FHH (1 in 78,000 in the west of Scotland [0.001%])[386]. The functional effect of this variant was predicted to be benign by two of the three prediction tools (PolyPhen-2 and Provean Protein) and disease causing by MutationTaster, therefore overall this variant was predicted to be probably benign (Table 29). Evolutionary conservartion of the WT asparagine residue in 8 orthologs (chimpanzee, mouse, cow, chicken, elephant, anole lizard, xenopus and zebrafish) showed that it is conserved (7/8) suggesting this variant may be pathogenic (Figure 68). Thus, overall, the Asn607Asp variant was predicted to be likely pathogenic (Table 29).

Figure 68. Confirmation of an Asn607Asp variant, in Klotho in a patient diagnosed with FHH

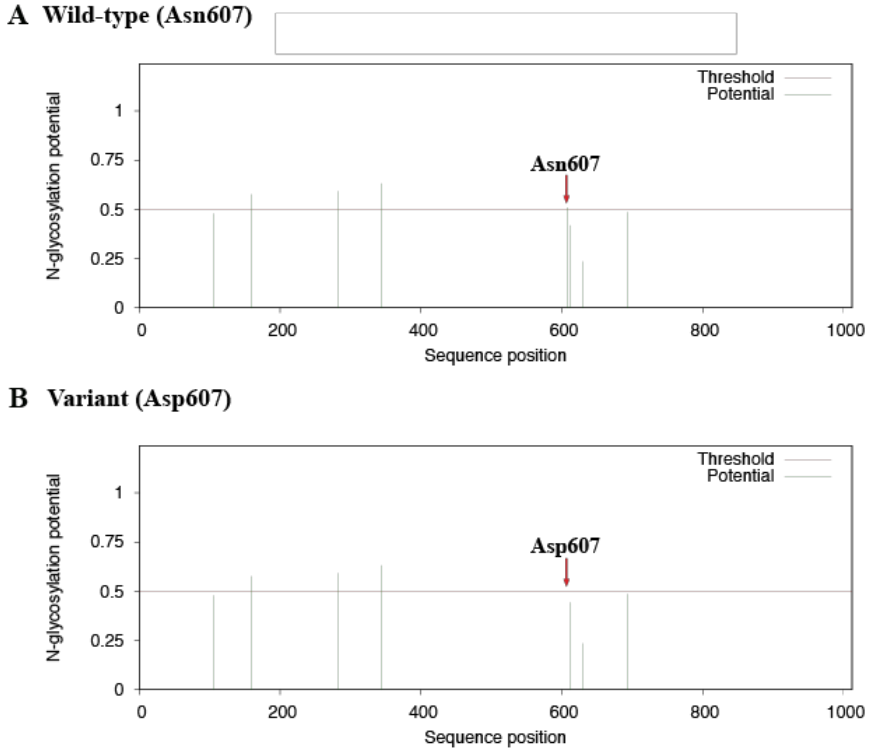


In silico analysis of the Asn607Asp Klotho variant identified in patient 4 by WES. (A) A heterozygous A-to-G transition at nucleotide c.1819 was identified in patient 4 within the FHH cohort (N=5). (B) This A-to-G transition (AAC to GAC) is predicted to result in a missense amino acid change from asparagine (ASN) to aspartic acid (Asp) at codon 607 of the Klotho protein. (C) Multiple sequence alignment of residues surrounding the human Asn607 residue of the Klotho protein sequence in eight orthologs using Clustal Omega[247], accessed September 2015 and May 2018. The Asp607 residue identified in the proband is shown in red. Residues conserved across all of the orthologs studied are highlighted in grey, the Asn607 residue was conserved across seven of the eight orthologs. Codon numbers are displayed for the human sequence.

Asparagine residues are often involved in glycosylation and the Academic Endocrine Unit, University of Oxford has previously been involved in describing a Klotho mouse model with mutation of an Asn residue that affects N-glycosylation (Ile604Asn)[381]. N-glycosylation is an important post-translational modification that has been shown to be important for processes such as protein folding and stability, ER-to-Golgi trafficking, apical sorting and quality control[255]. To assess the effect of the Asn607 Klotho variant on glycosylation the NetNGlyc 1.0 server was used to predict potential

N-glycosylation sites (Figure 69). In total, four sites were predicted to be N-glycosylated in the WT sequence, including Asn607 (0.51) (Figure 69A), as their N-glycosylation potentials were above the threshold (0.5). The other three sites were: Asn159 (0.58), Asn283 (0.59) and Asn344 (0.63) (Figure 69A). Furthermore, the Asp607 variant was predicted to result in the loss of this N-glycosylation site (Figure 69B). Therefore, these results predict loss of an N-glycosylation site and support the potential pathogenicity of this.

Figure 69. The rare Klotho variant, Asn607Asp, is predicted to disrupt an N-glycosylation site

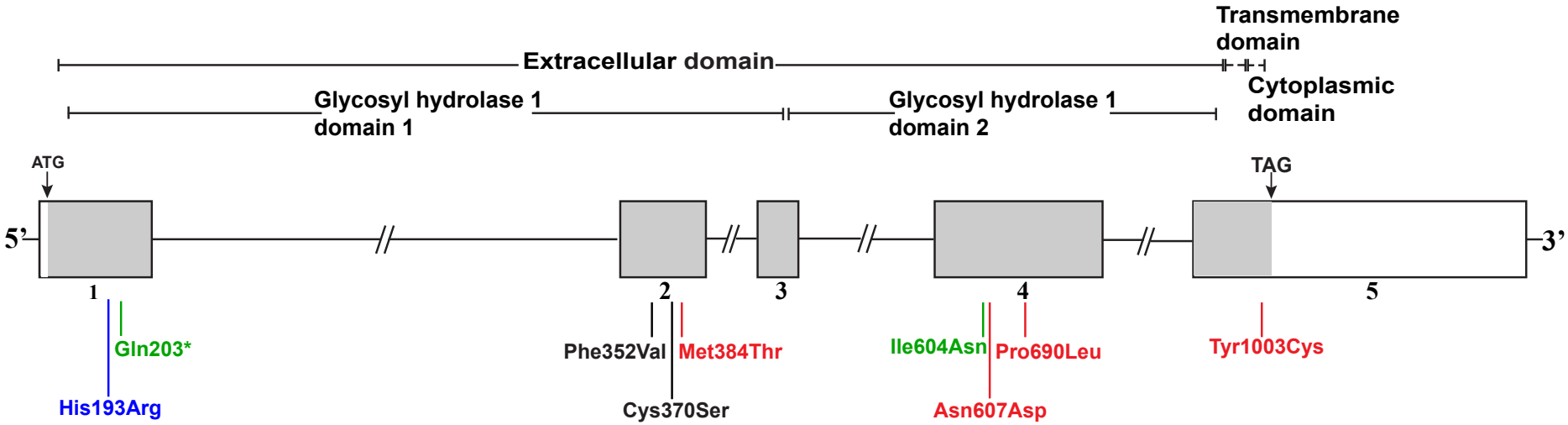


N-glycosylation site predictions were made using the NetNGlyc 1.0 server. If the N-glycosylation potential is greater than the threshold (0.5), sites are predicted to be glycosylated and if the potential is below the threshold (0.5) sites are predicted to not be glycosylated[256]. (A) The potential N-glycosylation sites present in the WT (Asn607) protein sequence and their averaged N-glycosylation potential scores. The following sites are predicted to be N-glycosylated: Asn159 (0.58), Asn283 (0.59), Asn344 (0.63) and Asn607 (0.51). The following sites are predicted to not be N-glycosylated: Asn106 (0.48), Asn612 (0.42), Asn630 (0.24) and Asn694 (0.49). (B) The potential N-glycosylation sites present in the variant (Asp607) protein sequence and their averaged N-glycosylation potential scores. The following sites are predicted to be N-glycosylated: Asn159 (0.58), Asn283 (0.59) and Asn344 (0.63). The following sites are predicted to not be N-glycosylated: Asn106 (0.48), Asn612 (0.44), Asn630 (0.24) and Asn694 (0.49).

9.2.3 Identification of three additional rare nonsynonymous Klotho variants in patients with FHH by Illumina TSCA analysis

To further study *KLOTHO* as a candidate gene for the pathogenicity of FHH, TSCA sequencing was performed using DNA samples, from 70 additional unrelated patients diagnosed with FHH and lacking mutations in *CASR, GNA11 and AP2S1,* as well as patient 4 as a positive control and patients 1-3 and 5 as negative controls. Limited clinical and biochemical, aside from a clinical diagnosis of FHH, were available for these patients (appendix, Table 49); therefore, additional clinical details, where available, for patients who were found to have rare nonsynonymous exonic *KLOTHO* variants, are given in Section 9.2.3.1 to 9.2.3.3. TSCA sequencing analysis identified two common nonsynonymous exonic *KLOTHO* variants in 25 FHH patients (Table 30), three additional rare nonsynonymous exonic *KLOTHO* variants in four additional patients with FHH (Table 31) and confirmed the presence of the Asn607Asp variant in patient 4 (Figure 70). Rare variants are defined as those with a vAF <1% and common variants as those with a vAF ≥1%[237].

Figure 70. Schematic representation of the genomic organisation of the human *KLOTHO* gene showing the location of variants identified in patients with FHH, TC-3 and mouse models of ectopic calcification



Schematic representation of the genomic organisation of the human and mouse *KLOTHO* gene showing the location of common (represented in black) and rare (represented in red) nonsynonymous exonic variants identified in FHH patients by WES and TSCA sequencing analysis. Also shown is the location of the His193Arg *KLOTHO* variant identified in a patient with TC-3[377] (represented in blue) and the two point mutations identified in *Klotho* in mouse models of ectopic calcification and reduced lifespan[381] (represented in green). The *KLOTHO* gene consists of five exons with the start (ATG) and stop (TAG) codons located in exons 1 and 5 respectively. The glycosyl hydrolase 1 domain (KL1) (encoded by exons 1-3) and glycosyl hydrolase 1 domain 2 (KL2) (encoded by the 3' portion of exon 3-exon 5) are located within the extracellular domain. The extracellular domain is followed by the transmembrane domain and cytoplasmic domain, both encoded by 3' portions of exon 5. The two common variants identified in patients with FHH, Phe352Val and Cys370Ser, are both located within exon 2, encoding the extracellular domain, KL1. The four rare variants identified in patients with FHH are spread across the extracellular and cytoplasmic domains. The Met384Thr variant is located within exon 2, encoding the extracellular domain, KL1. The Asn607Asp and Pro690Leu variants are both located within exon 4, encoding the extracellular domain, KL2. The Tyr1003Cys variant is located within exon 5, encoding the cytoplasmic domain. The rare variant identified in a patient with TC-3, His193Arg, is located within exon 1, encoding the extracellular domain KL1. The mouse model variants, Gln203* and Ile604Asn, are located in exon 1, encoding the extracellular domain, KL1 and exon 4, encoding the extracellular domain KL2, respectively.

Table 30. *In silico* analysis of two common nonsynonymous *KLOTHO* variants identified in patients with FHH by TSCA sequencing

Nucleotide change	Amino acid change	Patient cohort			^Reported vAF	^Reported genotype frequencies	MutationTaster	PolyPhen-2	Provean Protein	Evolutionary conservation	Combined *in silico* prediction
		Variant frequency	vAF	Genotype frequencies							
c.1054T>G	p.Phe352Val	28/75 (37.33%)	25.33% (G)	Heterozygotes (TG): 23 (30.67%) Homozygotes (GG): 5 (6.67%)	14.31% (G)	Heterozygotes (TG): 23.91% Homozygotes (GG): 2.35%	Polymorphism	Probably damaging (score 1.00)	Deleterious (score -6.994)	Conserved (8/8)	Likely pathogenic
c.1109G>C	p.Cys370Ser	28/75 (37.33%)	25.33% (C)	Heterozygotes (GC): 23 (30.67%) Homozygotes (CC): 5 (6.67%)	14.31% (C)	Heterozygotes (GC): 23.91% Homozygotes (CC): 2.36%	Polymorphism	Benign (score 0.00)	Neutral (score 4.026)	Not Conserved (1/8)	Benign

In silico analysis of the common (^reported vAF [ExAC] of ≥1%) nonsynonymous *KLOTHO* variants identified in FHH patients by TSCA sequencing. Eight orthologs were used to assess evolutionary conservation: chimpanzee, mouse, cow, chicken, elephant, anole lizard, xenopus and zebrafish. Variants were classified as conserved (≥6/8), partially conserved (3-5/8) or not conserved (≤2/8). A prediction of pathogenicity was made using a combined *in silico* analysis approach as described in Section 6.2.9.4.

Table 31. *In silico* analysis of three rare nonsynonymous *KLOTHO* variants identified in patients with FHH by TSCA sequencing

Nucleotide change	Amino acid change	Patient ID	Patient cohort			^Reported vAF	^Reported genotype frequencies	MutationTaster	PolyPhen-2	Provean Protein	Evolutionary conservation	Combined *in silico* prediction
			Variant frequency	vAF	Genotype frequencies							
c.1151T>C	*p.Met384Thr	6	1/75 (1.33%)	0.66% (C)	Heterozygotes (TC): 1 (1.33%)	0.016% (C)	Heterozygotes (TC): 0.031% Homozygotes (CC): 0%	Disease Causing	Possibly damaging (score: 0.561)	Neutral (score: -0.732)	Conserved (7/8)	Unknown significance
c.2069C>T	p.Pro690Leu	7	1/75 (1.33%)	0.66% (T)	Heterozygotes (CT): 1 (1.33%)	0.019% (T)	Heterozygotes (CT): 0.038% Homozygotes (TT): 0%	Disease Causing	Probably damaging (score: 1.00)	Deleterious (score: -8.028)	Conserved (8/8)	Likely pathogenic
c.3008A>G	p.Tyr10003Cys	8 and 9	2/75 (2.66%)	2.00% (G)	Heterozygotes (AG): 1 (1.33%) Homozygotes (GG): 1 (1.33%)	0.18% (G)	Heterozygotes (AG): 0.34% Homozygotes (GG): 0.0067%	Disease Causing	Probably damaging (score: 0.987)	Deleterious (score: -3.494)	Conserved (8/8)	Likely pathogenic

In silico analysis of the rare (^reported vAF [ExAC] of <1%) nonsynonymous *KLOTHO* variants identified in four FHH patients by TSCA sequencing. Eight orthologs were used to assess evolutionary conservation: chimpanzee, mouse, cow, chicken, elephant, anole lizard, xenopus and zebrafish. Variants were classified as conserved (≥6/8), partially conserved (3-5/8) or not conserved (≤2/8). A prediction of pathogenicity was made using a combined *in silico* analysis approach as described in Section 6.2.9.4. *Indicates a possible major amino acid change e.g. a hydrophobic amino acid for a hydrophilic amino acid.

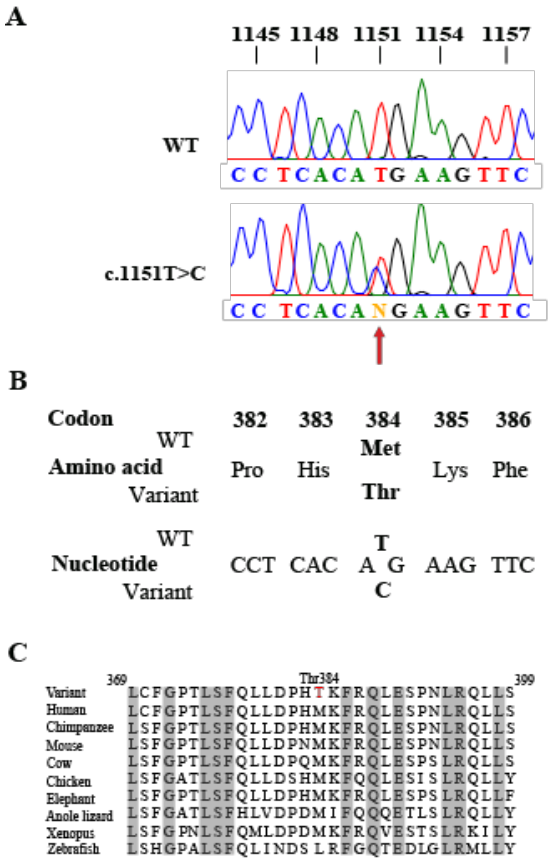
9.2.3.1 Identification of a Met384Thr variant in Klotho patient 6

A heterozygous T-to-C transition at nucleotide 1151 identified in patient 6, diagnosed with FHH, is predicted to result in the substitution of a methionine with a threonine at codon 384 (Figure 71). No further clinical or biochemical details were available for this patient. Confirmation of this variant was performed by Sanger DNA sequencing (Figure 71). *In silico* analysis revealed that this variant had a reported vAF of 0.016% on ExAC, had a predicted functional effect of unknown significance, and evolutionary conservation analysis of the WT methionine residue found it to be conserved across seven of the eight orthologs studied (Table 31 and Figure 71). Overall, combined *in silico* analysis classified this variant as being of unknown significance.

9.2.3.2 Identification of a Pro690Leu variant in Klotho in patient 7

A heterozygous C-to-T transition at nucleotide 2069 was identified in patient 7 by TSCA sequencing and is predicted to result in the substitution of a proline with a leucine at codon 690 (Figure 72). Whilst limited biochemical details were available, this patient is known to have mild asymptomatic hypercalcaemia, normal serum PTH levels and low-normal urinary Ca^{2+} excretion, consistent with a diagnosis of FHH. The variant was confirmed in patient 7 by Sanger DNA sequencing (Figure 72). *In silico* analysis revealed that this variant had a reported vAF of 0.019% (Table 31). Furthermore, the functional effect of this variant was predicted to be probably damaging by all three of the *in silico* tools (MutationTaster, PolyPhen-2 and Provean Protein) (Table 31). Evolutionary conservation analysis of the WT proline residue found it to fully conserved across the eight orthologs studied (Figure 72). Overall, combined *in silico* analysis predicted this variant to be likely pathogenic.

Figure 71. Confirmation of a Met384Thr variant in Klotho in patient 6



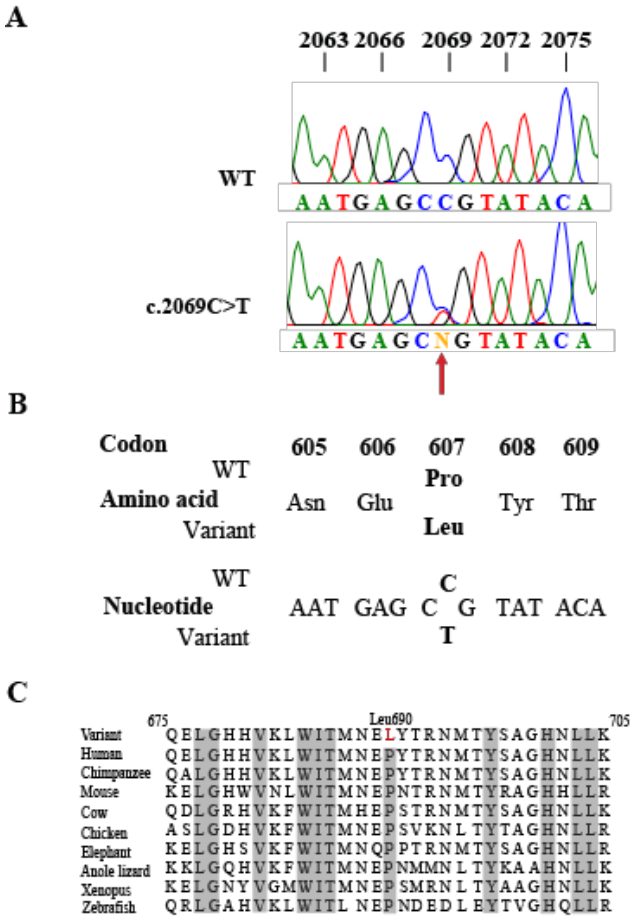
(A) A heterozygous T-to-C transition at nucleotide c.1151 was identified in patient 6 within the FHH cohort (N=75). (B) This T-to-C transition (ATG to ACG) is predicted to result in a missense amino acid change from methionine (Met) to threonine (Thr) at codon 384 of the Klotho protein. (C) Multiple sequence alignment of residues surrounding the human Met384 residue of the Klotho protein sequence in eight orthologs using Clustal Omega[247]. The Thr384 residue identified in patient 6 is shown in red. Residues conserved across all of the orthologs studied are highlighted in grey, the Met384 residue was conserved across seven of the eight orthologs. Codon numbers are displayed for the human sequence.

9.2.3.3 Identification of a Tyr1003Cys Klotho variant in two FHH patients

A G-to-A transition at nucleotide 3008 was identified in two patients (8 and 9), diagnosed with FHH, by TSCA sequencing and is predicted to result in the substitution of tyrosine with a cysteine at codon 1003 (Figure 73). The variant was identified as a heterozygous variant in patient 8 and a homozygous variant in patient 9 by TSCA sequencing and was confirmed in each patient by Sanger DNA sequencing (Figure 73). Whilst no additional clinical or biochemical details, aside from a clinical diagnosis of FHH were available for patient 8, patient 9 is known to have raised serum Ca^{2+} and

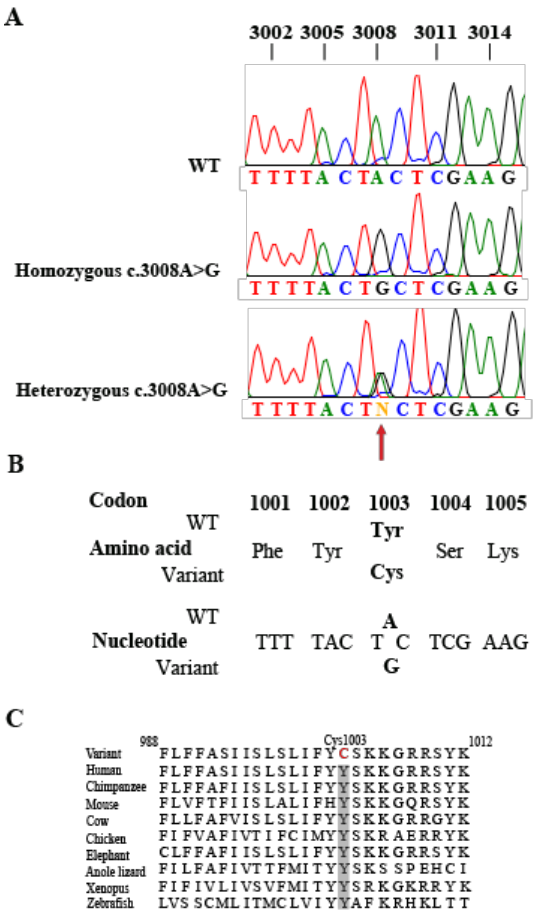
PTH levels, low fractional urinary Ca^{2+} excretion and a UCCR of <0.01, consistent with FHH. *In silico* analysis showed this variant had a reported vAF of 0.18% on ExAC (Table 31) and was predicted to be probably damaging by all three of the pathogenicity prediction software (MutationTaster, PolyPhen-2 and Provean Protein) (Table 31). Evolutionary conservation analysis of the WT tyrosine residue found it to be conserved across all of the eight orthologs studied (Figure 73). Overall, combined *in silico* analysis predicted this variant to be likely pathogenic.

Figure 72. Confirmation of a Pro690Leu variant in Klotho in patient 7



(A) A heterozygous C-to-T transition at nucleotide c.2069 was identified in patient 7 within the FHH cohort (N=75). (B) This C-to-T transition (CCG to CTG) is predicted to result in a missense amino acid change from proline (Pro) to leucine (Leu) at codon 690 of the Klotho protein. (C) Multiple sequence alignment of residues surrounding the human Met384 residue of the Klotho protein sequence in eight orthologs using Clustal Omega[247]. The Leu690 residue identified in patient 7 is shown in red. Residues conserved across all of the orthologs studied are highlighted in grey, the Pro690 residue was fully conserved across the eight orthologs. Codon numbers are displayed for the human sequence.

Figure 73. Confirmation of a Tyr1003Cys variant in Klotho in two patients diagnosed with FHH



(A) An A-to-G transition at nucleotide c.3008 was identified in two patients, as a heterozygote (patient 8) and homozygote (patient 9), within the FHH cohort (N=74). (B) This A-to-G transition (TAC to TGC) is predicted to result in a missense amino acid change from tyrosine (Tyr) to cysteine (Cys) at codon 1003 of the Klotho protein. (C) Multiple sequence alignment of residues surrounding the human Tyr1003 residue of the Klotho protein sequence in eight orthologu using Clustal Omega[247]. The Cys1003 residue identified in patients 8 and 9 is shown in red. Residues conserved across all of the orthologs studied are highlighted in grey, the Tyr1003 residue was fully conserved across the eight orthologs. Codon numbers are displayed for the human sequence.

9.2.3.4 Structural analysis of rare variants located in the extracellular Klotho domain

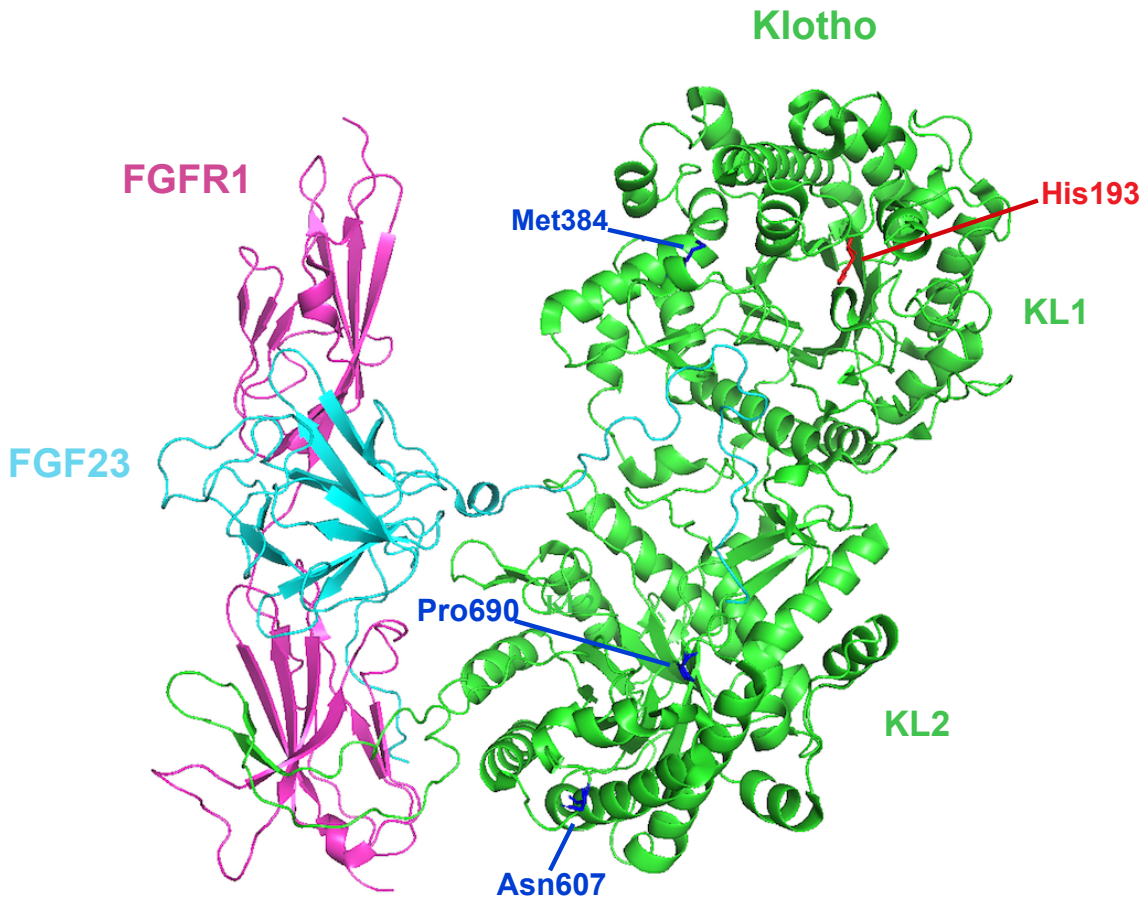
Recently, the crystal structure of the human Klotho-FGFR1c-FGF23 ternary complex was determined (PDB ID 5W21)[260] and I therefore performed structural modelling of the rare *KLOTHO* variants, identified in FHH patients in this study, and the His193Arg mutation identified in the patient with TC-3 (Figure 74 and Figure 75). However, the

structural impact of the Tyr1003Cys variant could not be assessed as the human Klotho-FGFR1c-FGF23 crystal structure does not contain this residue.

Structural analyses of the extracellular domain of Klotho (green), confirmed the location of both the His193 (red) and Met384 (blue) residues in the KL1 domain, and the Asn607 (blue) and Pro690 (blue) residues in the KL2 domain. Both the His193 and Pro690 residues were located more centrally in the triosephosphate isomerase (TIM) barrel of KL1 and KL2 respectively, compared to Met384 and Asn607 (Figure 74). The location of the Pro690 residue has previously been described as close to the C-terminal tail of FGF23 (cyan blue) (Figure 74), which has been reported to interact with Klotho within the KL1-KL2 cleft[260], therefore indicating that this variant may affect FGF23-Klotho binding. However, the structural analysis performed in this study and another previous study did not predict the WT (Pro690) or variant (Leu690) residues to interact with FGF23[260]. Rather, the formation of H^+ bonds between FGF23 and Klotho residues in the KL2 domain is predicted to occur further downstream from Pro690[260].

The impact of each variant on the tertiary structure of extracellular Klotho was also analysed using the human Klotho-FGFR1c-FGF23 ternary complex (PDB ID:5W21) (Figure 75). Analysis of the three-dimensional protein structure provides an insight into the interactions between amino acid residues, which are important for a protein's structure and stability. Thus, loss-or-gain of contacts between amino acid residues may indicate an impact on the structure or stability of Klotho.

Figure 74. Structural characterisation displaying the location of rare Klotho variants in the human Klotho:FGFR1c:FGF23 ternary complex

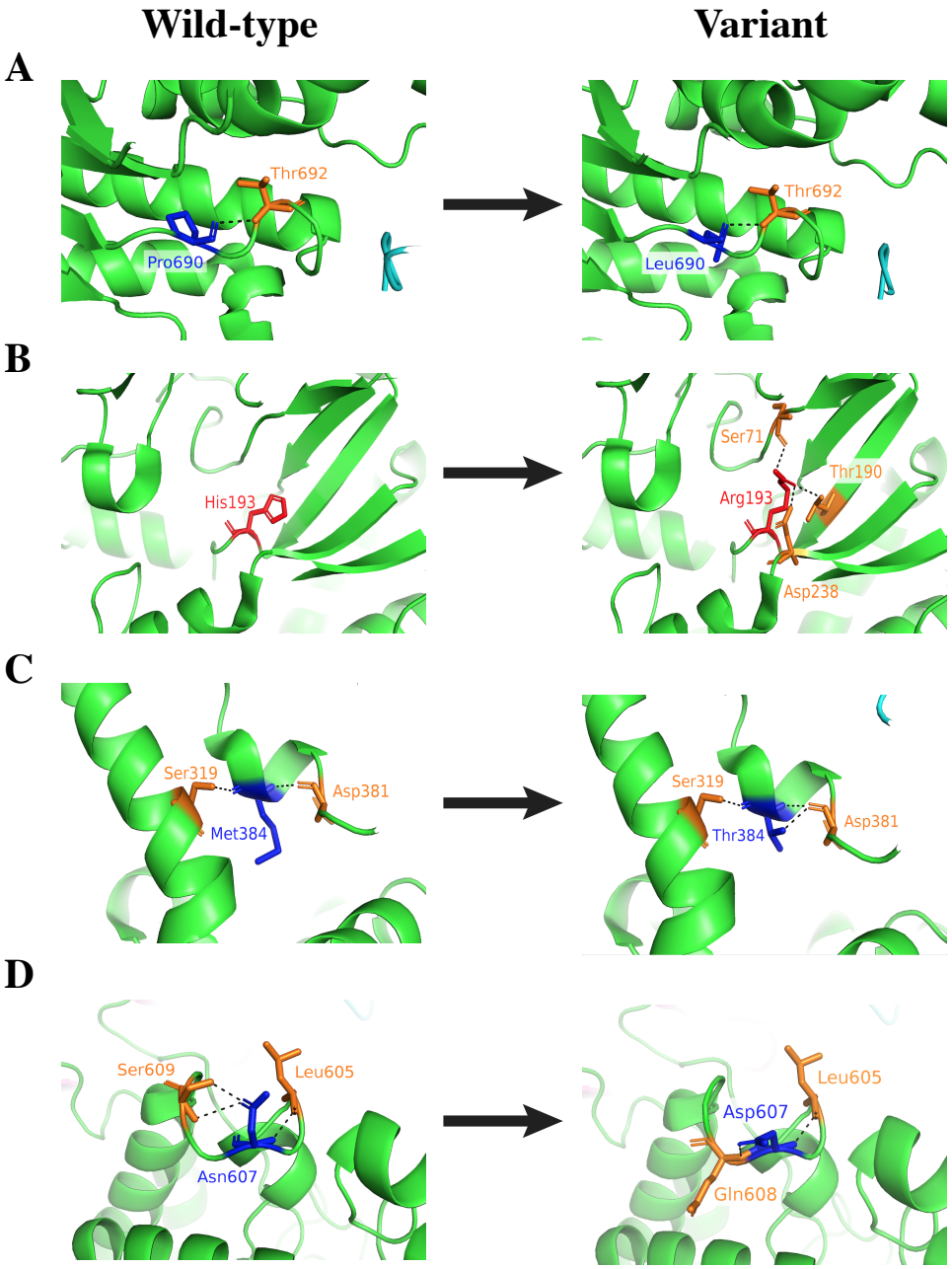


Overview of the position of WT residues affected by rare variants located in the extracellular domain of Klotho, using the human Klotho:FGFR1c;FGF23 crystal structure (PDB ID:5W21)[260]. A homozygous mutation affecting the His193 residue (highlighted in red) (His193Arg) was identified in a patient with TC-3[377]. Variants affecting the remaining three residues (highlighted in royal blue): Met384, Asn607 and Pro690, were identified in patients with FHH in this study (Met384Thr, Asn607Asp and Pro690Leu). The extracellular Klotho domain is displayed in green, the ligand-binding domain of FGFR1c is displayed in pink and FGF23 is displayed in cyan blue.

Whilst none of the variants are predicted to directly affect the interaction of Klotho with FGFR1c or FGF23 (Figure 75), all the variants, with the exception of Leu690 are predicted to alter the formation of contacts. The Leu690 variant is not predicted to alter the tertiary structure or stability of the Klotho protein, as mutation of the WT Pro690 residue to Leu690 was not predicted to disrupt the contact formed with the

Thr692 residue (Figure 75A). Conversely, whilst the WT His193 residue is not predicted to form contacts with any of the surrounding residues, the Arg193 variant is predicted to form contacts with three: Ser71, Thr190 and Asp238, therefore this variant may have an effect on the tertiary structure and stability of Klotho (Figure 75B). WT Met384 is predicted to form two polar contacts, one with Ser319 and the other with Asp381 (Figure 75C); and whilst the Thr384 variant is not predicted to disrupt either of these contacts, it is predicted to result in an additional contact with Asp381 (Figure 75C). Thus, indicating that this variant may also impact the tertiary structure of Klotho. Finally, the Asp607 variant is predicted to both disrupt and form new polar contacts with surrounding residues (Figure 75D). The Asn607 WT residue is predicted to form three polar contacts with neighbouring residues, two with Ser609 and one with Leu605 (Figure 75D). Mutation of the 607 residue to an aspartic acid is not predicted to disrupt the contact formed with Leu605 (Figure 75D). However, the Asp607 variant is predicted to disrupt the formation of the contacts with Ser609 (Figure 75D) and result in the formation of new contacts with Gln608 (Figure 75D), therefore indicating that this variant is likely to have an impact on the tertiary structure and stability of the Klotho protein.

Figure 75. Structural characterisation of rare *KLOTHO* variants located in the extracellular domain



Structural characterisation of rare variants located in the extracellular domain of Klotho, using the human Klotho:FGFR1c;FGF23 crystal structure (PDB ID 5W21)[260]. (A) Mutation of the WT Pro690 residue (blue) to Leu690 (blue) was not predicted to alter the formation of a polar contact with the Thr692 residue (orange). (B) Mutation of the WT His193 residue (red) (His193Arg) to Arg193 (red) was predicted to form new polar contacts with three surrounding residues: Ser71, Thr190 and Asp238, (all orange). (C) Mutation of the WT Met384 residue (blue) to Thr384 (blue) is not predicted to disrupt the formation of the polar contact formed with Ser319 and Asp381 (both orange). However, it is predicted to result in the formation of an additional polar contacts with Asp381 (orange). (D) Mutation of the WT Asn607 residue (blue) to Asp607 (blue) is not predicted to disrupt the formation of polar contacts with Leu605 (orange), but is predicted to disrupt the formation of polar contacts with Ser609 (orange). Furthermore, the Asp607 residue is predicted to form a polar contact with Gln608 (orange). The extracellular Klotho domain is displayed in green, FGF23 is displayed in cyan blue and polar contacts are displayed using black dashed lines.

9.2.4 *In vitro* functional analysis of the four rare Klotho variants identified in patients with FHH by NGS

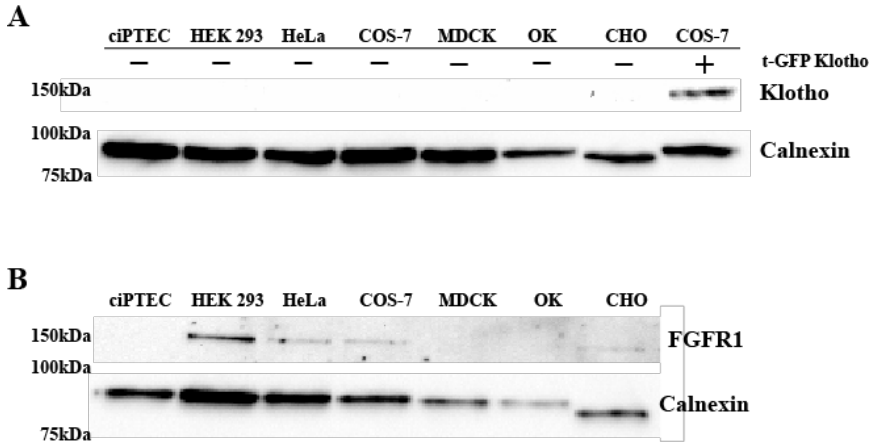
To determine whether the rare Klotho variants identified by NGS are pathogenic, *in vitro* functional studies are required. One of the most well documented functions of Klotho is its role as a co-receptor for FGF23, greatly increasing the affinity of FGF23 for its receptors (FGFRs)[35]. Binding of FGF23 to Klotho and FGFRs triggers downstream signalling of the ERK1/2 pathway, ultimately effecting the expression of downstream target genes such as *EGR1*[34]. Therefore, further analyses focussed on ERK1/2 signalling in response to FGF23.

9.2.4.1 Expression analysis of co-receptors Klotho and FGFR1

Whilst Klotho can bind multiple FGFRs including FGFR1c, 3c and 4[34,35], one in particular, FGFR1, has been described to activate ERK1/2 signalling resulting in *Egr-1* promoter activity[25]. To determine which cell-line was the most appropriate to study FGF23 signalling via co-receptors Klotho and FGFR1, Western blot analysis of Klotho and the FGFR1 was performed using lysates from a range of well-established mammalian cell-lines including a range of different human and non-human kidney cell-lines as well as cell-lines previously used to study Klotho and other renal disorders (Figure 76). Klotho expression was absent in all of the untransfected cell-line lysates analysed (Figure 76A). COS-7 cells transfected with a vector expressing the WT human Klotho-tGFP fusion protein were used as a positive control. Overexpression of Klotho was detected in the positive control lysate, confirming the detection capacity of the Klotho antibody (Figure 76A). Endogenous expression of FGFR1 was detected in 4 of the cell-lines analysed: HEK293, HeLa, COS-7 and CHO

cell-lines; and was absent from ciPTEC, MDCK and OK cell-line lysates (Figure 76B). Therefore, the HEK293 cell-line, an established human kidney cell-line, previously used for studies of Klotho function in response to FGF23[376,377,383,387], was chosen as the optimum cell-line for *in vitro* functional analysis of *KLOTHO* variants on ERK1/2 signalling in response to FGF23.

Figure 76. Expression of Klotho and FGFR1 in a panel of cell-lines



Western blot analysis of (A) Klotho and (B) co-receptor FGFR1 expression in a panel of lysates from a range of cell-lines: ciPTECs, HEK293 cells, HeLa cells, COS-7 cells, MDCK cells, Opossum Kidney (OK) cells and Chinese Hamster Ovary (CHO) cells. (A) Expression of endogenous Klotho was analysed in each of the untransfected cells lines and was shown to be absent from each. Expression of Klotho was also analysed in a positive control lysate from COS-7 cells transfected with t-GFP Klotho, where expression of Klotho was detected. (B) Expression of endogenous FGFR1 was analysed in the panel of cell-line lysates and was shown to be absent in ciPTEC, MDCK and OK cell lysates. Endogenous expression was detected in HEK293, HeLa, COS-7 and CHO cell-lines.

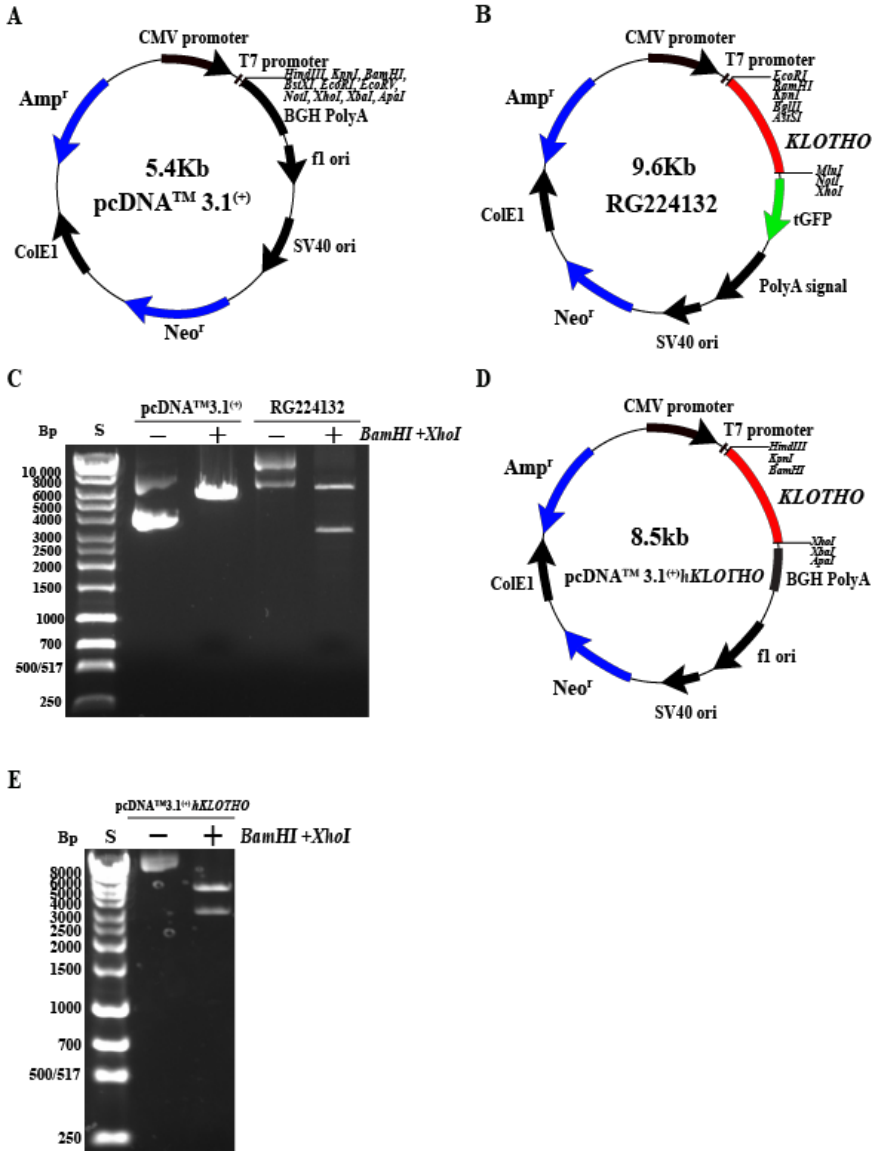
9.2.4.2 Generation of WT and mutant Klotho-expressing constructs

Vectors expressing untagged-WT Klotho were generated by sub-cloning full-length WT human *KLOTHO* cDNA (3Kb), from the RG224132 pCMV6-AC-tGFP vector (Origene™ Technologies) (Figure 77B), which encodes the Klotho-tGFP fusion protein into a pcDNA™ 3.1(+) vector (Invitrogen™) (5.4Kb) (Figure 77A) to prevent any activity interference by the tGFP tag. This was done using the REs *BamHI* and *XhoI* (Figure 77C), thus generating the untagged 8.5kb pcDNA™ 3.1(+) *hKLOTHO* vector

which was used in these studies expressing Klotho and the selective marker *Amp*^{r} that conferred resistance to ampicillin (Figure 77D). Sanger DNA sequencing (data not shown) and RED (Figure 77E) was used to confirm the presence and orientation of the WT *KLOTHO* insert in the pcDNA™ 3.1$^{(+)}$ *hKLOTHO* vector.

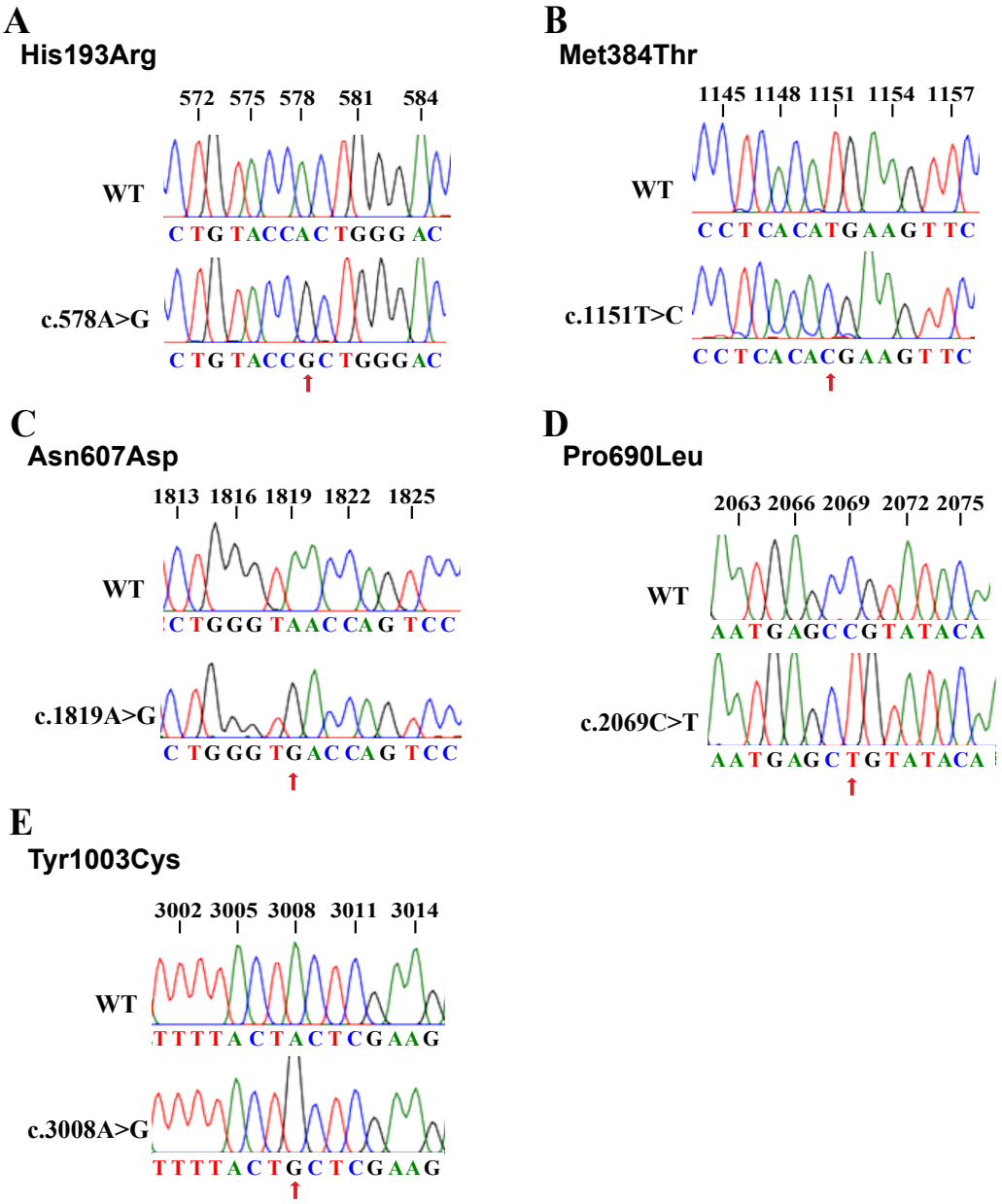
This vector was then used to generate five additional mutant plasmids by SDM as detailed in Section 5.4.1.3. The Leu690, Thr384, Asp607 and Cys1003 (Figure 78A,C-E) mutant plasmids were generated to express the four rare *KLOTHO* variants identified in the FHH patients in this study. The final mutant plasmid was generated to express the Arg193, previously reported in a patient with TC-3 and shown to result in reduced expression of *EGR1* (a downstream target of ERK1/2 signalling)[377], as a positive control (Figure 78A). Sanger DNA sequencing was performed to confirm the successful generation of mutant plasmids (Figure 78).

Figure 77. Generation and confirmation of the pcDNA™3.1(+)*hKLOTHO* vector



(A) Plasmid map of the pcDNA™3.1(+) mammalian expression vector used for the generation of the pcDNA™3.1(+)*hKLOTHO* vector. This vector encodes two selective markers: *Amp^r^* and *Neo^r^,* which confer resistance to the antibiotics ampicillin (for bacterial expression) and neomycin (for mammalian expression), respectively. (B) The 9.6Kb RG224132 expression vector encodes the human WT Klotho-tGFP fusion protein as well as the two selective markers *Amp^r^* and *Neo^r^.* (C) RED of the 5.4Kb pcDNA™3.1(+) vector by *BamHI* and *XhoI* was performed to linearise the receiving vector and generate compatible ends prior to ligation. Digestion of the 9.6kb RG224132 vector with *BamHI* and *XhoI* was performed to excise the human WT *KLOTHO* cDNA from the RG224132 vector, resulting in two bands of 3.1Kb (*KLOTHO*) and 6.5Kb (RG224132 vector without *KLOTHO*). (D) Plasmid map of the resulting pcDNA™3.1(+)*hKLOTHO* vector generated from sub-cloning human WT *KLOTHO* cDNA (from RG224132) into the pcDNA™3.1(+) vector. (E) Confirmation of the successful insertion of *KLOTHO* cDNA into the pcDNA™3.1(+) vector by restriction digest of the 8.5Kb pcDNA™3.1(+)*hKLOTHO* vector with *BamHI* and *XhoI*, resulting in two fragments of 3.1Kb and 5.4Kb representing the *KLOTHO* cDNA and pcDNA™3.1(+) vector respectively.

Figure 78. Confirmation of SDM in *KLOTHO*



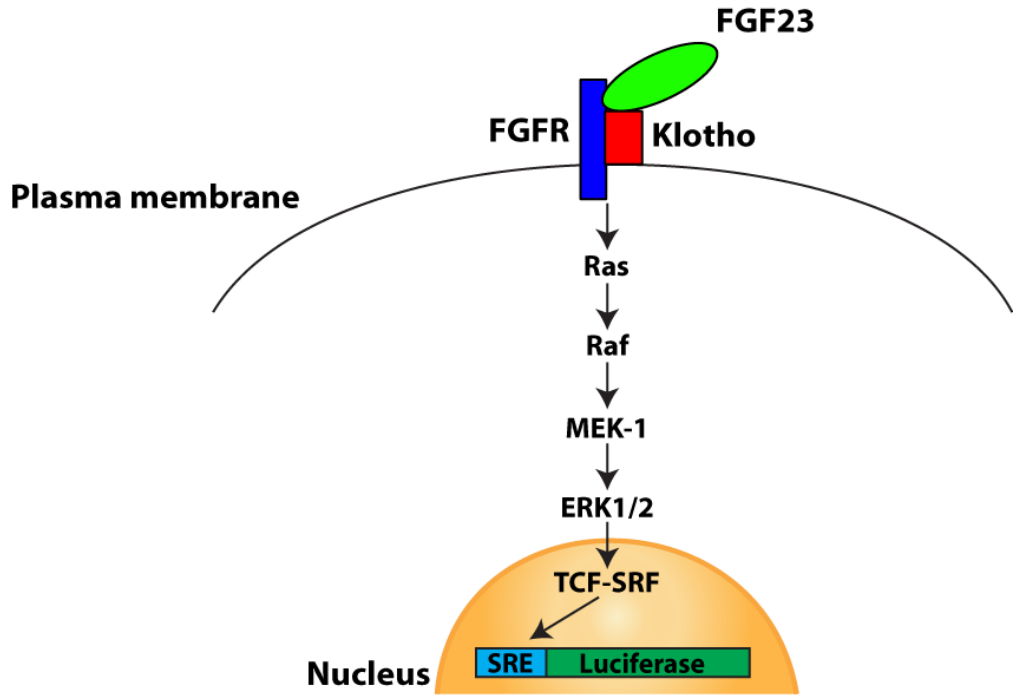
Nucleotide number is according to the *KLOTHO* transcript ENST00000380099.3. Successful mutagenesis in the six mutant Klotho constructs (A) His193Arg, (B) Met384Thr, (C) Asn607Asp, (D) Pro690Leu and (E) Tyr1003Cys as confirmed by Sanger DNA sequencing.

9.2.4.3 Effect of rare Klotho variants on ERK1/2 signalling in response to FGF23

Formation of the FGF23:Klotho:FGFR ternary complex triggers a downstream signalling response via ERK1/2, that subsequently regulates the expression of target genes (Figure 79)[34,388]. Phosphorylated ERK1/2 translocates to the nucleus where it

phosphorylates transcription factors such as Ternary Complex Factors (TCFs), which subsequently form a complex with Serum Response Factor (SRF) and binds to SREs in the promoters of target genes (Figure 79)[388,389]. Therefore, SRE-luciferase reporter assays, which generate a quantifiable intracellular luminescent response as a result of signalling via ERK1/2, were used to investigate the effect of *KLOTHO* variants on ERK1/2 signalling in response to FGF23.

Figure 79. Schematic representation of SRE-luciferase transcription induced by ERK1/2 signalling in response to FGF23



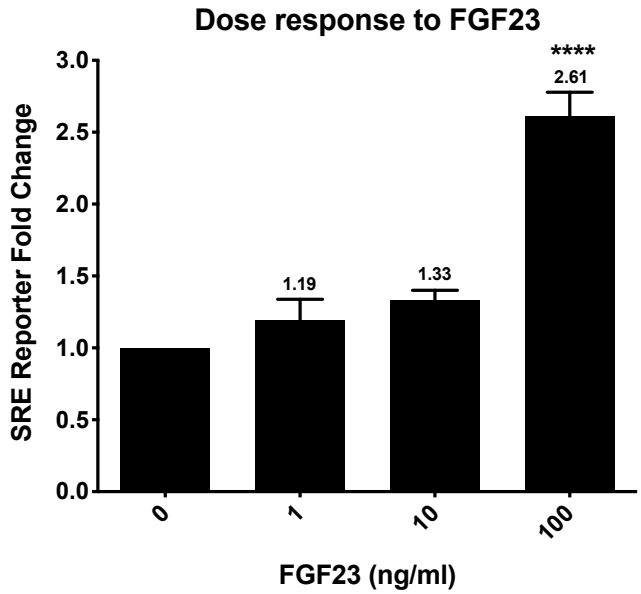
A schematic overview of the regulation of luciferase reporter gene expression via ERK1/2 signalling and in response to FGF23 in the SRE-luciferase reporter assay. FGF23 binding to the co-receptors FGFR and Klotho activates the ERK1/2 signalling pathway, which results in the regulation of target gene expression. Binding of FGF23 to FGFR and Klotho activates the intracellular tyrosine kinase domain by phosphorylation of specific tyrosine residues, recruiting the FGFR kinase substrate FRS2α and adapter proteins that then induce the activation of Ras at the plasma membrane[388-390]. Activated Ras then activates Rafs, which then go on to phosphorylate MEK-1. MEK-1 then activates its downstream target ERK1/2[388,389]. Phosphorylated ERK1/2 translocates to the nucleus where it is responsible for the phosphorylation of transcription factors such as Ternary Complex Factors (TCFs) (such as Elk-1)[388,389]. Phosphorylated TCFs are then able to bind to Serum Response Factors (SRFs), forming a complex which can subsequently bind to SREs located in the promoter regions of target genes[388,389]. Adapted from Ornitz and Itoh[390].

A dose-response assay to determine the optimum concentration of FGF23 to use to investigate the effect of *KLOTHO* variants on ERK1/2 signalling in response to FGF23 was performed using the SRE luciferase reporter assay (Figure 80). HEK293 cells were co-transfected with WT Klotho, pGL4.33-SRE (firefly) reporter and pRL (Renilla) control vectors and 24 hours later cells were treated with varying concentrations of recombinant human $FGF23^{Arg179Gln}$ (0-100ng/ml). The human recombinant FGF23, $FGF23^{Arg179Gln}$ is frequently used for studies of FGF23 signalling as the Arg179Gln variant, previously identified in patients with autosomal dominant hypophosphataemic rickets (ADHR), has been shown to protect FGF23 from proteolytic cleavage, whilst remaining active[65]. After incubation with $FGF23^{Arg179Gln}$ for a further 24 hours, cells were lysed and intracellular luciferase activity quantified (Figure 80). Only one concentration of $FGF23^{Arg179Gln}$ (100ng/ml) resulted in a statistically significant increase in SRE reporter activity compared to untreated ($p \leq 0.0001$, one-way ANOVA corrected for multiple comparisons) (Figure 80). Therefore, 100ng/ml $FGF23^{Arg179Gln}$ was used as the optimum concentration of $FGF23^{Arg179Gln}$ for studying the effects, if any, of the Klotho variants on SRE reporter activity.

Cells were co-transfected with WT or mutant *KLOTHO*, pGL4.33-SRE (firefly) reporter construct and pRL (Renilla) control vector and incubated for 24 hours with $FGF23^{Arg179Gln}$ prior to luciferase reporter assays being performed. Cells were incubated for a further 24 hours at 37°C, 5% CO_2 with $FGF23^{Arg179Gln}$ prior to cell lysis and quantification of intracellular luciferase activity. Intracellular firefly luciferase activity was normalised to Renilla luciferase activity for each well and the mean of the four technical replicates calculated. The results for each variant were normalised to

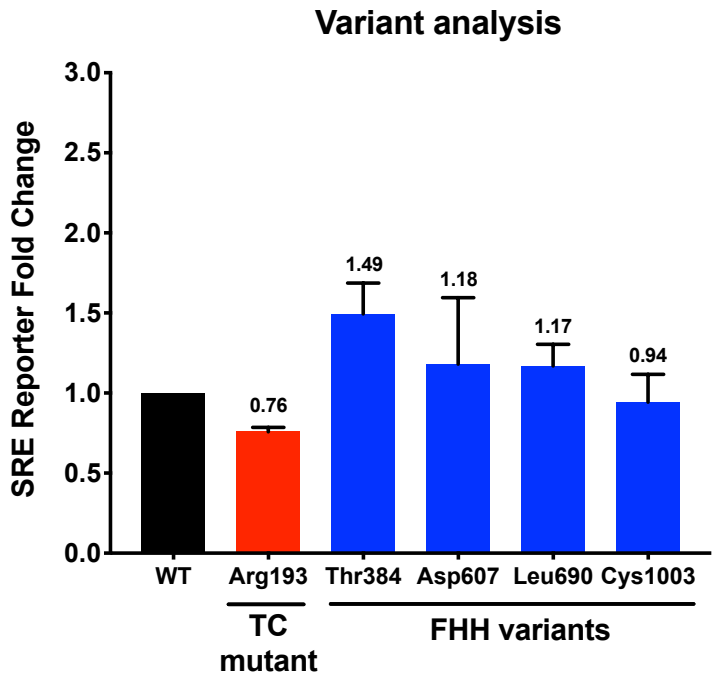
the WT (Figure 81). None of the variants had a significant effect on SRE reporter activity in response to treatment with FGF23^{Arg179Gln} when compared to the activity observed in cells expressing WT *KLOTHO* (Figure 81), thus indicating these variants do not alter ERK1/2 signalling in response to stimulation with FGF23^{Arg179Gln} and consequently, *KLOTHO* may not play a role via an FGF23- or ERK1/2 mechanism in the pathogenesis of FHH.

Figure 80. Dose-response of SRE-reporter activity to FGF23



Dose response to measure the optimum concentration of human recombinant FGF23^{Arg179Gln} to measure SRE reporter activity in cells expressing *KLOTHO*. Cells were treated with varying concentrations (0-100ng/ml) of FGF23^{Arg179Gln}, 24 hours post-transfection with WT *KLOTHO*, pGL4.33-SRE reporter (firefly) and pRL (Renilla) control vectors. SRE reporter activity was measured 24 hours post treatment with FGF23^{Arg179Gln} and showed only one concentration tested (100ng/ml) resulted in a statistically significant increase in SRE reporter activity compared to untreated ($p<0.0001$). The fold change was normalised to the untreated (0ng/ml) control. Statistical analysis was performed using a one-way ANOVA corrected for multiple comparisons using the Bonferroni method. ****$p<0.0001$ compared to the response at time 0. Results show the mean ±SEM for four technical replicates in four independent transfections.

Figure 81. SRE-reporter fold change in response to FGF23 in cells expressing WT or variant Klotho



HEK293 cells co-transfected with WT or mutant *KLOTHO,* representing the variants identified in the TC-3 and FHH patients. Cells were treated with 100ng/ml $FGF23^{Arg179Gln}$ and SRE reporter activity measured. None of the variants had any effect on the SRE reporter activity in response to FGF23. Fold change was normalised to the WT. Statistical analysis compared the fold change response of each of the variants to the WT and was calculated using a one-way ANOVA corrected for multiple comparisons using the Bonferroni method. Results show the mean ±SEM for four technical replicates in four independent transfections.

9.3. Discussion and future studies

FHH is a genetically heterogeneous disorder of Ca^{2+} homeostasis characterised by increased serum Ca^{2+}, decreased urinary Ca^{2+} excretion and normal or increased PTH[186]. To date, three subtypes have been identified, due to heterozygous loss of function mutations in *CASR* (FHH1)[183], *GNA11* (FHH2)[184] and *AP2S1* (FHH3)[185]. All three genes identified in FHH patients encode proteins involved in regulation of CaSR trafficking and signalling and consequently regulation of PTH secretion and renal tubular Ca^{2+} reabsorption and excretion[184-186,391,392]. Mutations in *CASR*, *GNA11* and *AP2S1* have been identified in approximately 75% of FHH patients, indicating a role

of an additional gene(s) in the pathogenesis of FHH in the remaining 25% of patients[183-186,372]. Therefore, WES of five patients with FHH, lacking mutations in *CASR*, *GNA11* and *AP2S1* was performed and bioinformatic analysis resulted in the identification of a heterozygous Asn607Asp variant in exon 4 of *KLOTHO* in proband 4. Notably, a homozygous mutation (His193Arg) in exon 1 of *KLOTHO* has previously been identified in a patient with TC-3[377]. Thus, it was initially hypothesised that the differences observed in phenotypes may be due to the genotype differences or differences in the location of the mutations, given that *KLOTHO* can generate multiple forms of the Klotho protein, which may have functional differences, due to alternative splicing in exon 3.

Combined *in silico* analysis of the Asn607Asp Klotho variant predicted it to be likely pathogenic due to it being rare and highly conserved. Furthermore, this variant was predicted to effect glycosylation, suggesting it may impact the stability and processing of the Klotho protein and supports the prediction of the *in silico* analysis. However, two of the three pathogenicity prediction programmes predicted the variant to be benign/neutral. Three-dimensional modelling of the Asn607Asp variant predicted it to disrupt the formation of two polar contacts with Ser609 and instead form new contacts with Gln608, suggesting this variant may impact the structure and stability of Klotho and therefore adding further support to the prediction made by the combined *in silico* analysis.

An additional five nonsynonymous exonic variants were identified in *KLOTHO* in 32 FHH patients by TSCA sequencing. *In silico* analysis of population genomics revealed that two of the variants were common variants, with reported vAFs ≥1% (Phe352Val

and Cys370Ser); and the remaining three variants (Met384Thr, Pro690Leu and Tyr1003Cys) were rare variants with reported vAFs <1%. Combined *in silico* analysis of the two common variants predicted Phe352Val to be likely pathogenic and Cys370Ser to be benign. Due to the relatively high vAFs of Phe352Val and Cys370Ser (both 14.31%) reported on ExAC, compared to the prevalence of FHH (estimated to be 1 in 78,000 in the west of Scotland [0.001%])[386] these variants were excluded from any further analysis. Furthermore, a literature search revealed that the two common variants had previously been identified as two of six single nucleotide polymorphism (SNPs) that make up the KL-VS haplotype, so named after the valine (V) and serine (S) of Phe352Val and Cys370Ser respectively[393]. The Phe352Val and Cys370Ser SNPs are the only two nonsynonymous SNPs in the KL-VS allele, the remaining four are comprised of a synonymous exonic variant (c.1155G>A) and three intronic variants (c.820-79C>T, c.820-46C>G and c.+143T>G). Only the three exonic Kl-VS SNPs were detected by the TSCA sequencing analysis performed in this study (data for the synonymous variant not shown) as the probes were designed to amplify and sequence the exonic regions and exon/intron boundaries and not the intronic regions. Consistent with previous reports, the KL-VS SNPs identified in this study were identified in the same patients as either homozygotes (five patients) or heterozygotes (23 patients). This haplotype has previously been associated with human longevity[393] and occult atherosclerosis (CAD) in a high-risk cohort[394]. However, it should be noted other studies have not reported an association with CAD[395] and whilst one study reported a survival advantage for individuals heterozygous for the KL-VS haplotype in a Bohemian Czech cohort[393], additional studies in two other populations did not observe this association, but instead a survival disadvantage was observed for individuals homozygous for this allele in three populations[393]. To date there is no data

regarding the KL-VS allele and Ca^{2+} homeostasis or renal diseases, therefore suggesting that neither of the variants are likely to play a role in the pathogenicity of FHH.

Of the three rare variants, two were detected as heterozygous variants only (Met384Thr in patient 6 and Pro690Leu in patient 7) and one (Tyr1003Cys) was identified as a heterozygous variant in patient 8 and a homozygous variant in patient 9. This suggests the initial hypothesis that the differences in the phenotypes observed between the FHH patients and the TC-3 patient may be due to gene dosage differences was unlikely. Furthermore, whilst the majority of mutations identified in the FHH patients were located in exons 4 and 5, encoding the KL2 domain; the Met384Thr variant was located in exon 3, encoding the KL1 domain. As the His193Arg variant identified in a TC-3 patient was located in exon 2, also encoding the KL1 domain, this suggests the hypothesis that differences in the phenotypes may be due to the differences in the location of the variants and therefore the affected forms of the Klotho protein, was also likely to be incorrect. Thus, further *in silico* and *in vitro* analysis was required to determine whether these variants were pathogenic.

Although all three variants had vAFs >0.001% reported on ExAC, combined *in silico* analysis predicted both the Pro690Leu and Tyr1003Cys variants to be likely pathogenic and the Met384Thr variant to be of unknown significance. Structural modelling using the Klotho-FGFR1c-FGF23 ternary complex (PDB ID:5W21) was used to indicate the potential impact of the Met384Thr and Pro690Leu variants on the three-dimensional structure of Klotho. Neither WT counterparts (Met384 and Pro690 respectively) directly impact the interaction between Klotho and FGF23. However,

mutation of the WT Met384 residue to Thr384 was predicted to result in an additional contact with Asp381, thus suggesting that whilst the Pro690Leu variant is not likely to impact the structure or stability of Klotho, the Met384Thr might.

Klotho has been shown to play at least two roles in Ca^{2+} homeostasis in both the kidney and parathyroid gland, although there remains some speculation as to the precise forms of Klotho and mechanisms employed. One of the most well documented roles of Klotho is its role facilitating FGF23 signalling by acting as a co-receptor for FGFRs, increasing their affinity for FGF23. Binding of FGF23 to Klotho and FGFRs (such as FGFR1c) triggers a downstream signalling response via ERK1/2, subsequently regulating the expression of target genes (Figure 79)[34,388]. Similarly, binding of extracellular Ca^{2+} to the CaSR triggers downstream signalling responses including the ERK1/2 pathway via the G-proteins $G_{q/11}$ and $G_{i/o}$ as well as via G-protein-independent mechanisms involving ß-arrestin proteins[396-399]. Furthermore, similarly to CaSR signalling, several studies have suggested that FGF23 is able to suppress PTH secretion in the parathyroid glands and is also able to reduce PTH gene expression[38,400]. However, one study has reported that this could be via a Klotho-independent mechanism[400]. Therefore, SRE-luciferase reporter assays were performed to investigate the effect of the *KLOTHO* variants on ERK/12 signalling in response to FGF23.

HEK293 cells were chosen as they do not endogenously express Klotho but do express FGFR1. Results of the dose-response assay showed that 100ng/ml $FGF23^{Arg179Gln}$ was sufficient to induce a significantly greater SRE-reporter response compared to WT and was the only concentration of $FGF23^{Arg179Gln}$ studied to do so. This is consistent

with previous studies, investigating the effects of the His193Arg variant on FGF23 signalling[377]. Thus, the effect of the variants on ERK1/2 signalling using the SRE-reporter assay was performed in response to 100ng/ml FGF23^{Arg179Gln}, and this revealed that none of the FHH variants resulted in a significantly different SRE reporter fold change response, when compared to WT. These findings suggest that none of the rare *KLOTHO* variants, identified in FHH patients, effect ERK1/2 signalling in response to FGF23. Furthermore, the positive control Arg193, representing the variant identified in the patient with TC-3, was also found not to result in a significant difference in SRE reporter fold change compared to WT, which would also suggest this variant does not affect ERK1/2 signalling in response to FG23 and via Klotho. However, this is inconsistent with the results of another study which reported a significant 6-fold decrease in *EGR1* expression, a known downstream target of the FGF23-ERK1/2 signalling pathway, in cells transfected with the Arg193 variant compared to WT[377]. The two studies had many similarities e.g. both used HEK293 cells, recombinant FGF23 harbouring the Arg179Gln ADHR mutation and the same concentration of FGF23 (100ng/ml); however, the methods used to detect changes in signalling were different, as was the duration of incubation with FGF23[377]. The previous study incubated cells for 30 mins with FGF23 before RNA was extracted for RT-qPCR analysis[377], compared to this study, which incubated the cells for 24 hours with FGF23 prior to measuring the luminescence response. The time taken to transcribe from RNA to protein by FGF23 is unknown, and therefore this study could not provide information on the timings for luciferase reporter activity. However, previous studies investigating luciferase reporter responses to FGF23 have reported responses in cells incubated with FGF23 for varying time periods for up-to 24 hours[67,401-403]. Furthermore, this study used an SRE-luciferase response to measure

signalling activity, whilst the previous study used RT-qPCR to quantify changes in *EGR1* expression[377]. An SRE-luciferase response was used as SRE sites are located within the *EGR1* promoter[404]; furthermore, the SRE-reporter assay would measure transcription of all ERK1/2 target genes rather than focusing on a single gene that may only be subtly affected. Thus, the differences in the findings in the two studies may be attributed to differences in the design of the studies. To overcome this, future studies could confirm the Arg193 variant results in a reduction in *EGR1* expression after incubation with FGF23 for 30 mins. Furthermore, a time-course SRE-luciferase reporter assay could be performed, incubating transfected cells with FGF23 for varying time intervals to determine which time point induces the greatest response and whether this may affect the results observed in this study.

The current findings suggest that the Klotho variants do not have an effect on FGF23 signalling and therefore indicate that this mechanism is likely not involved in the pathogenesis of FHH. This is supported by the three-dimensional structural analysis in which none of the variants were predicted to directly affect the interaction of Klotho with FGFR1c or FGF23 as none of the WT or mutant residues were predicted to form or disrupt polar contacts with residues in either protein. Therefore, these results would suggest that if these Klotho variants are involved in the pathogenesis of FHH, it is likely to be via an ERK1/2-FGF23-independent mechanism. In addition to its role as a co-receptor for FGF23, Klotho also has a key role in regulating the expression of TRPV5 at the plasma membrane in the DTs and therefore in the regulation of Ca^{2+} reabsorption[68-70]. Previous studies have shown that both extracellular and membrane-bound Klotho is able to increase the abundance of the TRPV5 channel at the plasma membrane, through its sialidase and ß-glucuronidase

activity, ultimately increasing TRPV5 activity[68-70]. Therefore, future studies could be performed to investigate the abundance of TRPV5 at the plasma membrane of cells overexpressing WT and mutant Klotho using Total Internal Reflection Fluorescence (TIRF) microscopy. Previous studies of the effects of Klotho on TRPV5 expression at the plasma membrane have used HEK293 cells[68-70], thereby suggesting that HEK293 cells may be the optimum cell-line to use for future studies investigating the effect, if any, the Klotho variants have on TRPV5 expression at the plasma membrane. However, due to time limitations I was unable to perform such TIRF experiments during the course of this project, although these would be appropriate future studies. Alternatively, these results may equally indicate that Klotho is not responsible for FHH in these patients and therefore an alternative gene(s) is responsible. Rare *KLOTHO* variants were not present in the remaining four FHH patients whose DNA was used for WES and the remaining 66 FHH patients whose DNA was used for TSCA analysis. Thus, future studies could investigate the results of the WES that was initially performed on the five FHH patients for novel candidates. However, none of the variants remained suitable candidates after applying a biological context filter (hypocalciuric hypercalcaemia or Ca^{2+} metabolism). Thus, future studies would need to investigate the biological relevance of these candidates in the literature in more detail and confirm their presence in each proband by Sanger DNA sequencing. TSCA sequencing and *in vitro* functional studies could then be performed for the most biologically relevant.

In conclusion, NGS identified *KLOTHO* as a novel candidate gene for FHH, identifying four rare variants in five patients with FHH. *In silico* analysis, using the criteria established in Section 6.2.9.4, predicted three of the four variants to be likely

pathogenic. However, *in vitro* functional analysis of the effect of these Klotho variants on FGF23-signalling showed they had no effect, therefore suggesting that either these variants act in an FGF-23/ERK1/2-independent manner in FHH patients or that Klotho is not involved in the pathogenesis of FHH. Thus, further study of the effects of these Klotho variants on the expression of TRPV5 at the plasma membrane by TIRF microscopy and re-analysis of the data generated by WES, using the *in silico* analysis criteria established in Section 6.2.9.4, would be appropriate future approaches. Overall these results show the value of NGS technologies at rapidly identifying genetic variants in large cohorts of patients; and indicate the importance of *in vitro* functional analysis as well as *in silico* analysis.

10 Discussion

Rare monogenic renal tubular disorders such as DD, FJHN and FHH, are valuable tools to gain insight into vital renal tubular processes, in addition to elucidating the mechanisms underpinning such disorders. Whilst the study of genes and pathways known to be associated with monogenic disorders builds on existing insight into the disorder, pathways and segment function; the identification of novel genes mutated in monogenic disorders may shed light on novel pathways and proteins previously unidentified or overlooked. Furthermore, as evidenced in this thesis, identification of such genes can have wide-ranging and lasting applications in the clinic including: ensuring an accurate diagnosis, informing prognosis, aiding familial and reproductive counselling, guiding clinical management and providing novel targets for therapeutics.

Whilst, the individual diseases studied in this thesis (DD, FJHN and FHH) are rare (as defined by effecting <200,000 people in the USA or <1 in 2000 in Europe), collectively, rare disorders affect millions of people worldwide[216]. In fact, the total number of rare genetic diseases is estimated to be between 6000 and 7000[110]; thus the impact on healthcare costs, mortality and morbidity is expected to be significant[110,216]. Specifically, there are estimated to be at least 150 different rare renal disorders that have a collective prevalence of 60-80 cases per 100,000 in Europe and the USA[405]. Furthermore, inherited renal disorders are thought to account for approximately 10% of adult end-stage renal disease and 70% of paediatric nephropathy[213]. It has been suggested that up-to 50% of patients with a rare genetic disorder do not receive a diagnosis using 'traditional approaches' such as clinical assessment, chromosomal analysis and single-gene/gene-panel sequencing[406]. As a result, patients and clinicians often have little choice but to undertake a 'diagnostic odyssey' which can be time- and

cost-intensive, with the time to diagnosis ranging from 5-30 years in approximately 25% of patients surveyed by Eurodis (EurodisCare2)[110,407]. This emphasises the need for 'gene-discovery' studies such as the ones performed in this thesis, to provide novel candidates for the aetiology of rare diseases. Furthermore, effective therapies for rare diseases are often themselves equally rare[216], highlighting the importance of identifying novel therapeutic targets and pathways. Additionally, the study of rare monogenic diseases provides important insights into more common and complex disorders. For example, whilst nephrolithiasis is a common disorder world-wide, with an estimated prevalence of 8.8% in the USA, using data collected from the National Health And Nutrition Examination Survey (NHANES), between 2007-2010 (10.6% in males, 7.1% in females)[408]; rare monogenic disorders such as DD can increase an individual's risk of developing nephrolithiasis, with an estimated prevalence of approximately 50% in males with DD[98,101,102]. Although in reality, the prevalence of nephrolithiasis in the general population is likely higher than indicated by NHANES as patients only recall symptomatic events and asymptomatic stone events are thought to be relatively common[408]. With the prevalence and incidence of nephrolithiasis demonstrated to have risen in the last few decades; and the rising prevalence of obesity and diabetes (in addition to population growth), the cumulative costs are predicted to increase by approximately US$1.24billion per year by 2030 (from an estimated cost of US$2.1billion in 2000)[408]. These reports highlight the current and future impact common disorders such as nephrolithiasis have on the healthcare systems and economies worldwide; and therefore the requirement to improve understanding of the molecular mechanisms underlying such disorders. Monogenic diseases such as DD1, where a single gene gives rise to the phenotype of

interest, can provide excellent models of simplified aetiology to study these mechanisms, that can subsequently be applied to more common and complex disorders.

Whilst 'gene-discovery' studies historically relied on Sanger DNA sequencing, NGS techniques such as WGS and WES, are more frequently being used in both the laboratory and clinic[110,210,213,214]. However, due to the identification of vast numbers of variants, the rate-limiting step in this process is the accurate interpretation of variants[210,213,219,265,266]. Therefore, this thesis investigated the effectiveness of commonly used *in silico* analyses at identifying pathogenic variants and distinguishing between pathogenic and benign variants. Parameters were optimised for population genomics using ExAC, prediction of functional effects using MutationTaster, PolyPhen-2 and Provean Protein, evolutionary conservation and a combined *in silico* approach. These parameters were then applied to the 'gene-discovery' studies included in this thesis to identify potential candidate genes and variants in each of the disorders. It is hoped these findings can be applied to both future NGS and Sanger DNA sequencing studies, providing clear guidelines for the interpretation of variants that can be used alone or in combination with existing guidelines[237], thereby improving the effectiveness and transparency of sequencing studies. However, future study is required to optimise new parameters for common disorders and non-coding variants as this study focused on coding variants associated with rare monogenic renal tubular disorders.

To gain new insight into the pathways involved in reabsorption and secretion processes in the different segments of the renal tubule, 'gene-discovery' studies were

performed for three monogenic disorders affecting different renal segments: DD, FJHN and FHH. These studies identified four novel candidate genes for these disorders: *CLCNKA* for DD, *CLDN3* and *DENND4C* for FJHN and *KLOTHO* for FHH. *In vitro* functional analysis of rare *KLOTHO* variants highlighted the importance of functional studies in determining pathogenicity; and whilst functional studies were not performed during the course of this thesis for *CLCNKA*, *CLDN3* and *DENND4C*, future studies of these genes may provide important insights into renal tubule biology and the aetiology of their respective disorders.

Currently, although three genes have been identified for FJHN, little is known about the molecular mechanisms underlying the pathogenesis of FJHN. Therefore, identification of additional genes responsible for the aetiology of FJHN may provide a greater insight into the underlying molecular mechanisms of the disease. Despite FJHN3 being mapped to SNPs in chromosome 2p22.1-p21.2 in five families shared with this study (families 2,3,5,6 and 7)[147], WGS identified no novel or very rare variants in that region in any of the probands. *In silico* and *in vitro* analysis of variants and genes identified by WGS resulted in *CLDN3* (family 5) and *DENND4C* (families 6 and 7) being identified and prioritised as good candidates for FJHN. Whilst *CLDN3*, encoding claudin 3, has well characterised roles in paracellular transport in the renal tubules, very little is known about *DENND4C*, encoding Dennd4C, with just four reports on PubMed to date[327,330,370,409]. Thus, whilst further study may prove more difficult for *DENND4C,* due to limited resources and functional information, such studies would provide novel insights into the function of Dennd4C, its role in the renal tubules and its potential role in FJHN.

In addition to providing further evidence for the genetic heterogeneity of a disorder, this thesis has demonstrated the utility of NGS in the correct diagnosis of complex disorders with multiple phenotypes (RCS with hyperuricaemia and gout); and how single genes may give rise to multiple disorders and phenotypes (*CLCNKA* and *KLOTHO*). This provides further evidence that many disorders may exist on a phenotypic spectrum rather than as distinct entities[210,213], in contrast to the classical Mendelian view of a one-to-one relationship between disease/phenotype and gene, which is reflected in recent literature[213].

WGS of two brothers diagnosed with FJHN, but lacking mutations in *UMOD*, *REN* and *HNF1ß*, identified a novel Gly76Arg variant in *PAX2*, a gene associated with RCS[347]. As RCS is characterised by both renal and ocular anomalies[348,351,352], ophthalmological examinations were subsequently performed, identifying optic pits in both brothers; and resulting in a revised diagnosis of RCS in this family. In addition to providing a genetic diagnosis for this family, allowing for familial and reproductive genetic screening; a revised diagnosis of RCS may alter the clinical management of the patients and affected family members, to prevent complications associated with retinal detachment and to monitor visual acuity, a reduction in which can be progressive over time in RCS patients[349,352]. Furthermore, these findings indicate hyperuricaemia and gout may be more prevalent in RCS than previously thought[349-352]. Similar findings have been observed in a range of disorders, including DD1, due to mutations in *CLCN5,* which is also associated with a vast range of inter- and intra-familial phenotypic variability[98,101,102].

Mutations in a single gene have been shown to give rise to multiple disorders, with varied phenotypes and severity[210]. This may be due to the location or type of mutation, whether the variant is heterozygous or homozygous, or due to an additional unknown or undetermined cause[210], and this is a relatively well reported phenomenon in the literature. For example, differences in the location of mutations in *OCRL1* are thought to be behind the phenotypic differences associated with DD2 and Lowe syndrome[98,121]. Whilst almost all mutations associated with Lowe syndrome have been reported to be located in exons 8-23, mutations associated with the milder DD2, are mostly located in exons 1-7[121]. This is in contrast to *COL4A3*, *COL4A4* and *COL4A5* mutations which cause a spectrum of diseases including Alport syndrome, thin basement membrane disease (TBMD) and focal segmental glomerulosclerosis (FSGS) in a seemingly sporadic manner[213,410,411]. Whilst mutations in *COL4A5* appear to be exclusive to Alport syndrome[412,413], there is little evidence for differences in the location or genotype of mutations in *COL4A3* and *COL4A4* in Alport syndrome[412,414-416], TBMD[417-420] or FSGS[411]. Reflecting the growing view that genetic disorders may exist on a phenotypic spectrum, disorders associated with mutations in *HNF1ß* have recently been termed *HNF1ß*-associated renal and extra-renal disease to describe the different symptoms associated with *HNF1ß* mutations[162,421]. It is likely that as more genetic variation is revealed by NGS projects, more genes will be associated with spectrums of clinical disorders. However, such overlap in genetic origins for phenotypically distinct disorders adds to the complexity of diagnosis in the clinic, thus highlighting how both clinical assessment and the use of NGS in the clinic may be beneficial for an accurate diagnosis[210,213], as demonstrated by our studies in RCS.

CLCNKA and *KLOTHO* were not excluded as candidate genes in DD and FHH, respectively; despite previously being associated with Bartter syndrome type 4b[134] and TC[377], respectively. Mutations in both *CLCNKA* and *CLCNKB* in combination are required for the pathogenesis of Bartter syndrome type 4b[134]. Therefore, after the identification of a homozygous variant in *CLCNKA*, it was hypothesised that homozygous variants in *CLCNKA,* encoding ClC-Ka, alone may be sufficient to cause DD. However, neither of the rare *CLCNKA* variants identified by Sanger DNA sequencing were homozygous or compound heterozygous. Additionally, the mechanisms by which ClC-Ka may cause both Bartter syndrome type 4b and DD is complicated as the reported expression profile of ClC-Ka in the renal tubules is not consistent with a renal Fanconi syndrome. DD is a well characterised renal Fanconi syndrome characterised by PT dysfunction. However, to date, most papers report the expression of ClC-Ka (or its rat ortholog ClC-K1) to be almost exclusively expressed in the thin limbs of the LOH (principally the tAL)[143,304,306]; with mice lacking ClC-K1 (homozygous) exhibiting polyuria and decreased urinary concentration, indicating nephrogenic diabetes insipidus[130]. These reports would therefore suggest that if ClC-Ka is involved in the aetiology of DD there may be a role for the LOH in DD; or alternatively may indicate a degree of cross-talk between the nephron segments, that as yet is uncharacterised. However, it has been reported that there is some expression of ClC-K1 in the S3 segment of the PT, which may indicate a direct role for ClC-Ka in reabsorption of Cl^- in the PT[273]. This highlights the importance of further studies to confirm these findings and to determine the effect, if any, these variants have on *CLCNKA* function and its role in relation to DD.

In addition to being a prime example of how variants in a single gene may give rise to disorders of varying severity, the investigation of *KLOTHO* as a candidate gene for FHH highlighted the importance of functional studies in determining the pathogenicity of a variant. *In silico* analysis of WES and targeted panel sequencing identified *KLOTHO* as a candidate gene for FHH4 in five patients with FHH that lacked mutations in *CASR*, *GNA11* and *AP2S1*. A homozygous His193Arg mutation in *KLOTHO* has previously been shown to cause TC[377] and it was therefore hypothesised that this study may be a further example of a single gene giving rise to multiple disorders that vary in severity. However, *in vitro* functional analysis showed no effect of Klotho variants on FGF23 signalling via ERK1/2 using SRE luciferase assays. Notably, no significant difference in SRE reporter activity was observed in the positive control, Arg193. In addition to mediating FGF23 signalling via FGFR1, Klotho also plays an important role in regulating TRPV5 expression in the DTs[68-70]. Therefore, further functional studies are required to determine whether the *KLOTHO* variants identified in this study effect TRPV5 regulation. Much of the current understanding of the molecular mechanisms underlying FHH signifies the role of the parathyroid glands and the role of CaSR trafficking and signalling in the regulation of PTH secretion[182]. Therefore, further study of Klotho and its role in the DTs may provide evidence for a distinct renal tubular role in FHH.

In conclusion, four novel candidate genes were identified for three rare monogenic renal tubular disorders: *CLCNKA* for DD; *CLDN3* and *DENND4C* for FJHN; and *KLOTHO* for FHH. It is hoped that future functional studies will ultimately provide the *in vitro* evidence for the determination of pathogenicity, or lack of, for each of the genes in their respective disorders. This, provides new insights into the molecular

mechanisms underlying each disorder and the function of the renal tubules in both health and disease. Finally, this thesis provides further evidence of the successful use of NGS methods to provide an accurate clinical diagnosis, distinguishing between overlapping clinical phenotypes; and guiding the future clinical management of patients.

11 Appendix

11.1. Materials and methods

Table 32. SDM primers

Gene	Variant	Forward primer	Reverse primer
CLDN3	p.Trp17Cys	cgtgctgggctgtctgggcaccatc	gatggtgcccagacagcccagcacg
KLOTHO	p.His193Arg	gtcaccctgtaccgctgggacctgccc	gggcaggtcccagcggtacagggtgac
	p.Met384Thr	acttttggaccctcacacgaagttccgccaattgg	ccaattggcggaacttcgtgtgagggtccaaaagt
	p.Asn607Asp	cctgattctccctctgggtgaccagtcccagg	cctgggactggtcacccagagggagaatcagg
	p.Pro690Leu	ctttggataacgatgaatgagctgtatacaaggaatatgacatac	gtatgtcatattccttgtatacagctcattcatcgttatccaaag
	p.Tyr1003Cys	ctctctcccttatattttactgctcgaagaaaggcagaag	cttctgcctttcttcgagcagtaaaatataagggagagag

Primers used for the generation of mutant *CLDN3* and *KLOTHO* plasmids by SDM.

Table 33. cDNA/plasmid sequencing primers

Plasmid	Section	Forward primer	Reverse primer
pCMV6-AC-tGFP	N/A	GGACTTTCCAAAATGTCG	ATTAGGACAAGGCTGGTGGG
CLDN3 (internal)	1	N/A	GATGATGTTGCTGCCGATG
	2	CTGGAGATCACGGGCACC	GATGGTGATCTTGGCCTTGG
	3	CCTTCGGGCTGCTAGTGG	CGTGTACTTCTTCTCGCGTG
	4	GGGCCTGTACGTGGGCTG	N/A
KLOTHO (internal)	1	N/A	CGAGATGGAGAAGCGGTAGT
	2	GCGACAGCTACAACAACG	CAGGAGGAGGTTGTGCG
	3	ATCACCATCGACAACCCCT	TGAAAACTCAAGGTGGGTC
	4	GGTGACTATCCCGAGAGCAT	GATGCTGTAACCTCTGTGCCA
	5	GGTGGATGTCATCGGGTAT	GGCAGCAAAGTCAACACAGT
	6	TGTCCACCACAGTAAAAGGC	GAAAGCACAGTCGGGCATAC
	7	CCCTGTGGCAGCCTATGG	CCAGTCCCTCATCACCCA
	8	AGGACAAAGAGGTGGCCGAG	CGATATAATACACCCTCAGCT
	9	GCTGAAGTTCAAGTACGGAG	N/A
DENND4C	1	CCGGGAATTCGTCGACTGG	TGTCTTGACTGGGGTAGCTG

Primers used for Sanger DNA sequencing of cDNA plasmids.

Table 34. Genomic DNA sequencing and PCR primers and their corresponding annealing temperatures

Gene	Exon	Variant	Forward primer	Reverse primer	PCR annealing temperature (°C)
CLCNKA	1	N/A	ggcagggagagagtgatgat	aaagccaaagtgaggtgctg	58°C
	2	N/A	cctcttcatttgggtgggga	gttcctgggcagagaggtg	58°C
	3	N/A	cccagactcaactaccaggg	agcaaatcaggagtagagcca	58°C
	4	N/A	ctggtcagtaagtgggcac	agaagccccctgggatctg	64°C
	5	N/A	aactcctgacctcgcgatc	aagactgagctccctgaagg	64°C
	6-7	N/A	ctacctgaggacagccct	ggtggctatacccaaagcg	54°C
	8	N/A	ccctacagccacaggt	acacggaggagggaaaagag	58°C
	9-10	N/A	cagattccgagtcaggacct	acaagggactcactgagatg	58°C
	11	N/A	gggatgtaggaaagggaggg	gaatgatgcccaggtgtcac	64°C
	12	N/A	aagtggcaggggaggattc	aaggaagtgtgggtgagagg	58°C
	13-14	N/A	gtcccctgtcctgtcttctc	gaaccaccagccaattctcc	58°C
	15	N/A	tacaattcccaccctagccc	ctggggagagtggagatgaga	58°C
	16	N/A	ccactgtgggttctaggagt	tcaagaaggaggcagagggcat	58°C
	17-18	N/A	ggaagcttggccctcaggcct	agcaggataagatgggcg	58°C
	19	N/A	tgcctcccacacatatcagg	catctccccagccttctcag	58°C
	20	N/A	tcagcctggaaatgaacctt	ttctcacactcagctctgcc	58°C
ANKRD11	9.1	p.Val454Met	CATCGTATCCTGTCAGACACG	AGAGAGTCCCTGTCATCCTCC	58°C
BSN	5.1	p.His1842Arg	CAGACAGCCCCATACCGAAG	CTGCCAAAGGGGAGCTTGTA	58°C
	5.2	p.Val2236Met	CTCAGACCTGGACTCCTTGG	caatgggaaatctacttggtgc	58°C
CLCN6	11	p.Trp303Arg	TCCATGTCTGCCACCTTCAC	TGTACCTAGCCCTCTGCTCA	58°C
CLDN3	1	p.Trp17Cys	TATGGAGCCGAGCCGTTAGC	tgaaggtcctgtggcagtgc	58°C
DENND4C	18.3	p.Ser1251Phe	GAGGGAAGATGTTGAAACTGG	GGGTTTGCTGCTTGAAACGC	58°C
	18.4	p.Arg1317Gln	TCACCAGCACAGGAAAATCC	cctgggcacagaaatctctg	58°C
FAT1	2	p.Pro714Leu	TGAGAATCACAGCTACAGATGG	GAAGCAACTATCCTCATTTCC	58°C
	10	p.Asp1930His	ATGAAGCATCTCTTTTGTTACC	TCCCAATAGCAGTAATGACAGC	58°C
FMOD	2.1	p.Gly56Val	TACTCTGCCTCACTGCCTCT	TACTTCATGCGGGAGGGAAC	58°C
	2.2	p.Gly147Asp	ACACCTACGGCTCTCCATCC	TCTGGTTGTGGTCGAGATGG	58°C
	2.3	p.Arg236Gln	AAGGTCTTCTCCAAGCTGAGG	TGTTGGTTAGACTGTTGTGGG	58°C
IGFN1	4	p.Phe48Leu	aaatacctagatgaggaagacg	gtcttactcctctagggattgg	54°C
	12.2	p.Ser2463Cys	GTCACAGGTCAGGATATTGGG	TCTGGAGACCTATCCTTCACC	58°C
	12.3	p.Gln2789X	CTGGAATGGCTTAGATGGTCC	AGTTCTCTCCCATAGGCTGC	58°C
KDM4E	1	p.Val311Met and p.Arg240Trp	ATGTGGGGTTGTCATCGAGG	AAGCCGTGATTGAAGCCAG	58°C
MYO16	9	p.Pro338Ser	agatttatgtgctatcaccacc	tgttctaactctttggctgag	55°C
	15	p.Gly570X	gtattattcactgcatcgtcgc	gaataggttttctctcccagc	58°C
NEU2	2.1	p.Arg83Trp	cgatgacttttgactctaaccc	GCATCAGTGAGGTCTCTGGG	59°C
	2.2	p.Phe279_Gly287delfs	GACGGGCTTGATTTCCAGG	TGCTCTGGAGGTCTGAGTAGG	59°C
PAX2	3	p.Gly76Arg	GAAGTCAGCTCAGCCACACT	CTGGAAGCAGGGAGAAAGGG	58°C
PPRC1	5.1	p.Arg243His	gggtttcagaaactcccagg	GCTTTATCTTCCTCCTCAGGG	58°C
	5.2	p.Leu937Arg	TTGCAGCCTCCTAGTCTTCC	GAACAGTAGACCAGAATGGAGC	58°C
RP1L1	4.2	p.Glu2013Lys	AGTTATAGAGTCCCAGGAGGC	GGCATCCCCTTCTGTCTTC	66.4°C

Table 34. Genomic DNA sequencing and PCR primers and their corresponding annealing temperatures continued

Gene	Exon	Variant	Forward primer	Reverse primer	PCR annealing temperature (°C)
SLC13A5	2	p.Pro68Ser	agcactgtgtcttgacaatcc	atccacaaatgagggttttcc	58°C
	9	p.Pro394His	tgtcttctaatgctgctctgg	gttatacgaaggatgcaggc	55°C
KLOTHO	2	p.Met384Thr	GGTGACTATCCCGAGAGCAT	ccagaagattttggcaggaa	63°C
	4.1	p.Asn607Asp	TCCTACTGTGTTGACTTTGCTGCC	GGCAGTGTAGGGGTTCTCC	58°C
	4.2	p.Pro690Leu	TCCTACTGTGTTGACTTTGCTGCC	TGAGTCTACAAGGATGGTGGT	58°C
	5	p.Tyr1003Cys	TCACACCCGAAAGTCTTTACT	TGCCCATTTCAAAACCTCTGT	58°C

Primers used for amplification of genomic DNA by PCR and the Sanger DNA sequencing of PCR products and their corresponding annealing temperatures. Exon numbers with decimal points indicate those that were too large to sequence as a single product and therefore signify which part of the exon was sequenced. N/A, not applicable, this is s stated for the *CLCNKA* gene as the entire gene was sequenced by Sanger DNA sequencing in the probands.

Table 35. ARMS PCR primers and their corresponding annealing temperatures

Gene	Exon/region	Variant	WT primer	Variant Primer	PCR annealing temperature (°C)
CLCNKA	1	p.Phe285del	GTTCCCTTCGACCTGCCTGAGATCTTC	GTTCCCTTCGACCTGCCTGAGATCTTT	58°C
ANKRD11	9.1	p.Val454Met	CAGCAGAAGGAAAAAAATAAAG	CAGCAGAAGGAAAAAAATAAAA	56°C
BSN	5.1	p.His1842Arg	CCAGTGCCAGAGCCAGGTGCCGAGCCCTA	CCAGTGCCAGAGCCAGGTGCCGAGCCCTG	52°C
	5.2	p.Val2236Met	TCTGGTGGAATCACAGCCG	TCTGGTGGAATCACAGCCA	58°C
CLCN6	11	p.Trp303Arg	CTGGGATTCAGTTTGGAAGCT	CTGGGATTCAGTTTGGAAGCC	61°C
CLDN3	1	p.Trp17Cys	GGCCGTGCTGGGCTGG	GGCCGTGCTGGGCTGT	65°C
DENND4C	18.3	p.Ser1251Phe	AAGTCCCCTAGGTAGTAAATCTTC	AAGTCCCCTAGGTAGTAAATCTTT	61°C
	18.4	p.Arg1317Gln	CAGCAAACCCCCTCTCG	CAGCAAACCCCCTCTCA	58°C
FAT1	10	p.Asp1930	CGGGGAGAAGTTTTCTATGG	CGGGGAGAAGTTTTCTATGC	58°C
FMOD	2.1	p.Gly56Val	TACGAGCCTTACCCCTATGG	CTACGAGCCTTACCCCTATGT	58°C
IGFN1	4	p.Phe48Leu	CAGGGAAAAATGCTGTCTTT	CAGGGAAAAATGCTGTCTTA	61°C
	12.3	p.Gln2789*	GCTGAGAATGGTGAGGTCC	CTGAGAATGGTGAGGTCT	58°C
KDM4E	1	p.Arg240Trp	GCTGTGAGGCCTTCCTGC	GCTGTGAGGCCTTCCTGT	65°C
MYO16	9	p.Pro338Ser	GAAGAGATCATTCACGATCTTC	GAAGAGATCATTCACGATCTTT	61°C
PAX2	3	p.Gly76Arg	CTTTCCCGGCGCAGGTACTACGAGACAG	CTTTCCCGGCGCAGGTACTACGAGACAC	66°C
SLC13A5	2	p.Pro68Ser	CATGCCTGTCTTGCTTTTCC	CATGCCTGTCTTGCTTTTCT	61°C
	9	p.Pro394His	GAAAACTCCATTTTATCCCCC	GAAAACTCCATTTTATCCCCA	58°C

The internal primers used for amplification of genomic DNA and identification of variants by ARMS PCR and their corresponding annealing temperatures. External forward and reverse primers also used for the amplification of genomic DNA by ARMS PCR and their corresponding annealing temperatures are detailed in appendix Table 34.

Table 36. Reverse Transcription (RT)-PCR primers and their corresponding annealing temperatures

Gene	Forward primer	Reverse primer	PCR annealing temperature (°C)
ANKRD11	CCGAGGAGTCTGCCAACA	GTGTTCACCTCCGCACCT	58°C
CLDN3	AAGGTGTACGACTCGCTGC	GTCCCGGATAATGGTGTTGG	58°C
DENND4C	GTTCACCAGCACAGGAAAATC	TCTGATAGATGCTAGACATGCTG	58°C
FMOD	CCCACAACAGTCTAACCAACA	GCTTGGAGAAGTTCACGACG	58°C
MYO16	ACGATGAAGGAGTAACCC	TCCTGAGACTGCTGCTTAC	58°C
GAPDH	Not specified	Not specified	55°C
DENND4C (insert)	GAATACTAGCGATCGCATGATAGAAGACAAAGGACCAAGAG	GAATACTACGCTAGCGAGGAAGGCAGAAAAGAGGTACATCT	58°C

Primers used for amplification of cDNA for RT-PCR and their corresponding annealing temperatures. GAPDH primers were purchased from Qiagen and the sequences were not specified.

Table 37. REs and their corresponding buffers and incubation temperatures

REs	Buffer	Incubation temperature (°C)
AcuI	CutSmart® + S-adenosylmethionine (SAM)	37°C
NaeI	CutSmart®	37°C
BsaAI	CutSmart®	37°C
BsaWI	CutSmart®	60°C
BsgI	CutSmart® + SAM	37°C
PstI	NEB 3.1	37°C
EarI	CutSmart®	37°C
DrdI	CutSmart®	37°C
MslI	CutSmart®	37°C
NspI	CutSmart®	37°C
BamHI + XhoI	NEB 3.1	37°C
AsiSI	CutSmart®	37°C
KpnI + XhoI	NEB 3.1	37°C

REs and their corresponding buffers and incubation temperatures used for the digestion of PCR products and cDNA plasmids.

Table 38. Antibodies used for Western blot analysis

Primary antibody	Manufacturer/ product code	Concentration	Secondary antibody	Concentration
Claudin-3	Abcam/ab214487	1 in 1000	Goat-anti-rabbit HRP	1 in 1000
Flg (FGFR1)	Santa Cruz Biotechnology/ Flg C-15 Sc121	1 in 100	Goat-anti-rabbit HRP	1 in 1000
TRPV5	Santa Cruz Biotechnology /R-98 Sc30187	1 in 100	Goat-anti-rabbit HRP	1 in 1000
Klotho	Santa Cruz Biotechnology /E21 Sc2220	1 in 200	Donkey-anti-goat HRP	1 in 1000
Calnexin	Abcam/ AB2301	1 in 1000	Goat-anti-rabbit HRP	1 in 2000

Antibodies and their corresponding concentrations and secondary antibodies used for the detection of specific proteins in cell lysates by Western blot analysis.

11.2. Results

Table 39. *In silico* analysis of *CASR* variants obtained from HGMD

Nucleotide change	Amino acid change	Phenotype/ disorder	Reference	*Reported vAF	Prediction of functional effects			Evolutionary conservation		Combined analysis	
					MutationTaster	PolyPhen-2	Provean Protein	4 Orthologs	8 Orthologs	1	2
c.2T>G	p.Met1Arg	Hypercalcaemia, hypocalciuric and hyperparathyroidism	Andrade et al.,[422]	0%	Disease causing	Possibly damaging (score 0.693)	Neutral (score -1.590)	3	6	Pathogenic	Likely pathogenic
c.32T>C	p.Leu11Ser	Hypercalcaemia, hypocalciuric	Pidasheva et al.,[423]	0.00082%	Disease causing	Benign (score 0.350)	Neutral (score -1.022)	4	7	Pathogenic	Likely pathogenic
c.38T>C	p.Leu13Pro	Hypercalcaemia, hypocalciuric	Miyashiro et al.,[424]	0%	Disease causing	Possibly damaging (score 0.610)	Neutral (score -0.979)	3	3	Pathogenic	Unknown significance
c.60C>A	p.Tyr20*	Hypercalcaemia, hypocalciuric	Nissen et al.,[425]	0%	Disease causing	N/A	N/A	4	8	Pathogenic	Pathogenic
c.61G>A	p.Gly21Arg	Hypercalcaemia, hypocalciuric	Nissen et al[426]	0%	Disease causing	Benign (score 0.347)	Neutral (score -1.207)	4	8	Pathogenic	Likely pathogenic
c.73C>T	p.Arg25*	Hypercalcaemia, hypocalciuric	Ward et al.,[427]	0.00164%	Disease causing	N/A	N/A	4	8	Pathogenic	Likely pathogenic
c.77C>G	p.Ala26Gly	Hypercalcaemia, hypocalciuric	Nissen et al.,[425]	0%	Disease causing	Benign (score 0.064)	Neutral (score -1.083)	4	8	Pathogenic	Likely pathogenic
c.79A>G	p.Gln27Arg	Hypercalcaemia, hypocalciuric	Chikatsu et al.,[428]	0%	Disease causing	Benign (score 0.070)	Neutral (score -0.968)	4	8	Pathogenic	Likely pathogenic
c.85A>G	p.Lys29Glu	Hypocalcaemia	Hu et al.,[429]	0%	Disease causing	Benign (score 0.014)	Neutral (score -0.353)	4	7	Pathogenic	Likely pathogenic
c.115C>G	p.Pro39Ala	Hypercalcaemia, hypocalciuric	Aida et al.,[430]	0%	Disease causing	Benign (score 0.195)	Deleterious (score -4.365)	4	8	Pathogenic	Pathogenic
c.118A>T	p.Ile40Phe	Hypercalcaemia, hypocalciuric	Vargas-Poussou et al.,[431]	0%	Disease causing	Benign (score 0.330)	Neutral (score -2.436)	4	7	Pathogenic	Likely pathogenic
c.125T>C	p.Phe42Ser	Hypercalcaemia, hypocalciuric	Cole et al.,[432]	0%	Disease causing	Benign (score 0.101)	Neutral (score -1.483)	4	8	Pathogenic	Likely pathogenic
c.141A>C	p.Lys47Asn	Hypocalcaemia	Okazaki et al.,[433]	0%	Disease causing	Benign (score 0.062)	Neutral (score-0.866)	4	8	Pathogenic	Likely pathogenic
c.157T>C	p.Ser53Pro	Hypercalcaemia, hypocalciuric	Heath et al.,[434]	0%	Disease causing	Benign (score 0.248)	Deleterious (score -2.596)	4	7	Pathogenic	Likely pathogenic

Nucleotide change	Amino acid change	Phenotype/ disorder	Reference	*Reported vAF	Prediction of functional effects			Evolutionary conservation		Combined analysis	
					MutationTaster	PolyPhen-2	Provean Protein	4 Orthologs	8 Orthologs	1	2
c.164C>T	p.Pro55Leu	Hypercalcaemia, hypocalciuric	Pearce et al.,[435]	0%	Disease causing	Possibly damaging (score 0.837)	Deleterious (score -8.153)	4	8	Pathogenic	Pathogenic
c.179G>T	p.Cys60Phe	Hypercalcaemia, hypocalciuric	Waller et al.,[436]	0%	Disease causing	Possibly damaging (score 0.696)	Deleterious (score -9.164)	4	8	Pathogenic	Pathogenic
c.185G>T	p.Arg62Met	Hypercalcaemia, hypocalciuric	Chou et al.,[437]	0%	Disease causing	Benign (score 0.358)	Neutral (score -2.419)	4	8	Pathogenic	Likely pathogenic
c.196C>T	p.Arg66Cys	Hypercalcaemia, hypocalciuric	Pidasheva et al.,[438]	0%	Disease causing	Possibly damaging (score 0.617)	Deleterious (score -3.445)	4	8	Pathogenic	Pathogenic
c.197G>A	p.Arg66His	Hypercalcaemia, hypocalciuric	Chou et al.,[437]	0%	Disease causing	Probably damaging (score 0.981)	Deleterious (score -5.336)	4	8	Pathogenic	Pathogenic
c.205C>T	p.Arg69Cys	Hyperparathyroidism, neonatal primary	Wilhelm-Bals et al.,[439]	0.00164%	Disease causing	Possibly damaging (score 0.615)	Deleterious (score -4.205)	4	8	Pathogenic	Likely pathogenic
c.206G>A	p.Arg69His	Hypercalcaemia, hypocalciuric	Hannan et al.,[372]	0%	Disease causing	Possibly damaging (score 0.849)	Deleterious (score -6.966)	4	8	Pathogenic	Pathogenic
c.242T>C	p.Ile81Thr	Hypercalcaemia, hypocalciuric	Nissen et al.,[425]	0%	Disease causing	Probably damaging (score 0.936)	Deleterious (score -4.742)	4	8	Pathogenic	Pathogenic
c.243A>G	p.Ile81Met	Hypercalcaemia, hypocalciuric	Cole et al.,[432]	0%	Disease causing	Probably damaging (score 0.957)	Deleterious (score -2.852)	4	8	Pathogenic	Pathogenic
c.269A>C	p.Asn90Thr	Hypercalcaemia, hypocalciuric	Nissen et al.,[425]	0.00082%	Disease causing	Probably damaging (score 0.948)	Deleterious (score -5.248)	4	8	Pathogenic	Pathogenic
c.280G>T	p.Gly94*	Hyperparathyroidism	Ward et al.,[440]	0%	Disease causing	N/A	N/A	4	8	Pathogenic	Pathogenic
c.299C>T	p.Thr100Ile	Hyperparathyroidism	Warner (et al.,[441]	0%	Disease causing	Benign (score 0.219)	Deleterious (score -4.737)	4	8	Pathogenic	Likely pathogenic
c.310G>A	p.Val104Ile	Hypercalciuria, hypocalcaemic	Hannan et al.,[372]	0%	Disease causing	Benign (score 0.017)	Neutral (score 0.099)	3	7	Pathogenic	Likely pathogenic
c.328G>A	p.Ala110Thr	Hypercalcaemia, hypocalciuric	Nakamura et al.,[442]	0%	Disease causing	Benign (score 0.219)	Neutral (score -1.727)	4	8	Pathogenic	Likely pathogenic
c.346G>A	p.Ala116Thr	Hypoparathyroidism	Baron et al.,[443]	0%	Disease causing	Benign (score 0.012)	Neutral (score 0.234)	4	8	Pathogenic	Likely pathogenic
c.346G>C	p.Asn116Pro	Hypercalciuria, hypocalcaemic	Hannan et al.,[372]	0%	Disease causing	Benign (score 0.064)	Deleterious (score -2.523)	4	8	Pathogenic	Pathogenic

Nucleotide change	Amino acid change	Phenotype/ disorder	Reference	*Reported vAF	Prediction of functional effects			Evolutionary conservation		Combined analysis	
					MutationTaster	PolyPhen-2	Provean Protein	4 Orthologs	8 Orthologs	1	2
c.354C>A	p.Asn118Ly	Hypocalcaemia with hypercalciuria	Pearce et al.,[444]	0%	Disease causing	Benign (score 0.007)	Neutral (score -1.398)	4	8	Pathogenic	Likely pathogenic
c.365C>G	p.Ser122Cys	Hypoparathyroidism, autosomal dominant	Nakamura et al.,[442]	0%	Disease causing	Benign (score 0.250)	Neutral (score -2.204)	4	8	Pathogenic	Likely pathogenic
c.372C>A	p.Asn124Lys	Hypocalcaemia	Hu et al.,[445]	0%	Disease causing	Possibly damaging (score 0.600)	Neutral (score -1.350)	4	8	Pathogenic	Likely pathogenic
c.373C>T	p.Leu125Phe	Hypoparathyroidism	Hendy et al.,[446]	0%	Disease causing	Benign (score 0.075)	Neutral (score -1.423)	4	8	Pathogenic	Likely pathogenic
c.374T>C	p.Leu125Pro	Hypocalcaemia	Cole et al.,[432]	0%	Disease causing	Benign (score 0.062)	Neutral (score -0.422)	4	8	Pathogenic	Likely pathogenic
c.379G>A	p.Glu127Lys	Hypoparathyroidism	Lienhardt et al,.[447]	0%	Disease causing	Benign (score 0.113)	Neutral (score -1.300)	4	8	Pathogenic	Likely pathogenic
c.380A>C	p.Glu127Ala	Hypocalcaemia	Pollak et al.,[190]	0%	Disease causing	Benign (score 0.070)	Neutral (score -1.841)	4	8	Pathogenic	Likely pathogenic
c.380A>G	p.Glu127Gly	Hypercalciuria, hypocalcaemic	Hannan et al.,[372]	0%	Disease causing	Benign (score 0.039)	Neutral (score -1.387)	4	8	Pathogenic	Likely pathogenic
c.382T>C	p.Phe128Leu	Hypocalcaemia with hypercalciuria	Pearce et al.,[444]	0%	Disease causing	Benign (score 0.032)	Neutral (score -0.837)	4	8	Pathogenic	Likely pathogenic
c.385T>A	p.Cys129Ser	Hypocalcaemia	Hirai et al.,[448]	0%	Disease causing	Possibly damaging (score 0.510)	Neutral (score -2.444)	4	8	Pathogenic	Likely pathogenic
c.385T>C	p.Cys129Arg	Hypocalcaemia	Cole et al.,[432]	0%	Disease causing	Possibly damaging (score 0.600)	Neutral (score -2.420)	4	8	Pathogenic	Likely pathogenic
c.386G>A	p.Cys129Tyr	Hypocalcaemia with hypercalciuria	Burren et al.,[449]	0%	Disease causing	Possibly damaging (score 0.6)	Neutral (score -1.957)	4	8	Pathogenic	Likely pathogenic
c.386G>T	p.Cys129Phe	Hypocalcaemia	Hendy et al.,[446]	0%	Disease causing	Possibly damaging (score 0.696)	Neutral (score -2.355)	4	8	Pathogenic	Likely pathogenic
c.391T>A	p.Cys131Ser	Hypercalciuria, hypocalcaemic	Hannan et al.,[372]	0%	Disease causing	Possibly damaging (score 0.604)	Neutral (score -2.067)	4	8	Pathogenic	Likely pathogenic
c.392G>A	p.Cys131Tyr	Hypercalciuria, hypocalcaemic	Hannan et al.,[372]	0%	Disease causing	Benign (score 0.377)	Deleterious (score -4.217)	4	8	Pathogenic	Pathogenic
c.392G>T	p.Cys131Phe	Hypocalcaemia	Watanabe et al.,[450]	0%	Disease causing	Probably damaging (score 0.986)	Deleterious (score -4.449)	4	8	Pathogenic	Pathogenic

Nucleotide change	Amino acid change	Phenotype/ disorder	Reference	*Reported vAF	Prediction of functional effects			Evolutionary conservation		Combined analysis	
					MutationTaster	PolyPhen-2	Provean Protein	4 Orthologs	8 Orthologs	1	2
c.393C>G	p.Cys131Trp	Hypercalcaemia, hypocalciuric & hypoparathyroidism	Suzuki et al.,[451]	0%	Disease causing	Possibly damaging (score 0.758)	Deleterious (score -4.077)	4	8	Pathogenic	Pathogenic
c.407C>T	p.Pro136Leu	Hypocalcaemia	Gupta et al.,[452]	0%	Disease causing	Possibly damaging (score 0.696)	Deleterious (score -5.679)	4	8	Pathogenic	Pathogenic
c.409T>C	p.Ser137Pro	Hypercalcaemia, hypocalciuric	Soei et al.,[453]	0%	Disease causing	Benign (score 0.019)	Neutral (score 0.436)	4	8	Pathogenic	Likely pathogenic
c.413C>T	p.Thr138Met	Hypercalcaemia, hypocalciuric	Chou et al.,[437]	0%	Disease causing	Benign (score 0.404)	Neutral (score 0.296)	4	8	Pathogenic	Likely pathogenic
c.427G>A	p.Gly143Arg	Hypercalcaemia, hypocalciuric	Cole et al.,[432]	0.00082%	Disease causing	Probably damaging (score 0.992)	Deleterious (score -7.604)	4	8	Pathogenic	Pathogenic
c.428G>A	p.Gly143Glu	Hypercalcaemia, hypocalciuric	Chou et al.,[437]	0%	Disease causing	Probably damaging (score 0.957)	Deleterious (score -7.543)	4	8	Pathogenic	Pathogenic
c.445G>C	p.Val149Leu	Hypercalcaemia, hypocalciuric	Nissen et al.,[425]	0%	Disease causing	Benign (score 0)	Neutral (score 0.196)	4	7	Pathogenic	Likely pathogenic
c.452C>G	p.Thr151Arg	Hypocalcaemia	Letz et al.,[454]	0%	Disease causing	Benign (score 0.008)	Neutral (score -2.294)	4	8	Pathogenic	Likely pathogenic
c.452C>T	p.Thr151Met	Hypoparathyroidism	Lovlie et al.,[455]	0%	Disease causing	Benign (score 0.002)	Neutral (score 0.602)	4	8	Pathogenic	Likely pathogenic
c.472G>A	p.Gly158Arg	Hypercalcaemia, hypocalciuric	Cole et al.,[432]	0%	Disease causing	Benign (score 0.171)	Deleterious (score -6.456)	4	8	Pathogenic	Pathogenic
c.473G>A	p.Gly158Glu	Hypercalcaemia, hypocalciuric	Hannan et al.,[372]	0%	Disease causing	Benign (score 0.053)	Deleterious (score -6.339)	4	8	Pathogenic	Pathogenic
c.476T>C	p.Leu159Pro	Hyperparathyroidism	Simonds et al.,[456]	0%	Disease causing	Benign (score 0.032)	Deleterious (score -4.536)	4	8	Pathogenic	Pathogenic
c.476T>G	p.Leu159Arg	Hypercalcaemia, hypocalciuric	Ho et al.,[457]	0%	Disease causing	Possibly damaging (score 0.470)	Deleterious (score -4.616)	4	8	Pathogenic	Pathogenic
c.482A>G	p.Tyr161Cys	Hyperparathyroidism	Rajguru (2001) CASR Locus-specific database Unpublished 61	0%	Disease causing	Benign (score 0.278)	Deleterious (score -4.447)	3	7	Pathogenic	Pathogenic
c.490C>T	p.Gln164*	Hypercalcaemia, hypocalciuric	Waller et al.,[436]	0%	Disease causing	N/A	N/A	3	7	Pathogenic	Likely pathogenic
c.494T>A	p.Val165Asp	Hypercalcaemia, hypocalciuric	Nissen et al.,[425]	0%	Disease causing	Probably damaging (score 0.944)	Deleterious (score -6.507)	4	7	Pathogenic	Pathogenic
c.496A>G	p.Ser166Gly	Hypercalcaemia, hypocalciuric	Cole et al.,[432]	0%	Disease causing	Benign (score 0.365)	Neutral (score -2.217)	4	8	Pathogenic	Likely pathogenic

Nucleotide change	Amino acid change	Phenotype/ disorder	Reference	*Reported vAF	Prediction of functional effects			Evolutionary conservation		Combined analysis	
					MutationTaster	PolyPhen-2	Provean Protein	4 Orthologs	8 Orthologs	1	2
c.512G>A	p.Ser171Asn	Hypercalcaemia, hypocalciuric	Nissen et al.,[426]	0%	Disease causing	Benign (score 0.016)	Neutral (score -2.190)	4	8	Pathogenic	Likely pathogenic
c.514A>G	p.Arg172Gly	Hypercalcaemia, hypocalciuric	Hinnie et al.,[458]	0%	Disease causing	Benign (score 0.001)	Neutral (score -1.235)	4	8	Pathogenic	Likely pathogenic
c.517C>T	p.Leu173Pro	Hypercalcaemia, hypocalciuric	Felderbauer et al., [459]	0%	Disease causing	Benign (score 0.126)	Deleterious (score -3.627)	4	8	Pathogenic	Pathogenic
c.518T>C	p.Leu173Phe	Hypercalciuria, hypocalcaemic	Hannan et al.,[372]	0%	Disease causing	Benign (score 0.064)	Neutral (score -1.964)	4	8	Pathogenic	Likely pathogenic
c.521T>G	p.Leu174Arg	Hypercalcaemia, hypocalciuric	Ward et al.,[460]	0%	Disease causing	Probably damaging (score 0.979)	Deleterious (score -5.699)	4	8	Pathogenic	Pathogenic
c.532A>G	p.Asn178Asp	Hypercalcaemia, hypocalciuric	Pearce et al.,[188]	0%	Disease causing	Benign (score 0.016)	Neutral (score -1.725)	4	8	Pathogenic	Likely pathogenic
c.539T>G	p.Phe180Cys	Hypercalcaemia, hypocalciuric	Zajickova et al.,[461]	0%	Disease causing	Benign (score 0.186)	Deleterious (score -6.469)	3	5	Pathogenic	Likely pathogenic
c.553C>T	p.Arg185*	Hypercalcaemia, hypocalciuric	Kobayashi et al.,[462]	0%	Disease causing	N/A	N/A	4	8	Pathogenic	Pathogenic
c.554G>A	p.Arg185Gln	Hypercalcaemia, hypocalciuric	Pollak et al.,[183]	0%	Disease causing	Possibly damaging (score 0.485)	Deleterious (score -3.884)	4	8	Pathogenic	Pathogenic
c.569A>G	p.Asp190Gly	Hypercalcaemia, hypocalciuric	Nanjo et al.,[463]	0%	Disease causing	Benign (score 0.446)	Deleterious (score -6.796)	4	8	Pathogenic	Pathogenic
c.571G>A	p.Glu191Lys	Hypocalcaemia with hypercalciuria	Pearce et al.,[444]	0%	Disease causing	Benign (score 0.016)	Neutral (score -0.779)	4	8	Pathogenic	Likely pathogenic
c.613C>T	p.Arg205Cys	Hypercalcaemia, hypocalciuric	Nissen et al.,[425]	0.00082%	Disease causing	Benign (score 0.416)	Neutral (score -2.337)	3	5	Pathogenic	Likely benign
c.623G>C	p.Trp208Ser	Hypercalcaemia, hypocalciuric	Demedts et al.,[464]	0%	Disease causing	Probably damaging (score 0.998)	Deleterious (score -13.602)	4	8	Pathogenic	Pathogenic
c.624G>C	p.Trp208Cys	Hypercalcaemia, hypocalciuric	Hannan et al.,[372]	0%	Disease causing	Probably damaging (score 0.999)	Deleterious (score -12.631)	4	8	Pathogenic	Pathogenic
c.635T>C	p.Ile212Thr	Hypercalcaemia, hypocalciuric	Marcocci et al.,[465]	0%	Disease causing	Possibly damaging (score 0.575)	Deleterious (score -3.698)	4	8	Pathogenic	Pathogenic
c.635T>G	p.Ile212Ser	Hyperparathyroidism, neonatal primary	Hannan et al.,[372]	0%	Disease causing	Possibly damaging (score 0.719)	Deleterious (score -4.935)	4	8	Pathogenic	Pathogenic
c.638C>A	p.Ala213Glu	Hypercalcaemia, hypocalciuric	Elamin and de Buyl [466]	0%	Disease causing	Possibly damaging (score 0.480)	Deleterious (score -3.516)	4	8	Pathogenic	Pathogenic

Nucleotide change	Amino acid change	Phenotype/ disorder	Reference	*Reported vAF	Prediction of functional effects			Evolutionary conservation		Combined analysis	
					MutationTaster	PolyPhen-2	Provean Protein	4 Orthologs	8 Orthologs	1	2
c.644A>G	p.Asp215Gly	Hypercalcaemia, hypocalciuric	Heath et al.,[434]	0%	Disease causing	Benign (score 0.346)	Deleterious (score -6.347)	4	8	Pathogenic	Pathogenic
c.652T>C	p.Tyr218His	Hypercalcaemia, hypocalciuric	Hannan et al.,[372]	0%	Disease causing	Benign (score 0.368)	Deleterious (score -4.830)	4	8	Pathogenic	Pathogenic
c.653A>C	p.Tyr218Ser	Hypercalcaemia, hypocalciuric	Pearce et al.,[435]	0%	Disease causing	Benign (score 0.064)	Deleterious (score -8.689)	4	8	Pathogenic	Pathogenic
c.653A>G	p.Tyr218Cys	Hypercalcaemia, hypocalciuric	Cetani et al.,[467]	0%	Disease causing	Possibly damaging (score 0.887)	Deleterious (score -8.700)	4	8	Pathogenic	Pathogenic
c.658C>T	p.Arg22Trp	Hypercalcaemia, hypocalciuric	Pearce et al.,[188]	0%	Disease causing	Benign (score 0.013)	Neutral (score -1.874)	4	8	Pathogenic	Likely pathogenic
c.659G>A	p.Arg220Gln	Hypercalcaemia, hypocalciuric	Hannan et al.,[372]	0%	Disease causing	Benign (score 0.112)	Deleterious (score -3.958)	4	8	Pathogenic	Pathogenic
c.659G>C	p.Arg220Pro	Hypercalcaemia, hypocalciuric	D'Souza-Li et al.,[468]	0%	Disease causing	Possibly damaging (score 0.775)	Deleterious (score -4.652)	4	8	Pathogenic	Pathogenic
c.661C>T	p.Pro221Ser	Hypercalcaemia, hypocalciuric	Nissen et al.,[426]	0%	Disease causing	Benign (score 0.001)	Neutral (score -0.856)	4	8	Pathogenic	Likely pathogenic
c.662C>A	p.Pro221Gln	Hypocalcaemia	Conley et al.,[469]	0%	Disease causing	Benign (score 0.001)	Neutral (score -1.701)	4	8	Pathogenic	Likely pathogenic
c.662C>T	p.Pro221Ser	Hypercalcaemia, hypocalciuric	Pearce et al.,[188]	0%	Disease causing	Benign (score 0.001)	Neutral (score -0.890)	4	8	Pathogenic	Likely pathogenic
c.674A>C	p.Lys674Thr	Hypercalcaemia, hypocalciuric	Nissen et al.,[426]	0%	Disease causing	Benign (score 0.001)	Neutral (score -0.263)	4	8	Pathogenic	Likely pathogenic
c.679C>T	p.Arg227*	Hypercalcaemia, hypocalciuric	Chou et al.,[437]	0.00082%	Disease causing	Benign (score 0.007)	Neutral (score -0.179)	4	7	Pathogenic	Likely pathogenic
c.680G>A	p.Arg227Gln	Hyperparathyroidism	Pearce et al.,[435]	0%	Disease causing	Benign (score 0.007)	Neutral (score -2.100)	4	7	Pathogenic	Likely pathogenic
c.680G>T	p.Arg2227Leu	Hyperparathyroidism	Al-Khalaf et al.,[470]	0%	Disease causing	N/A	N/A	4	7	Pathogenic	Pathogenic
c.682G>A	p.Glu228Lys	Hypocalcaemia	Cole et al.,[432]	0%	Disease causing	Benign (score 0.005)	Neutral (score -1.192)	4	7	Pathogenic	Likely pathogenic
c.682G>C	p.Glu228Gln	Hypocalcaemia	Conley et al.,[469]	0%	Disease causing	Benign (score 0.015)	Neutral (score -1.213)	4	7	Pathogenic	Likely pathogenic
c.683A>G	p.Glu228Gly	Hypocalcaemia	Nakajima et al.,[471]	0%	Disease causing	Benign (score 0.015)	Deleterious (score -3.937)	4	7	Pathogenic	Pathogenic
c.706T>G	p.Cys236Gly	Hypercalcaemia, hypocalciuric	Hannan et al.,[372]	0%	Disease causing	Probably damaging (score 0.998)	Deleterious (score -11.090)	4	8	Pathogenic	Pathogenic
c.721G>A	p.Glu241Lys	Hypercalciuria, hypocalcaemic	Hannan et al.,[372]	0%	Disease causing	Benign (score 0.035)	Deleterious (score -3.004)	4	7	Pathogenic	Pathogenic

Nucleotide change	Amino acid change	Phenotype/ disorder	Reference	*Reported vAF	Prediction of functional effects			Evolutionary conservation		Combined analysis	
					MutationTaster	PolyPhen-2	Provean Protein	4 Orthologs	8 Orthologs	1	2
c.734A>G	p.Gln245Arg	Hypocalcaemia	Perry et al.,[472]	0%	Disease causing	Benign (score 0.007)	Neutral (score -0.458)	4	8	Pathogenic	Likely pathogenic
c.740C>T	p.Ser247Phe	FIH	Nissen et al.,[425]	0.00329%	Disease causing	Benign (score 0.002)	Neutral (score 0.249)	3	5	Pathogenic	Benign
c.748G>A	p.Glu250Lys	Hyperparathyroidism	Simonds et al.,[456]	0.18%	Polymorphism	Benign (score 0.001)	Neutral (score -1.312)	4	6	Pathogenic	Likely benign
c.759G>C	p.Gln253His	FHH	Nissen et al.,[425]	0%	Polymorphism	Benign (score 0.002)	Neutral (score -2.190)	3	6	Pathogenic	Likely pathogenic
c.788C>T	p.Thr263Met	Hypercalcaemia, hypocalciuric	Guarnieri et al.,[473]	0%	Disease causing	Benign (score 0.326)	Deleterious (score -3.950)	4	7	Pathogenic	Pathogenic
c.812C>T	p.Ser271Phe	FHH	Nissen et al.,[426]	0%	Disease causing	Benign (score 0.053)	Deleterious (score -4.099)	4	7	Pathogenic	Pathogenic
c.848T>C	p.Ile283Thr	Hyperparathyroidism	Guarnieri et al.,[473]	0.0132%	Disease causing	Benign (score 0.036)	Deleterious (score -3.077)	4	7	Pathogenic	Likely pathogenic
c.862A>G	p.Ile288Val	FHH	Nissen et al.,[425]	0%	Disease causing	Benign (score 0.012)	Neutral (score -0.240)	4	8	Pathogenic	Likely pathogenic
c.887G>A	p.Ser296Asn	Hypercalcaemia, hypocalciuric	Hannan et al.,[372]	0%	Disease causing	Benign (score 0.197)	Deleterious (score -2.866)	4	8	Pathogenic	Pathogenic
c.889G>A	p.Glu297Lys	Hypercalcaemia, hypocalciuric	Pollak et al.,[183]	0%	Disease causing	Benign (score 0.227)	Deleterious (score -3.941)	4	8	Pathogenic	Pathogenic
c.892G>A	p.Ala298Thr	Hyperparathyroidism	Starker et al.,[474]	0%	Disease causing	Benign (score 0.040)	Deleterious (score -3.793)	4	8	Pathogenic	Pathogenic
c.967A>T	p.Lys323*	Hypercalcaemia, hypocalciuric	Ward et al.,[427]	0%	Disease causing	N/A	N/A	3	6	Pathogenic	Likely pathogenic
c.1015C>A	p.Pro339Thr	Hyperparathyroidism	Hannan et al.,[475]	0%	Disease causing	Benign (score 0.341)	Deleterious (score -7.395)	3	7	Pathogenic	Pathogenic
c.1051T>G	p.Phe351Val	Hypercalcaemia, hypocalciuric	Guarnieri et al.,[473]	0%	Disease causing	Benign (score 0.265)	Deleterious (score -5.989)	4	8	Pathogenic	Pathogenic
c.1056G>A	p.Trp352*	Hypercalcaemia, hypocalciuric	Nissen et al.,[426]	0%	Disease causing			4	8	Pathogenic	Pathogenic
c.1073G>C	p.Cys358Ser	FHH	Nissen et al.,[425]	0%	Disease causing	Probably damaging (score 0.970)	Deleterious (score -9.810)	4	8	Pathogenic	Pathogenic
c.1174C>T	p.Arg392*	Hyperparathyroidism, neonatal primary	Hannan et al.,[372]	0%	Disease causing	N/A	N/A	4	8	Pathogenic	Pathogenic
c.1183T>C	p.Cys395Arg	Hypercalcaemia, hypocalciuric	Vigouroux et al[476]	0%	Disease causing	Possibly damaging (score 0.796)	Deleterious (score -11.353)	4	8	Pathogenic	Pathogenic
c.1189G>A	p.Gly397Arg	FHH	Nissen et al.,[426]	0%	Disease causing	Benign (score 0.171)	Deleterious (score -7.606)	4	8	Pathogenic	Pathogenic
c.1230T>A	p.Asp410Glu	Hypocalcaemia	Park et al.,[477]	0%	Disease causing	Benign (score 0.006)	Deleterious (score -3.547)	4	8	Pathogenic	Pathogenic

Nucleotide change	Amino acid change	Phenotype/ disorder	Reference	*Reported vAF	Prediction of functional effects			Evolutionary conservation		Combined analysis	
					MutationTaster	PolyPhen-2	Provean Protein	4 Orthologs	8 Orthologs	1	2
c.1256A>G	p.Asn419Ser	Hypercalciuria, hypocalcaemic	Hannan et al.,[372]	0%	Disease causing	Benign (score 0.030)	Deleterious (score -4.350)	4	8	Pathogenic	Pathogenic
c.1370C>T	p.Ala457Val	FHH	Nissen et al.,[425]	0%	Disease causing	Benign (score 0.029)	Neutral (score -1.535)	4	8	Pathogenic	Likely pathogenic
c.1376A>G	p.Gln459Arg	Hypercalcaemia, hypocalciuric	Lietman et al.,[478]	0%	Disease causing	Benign (score 0.142)	Deleterious (score -3.833)	4	8	Pathogenic	Pathogenic
c.1382T>C	p.Leu461Pro	Hypercalcaemia, hypocalciuric	Hannan et al.,[372]	0%	Disease causing	Possibly damaging (score 0.887)	Deleterious (score -4.745)	4	8	Pathogenic	Pathogenic
c.1389C>A	p.His463Gln	Hypercalcaemia, hypocalciuric	Nissen et al.,[425]	0.00412%	Disease causing	Benign (score 0.015)	Deleterious (score -2.558)	4	7	Pathogenic	Likely pathogenic
c.1393C>T	p.Arg465Trp	Hypercalcaemia, hypocalciuric	Leech et al.,[479]	0%	Disease causing	Benign (score 0.015)	Neutral (score -0.229)	4	8	Pathogenic	Likely pathogenic
c.1394G>A	p.Arg465Gln	Hypercalcaemia, hypocalciuric	Guarnieri et al.,[473]	0.00164%	Disease causing	Benign (score 0.052)	Deleterious (score -4.335)	4	8	Pathogenic	Likely pathogenic
c.1525G>A	p.Gly509Arg	Hypercalcaemia, hypocalciuric	Nissen et al.,[426]	0.00082%	Disease causing	Possibly damaging (score 0.844)	Deleterious (score -7.281)	4	8	Pathogenic	Pathogenic
c.1526G>C	p.Gly509Ala	Hypercalcaemia	Koltin et al.,[480]	0%	Disease causing	Possibly damaging (score 0.710)	Deleterious (score -5.621)	4	8	Pathogenic	Pathogenic
c.1541A>G	p.Tyr514Cys	Hypoparathyroidism	Nissen et al.,[425]	0%	Disease causing	Benign (score 0.342)	Neutral (score -0.759)	4	7	Pathogenic	Likely pathogenic
c.1555G>T	p.Glu519*	Hypercalcaemia, hypocalciuric	Rodrigues et al.,[481]	0%	Disease causing	N/A	N/A	4	7	Pathogenic	Pathogenic
c.1588T>G	p.Trp530Gly	Hypercalcaemia, hypocalciuric	Rus et al.,[482]	0%	Disease causing	Probably damaging (score 0.940)	Deleterious (score -12.004)	4	8	Pathogenic	Pathogenic
c.1589G>A	p.Trp530*	Hypercalcaemia, hypocalciuric	Nissen et al.,[425]	0%	Disease causing	N/A	N/A	4	8	Pathogenic	Pathogenic
c.1631G>A	p.Arg544Gln	Hypercalcaemia, hypocalciuric	Nissen et al.,[425]	0.08%	Disease causing	Benign (score 0)	Neutral (score 0.627)	3	6	Pathogenic	Likely benign
c.1645G>A	p.Gly549Arg	Hypercalcaemia, hypocalciuric	D'Souza-Li et al.,[483]	0%	Disease causing	Probably damaging (score 0.969)	Deleterious (score -.406)	4	8	Pathogenic	Pathogenic
c.1649C>T	p.Thr550Ile	Hypercalcaemia, hypocalciuric	Al-Salameh et al.,[484]	0%	Disease causing	Benign (score 0.22)	Deleterious (score -4.497)	3	7	Pathogenic	Pathogenic
c.1652G>A	p.Arg551Lys	Hyperparathyroidism	Toke et al.,[485]	0%	Disease causing	Benign (score 0.153)	Deleterious (score -2.588)	3	7	Pathogenic	Pathogenic
c.1657G>A	p.Gly553Arg	Hypercalcaemia, hypocalciuric	Schwarz et al.,[486]	0%	Disease causing	Benign (score 0.013)	Deleterious (score -3.749)	3	7	Pathogenic	Pathogenic
c.1663A>G	p.Ile555Val	Hypercalcaemia, hypocalciuric	Nissen et al.,[426]	0.0008%	Disease causing	Benign (score 0.002)	Neutral (score -0.164)	3	7	Pathogenic	Likely pathogenic

Nucleotide change	Amino acid change	Phenotype/ disorder	Reference	*Reported vAF	Prediction of functional effects			Evolutionary conservation		Combined analysis	
					MutationTaster	PolyPhen-2	Provean Protein	4 Orthologs	8 Orthologs	1	2
c.1664T>C	p.Ile555Thr	Hypercalcaemia, hypocalciuric	Tonyushkina, O'Connor and Dunbar[487]	0%	Disease causing	Benign (score 0.008)	Neutral (score -0.247)	3	7	Pathogenic	Likely pathogenic
c.1666G>A	p.Glu556Lys	Hypocalcaemia	Livadariu et al.,[488]	0%	Disease causing	Benign (score 0.004)	Neutral (score 0.121)	3	6	Pathogenic	Likely pathogenic
c.1670G>A	p.Gly557Glu	Hypercalcaemia, hypocalciuric	Nakayama et al.,[489]	0%	Disease causing	Benign (score 0.245)	Deleterious (score -6.275)	3	7	Pathogenic	Pathogenic
c.1685G>A	p.Cys562Tyr	Hypercalcaemia, hypocalciuric	Burski et al.,[490]	0%	Disease causing	Possibly damaging (score 0.871)	Deleterious (score -10.527)	3	7	Pathogenic	Pathogenic
c.1693T>G	p.Cys565Gly	Hypercalcaemia, hypocalciuric	Cole et al.,[432]	0%	Disease causing	Probably damaging (score 0.983)	Deleterious (score -11.484)	3	7	Pathogenic	Pathogenic
c.1703G>A	p.Cys568Tyr	Hypercalcaemia, hypocalciuric	Rus et al.,[482]	0%	Disease causing	Probably damaging (score 0.977)	Deleterious (score -10.512)	3	7	Pathogenic	Pathogenic
c.1706T>A	p.Pro569His	Hypoparathyroidism, autosomal dominant	Nakamura et al.,[442]	0%	Disease causing	Benign (score 0.154)	Neutral (score -1.650)	3	5	Pathogenic	Likely benign
c.1718A>G	p.Tyr573Cys	Hypercalcaemia, hypocalciuric	Hannan et al.,[372]	0%	Disease causing	Benign (score 0.401)	Neutral (score -1.857)	3	6	Pathogenic	Likely pathogenic
c.1719T>A	p.Tyr573*	Hypercalcaemia, hypocalciuric	Nissen et al.,[426]	0%	Disease causing	N/A	N/A	3	6	Pathogenic	Likely pathogenic
c.1745G>A	p.Cys582Tyr	Hyperparathyroidism	Pearce et al.,[435]	0%	Disease causing	Probably damaging (score 0.998)	Deleterious (score -10.711)	4	8	Pathogenic	Pathogenic
c.1745G>T	p.Cys582Phe	Hypercalcaemia, hypocalciuric	Nissen et al.,[426]	0%	Disease causing	Probably damaging (score 0.997)	Deleterious (score -10.677)	4	8	Pathogenic	Pathogenic
c.1765T>C	p.Phe589Leu	Hypocalcaemia	Lienhardt (2001) CASR Locus-specific database Unpublished 68	0%	Disease causing	Benign (score 0.006)	Deleterious (score -4.464)	3	6	Pathogenic	Likely pathogenic
c.1772C>G	p.Ser591Cys	Hypercalcaemia, hypocalciuric	Nyweide et al.,[491]	0%	Disease causing	Probably damaging (score 0.969)	Deleterious (score -4.611)	4	8	Pathogenic	Pathogenic
c.1783C>T	p.His595Tyr	Hypercalcaemia, hypocalciuric	Cetani et al.,[492]	0%	Disease causing	Benign (score 0.002)	Deleterious (score -2.641)	4	8	Pathogenic	Pathogenic
c.1810G>A	p.Glu604Lys	Hypocalcaemia	Tan et al.,[493]	0%	Disease causing	Benign (score 0.230)	Deleterious (score -3.823)	4	8	Pathogenic	Pathogenic
c.1820C>A	p.Ser607*	Hypercalcaemia, hypocalciuric	Pearce et al.,[435]	0%	Disease causing	N/A	N/A	3	7	Pathogenic	Pathogenic
c.1829A>G	p.Glu610Gly	Hypercalciuria, hypocalcaemic	Hannan et al.,[372]	0%	Disease causing	Possibly damaging (score 0.513)	Deleterious (score -5.338)	4	8	Pathogenic	Pathogenic

Nucleotide change	Amino acid change	Phenotype/ disorder	Reference	*Reported vAF	Prediction of functional effects			Evolutionary conservation		Combined analysis	
					MutationTaster	PolyPhen-2	Provean Protein	4 Orthologs	8 Orthologs	1	2
c.1835T>C	p.Phe612Ser	Hypocalcaemia with hypercalciuria	Pearce et al.,[444]	0%	Disease causing	Possibly damaging (score 0.581)	Deleterious (score -3.155)	4	8	Pathogenic	Pathogenic
c.1837G>A	p.Gly613Arg	Hypercalcaemia, hypocalciuric	Rasmussen, Jorgensen and Schwarz[494]	0%	Disease causing	Probably damaging (score 0.951)	Deleterious (score -7.788)	4	8	Pathogenic	Pathogenic
c.1846C>G	p.Leu616Val	Hypocalcaemia	Stock et al.,[495]	0%	Disease causing	Possibly damaging (score 0.807)	Deleterious (score -2.587)	4	8	Pathogenic	Pathogenic
c.1868G>A	p.Gly623Asp	Hypercalcaemia, hypocalciuric	Nissen et al.,[426]	0%	Disease causing	Probably damaging (score 0.961)	Deleterious (score -6.815)	4	8	Pathogenic	Pathogenic
c.1913G>T	p.Arg638Leu	Hypercalcaemia, hypocalciuric	D'Souza-Li (2006) CASR Locus-specific database Unpublished	0%	Disease causing	Benign (score 0.142)	Deleterious (score -4.897)	4	8	Pathogenic	Pathogenic
c.1934C>A	p.Ala645Asp	Hypercalcaemia, hypocalciuric	Hannan et al.,[372]	0%	Disease causing	Probably damaging (score 0.997)	Deleterious (score-5.322)	4	8	Pathogenic	Pathogenic
c.1942C>T	p.Arg648*	Hypercalcaemia, hypocalciuric	Jap et al.,[496]	0.00082%	Disease causing	N/A	N/A	4	8	Pathogenic	Pathogenic
c.1949T>C	p.Leu650Pro	Hyperparathyroidism	Warner et al.,[441]	0%	Disease causing	Probably damaging (score 0.992)	Deleterious (score -6.539)	4	8	Pathogenic	Pathogenic
c.1970C>A	p.Ser657Tyr	Hypercalcaemia, hypocalciuric	Heath et al.,[434]	0%	Disease causing	Probably damaging (score 0.973)	Deleterious (score -4.899)	4	8	Pathogenic	Pathogenic
c.1982G>A	p.Cys661Tyr	Hypercalcaemia, hypocalciuric	Cole et al.,[432]	0%	Disease causing	Probably damaging (score 0.969)	Deleterious (score -8.265)	4	8	Pathogenic	Pathogenic
c.2002T>C	p.Phe668Leu	Hypercalcaemia, hypocalciuric	Nissen et al.,[425]	0%	Disease causing	Probably damaging (score 0.927)	Deleterious (score -5.699)	4	8	Pathogenic	Pathogenic
c.2008G>A	p.Gly670Arg	Hypercalcaemia, hypocalciuric	Pearce et al.,[435]	0%	Disease causing	Probably damaging (score 0.978)	Deleterious (score -7.543_	4	8	Pathogenic	Pathogenic
c.2009G>A	p.Gly670Glu	Hypercalcaemia, hypocalciuric	Kobayashi et al.,[462]	0%	Disease causing	Probably damaging (score 0.993)	Deleterious (score -7.510)	4	8	Pathogenic	Pathogenic
c.2038C>T	p.Arg680Cys	Hypercalcaemia, hypocalciuric	Hendy et al.,[446]	0.00165%	Disease causing	Possibly damaging (score 0.891)	Deleterious (score -4.331)	4	8	Pathogenic	Likely pathogenic

Nucleotide change	Amino acid change	Phenotype/ disorder	Reference	*Reported vAF	Prediction of functional effects			Evolutionary conservation		Combined analysis	
					MutationTaster	PolyPhen-2	Provean Protein	4 Orthologs	8 Orthologs	1	2
c.2039G>A	p.Arg680His	Hypercalcaemia, hypocalciuric	Pearce et al.,[435]	0.00082%	Disease causing	Possibly damaging (score 0.746)	Deleterious (score -6.869)	4	8	Pathogenic	Pathogenic
c.2042A>G	p.Gln681Arg	Hypoparathyroidism	Baron et al.,[443]	0%	Disease causing	Benign (score 0.321)	Neutral (score 0.551)	4	8	Pathogenic	Likely pathogenic
c.2043G>T	p.Gln681His	Hypocalcaemia	Guarnieri et al.,[497]	0%	Disease causing	Possibly damaging (score 0.872)	Neutral (score -1.815)	4	8	Pathogenic	Likely pathogenic
c.2065G>A	p.Val689Met	Hyperparathyroidism	Warner et al.,[441]	0%	Disease causing	Benign (score 0.409)	Neutral (score -1.543)	4	8	Pathogenic	Likely pathogenic
c.2089G>A	p.Val697Met	Hypercalcaemia, hypocalciuric	Aparicio López et al.,[498]	0%	Disease causing	Benign (score 0.220)	Neutral (score -1.556)	4	8	Pathogenic	Likely pathogenic
c.2102G>C	p.Arg701Pro	Hypercalcaemia, hypocalciuric	Hannan et al.,[372]	0%	Disease causing	Benign (score 0.211)	Neutral (score -1.299)	4	8	Pathogenic	Likely pathogenic
c.2111T>C	p.Leu704Pro	Hyperparathyroidism	Starker et al.,[474]	0%	Disease causing	Probably damaging (score 0.959)	Deleterious (score -3.676)	4	8	Pathogenic	Pathogenic
c.2147G>A	p.Arg716His	Hypercalcaemia	Koltin et al.,[480]	0.00165	Disease causing	Possibly damaging (score 0.647)	Neutral (score -1.561)	4	8	Pathogenic	Unknown significance
c.2154G>A	p.Trp718*	Hypercalcaemia, hypocalciuric	Rus et al.,[482]	0%	Disease causing	N/A	N/A	4	8	Pathogenic	Pathogenic
c.2180T>A	p.Leu727Gln	Hypocalcaemia	Mittelman et al.,[499]	0%	Disease causing	Possibly damaging (score 0.539)	Deleterious (score -2.570)	4	8	Pathogenic	Pathogenic
c.2182G>T	p.Val728Phe	Hypercalcaemia, hypocalciuric	Nissen et al.,[426]	0%	Disease causing	Possibly damaging (score 0.776)	Deleterious (score -3.951)	4	8	Pathogenic	Pathogenic
c.2201T>C	p.Met734Thr	Hypoparathyroidism	Raue et al.,[500]	0%	Disease causing	Benign (score 0)	Neutral (score -1.522)	3	5	Pathogenic	Likely benign
c.2201T>G	p.Met734Arg	Hypercalcaemia, hypocalciuric	Rus et al.,[482]	0%	Disease causing	Benign (score 0.007)	Deleterious (score -3.497)	3	5	Pathogenic	Likely pathogenic
c.2204A>C	p.Gln735Pro	Hypocalcaemia	Wong et al.,[501]	0%	Disease causing	Possibly damaging (score 0.884)	Deleterious (score -5.419)	4	8	Pathogenic	Pathogenic
c.2224T>C	p.Trp742Arg	Hypercalcaemia, hypocalciuric	Nissen et al.,[426]	0%	Disease causing	Probably damaging (score 0.929)	Deleterious (score -10.967)	4	8	Pathogenic	Pathogenic
c.2254C>T	p.Arg752Cys	Hypercalcaemia, hypocalciuric	Hannan et al.,[372]	0%	Disease causing	Possibly damaging (score 0.648)	Deleterious (score -4.557)	4	8	Pathogenic	Pathogenic

Nucleotide change	Amino acid change	Phenotype/ disorder	Reference	*Reported vAF	Prediction of functional effects			Evolutionary conservation		Combined analysis	
					MutationTaster	PolyPhen-2	Provean Protein	4 Orthologs	8 Orthologs	1	2
c.2293T>C	p.Cys765Arg	Hypercalcaemia, hypocalciuric	Dixit and Penas[502]	0%	Disease causing	Probably damaging (score 0.999)	Deleterious (score -11.334)	4	8	Pathogenic	Pathogenic
c.2295C>G	p.Cys765Trp	Hypercalcaemia, hypocalciuric	Cetani et al.,[492]	0%	Disease causing	Probably damaging (score 1.000)	Deleterious (score -10.562)	4	8	Pathogenic	Pathogenic
c.2299G>A	p.Glu767Lys	Hypocalcaemia	Uckun-Kitapci et al.,[503]	0%	Disease causing	Benign (score 0.403)	Neutral (score -1.593)	4	8	Pathogenic	Likely pathogenic
c.2299G>C	p.Glu767Gln	Hypocalcaemia	Letz et al.,[454]	0%	Disease causing	Probably damaging (score 0.979)	Neutral (score -1.239)	4	8	Pathogenic	Pathogenic
c.2303G>T	p.Gly768Val	Hyperparathyroidism, neonatal primary	Hannan et al.,[372]	0.00414%	Disease causing	Probably damaging (score 0.936)	Deleterious (score -7.363)	4	8	Pathogenic	Likely pathogenic
c.2318T>G	p.Leu773Arg	Hypoparathyroidism	De Luca et al.,[504]	0%	Disease causing	Probably damaging (score 0.920)	Deleterious (score -3.923)	4	8	Pathogenic	Pathogenic
c.2332G>C	p.Gly778Arg	Hypercalcaemia, hypocalciuric	Hannan et al.,[372]	0%	Disease causing	Probably damaging (score 0.995)	Deleterious (score -6.835)	4	8	Pathogenic	Pathogenic
c.2333G>A	p.Gly778Asp	Hypercalcaemia, hypocalciuric	Ward et al.,[427]	0%	Disease causing	Probably damaging (score 0.988)	Deleterious (score -6.051)	4	8	Pathogenic	Pathogenic
c.2341T>C	p.Cys781Arg	Hypercalcaemia, hypocalciuric	Nissen et al.,[425]	0%	Disease causing	Benign (score 0.109)	Deleterious (score -2.641)	4	8	Pathogenic	Pathogenic
c.2362T>C	p.Phe788Leu	Hypocalcaemia	Hendy et al.,[505]	0%	Disease causing	Possibly damaging (score 0.641)	Deleterious (score -5.181)	4	8	Pathogenic	Pathogenic
c.2363T>G	p.Phe788Cys	Hypoparathyroidism	Watanabe et al.,[506]	0%	Disease causing	Probably damaging (score 0.955)	Deleterious (score -7.063)	4	8	Pathogenic	Pathogenic
c.2371G>C	p.Ala791Pro	Hypercalcaemia, hypocalciuric	Hannan et al.,[372]	0%	Disease causing	Probably damaging (score 0.996)	Deleterious (score -4.466)	4	8	Pathogenic	Pathogenic
c.2383C>T	p.Arg795Trp	Hypercalcaemia, hypocalciuric	Pollak et al.,[183]	0%	Disease causing	Probably damaging (score 1.000)	Deleterious (score -7.730)	4	8	Pathogenic	Pathogenic
c.2392C>A	Pro798Thr	Hypercalcaemia, hypocalciuric	Lam et al.,[507]	0%	Disease causing	Probably damaging (score 0.996)	Deleterious (score -7.197)	4	8	Pathogenic	Pathogenic

Nucleotide change	Amino acid change	Phenotype/ disorder	Reference	*Reported vAF	Prediction of functional effects			Evolutionary conservation		Combined analysis	
					MutationTaster	PolyPhen-2	Provean Protein	4 Orthologs	8 Orthologs	1	2
c.2393C>T	p.Pro798Leu	Hypercalcaemia, hypocalciuric	Hannan et al.,[372]	0%	Disease causing	Probably damaging (score 0.971)	Deleterious (score -9.129)	4	8	Pathogenic	Pathogenic
c.2395G>A	p.Glu799Lys	Hypoparathyroidism	Lienhardt et al.,[447]	0%	Disease causing	Benign (score 0.354)	Deleterious (score -2.947)	4	8	Pathogenic	Pathogenic
c.2399A>C	p.Asn800Thr	Hypercalciuria, hypocalcaemic	Hannan et al.,[372]	0%	Disease causing	Benign (score 0.083)	Deleterious (score -4.095)	4	8	Pathogenic	Pathogenic
c.2405A>G	p.Asn802Ser	Hypercalcaemia	Lia-Baldini et al.,[508]	0.00164%	Disease causing	Possibly damaging (score 0.892)	Deleterious (score -3.868)	4	8	Pathogenic	Likely pathogenic
c.2405A>T	p.Asn802Ile	Hypocalcaemia	Cole et al.,[432]	0%	Disease causing	Probably damaging (score 0.982)	Deleterious (score -7.369)	4	8	Pathogenic	Pathogenic
c.2411C>A	p.Ala804Asp	Hypercalcaemia, hypocalciuric	Miyashiro et al.,[509]	0%	Disease causing	Probably damaging (score 0.996)	Deleterious (score -5.000)	4	8	Pathogenic	Pathogenic
c.2417T>C	p.Phe806Ser	Hypoparathyroidism	Baron et al.,[443]	0%	Disease causing	Possibly damaging (score 0.729)	Deleterious (score -5.169)	4	8	Pathogenic	Pathogenic
c.2427C>G	p.Phe809Leu	Hypercalcaemia, hypocalciuric	Timmers et al.,[510]	0%	Disease causing	Probably damaging (score 0.950)	Deleterious (score -5.820)	4	8	Pathogenic	Pathogenic
c.2431A>G	p.Met811Val	Hypercalcaemia, hypocalciuric & hypoparathyroidism	Schouten et al.,[511]	0%	Disease causing	Probably damaging (score 0.982)	Deleterious (score -3.732)	4	8	Pathogenic	Pathogenic
c.2447T>C	p.Ile816Thr	Hypercalcaemia, hypocalciuric	Hannan et al.,[372]	0%	Disease causing	Benign (score 0.076)	Neutral (score -1.828)	4	8	Pathogenic	Likely pathogenic
c.2449G>A	p.Val817Ile	Hypercalcaemia, hypocalciuric	Pearce et al.,[435]	0%	Disease causing	Probably damaging (score 0.943)	Neutral (score -0.937)	4	8	Pathogenic	Pathogenic
c.2453G>T	p.Trp818Leu	Hypercalcaemia, hypocalciuric & hypoparathyroidism	Schouten et al.,[511]	0%	Disease causing	Probably damaging (score 0.999)	Deleterious (score -12.610)	4	8	Pathogenic	Pathogenic
c.2459C>T	p.Ser820Phe	Hypocalcaemia	Nagase et al.,[512]	0%	Disease causing	Possibly damaging (score 0.724)	Deleterious (score -4.401)	4	8	Pathogenic	Pathogenic
c.2461T>C	p.Phe821Leu	Hypoparathyroidism	Shiohara et al.,[513]	0%	Disease causing	Probably damaging (score 0.927)	Deleterious (score -5.753)	4	8	Pathogenic	Pathogenic
c.2470G>C	p.Ala824Pro	Hypercalciuria, hypocalcaemic	Hannan et al.,[372]	0%	Disease causing	Probably damaging (score 0.979)	Deleterious (score -4.540)	4	8	Pathogenic	Pathogenic

Nucleotide change	Amino acid change	Phenotype/ disorder	Reference	*Reported vAF	Prediction of functional effects			Evolutionary conservation		Combined analysis	
					MutationTaster	PolyPhen-2	Provean Protein	4 Orthologs	8 Orthologs	1	2
c.2470G>T	p.Ala824Ser	Hypoparathyroidism	Inoue et al.,[514]	0%	Disease causing	Possibly damaging (score 0.622)	Deleterious (score -2.740)	4	8	Pathogenic	Pathogenic
c.2483C>A	p.Thr828Asn	Hypercalciuria, hypocalcaemic	Hannan et al.,[372]	0%	Disease causing	Probably damaging (score 0.920)	Deleterious (score -2.540)	4	8	Pathogenic	Pathogenic
c.2488G>A	p.Gly830Ser	Hypocalcaemia	Letz et al.,[454]	0%	Disease causing	Probably damaging (score 0.997)	Deleterious (score -5.820)	4	8	Pathogenic	Pathogenic
c.2492A>C	p.Lys831Thr	Hypercalciuria, hypocalcaemic	Hannan et al.,[372]	0%	Disease causing	Probably damaging (score 0.918)	Deleterious (score -5.027)	4	8	Pathogenic	Pathogenic
c.2494T>C	p.Phe832Leu	Hypocalcaemia	Cole et al.,[432]	0%	Disease causing	Benign (score 0.047)	Deleterious (score -4.334)	4	8	Pathogenic	Pathogenic
c.2495T>C	p.Phe832Ser	Hypercalcaemia, hypocalciuric	Dreimane (2001) CASR Locus-specific database Unpublished	0%	Disease causing	Benign (score 0.122)	Deleterious (score -5.521)	4	8	Pathogenic	Pathogenic
c.2503G>A	p.Ala835Thr	Hypocalcaemia	D'Souza-Li et al.,[468]	0%	Disease causing	Possibly damaging (score 0.865)	Deleterious (Score -3.524)	4	8	Pathogenic	Pathogenic
c.2506G>C	p.Val836Leu	Hypoparathyroidism	Hu et al.,[515]	0%	Disease causing	Probably damaging (score 0.924)	Deleterious (Score -2.711)	4	8	Pathogenic	Pathogenic
c.2511G>C	p.Glu837Asp	Hypercalciuria, hypocalcaemic	Hannan et al.,[372]	0%	Disease causing	Probably damaging (score 0.995)	Deleterious (score -2.593)	4	8	Pathogenic	Pathogenic
c.2516T>C	p.Ile839Thr	Hypoparathyroidism, autosomal dominant	Nakamura et al.,[442]	0%	Disease causing	Possibly damaging (score 0.659)	Deleterious (score -2.536)	4	8	Pathogenic	Pathogenic
c.2528C>A	p.Ala843Thr	Hypocalcaemia	Zhao et al.,[516]	0%	Disease causing	Probably damaging (score 0.961)	Deleterious (score -4.418)	4	8	Pathogenic	Pathogenic
c.2530G>A	p.Ala844Thr	Hypocalcaemia	Letz et al.,[454]	0%	Disease causing	Benign (score 0.008)	Neutral (score -0.261)	3	6	Pathogenic	Likely pathogenic
c.2530G>C	p.Ala844Pro	Hypocalcaemia	Nakajima et al.,[471]	0%	Disease causing	Benign (score 0.125)	Neutral (score -2.103)	3	6	Pathogenic	Likely pathogenic
c.2534G>A	p.Ser845Asn	Hypercalciuria, hypocalcaemic	Hannan et al.,[372]	0%	Disease causing	Possibly damaging (score 0.758)	Deleterious (score -2.723)	4	8	Pathogenic	Pathogenic
c.2546T>C	p.Leu849Pro	Hypercalcaemia, hypocalciuric	Rus et al.,[482]	0%	Disease causing	Probably damaging (score 0.997)	Deleterious (score -6.673)	4	8	Pathogenic	Pathogenic

Nucleotide change	Amino acid change	Phenotype/ disorder	Reference	*Reported vAF	Prediction of functional effects			Evolutionary conservation		Combined analysis	
					MutationTaster	PolyPhen-2	Provean Protein	4 Orthologs	8 Orthologs	1	2
c.2551T>A	p.Cys851Ser	Hypoparathyroidism	Baron et al.,[443]	0.00164%	Disease causing	Possibly damaging (score 0.841)	Deleterious (score -6.410)	4	8	Pathogenic	Likely pathogenic
c.2641T>C	p.Phe881Leu	Hypercalcaemia and hypercalciuria	Carling et al.,[517]	0%	Disease causing	Benign (score 0.077)	Neutral (score -0.897)	4	8	Pathogenic	Likely pathogenic
c.2647G>A	p.Val883Met	Hypercalciuria, hypocalcaemic	Hannan et al.,[372]	0%	Disease causing	Benign (score 0.341)	Neutral (score -0.864)	4	7	Pathogenic	Likely pathogenic
c.2654C>A	p.Ala885Asp	Hypercalcaemia, hypocalciuric	Hannan et al.,[372]	0%	Disease causing	Possibly damaging (score 0.9)	Neutral (score -1.206)	4	8	Pathogenic	Likely pathogenic
c.2656C>T	p.Arg886Trp	Hypercalcaemia, hypocalciuric	Nissen et al.,[426]	0%	Disease causing	Probably damaging (score 0.957)	Neutral (score -1.964)	4	7	Pathogenic	Pathogenic
c.2657G>C	p.Arg886Pro	Hyperparathyroidism	Simonds et al.,[456]	0%	Disease causing	Possibly damaging (score 0.854)	Neutral (score -0.801)	4	7	Pathogenic	Likely pathogenic
c.2663C>T	p.Thr888Met	Hypocalcaemia	Lazarus et al.,[518]	0%	Disease causing	Probably damaging (score 0.938)	Neutral (score -1.459)	4	8	Pathogenic	Pathogenic
c.2777A>G	p.Gln926Arg	Hypercalcaemia, hypocalciuric	Rus et al.,[482]	0.01323%	Polymorphism	Benign (score 0.001)	Neutral (score -0.376)	2	4	Unknown significance	Benign
c.2980C>T	p.His994Tyr	Hypercalcaemia, hypocalciuric	Christie (2002) CASR Locus-specific database Unpublished 173	0%	Polymorphism	Benign (score 0.019)	Neutral (score -0.400)	1	4	Benign	Likely benign
c.3013G>A	p.Asp1005Asn	Hypercalcaemia, hypocalciuric	Rus et al.,[482]	0.00329%	Disease causing	Benign (score 0.070)	Neutral (score -0.648)	4	6	Pathogenic	Likely benign

CASR variants obtained from HGMD[235] that were used to investigate the effectiveness of *in silico* methods for variant analysis (Chapter 6). Nucleotide number is according to transcript ENST00000639785 and amino acid number is according to the 1078 amino acid protein (NCBI, NP_000379; UniProt P41180) as displayed on HGMD. *Reported vAFs were obtained from ExAC[236]. Evolutionary conservation scores were based on the number of orthologs each WT residue was conserved in, the number of orthologs studied in each analysis is detailed in the column heading, as detailed in Chapter 6. Combined analysis 1 and 2 are based on the criteria detailed in Chapter 6. N/A, not applicable.

Table 40. *In silico* analysis of *CLCN5* variants obtained from HGMD

Nucleotide change	Amino acid change	Phenotype/ disorder	Reference	*Reported vAFs	Prediction of functional effects			Evolutionary conservation		Combined analysis	
					MutationTaster	PolyPhen-2	Provean Protein	4 Orthologs	8 Orthologs	1	2
c.64T>G	p.Trp22Gly	Low molecular weight proteinuria	Morimoto et al.,[519]	0%	Disease causing	Probably damaging (score 0.970)	Deleterious (score -12.302)	4	8	Pathogenic	Pathogenic
c.82C>T	p.Arg28*	Dent's disease	Hoopes et al.,[520]	0%	Disease causing	N/A	N/A	4	8	Pathogenic	Pathogenic
c.100C>T	p.Arg34*	Dent's disease	Hoopes et al.,[520]	0%	Disease causing	N/A	N/A	4	8	Pathogenic	Pathogenic
c.134G>A	p.Trp45*	Dent's disease	Hoopes et al.,[104]	0%	Disease causing	N/A	N/A	3	7	Pathogenic	Pathogenic
c.169G>T	p.Gly57Val	Nephrolithiasis, hypercalciuric	Lloyd et al.,[521]	0%	Disease causing	Possibly damaging (score 0.826)	Deleterious (score-8.161)	3	7	Pathogenic	Pathogenic
c.173G>T	p.Trp58Leu	Dent's disease	Tosetto et al.,[522]	0%	Disease causing	Probably damaging (score 0.978)	Deleterious (score -12.332)	3	7	Pathogenic	Pathogenic
c.174G>C	p.Trp58Cys	Dent's disease	Sethi et al.,[523]	0%	Disease causing	Probably damaging (score 0.998)	Deleterious (score -12.321)	3	7	Pathogenic	Pathogenic
c.263G>A	p.Gly88Asp	Dent's disease	Ludwig et al.,[524]	0%	Disease causing	Probably damaging (score 1.000)	Deleterious (score -6.846)	4	8	Pathogenic	Pathogenic
c.263G>T	p.Gly88Val	Dent's disease	Sekine et al.,[292]	0%	Disease causing	Probably damaging (score 1.000)	Deleterious (score -8.802)	4	8	Pathogenic	Pathogenic
c.270C>G	p.Cys90Trp	Dent's disease	Sekine et al.,[292]	0%	Disease causing	Probably damaging (score 1.000)	Deleterious (score -10.757)	4	8	Pathogenic	Pathogenic
c.277G>T	p.Gly93*	Dent's disease	Sekine et al.,[292]	0%	Disease causing	N/A	N/A	3	6	Pathogenic	Pathogenic
c.284G>A	p.Trp95*	Dent's disease	Ludwig et al.,[524]	0%	Disease causing	N/A	N/A	4	8	Pathogenic	Pathogenic
c.302G>A	p.Cys101Tyr	Dent's disease	Cho et al.,[525]	0%	Disease causing	Probably damaging (score 1.000)	Deleterious (score -10.757)	4	8	Pathogenic	Pathogenic
c.307T>C	p.Trp103Arg	Dent's disease	Sekine et al.,[292]	0%	Disease causing	Probably damaging (score 0.942)	Deleterious (score -12.838)	4	8	Pathogenic	Pathogenic
c.352G>T	p.Glu118*	Low molecular weight proteinuria	Morimoto et al., [519]	0%	Disease causing	N/A	N/A	4	7	Pathogenic	Pathogenic
c.366G>A	p.Trp122*	Dent's disease	Frishberg et al.,[526]	0%	Disease causing	N/A	N/A	4	8	Pathogenic	Pathogenic
c.370C>T	p.Gln124*	Dent's disease	Sekine et al.,[292]	0%	Disease causing	N/A	N/A	4	7	Pathogenic	Pathogenic
c.420T>G	p.Tyr140*	Dent's disease	Ramos-Trujillo et al.,[527]	0%	Disease causing	N/A	N/A	4	8	Pathogenic	Pathogenic
c.527T>A	p.Ile176Asn	Dent's disease	Sekine et al.,[292]	0%	Disease causing	Probably damaging (score 0.995)	Deleterious (score-6.448)	4	8	Pathogenic	Pathogenic
c.536G>A	p.Gly179Asp	Dent's disease	Grand et al.,[528]	0%	Disease causing	Probably damaging (score 0.998)	Deleterious (score -6.712)	4	8	Pathogenic	Pathogenic
c.566G>A	p.Trp189*	Dent's disease	Sekine et al.,[292]	0%	Disease causing	N/A	N/A	4	8	Pathogenic	Pathogenic
c.599T>G	p.Leu200Arg	Dent's disease	Lloyd et al.,[99]	0%	Disease causing	Probably damaging (score 0.997)	Deleterious (score -5.435)	4	8	Pathogenic	Pathogenic
c.608C>T	p.Ser203Leu	Dent's disease	Grand et al.,[528]	0%	Disease causing	Possibly damaging (score 0.794)	Deleterious (score -4.010)	4	8	Pathogenic	Pathogenic

Nucleotide change	Amino acid change	Phenotype/ disorder	Reference	*Reported vAFs	Prediction of functional effects			Evolutionary conservation		Combined analysis	
					MutationTaster	PolyPhen-2	Provean Protein	4 Orthologs	8 Orthologs	1	2
c.631G>C	p.Glu211Gln	Dent's disease	Sekine et al.,[292]	0%	Disease causing	Probably damaging (score 0.993)	Deleterious (score -2.878)	4	8	Pathogenic	Pathogenic
c.634G>A	p.Gly212Ser	Dent's disease	Sekine et al.,[292]	0.00114%	Disease causing	Probably damaging (score 0.999)	Deleterious (score -5.755)	4	8	Pathogenic	Likely pathogenic
c.635G>C	p.Gly212Ala	Dent's disease	Grand et al.,[528]	0%	Disease causing	Probably damaging (score 0.998)	Deleterious (score -5.755)	4	8	Pathogenic	Pathogenic
c.638C>T	p.Pro213Leu	Dent's disease	Sekine et al.,[292]	0%	Disease causing	Probably damaging (score 0.997)	Deleterious (score -9.52)	4	8	Pathogenic	Pathogenic
c.655T>C	p.Cys219Arg	Dent's disease	Ramos-Trujillo et al.,[527]	0%	Disease causing	Possibly damaging (score 0.862)	Deleterious (score -7.685)	4	8	Pathogenic	Pathogenic
c.661T>C	p.Cys221Arg	Dent's disease	Hoopes et al.,[104]	0%	Disease causing	Probably damaging (score 0.961)	Deleterious (score -7.685)	4	8	Pathogenic	Pathogenic
c.663T>A	p.Cys221*	Dent's disease	Hoopes et al.,[104]	0%	Disease causing	N/A	N/A	4	8	Pathogenic	Pathogenic
c.674T>C	p.Leu225Pro	Dent's disease	Ramos-Trujillo et al.,[529]	0%	Disease causing	Probably damaging (score 0.934)	Deleterious (score -4.832)	4	8	Pathogenic	Pathogenic
c.731C>T	p.Ser244Leu	Dent's disease	Lloyd et al.,[99]	0%	Disease causing	Probably damaging (score 0.931)	Deleterious (score -5.500)	4	8	Pathogenic	Pathogenic
c.779G>T	p.Gly260Val	Dent's disease	Tosetto et al.,[530]	0%	Disease causing	Probably damaging (score 0.986)	Deleterious (score -7.713)	4	8	Pathogenic	Pathogenic
c.781G>A	p.Gly261Arg	Dent's disease	Tosetto et al.,[522]	0%	Disease causing	Probably damaging (score 0.999)	Deleterious (score -7.047)	4	8	Pathogenic	Pathogenic
c.782G>A	p.Gly261Glu	Dent's disease	Bogdanovic et al.,[531]	0%	Disease causing	Probably damaging (score 0.999	Deleterious (score -7.014)	4	8	Pathogenic	Pathogenic
c.796C>T	p.Leu266Val	Dent's disease	Sekine et al.,[292]	0%	Disease causing	Possibly damaging (score 0.903)	Deleterious (score -2.664)	4	8	Pathogenic	Pathogenic
c.800A>C	p.Glu267Ala	Dent's disease	Hoopes et al.,[104]	0%	Disease causing	Probably damaging (score 0.989)	Deleterious (score -5.269)	4	8	Pathogenic	Pathogenic
c.808A>C	p.Ser270Arg	Dent's disease	Igarashi et al.,[532]	0%	Disease causing	Possibly damaging (score 0.792)	Deleterious (score -4.734)	3	7	Pathogenic	Pathogenic
c.808A>G	p.Ser270Gly	Dent's disease	Hoopes et al.,[104]	0%	Disease causing	Probably damaging (score 0.976)	Deleterious (score -3.787)	3	7	Pathogenic	Pathogenic
c.814T>A	p.Tyr272Asn	Dent's disease	Sekine et al.,[292]	0%	Disease causing	Benign (score 0.285)	Deleterious (score -8.521)	3	7	Pathogenic	Pathogenic
c.815A>G	p.Tyr272Cys	Dent's disease	Tosetto et al.,[533]	0%	Disease causing	Probably damaging (score 0.950)	Deleterious (score -8.521)	3	7	Pathogenic	Pathogenic
c.817T>C	p.Phe273Leu	Dent's disease	Ramos-Trujillo et al.,[527]	0%	Disease causing	Probably damaging (score 0.997)	Deleterious (score -5.580)	3	7	Pathogenic	Pathogenic
c.833T>G	p.Leu278Trp	Dent's disease	Vaisbich et al.,[534]	0%	Disease causing	Probably damaging (score 0.998)	Deleterious (score -5.330)	4	8	Pathogenic	Pathogenic
c.834G>C	p.Leu278Phe	Dent's disease	Igarashi et al.,[532]	0%	Disease causing	Possibly damaging (score 0.905)	Deleterious (score -3.554)	4	8	Pathogenic	Pathogenic

Nucleotide change	Amino acid change	Phenotype/ disorder	Reference	*Reported vAFs	Prediction of functional effects			Evolutionary conservation		Combined analysis	
					MutationTaster	PolyPhen-2	Provean Protein	4 Orthologs	8 Orthologs	1	2
c.836G>A	p.Trp279*	Dent's disease	Sekine et al.,[292]	0%	Disease causing	N/A	N/A	3	7	Pathogenic	Pathogenic
c.837G>A	p.Trp279*	Dent's disease	Lloyd et al.,[99]	0%	Disease causing	N/A	N/A	3	7	Pathogenic	Pathogenic
c.839G>C	p.Arg280Pro	Dent's disease	Lloyd et al.,[535]	0%	Disease causing	Probably damaging (score 0.996)	Deleterious (score -6.627)	3	7	Pathogenic	Pathogenic
c.942G>A	p.Trp314*	Dent's disease	Ramos-Trujillo et al.,[527]	0%	Disease causing	N/A	N/A	3	7	Pathogenic	Pathogenic
c.971T>G	p.Leu324Arg	Dent's disease	Ludwig et al.,[536]	0%	Disease causing	Probably damaging (score 0.964)	Deleterious (score -3.523)	2	6	Pathogenic	Pathogenic
c.986G>A	p.Gly329Asp	Dent's disease	Vaisbich et al.,[534]	0%	Disease causing	Probably damaging (score 0.994)	Deleterious (score -6.365)	3	7	Pathogenic	Pathogenic
c.995G>A	p.Trp332*	Dent's disease	Ludwig et al.,[536]	0%	Disease causing	N/A	N/A	3	7	Pathogenic	Pathogenic
c.997G>A	p.Gly333Arg	Dent's disease	Tanuma et al.,[537]	0%	Disease causing	Probably damaging (score 0.997)	Deleterious (score -5.962)	4	8	Pathogenic	Pathogenic
c.1020C>G	p.Asn340Lys	Dent's disease	Tosetto et al.,[533]	0%	Disease causing	Probably damaging (score 0.982)	Deleterious (score -5.455)	3	7	Pathogenic	Pathogenic
c.1028G>A	p.Trp343*	Dent's disease	Lloyd et al.,[535]	0%	Disease causing	N/A	N/A	3	7	Pathogenic	Pathogenic
c.1039C>T	p.Arg347*	Low molecular weight proteinuria	Akuta et al.,[538]	0%	Disease causing	N/A	N/A	4	8	Pathogenic	Pathogenic
c.1292T>G	p.Leu433*	Dent's disease	Carballo-Trujillo et al.,[539]	0%	Disease causing	N/A	N/A	4	8	Pathogenic	Pathogenic
c.1385G>A	p.Gly462Asp	Dent's disease	Hoopes et al.,[104]	0%	Disease causing	Probably damaging (score 0.998)	Deleterious (score -6.365)	4	8	Pathogenic	Pathogenic
c.1385G>T	p.Gly462Val	Dent's disease	Ludwig et al.,[536]	0%	Disease causing	Probably damaging (score 0.998)	Deleterious (score -8.099)	4	8	Pathogenic	Pathogenic
c.1396G>C	p.Gly466Arg	Dent's disease	Valina et al.,[540]	0%	Disease causing	Probably damaging (score 0.998)	Deleterious (score -7.210)	4	8	Pathogenic	Pathogenic
c.1399C>T	p.Arg467*	Dent's disease	Ludwig et al.,[536]	0%	Disease causing	N/A	N/A	4	8	Pathogenic	Pathogenic
c.1403T>C	p.Leu468Pro	Dent's disease	Sekine et al.,[292]	0%	Disease causing	Possibly damaging (score 0.863)	Deleterious (score -4.594)	4	8	Pathogenic	Pathogenic
c.1406T>C	p.Leu469Pro	Dent's disease	Grand et al.,[528]	0%	Disease causing	Probably damaging (score 0.976)	Deleterious (score -3.733)	4	8	Pathogenic	Pathogenic
c.1467G>A	p.Trp489*	Dent's disease	Sekine et al.,[292]	0%	Disease causing	N/A	N/A	4	8	Pathogenic	Pathogenic
c.1505A>G	p.Tyr502Cys	Dent's disease	Sekine et al.,[292]	0%	Disease causing	Probably damaging (score 1.000)	Deleterious (score -7.763)	4	8	Pathogenic	Pathogenic
c.1506T>G	p.Tyr502*	Dent's disease	Ramos-Trujillo et al.,[529]	0%	Disease causing	N/A	N/A	4	8	Pathogenic	Pathogenic
c.1511T>A	p.Met504Lys	Dent's disease	Sethi et al.,[523]	0%	Disease causing	Probably damaging (score 0.962)	Deleterious (score -5.129)	4	8	Pathogenic	Pathogenic
c.1514T>G	p.Val505Gly	Dent's disease	Zhu et al.,[541]	0%	Disease causing	Probably damaging (score 0.930)	Deleterious (score -6.039)	4	8	Pathogenic	Pathogenic

Nucleotide change	Amino acid change	Phenotype/ disorder	Reference	*Reported vAFs	Prediction of functional effects			Evolutionary conservation		Combined analysis	
					MutationTaster	PolyPhen-2	Provean Protein	4 Orthologs	8 Orthologs	1	2
c.1516G>A	p.Gly506Arg	Dent's disease	Matsuyama et al.,[542]	0%	Disease causing	Probably damaging (score 0.999)	Deleterious (score -6.644)	4	8	Pathogenic	Pathogenic
c.1517G>A	p.Gly506Glu	Dent's disease	Lloyd et al.,[99]	0%	Disease causing	Probably damaging (score 0.999)	Deleterious (score -6.644)	4	8	Pathogenic	Pathogenic
c.1534G>C	p.Gly512Arg	Nephrolithiasis, hypercalciuric	Lloyd et al.,[535]	0%	Disease causing	Probably damaging (score 0.989)	Deleterious (score -6.596)	4	8	Pathogenic	Pathogenic
c.1535G>A	p.Gly512Asp	Dent's disease	Tosetto et al.,[522]	0%	Disease causing	Possibly damaging (score 0.568)	Deleterious (score -5.811)	4	8	Pathogenic	Pathogenic
c.1537G>A	p.Gly513Arg	Dent's disease	Hoopes et al.,[104]	0%	Disease causing	Probably damaging (score 0.998)	Deleterious (score -6.543)	4	8	Pathogenic	Pathogenic
c.1538G>A	p.Gly513Glu	Dent's disease	Akuta et al.,[538]	0%	Disease causing	Probably damaging (score 0.998)	Deleterious (score -6.544)	4	8	Pathogenic	Pathogenic
c.1547G>A	p.Arg516Gln	Dent's disease	Sekine et al.,[292]	0%	Disease causing	Possibly damaging (score 0.746)	Deleterious (score -2.801)	4	8	Pathogenic	Pathogenic
c.1546C>T	p.Arg516Trp	Dent's disease	Akuta et al.,[538]	0%	Disease causing	Probably damaging (score 0.993)	Deleterious (score -5.827)	4	8	Pathogenic	Pathogenic
c.1556T>A	p.Val519Asp	Dent's disease	Tosetto et al.,[522]	0%	Disease causing	Probably damaging (score 0.998)	Deleterious (score -5.392)	4	8	Pathogenic	Pathogenic
c.1558T>C	P.Ser520Pro	Dent's disease	Lloyd et al.,[99]	0%	Disease causing	Probably damaging (score 0.993)	Deleterious (score -3.900)	4	8	Pathogenic	Pathogenic
c.1571T>A	p.Ile524Lys	Low molecular weight proteinuria	Takemura et al.,[543]	0%	Disease causing	Probably damaging (score 0.999)	Deleterious (score -5.628)	4	8	Pathogenic	Pathogenic
c.1581A>T	p.Glu527Asp	Nephrolithiasis, hypercalciuric	Lloyd et al.,[535]	0%	Disease causing	Probably damaging (score 1.000)	Neutral (score -2.474)	4	8	Pathogenic	Pathogenic
c.1634G>A	p.Ser545Asn	Dent's disease	Hoopes et al.,[104]	0%	Disease causing	Probably damaging (score 0.944)	Neutral (score -2.471)	4	8	Pathogenic	Pathogenic
c.1636A>G	p.Lys546Glu	Dent's disease	Hoopes et al.,[104]	0%	Disease causing	Probably damaging (score 0.996)	Deleterious (score -3.288)	4	8	Pathogenic	Pathogenic
c.1639T>C	p.Trp547Arg	Dent's disease	Tosetto et al.,[522]	0%	Disease causing	Probably damaging (score 0.979)	Deleterious (score -11.632)	4	8	Pathogenic	Pathogenic
c.1639T>G	p.Trp547Gly	Dent's disease	Ramos-Trujillo et al.,[527]	0%	Disease causing	Benign (score 0.414)	Deleterious (score-10.817)	4	8	Pathogenic	Pathogenic
c.1641G>A	p.Trp547*	Dent's disease	Tosetto et al.,[533]	0%	Disease causing	N/A	N/A	4	8	Pathogenic	Pathogenic
c.1701C>A	p.Tyr567*	Dent's disease	Okamoto et al.,[544]	0%	Disease causing	N/A	N/A	4	8	Pathogenic	Pathogenic
c.1798C>T	p.Gln600*	Dent's disease	Tosetto et al.,[533]	0%	Disease causing	N/A	N/A	4	8	Pathogenic	Pathogenic
c.1825G>T	p.Glu609*	Dent's disease	Cheong et al.,[545]	0%	Disease causing	N/A	N/A	4	8	Pathogenic	Pathogenic
c.1851C>A	p.Tyr617*	Dent's disease	Yamamoto et al.,[546]	0%	Disease causing	N/A	N/A	4	8	Pathogenic	Pathogenic
c.1862C>T	p.Pro621Leu	Dent's disease	Tosetto et al.,[522]	0%	Disease causing	Probably damaging (score 1.000)	Deleterious (score-8.736)	4	8	Pathogenic	Pathogenic
c.1885C>T	p.Gln629*	Dent's disease	Sekine et al.,[292]	0%	Disease causing	N/A	N/A	4	8	Pathogenic	Pathogenic

Nucleotide change	Amino acid change	Phenotype/ disorder	Reference	*Reported vAFs	Prediction of functional effects			Evolutionary conservation		Combined analysis	
					MutationTaster	PolyPhen-2	Provean Protein	4 Orthologs	8 Orthologs	1	2
c.1909C>T	p.Arg637*	Low molecular weight proteinuria	Takemura et al.,[543]	0%	Disease causing	N/A	N/A	4	8	Pathogenic	Pathogenic
c.1942C>T	p.Arg648*	Dent's disease	Lloyd et al.,[99]	0%	Disease causing	N/A	N/A	4	8	Pathogenic	Pathogenic
c.2108T>C	p.Phe703Ser	Dent's disease	Sekine et al.,[292]	0%	Disease causing	Probably damaging (score 1.000)	Deleterious (score -7.225)	4	8	Pathogenic	Pathogenic
c.2110C>T	p.Arg704*	Dent's disease	Lloyd et al.,[99]	0%	Disease causing	N/A	N/A	4	8	Pathogenic	Pathogenic
c.2117T>C	p.Leu706Pro	Dent's disease	Sekine et al.,[292]	0%	Disease causing	Probably damaging (score 0.998)	Deleterious (score -6.160)	4	8	Pathogenic	Pathogenic
c.2133C>G	p.Cys711Trp	Dent's disease	Sekine et al.,[292]	0%	Disease causing	Probably damaging (score 0.942)	Deleterious (score -4.240)	4	7	Pathogenic	Pathogenic
c.2152C>T	p.Arg718*	Dent's disease	Carballo-Trujillo et al.,[539]	0%	Disease causing	N/A	N/A	3	7	Pathogenic	Pathogenic
c.2173A>G	p.Lys725Glu	Dent's disease	Ludwig et al.,[524]	0%	Disease causing	Possibly damaging (score 0.839)	Deleterious (score -3.594)	4	8	Pathogenic	Pathogenic
c.2186T>G	p.Leu729*	Dent's disease	Sethi et al.,[523]	0%	Disease causing	N/A	N/A	4	8	Pathogenic	Pathogenic

CLCN5 variants obtained from HGMD[235] that were used to investigate the effectiveness of *in silico* methods for variant analysis (Chapter 6). Nucleotide number is according to transcript ENST00000376108.7 and amino acid number according to the 746 amino acid protein (NCBI NP_000075; UniProt P51795) as displayed on HGMD. *Reported vAFs were obtained from ExAC[236]. Evolutionary conservation scores were based on the number of orthologs each WT residue was conserved in, the number of orthologs studied in each analysis is detailed in the column heading, as detailed in Chapter 6. Combined analysis 1 and 2 are based on the criteria detailed in Chapter 6. N/A, not applicable.

Table 41. *In silico* analysis of *CLCNKB* variants obtained from HGMD

Nucleotide change	Amino Acid change	Phenotype/ disorder	Reference	*Reported vAFs	Prediction of functional effects			Evolutionary conservation		Combined analysis	
					MutationTaster	PolyPhen-2	Provean Protein	4 Orthologs	8 Orthologs	1	2
c.88C>T	p.Arg30*	Bartter syndrome	Yu et al.,[547]	0.00305%	Disease causing	N/A	N/A	3	7	Pathogenic	Likely pathogenic
c.182C>A	p.Ala61Asp	Bartter syndrome 3	Bettinelli et al.,[548]	0.00082%	Disease causing	Probably damaging (score 1.000)	Deleterious (score -5.337)	4	8	Pathogenic	Pathogenic
c.226C>T	p.Arg76*	Salt-losing tubulopathy	Nozu et al.,[549]	0.00082%	Disease causing	N/A	N/A	3	6	Pathogenic	Pathogenic
c.229G>A	p.Ala77Thr	Bartter syndrome 3	Konrad et al.,[550]	0%	Disease causing	Possibly damaging (score 0.890)	Deleterious (score -3.216)	4	8	Pathogenic	Pathogenic
c.229G>C	p.Ala77Pro	Bartter syndrome 3	Robitaille et al.,[551]	0%	Disease causing	Probably damaging (score 0.918)	Deleterious (score -4.115)	4	8	Pathogenic	Pathogenic
c.242T>C	p.Leu81Pro	Bartter syndrome 3	Keck et al.,[552]	0%	Disease causing	Probably damaging (score 0.929)	Deleterious (score -5.014)	3	7	Pathogenic	Pathogenic
c.274C>T	p.Arg92Trp	Bartter syndrome 3	Vargas-Poussou et al.,[553]	0.00082%	Disease causing	Benign (score 4.37)	Deleterious (score -4.139)	2	4	Pathogenic	Likely pathogenic
c.343A>C	p.Thr115Pro	Bartter syndrome 3	Brochard et al.,[554]	0%	Disease causing	Possibly damaging (score 0.903)	Deleterious (score -2.678)	3	6	Pathogenic	Pathogenic
c.359G>T	p.Gly120Val	Bartter syndrome antenatal	Lee et al.,[555]	0%	Disease causing	Probably damaging (score 1.000)	Deleterious (score -8.062)	4	8	Pathogenic	Pathogenic
c.371C>T	p.Pro124Leu	Bartter syndrome 3	Simon et al.,[270]	0.00164%	Disease causing	Probably damaging (score 0.991)	Deleterious (score -8.802)	4	8	Pathogenic	Likely pathogenic
c.416T>C	p.Leu139Pro	Bartter syndrome 3	Konrad et al.,[550]	0%	Disease causing	Probably damaging (score 0.993)	Deleterious (score -6.446)	3	7	Pathogenic	Pathogenic
c.446T>A	p.Val149Glu	Bartter syndrome 3	Bettinelli et al.,[548]	0%	Disease causing	Possibly damaging (score 0.580)	Deleterious (score -5.033)	3	6	Pathogenic	Pathogenic
c.508G>T	p.Val170Met	Bartter syndrome 3	Vargas-Poussou et al.,[553]	0.02072%	Disease causing	Probably damaging (score 0.975)	Deleterious (score -2.613)	4	8	Pathogenic	Likely pathogenic
c.610G>A	p.Ala204Thr	Bartter syndrome 3	Simon et al.,[270]	0.00757%	Disease causing	Probably damaging (score 0.936)	Deleterious (score -3.003)	2	3	Pathogenic	Likely benign
c.629C>T	p.Ala210Val	Bartter syndrome	Yu et al.,[547]	0%	Disease causing	Probably damaging (score 0.964)	Deleterious (score -3.120)	4	8	Pathogenic	Pathogenic
c.647C>T	p.Pro216Leu	Bartter syndrome	Lee et al.,[555]	0%	Disease causing	Probably damaging (score 1.000)	Deleterious (score -8.864)	4	8	Pathogenic	Pathogenic
c.725C>A	p.Ala242Glu	Bartter syndrome 3	Bettinelli et al[556]	0%	Disease causing	Probably damaging (score 0.982)	Deleterious (score -3.447)	4	7	Pathogenic	Pathogenic
c.736G>C	p.Gly246Arg	Bartter syndrome 3	Keck et al.,[552]	0%	Disease causing	Probably damaging (score 0.969)	Deleterious (score -4.087)	3	7	Pathogenic	Pathogenic

Nucleotide change	Amino Acid change	Phenotype/ disorder	Reference	*Reported vAFs	Prediction of functional effects			Evolutionary conservation		Combined analysis	
					MutationTaster	PolyPhen-2	Provean Protein	4 Orthologs	8 Orthologs	1	2
c.887G>A	p.Gly296Asp	Bartter syndrome 3	Vargas-Poussou et al.,[553]	0%	Disease causing	Benign (score 0.013)	Deleterious (score -4.002)	1	1	Pathogenic	Likely pathogenic
c.891C>A	p.Ser297Arg	Bartter syndrome 3	Konrad et al.,[550]	0.00082%	Polymorphism	Benign (score 0.340)	Neutral (score -1.872)	1	1	Benign	Likely benign
c.908A>C	p.Gln303Pro	Bartter syndrome	Urbanová et al.,[557]	0.00164%	Disease causing	Probably damaging (score 0.935)	Deleterious (score -3.094)	3	6	Pathogenic	Likely pathogenic
c.1004T>C	p.Leu335Pro	Bartter syndrome	Chiang et al.,[558]	0%	Disease causing	Probably damaging (score 0.998)	Deleterious (score -5.149)	4	8	Pathogenic	Pathogenic
c.1010C>T	p.Ser337Phe	Bartter syndrome 3	Konrad et al.,[550]	0%	Disease causing	Probably damaging (score 0.997)	Deleterious (score -4.835)	4	7	Pathogenic	Pathogenic
c.1046C>A	p.Ala349Asp	Bartter syndrome 3	Simon et al.,[270]	0%	Disease causing	Probably damaging (score 0.999)	Deleterious (score -5.573)	3	7	Pathogenic	Pathogenic
c.1051C>T	p.Arg351Trp	Bartter syndrome	Yu et al.,[547]	0.00082%	Disease causing	Probably damaging (score 0.997)	Deleterious (score -4.685)	4	7	Pathogenic	Pathogenic
c.1052G>C	p.Arg351Pro	Bartter syndrome 3	Keck et al.,[552]	0%	Disease causing	Probably damaging (score 0.996)	Deleterious (score -3.236)	4	7	Pathogenic	Pathogenic
c.1071T>A	p.His357Gln	Bartter syndrome 3	Konrad et al.,[550]	0%	Polymorphism	Benign (score 0.031)	Neutral (score -0.742)	4	4	Pathogenic	Likely benign
c.1172G>A	p.Trp391*	Bartter syndrome 3	Nozu et al.,[549]	0.00247%	Disease causing	N/A	N/A	4	8	Pathogenic	Likely pathogenic
c.1173G>A	p.Trp391*	Bartter syndrome 3	Vargas-Poussou et al.,[553]	0.00247%	Disease causing	N/A	N/A	4	8	Pathogenic	Likely pathogenic
c.1236G>A	p.Met412Ile	Bartter syndrome 3	Bettinelli et al.,[556]	0%	Disease causing	Probably damaging (score 0.930)	Deleterious (score -3.218)	4	7	Pathogenic	Pathogenic
c.1270G>A	p.Gly424Arg	Bartter syndrome 3	Vargas-Poussou et al.,[553]	0.00494%	Disease causing	Probably damaging (score 1.000)	Deleterious (score -7.768)	4	8	Pathogenic	Likely pathogenic
c.1271G>A	p.Gly424Glu	Bartter syndrome 3	Vargas-Poussou et al.,[553]	0%	Disease causing	Probably damaging (score 1.000)	Deleterious (score -7.768)	4	8	Pathogenic	Pathogenic
c.1294T>C	p.Tyr432His	Bartter syndrome 3	Simon et al.,[270]	0%	Disease causing	Possibly damaging (score 0.869)	Deleterious (score -2.939)	4	7	Pathogenic	Pathogenic
c.1298G>A	p.Gly433Glu	Bartter syndrome 3	Bettinelli et al.,[556]	0.00082%	Disease causing	Probably damaging (score 1.000)	Deleterious (score -7.702)	4	8	Pathogenic	Pathogenic
c.1309G>A	p.Gly437Arg	Bartter syndrome	Lee et al.,[555]	0.00412%	Disease causing	Possibly damaging (score 0.750)	Deleterious (score -7.462)	4	8	Pathogenic	Likely pathogenic
c.1312C>T	p.Arg438Cys	Bartter syndrome 3	Simon et al.,[270]	0.00082%	Disease causing	Probably damaging (score 0.999)	Deleterious (score -7.471)	4	8	Pathogenic	Pathogenic
c.1313G>A	p.Arg438His	Bartter syndrome 3	Konrad et al.,[550]	0.00164%	Disease causing	Probably damaging (score 0.999)	Deleterious (score -4.67)	4	8	Pathogenic	Likely pathogenic
c.1316T>C	p.Leu439Pro	Bartter syndrome 3	Keck et al.,[552]	0.00082%	Disease causing	Probably damaging (score 0.994)	Deleterious (score -5.837)	4	7	Pathogenic	Pathogenic

Nucleotide change	Amino Acid change	Phenotype/ disorder	Reference	*Reported vAFs	Prediction of functional effects			Evolutionary conservation		Combined analysis	
					MutationTaster	PolyPhen-2	Provean Protein	4 Orthologs	8 Orthologs	1	2
c.1325A>G	p.Glu442Gly	Bartter syndrome 3	García Castaño et al.,[559]	0%	Disease causing	Probably damaging (score 0.999)	Deleterious (score -6.537)	4	8	Pathogenic	Pathogenic
c.1340T>C	p.Ile447Thr	Bartter syndrome 3	Vargas-Poussou et al.,[553]	0.00165%	Polymorphism	Benign (score 0.005)	Neutral (score -1.411)	2	2	Unknown significance	Benign
c.1409G>A	p.Gly470Glu	Bartter syndrome	Lin et al.,[560]	0%	Disease causing	Probably damaging (score 1.000)	Deleterious (score -7.51)	4	8	Pathogenic	Pathogenic
c.1537C>T	p.Gln513*	Bartter syndrome 3	Simon et al.,[270]	0%	Disease causing	N/A	N/A	4	7	Pathogenic	Pathogenic
c.1613G>C	p.Arg538Pro	Bartter syndrome 3	Martinez and Maduke[561]	0%	Polymorphism	Possibly damaging (score 0.885)	Deleterious (score -2.562)	3	6	Pathogenic	Likely pathogenic
c.1679A>T	p.Lys560Met	Bartter syndrome 3	Konrad et al.,[550]	0%	Disease causing	Probably damaging (score 0.968)	Neutral (score -1.525)	4	6	Pathogenic	Pathogenic
c.1718C>A	p.Ser573Tyr	Bartter syndrome 3	Konrad et al.,[550]	0%	Disease causing	Possibly damaging (score 0.828)	Deleterious (score -3.825)	3	6	Pathogenic	Pathogenic
c.1783C>T	p.Arg595*	Bartter syndrome 3	Bettinelli et al.,[556]	0.00672%	Disease causing	N/A	N/A	1	3	Pathogenic	Likely benign
c.1830G>A	p.Trp610*	Bartter syndrome 3	Fukuyama et al.,[562]	0.01652%	Disease causing	N/A	N/A	2	4	Pathogenic	Likely benign
c.1877G>A	p.Cys626Tyr	Bartter syndrome 3	Vargas-Poussou et al.,[553]	2.29%	Polymorphism	Probably damaging (score 0.998)	Deleterious (score -5.327)	3	7	Pathogenic	Likely pathogenic
c.2001C>A	p.Cys667*	Bartter syndrome 3	Bettinelli et al.,[556]	0%	Disease causing	N/A	N/A	1	1	Pathogenic	Likely pathogenic

CLCNKB variants obtained from HGMD[235] that were used to investigate the effectiveness of *in silico* methods for variant analysis (Chapter 6). Nucleotide number is according to transcript ENST00000375679 and amino acid number is according to the full-length 687 amino acid protein (NCBI NP_000076; UniProt P518010 as displayed on HGMD. *Reported vAFs were obtained from ExAC[236]. Evolutionary conservation scores were based on the number of orthologs each WT residue was conserved in, the number of orthologs studied in each analysis is detailed in the column heading as detailed in Chapter 6. Combined analysis 1 and 2 are based on the criteria detailed in Chapter 6. N/A, not applicable.

Table 42. *In silico* analysis of *OCRL1* variants obtained from HGMD

Nucleotide change	Amino acid change	Phenotype/ disorder	Reference	*Reported vAFs	Prediction of functional effects			Evolutionary conservation		Combined analysis	
					MutationTaster	PolyPhen-2	Provean Protein	4 Orthologs	8 Orthologs	1	2
c.46G>C	p.Glu16Gln	Dent's disease	Sekine et al.,[292]	0%	Polymorphism	Benign (score 0.000)	Neutral (score: 0.079)	1	2	Benign	Likely benign
c.314T>A	p.Leu105*	Dent's disease	Tosetto et al.,[124]	0%	Disease causing	N/A	N/A	3	4	Pathogenic	Likely pathogenic
c.497C>A	p.Ser166*	Dent's disease	Shrimpton et al.,[563]	0%	Disease causing	N/A	N/A	1	2	Pathogenic	Likely pathogenic
c.595C>T	p.Gln199*	Lowe oculocerebrorenal syndrome without cataracts	Pasternack et al.,[564]	0%	Disease causing	N/A	N/A	3	5	Pathogenic	Likely pathogenic
c.643C>T	p.Gln215*	Lowe oculocerebrorenal syndrome	Bockenhauer et al.,[565]	0%	Disease causing	N/A	N/A	4	7	Pathogenic	Pathogenic
c.688C>T	p.Arg230*	Lowe oculocerebrorenal syndrome	Hichri et al.,[566]	0%	Disease causing	N/A	N/A	3	6	Pathogenic	Pathogenic
c.702T>G	p.Tyr234*	Lowe oculocerebrorenal syndrome	Hichri et al.,[566]	0%	Disease causing	N/A	N/A	4	8	Pathogenic	Pathogenic
c.725T>C	p.Phe242Ser	Lowe oculocerebrorenal syndrome	Hichri et al.,[566]	0%	Disease causing	Probably damaging (score 0.978)	Deleterious (score -5.155)	4	8	Pathogenic	Pathogenic
c.728T>C	p.Phe243Ser	Dent's disease	Cho et al.,[525]	0%	Disease causing	Probably damaging (score 0.997)	Deleterious (score -7.021)	4	8	Pathogenic	Pathogenic
c.740G>A	p.Trp247*	Lowe oculocerebrorenal syndrome	Roa (2006) OCRL Locus-specific database Unpublished.	0%	Disease causing	N/A	N/A	4	8	Pathogenic	Pathogenic
c.741G>C	p.Trp247Cys	Lowe oculocerebrorenal syndrome	Addis et al.,[567]	0%	Disease causing	Probably damaging (score 0.996)	Deleterious (score -8.517)	4	8	Pathogenic	Pathogenic
c.783G>C	p.Trp261Cys	Lowe oculocerebrorenal syndrome	Roa (2006) OCRL Locus-specific database Unpublished.	0%	Disease causing	Probably damaging (score 1.000)	Deleterious (score -11.691)	4	8	Pathogenic	Pathogenic
c.814T>C	p.Tyr272His	Lowe oculocerebrorenal syndrome	No author given (2006) OCRL Locus-specific database Unpublished.	0%	Disease causing	Probably damaging (score 1.000)	Deleterious (score -4.512)	4	8	Pathogenic	Pathogenic
c.821T>C	p.Ile274Thr	Dent's disease	Utsch et al.,[568]	0%	Disease causing	Probably damaging (score 0.833)	Deleterious (score -3.606)	4	6	Pathogenic	Pathogenic
c.827T>C	p.Phe276Ser	Lowe oculocerebrorenal syndrome	Chabaa et al.,[569]	0%	Disease causing	Probably damaging (score 1.000)	Deleterious (score -7.313)	4	8	Pathogenic	Pathogenic

Nucleotide change	Amino acid change	Phenotype/ disorder	Reference	*Reported vAFs	Prediction of functional effects			Evolutionary conservation		Combined analysis	
					MutationTaster	PolyPhen-2	Provean Protein	4 Orthologs	8 Orthologs	1	2
c.830A>G	p.Gln277Arg	Lowe oculocerebrorenal syndrome	Sethi et al.,[570]	0%	Disease causing	Probably damaging (score 1.000)	Deleterious (score -3.826)	4	8	Pathogenic	Pathogenic
c.829C>G	p.Gln277Glu	Lowe oculocerebrorenal syndrome	Cho et al.,[525]	0%	Disease causing	Probably damaging (score 1.000)	Deleterious (score -2.869)	4	8	Pathogenic	Pathogenic
c.850G>A	p.Glu284Lys	Congenital cataract	Craigen et al.,[571]	0%	Disease causing	Probably damaging (score 0.959)	Deleterious (score -3.826)	4	8	Pathogenic	Pathogenic
c.860T>C	p.Phe287Ser	Dent's disease	Tosetto et al.,[124]	0%	Disease causing	Probably damaging (score 0.956)	Deleterious (score -5.285)	4	8	Pathogenic	Pathogenic
c.877A>G	p.Lys293Glu	Dent's disease	Sekine et al.,[292]	0%	Disease causing	Probably damaging (score 0.927)	Deleterious (score -3.323)	4	8	Pathogenic	Pathogenic
c.880G>T	p.Glu294*	Lowe oculocerebrorenal syndrome	Ke et al.,[572]	0%	Disease causing	N/A	N/A	4	8	Pathogenic	Pathogenic
c.883C>T	p.Gln295*	Lowe oculocerebrorenal syndrome	Lin et al.,[573]	0%	Disease causing	N/A	N/A	4	8	Pathogenic	Pathogenic
c.890G>A	p.Trp297*	Lowe oculocerebrorenal syndrome	Gal (2001) OCRL Locus-specific database Unpublished	0%	Disease causing	N/A	N/A	4	8	Pathogenic	Pathogenic
c.904G>T	p.Glu302*	Lowe oculocerebrorenal syndrome	Sethi et al.,[570]	0%	Disease causing	N/A	N/A	4	8	Pathogenic	Pathogenic
c.953G>A	p.Arg318His	Dent's disease	Shrimpton et al.,[563]	0%	Disease causing	Probably damaging (score 0.982)	Deleterious (score -4.966)	4	8	Pathogenic	Pathogenic
c.952C>T	p.Arg318Cys	Dent's disease	Hoopes et al.,[100]	0%	Disease causing	Probably damaging (score 1.000)	Deleterious (score -4.966)	4	8	Pathogenic	Pathogenic
c.962G>A	p.Gly321Glu	Dent's disease	Shrimpton et al.,[563]	0%	Disease causing	Probably damaging (score 1.000)	Deleterious (score -7.945)	4	8	Pathogenic	Pathogenic
c.982G>C	p.Ala328Pro	Lowe oculocerebrorenal syndrome	Bockenhauer et al.,[565]	0%	Disease causing	Probably damaging (score 0.961)	Deleterious (score -2.739)	4	7	Pathogenic	Pathogenic
c.1001G>C	p.Arg334Pro	Lowe oculocerebrorenal syndrome	Gal (2001) OCRL Locus-specific database Unpublished	0%	Polymorphism	Benign (score 0.000)	Neutral (score 0.919)	1	3	Benign	Likely benign
c.1000C>T	p.Arg334*	Lowe oculocerebrorenal syndrome	Satre et al.,[574]	0%	Disease causing	N/A	N/A	1	3	Pathogenic	Likely pathogenic
c.1005C>G	p.Tyr335*	Lowe oculocerebrorenal syndrome	Hichri et al.,[566]	0%	Disease causing	N/A	N/A	2	5	Pathogenic	Likely pathogenic
c.1060A>C	p.Asn354His	Dent's disease	Hichri et al.,[566]	0%	Disease causing	Probably damaging (score 0.999)	Deleterious (score -4.889)	4	8	Pathogenic	Pathogenic
c.1070G>A	p.Gly357Glu	Lowe oculocerebrorenal syndrome	Monnier et al.,[575]	0%	Disease causing	Probably damaging (score 1.000)	Deleterious (score -6.762)	4	8	Pathogenic	Pathogenic

Nucleotide change	Amino acid change	Phenotype/ disorder	Reference	*Reported vAFs	Prediction of functional effects			Evolutionary conservation		Combined analysis	
					MutationTaster	PolyPhen-2	Provean Protein	4 Orthologs	8 Orthologs	1	2
c.1115T>G	p.Val372Gly	Lowe oculocerebrorenal syndrome	Hichri et al.,[566]	0%	Disease causing	Probably damaging (score 1.000)	Deleterious (score -6.961)	4	8	Pathogenic	Pathogenic
c.1117A>T	p.Asn373Tyr	Lowe oculocerebrorenal syndrome	Hichri et al.,[566]	0%	Disease causing	Probably damaging (score 1.000)	Deleterious (score -7.956)	4	8	Pathogenic	Pathogenic
c.1120T>C	p.Ser374Pro	Lowe oculocerebrorenal syndrome	Cho et al.,[525]	0%	Disease causing	Probably damaging (score 0.999)	Deleterious (score -4.472)	4	8	Pathogenic	Pathogenic
c.1121C>T	p.Ser374Phe	Lowe oculocerebrorenal syndrome	Hichri et al.,[566]	0%	Disease causing	Probably damaging (score 1.000)	Deleterious (score -5.400)	4	8	Pathogenic	Pathogenic
c.1123C>T	p.His375Tyr	Lowe oculocerebrorenal syndrome	Lin et al.,[576]	0%	Disease causing	Probably damaging (score 1.000)	Deleterious (score -5.967)	4	8	Pathogenic	Pathogenic
c.1162C>T	p.Gln388*	Lowe oculocerebrorenal syndrome	Lin et al.,[573]	0%	Disease causing	N/A	N/A	4	8	Pathogenic	Pathogenic
c.1177A>T	p.Ile393Phe	Dent's disease	Bockenhauer et al.,[577]	0%	Disease causing	Probably damaging (score 0.999)	Deleterious (score -3.978)	4	8	Pathogenic	Pathogenic
c.1222C>T	p.Gln408*	Lowe oculocerebrorenal syndrome	Kubota et al.,[578]	0%	Disease causing	N/A	N/A	3	6	Pathogenic	Pathogenic
c.1241A>G	p.His414Arg	Lowe oculocerebrorenal syndrome	Hichri et al.,[566]	0%	Disease causing	Probably damaging (score 0.999)	Deleterious (score -7.722)	4	8	Pathogenic	Pathogenic
c.1262G>A	p.Gly421Glu	Lowe oculocerebrorenal syndrome	Monnier et al.,[575]	0%	Disease causing	Probably damaging (score 1.000)	Deleterious (score -7.956)_	4	8	Pathogenic	Pathogenic
c.1264G>A	p.Asp422Asn	Lowe oculocerebrorenal syndrome	Roa (2005) OCRL Locus-specific database Unpublished .	0%	Disease causing	Probably damaging (score 0.998)	Deleterious (score -4.972)	4	8	Pathogenic	Pathogenic
c.1270A>G	p.Asn424Asp	Lowe oculocerebrorenal syndrome	Monnier et al.,[575]	0%	Disease causing	Probably damaging (score 1.000)	Deleterious (score -4.972)	4	8	Pathogenic	Pathogenic
c.1351G>A	p.Asp451Asn	Lowe oculocerebrorenal syndrome	Hichri et al.,[566]	0%	Disease causing	Probably damaging (score 1.000)	Deleterious (score -4.972)	4	8	Pathogenic	Pathogenic
c.1352A>G	p.Asp451Gly	Lowe oculocerebrorenal syndrome	Lin et al.,[573]	0%	Disease causing	Probably damaging (score 1.000)	Deleterious (score -6.961)	4	8	Pathogenic	Pathogenic
c.1369C>G	p.Arg457Gly	Lowe oculocerebrorenal syndrome	Hichri et al.,[566]	0%	Disease causing	Probably damaging (score 0.917)	Deleterious (score -3.654)	4	8	Pathogenic	Pathogenic
c.1378A>T	p.Lys460*	Lowe oculocerebrorenal syndrome	Hichri et al.,[566]	0%	Disease causing	N/A	N/A	4	8	Pathogenic	Pathogenic
c.1388T>C	p.Phe463Ser	Lowe oculocerebrorenal syndrome	Lin et al.,[573]	0%	Disease causing	Probably damaging (score 1.00)	Deleterious (score -6.972)	4	8	Pathogenic	Pathogenic
c.1402G>A	p.Glu468Lys	Lowe oculocerebrorenal syndrome	Hichri et al.,[566]	0%	Disease causing	Probably damaging (score 1.00)	Deleterious (score -3.778)	4	8	Pathogenic	Pathogenic
c.1403A>G	p.Glu468Gly	Lowe oculocerebrorenal syndrome	Hichri et al.,[566]	0%	Disease causing	Probably damaging (score 1.00)	Deleterious (score -6.611)	4	8	Pathogenic	Pathogenic

Nucleotide change	Amino acid change	Phenotype/ disorder	Reference	*Reported vAFs	Prediction of functional effects			Evolutionary conservation		Combined analysis	
					MutationTaster	PolyPhen-2	Provean Protein	4 Orthologs	8 Orthologs	1	2
c.1424C>A	p.Pro475His	Lowe oculocerebrorenal syndrome	Chou et al.,[579]	0%	Disease causing	Probably damaging (score 1.00)	Deleterious (score -8500)	4	8	Pathogenic	Pathogenic
c.1431T>G	p.Tyr477*	Lowe oculocerebrorenal syndrome	Addis et al.,[567]	0%	Disease causing	N/A	N/A	4	8	Pathogenic	Pathogenic
c.1436A>G	p.Tyr479Cys	Dent's disease	Hoopes et al.,[563]	0%	Disease causing	Probably damaging (score 1.000)	Deleterious (score -8.196)	3	6	Pathogenic	Pathogenic
c.1477C>T	p.Arg493Trp	Dent's disease	Utsch et al.,[568]	0%	Disease causing	Probably damaging (score 1.000)	Deleterious (score -7.873)	4	8	Pathogenic	Pathogenic
c.1484C>T	p.Pro495Leu	Lowe oculocerebrorenal syndrome	Tasic et al.,[580]	0%	Disease causing	Probably damaging (score 1.000)	Deleterious (score -9.819)	4	8	Pathogenic	Pathogenic
c.1489T>G	p.Trp497Gly	Lowe oculocerebrorenal syndrome	Schneider (2001) OCRL Locus-specific database Unpublished .	0%	Disease causing	Probably damaging (score 1.000)	Deleterious (score -12.737)	4	8	Pathogenic	Pathogenic
c.1490G>A	p.Trp497*	Lowe oculocerebrorenal syndrome	Gal (2001) OCRL Locus-specific database Unpublished	0%	Disease causing	N/A	N/A	4	8	Pathogenic	Pathogenic
c.1493G>A	p.Cys498Tyr	Lowe oculocerebrorenal syndrome	Monnier et al.,[575]	0%	Disease causing	Probably damaging (score 1.000)	Deleterious (score -10.491)	4	8	Pathogenic	Pathogenic
c.1495G>C	p.Asp499His	Lowe oculocerebrorenal syndrome	Hichri et al.,[566]	0%	Disease causing	Probably damaging (score 1.000)	Deleterious (score -6900)	4	8	Pathogenic	Pathogenic
c.1499G>A	p.Arg500Gln	Lowe oculocerebrorenal syndrome	Kawano et al.,[581]	0%	Disease causing	Probably damaging (score 1.000)	Deleterious (score -3.931)	4	8	Pathogenic	Pathogenic
c.1498C>G	p.Arg500Gly	Lowe oculocerebrorenal syndrome	Satre et al.,[574]	0%	Disease causing	Probably damaging (score 1.000)	Deleterious (score -6.806)	4	8	Pathogenic	Pathogenic
c.1498C>T	p.Arg500*	Lowe oculocerebrorenal syndrome	Monnier et al.,[575]	0%	Disease causing	N/A	N/A	4	8	Pathogenic	Pathogenic
c.1507T>C	p.Trp503Arg	Lowe oculocerebrorenal syndrome	Hichri et al.,[566]	0%	Disease causing	Probably damaging (score 0.999)	Deleterious (score -12.556)	4	8	Pathogenic	Pathogenic
c.1523T>A	p.Val508Asp	Lowe oculocerebrorenal syndrome	Lin et al.,[576]	0%	Disease causing	Probably damaging (score 0.962)	Deleterious (score -6.317)	2	6	Pathogenic	Pathogenic
c.1528C>T	p.Gln510*	Lowe oculocerebrorenal syndrome	Simsek et al.,[582]	0%	Disease causing	N/A	N/A	4	8	Pathogenic	Pathogenic
c.1538A>G	p.Tyr513Cys	Lowe oculocerebrorenal syndrome	Lin et al.,[576]	0%	Disease causing	Probably damaging (score 1.000)	Deleterious (score -8.590)	4	8	Pathogenic	Pathogenic
c.1566C>G	p.Ser522Arg	Lowe oculocerebrorenal syndrome	Kubota et al.,[578]	0%	Disease causing	Probably damaging (score 1.000)	Deleterious (score -4.976)	4	8	Pathogenic	Pathogenic
c.1567G>A	p.Asp523Asn	Dent's disease	Tosetto et al.,[124]	0%	Disease causing	Probably damaging (score 1.000)	Deleterious (score-4.976)	4	8	Pathogenic	Pathogenic

Nucleotide change	Amino acid change	Phenotype/ disorder	Reference	*Reported vAFs	Prediction of functional effects			Evolutionary conservation		Combined analysis	
					MutationTaster	PolyPhen-2	Provean Protein	4 Orthologs	8 Orthologs	1	2
c.1568A>G	p.Asp523Gly	Lowe oculocerebrorenal syndrome	Roa (2005) OCRL Locus-specific database Unpublished .	0%	Disease causing	Probably damaging (score 1.000)	Deleterious (score -6.966)	4	8	Pathogenic	Pathogenic
c.1572C>G	p.His524Gln	Lowe oculocerebrorenal syndrome	Kawano et al.,[581]	0%	Disease causing	Probably damaging (score 1.000)	Deleterious (score -7.961)	4	8	Pathogenic	Pathogenic
c.1571A>G	p.His524Arg	Lowe oculocerebrorenal syndrome	Lin et al.,[573]	0%	Disease causing	Probably damaging (score 1.000)	Deleterious (score -7.961)	4	8	Pathogenic	Pathogenic
c.1576C>A	p.Pro526Thr	Lowe oculocerebrorenal syndrome	Roa (2005) OCRL Locus-specific database Unpublished .	0%	Disease causing	Probably damaging (score 1.000)	Deleterious (score -7.961)	4	8	Pathogenic	Pathogenic
c.1577C>T	p.Pro526Leu	Lowe oculocerebrorenal syndrome	Roschinger et al.,[583]	0%	Disease causing	Probably damaging (score 1.000)	Deleterious (score -9.923)	4	8	Pathogenic	Pathogenic
c.1576C>T	p.Pro526Ser	Dent's disease	Kaneko et al.,[584]	0%	Disease causing	Probably damaging (score 1.000)	Deleterious (score -7.961)	4	8	Pathogenic	Pathogenic
c.1580T>A	p.Val527Asp	Lowe oculocerebrorenal syndrome	Addis et al.,[567]	0%	Disease causing	Probably damaging (score 1.000)	Deleterious (score -6.762)	4	8	Pathogenic	Pathogenic
c.1598T>C	p.Ile533Thr	Dent's disease	Bockenhauer et al.,[577]	0%	Disease causing	Probably damaging (score 0.908)	Deleterious (score -3.130)	4	8	Pathogenic	Pathogenic
c.1598T>G	p.Ile533Ser	Lowe oculocerebrorenal syndrome	Lin (2001) OCRL Locus-specific database Unpublished	0%	Disease causing	Probably damaging (score 0.911)	Deleterious (score -3.463)	4	8	Pathogenic	Pathogenic
c.1621C>T	p.Arg541*	Lowe oculocerebrorenal syndrome	Roa (2005) OCRL Locus-specific database Unpublished .	0%	Disease causing	N/A	N/A	3	6	Pathogenic	Pathogenic
c.1723G>T	p.Glu575*	Lowe oculocerebrorenal syndrome	Satre et al.,[574]	0%	Disease causing	N/A	N/A	4	7	Pathogenic	Pathogenic
c.1730T>A	p.Val577Glu	Lowe oculocerebrorenal syndrome	Addis et al.,[567]	0%	Disease causing	Probably damaging (score 0.999)	Deleterious (score -5.771)	4	8	Pathogenic	Pathogenic
c.1773C>A	p.Asn591Lys	Lowe oculocerebrorenal syndrome	Yuksel, Karaca and Albayram[585]	0%	Disease causing	Probably damaging (score 0.999)	Deleterious (score -4.463)	4	8	Pathogenic	Pathogenic
c.1780C>T	p.Gln594*	Lowe oculocerebrorenal syndrome	Hichri et al.,[566]	0%	Disease causing	N/A	N/A	4	8	Pathogenic	Pathogenic
c.1830C>G	p.Tyr610*	Lowe oculocerebrorenal syndrome	Gal (2001) OCRL Locus-specific database Unpublished	0%	Disease causing	N/A	N/A	4	8	Pathogenic	Pathogenic

Nucleotide change	Amino acid change	Phenotype/ disorder	Reference	*Reported vAFs	Prediction of functional effects			Evolutionary conservation		Combined analysis	
					MutationTaster	PolyPhen-2	Provean Protein	4 Orthologs	8 Orthologs	1	2
c.1901T>C	p.Leu634Pro	Lowe oculocerebrorenal syndrome	Bockenhauer et al.,[565]	0%	Disease causing	Probably damaging (score 1.000)	Deleterious (score -6.470)	4	8	Pathogenic	Pathogenic
c.1987C>T	p.Arg663*	Lowe oculocerebrorenal syndrome	Lin et al.,[573]	0%	Disease causing	N/A	N/A	4	8	Pathogenic	Pathogenic
c.2039T>C	p.Phe680Ser	Dent's disease	Sekine et al.,[292]	0%	Disease causing	Probably damaging (score 1.000)	Deleterious (score -7.561)	4	8	Pathogenic	Pathogenic
c.2051T>G	p.Leu684*	Lowe oculocerebrorenal syndrome	Roa (2005) OCRL Locus-specific database Unpublished .	0%	Disease causing	N/A	N/A	4	8	Pathogenic	Pathogenic
c.2060T>C	p.Leu687Pro	Lowe oculocerebrorenal syndrome	Roa (2005) OCRL Locus-specific database Unpublished .	0%	Disease causing	Probably damaging (score 0.984)	Deleterious (score -6.966)	4	8	Pathogenic	Pathogenic
c.2071A>T	p.Lys691*	Lowe oculocerebrorenal syndrome	Bockenhauer et al.,[565]	0%	Disease causing	N/A	N/A	3	7	Pathogenic	Pathogenic
c.2083C>T	p.Arg695*	Lowe oculocerebrorenal syndrome	Lin et al.,[576]	0%	Disease causing	N/A	N/A	4	8	Pathogenic	Pathogenic
c.2086G>T	p.Glu696*	Lowe oculocerebrorenal syndrome	Hichri et al.,[566]	0%	Disease causing	N/A	N/A	4	8	Pathogenic	Pathogenic
c.2211G>C	p.Glu737Asp	Dent's disease	Tosetto et al.,[124]	0%	Disease causing	Probably damaging (score 0.999)	Deleterious (score -2.936)	4	8	Pathogenic	Pathogenic
c.2244C>G	p.Tyr748*	Lowe oculocerebrorenal syndrome	Addis (2005) OCRL Locus-specific database Unpublished .	0%	Disease causing	N/A	N/A	2	4	Pathogenic	Likely pathogenic
c.2269C>T	p.Gln757*	Lowe oculocerebrorenal syndrome	Monnier et al.,[575]	0%	Disease causing	N/A	N/A	4	8	Pathogenic	Pathogenic
c.2303T>A	p.Ile768Asn	Lowe oculocerebrorenal syndrome	Monnier et al.,[575]	0%	Disease causing	Probably damaging (score 0.996)	Deleterious (score -6.748)	4	8	Pathogenic	Pathogenic
c.2363C>A	p.Ala788Asp	Lowe oculocerebrorenal syndrome	Topaloğlu, Ludwig and Celebi Tayfur[586]	0%	Disease causing	Probably damaging (score 0.999)	Deleterious (score -5.147)	4	7	Pathogenic	Pathogenic
c.2389G>C	p.Ala797Pro	Lowe oculocerebrorenal syndrome	Monnier et al.,[575]	0%	Disease causing	Probably damaging (score 0.992)	Deleterious (score -2.974)	4	7	Pathogenic	Pathogenic
c.2415C>G	p.Tyr805*	Lowe oculocerebrorenal syndrome	Monnier et al.,[575]	0%	Disease causing	N/A	N/A	4	7	Pathogenic	Pathogenic
c.2416G>T	p.Glu806*	Lowe oculocerebrorenal syndrome	Roa (2005) OCRL Locus-specific database Unpublished .	0%	Disease causing	N/A	N/A	4	7	Pathogenic	Pathogenic

Nucleotide change	Amino acid change	Phenotype/ disorder	Reference	*Reported vAFs	Prediction of functional effects			Evolutionary conservation		Combined analysis	
					MutationTaster	PolyPhen-2	Provean Protein	4 Orthologs	8 Orthologs	1	2
c.2428C>T	p.Arg810*	Lowe oculocerebrorenal syndrome	Monnier et al.,[575]	0%	Disease causing	N/A	N/A	4	7	Pathogenic	Pathogenic
c.2433T>A	p.Cys811*	Lowe oculocerebrorenal syndrome	Gal (2001) OCRL Locus-specific database Unpublished	0%	Disease causing	N/A	N/A	4	7	Pathogenic	Pathogenic
c.2464C>T	p.Arg822*	Lowe oculocerebrorenal syndrome	Hichri et al.,[566]	0%	Disease causing	N/A	N/A	3	5	Pathogenic	Likely pathogenic
c.2467C>T	p.Gln823*	Lowe oculocerebrorenal syndrome	Lin et al.,[576]	0%	Disease causing	N/A	N/A	4	7	Pathogenic	Pathogenic
c.2486C>T	p.Pro829Leu	Dent's disease	Sekine et al.,[292]	0%	Disease causing	Probably damaging (score 0.998)	Deleterious (score -8.343)	4	7	Pathogenic	Pathogenic
c.2530C>T	p.Arg844*	Lowe oculocerebrorenal syndrome	Leahey, Charnas and Nussbaum[587]	0%	Disease causing	N/A	N/A	2	5	Pathogenic	Likely pathogenic
c.2533G>T	p.Glu845*	Lowe oculocerebrorenal syndrome	Monnier et al.,[575]	0%	Disease causing	N/A	N/A	3	6	Pathogenic	Pathogenic
c.2581G>A	p.Ala861Thr	Lowe oculocerebrorenal syndrome	Bockenhauer et al.,[565]	0%	Disease causing	Probably damaging (score 0.996)	Deleterious (score -2.912)	2	5	Pathogenic	Likely pathogenic
c.2672T>G	p.Leu891Arg	Lowe oculocerebrorenal syndrome	Hichri et al.,[566]	0%	Disease causing	Possibly damaging (score 0.707)	Deleterious (score -4.140)	2	5	Pathogenic	Likely pathogenic

OCRL1 variants obtained from HGMD[235] that were used to investigate the effectiveness of *in silico* methods for variant analysis (Chapter 6). Nucleotide number is according to transcript ENST00000371113 and amino acid number is according to the full-length 901 amino acid protein (NCBI NP_000267; UniProt Q01968) as displayed on HGMD. *Reported vAFs were obtained from ExAC[236]. Evolutionary conservation scores were based on the number of orthologs each WT residue was conserved in, the number of orthologs studied in each analysis is detailed in the column heading, as detailed in Chapter 6. Combined analysis 1 and 2 are based on the criteria detailed in Chapter 6. N/A, not applicable.

Table 43. *In silico* analysis of *UMOD* variants obtained from HGMD

Nucleotide change	Amino acid change	Phenotype/ disorder	Reference	*Reported vAFs	Prediction of functional effects			Evolutionary conservation		Combined analysis	
					MutationTaster	PolyPhen-2	Provean Protein	4 Orthologs	8 Orthologs	1	2
c.95G>A	p.Cys32Tyr	FJHN/MCKD syndrome	Vylet'al et al.,[156]	0%	Disease causing	Probably damaging (score 0.999)	Deleterious (score -4.207)	4	7	Pathogenic	Pathogenic
c.96C>G	p.Cys32Trp	Hyperuricaemic nephropathy, juvenile	Williams et al.,[155]	0%	Disease causing	Probably damaging (score 0.999)	Deleterious (score -4.653)	4	7	Pathogenic	Pathogenic
c.101G>A	p.Glu34Lys	Tubulointerstitial nephritis	Bollée et al.,[588]	0%	Polymorphism	Benign (score 0.019)	Neutral (score -1.255)	3	3	Pathogenic	Likely benign
c.149G>C	p.Cys50Ser	Reduced kidney function, hyperuricaemia, impaired urine-concentrating ability	Benetti et al.,[589]	0%	Disease causing	Probably damaging (score 0.998)	Deleterious (score -4.075)	4	7	Pathogenic	Pathogenic
c.156T>G	p.Cys52Trp	Hyperuricaemic nephropathy, juvenile	Kudo et al.,[590]	0%	Disease causing	Probably damaging (score 0.999)	Deleterious (score -4.764)	4	7	Pathogenic	Pathogenic
c.172G>T	p.Gly58Cys	Uromodulin-associated kidney disease	Zaucke et al.,[591]	0%	Disease causing	Probably damaging (score 1.000)	Deleterious (score -3.615)	4	6	Pathogenic	Pathogenic
c.176A>C	p.Asp59Ala	Hyperuricaemic nephropathy, juvenile	Dahan et al.,[592]	0%	Disease causing	Possibly damaging (score 0.492)	Deleterious (score -3.448)	4	7	Pathogenic	Pathogenic
c.187T>C	p.Cys63Arg	Hyperuricaemic nephropathy, juvenile	Lee et al.,[593]	0%	Disease causing	Probably damaging (score 0.999)	Deleterious (score -4.780)	4	6	Pathogenic	Pathogenic
c.205T>C	p.Cys69Arg	Tubulointerstitial nephritis	Bollée et al.,[588]	0%	Disease causing	Probably damaging (score 0.999)	Deleterious (score -4.350)	4	6	Pathogenic	Pathogenic
c.206G>A	p.Cys69Tyr	Uromodulin-associated kidney disease	Zaucke et al.,[591]	0%	Disease causing	Probably damaging (score 0.999)	Deleterious (score -3.807)	4	6	Pathogenic	Pathogenic
c.229T>G	p.Cys77Gly	FJHN/MCKD syndrome	Wolf et al.,[594]	0%	Disease causing	Probably damaging (score 0.998)	Deleterious (score -4.421)	4	6	Pathogenic	Pathogenic
c.230G>A	p.Cys77Tyr	Hyperuricaemic nephropathy, juvenile	Turner et al.,[140]	0%	Disease causing	Probably damaging (score 0.999)	Deleterious (score -3.797)	4	6	Pathogenic	Pathogenic
c.307G>T	p.Gly103Cys	Medullary cystic kidney disease 2	Hart et al.,[595]	0%	Disease causing	Possibly damaging (score 0.897)	Neutral (score -1.703)	2	3	Unknown significance	Unknown significance
c.317G>A	p.Cys106Tyr	Uromodulin-associated kidney disease	Zaucke ert al.,[591]	0%	Disease causing	Probably damaging (score 0.999)	Deleterious (score -4.419)	4	5	Pathogenic	Likely pathogenic
c.326T>A	p.Val109Glu	Hyperuricaemic nephropathy, juvenile	Liu et al.,[596]	0%	Disease causing	Probably damaging (score 0.982)	Neutral (score -2.300)	3	6	Pathogenic	Pathogenic
c.334T>C	p.Cys112Arg	Hyperuricaemic nephropathy, juvenile	Dahan et al.,[592]	0%	Disease causing	Probably damaging (score 0.999)	Deleterious (score -4.781)	4	7	Pathogenic	Pathogenic
c.376T>C	p.Cys126Arg	Hyperuricaemic nephropathy, juvenile	Turner et al.,[140]	0%	Disease causing	Probably damaging (score 0.999)	Deleterious (score -5.459)	4	7	Pathogenic	Pathogenic
c.383A>G	p.Asn128Ser	Hyperuricaemic nephropathy, juvenile	Turner et al.,[140]	0%	Disease causing	Probably damaging (score 0.996)	Neutral (score -1.913)	4	7	Pathogenic	Pathogenic
c.404T>A	p.Cys135Ser	Hyperuricaemic nephropathy, juvenile	Kudo et al.,[590]	0%	Disease causing	Probably damaging (score 0.933)	Deleterious (score -4.340)	4	7	Pathogenic	Pathogenic

Nucleotide change	Amino acid change	Phenotype/ disorder	Reference	*Reported vAFs	Prediction of functional effects			Evolutionary conservation		Combined analysis	
					MutationTaster	PolyPhen-2	Provean Protein	4 Orthologs	8 Orthologs	1	2
c.442T>C	p.Cys148Arg	Tubulointerstitial nephritis	Bollée et al.,[588]	0%	Disease causing	Benign (score 0.223)	Deleterious (score -4.551)	4	7	Pathogenic	Pathogenic
c.443G>A	p.Cys148Tyr	Hyperuricaemic nephropathy, juvenile	Hart et al.,[595]	0%	Disease causing	Probably damaging (score 0.961)	Deleterious (score -4.143)	4	7	Pathogenic	Pathogenic
c.444T>G	p.Cys148Trp	Medullary cystic kidney disease 2	Rampoldi et al.,[597]	0%	Disease causing	Probably damaging (score 0.986)	Deleterious (score -4.396)	4	7	Pathogenic	Pathogenic
c.448T>A	p.Cys150Ser	Uromodulin-associated kidney disease	Zaucke et al.,[591]	0%	Disease causing	Benign (score 0.160)	Deleterious (score -2.643)	3	5	Pathogenic	Likely pathogenic
c.449G>C	p.Cys150Ser	Medullary cystic kidney disease 2	Rampoldi et al.,[597]	0%	Disease causing	Benign (score 0.160)	Deleterious (score -2.643)	3	5	Pathogenic	Likely pathogenic
c.509G>A	p.Cys170Tyr	Hyperuricaemic nephropathy, juvenile	Dahan et al.,[592]	0%	Polymorphism	Probably damaging (score 0.999)	Deleterious (score -6.817)	4	7	Pathogenic	Pathogenic
c.514G>C	p.Asp172His	Tubulointerstitial nephritis	Bollée et al.,[588]	0%	Disease causing	Probably damaging (score 1.000)	Deleterious (score -4.950)	4	8	Pathogenic	Pathogenic
c.520T>C	p.Cys174Arg	Uromodulin-associated kidney disease	Moskowitz et al.,[598]	0%	Disease causing	Probably damaging (score 0.999)	Deleterious (score -8.999)	4	8	Pathogenic	Pathogenic
c.552G>C	p.Trp184Cys	Tubulointerstitial nephritis	Bollée et al.,[588]	0%	Disease causing	Probably damaging (score 0.948)	Deleterious (score -6.092)	4	8	Pathogenic	Pathogenic
c.553C>A	p.Arg185Ser	Hyperuricaemic nephropathy, juvenile	Dahan et al.,[592]	0%	Disease causing	Probably damaging (score 0.995)	Deleterious (score -4.213)	4	8	Pathogenic	Pathogenic
c.553C>G	p.Arg185Gly	Hyperuricaemic nephropathy, juvenile	Bleyer et al.,[599]	0%	Disease causing	Probably damaging (score 0.995)	Deleterious (score 5.032)	4	8	Pathogenic	Pathogenic
c.553C>T	p.Arg185Cys	Tubulointerstitial nephritis	Bollée et al.,[588]	0%	Disease causing	Probably damaging (score 0.998)	Deleterious (score -5.670)	4	8	Pathogenic	Pathogenic
c.554G>A	p.Arg185His	Tubulointerstitial nephritis	Bollée et al.,[588]	0%	Disease causing	Probably damaging (score 0.998)	Deleterious (score -3.320)	4	8	Pathogenic	Pathogenic
c.584G>T	p.Cys195Phe	Hyperuricaemic nephropathy, juvenile	Kudo et al.,[590]	0%	Disease causing	Probably damaging (score 0.999)	Deleterious (score -7.362)	4	8	Pathogenic	Pathogenic
c.586G>A	p.Asp196Asn	Hyperuricaemic nephropathy, juvenile	Williams et al.,[155]	0%	Disease causing	Probably damaging (score 1.000)	Deleterious (score -3.550)	4	8	Pathogenic	Pathogenic
c.586G>T	p.Asp196Tyr	Hyperuricaemic nephropathy, juvenile	Lhotta et al.,[600]	0%	Disease causing	Probably damaging (score 1.000)	Deleterious (score -6.433)	4	8	Pathogenic	Pathogenic
c.605G>C	p.Trp202Ser	Hyperuricaemic nephropathy, juvenile	Kudo et al.,[590]	0%	Disease causing	Probably damaging (score 0.999)	Deleterious (score -10.174)	4	8	Pathogenic	Pathogenic
c.610C>G	p.Arg204Gly	Hyperuricaemic nephropathy, juvenile	Dahan et al.,[592]	0%	Disease causing	Probably damaging (score 0.999)	Deleterious (score -4.669)	4	8	Pathogenic	Pathogenic
c.628G>A	p.Gly210Ser	Tubulointerstitial nephritis	Bollée et al.,[588]	0%	Disease causing	Probably damaging (score 1.000)	Deleterious (score -2.862)	4	7	Pathogenic	Pathogenic
c.634C>T	p.Arg212Cys	Uromodulin-associated kidney disease	Schaeffer et al.,[601]	0%	Disease causing	Possibly damaging (score 0.694)	Deleterious (score -4.631)	4	7	Pathogenic	Pathogenic

Nucleotide change	Amino acid change	Phenotype/ disorder	Reference	*Reported vAFs	Prediction of functional effects			Evolutionary conservation		Combined analysis	
					MutationTaster	PolyPhen-2	Provean Protein	4 Orthologs	8 Orthologs	1	2
c.649T>C	p.Cys217Arg	Hyperuricaemic nephropathy, juvenile	Hart et al.,[595]	0%	Disease causing	Probably damaging (score 0.998)	Deleterious (score -8.243)	4	8	Pathogenic	Pathogenic
c.649T>G	p.Cys217Gly	Hyperuricaemic nephropathy, juvenile	Dahan et al.,[592]	0%	Disease causing	Probably damaging (score 0.997)	Deleterious (score -8.178)	4	8	Pathogenic	Pathogenic
c.651C>G	p.Cys217Trp	Hyperuricaemic nephropathy, juvenile	Williams et al.,[155]	0%	Disease causing	Probably damaging (score 1.000)	Deleterious (score -7.458)	4	8	Pathogenic	Pathogenic
c.665G>C	p.Arg222Pro	Hyperuricaemic nephropathy, juvenile	Dahan et al.,[592]	0%	Polymorphism	Probably damaging (score 0.956)	Deleterious (score -4.067)	3	7	Pathogenic	Pathogenic
c.667T>C	p.Cys223Arg	Hyperuricaemic nephropathy, juvenile	Williams et al.,[155]	0%	Disease causing	Probably damaging (score 0.999)	Deleterious (score -8.167)	4	8	Pathogenic	Pathogenic
c.668G>A	p.Cys223Tyr	Hyperuricaemic nephropathy, juvenile	Bleyer et al.,[602]	0%	Disease causing	Probably damaging (score 0.999)	Deleterious (score -7.334)	4	8	Pathogenic	Pathogenic
c.674C>A	p.Thr225Lys	Medullary cystic kidney disease 2	Wolf et al.,[603]	0%	Disease causing	Probably damaging (score 0.994)	Deleterious (score -3.803)	4	8	Pathogenic	Pathogenic
c.674C>T	p.Thr225Met	Hyperuricaemic nephropathy, juvenile	Dahan et al.,[592]	0%	Disease causing	Probably damaging (score 0.995)	Deleterious (score -3.739)	4	8	Pathogenic	Pathogenic
c.686T>G	p.Met229Arg	FJHN/MCKD syndrome	Vylet'al et al.,[156]	0%	Disease causing	Possibly damaging (score 0.548)	Deleterious (score -3.668)	4	7	Pathogenic	Pathogenic
c.688T>C	p.Trp230Arg	Uromodulin-associated kidney disease	Zaucke et al.,[591]	0%	Disease causing	Probably damaging (score 0.999)	Deleterious (score -9.387)	4	8	Pathogenic	Pathogenic
c.707C>A	p.Pro236Gln	Hyperuricaemic nephropathy, juvenile	Liu et al.,[596]	0%	Disease causing	Probably damaging (score 1.000)	Deleterious (score -5.643)	4	8	Pathogenic	Pathogenic
c.707C>G	p.Pro236Arg	Hyperuricaemic nephropathy, juvenile	Bernascone et al.,[604]	0%	Disease causing	Probably damaging (score 1.000)	Deleterious (score -6.356)	4	8	Pathogenic	Pathogenic
c.707C>T	p.Pro236Leu	Hyperuricaemic nephropathy, juvenile	Kudo et al.,[590]	0%	Disease causing	Probably damaging (score 1.000)	Deleterious (score -7.196)	4	8	Pathogenic	Pathogenic
c.710C>G	p.Ser237Cys	Tubulointerstitial nephritis	Bollée et al.,[588]	0%	Polymorphism	Possibly damaging (score 0.711)	Neutral (score -2.092)	3	5	Pathogenic	Likely benign
c.743G>C	p.Cys248Ser	Uromodulin-associated kidney disease	Zaucke et al.,[591]	0%	Disease causing	Probably damaging (score 0.998)	Deleterious (score -7.073)	4	8	Pathogenic	Pathogenic
c.744C>G	p.Cys248Trp	Medullary cystic kidney disease 2	Wolf et al.,[603]	0%	Disease causing	Probably damaging (score 1.000)	Deleterious (score -7.797)	4	8	Pathogenic	Pathogenic
c.749A>T	p.His250Leu	Tubulointerstitial nephritis	Bollée et al.,[588]	0%	Disease causing	Probably damaging (score 0.913)	Deleterious (score -6.706)	4	7	Pathogenic	Pathogenic
c.764G>A	p.Cys255Tyr	Hyperuricaemic nephropathy, juvenile	Turner et al.,[140]	0%	Disease causing	Probably damaging (score 0.998)	Deleterious (score -7.804)	4	8	Pathogenic	Pathogenic
c.767G>A	p.Cys256Tyr	Uromodulin-associated kidney disease	Schaeffer et al.,[601]	0%	Disease causing	Probably damaging (score 0.999)	Deleterious (score -7.696)	4	8	Pathogenic	Pathogenic
c.808G>T	p.Gly270Cys	Uromodulin-associated kidney disease	Nasr et al.,[605]	0%	Disease causing	Probably damaging (score 0.999)	Deleterious (score -5.744)	4	7	Pathogenic	Pathogenic

Nucleotide change	Amino acid change	Phenotype/ disorder	Reference	*Reported vAFs	Prediction of functional effects			Evolutionary conservation		Combined analysis	
					MutationTaster	PolyPhen-2	Provean Protein	4 Orthologs	8 Orthologs	1	2
c.817G>T	p.Val273Phe	FJHN/MCKD syndrome	Vylet'al et al.,[156]	0%	Disease causing	Probably damaging (score 0.964)	Deleterious (score -3.520)	3	7	Pathogenic	Pathogenic
c.821A>G	p.Tyr274Cys	Uromodulin-associated kidney disease	Zaucke et al.,[591]	0%	Disease causing	Probably damaging (score 0.999)	Deleterious (score -6.576)	4	8	Pathogenic	Pathogenic
c.844T>C	p.Cys282Arg	Hyperuricaemic nephropathy, juvenile	Dahan et al.,[592]	0%	Disease causing	Probably damaging (score 0.999)	Deleterious (score +8.890)	4	8	Pathogenic	Pathogenic
c.890G>A	p.Cys297Tyr	Tubulointerstitial nephritis	Bollée et al.,[588]	0%	Disease causing	Probably damaging (score 0.999)	Deleterious (score -6.856)	4	7	Pathogenic	Pathogenic
c.898T>G	p.Cys300Gly	Hyperuricaemic nephropathy, juvenile	Turner et al.,[140]	0%	Disease causing	Probably damaging (score 0.999)	Deleterious (score -7.652)	4	7	Pathogenic	Pathogenic
c.899G>A	p.Cys300Tyr	Medullary cystic kidney disease 2	Bleyer et al.,[606]	0%	Disease causing	Probably damaging (score 0.999)	Deleterious (score -7.598)	4	7	Pathogenic	Pathogenic
c.919A>C	p.Lys307Thr	Hyperuricaemic nephropathy, juvenile	Calado et al.,[607]	0%	Polymorphism	Benign (score 0.138)	Neutral (score -1.712)	2	3	Unknown significance	Likely benign
c.943T>C	p.Cys315Arg	Glomerulocystic kidney disease	Rampoldi et al.,[597]	0%	Disease causing	Probably damaging (score 0.999)	Deleterious (score -10.176)	4	7	Pathogenic	Pathogenic
c.944G>A	p.Cys315Tyr	Tubulointerstitial nephritis	Bollée et al.,[588]	0%	Disease causing	Probably damaging (score 0.999)	Deleterious (score -9.378)	4	7	Pathogenic	Pathogenic
c.947A>C	p.Gln316Pro	Hyperuricaemic nephropathy, juvenile	Lens et al.,[608]	0%	Polymorphism	Possibly damaging (score 0.610)	Neutral (score -2.247)	3	5	Pathogenic	Likely benign
c.950G>A	p.Cys317Tyr	Medullary cystic kidney disease 2	Rampoldi et al.,[597]	0%	Disease causing	Probably damaging (score 0.999)	Deleterious (score -8.945)	4	7	Pathogenic	Pathogenic
c.1039T>G	p.Cys347Gly	Hyperuricaemic nephropathy, juvenile	Tinschert et al.,[609]	0%	Disease causing	Probably damaging (score 0.983)	Deleterious (score -9.406)	4	7	Pathogenic	Pathogenic
c.1382C>A	p.Ala461Glu	Hyperuricaemic nephropathy, juvenile	Lee et al.,[610]	0%	Disease causing	Probably damaging (score 0.999)	Deleterious (score -4.304)	4	7	Pathogenic	Pathogenic
c.1406C>T	p.Thr469Met	Tubulointerstitial nephritis	Bollée et al.,[588]	0%	Polymorphism	Probably damaging (score 0.998)	Deleterious (score -4.118)	3	7	Pathogenic	Pathogenic
c.1462G>C	p.Gly488Arg	Hyperuricaemic nephropathy, juvenile	Williams et al.,[155]	0%	Disease causing	Probably damaging (score 1.000)	Deleterious (score -6.943)	4	7	Pathogenic	Pathogenic
c.1813A>G	p.Thr605Ala	Hyperuricaemic nephropathy, juvenile	Wei et al.,[611]	0%	Polymorphism	Benign (score 0.061)	Neutral (score -2.202)	3	5	Pathogenic	Likely benign

UMOD variants obtained from HGMD[235] used to investigate the effectiveness of *in silico* methods for variant analysis Chapter 6. Nucleotide number is according to transcript ENST00000302509 and amino acid number is according to the 640 amino acid protein (NCBI NP_003352; UniProt P07911) as displayed on HGMD. *Reported vAFs were obtained from ExAC[236]. Evolutionary conservation scores were based on the number of orthologs each WT residue was conserved in, the number of orthologs studied in each analysis is detailed in the column heading, as detailed Chapter 6. Combined analysis 1 and 2 are based on the criteria detailed in Chapter 6. N/A, not applicable.

Table 44. *In silico* analysis of *CASR* variants obtained from ExAC

Nucleotide change	Amino acid change	*Reported vAFs	Prediction of functional effects			Evolutionary conservation		Combined analysis	
			MutationTaster	PolyPhen-2	Provean Protein	4 Orthologs	8 Orthologs	1	2
c.32T>C	p.Leu11Ser	0.000824307%	Disease causing	Benign (score 0.062)	Neutral (score -1.088)	4	7	Pathogenic	Likely pathogenic
c.40A>G	p.Thr14Ala	0.001648451%	Polymorphism	Benign (score 0)	Neutral (score -0.076)	3	5	Pathogenic	Benign
c.46C>T	p.His16Tyr	0.000824212%	Polymorphism	Benign (score 0.016)	Neutral (score -0.32)	3	4	Pathogenic	Likely benign
c.53C>T	p.Ser18Phe	0.001648343%	Disease causing	Benign (score 0.186)	Neutral (score -2.068)	3	6	Pathogenic	Likely benign
c.73C>T	p.Arg25*	0.001649077%	Disease causing	N/A	N/A	4	8	Pathogenic	Likely pathogenic
c.74G>A	p.Arg25Gln	0.001649077%	Disease causing	Probably damaging (score 0.978)	Neutral (score -0.665)	4	8	Pathogenic	Likely pathogenic
c.93C>A	p.Asp31Glu	0.0008250 83%	Disease causing	Probably damaging (score 0.978)	Deleterious (score -2.543)	4	8	Pathogenic	Pathogenic
c.98T>G	p.Ile33Ser	0.003300602%	Disease causing	Possibly damaging (score 0.676)	Deleterious (score -3.598)	4	8	Pathogenic	Likely pathogenic
c.134C>G	p.Ala45Gly	0.000826665%	Disease causing	Benign (score 0.137)	Neutral (score -1.962)	4	8	Pathogenic	Likely pathogenic
c.134C>A	p.Ala45Glu	0.000826665%	Disease causing	Benign (score 0.323)	Neutral (score -1.096)	4	8	Pathogenic	Likely pathogenic
c.179G>A	p.Cys60Tyr	0.000830372%	Disease causing	Probably damaging (score 0.991)	Deleterious (score -9.083)	4	8	Pathogenic	Pathogenic
c.206G>A	p.Arg69His	0.001647935%	Disease causing	Probably damaging (score 0.996)	Deleterious (score -4.072	4	8	Pathogenic	Likely pathogenic
c.220A>C	p.Met74Leu	0.000823873%	Disease causing	Possibly damaging (score 0.829)	Deleterious (score -2.552)	4	8	Pathogenic	Pathogenic
c.232A>G	p.Ile78Val	0.001647609%	Disease causing	Possibly damaging (score 0.854)	Neutral (score -0.636)	4	8	Pathogenic	Unknown significance
c.266C>G	p.Pro89Arg	0.000823683%	Disease causing	Probably damaging (score 0.999)	Deleterious (score -8.355)	4	8	Pathogenic	Pathogenic
c.269A>C	p.Asn90Thr	0.000823683%	Disease causing	Probably damaging (score 0.995)	Deleterious (score -5.248)	4	8	Pathogenic	Pathogenic
c.275C>T	p.Thr92Met	0.000823669%	Disease causing	Probably damaging (score 0.980)	Deleterious (score -34.721)	4	8	Pathogenic	Pathogenic
c.303C>A	p.Cys101*	0.000823655%	Disease causing	N/A	N/A	4	8	Pathogenic	Pathogenic
c.308C>T	p.Thr103Ile	0.002470966%	Disease causing	Probably damaging (score 0.998)	Deleterious (score -3.835)	4	8	Pathogenic	Likely pathogenic
c.365C>A	p.Ser122Tyr	0.000823805%	Disease causing	Probably damaging (score 0.996)	Neutral (score -1.541)	4	8	Pathogenic	Pathogenic
c.419C>T	p.Ala140Val	0.000824375%	Disease causing	Probably damaging (score 0.996)	Neutral (score -2.311)	4	8	Pathogenic	Pathogenic
c.427G>A	p.Gly143Arg	0.000824688%	Disease causing	Probably damaging (score 0.999)	Deleterious (score -7.604)	4	8	Pathogenic	Pathogenic
c.430G>A	p.Ala144Thr	0.000824701%	Disease causing	Probably damaging (score 0.994)	Neutral (score -1.337)	4	8	Pathogenic	Pathogenic
c.445G>A	p.Val149Ile	0.000825682%	Disease causing	Benign (score 0.003)	Neutral (score 0.060)	4	5	Pathogenic	Likely benign
c.455C>T	p.Ala152Val	0.001652975%	Disease causing	Probably damaging (score 0.987)	Deleterious (score -2.526)	4	8	Pathogenic	Likely pathogenic
c.475C>G	p.Leu159Val	0.0008282 53%	Disease causing	Possibly damaging (score 0.897)	Neutral (score -1.396)	4	8	Pathogenic	Likely pathogenic
c.525C>G	p.Ser175Arg	0.00082511%	Disease causing	Probably damaging (score 0.996)	Deleterious (score -4.153)	4	8	Pathogenic	Pathogenic
c.528C>G	p.Asn176Lys	0.001650029%	Disease causing	Probably damaging (score 0.996)	Deleterious (score -3.759)	4	8	Pathogenic	Likely pathogenic
c.560T>C	p.Ile187Thr	0.000824525%	Disease causing	Possibly damaging (score 0.596)	Deleterious (score -4.453)	3	7	Pathogenic	Pathogenic
c.566A>G	p.Asn189Ser	0.000824402%	Disease causing	Possibly damaging (score 0.468)	Neutral (score 1.079)	4	7	Pathogenic	Likely pathogenic
c.572A>G	p.Glu191Gly	0.000824389%	Disease causing	Probably damaging (score 0.996)	Neutral(score -2.354)	4	8	Pathogenic	Pathogenic
c.613C>T	p.Arg205Cys	0.000824525%	Disease causing	Possibly damaging (score 0.761)	Neutral (score -2.337)	3	5	Pathogenic	Unknown significance
c.614G>A	p.Arg205His	0.001649049%	Disease causing	Benign (score 0.435)	Neutral (score -0.510)	3	5	Pathogenic	Benign
c.646G>A	p.Asp216Asn	0.00082447%	Disease causing	Probably damaging (score 0.997)	Deleterious (score -3.645)	4	8	Pathogenic	Pathogenic
c.649G>A	p.Asp217Asn	0.001649022%	Disease causing	Benign (score 0.033)	Deleterious (score -3.968)	4	6	Pathogenic	Likely pathogenic
c.680G>A	p.Arg227Gln	0.000824402%	Disease causing	Possibly damaging (score 0.588)	Neutral (score -0.146)	4	7	Pathogenic	Likely pathogenic
c.705C>G	p.Ile235Met	0.001648207%	Disease causing	Probably damaging (score 0.998)	Neutral (score -1.162)	4	8	Pathogenic	Likely pathogenic
c.712G>A	p.Asp238Asn	0.002472229%	Disease causing	Benign (score 0.01)	Neutral (score -0.615)	4	8	Pathogenic	Likely benign
c.719G>C	p.Ser240Thr	0.001647935%	Disease causing	Possibly damaging (score 0.554)	Neutral (score -1.195)	4	7	Pathogenic	Unknown significance
c.740C>T	p.Ser247Phe	0.003295056%	Disease causing	Benign (score 0.003)	Neutral (score 0.249)	3	5	Pathogenic	Benign
c.748G>A	p.Glu250Lys	0.183696333%	Polymorphism	Benign (score 0.001)	Neutral (score -1.445)	4	6	Pathogenic	Likely benign

Nucleotide change	Amino acid change	*Reported vAFs	Prediction of functional effects			Evolutionary conservation		Combined analysis	
			MutationTaster	PolyPhen-2	Provean Protein	4 Orthologs	8 Orthologs	1	2
c.752A>G	p.Glu251Gly	0.001647528%	Disease causing	Benign (score 0.158)	Deleterious (score -3.612)	4	6	Pathogenic	Likely pathogenic
c.757C>A	p.Gln253Lys	0.009061403%	Polymorphism	Benign (score 0.018)	Neutral (score -0.957)	3	6	Pathogenic	Likely benign
c.758A>T	p.Gln253Leu	0.000823764%	Disease causing	Benign (score 0.412)	Deleterious (score -3.612)	3	6	Pathogenic	Pathogenic
c.770A>G	p.Glu257Gly	0.000823805%	Disease causing	Benign (score 0.005)	Neutral (score -2.306)	3	6	Pathogenic	Likely pathogenic
c.773T>C	p.Val258Ala	0.000823832%	Disease causing	Possibly damaging (score 0.630)	Neutral (score -0.952)	4	7	Pathogenic	Likely pathogenic
c.779A>G	p.Gln260Arg	0.012357681%	Disease causing	Possibly damaging (score 0.578)	Neutral (score -0.247)	4	8	Pathogenic	Unknown significance
c.788C>T	p.Thr263Met	0.0008239%	Disease causing	Probably damaging (score 0.949)	Deleterious (score -3.950)	4	7	Pathogenic	Pathogenic
c.788C>A	p.Thr263Lys	0.0008239%	Disease causing	Possibly damaging (score 0.779)	Deleterious (score -3.585)	4	7	Pathogenic	Pathogenic
c.814A>G	p.Ser272Gly	0.000824266%	Disease causing	Benign (score 0.386)	Neutral (score -2.132)	4	8	Pathogenic	Likely pathogenic
c.835C>G	p.Leu279Val	0.000824701%	Disease causing	Possibly damaging (score 0.472)	Neutral (score -1.998)	4	8	Pathogenic	Likely pathogenic
c.845A>G	p.Glu282Gly	0.001649648%	Disease causing	Probably damaging (score 0.996)	Deleterious (score -6.022)	4	8	Pathogenic	Likely pathogenic
c.848T>C	p.Ile283Thr	0.013198053%	Disease causing	Possibly damaging (score 0.721)	Deleterious (score -3.077)	4	7	Pathogenic	Likely pathogenic
c.854G>C	p.Arg285Pro	0.000825042%	Disease causing	Possibly damaging (score 0.811)	Deleterious (score -3.453)	3	6	Pathogenic	Pathogenic
c.866C>T	p.Thr289Met	0.000825928%	Disease causing	Probably damaging (score 0.999)	Deleterious (score -5.217)	4	8	Pathogenic	Pathogenic
c.873G>C	p.Lys291Asn	0.000826925%	Polymorphism	Benign (score 0.076)	Neutral (score -2.050)	2	2	Unknown significance	Likely benign
c.913A>G	p.Ile305Val	0.00082605%	Disease causing	Benign (score 0.079)	Neutral (score -0.793)	4	7	Pathogenic	Likely pathogenic
c.921G>A	p.Met307Ile	0.002478519%	Disease causing	Benign (score 0.056)	Neutral (score -1.174)	3	6	Pathogenic	Likely benign
c.923C>T	p.Pro308Leu	0.00082616%	Disease causing	Probably damaging (score 0.999)	Deleterious (score -7.074)	4	8	Pathogenic	Pathogenic
c.946G>A	p.Gly316Ser	0.000826474%	Disease causing	Benign (score 0.227)	Deleterious (score -5.713)	4	8	Pathogenic	Pathogenic
c.952A>G	p.Ile318Val	0.000826337%	Disease causing	Probably damaging (score 0.970)	Neutral(score -0.756)	4	8	Pathogenic	Pathogenic
c.970G>C	p.Ala324Pro	0.000826364%	Disease causing	Possibly damaging (score 0.845)	Neutral (score -1.748)	4	8	Pathogenic	Likely pathogenic
c.973G>C	p.Gly325Arg	0.000826351%	Disease causing	Probably damaging (score 1.000)	Deleterious (score -5.011)	4	8	Pathogenic	Pathogenic
c.992G>A	p.Arg331Gln	0.000826351%	Disease causing	Benign (score 0.432)	Neutral (score -1.075)	4	7	Pathogenic	Likely pathogenic
c.1008G>T	p.Lys336Asn	0.001651855%	Disease causing	Benign (score 0.007)	Neutral (score -0.417)	3	6	Pathogenic	Likely benign
c.1008G>C	p.Lys336Asn	0.000825928%	Disease causing	Benign (score 0.007)	Neutral (score -0.417)	3	6	Pathogenic	Likely pathogenic
c.1009G>T	p.Val337Phe	0.0008259%	Disease causing	Probably damaging (score 0.999)	Deleterious (score -3.060)	4	8	Pathogenic	Pathogenic
c.1013A>G	p.His338Arg	0.000825846%	Disease causing	Benign (score 0.265)	Neutral (score -2.394)	3	7	Pathogenic	Likely pathogenic
c.1019G>A	p.Arg340Lys	0.001651582%	Disease causing	Benign (score 0.001)	Neutral (score 0.517)	2	4	Unknown significance	Benign
c.1027G>A	p.Val343Ile	0.001650901%	Polymorphism	Benign (score 0.023)	Neutral (score -0.522)	2	5	Unknown significance	Benign
c.1028T>C	p.Val343Ala	0.000825437%	Polymorphism	Benign (score 0)	Neutral (score 0.417)	2	5	Unknown significance	Likely benign
c.1033A>G	p.Asn345Asp	0.000825314%	Disease causing	Probably damaging (score 0.995)	Neutral (score -1.141)	4	8	Pathogenic	Pathogenic
c.1078C>T	p.Leu360Phe	0.000824212%	Disease causing	Benign (score 0.066)	Neutral (score 0.159)	4	8	Pathogenic	Likely pathogenic
c.1087G>A	p.Gly363Ser	0.000824103%	Disease causing	Benign (score 0.008)	Neutral (score 0.397)	2	4	Unknown significance	Likely benign
c.1091C>A	p.Ala364Glu	0.001648125%	Polymorphism	Benign (score 0.038)	Neutral (score -0.611)	2	4	Unknown significance	Benign
c.1097G>A	p.Gly366Glu	0.000824008%	Disease causing	Benign (score 0.096)	Neutral (score -0.614)	2	4	Unknown significance	Likely benign

Nucleotide change	Amino acid change	*Reported vAFs	Prediction of functional effects			Evolutionary conservation		Combined analysis	
			MutationTaster	PolyPhen-2	Provean Protein	4 Orthologs	8 Orthologs	1	2
c.1099C>T	p.Pro367Ser	0.001647962%	Polymorphism	Benign (score 0.001)	Neutral (score 0.074)	2	4	Unknown significance	Benign
c.1111G>A	p.Asp371Asn	0.00082394%	Polymorphism	Benign (score 0.001)	Neutral (score 0.133)	2	4	Unknown significance	Likely benign
c.1114A>G	p.Thr372Ala	0.000823927%	Polymorphism	Benign (score 0.014)	Neutral (score -0.764)	2	3	Unknown significance	Likely benign
c.1124G>A	p.Arg375Lys	0.002471862%	Polymorphism	Benign (score 0.001)	Neutral (score -0.423)	2	4	Unknown significance	Benign
c.1144G>A	p.Asp382Asn	0.003295164%	Polymorphism	Benign (score 0.001)	Neutral (score 0.107)	1	1	Benign	Benign
c.1159A>G	p.Ser387Gly	0.00082371%	Polymorphism	Benign (score 0.001)	Neutral (score -0.820)	2	4	Unknown significance	Likely benign
c.1163C>G	p.Ser388Trp	0.001647446%	Disease causing	Possibly damaging (score 0.753)	Neutral (score -2.230)	3	5	Pathogenic	Likely benign
c.1169C>G	p.Ala390Gly	0.000823723%	Disease causing	Benign (score 0.055)	Neutral (score -0.590)	3	6	Pathogenic	Likely pathogenic
c.1192G>A	p.Asp398Asn	0.048597269%	Disease causing	Benign (score 0.037)	Neutral (score -0.704)	3	4	Pathogenic	Benign
c.1193A>G	p.Asp398Gly	0.00329473%	Disease causing	Benign (score 0.037)	Deleterious (score -2.633)	3	4	Pathogenic	Likely benign
c.1199A>T	p.Asn400Ile	0.003294784%	Disease causing	Probably damaging (score 0.948)	Deleterious (score -4.340)	4	7	Pathogenic	Likely pathogenic
c.1206C>G	p.Ser402Arg	0.000823696%	Disease causing	Benign (score 0.055)	Neutral (score -0.418)	2	5	Unknown significance	Likely benign
c.1207A>T	p.Ser403Cys	0.000823696%	Disease causing	Probably damaging (score 0.923)	Deleterious (score -3.207)	4	8	Pathogenic	Pathogenic
c.1285C>T	p.His429Tyr	0.179710814%	Disease causing	Benign (score 0.011)	Deleterious (score -2.755)	3	6	Pathogenic	Likely pathogenic
c.1287C>A	p.His429Gln	0.002473166%	Disease causing	Benign (score 0.060)	Deleterious (score -5.048)	3	6	Pathogenic	Likely pathogenic
c.1297G>C	p.Asp433His	0.01979806%	Disease causing	Possibly damaging (score 0.897)	Deleterious (score -3.258)	4	8	Pathogenic	Likely pathogenic
c.1297G>T	p.Asp433Tyr	0.000824919%	Disease causing	Probably damaging (score 0.947)	Deleterious (score -5.268)	4	8	Pathogenic	Pathogenic
c.1333A>G	p.Thr445Ala	2.380044434%	Polymorphism	Benign (score 0.008)	Neutral (score -0.113)	3	6	Benign	Likely benign
c.1340G>A	p.Gly447Asp	0.000829917%	Disease causing	Possibly damaging (score 0.842)	Neutral (score -1.395)	3	7	Pathogenic	Likely pathogenic
c.1351G>A	p.Asp451Asn	0.000831269%	Disease causing	Probably damaging (score 0.997)	Neutral (score -1.587)	4	8	Pathogenic	Pathogenic
c.1354A>G	p.Ile452Val	0.000831684%	Disease causing	Benign (score 0.265)	Neutral (score -0.760)	4	8	Pathogenic	Likely pathogenic
c.1378G>A	p.Val460Ile	0.000824661%	Disease causing	Benign (score 0.334)	Neutral(score 0.471)	3	7	Pathogenic	Likely pathogenic
c.1389C>A	p.His463Gln	0.004121128%	Disease causing	Benign (score 0.084)	Deleterious (score -2.558)	4	7	Pathogenic	Likely pathogenic
c.1390C>G	p.Leu464Val	0.000824198%	Disease causing	Probably damaging (score 0.994)	Neutral (score -2.006)	4	8	Pathogenic	Pathogenic
c.1393C>T	p.Arg465Trp	0.001648288%	Disease causing	Probably damaging (score 0.916)	Deleterious (score -4.335)	4	8	Pathogenic	Likely pathogenic
c.1396C>T	p.His466Tyr	0.000824049%	Disease causing	Probably damaging (score 0.992)	Deleterious (score -2.505)	4	8	Pathogenic	Pathogenic
c.1398T>A	p.His466Gln	0.000823995%	Disease causing	Probably damaging (score 0.996)	Neutral (score -1.019)	4	8	Pathogenic	Pathogenic
c.1405T>C	p.Phe469Leu	0.000823886%	Disease causing	Possibly damaging (score 0.524)	Deleterious (score -5.243)	4	7	Pathogenic	Pathogenic
c.1412A>T	p.Asn471Ile	0.000823859%	Disease causing	Possibly damaging (score 0.476)	Neutral (score -2.210)	3	6	Pathogenic	Likely pathogenic
c.1427A>G	p.Gln476Arg	0.00082375%	Disease causing	Benign (score 0.018)	Neutral (score -1.289)	4	7	Pathogenic	Likely pathogenic
c.1430T>C	p.Val477Ala	0.000823764%	Disease causing	Possibly damaging (score 0.554)	Deleterious (score -2.277)	4	8	Pathogenic	Pathogenic
c.1444T>A	p.Cys482Ser	0.000823764%	Disease causing	Benign (score 0.001)	Neutral (score 2.607)	2	4	Unknown significance	Likely benign
c.1445G>A	p.Cys482Tyr	0.000823737%	Disease causing	Benign (score 0.038)	Neutral (score 0.121)	2	4	Unknown significance	Likely benign
c.1456G>T	p.Val486Leu	0.0008237235	Disease causing	Benign (score 0.005)	Neutral (score -0.449)	4	5	Pathogenic	Likely benign
c.1463A>G	p.Asn488Ser	0.000823723%	Disease causing	Probably damaging (score 0.992)	Neutral (score 0.051)	4	8	Pathogenic	Pathogenic

Nucleotide change	Amino acid change	*Reported vAFs	Prediction of functional effects			Evolutionary conservation		Combined analysis	
			MutationTaster	PolyPhen-2	Provean Protein	4 Orthologs	8 Orthologs	1	2
c.1471A>G	p.Ile491Val	0.000823683%	Disease causing	Benign (score 0.265)	Neutral (score -0.600)	4	8	Pathogenic	Likely pathogenic
c.1486C>T	p.Leu496Phe	0.000823655%	Disease causing	Possibly damaging (score 0.853)	Neutral (score -0.873)	4	7	Pathogenic	Likely pathogenic
c.1507A>G	p.Ile503Val	0.000823669%	Disease causing	Benign (score 0.001)	Neutral (score -0.124)	3	6	Pathogenic	Likely pathogenic
c.1510G>A	p.Val504Met	0.004118345%	Disease causing	Benign (score 0.026)	Neutral(score 0.041)	4	8	Pathogenic	Likely benign
c.1517A>C	p.Lys506Thr	0.000823683%	Disease causing	Benign (score 0.014)	Neutral (score -0.062)	2	5	Unknown significance	Likely benign
c.1525G>A	p.Gly509Arg	0.000823669%	Disease causing	Probably damaging (score 0.999)	Deleterious (score -7.281)	4	8	Pathogenic	Pathogenic
c.1529A>G	p.Tyr510Cys	0.000823669%	Disease causing	Benign (score 0.293)	Neutral(score -2.455)	3	6	Pathogenic	Likely pathogenic
c.1549A>G	p.Lys517Glu	0.001647609%	Polymorphism	Benign (score 0.053)	Neutral (score -0.798)	3	6	Pathogenic	Likely benign
c.1551G>T	p.Lys517Asn	0.001647664%	Disease causing	Benign (score 0.003)	Neutral (score -1.296)	3	6	Pathogenic	Likely benign
c.1553G>A	p.Gly518Glu	0.000823845%	Disease causing	Possibly damaging (score 0.541)	Deleterious (score -3.244)	4	7	Pathogenic	Pathogenic
c.1560A>T	p.Arg520Ser	0.000824063%	Disease causing	Benign (score 0.185)	Neutral(score -1.258)	4	7	Pathogenic	Likely pathogenic
c.1564T>C	p.Phe522Leu	0.000824144%	Disease causing	Benign (score 0.003)	Neutral (score 0.613)	4	7	Pathogenic	Likely pathogenic
c.1566C>A	p.Phe522Leu	0.000824239%	Disease causing	Benign (score 0.003)	Neutral (score 0.613)	4	7	Pathogenic	Likely pathogenic
c.1573G>A	p.Glu525Lys	0.001648913%	Disease causing	Benign (score 0.001)	Neutral (score -1.916)	4	6	Pathogenic	Likely benign
c.1592G>A	p.Ser531Asn	0.000826023%	Disease causing	Benign (score 0.001)	Neutral (score 2.223)	3	6	Pathogenic	Likely pathogenic
c.1605G>C	p.Arg535Ser	0.000829765%	Disease causing	Benign (score 0.004)	Neutral (score 0.192)	3	5	Pathogenic	Likely benign
c.1609C>A	p.Pro537Thr	0.000823886%	Polymorphism	Benign (score 0)	Neutral (score -1.901)	1	2	Benign	Likely benign
c.1612C>T	p.Leu538Phe	0.009062001%	Polymorphism	Benign (score 0.001)	Neutral (score -0.113)	1	1	Benign	Benign
c.1616C>T	p.Thr539Ile	0.000823764%	Polymorphism	Benign (score 0.001)	Neutral (score -0.208)	1	1	Benign	Likely benign
c.1618T>C	p.Phe540Leu	0.000823723%	Polymorphism	Benign (score 0)	Neutral (score -0.075)	1	1	Benign	Likely benign
c.1628C>T	p.Ser543Phe	0.000823669%	Polymorphism	Benign (score 0)	Neutral (score -0.276)	1	1	Benign	Likely benign
c.1647C>G	p.Phe549Leu	0.000823655%	Disease causing	Benign (score 0.022)	Neutral (score -0.240)	3	7	Pathogenic	Likely pathogenic
c.1652A>G	p.Asn551Ser	0.000823655%	Disease causing	Probably damaging (score 0.994)	Neutral (score -0.105)	4	8	Pathogenic	Pathogenic
c.1661G>A	p.Arg554Gln	0.079070917%	Disease causing	Benign (score 0.089)	Neutral (score 0.694)	3	6	Pathogenic	Likely benign
c.1661G>T	p.Arg554Leu	0.000823655%	Disease causing	Benign (score 0.022)	Neutral (score -2.419)	3	6	Pathogenic	Likely pathogenic
c.1672G>A	p.Ala558Thr	0.001647284%	Disease causing	Benign (score 0.006)	Neutral (score -0.151)	2	4	Unknown significance	Benign
c.1693A>G	p.Ile565Val	0.000823642%	Disease causing	Possibly damaging (score 0.533)	Neutral (score -0.131)	3	7	Pathogenic	Likely pathogenic
c.1706C>T	p.Pro569Leu	0.000823655%	Disease causing	Probably damaging (score 1.000)	Deleterious (score 8.803)	4	8	Pathogenic	Pathogenic
c.1708A>C	p.Thr570Pro	0.000823655%	Disease causing	Probably damaging (score 0.948)	Neutral (score -2.420)	3	7	Pathogenic	Pathogenic
c.1805A>G	p.Asn602Ser	0.329489292%	Disease causing	Benign (score 0.004)	Deleterious (score -3.738)	4	8	Pathogenic	Likely pathogenic
c.1811A>G	p.Asn604Ser	0.00082371%	Disease causing	Probably damaging (score 0.978)	Neutral (score -1.708)	4	8	Pathogenic	Pathogenic
c.1842G>C	p.Glu614Asp	0.000823696%	Disease causing	Probably damaging (score 0.978)	Neutral (score -2.417)	4	8	Pathogenic	Pathogenic
c.1855A>G	p.Thr619Ala	0.0008236965	Disease causing	Benign (score 0.366)	Neutral (score -0.646)	4	8	Pathogenic	Likely pathogenic
c.1856C>T	p.Thr619Met	0.001647419%	Disease causing	Probably damaging (score 0.945)	Neutral(score -1.457)	4	8	Pathogenic	Likely pathogenic
c.1873G>A	p.Ala625Thr	0.001647501%	Disease causing	Probably damaging (score 0.993)	Neutral (score 0.406)	4	8	Pathogenic	Likely pathogenic
c.1891G>A	p.Val631Met	0.004118888%	Disease causing	Possibly damaging (score 0.565)	Neutral (score -1.098)	3	7	Pathogenic	Unknown significance
c.1921C>G	p.Leu641Val	0.000824008%	Disease causing	Possibly damaging (score 0.575)	Neutral (score -0.660)	4	8	Pathogenic	Likely pathogenic
c.1936A>G	p.Lys646Glu	0.000824063%	Disease Causing	Benign (score 0.320)	Neutral (score -1.428)	4	6	Pathogenic	Likely pathogenic
c.1943G>A	p.Arg648His	0.002472432%	Disease causing	Benign (score 0.089)	Deleterious (score -3.409)	4	8	Pathogenic	Likely pathogenic
c.1972C>G	p.Arg658Gly	0.000824443%	Disease causing	Probably damaging (score 0.998)	Neutral (score -2.473)	4	8	Pathogenic	Pathogenic
c.1972C>T	p.Arg658*	0.000824443%	Disease causing	N/A	N/A	4	8	Pathogenic	Pathogenic

Nucleotide change	Amino acid change	*Reported vAFs	Prediction of functional effects			Evolutionary conservation		Combined analysis	
			MutationTaster	PolyPhen-2	Provean Protein	4 Orthologs	8 Orthologs	1	2
c.1973G>T	p.Arg658Leu	0.003298044%	Disease causing	Probably damaging (score 0.998)	Deleterious (score -2.926)	4	8	Pathogenic	Likely pathogenic
c.2042A>T	p.Glu681Val	0.000824906%	Disease causing	Probably damaging (score 0.956)	Deleterious (score -3.723)	4	8	Pathogenic	Pathogenic
c.2057C>T	p.Thr686Met	0.000825014%	Disease causing	Benign (score 0.116)	Deleterious (score -2.940)	4	7	Pathogenic	Pathogenic
c.2057C>G	p.Thr686Arg	0.000825014%	Disease causing	Possibly damaging (score 0.759)	Deleterious (score -3.083)	4	7	Pathogenic	Pathogenic
c.2068C>T	p.Arg690Cys	0.000825014%	Disease causing	Probably damaging (score 0.999)	Deleterious (score -6.869)	4	8	Pathogenic	Pathogenic
c.2069G>A	p.Arg690His	0.001650219%	Disease causing	Probably damaging (score 0.998)	Deleterious (score -4.331)	4	8	Pathogenic	Likely pathogenic
c.2086A>G	p.Ile696Val	0.003299241%	Disease causing	Benign (score 0.026)	Neutral (score -0.701)	4	8	Pathogenic	Likely benign
c.2093T>G	p.Phe698Cys	0.000824715%	Disease causing	Probably damaging (score 0.999)	Deleterious (score -7.710)	4	8	Pathogenic	Pathogenic
c.2113A>G	p.Ile705Val	0.000824606%	Disease causing	Probably damaging (score 0.978)	Neutral (score -0.622)	4	8	Pathogenic	Pathogenic
c.2131C>T	p.Arg711Cys	0.001649104%	Disease causing	Benign (score 0.037)	Neutral (score -0.865)	3	7	Pathogenic	Likely benign
c.2134G>A	p.Val712Ile	0.000824552%	Disease causing	Benign (score 0.024)	Neutral (score -0.516)	3	7	Pathogenic	Likely pathogenic
c.2165C>A	p.Thr722Asn	0.000825137%	Disease causing	Probably damaging (score 0.998)	Neutral (score -0.071)	4	8	Pathogenic	Pathogenic
c.2167A>G	p.Ser723Gly	0.000825137%	Disease causing	Benign (score 0.026)	Neutral (score -1.071)	4	8	Pathogenic	Likely pathogenic
c.2177G>A	p.Arg726His	0.001651609%	Disease causing	Probably damaging (score 0.998)	Neutral (score -1.561)	4	8	Pathogenic	Likely pathogenic
c.2196C>G	p.Asn732Lys	0.002478724%	Disease causing	Probably damaging (score 0.997)	Neutral (score -0.436)	4	8	Pathogenic	Likely pathogenic
c.2237T>C	p.Ile746Thr	0.000826979%	Disease causing	Benign (score 0.418)	Neutral (score -1.840)	4	7	Pathogenic	Likely pathogenic
c.2239G>A	p.Val747Ile	0.001654013%	Disease causing	Benign (score 0.068)	Neutral (score -0.469)	4	6	Pathogenic	Likely benign
c.2243T>C	p.Ile748Thr	0.000827185%	Disease causing	Benign (score 0.017)	Deleterious (score -3.696)	3	7	Pathogenic	Pathogenic
c.2246G>A	p.Cys749Tyr	0.002481554%	Disease causing	Probably damaging (score 0.998)	Deleterious (score -9.629)	4	8	Pathogenic	Likely pathogenic
c.2261A>T	p.Tyr754Phe	0.000828569%	Disease causing	Possibly damaging (score 0.466)	Neutral (score -0.467)	4	7	Pathogenic	Likely pathogenic
c.2266G>A	p.Ala756Thr	0.001659421%	Disease causing	Probably damaging (score 0.998)	Neutral (score -1.832)	4	8	Pathogenic	Likely pathogenic
c.2267C>T	p.Ala756Val	0.004978923%	Disease causing	Probably damaging (score 0.997)	Neutral (score -2.151)	4	8	Pathogenic	Likely pathogenic
c.2275T>G	p.Ser759Ala	0.00083033%	Polymorphism	Benign (score 0.025)	Neutral (score -0.721)	3	6	Pathogenic	Likely pathogenic
c.2285G>A	p.Arg762His	0.002491984%	Disease causing	Possibly damaging (score 0.897)	Deleterious (score -2.525)	4	7	Pathogenic	Likely pathogenic
c.2291A>G	p.Gln764Arg	0.000830358%	Polymorphism	Benign (score 0.032)	Neutral (score -0.389)	1	1	Benign	Likely benign
c.2295G>T	p.Glu765Asp	0.002490991%	Disease causing	Benign (score 0.025)	Neutral (score -0.858)	3	6	Pathogenic	Likely benign
c.2321C>T	p.Thr774Met	0.000829531%	Disease causing	Probably damaging (score 0.999)	Neutral (score -1.543)	4	8	Pathogenic	Pathogenic
c.2326C>T	p.His776Tyr	0.000829407%	Disease causing	Possibly damaging (score 0.471)	Neutral (score -1.866)	3	5	Pathogenic	Unknown significance
c.2333G>T	p.Gly778Val	0.004144288%	Disease causing	Probably damaging (score 1.000)	Deleterious (score -7.696)	4	8	Pathogenic	Likely pathogenic
c.2344G>A	p.Ala782Thr	0.000828514%	Disease causing	Probably damaging (score 0.998)	Neutral (score -1.906)	4	8	Pathogenic	Pathogenic
c.2365T>C	p.Tyr789His	0.00082802%	Disease causing	Probably damaging (score 0.999)	Deleterious (score -4.536)	4	8	Pathogenic	Pathogenic
c.2369C>T	p.Thr790Ile	0.000827732%	Disease causing	Probably damaging (score 0.998)	Neutral (score 0.768)	4	8	Pathogenic	Pathogenic
c.2386A>G	p.Ile796Val	0.002480077%	Disease causing	Benign (score 0.026)	Neutral (score -0.441)	3	7	Pathogenic	Likely benign
c.2435A>G	p.Asn812Ser	0.001648642%	Disease causing	Possibly damaging (score 0.550)	Deleterious (score -3.868)	4	7	Pathogenic	Likely pathogenic
c.2440G>T	p.Ala814Ser	0.001648478%	Disease causing	Probably damaging (score 0.997)	Neutral (score -2.287)	4	8	Pathogenic	Likely pathogenic
c.2467A>G	p.Ile823Val	0.002471821%	Disease causing	Probably damaging (score 0.978)	Neutral (score -0.448)	4	8	Pathogenic	Likely pathogenic
c.2487C>G	p.Ile829Met	0.000823832%	Disease causing	Probably damaging (score 0.998)	Neutral (score -2.178)	4	8	Pathogenic	Pathogenic
c.2504A>G	p.Tyr835Cys	0.000823737%	Disease causing	Probably damaging (score 0.999)	Deleterious (score -8.596)	4	8	Pathogenic	Pathogenic
c.2579C>A	p.Ala860Glu	0.000824022%	Disease causing	Probably damaging (score 0.958)	Neutral (score -2.379)	4	8	Pathogenic	Pathogenic
c.2581T>A	p.Cys861Ser	0.001648125%	Disease causing	Probably damaging (score 0.996)	Deleterious (score -6.910)	4	8	Pathogenic	Likely pathogenic
c.2600T>C	p.Ile867Thr	0.000824389%	Polymorphism	Benign (score 0.008)	Neutral (score -0.450)	1	1	Benign	Likely benign
c.2602T>G	p.Tyr868Asp	0.000824375%	Disease causing	Probably damaging (score 0.999)	Deleterious (score -9.087)	4	8	Pathogenic	Pathogenic
c.2615T>C	p.Phe872Ser	0.011543916%	Disease causing	Possibly damaging (score 0.811)	Deleterious (score -3.355)	4	7	Pathogenic	Likely pathogenic

Nucleotide change	Amino acid change	*Reported vAFs	Prediction of functional effects			Evolutionary conservation		Combined analysis	
			MutationTaster	PolyPhen-2	Provean Protein	4 Orthologs	8 Orthologs	1	2
c.2668G>T	p.Ala890Ser	0.001653658%	Disease causing	Benign (score 0.152)	Neutral (score -0.003)	4	8	Pathogenic	Likely benign
c.2698C>T	p.Arg900Cys	0.000830151%	Disease causing	Possibly damaging (score 0.482)	Neutral (score -1.490)	4	8	Pathogenic	Likely pathogenic
c.2699G>A	p.Arg900His	0.000830041%	Disease causing	Possibly damaging (score 0.482)	Neutral (score -0.942)	4	8	Pathogenic	Likely pathogenic
c.2702G>A	p.Arg901His	0.0016603025	Disease causing	Benign (score 0.018)	Neutral (score -0.145)	4	7	Pathogenic	Likely benign
c.2710G>T	p.Val904Phe	0.002489585%	Disease causing	Benign (score 0.06)	Neutral (score -0.822)	3	6	Pathogenic	Likely benign
c.2716C>G	p.Arg906Gly	0.000830013%	Disease causing	Benign (score 0.410)	Neutral (score -1.255)	3	7	Pathogenic	Likely pathogenic
c.2716C>T	p.Arg906Cys	0.000830013%	Disease causing	Possibly damaging (score 0.791)	Neutral (score -1.488)	3	7	Pathogenic	Likely pathogenic
c.2717G>T	p.Arg906Leu	0.000829917%	Disease causing	Possibly damaging(score 0.492)	Neutral(score -1.043)	3	7	Pathogenic	Likely pathogenic
c.2723G>A	p.Arg908Gln	0.003319612%	Disease causing	Benign (score 0.067)	Neutral(score -0.422)	4	8	Pathogenic	Likely benign
c.2725T>C	p.Ser909Pro	0.000829628%	Disease causing	Benign (score 0.132)	Neutral(score -1.221)	4	8	Pathogenic	Likely pathogenic
c.2741G>C	p.Gly914Ala	0.000829407%	Disease causing	Possibly damaging(score 0.631)	Neutral(score -1.146)	4	8	Pathogenic	Likely pathogenic
c.2750G>C	p.Gly917Ala	0.000829215%	Disease causing	Benign (score 0.021)	Neutral(score -0.148)	4	7	Pathogenic	Likely pathogenic
c.2753C>A	p.Ser918Tyr	0.000829146%	Disease causing	Probably damaging(score 0.956)	Neutral(score -1.859)	4	8	Pathogenic	Pathogenic
c.2768C>T	p.Ser923Phe	0.001657358%	Disease causing	Probably damaging(score 0.942)	Neutral(score -1.426)	4	8	Pathogenic	Likely pathogenic
c.2789G>A	p.Ser930Asn	0.000827595%	Disease causing	Benign (score 0.003)	Neutral(score -0.390)	2	4	Unknown significance	Likely benign
c.2790C>G	p.Ser930Arg	0.001655547%	Disease causing	Benign (score 0.138)	Neutral(score -0.860)	2	4	Unknown significance	Benign
c.2791G>A	p.Glu931Lys	0.001655054%	Disease causing	Benign (score 0.005)	Neutral(score -0.245)	3	6	Pathogenic	Likely benign
c.2794G>C	p.Asp932His	0.000827513%	Disease causing	Possibly damaging(score 0.671)	Neutral(score -0.987)	3	6	Pathogenic	Likely pathogenic
c.2797C>G	p.Pro933Ala	0.002482211%	Polymorphism	Benign (score 0)	Neutral(score -0.523)	2	5	Unknown significance	Benign
c.2800T>C	p.Phe934Leu	0.000827349%	Disease causing	Benign (score 0.026)	Neutral(score -0.889)	4	7	Pathogenic	Likely pathogenic
c.2807A>G	p.Gln936Arg	0.013236267%	Polymorphism	Benign (score 0)	Neutral(score -0.376)	2	4	Unknown significance	Benign
c.2821A>C	p.Lys941Gln	0.000827842%	Polymorphism	Benign (score 0.001)	Neutral(score -0.445)	2	4	Unknown significance	Likely benign
c.2840C>G	p.Ala947Gly	0.000826556%	Disease causing	Benign (score 0.010)	Neutral(score -0.155)	2	4	Unknown significance	Likely benign
c.2854G>A	p.Glu952Lys	0.082658291%	Polymorphism	Benign (score 0)	Neutral(score -0.297)	2	3	Unknown significance	Benign
c.2869C>T	p.Pro957Ser	0.000825682%	Polymorphism	Benign (score 0.064)	Neutral(score -0.801)	2	4	Unknown significance	Likely benign
c.2870C>T	p.Pro957Leu	0.000825614%	Disease causing	Benign (score 0.001)	Neutral(score -0.927)	2	4	Unknown significance	Likely benign
c.2873T>C	p.Leu958Pro	0.000825559%	Polymorphism	Benign (score 0)	Neutral(score -0.806)	2	3	Unknown significance	Likely benign
c.2879T>C	p.Leu960Pro	0.003301856%	Polymorphism	Benign (score 0)	Neutral(score -0.459)	2	3	Unknown significance	Benign
c.2887C>G	p.Gln963Glu	0.0024756975	Polymorphism	Benign (score 0)	Neutral (score -0.240)	2	4	Unknown significance	Benign
c.2900A>G	p.Gln967Arg	0.003299078%	Polymorphism	Benign (score 0.014)	Neutral (score -0.258)	2	5	Unknown significance	Benign

Nucleotide change	Amino acid change	*Reported vAFs	Prediction of functional effects			Evolutionary conservation		Combined analysis	
			MutationTaster	PolyPhen-2	Provean Protein	4 Orthologs	8 Orthologs	1	2
c.2914T>C	p.Cys972Arg	0.000824497%	Disease causing	Benign (score 0.120)	Neutral (score -0.724)	4	7	Pathogenic	Likely pathogenic
c.2929A>G	p.Ile977Val	0.000824307%	Disease causing	Benign (score 0.051)	Neutral (score -0.113)	2	4	Unknown significance	Likely benign
c.2945C>T	p.Thr982Met	0.004121128%	Disease causing	Probably damaging (score 0.959)	Neutral (score -1.061)	4	8	Pathogenic	Likely pathogenic
c.2951C>T	p.Thr984Ile	0.002472555%	Disease causing	Benign (score 0.254)	Neutral (score -0.996)	4	7	Pathogenic	Likely benign
c.2984A>C	p.Asn995Thr	0.000824198%	Polymorphism	Benign (score 0.001)	Neutral (score -0.701)	4	6	Pathogenic	Likely pathogenic
c.2986G>T	p.Ala996Ser	12.6931895%	Polymorphism	Benign (score 0.041)	Neutral (score -0.324)	4	7	Benign	Likely benign
c.2993C>T	p.Ala998Val	0.001648669%	Polymorphism	Benign (score 0.006)	Neutral (score -0.135)	3	6	Pathogenic	Likely benign
c.2998A>G	p.Arg1000Gly	14.51429232%	Polymorphism	Benign (score 0.051)	Neutral (score -0.791)	4	6	Benign	Likely benign
c.3008C>T	p.Thr1003Met	0.001649022%	Polymorphism	Benign (score 0.001)	Neutral (score -0.020)	1	3	Benign	Benign
c.3031C>A	p.Gln1011Lys	0.000824783%	Disease causing	Benign (score 0.001)	Neutral (score -0.411)	1	4	Benign	Likely benign
c.3040A>C	p.Ser1014Arg	0.000824606%	Polymorphism	Benign (score 0.008)	Neutral (score -0.411)	4	4	Pathogenic	Likely benign
c.3043G>A	p.Asp1015Asn	0.00329886%	Disease causing	Benign (score 0.060)	Neutral (score -0.648)	4	6	Pathogenic	Likely benign
c.3043G>T	p.Asp1015Tyr	0.000824715%	Disease causing	Possibly damaging (score 0.673)	Neutral (score -1.167)	2	4	Unknown significance	Unknown significance
c.3047C>T	p.Thr1016Met	0.000824769%	Polymorphism	Benign (score 0.002)	Neutral (score -0.495)	4	4	Pathogenic	Likely benign
c.3056G>A	p.Arg1019Gln	0.000825164%	Disease causing	Benign (score 0.045)	Neutral (score -0.336)	4	5	Pathogenic	Likely benign
c.3056G>T	p.Arg1019Leu	0.000825164%	Disease causing	Benign (score 0.056)	Neutral (score -0.849)	4	5	Pathogenic	Likely benign
c.3058C>T	p.His1020Tyr	0.000824865%	Disease causing	Benign (score 0.026)	Neutral (score -0.713)	4	7	Pathogenic	Likely pathogenic
c.3060C>G	p.His1020Gln	0.0008253%	Disease causing	Benign (score 0.018)	Neutral (score -0.865)	4	7	Pathogenic	Likely pathogenic
c.3061G>C	p.Glu1021Gln	94.46247899%	Polymorphism	Benign (score 0)	Neutral(score 0.255)	0	0	Benign	Benign
c.3064C>A	p.Pro1022Thr	0.00082409%	Polymorphism	Benign (score 0)	Neutral (score 0.180)	1	1	Benign	Likely benign
c.3068T>C	p.Leu1023Ser	0.000824103%	Polymorphism	Probably damaging (score 0.979)	Neutral (score -0.425)	4	7	Pathogenic	Likely pathogenic
c.3070C>A	p.Leu1024Ile	0.001648261%	Disease causing	Benign (score 0.007)	Neutral (score -0.064)	4	7	Pathogenic	Likely benign
c.3074C>T	p.Pro1025Leu	0.000824131%	Disease causing	Benign (score 0.105)	Neutral (score -1.023)	3	6	Pathogenic	Likely pathogenic
c.3077T>C	p.Leu1026Pro	0.000824035%	Disease causing	Benign (score 0)	Neutral (score -0.379)	4	7	Pathogenic	Likely pathogenic
c.3080A>G	p.Gln1027Arg	0.000824063%	Disease causing	Benign (score 0.001)	Neutral (score -0.456)	4	7	Pathogenic	Likely pathogenic
c.3092C>A	p.Thr1031Lys	0.000824212%	Polymorphism	Benign (score 0.012)	Neutral (score -0.360)	1	2	Benign	Likely benign
c.3109G>A	p.Val1037Ile	0.000824633%	Polymorphism	Benign (score 0)	Neutral (score -0.046)	1	1	Benign	Likely benign
c.3110T>C	p.Val1037Ala	0.000824701%	Polymorphism	Benign (score 0)	Neutral (score -0.259)	1	1	Benign	Likely benign
c.3117A>T	p.Glu1039Asp	0.000825055%	Polymorphism	Benign (score 0)	Neutral (score -0.001)	4	5	Pathogenic	Likely benign
c.3121G>A	p.Gly1041Ser	0.022284582%	Polymorphism	Benign (score 0.002)	Neutral (score -0.562)	3	4	Pathogenic	Benign
c.3133C>T	p.Pro1045Ser	0.001652046%	Polymorphism	Benign (score 0)	Neutral (score -0.390)	2	4	Unknown significance	Benign
c.3142G>A	p.Gly1048Arg	0.000826228%	Polymorphism	Benign (score 0.084)	Neutral (score -0.695)	3	5	Pathogenic	Likely benign
c.3151C>T	p.Arg1051Trp	0.002479667%	Polymorphism	Benign (score 0.109)	Neutral (score -0.607)	1	1	Benign	Benign
c.3158A>T	p.Glu1053Val	0.000826788%	Disease causing	Benign (score 0.193)	Neutral (score 0.507)	4	6	Pathogenic	Likely pathogenic
c.3165G>C	p.Glu1055Asp	0.000827157%	Polymorphism	Benign (score 0.007)	Neutral (score -0.084)	2	4	Unknown significance	Likely benign
c.3172G>A	p.Glu1058Lys	0.000827691%	Disease causing	Benign (score 0.057)	Neutral (score -0.266)	2	5	Unknown significance	Likely benign
c.3181T>C	p.Ser1061Pro	0.000828555%	Polymorphism	Benign (score 0)	Neutral (score -0.403)	2	3	Unknown significance	Likely benign

Nucleotide change	Amino acid change	*Reported vAFs	Prediction of functional effects			Evolutionary conservation		Combined analysis	
			MutationTaster	PolyPhen-2	Provean Protein	4 Orthologs	8 Orthologs	1	2
c.3217G>A	p.Val1073Ile	0.000834251%	Disease causing	Benign (score 0.001)	Neutral (score -0.077)	2	3	Unknown significance	Likely benign
c.3223A>G	p.Ser1075Gly	0.006682928%	Disease causing	Benign (score 0.076)	Neutral (score -0.408)	2	4	Unknown significance	Benign
c.3227G>A	p.Gly1076Asp	0.000836638%	Polymorphism	Benign (score 0.053)	Neutral (score -0.400)	2	3	Unknown significance	Likely benign
c.3250A>G	p.Asn1084Asp	0.000846382%	Disease causing	Benign (score 0.034)	Neutral (score -0.571)	4	7	Pathogenic	Likely pathogenic
c.3253G>C	p.Val1085Leu	0.000847989%	Polymorphism	Benign (score 0.001)	Neutral (score -0.196)	1	1	Benign	Likely benign

CASR variants obtained from ExAC[236] used to investigate the effectiveness of *in silico* methods for variant analysis (Chapter 6). Nucleotide number is according to transcript ENST00000498619 and amino acid number is according to the full length 1088 amino acid protein (NCBI NP_001171536; UniProt P41180) as displayed on ExAC. *Reported vAFs were also obtained from ExAC[236]. Evolutionary conservation scores were based on the number of orthologs each WT residue was conserved in, the number of orthologs studied in each analysis is detailed in the column heading, as detailed in Chapter 6. Combined analysis 1 and 2 are based on the criteria detailed in Chapter 6. N/A, not applicable.

Table 45. *In silico* analysis of *CLCN5* variants obtained from ExAC

Nucleotide change	Amino acid change	*Reported vAFs	Prediction of functional effects			Evolutionary conservation		Combined analysis	
			MutationTaster	PolyPhen-2	Provean Protein	4 Orthologs	8 Orthologs	1	2
c.7A>G	p.Met3Val	0.001153988%	Polymorphism	Benign (score 0.000)	Neutral(score -0.330)	1	1	Benign	Benign
c.11G>C	p.Trp4Ser	0.001153988%	Disease causing	Possibly damaging(score 0.607)	Neutral(score 1.382)	1	1	Unknown significance	Likely benign
c.22A>G	p.Met8Val	0.003248652%	Disease causing	Possibly damaging(score 0.455)	Neutral(score 0.000)	3	7	Pathogenic	Unknown significance
c.56G>A	p.Ser19Asn	0.013387777%	Polymorphism	Benign (score 0.000)	Neutral(score 0.041)	1	2	Benign	Benign
c.95A>G	p.Asp32Gly	0.130618863%	Disease causing	Benign (score 0.136)	Neutral(score -1.844)	1	3	Benign	Benign
c.116A>G	p.Asp39Gly	0.005695409%	Disease causing	Probably damaging(score 0.990)	Neutral(score -0.901)	3	7	Pathogenic	Likely pathogenic
c.179A>G	p.Asn60Ser	0.001599105%	Disease causing	Benign (score 0.059)	Neutral(score -0.667)	3	6	Pathogenic	Likely benign
c.184G>A	p.Gly62Arg	0.001513134%	Disease causing	Benign (score 0.081)	Neutral(score -1.382)	2	4	Unknown significance	Benign
c.185G>A	p.Gly62Glu	0.001497409%	Disease causing	Benign (score 0.002)	Neutral(score -1.124)	2	4	Unknown significance	Benign
c.232A>G	p.Ile78Val	0.009759668%	Polymorphism	Benign (score 0.000)	Neutral(score -0.478)	2	3	Unknown significance	Benign
c.293G>A	p.Arg98Gln	0.001238436%	Disease causing	Benign (score 0.005)	Deleterious (score -3.267)	4	7	Pathogenic	Likely pathogenic
c.298C>T	p.Arg100Trp	0.006242899%	Disease causing	Probably damaging(score 0.996)	Deleterious (score -6.640)	4	8	Pathogenic	Likely pathogenic
c.299G>A	p.Arg100Gln	0.002501626%	Disease causing	Probably damaging(score 0.986)	Deleterious (score -3.219)	4	8	Pathogenic	Likely pathogenic
c.323A>G	p.Asn108Ser	0.001142713%	Polymorphism	Benign (score 0.001)	Neutral(score 0.229)	2	4	Unknown significance	Benign
c.331A>C	p.Lys111Gln	0.001142009%	Disease causing	Benign (score 0.425)	Neutral(score -1.151)	3	7	Pathogenic	Likely benign
c.361G>A	p.Val121Met	0.002281959%	Disease causing	Possibly damaging(score 0.576)	Neutral(score 0.091)	2	5	Unknown significance	Likely benign
c.379G>A	p.Gly127Ser	0.002282636%	Disease causing	Probably damaging(score 0.999)	Deleterious (score -5.549)	3	7	Pathogenic	Likely pathogenic
c.401T>C	p.Ile134Thr	0.002284122%	Disease causing	Benign (score 0.088)	Neutral(score -2.386)	3	6	Pathogenic	Likely benign
c.449A>G	p.His150Arg	0.001139835%	Disease causing	Probably damaging(score 0.985)	Neutral(score 0.104)	4	8	Pathogenic	Likely pathogenic
c.503A>G	p.His168Arg	0.001140706%	Disease causing	Benign (score 0.009)	Neutral(score 0.664)	4	7	Pathogenic	Likely benign
c.506A>T	p.Glu169Val	0.002281803%	Disease causing	Probably damaging(score 0.994)	Deleterious (score -6.445)	4	8	Pathogenic	Likely pathogenic
c.514T>C	p.Cys172Arg	0.001141566%	Disease causing	Probably damaging(score 0.994)	Deleterious (score -11.735)	4	8	Pathogenic	Likely pathogenic
c.526G>A	p.Glu176Lys	0.002286158%	Polymorphism	Benign (score 0.000)	Neutral(score -0.152)	2	2	Unknown significance	Benign
c.530A>C	p.His177Pro	0.002287544%	Disease causing	Benign (score 0.000)	Neutral(score -1.094)	2	4	Unknown significance	Benign
c.547A>G	p.Arg183Gly	0.002297213%	Disease causing	Probably damaging(score 0.985)	Neutral(score 0.422)	4	7	Pathogenic	Likely pathogenic
c.548G>C	p.Arg183Thr	0.001148937%	Disease causing	Probably damaging(score 0.985)	Neutral(score -1.921)	4	7	Pathogenic	Likely pathogenic
c.554A>G	p.Lys185Arg	0.036829869%	Disease causing	Benign (score 0.001)	Neutral(score -0.968)	3	7	Pathogenic	Likely benign
c.584T>G	p.Leu195Arg	0.001170234%	Disease causing	Probably damaging(score 0.925)	Deleterious (score -4.742)	4	8	Pathogenic	Likely pathogenic
c.596C>G	p.Thr199Arg	0.001187507%	Polymorphism	Benign (score 0.001)	Neutral(score -0.126)	2	5	Unknown significance	Benign
c.619A>G	p.Ile207Val	0.001284324%	Disease causing	Benign (score 0.080)	Neutral(score -0.320)	4	8	Pathogenic	Likely benign
c.634A>G	p.Met212Val	0.001214359%	Disease causing	Benign (score 0.015)	Neutral(score -1.276)	4	7	Pathogenic	Likely benign
c.634A>T	p.Met212Leu	0.001214359%	Disease causing	Benign (score 0.001)	Neutral(score -0.584)	4	7	Pathogenic	Likely benign
c.636G>A	p.Met212Ile	0.296757383%	Polymorphism	Benign (score 0.003)	Neutral(score -0.870)	4	7	Pathogenic	Likely benign
c.640G>A	p.Val214Ile	0.005927682%	Disease causing	Benign (score 0.009)	Neutral(score -0.214)	4	8	Pathogenic	Likely benign
c.656T>C	p.Leu219Pro	0.001152578%	Disease causing	Possibly damaging(score 0.777)	Deleterious (score -3.519)	4	8	Pathogenic	Likely pathogenic
c.673G>A	p.Val225Ile	0.003429747%	Disease causing	Probably damaging(score 0.981)	Neutral(score -0.976)	4	8	Pathogenic	Likely pathogenic
c.677C>T	p.Ser226Phe	0.001142413%	Disease causing	Benign (score 0.081)	Neutral(score -1.981)	2	5	Unknown significance	Benign
c.682G>A	p.Val228Ile	0.001141618%	Disease causing	Probably damaging(score 0.980)	Neutral(score -0.976)	4	8	Pathogenic	Likely pathogenic
c.695C>T	p.Ala232Val	0.002281204%	Disease causing	Probably damaging(score 0.991)	Deleterious (score -3.904)	4	8	Pathogenic	Likely pathogenic

Nucleotide change	Amino acid change	*Reported vAFs	Prediction of functional effects			Evolutionary conservation		Combined analysis	
			MutationTaster	PolyPhen-2	Provean Protein	4 Orthologs	8 Orthologs	1	2
c.730A>G	p.Lys244Glu	0.001141644%	Disease causing	Probably damaging(score 0.987)	Deleterious (score -3.770)	4	8	Pathogenic	Likely pathogenic
c.787A>G	p.Ile263Val	0.001139874%	Disease causing	Benign (score 0.074)	Neutral(score -0.765)	4	8	Pathogenic	Likely benign
c.796A>G	p.Ile266Val	0.011400299%	Disease causing	Benign (score 0.001)	Neutral(score 0.160)	3	6	Pathogenic	Likely benign
c.892T>G	p.Cys298Gly	0.001219497%	Polymorphism	Benign (score 0.065)	Deleterious (score -3.021)	2	4	Unknown significance	Benign
c.844G>A	p.Gly282Ser	0.001148528%	Disease causing	Probably damaging(score 0.999)	Deleterious (score -5.855)	4	8	Pathogenic	Likely pathogenic
c.853G>C	p.Val285Leu	0.001153376%	Disease causing	Benign (score 0.128)	Deleterious (score -2.900)	3	7	Pathogenic	Likely pathogenic
c.859G>A	p.Val287Met	0.001159958%	Disease causing	Probably damaging(score 0.996)	Neutral(score -2.007)	4	8	Pathogenic	Likely pathogenic
c.866G>C	p.Cys289Ser	0.001167951%	Disease causing	Probably damaging(score 0.985)	Deleterious (score -5.335)	4	8	Pathogenic	Likely pathogenic
c.901A>G	p.Lys301Glu	0.001253007%	Disease causing	Probably damaging(score 0.987)	Deleterious (score -3.870)	4	8	Pathogenic	Likely pathogenic
c.902A>G	p.Lys301Arg	0.001252913%	Disease causing	Probably damaging(score 0.987)	Deleterious (score -2.903)	4	8	Pathogenic	Likely pathogenic
c.925C>T	p.Arg309Cys	0.004276489%	Disease causing	Probably damaging(score 0.911)	Deleterious (score -5.367)	4	8	Pathogenic	Likely pathogenic
c.926G>A	p.Arg309His	0.015924028%	Disease causing	Probably damaging(score 0.911)	Deleterious (score -3.255)	4	8	Pathogenic	Likely pathogenic
c.926G>T	p.Arg309Leu	0.001447639%	Disease causing	Possibly damaging(score 0.653)	Deleterious (score -4.400)	4	8	Pathogenic	Likely pathogenic
c.1103T>C	p.Phe368Ser	0.001212386%	Disease causing	Possibly damaging(score 0.648)	Deleterious (score -7.304)	3	7	Pathogenic	Likely pathogenic
c.1049G>A	p.Arg350His	0.001447471%	Disease causing	Possibly damaging(score 0.681)	Deleterious (score -4.817)	3	7	Pathogenic	Likely pathogenic
c.1087C>T	p.Arg363Cys	0.002550467%	Disease causing	Probably damaging(score 0.996)	Deleterious (score -6.787)	4	8	Pathogenic	Likely pathogenic
c.1093A>G	p.Ile365Val	0.001242576%	Disease causing	Benign (score 0.074)	Neutral(score -0.830)	3	7	Pathogenic	Likely benign
c.1094T>G	p.Ile365Ser	0.00123948%	Disease causing	Possibly damaging(score 0.648)	Deleterious (score -5.215)	3	7	Pathogenic	Likely pathogenic
c.1099C>G	p.Pro367Ala	0.001222972%	Disease causing	Possibly damaging(score 0.520)	Deleterious (score -7.707)	3	7	Pathogenic	Likely pathogenic
c.1114C>T	p.Arg372Cys	0.010684649%	Disease causing	Possibly damaging(score 0.855)	Deleterious (score -4.262)	3	7	Pathogenic	Likely pathogenic
c.1137G>T	p.Glu379Asp	0.001155495%	Disease causing	Benign (score 0.164)	Neutral(score -1.636)	3	7	Pathogenic	Likely benign
c.1168G>A	p.Val390Met	0.00114478%	Polymorphism	Benign (score 0.249)	Neutral(score -0.978)	3	6	Pathogenic	Likely benign
c.1222C>T	p.Arg408Cys	0.003427083%	Disease causing	Possibly damaging(score 0.809)	Deleterious (score -5.409)	3	7	Pathogenic	Likely pathogenic
c.1223G>A	p.Arg408His	0.019422578%	Disease causing	Possibly damaging(score 0.681)	Deleterious (score -2.647)	3	7	Pathogenic	Likely pathogenic
c.1243C>T	p.Arg415Trp	0.003428376%	Disease causing	Possibly damaging(score 0.653)	Deleterious (score -6.793)	3	7	Pathogenic	Likely pathogenic
c.1244G>A	p.Arg415Gln	0.031998903%	Disease causing	Benign (score 0.005)	Deleterious (score -3.028)	3	7	Pathogenic	Likely pathogenic
c.1244G>T	p.Arg415Leu	0.003428454%	Disease causing	Benign (score 0.151)	Deleterious (score -5.851)	3	7	Pathogenic	Likely pathogenic
c.1274A>G	p.Tyr425Cys	0.001142635%	Disease causing	Possibly damaging(score 0.789)	Deleterious (score -7.823)	3	6	Pathogenic	Likely pathogenic
c.1282A>C	p.Ile428Leu	0.00114274%	Polymorphism	Benign (score 0.000)	Neutral(score 0.214)	1	2	Benign	Benign
c.1294G>A	p.Val432Ile	0.001142922%	Polymorphism	Benign (score 0.001)	Neutral(score -0.177)	3	5	Pathogenic	Benign
c.1297G>A	p.Val433Met	0.00914129%	Disease causing	Possibly damaging(score 0.759)	Neutral(score -2.375)	2	6	Unknown significance	Unknown significance
c.1331A>G	p.Asn444Ser	0.011414613%	Disease causing	Benign (score 0.269)	Deleterious (score -4.736)	3	7	Pathogenic	Likely pathogenic
c.1343G>A	p.Arg448Gln	0.001141005%	Disease causing	Benign (score 0.383)	Deleterious (score -3.619)	3	7	Pathogenic	Likely pathogenic
c.1354A>G	p.Ser452Gly	0.00456246%	Disease causing	Benign (score 0.164)	Deleterious (score -3.470)	3	7	Pathogenic	Likely pathogenic
c.1397A>C	p.Asp466Ala	0.001140017%	Disease causing	Benign (score 0.006)	Deleterious (score -4.791)	3	7	Pathogenic	Likely pathogenic
c.1423A>G	p.Asn475Asp	0.001140082%	Disease causing	Benign (score 0.025)	Neutral(score -2.222)	3	7	Pathogenic	Likely benign
c.1426C>T	p.Arg476Cys	0.001140147%	Polymorphism	Benign (score 0.258)	Neutral(score -2.343)	1	3	Benign	Benign
c.1427G>A	p.Arg476His	0.001140069%	Polymorphism	Benign (score 0.064)	Neutral(score -0.293)	1	3	Benign	Benign
c.1460A>T	p.Asp487Val	0.001140537%	Disease causing	Benign (score 0.398)	Neutral(score -0.968)	3	6	Pathogenic	Likely benign
c.1466C>T	p.Pro489Leu	0.001140862%	Disease causing	Benign (score 0.039)	Deleterious (score -4.688)	2	5	Pathogenic	Likely benign
c.1474G>A	p.Val492Met	0.003424306%	Polymorphism	Benign (score 0.135)	Neutral(score -0.301)	2	3	Unknown significance	Benign

Nucleotide change	Amino acid change	*Reported vAFs	Prediction of functional effects			Evolutionary conservation		Combined analysis	
			MutationTaster	PolyPhen-2	Provean Protein	4 Orthologs	8 Orthologs	1	2
c.1474G>T	p.Val492Leu	0.012555788%	Polymorphism	Benign (score 0.018)	Neutral(score -0.850)	2	3	Unknown significance	Benign
c.1478G>A	p.Gly493Glu	0.001141396%	Disease causing	Possibly damaging(score 0.659)	Deleterious (score -6.282)	4	7	Pathogenic	Likely pathogenic
c.1484A>G	p.Tyr495Cys	0.003424697%	Disease causing	Benign (score 0.005)	Deleterious (score -5.832)	4	7	Pathogenic	Likely pathogenic
c.1504G>C	p.Ala502Pro	0.001143537%	Disease causing	Benign (score 0.407)	Deleterious (score -2.874)	3	6	Pathogenic	Likely pathogenic
c.1635G>T	p.Gln545His	0.005699305%	Disease causing	Probably damaging(score 0.991)	Deleterious (score -4.068)	4	8	Pathogenic	Likely pathogenic
c.1654G>A	p.Glu552Lys	0.001140004%	Disease causing	Benign (score 0.006)	Neutral(score -1.448)	1	1	Benign	Benign
c.1628T>C	p.Met543Thr	0.001139822%	Disease causing	Benign (score 0.005)	Deleterious (score -2.800)	4	6	Pathogenic	Likely pathogenic
c.1639G>T	p.Ala547Ser	0.001139926%	Disease causing	Benign (score 0.030)	Neutral(score -2.362)	3	7	Pathogenic	Likely benign
c.1663G>A	p.Val555Ile	0.015961874%	Polymorphism	Benign (score 0.000)	Neutral(score 0.523)	1	1	Benign	Benign
c.1816G>A	p.Val606Met	0.00456142%	Disease causing	Probably damaging(score 0.996)	Neutral(score -2.223)	4	8	Pathogenic	Likely pathogenic
c.1828G>A	p.Ala610Thr	0.002280918%	Disease causing	Possibly damaging(score 0.677)	Neutral(score -1.791)	4	8	Pathogenic	Unknown significance
c.1837A>G	p.Met613Val	0.001140511%	Disease causing	Benign (score 0.003)	Deleterious (score -2.595)	4	8	Pathogenic	Likely pathogenic
c.1852G>A	p.Val618Met	0.007985034%	Disease causing	Probably damaging(score 0.996)	Neutral(score -2.179)	4	8	Pathogenic	Likely pathogenic
c.1862C>T	p.Ala621Val	0.001141123%	Disease causing	Probably damaging(score 0.990)	Deleterious (score -3.107)	4	8	Pathogenic	Likely pathogenic
c.1894A>G	p.Ile632Val	0.001141474%	Disease causing	Probably damaging(score 0.927)	Neutral(score -0.874)	4	8	Pathogenic	Likely pathogenic
c.1898G>A	p.Arg633His	0.0011415%	Disease causing	Benign (score 0.008)	Neutral(score 0.379)	3	7	Pathogenic	Likely benign
c.1942C>T	p.His648Tyr	0.003430257%	Disease causing	Probably damaging(score 0.979)	Deleterious (score -4.152)	4	8	Pathogenic	Likely pathogenic
c.1943A>G	p.His648Arg	0.001143275%	Disease causing	Probably damaging(score 0.985)	Deleterious (score -5.915)	4	8	Pathogenic	Likely pathogenic
c.1972C>A	p.Pro658Thr	0.001147078%	Disease causing	Probably damaging(score 0.998)	Deleterious (score -7.267)	4	8	Pathogenic	Likely pathogenic
c.1975C>T	p.Arg659Trp	0.002295447%	Disease causing	Probably damaging(score 0.997)	Deleterious (score -6.052)	4	8	Pathogenic	Likely pathogenic
c.1976G>A	p.Arg659Gln	0.00573954%	Disease causing	Probably damaging(score 0.977)	Neutral(score -2.420)	4	8	Pathogenic	Likely pathogenic
c.1979G>A	p.Arg660Lys	0.001148528%	Disease causing	Benign (score 0.002)	Neutral(score -1.500)	4	8	Pathogenic	Likely benign
c.2012A>G	p.Asp671Gly	0.005837916%	Disease causing	Benign (score 0.305)	Deleterious (score -5.049)	4	8	Pathogenic	Likely pathogenic
c.2014A>G	p.Ser672Gly	0.001170604%	Disease causing	Benign (score 0.001)	Neutral(score -0.001)	4	7	Pathogenic	Likely benign
c.2031T>G	p.Asp677Glu	0.00120097%	Disease causing	Benign (score 0.000)	Neutral(score -1.475)	4	7	Pathogenic	Likely benign
c.2074G>A	p.Val692Met	0.001337703%	Disease causing	Possibly damaging(score 0.838)	Neutral(score -2.153)	3	7	Pathogenic	Unknown significance
c.2074G>C	p.Val692Leu	0.001337703%	Disease causing	Benign (score 0.092)	Neutral(score -2.051)	3	7	Pathogenic	Likely benign
c.2086C>T	p.Arg696Trp	0.002791503%	Disease causing	Possibly damaging(score 0.622)	Deleterious (score -4.775)	4	7	Pathogenic	Likely pathogenic
c.2104G>A	p.Val702Met	0.001471714%	Disease causing	Benig(score 0.089)	Neutral(score -2.322)	4	8	Pathogenic	Likely benign
c.2131A>G	p.Ile711Val	0.001671794%	Disease causing	Benign (score 0.000)	Neutral(score 0.106)	4	7	Pathogenic	Likely benign
c.2140A>G	p.Ile714Val	0.017393724%	Disease causing	Benign (score 0.000)	Neutral(score -0.840)	3	7	Pathogenic	Likely benign
c.2168G>C	p.Gly723Ala	0.001596526%	Disease causing	Possibly damaging(score 0.835)	Deleterious (score -3.689)	4	8	Pathogenic	Likely pathogenic
c.2180C>G	p.Thr727Ser	0.028156074%	Disease causing	Benign (score 0.006)	Neutral(score 1.412)	4	7	Pathogenic	Likely benign
c.2188A>G	p.Ile730Val	0.001423771%	Disease causing	Benign (score 0.002)	Neutral(score 0.810)	4	8	Pathogenic	Likely benign
c.2198C>T	p.Thr733Met	0.001361248%	Disease causing	Probably damaging(score 0.952)	Deleterious (score -3.395)	4	8	Pathogenic	Likely pathogenic
c.2201A>C	p.Glu734Ala	0.005357191%	Disease causing	Benign (score 0.170)	Neutral(score -1.097)	3	6	Pathogenic	Likely benign
c.2221C>T	p.Pro741Ser	0.001254296%	Disease causing	Benign (score 0.003)	Neutral(score 0.243)	4	8	Pathogenic	Likely benign
c.2237C>T	p.Thr746Ile	0.001209687%	Polymorphism	Benign (score 0.007)	Neutral(score -1.687)	2	4	Unknown significance	Benign
c.2248C>T	p.Arg750Trp	0.001186887%	Disease causing	Probably damaging(score 0.999)	Deleterious (score -5.150)	4	8	Pathogenic	Likely pathogenic
c.2260G>A	p.Asp754Asn	0.001168429%	Disease causing	Probably damaging(score 0.988)	Deleterious (score -3.428)	4	8	Pathogenic	Likely pathogenic
c.2293C>G	p.Pro765Ala	0.001154028%	Disease causing	Benign (score 0.005)	Deleterious (score -7.087)	4	7	Pathogenic	Likely pathogenic

Nucleotide change	Amino acid change	*Reported vAFs	Prediction of functional effects			Evolutionary conservation		Combined analysis	
			MutationTaster	PolyPhen-2	Provean Protein	4 Orthologs	8 Orthologs	1	2
c.2305G>A	p.Val769Ile	0.004617551%	Disease causing	Benign (score 0.025)	Neutral (score -0.937)	4	8	Pathogenic	Likely benign
c.2321G>A	p.Arg774Gln	0.001158708%	Disease causing	Probably damaging(score 0.975)	Deleterious (score -3.429)	4	8	Pathogenic	Likely pathogenic
c.2363G>A	p.Arg788Gln	0.003538403%	Disease causing	Benign (score 0.144)	Deleterious (score -2.788)	3	6	Pathogenic	Likely pathogenic
c.2369T>G	p.Leu790Arg	0.001170015%	Disease causing	Probably damaging(score 0.995)	Deleterious (score -4.861)	4	8	Pathogenic	Likely pathogenic
c.2390A>T	p.Asp797Val	0.001157515%	Disease causing	Probably damaging(score 0.998)	Deleterious (score -8.132)	4	8	Pathogenic	Likely pathogenic
c.2417C>T	p.Ala806Val	0.00115977%	Disease causing	Probably damaging(score 0.941)	Neutral(score -1.764)	4	8	Pathogenic	Likely pathogenic
c.2444T>A	p.Phe815Tyr	0.001179078%	Disease causing	Possibly damaging(score 0.815)	Neutral(score -1.919)	4	8	Pathogenic	Unknown significance

CLCN5 variants obtained from the ExAC[236] used to investigate the effectiveness of *in silico* methods for variant analysis (Chapter 6). Nucleotide number is according to transcript ENST00000376088 and amino acid number is according to the 816 amino acid protein (NCBI NP_0011213170; UniProt P51795) as displayed on ExAC. Reported vAFs were also obtained from ExAC[236]. Evolutionary conservation scores were based on the number of orthologs each WT residue was conserved in, the number of orthologs studied in each analysis is detailed in the column heading, as detailed in Chapter 6. Combined analysis 1 and 2 are based on the criteria detailed in Chapter 6.

Table 46. *In silico* analysis of *CLCNKB* variants obtained from ExAC

Nucleotide change	Amino acid change	*Reported vAFs	Prediction of functional effects			Evolutionary conservation		Combined analysis	
			MutationTaster	PolyPhen-2	Provean Protein	4 Orthologs	8 Orthologs	1	2
c.9G>T	p.Glu3Asp	0.018315628%	Polymorphism	Benign (score 0.036)	Neutral (score -1.441)	2	4	Unknown significance	Benign
c.12T>G	p.Phe4Leu	0.535036804%	Polymorphism	Benign (score 0.000)	Neutral (score 0.639)	1	1	Benign	Benign
c.17G>A	p.Gly6Glu	0.001569662%	Disease Causing	Probably damaging (score 1.000)	Neutral (score -0.571)	2	5	Pathogenic	Likely benign
c.23G>A	p.Arg8His	0.010509564%	Polymorphism	Benign (score 0.008)	Neutral (score -2.396)	2	4	Unknown significance	Benign
c.32C>T	p.Ser11Phe	0.002858695%	Polymorphism	Benign (score 0.005)	Neutral (score -2.410)	1	3	Benign	Benign
c.71C>T	p.Pro24Leu	0.00131527%	Disease Causing	Possibly damaging (score 0.801)	Deleterious (score -4.566)	3	7	Pathogenic	Likely pathogenic
c.79C>T	p.Arg27Cys	0.001308798%	Disease Causing	Possibly damaging (score 0.591)	Neutral (score -2.329)	2	5	Unknown significance	Likely benign
c.80G>A	p.Arg27His	0.00108394%	Polymorphism	Benign (score 0.006)	Neutral (score -2.189)	2	5	Unknown significance	Benign
c.80G>C	p.Arg27Pro	0.00108394%	Polymorphism	Benign (score 0.379)	Deleterious (score -2.680)	2	5	Unknown significance	Benign
c.80G>T	p.Arg27Leu	64.13024627%	Polymorphism	Benign (score 0.162)	Deleterious (score -3.053)	2	5	Benign	Benign
c.85C>T	p.Arg29Cys	0.002889004%	Disease Causing	Possibly damaging (score 0.575)	Deleterious (score -2.718)	3	6	Pathogenic	Likely pathogenic
c.86G>A	p.Arg29His	0.001456792%	Disease Causing	Benign (score 0.421)	Neutral (score -2.257)	3	6	Pathogenic	Likely benign
c.88C>T	p.Arg30*	0.003056702%	Disease Causing	N/A	N/A	3	6	Pathogenic	Likely pathogenic
c.92G>C	p.Gly31Ala	0.001539409%	Polymorphism	Benign (score 0.001)	Neutral (score 0.094)	1	3	Benign	Benign
c.97C>T	p.Arg33*	0.003214504%	Disease Causing	N/A	N/A	2	6	Pathogenic	Likely pathogenic
c.98G>A	p.Arg33Gln	0.009745955%	Disease Causing	Benign (score 0.007)	Neutral (score -0.597)	2	6	Unknown significance	Likely benign
c.101G>A	p.Gly34Asp	0.000830165%	Disease Causing	Benign (score 0.015)	Neutral (score -0.893)	3	5	Pathogenic	Likely benign
c.101G>T	p.Gly34Val	0.000830165%	Disease Causing	Benign (score 0.111)	Neutral(score -1.954)	3	5	Pathogenic	Likely benign
c.112T>C	p.Trp38Arg	0.018240005%	Disease Causing	Benign (score 0.006)	Deleterious (score -2.887)	2	4	Pathogenic	Likely benign
c.122A>G	p.Gln41Arg	0.000828336%	Polymorphism	Benign (score 0.001)	Neutral (score 0.151)	1	2	Benign	Likely benign
c.127C>A	p.Leu43Ile	0.000828061%	Disease Causing	Benign (score 0.188)	Neutral (score -0.321)	4	8	Pathogenic	Likely pathogenic
c.127C>G	p.Leu43Val	0.000828061%	Disease Causing	Benign (score 0.051)	Neutral (score -0.709)	4	8	Pathogenic	Likely pathogenic
c.131T>A	p.Phe44Tyr	0.001655684%	Disease Causing	Probably damaging (score 0.958)	Neutral (score -1.209)	3	6	Pathogenic	Likely pathogenic
c.133C>T	p.Arg45Cys	0.009105659%	Disease Causing	Benign (score 0.064)	Deleterious (score -4.540)	2	3	Pathogenic	Likely benign
c.134G>A	p.Arg45His	0.004966476%	Disease Causing	Benign (score 0.064)	Deleterious (score -3.244)	4	5	Pathogenic	Likely benign
c.140G>A	p.Gly47Asp	0.000827431%	Disease Causing	Probably damaging (score 0.970)	Deleterious (score -5.634)	4	7	Pathogenic	Pathogenic
c.142G>A	p.Glu48Lys	0.002481964%	Disease Causing	Possibly damaging (score 0.797)	Deleterious (score -3.103)	4	6	Pathogenic	Likely pathogenic
c.169G>A	p.Gly57Arg	0.001653795%	Disease Causing	Benign (score 0.431)	Deleterious (score -7.000)	4	8	Pathogenic	Likely pathogenic
c.172G>T	p.Val58Leu	0.04381976%	Disease Causing	Possibly damaging (score 0.688)	Neutral (score -0.636)	3	6	Pathogenic	Unknown significance
c.176T>G	p.Leu59Arg	0.000826638%	Disease Causing	Probably damaging (score 0.957)	Deleterious (score -4.204)	3	6	Pathogenic	Pathogenic
c.179T>C	p.Met60Thr	0.001653384%	Disease Causing	Benign (score 0.145)	Deleterious (score -4.507)	4	7	Pathogenic	Likely pathogenic
c.182C>A	p.Ala61Asp	0.00082672%	Disease Causing	Probably damaging (score 1.000)	Deleterious (score -5.337)	4	8	Pathogenic	Pathogenic
c.196G>A	p.Ala66Thr	0.002480405%	Polymorphism	Benign (score 0.003)	Neutral (score -1.442)	2	4	Unknown significance	Benign
c.196G>T	p.Ala66Ser	0.002480405%	Polymorphism	Benign (score 0.066)	Neutral (score -1.272)	2	4	Unknown significance	Benign
c.197C>G	p.Ala66Gly	0.000826788%	Polymorphism	Benign (score 0.003)	Neutral (score -2.217)	2	4	Unknown significance	Likely benign
c.199A>G	p.Met67Val	0.000826856%	Disease Causing	Benign (score 0.348)	Deleterious (score -2.733)	3	7	Pathogenic	Pathogenic
c.209C>A	p.Ala70Asp	0.000827075%	Polymorphism	Benign (score 0.224)	Deleterious (score -3.003)	1	2	Benign	Likely benign
c.220G>A	p.Val74Met	0.000827746%	Polymorphism	Benign (score 0.037)	Neutral (score -0.426)	2	5	Unknown significance	Likely benign
c.227G>A	p.Arg76Gln	0.048870188%	Polymorphism	Benign (score 0.004)	Neutral(score 0.203)	3	4	Pathogenic	Benign

Nucleotide change	Amino acid change	*Reported vAFs	Prediction of functional effects			Evolutionary conservation		Combined analysis	
			MutationTaster	PolyPhen-2	Provean Protein	4 Orthologs	8 Orthologs	1	2
c.230C>T	p.Ala77Val	0.004971167%	Disease Causing	Possibly damaging (score 0.882)	Deleterious (score -3.397)	4	8	Pathogenic	Likely pathogenic
c.232C>T	p.His78Tyr	0.001656617%	Disease Causing	Possibly damaging (score 0.825)	Neutral (score -2.402)	3	7	Pathogenic	Unknown significance
c.240G>C	p.Trp80Cys	0.000828061%	Disease Causing	Possibly damaging (score 0.898)	Deleterious (score -11.306)	4	8	Pathogenic	Pathogenic
c.254T>C	p.Ile85Thr	0.000827185%	Polymorphism	Benign (score 0.075)	Deleterious (score -3.034)	2	4	Unknown significance	Likely benign
c.255T>G	p.Ile85Met	0.002481472%	Polymorphism	Benign (score 0.352)	Neutral(score -0.718)	2	4	Unknown significance	Benign
c.262A>C	p.Ser88Arg	1.15000496%	Polymorphism	Benign (score 0.027)	Neutral(score -1.560)	1	4	Benign	Benign
c.271C>T	p.Leu91Phe	0.000825668%	Disease Causing	Probably damaging (score 0.918)	Deleterious (score -3.257)	4	8	Pathogenic	Pathogenic
c.274C>T	p.Arg92Trp	0.000825505%	Disease Causing	Benign (score 0.437)	Deleterious (score -4.139)	2	4	Pathogenic	Likely pathogenic
c.275G>A	p.Arg92Gln	0.000825437%	Disease Causing	Benign (score 0.014)	Neutral (score 0.996)	2	4	Unknown significance	Likely benign
c.280C>A	p.Leu94Ile	0.027234014%	Disease Causing	Benign (score 0.023)	Neutral (score -1.569)	3	7	Pathogenic	Likely benign
c.280C>G	p.Leu94Val	0.000825273%	Disease Causing	Benign (score 0.071)	Neutral (score -2.455)	3	7	Pathogenic	Likely pathogenic
c.290C>G	p.Thr97Ser	0.000825069%	Disease Causing	Benign (score 0.388)	Neutral (score -2.381)	3	7	Pathogenic	Likely pathogenic
c.295T>C	p.Tyr99His	0.002474757%	Disease Causing	Possibly damaging (score 0.905)	Deleterious (score -3.975)	4	8	Pathogenic	Likely pathogenic
c.304G>A	p.Ala102Thr	0.002474268%	Disease Causing	Possibly damaging (score 0.542)	Neutral(score -1.312)	3	6	Pathogenic	Unknown significance
c.310G>A	p.Val104Ile	0.245740768%	Polymorphism	Benign (score 0.004)	Neutral(score 0.205)	1	2	Benign	Benign
c.323C>T	p.Ser108Leu	0.002473248%	Disease Causing	Possibly damaging (score 0.696)	Deleterious (score -2.710)	2	4	Pathogenic	Likely benign
c.338G>C	p.Ser113Thr	0.00164837%	Disease Causing	Probably damaging (score 0.974)	Neutral (score -0.553)	3	7	Pathogenic	Likely pathogenic
c.350C>T	p.Ser117Phe	0.000824266%	Polymorphism	Benign (score 0.004)	Neutral(score -1.238)	2	3	Unknown significance	Likely benign
c.356G>A	p.Gly119Glu	0.008245791%	Disease Causing	Probably damaging (score 0.993)	Neutral(score -1.869)	3	6	Pathogenic	Likely pathogenic
c.371C>T	p.Pro124Leu	0.001648098%	Disease Causing	Probably damaging (score 0.991)	Deleterious (score -8.802)	4	8	Pathogenic	Likely pathogenic
c.392C>T	p.Ala131Val	0.018129677%	Polymorphism	Benign (score 0.105)	Neutral(score -1.874)	1	1	Benign	Benign
c.394G>T	p.Gly132Cys	0.000824035%	Disease Causing	Probably damaging (score 1.000)	Deleterious (score -8.250)	4	8	Pathogenic	Pathogenic
c.397G>A	p.Val133Met	0.000824063%	Disease Causing	Probably damaging (score 0.943)	Deleterious (score -2.621)	4	8	Pathogenic	Pathogenic
c.408G>T	p.Glu136Asp	0.010712991%	Polymorphism	Possibly damaging (score 0.880)	Neutral(score -2.041)	3	6	Pathogenic	Likely benign
c.409G>T	p.Asp137Tyr	0.000824076%	Disease Causing	Possibly damaging (score 0.877)	Deleterious (score 4.782)	2	5	Pathogenic	Likely pathogenic
c.410A>T	p.Asp137Val	0.000824076%	Disease Causing	Benign (score 0.385)	Deleterious (score -4.976)	2	5	Pathogenic	Likely pathogenic
c.416T>G	p.Leu139Arg	0.00164818%	Disease Causing	Probably damaging (score 0.993)	Deleterious (score -5.529)	3	7	Pathogenic	Likely pathogenic
c.418G>A	p.Asp140Asn	0.000824063%	Polymorphism	Possibly damaging (score 0.574)	Neutral(score -0.539)	2	4	Unknown significance	Likely benign
c.422T>C	p.Ile141Thr	0.00164818%	Disease Causing	Possibly damaging (score 0.672)	Deleterious (score -3.011)	3	6	Pathogenic	Likely pathogenic
c.454T>C	p.Ser152Pro	0.000824552%	Polymorphism	Benign (score 0.005)	Neutral (score -1.530)	2	2	Unknown significance	Likely benign
c.458G>T	p.Cys153Phe	0.001649267%	Disease Causing	Possibly damaging (score 0.878)	Deleterious (score -5.590)	4	8	Pathogenic	Likely pathogenic
c.463C>G	p.Leu155Val	0.00247386%	Disease Causing	Benign (score 0.120)	Neutral (score -1.381)	4	8	Pathogenic	Likely benign
c.464T>G	p.Leu155Arg	0.000824647%	Disease Causing	Benign (score 0.182)	Deleterious (score -2.961)	4	8	Pathogenic	Pathogenic
c.507C>A	p.Phe169Leu	0.000829064%	Disease Causing	Possibly damaging (score 0.872)	Deleterious (score -4.837)	4	8	Pathogenic	Pathogenic
c.508G>A	p.Val170Met	0.020722812%	Disease Causing	Probably damaging (score 0.975)	Deleterious (score -2.613)	4	8	Pathogenic	Likely pathogenic
c.527T>C	p.Met176Thr	0.000826733%	Polymorphism	Benign (score 0.002)	Neutral (score -0.903)	1	1	Benign	Likely benign
c.528G>C	p.Met176Ile	0.00082672%	Polymorphism	Benign (score 0.001)	Neutral (score 0.607)	1	1	Benign	Likely benign
c.533C>T	p.Ala178Val	0.000826638%	Disease Causing	Probably damaging (score 0.967)	Deleterious (score -2.814)	3	7	Pathogenic	Pathogenic
c.542G>A	p.Gly181Asp	0.000826624%	Disease Causing	Probably damaging (score 0.973)	Neutral (score -2.124)	4	6	Pathogenic	Pathogenic
c.554C>A	p.Thr185Asn	0.000826843%	Polymorphism	Probably damaging (score 0.912)	Neutral (score -2.420)	3	5	Pathogenic	Likely benign
c.610G>A	p.Ala204Thr	0.007573463%	Disease Causing	Probably damaging (score 0.936)	Deleterious (score -3.003)	2	3	Pathogenic	Likely benign

Nucleotide change	Amino acid change	*Reported vAFs	Prediction of functional effects			Evolutionary conservation		Combined analysis	
			MutationTaster	PolyPhen-2	Provean Protein	4 Orthologs	8 Orthologs	1	2
c.639T>G	p.Phe213Leu	0.000830372%	Disease Causing	Benign (score 0.167)	Deleterious (score -5.331)	4	8	Pathogenic	Pathogenic
c.641C>G	p.Ala214Gly	90.06240482%	Polymorphism	Benign (score 0.000)	Neutral(score 0.818)	1	2	Benign	Benign
c.653G>T	p.Ser218Ile	0.002490205%	Disease Causing	Probably damaging (score 0.982)	Deleterious (score -4.275)	4	8	Pathogenic	Likely pathogenic
c.666C>G	p.Phe222Leu	0.000824661%	Disease Causing	Possibly damaging (score 0.782)	Deleterious (score -5.153)	4	8	Pathogenic	Pathogenic
c.672C>G	p.Ile224Met	0.000824633%	Disease Causing	Probably damaging (score 0.972)	Neutral(score -2.463)	3	6	Pathogenic	Pathogenic
c.688C>T	p.His230Tyr	0.004947964%	Disease Causing	Probably damaging (score 1.000)	Neutral (score 0.211)	4	8	Pathogenic	Likely pathogenic
c.707A>C	p.Tyr236Ser	0.000825382%	Disease Causing	Probably damaging (score 1.000)	Deleterious (score -7.629)	4	8	Pathogenic	Pathogenic
c.708C>A	p.Tyr236*	0.000825505%	Disease Causing	N/A	N/A	4	8	Pathogenic	Pathogenic
c.725C>T	p.Ala242Val	0.000827527%	Disease Causing	Probably damaging (score 0.977)	Deleterious (score -3.220)	4	7	Pathogenic	Pathogenic
c.735C>A	p.Cys245*	0.001657028%	Disease Causing	N/A	N/A	4	8	Pathogenic	Likely pathogenic
c.735C>G	p.Cys245Trp	0.001657028%	Disease Causing	Probably damaging (score 1.000)	Deleterious (score -4.295)	4	8	Pathogenic	Likely pathogenic
c.739G>T	p.Ala247Ser	0.000828981%	Disease Causing	Probably damaging (score 1.000)	Deleterious (score -2.554)	4	8	Pathogenic	Pathogenic
c.740C>T	p.Ala247Val	0.000829504%	Disease Causing	Probably damaging (score 1.000)	Deleterious (score -3.433)	4	8	Pathogenic	Pathogenic
c.751C>T	p.Arg251Trp	0.001662538%	Disease Causing	Probably damaging (score 0.997)	Deleterious (score -6.645)	3	7	Pathogenic	Likely pathogenic
c.761C>T	p.Ala254Val	0.007495752%	Disease Causing	Possibly damaging (score 0.532)	Deleterious (score -3.072)	4	7	Pathogenic	Likely pathogenic
c.860C>T	p.Ala287Val	90.96297306%	Polymorphism	Benign (score 0.006)	Neutral (score 1.603)	1	2	Benign	Benign
c.869G>T	p.Gly290Val	0.046950677%	Disease Causing	Benign (score 0.004)	Neutral(score 2.918)	1	1	Benign	Benign
c.875G>T	p.Cys292Phe	0.000823696%	Disease Causing	Probably damaging (score 0.998)	Deleterious (score-7.217)	3	7	Pathogenic	Pathogenic
c.877G>A	p.Gly293Ser	0.00082371%	Disease Causing	Probably damaging (score 0.971)	Deleterious (score -5.126)	3	6	Pathogenic	Pathogenic
c.886G>A	p.Gly296Ser	0.00082371%	Polymorphism	Benign (score 0.001)	Neutral (score -2.048)	1	1	Benign	Likely benign
c.889A>G	p.Ser297Gly	0.053541128%	Polymorphism	Benign (score 0.116)	Neutral (score -1.359	1	1	Benign	Benign
c.891C>A	p.Ser297Arg	0.00082371%	Polymorphism	Benign (score 0.340)	Neutral (score -1.872)	1	1	Benign	Likely benign
c.905G>A	p.Cys302Tyr	0.00082375%	Disease Causing	Probably damaging (score 0.981)	Deleterious (score -4.439)	2	6	Pathogenic	Pathogenic
c.908A>C	p.Gln303Pro	0.001647528%	Disease Causing	Probably damaging (score 0.935)	Deleterious (score -3.094)	3	5	Pathogenic	Likely benign
c.908A>T	p.Gln303Leu	0.001647528%	Disease Causing	Benign (score 0.199)	Deleterious (score -4.034)	3	5	Pathogenic	Likely benign
c.910C>T	p.Arg304*	0.00411882%	Disease Causing	N/A	N/A	3	7	Pathogenic	Likely pathogenic
c.911G>A	p.Arg304Gln	0.000823764%	Disease Causing	Probably damaging (score 0.998)	Deleterious (score -3.527)	3	7	Pathogenic	Pathogenic
c.928A>C	p.Ile310Leu	0.000823845%	Polymorphism	Benign (score 0.004)	Neutral (score -0.431)	1	1	Benign	Likely benign
c.944T>G	p.Phe315Cys	0.000824144%	Polymorphism	Benign (score 0.021)	Neutral(score -1.188)	2	4	Unknown significance	Likely benign
c.973C>G	p.Pro325Ala	0.000824429%	Disease Causing	Possibly damaging (score 0.585)	Neutral (score -1.914)	3	6	Pathogenic	Likely pathogenic
c.985G>C	p.Ala329Pro	0.0008243625	Disease Causing	Probably damaging (score 0.997)	Deleterious (score -3.772)	3	7	Pathogenic	Pathogenic
c.986C>T	p.Ala329Val	0.000824375%	Disease Causing	Possibly damaging (score 0.708)	Deleterious (score -2.928)	3	7	Pathogenic	Pathogenic
c.992C>G	p.Ala331Gly	0.002473125%	Polymorphism	Possibly damaging (score 0.705)	Deleterious (score -3.098)	2	3	Unknown significance	Likely benign
c.1000G>C	p.Val334Leu	0.041220795%	Polymorphism	Benign (score 0.003)	Neutral (score 0.140)	3	4	Pathogenic	Benign
c.1006G>A	p.Ala336Thr	0.000824416%	Disease Causing	Probably damaging (score 0.985)	Deleterious (score -2.536)	4	8	Pathogenic	Pathogenic
c.1013T>A	p.Ile338Asn	0.001649049%	Disease Causing	Probably damaging (score 0.971)	Deleterious (score -5.288)	4	6	Pathogenic	Likely pathogenic
c.1024C>T	p.Pro342Ser	0.004947882%	Polymorphism	Possibly damaging (score 0.593)	Deleterious (score -4.796)	3	5	Pathogenic	Likely benign
c.1028G>A	p.Ser343Asn	0.000824838%	Polymorphism	Possibly damaging (score 0.513)	Neutral (score -0.608)	1	3	Benign	Likely benign
c.1029C>G	p.Ser343Arg	0.001649648%	Polymorphism	Possibly damaging (score 0.902)	Neutral (score -2.454)	1	3	Benign	Benign
c.1030G>A	p.Ala344Thr	0.001649702%	Polymorphism	Benign (score 0.105)	Neutral (score -0.502)	1	3	Benign	Benign
c.1033G>A	p.Gly345Ser	0.002474757%	Disease Causing	Probably damaging (score 1.000)	Deleterious (score -5.740)	4	8	Pathogenic	Likely pathogenic

Nucleotide change	Amino acid change	*Reported vAFs	Prediction of functional effects			Evolutionary conservation		Combined analysis	
			MutationTaster	PolyPhen-2	Provean Protein	4 Orthologs	8 Orthologs	1	2
c.1036C>T	p.Arg346Cys	0.001650083%	Disease Causing	Possibly damaging (score 0.832)	Deleterious (score -4.695)	1	1	Pathogenic	Likely benign
c.1037G>A	p.Arg346His	0.003300439%	Polymorphism	Benign (score 0.008)	Neutral (score -1.192)	1	3	Benign	Benign
c.1039T>A	p.Phe347Ile	0.00082511%	Disease Causing	Possibly damaging (score 0.452)	Deleterious (score -5.268)	2	6	Pathogenic	Pathogenic
c.1051C>T	p.Arg351Trp	0.000825655%	Disease Causing	Probably damaging (score 0.97)	Deleterious (score -4.685)	4	7	Pathogenic	Pathogenic
c.1112C>T	p.Thr371Ile	0.001657852%	Polymorphism	Possibly damaging (score 0.821)	Neutral (score -2.156)	2	4	Unknown significance	Benign
c.1125C>A	p.Ser375Arg	0.000828212%	Disease Causing	Probably damaging (score 0.980)	Neutral (score -2.114)	3	7	Pathogenic	Pathogenic
c.1138G>A	p.Glu380Lys	0.002481677%	Polymorphism	Benign (score 0.004)	Neutral (score -1.687)	1	1	Benign	Benign
c.1147G>A	p.Asp383Asn	0.004960153%	Disease Causing	Probably damaging (score 0.985)	Neutral (score -1.760)	3	6	Pathogenic	Likely pathogenic
c.1153C>T	p.Gln385*	0.000826515%	Disease Causing	N/A	N/A	2	5	Pathogenic	Likely pathogenic
c.1154A>G	p.Gln385Arg	0.071905581%	Polymorphism	Benign (score 0.026)	Neutral (score -1.110)	2	5	Unknown significance	Benign
c.1160T>C	p.Leu387Pro	0.00082646%	Disease Causing	Probably damaging (score 0.997)	Deleterious (score -3.317)	3	6	Pathogenic	Pathogenic
c.1171T>C	p.Trp391Arg	0.004132846%	Disease Causing	Probably damaging (score 1.000)	Deleterious (score -7.970)	4	8	Pathogenic	Likely pathogenic
c.1172G>A	p.Trp391*	0.002479872%	Disease Causing	N/A	N/A	4	8	Pathogenic	Likely pathogenic
c.1183C>T	p.Arg395Trp	0.217427249%	Polymorphism	Possibly damaging (score 0.670)	Deleterious (score -3.083)	0	0	Unknown significance	Likely benign
c.1184G>A	p.Arg395Gln	0.001653576%	Polymorphism	Benign (score 0.003)	Neutral (score 0.415)	0	0	Benign	Benign
c.1184G>C	p.Arg395Pro	0.000826788%	Polymorphism	Benign (score 0.006)	Neutral (score -2.230)	0	0	Benign	Likely benign
c.1184G>T	p.Arg395Leu	0.00413394%	Polymorphism	Benign (score 0.112)	Deleterious (score -2.915)	0	0	Benign	Benign
c.1192A>G	p.Ile398Val	0.008270067%	Disease Causing	Benign (score 0.014)	Neutral (score 0.118)	2	3	Unknown significance	Benign
c.1202C>A	p.Thr401Asn	0.00082728%	Disease Causing	Probably damaging (score 0.989)	Deleterious (score -3.649)	3	7	Pathogenic	Pathogenic
c.1244T>A	p.Leu415Gln	0.00082371%	Disease Causing	Probably damaging (score 0.998)	Deleterious (score -4.876)	3	6	Pathogenic	Pathogenic
c.1255A>G	p.Ile419Val	10.1520543%	Polymorphism	Benign (score 0.050)	Neutral (score -0.653)	1	3	Benign	Benign
c.1261A>G	p.Met421Val	0.00082371%	Disease Causing	Benign (score 0.007)	Neutral (score 0.277)	2	5	Unknown significance	Likely benign
c.1270G>A	p.Gly424Arg	0.0049422585	Disease Causing	Probably damaging (score 1.000)	Deleterious (score -7.768)	4	8	Pathogenic	Likely pathogenic
c.1286T>A	p.Ile429Asn	0.00082371%	Disease Causing	Possibly damaging (score 0.776)	Deleterious (score -6.069)	2	3	Pathogenic	Likely pathogenic
c.1295A>C	p.Tyr432Ser	0.0024710885	Polymorphism	Possibly damaging (score 0.704)	Deleterious (score -3.559)	4	7	Pathogenic	Unknown significance
c.1298G>A	p.Gly433Glu	0.000824606%	Disease Causing	Probably damaging (score 1.000)	Deleterious (score -7.702)	4	8	Pathogenic	Pathogenic
c.1309G>A	p.Gly437Arg	0.004123575%	Disease Causing	Possibly damaging (score 0.750)	Deleterious (score -7.462)	4	8	Pathogenic	Likely pathogenic
c.1312C>A	p.Arg438Ser	0.014846585%	Disease Causing	Probably damaging (score 0.987)	Deleterious (score -5.603)	4	8	Pathogenic	Likely pathogenic
c.1312C>T	p.Arg438Cys	0.00082481%	Disease Causing	Probably damaging (score 0.999)	Deleterious (score -7.471)	4	8	Pathogenic	Pathogenic
c.1313G>A	p.Arg438His	0.001649593%	Disease Causing	Probably damaging (score 0.999)	Deleterious (score -4.670)	4	8	Pathogenic	Likely pathogenic
c.1316T>C	p.Leu439Pro	0.00082481%	Disease Causing	Probably damaging (score 0.994)	Deleterious (score -5.837)	4	7	Pathogenic	Pathogenic
c.1339A>G	p.Ile447Val	0.000825246%	Polymorphism	Benign (score 0.007)	Neutral (score -0.403)	1	1	Benign	Likely benign
c.1340T>C	p.Ile447Thr	0.001650465%	Polymorphism	Benign (score 0.005)	Neutral(score -1.411)	2	2	Unknown significance	Benign
c.1348G>A	p.Glu450Lys	0.001650846%	Polymorphism	Possibly damaging (score 0.675)	Neutral(score -2.358)	2	4	Unknown significance	Benign
c.1350G>C	p.Glu450Asp	0.0008256%	Polymorphism	Possibly damaging (score 0.747)	Neutral(score -0.194)	2	4	Unknown significance	Likely benign
c.1357G>A	p.Val453Met	0.009909657%	Polymorphism	Benign (score 0.223)	Neutral (score -0.164)	3	5	Pathogenic	Benign
c.1357G>T	p.Val453Leu	0.001651609%	Polymorphism	Benign (score 0.214)	Neutral (score -0.290)	3	5	Pathogenic	Benign
c.1360G>T	p.Ala454Ser	0.0008259%	Disease Causing	Benign (score 0.048)	Neutral(score -0.262)	3	5	Pathogenic	Likely benign
c.1369A>G	p.Ile457Val	0.000826132%	Polymorphism	Benign (score 0.001)	Neutral (score 0.054)	2	2	Unknown significance	Likely benign
c.1375A>C	p.Asn459His	0.009088956%	Polymorphism	Possibly damaging (score 0.707)	Neutral (score 0.009)	2	3	Unknown significance	Benign
c.1384A>T	p.Met462Leu	0.001653466%	Polymorphism	Benign (score 0.004)	Neutral (score -0.173)	2	3	Unknown significance	Benign

Nucleotide change	Amino acid change	*Reported vAFs	Prediction of functional effects			Evolutionary conservation		Combined analysis	
			MutationTaster	PolyPhen-2	Provean Protein	4 Orthologs	8 Orthologs	1	2
c.1391G>A	p.Gly464Glu	0.000827171%	Disease Causing	Probably damaging (score 0.998)	Deleterious (score -7.377)	3	7	Pathogenic	Pathogenic
c.1393G>A	p.Gly465Arg	0.001654588%	Disease Causing	Probably damaging (score 0.986)	Deleterious (score -6.712)	3	7	Pathogenic	Likely pathogenic
c.1393G>C	p.Gly465Arg	0.000827294%	Disease Causing	Probably damaging (score 0.986)	Deleterious (score -6.712)	3	6	Pathogenic	Pathogenic
c.1394G>A	p.Gly465Glu	0.000827554%	Disease Causing	Probably damaging (score 0.973)	Deleterious (score -6.710)	3	6	Pathogenic	Pathogenic
c.1394G>C	p.Gly465Ala	0.000827554%	Disease Causing	Benign (score 0.341)	Deleterious (score -4.496)	3	6	Pathogenic	Pathogenic
c.1405G>A	p.Ala469Thr	0.008282671%	Disease Causing	Probably damaging (score 0.986)	Neutral (score -1.724)	4	8	Pathogenic	Likely pathogenic
c.1414G>A	p.Ala472Thr	0.000839109%	Disease Causing	Probably damaging (score 0.994)	Deleterious (score -3.688)	4	8	Pathogenic	Pathogenic
c.1418C>A	p.Ala473Asp	0.000838392%	Disease Causing	Probably damaging (score 1.000)	Deleterious (score -5.466)	4	8	Pathogenic	Pathogenic
c.1429G>A	p.Ala477Thr	0.0008364%	Disease Causing	Probably damaging (score 0.954)	Deleterious (score -3.483)	4	8	Pathogenic	Pathogenic
c.1441A>C	p.Thr481Pro	0.0008335%	Disease Causing	Probably damaging (score 0.968)	Deleterious (score -4.948)	2	4	Pathogenic	Likely pathogenic
c.1441A>T	p.Thr481Ser	10.17120091%	Polymorphism	Benign (score 0.186)	Deleterious (score -2.558)	2	4	Benign	Benign
c.1442C>T	p.Thr481Ile	0.000833528%	Disease Causing	Probably damaging (score 0.968)	Deleterious (score -5.117)	2	4	Pathogenic	Likely pathogenic
c.1451C>T	p.Thr484Met	0.004164584%	Disease Causing	Probably damaging (score 0.999)	Deleterious (score -4.566)	4	7	Pathogenic	Likely pathogenic
c.1454C>T	p.Ala485Val	0.033309462%	Disease Causing	Probably damaging (score 0.954)	Deleterious (score -3.222)	4	8	Pathogenic	Likely pathogenic
c.1463C>A	p.Ala488Asp	0.050747063%	Disease Causing	Probably damaging (score 0.992)	Deleterious (score -3.907)	2	6	Pathogenic	Likely pathogenic
c.1465T>G	p.Phe489Val	0.002495508%	Disease Causing	Benign (score 0.264)	Deleterious (score -5.337	3	6	Pathogenic	Likely pathogenic
c.1468G>A	p.Glu490Lys	0.000831822%	Disease Causing	Probably damaging (score 1.000)	Deleterious (score -3.755)	4	8	Pathogenic	Pathogenic
c.1477G>A	p.Gly493Ser	0.00249501%	Disease Causing	Probably damaging (score 1.000)	Deleterious (score -5.632)	4	8	Pathogenic	Likely pathogenic
c.1484T>G	p.Ile495Arg	0.000831698%	Disease Causing	Possibly damaging (score 0.824)	Deleterious (score -5.953)	1	4	Pathogenic	Likely pathogenic
c.1486G>A	p.Val496Met	0.000831628%	Polymorphism	Possibly damaging (score 0.707)	Neutral (score -0.614)	2	3	Unknown significance	Likely benign
c.1487T>C	p.Val496Ala	0.000831725%	Polymorphism	Benign (score 0.034)	Neutral (score 0.783)	2	3	Unknown significance	Likely benign
c.1490A>C	p.His497Pro	0.000831656%	Disease Causing	Probably damaging (score 0.998)	Deleterious (score -9.219)	4	7	Pathogenic	Pathogenic
c.1490A>G	p.His497Arg	0.001663312%	Disease Causing	Probably damaging (score 0.998)	Deleterious (score -7.376	4	7	Pathogenic	Likely pathogenic
c.1498C>A	p.Pro500Thr	0.00083221%	Disease Causing	Probably damaging (score 1.000)	Deleterious (score -7.509)	4	8	Pathogenic	Pathogenic
c.1498C>T	p.Pro500Ser	0.004993259%	Disease Causing	Probably damaging (score 1.000)	Deleterious (score -7.509)	4	8	Pathogenic	Likely pathogenic
c.1501G>A	p.Val501Met	0.009158882%	Disease Causing	Probably damaging (score 0.998)	Neutral (score -1.461)	4	7	Pathogenic	Likely pathogenic
c.1511C>T	p.Ala504Val	0.006701178%	Disease Causing	Probably damaging (score 0.962)	Deleterious (score -3.611)	4	8	Pathogenic	Likely pathogenic
c.1513G>T	p.Val505Leu	0.000837423%	Disease Causing	Probably damaging (score 0.976)	Deleterious (score -2.681)	4	7	Pathogenic	Pathogenic
c.1528G>A	p.Ala510Thr	0.001674173%	Disease Causing	Probably damaging (score 0.937)	Deleterious (score -2.905)	4	8	Pathogenic	Likely pathogenic
c.1535C>T	p.Ala512Val	0.000836694%	Disease Causing	Possibly damaging (score 0.595)	Deleterious (score -3.060)	1	4	Pathogenic	Likely pathogenic
c.1547A>G	p.Gln516Arg	0.000835687%	Disease Causing	Probably damaging (score 0.971)	Deleterious (score -3.216)	4	7	Pathogenic	Pathogenic
c.1549C>A	p.Pro517Thr	0.000835548%	Disease Causing	Possibly damaging (score 0.780)	Deleterious (score -7.491)	3	6	Pathogenic	Pathogenic
c.1565G>A	p.Gly522Asp	0.005013285%	Disease Causing	Possibly damaging (score 0.852)	Neutral (score -2.467)	3	7	Pathogenic	Unknown significance
c.1570G>A	p.Val524Ile	0.530750071%	Polymorphism	Benign (score 0.000)	Neutral (score 0.798)	1	1	Benign	Benign
c.1574T>C	p.Ile525Thr	0.0050091%	Polymorphism	Possibly damaging (score 0.603)	Neutral (score -1.285)	4	7	Pathogenic	Likely benign
c.1584G>C	p.Lys528Asn	0.000837058%	Disease Causing	Possibly damaging (score 0.881)	Deleterious (score -4.160)	4	7	Pathogenic	Pathogenic
c.1589C>T	p.Pro530Leu	0.003339233%	Disease Causing	Probably damaging (score 1.000)	Deleterious (score -9.387)	4	8	Pathogenic	Likely pathogenic
c.1593C>A	p.Tyr531*	0.000833181%	Disease Causing	N/A	N/A	4	7	Pathogenic	Pathogenic
c.1600C>T	p.Arg534Trp	0.00333139%	Polymorphism	Benign (score 0.001)	Neutral (score -2.027)	1	2	Benign	Benign
c.1613G>A	p.Arg538His	0.002502252%	Polymorphism	Possibly damaging (score 0.858)	Neutral(score -1.230)	3	6	Pathogenic	Likely benign
c.1613G>T	p.Arg538Leu	0.000834084%	Polymorphism	Possibly damaging (score 0.458)	Deleterious (score -3.063)	3	6	Pathogenic	Likely pathogenic

Nucleotide change	Amino acid change	*Reported vAFs	Prediction of functional effects			Evolutionary conservation		Combined analysis	
			MutationTaster	PolyPhen-2	Provean Protein	4 Orthologs	8 Orthologs	1	2
c.1619T>G	p.Ile540Ser	0.00166853%	Polymorphism	Benign (score 0.065)	Neutral (score -1.330)	3	6	Pathogenic	Likely benign
c.1620C>G	p.Ile540Met	0.000834446%	Polymorphism	Possibly damaging (score 0.703)	Neutral (score -0.556)	3	6	Pathogenic	Likely pathogenic
c.1621G>A	p.Gly541Ser	0.004173065%	Polymorphism	Benign (score 0.001)	Neutral (score -0.279)	2	3	Unknown significance	Benign
c.1621G>C	p.Gly541Arg	0.000834613%	Polymorphism	Benign (score 0.002)	Neutral (score -1.430)	2	3	Unknown significance	Likely benign
c.1628A>G	p.His543Arg	0.000828171%	Polymorphism	Benign (score 0.001)	Deleterious (score -4.073)	2	3	Unknown significance	Likely benign
c.1630C>T	p.Arg544Cys	0.003312575%	Disease Causing	Benign (score 0.001)	Neutral (score -2.186)	3	4	Pathogenic	Benign
c.1631G>A	p.Arg544His	0.04803074%	Polymorphism	Benign (score 0.001)	Neutral (score -0.120)	3	4	Pathogenic	Benign
c.1633G>A	p.Val545Met	0.000827979%	Polymorphism	Possibly damaging (score 0.864)	Neutral (score -2.327)	4	8	Pathogenic	Likely pathogenic
c.1657C>A	p.His553Asn	0.000827678%	Polymorphism	Benign (score 0.036)	Neutral (score -0.297)	2	2	Unknown significance	Likely benign
c.1669A>C	p.Thr557Pro	0.013241525%	Polymorphism	Possibly damaging (score 0.894)	Deleterious (score -2.717)	3	6	Pathogenic	Unknown significance
c.1670C>T	p.Thr557Ile	0.000827554%	Polymorphism	Benign (score 0.136)	Neutral (score -0.772)	3	6	Pathogenic	Likely pathogenic
c.1675G>A	p.Ala559Thr	0.000827582%	Disease Causing	Benign (score 0.177)	Neutral (score -0.516)	3	5	Pathogenic	Likely benign
c.1685T>C	p.Met562Thr	93.10119785%	Polymorphism	Benign (score 0.000)	Neutral (score 0.223]	2	2	Benign	Benign
c.1686G>A	p.Met562Ile	0.002482498%	Polymorphism	Benign (score 0.030)	Neutral (score -0.989)	2	2	Unknown significance	Benign
c.1717T>C	p.Ser573Pro	0.011592859%	Disease Causing	Possibly damaging (score 0.657)	Deleterious (score -2.988)	3	6	Pathogenic	Likely pathogenic
c.1724A>T	p.Asp575Val	0.00082802%	Polymorphism	Benign (score 0.064)	Deleterious (score -2.805)	2	4	Unknown significance	Likely benign
c.1726G>A	p.Val576Met	0.000827993%	Polymorphism	Benign (score 0.008)	Neutral (score -0.348)	2	3	Unknown significance	Likely benign
c.1726G>C	p.Val576Leu	0.001655986%	Polymorphism	Benign (score 0.000)	Neutral (score -0.116)	2	3	Unknown significance	Benign
c.1732A>G	p.Lys578Glu	65.85726386%	Polymorphism	Benign (score 0.000)	Neutral (score 1.116)	0	0	Benign	Benign
c.1762C>T	p.Gln588*	0.000841694%	Disease Causing	N/A	N/A	2	4	Pathogenic	Likely pathogenic
c.1764G>C	p.Gln588His	0.000841468%	Polymorphism	Benign (score 0.098)	Neutral (score -2.490)	2	4	Unknown significance	Likely benign
c.1780G>C	p.Val594Leu	0.003361966%	Polymorphism	Benign (score 0.004)	Neutral (score -1.579)	2	4	Unknown significance	Benign
c.1783C>T	p.Arg595*	0.00672461%	Disease Causing	N/A	N/A	1	3	Pathogenic	Likely benign
c.1784G>A	p.Arg595Gln	0.0084077425	Polymorphism	Benign (score 0.002)	Neutral (score 13.65)	1	3	Benign	Benign
c.1788G>C	p.Arg596Ser	0.000841%	Disease Causing	Possibly damaging (score 0.849)	Deleterious (score -5.246)	4	8	Pathogenic	Pathogenic
c.1790C>T	p.Ala597Val	0.000841156%	Polymorphism	Benign (score 0.003)	Neutral (score -1.648)	2	4	Unknown significance	Likely benign
c.1802A>G	p.Gln601Arg	0.000844894%	Polymorphism	Benign (score 0.053)	Neutral (score -0.751)	2	4	Unknown significance	Likely benign
c.1830G>A	p.Trp610*	0.016524038%	Disease Causing	N/A	N/A	2	4	Pathogenic	Likely benign
c.1834C>T	p.Pro612Ser	0.000874875%	Polymorphism	Benign (score 0.004)	Neutral (score -1.892)	3	6	Pathogenic	Likely pathogenic
c.1846C>T	p.Gln616*	0.000829518%	Disease Causing	N/A	N/A	1	2	Pathogenic	Likely pathogenic
c.1850G>A	p.Cys617Tyr	0.000829229%	Polymorphism	Benign (score 0.002)	Neutral (score -0.716)	2	4	Unknown significance	Likely benign
c.1856A>G	p.Gln619Arg	0.000829091%	Polymorphism	Benign (score 0.030)	Neutral (score -0.836)	2	4	Unknown significance	Likely benign
c.1858G>A	p.Asp620Asn	0.000829091%	Polymorphism	Benign (score 0.015)	Neutral (score -0.965)	2	4	Unknown significance	Likely benign
c.1863C>G	p.Ile621Met	0.000829009%	Polymorphism	Benign (score 0.070)	Neutral(score -0.594)	2	4	Unknown significance	Likely benign
c.1870G>T	p.Ala624Ser	0.00082894%	Polymorphism	Benign (score 0.030)	Neutral(score 0.942)	1	1	Benign	Likely benign
c.1874G>T	p.Gly625Val	0.004145043%	Disease Causing	Benign (score 0.091)	Neutral (score -2.466)	2	5	Unknown significance	Benign
c.1877G>A	p.Cys626Tyr	2.291455953%	Polymorphism	Probably damaging (score 0.998)	Deleterious (score -5.327)	3	7	Pathogenic	Likely pathogenic
c.1877G>T	p.Cys626Phe	0.000829036%	Disease Causing	Probably damaging (score 0.997)	Deleterious (score -5.512)	3	7	Pathogenic	Pathogenic
c.1879C>A	p.Pro627Thr	0.004145593%	Polymorphism	Benign (score 0.017)	Neutral (score -0.717)	2	4	Unknown significance	Benign
c.1879C>T	p.Pro627Ser	0.000829119%	Polymorphism	Benign (score 0.017)	Neutral (score -0.601)	2	4	Unknown significance	Likely benign
c.1915A>G	p.Thr639Ala	0.000831131%	Disease Causing	Benign (score 0.025)	Deleterious (score -2.546)	3	6	Pathogenic	Pathogenic

Nucleotide change	Amino acid change	*Reported vAFs	Prediction of functional effects			Evolutionary conservation		Combined analysis	
			MutationTaster	PolyPhen-2	Provean Protein	4 Orthologs	8 Orthologs	1	2
c.1919C>T	p.Ser640Phe	0.000831711%	Disease Causing	Possibly damaging (score 0.583)	Deleterious (score -3.906)	3	6	Pathogenic	Pathogenic
c.1921C>G	p.Leu641Val	0.000832196%	Disease Causing	Benign (score 0.044)	Neutral (score -1.435)	3	6	Pathogenic	Likely pathogenic
c.1929G>C	p.Glu643Asp	0.000834516%	Disease Causing	Benign (score 0.111)	Neutral (score -1.597)	2	2	Unknown significance	Likely benign
c.1930G>A	p.Ala644Thr	0.000824253%	Disease Causing	Possibly damaging (score 0.671)	Neutral (score 0.032)	2	6	Unknown significance	Likely pathogenic
c.1931C>T	p.Ala644Val	0.000824239%	Disease Causing	Possibly damaging (score 0.467)	Neutral (score -0.829)	2	6	Unknown significance	Likely pathogenic
c.1940T>C	p.Leu647Pro	0.000824266%	Disease Causing	Probably damaging (score 0.998)	Deleterious (score -4.071)	3	6	Pathogenic	Pathogenic
c.1943T>C	p.Phe648Ser	0.000824253%	Disease Causing	Probably damaging (score 1.000)	Deleterious (score -4.959)	3	6	Pathogenic	Pathogenic
c.1944T>G	p.Phe648Leu	0.004121264%	Disease Causing	Benign (score 0.412)	Deleterious (score -3.739)	3	6	Pathogenic	Likely pathogenic
c.1952T>G	p.Leu651Trp	0.003296903%	Disease Causing	Probably damaging (score 0.988)	Deleterious (score -3.884)	3	5	Pathogenic	Likely benign
c.1955A>G	p.Asn652Ser	0.000824212%	Polymorphism	Benign (score 0.005)	Neutral (score -0.466)	2	4	Unknown significance	Likely benign
c.1960C>T	p.His654Tyr	0.000824212%	Polymorphism	Benign (score 0.121)	Neutral (score -1.164)	1	1	Benign	Likely benign
c.1964C>T	p.Ser655Phe	0.005769389%	Polymorphism	Benign (score 0.396)	Neutral (score -1.310)	1	3	Benign	Benign
c.1976C>T	p.Thr659Met	0.009065884%	Disease Causing	Probably damaging (score 0.999)	Deleterious (score -3.864)	3	7	Pathogenic	Likely pathogenic
c.1979C>T	p.Ser660Leu	0.499431341%	Polymorphism	Benign (score 0.024)	Deleterious (score -3.270)	2	5	Unknown significance	Benign
c.1981C>T	p.Arg661Trp	0.001648315%	Polymorphism	Benign (score 0.011)	Neutral (score -1.870)	2	3	Unknown significance	Benign
c.1982G>A	p.Arg661Gln	0.000824144%	Polymorphism	Benign (score 0.005)	Neutral (score -0.343)	2	3	Unknown significance	Likely benign
c.1984G>C	p.Gly662Arg	0.000824144%	Disease Causing	Probably damaging (score 1.000)	Deleterious (score -5.722)	3	7	Pathogenic	Pathogenic
c.1990G>T	p.Ala664Ser	0.000824185%	Polymorphism	Possibly damaging (score 0.754)	Neutral (score -1.011)	2	4	Unknown significance	Likely benign
c.2002G>A	p.Val668Met	0.002473166%	Disease Causing	Probably damaging (score 0.984)	Neutral (score -1.541)	3	6	Pathogenic	Likely pathogenic
c.2002G>C	p.Val668Leu	0.011541442%	Disease Causing	Possibly damaging (score 0.605)	Neutral (score -1.094)	3	6	Pathogenic	Unknown significance
c.2005T>G	p.Ser669Ala	0.000824389%	Polymorphism	Possibly damaging (score 0.700)	Neutral (score -0.966)	2	5	Unknown significance	Likely benign
c.2026G>A	p.Ala676Thr	0.000873607%	Disease Causing	Possibly damaging (score 0.815)	Neutral (score -2.158)	2	5	Unknown significance	Unknown significance
c.2027C>T	p.Ala676Val	0.0008719%	Disease Causing	Benign (score 0.071)	Neutral (score -1.906)	2	5	Unknown significance	Likely benign
c.2048C>T	p.Pro683Leu	0.001691218%	Disease Causing	Possibly damaging (score 0.866)	Deleterious (score -2.615)	2	5	Pathogenic	Likely benign
c.2053G>A	p.Ala685Thr	0.000842105%	Polymorphism	Benign (score 0.005)	Neutral (score -0.917	2	5	Unknown significance	Likely benign
c.2054C>A	p.Ala685Asp	0.000841637%	Disease Causing	Benign (score 0.243)	Neutral (score -1.948	2	5	Unknown significance	Likely benign

CLCNKB variants obtained from ExAC[236] used to investigate the effectiveness of *in silico* methods for variant analysis (Chapter 6). Nucleotide number is according to transcript ENST00000375679 and amino acid is according to the full-length 687 amino acid protein (NCBI NP_000076; UniProt P51801) as displayed on ExAC. *Reported vAFs were also obtained from ExAC[236]. Evolutionary conservation scores were based on the number of orthologs each WT residue was conserved in, the number of orthologs studied in each analysis is detailed in the column heading, as detailed in Chapter 6. Combined analysis 1 and 2 are based on the criteria detailed in Chapter 6. N/A, not applicable.

Table 47. *In silico* analysis of *OCRL1* variants obtained from ExAC

Nucleotide change	Amino acid change	*Reported vAFs	Prediction of functional effects			Evolutionary conservation		Combined analysis	
			MutationTaster	PolyPhen-2	Provean Protein	4 Orthologs	8 Orthologs	1	2
c.17C>T	p.Pro6Leu	0.014186409%	Disease Causing	Benign (score 0.113)	Neutral (score -0.414)	2	4	Unknown significance	Benign
c.40A>G	p.Thr14Ala	0.001147421%	Polymorphism	Benign (score 0.001)	Neutral (score -0.138)	1	3	Benign	Benign
c.41C>T	p.Thr14Ile	0.534673459%	Polymorphism	Benign (score 0.000)	Neutral (score -0.666)	1	3	Benign	Benign
c.50G>C	p.Gly17Ala	0.003438317%	Disease Causing	Benign (score 0.081)	Neutral (score -1.478)	4	8	Pathogenic	Likely benign
c.52A>G	p.Met18Val	0.001145672%	Polymorphism	Benign (score 0.000)	Neutral (score 0.006)	1	3	Benign	Benign
c.67C>T	p.Pro23Ser	0.004579908%	Polymorphism	Benign (score 0.014)	Neutral (score 0.268)	2	4	Unknown significance	Benign
c.74G>C	p.Arg25Pro	0.001144951%	Disease Causing	Benign (score 0.055)	Neutral (score -0.996)	3	6	Pathogenic	Likely benign
c.86C>T	p.Ala29Val	0.001145357%	Polymorphism	Benign (score 0.001)	Neutral (score 0.273)	2	4	Unknown significance	Benign
c.91A>T	p.Thr31Ser	0.0011456075	Polymorphism	Benign (score 0.001)	Neutral (score 0.511)	2	4	Unknown significance	Benign
c.92C>T	p.Thr31Ile	0.0011456335	Disease Causing	Benign (score 0.038	Neutral (score -0.536)	2	4	Unknown significance	Benign
c.97G>T	p.Ala33Ser	0.001146053%	Disease Causing	Benign (score 0.012)	Neutral (score -0.669)	3	5	Pathogenic	Benign
c.101A>G	p.Gln34Arg	0.001146158%	Polymorphism	Benign (score 0.000)	Neutral (score -0.168)	3	5	Pathogenic	Benign
c.109G>A	p.Gly37Arg	0.006882234%	Disease Causing	Benign (score 0.224)	Neutral (score -0.787)	4	8	Pathogenic	Likely benign
c.109G>C	p.Gly37Arg	0.002294078%	Disease Causing	Benign (score 0.224)	Neutral (score -0.787)	4	8	Pathogenic	Likely benign
c.115T>C	p.Tyr39His	0.001148119%	Disease Causing	Benign (score 0.377)	Neutral (score 0.322)	4	7	Pathogenic	Likely benign
c.152A>G	p.His51Arg	0.02646629%	Polymorphism	Benign (score 0.000)	Neutral (score -0.059)	2	3	Unknown significance	Benign
c.172A>G	p.Ile58Val	0.003456341%	Disease Causing	Benign (score 0.394)	Neutral (score -0.236)	4	8	Pathogenic	Likely benign
c.175A>G	p.Asn59Asp	0.001152592%	Disease Causing	Benign (score 0.164)	Neutral (score -0.429)	3	7	Pathogenic	Likely benign
c.180C>G	p.Ser60Arg	0.001154588%	Disease Causing	Benign (score 0.246)	Neutral (score -0.358)	4	7	Pathogenic	Likely benign
c.197A>G	p.Gln66Arg	0.001164727%	Disease Causing	Benign (score 0.107)	Neutral (score -0.419)	4	7	Pathogenic	Likely benign
c.205G>A	p.Glu69Lys	0.001139835%	Disease Causing	Benign (score 0.093)	Neutral (score -0.825)	4	8	Pathogenic	Likely benign
c.235A>G	p.Asn79Asp	0.002279982%	Disease Causing	Benign (score 0.004)	Neutral (score -0.106)	4	7	Pathogenic	Likely benign
c.244T>C	p.Cys82Arg	0.001157501%	Disease Causing	Probably damaging (score 0.964)	Neutral (score -1.373)	4	7	Pathogenic	Likely pathogenic
c.265G>C	p.Asp89His	0.005746268%	Disease Causing	Possibly damaging (score 0.774)	Neutral (score -1.010)	4	7	Pathogenic	Unknown significance
c.283C>T	p.Arg95Cys	0.002300516%	Disease Causing	Benign (score 0.175)	Neutral (score -0.514)	2	3	Unknown significance	Benign
c.284G>A	p.Arg95His	0.003451053%	Polymorphism	Benign (score 0.000)	Neutral (score -0.750)	2	3	Unknown significance	Benign
c.350C>T	p.Ala117Val	0.001139432%	Disease Causing	Benign (score 0.053)	Neutral (score -0.462)	3	6	Pathogenic	Likely benign
c.375G>T	p.Glu125Asp	0.097988948%	Polymorphism	Benign (score 0.002)	Neutral (score -0.252)	4	5	Pathogenic	Benign
c.428C>T	p.Ser143Phe	0.001139666%	Polymorphism	Benign (score 0.000)	Neutral (score -1.204)	1	2	Benign	Benign
c.446T>A	p.Leu149His	0.003442696%	Disease Causing	Possibly damaging (score 0.641)	Neutral (score -0.902)	4	6	Pathogenic	Unknown significance
c.481G>A	p.Asp161Asn	0.003439618%	Disease Causing	Benign (score 0.003)	Neutral (score -1.040)	2	4	Unknown significance	Benign
c.523C>T	p.Arg175Trp	0.00343383%	Disease Causing	Possibly damaging (score 0.820)	Neutral (score -1.751)	4	8	Pathogenic	Unknown significance
c.524G>A	p.Arg175Gln	0.002289351%	Disease Causing	Benign (score 0.011)	Neutral (score -0.358)	4	8	Pathogenic	Likely benign
c.529C>A	p.Pro177Thr	0.001143995%	Disease Causing	Probably damaging (score 0.963)	Neutral (score -1.313)	4	8	Pathogenic	Likely pathogenic
c.533C>G	p.Pro178Arg	0.001143824%	Disease Causing	Probably damaging (score 0.975)	Neutral (score -1.650)	4	8	Pathogenic	Likely pathogenic
c.568C>T	p.Arg190Cys	0.002282662%	Disease Causing	Benign (score 0.055)	Neutral (score -2.411)	4	7	Pathogenic	Likely benign
c.569G>A	p.Arg190His	0.001141266%	Disease Causing	Possibly damaging (score 0.899)	Neutral (score -1.718)	4	7	Pathogenic	Unknown significance
c.569G>T	p.Arg190Leu	0.001141266%	Disease Causing	Possibly damaging (score 0.621)	Neutral (score -2.243)	4	7	Pathogenic	Unknown significance
c.586A>G	p.Asn196Asp	0.003421494%	Polymorphism	Benign (score 0.019)	Neutral (score -0.623)	2	4	Unknown significance	Benign
c.587A>G	p.Asn196Ser	0.001140407%	Polymorphism	Benign (score 0.001)	Neutral (score 0.017)	2	4	Unknown significance	Benign
c.619C>T	p.Arg207Trp	0.00113977%	Disease Causing	Probably damaging (score 0.952)	Deleterious (score -2.663)	4	8	Pathogenic	Likely pathogenic
c.620G>A	p.Arg207Gln	0.002279592%	Disease Causing	Benign (score 0.158)	Neutral (score -1.150)	4	8	Pathogenic	Likely benign
c.655C>T	p.Arg219Trp	0.001139874%	Disease Causing	Probably damaging (score 0.999)	Deleterious (score -6.488)	4	8	Pathogenic	Likely pathogenic
c.662G>T	p.Gly221Val	0.00228019%	Disease Causing	Benign (score 0.048)	Neutral (score -1.203)	4	8	Pathogenic	Likely benign

Nucleotide change	Amino acid change	*Reported vAFs	Prediction of functional effects			Evolutionary conservation		Combined analysis	
			MutationTaster	PolyPhen-2	Provean Protein	4 Orthologs	8 Orthologs	1	2
c.677T>C	p.Ile226Thr	0.001141071%	Disease Causing	Benign (score 0.045)	Neutral (score 0.407)	3	4	Pathogenic	Benign
c.692A>G	p.Glu231Gly	0.001142674%	Polymorphism	Probably damaging (score 0.973)	Deleterious (score -6.464)	4	8	Pathogenic	Likely pathogenic
c.693G>C	p.Glu231Asp	0.001142792%	Disease Causing	Probably damaging (score 0.980)	Deleterious (score -2.869)	4	8	Pathogenic	Likely pathogenic
c.696A>C	p.Lys232Asn	0.001143223%	Disease Causing	Benign (score 0.003)	Neutral (score -0.533)	3	7	Pathogenic	Likely benign
c.775G>C	p.Glu259Gln	0.001141097%	Disease Causing	Benign (score 0.038)	Neutral (score 0.015)	4	7	Pathogenic	Likely benign
c.778C>T	p.Pro260Ser	0.00114124%	Disease Causing	Benign (score 0.420)	Deleterious (score -3.762)	4	8	Pathogenic	Likely pathogenic
c.800A>G	p.Asn267Ser	0.003429081%	Polymorphism	Benign (score 0.001)	Neutral (score -0.153)	2	4	Unknown significance	Benign
c.880G>C	p.Glu294Gln	0.001139861%	Disease Causing	Probably damaging (score 0.997)	Deleterious (score -2.836)	4	8	Pathogenic	Likely pathogenic
c.897G>A	p.Met299Ile	0.595088807%	Polymorphism	Benign (score 0.001)	Neutral (score -1.763)	1	2	Benign	Benign
c.944A>G	p.Gln315Arg	0.001140121%	Disease Causing	Benign (score 0.001)	Neutral (score 0.341)	3	6	Pathogenic	Likely benign
c.983C>T	p.Ala328Val	0.001139705%	Disease Causing	Benign (score 0.040)	Neutral (score 1.756)	4	7	Pathogenic	Likely benign
c.1001G>A	p.Arg334Gln	0.001139588%	Polymorphism	Benign (score 0.000)	Neutral (score 0.738)	1	3	Benign	Benign
c.1009C>A	p.Arg337Ser	0.001139627%	Disease Causing	Benign (score 0.008)	Neutral (score 0.149)	4	8	Pathogenic	Likely benign
c.1010G>A	p.Arg337His	0.001139614%	Disease Causing	Benign (score 0.005)	Neutral (score -1.907)	4	8	Pathogenic	Likely benign
c.1031T>C	p.Val344Ala	0.001139588%	Disease Causing	Possibly damaging (score 0.828)	Deleterious (score -3.950)	3	7	Pathogenic	Likely pathogenic
c.1063A>G	p.Lys355Glu	0.001140121%	Disease Causing	Probably damaging (score 1.000)	Deleterious (score -3.911)	4	8	Pathogenic	Likely pathogenic
c.1184C>T	p.Ala395Val	0.009121487%	Disease Causing	Possibly damaging (score 0.684)	Deleterious (score -3.226)	4	8	Pathogenic	Likely pathogenic
c.1220C>G	p.Pro407Arg	0.001141409%	Disease Causing	Benign (score 0.311)	Deleterious (score -5.520)	4	8	Pathogenic	Likely pathogenic
c.1220C>T	p.Pro407Leu	0.002282818%	Disease Causing	Benign (score 0.205)	Deleterious (score -6.431)	4	8	Pathogenic	Likely pathogenic
c.1245G>T	p.Glu415Asp	0.001141852%	Polymorphism	Benign (score 0.000)	Neutral (score 3.287)	1	1	Benign	Benign
c.1285A>C	p.Met429Leu	0.001142152%	Disease Causing	Benign (score 0.004)	Neutral (score -0.832)	2	4	Unknown significance	Benign
c.1287G>C	p.Met429Ile	0.001142113%	Disease Causing	Benign (score 0.004)	Neutral (score -0.715)	2	4	Unknown significance	Benign
c.1291G>A	p.Asp431Asn	0.054846487%	Disease Causing	Benign (score 0.033)	Deleterious (score -3.672)	4	8	Pathogenic	Likely pathogenic
c.1336A>G	p.Arg446Gly	0.001149174%	Disease Causing	Benign (score 0.027)	Neutral (score -1.968)	1	5	Benign	Benign
c.1391T>C	p.Val464Ala	0.005996642%	Polymorphism	Benign (score 0.003)	Neutral (score 0.522)	1	1	Benign	Benign
c.1399A>T	p.Asn467Tyr	0.001198279%	Disease Causing	Benign (score 0.217)	Neutral (score -1.409)	2	2	Unknown significance	Benign
c.1400A>G	p.Asn467Ser	0.001197863%	Polymorphism	Benign (score 0.007)	Neutral (score 0.464)	2	2	Unknown significance	Benign
c.1516A>G	p.Thr506Ala	0.002278813%	Polymorphism	Benign (score 0.004)	Neutral (score -0.660)	2	4	Unknown significance	Benign
c.1526A>C	p.Asn509Thr	0.002278813%	Disease Causing	Benign (score 0.003)	Neutral (score 0.770)	3	6	Pathogenic	Likely benign
c.1536T>G	p.Asn512Lys	0.001139406%	Polymorphism	Benign (score 0.000)	Neutral (score -0.105)	1	1	Benign	Benign
c.1540C>T	p.Arg514Trp	0.001139406%	Disease Causing	Benign (score 0.220)	Deleterious (score -5.752)	4	8	Pathogenic	Likely pathogenic
c.1622G>A	p.Arg541Gln	0.00114167%	Disease Causing	Benign (score 0.000)	Neutral (score 0.881)	3	6	Pathogenic	Likely benign
c.1625G>A	p.Arg542Lys	0.001141592%	Disease Causing	Benign (score 0.000)	Neutral (score 0.187)	4	8	Pathogenic	Likely benign
c.1657A>G	p.Ile553Val	0.002284305%	Polymorphism	Benign (score 0.000)	Neutral (score 0.194)	2	4	Unknown significance	Benign
c.1739G>A	p.Arg580Gln	0.001139614%	Disease Causing	Benign (score 0.016)	Neutral (score -0.604)	4	8	Pathogenic	Likely benign
c.1846C>T	p.Arg616Trp	0.001141149%	Disease Causing	Possibly damaging (score 0.702)	Deleterious (score -4.291)	4	8	Pathogenic	Likely pathogenic
c.1877C>T	p.Pro626Leu	0.001143406%	Disease Causing	Possibly damaging (score 0.819)	Deleterious (score -8.869)	4	8	Pathogenic	Likely pathogenic
c.1889T>C	p.Val630Ala	0.001153669%	Disease Causing	Benign (score 0.004)	Neutral (score -2.517)	3	6	Pathogenic	Likely benign
c.1893C>A	p.Asp631Glu	0.005755528%	Disease Causing	Benign (score 0.000)	Neutral (score -0.073)	4	7	Pathogenic	Likely benign
c.1943C>T	p.Ser648Leu	0.002284226%	Disease Causing	Possibly damaging (score 0.900)	Deleterious (score -5.104)	4	8	Pathogenic	Likely pathogenic
c.1972G>C	p.Val658Leu	0.001141474%	Disease Causing	Possibly damaging (score 0.664)	Deleterious (score -2.611)	4	8	Pathogenic	Likely pathogenic
c.1988G>A	p.Arg663Gln	0.001141435%	Disease Causing	Benign (score 0.003)	Neutral (score -2.047)	4	8	Pathogenic	Likely benign
c.2066G>A	p.Arg689His	0.001146487%	Disease Causing	Benign (score 0.005)	Neutral (score 0.929)	4	8	Pathogenic	Likely benign
c.2070G>A	p.Met690Ile	0.001147579%	Disease Causing	Benign (score 0.041)	Neutral (score -2.431)	4	8	Pathogenic	Likely benign
c.2084G>A	p.Arg695Gln	0.002310403%	Disease Causing	Benign (score 0.149)	Neutral (score -1.114)	4	8	Pathogenic	Likely benign
c.2107A>G	p.Ile703Val	0.001184581%	Disease Causing	Benign (score 0.032)	Neutral (score -0.360)	4	8	Pathogenic	Likely benign

Nucleotide change	Amino acid change	*Reported vAFs	Prediction of functional effects			Evolutionary conservation		Combined analysis	
			MutationTaster	PolyPhen-2	Provean Protein	4 Orthologs	8 Orthologs	1	2
c.2138A>G	p.Lys713Arg	0.002291029%	Disease Causing	Benign (score 0.140)	Neutral (score -0.057)	4	6	Pathogenic	Likely benign
c.2160G>A	p.Met720Ile	0.001139705%	Disease Causing	Benign (score 0.001)	Neutral (score -0.415)	3	6	Pathogenic	Likely benign
c.2171A>G	p.Asp724Gly	0.00227941%	Disease Causing	Benign (score 0.003)	Neutral (score -1.738)	2	5	Unknown significance	Benign
c.2177G>T	p.Gly726Val	0.051286142%	Disease Causing	Benign (score 0.004)	Deleterious (score -2.965)	2	5	Pathogenic	Likely benign
c.2179G>A	p.Ala727Thr	0.001139679%	Polymorphism	Benign (score 0.000)	Neutral (score -0.022)	2	4	Unknown significance	Benign
c.2191C>A	p.Pro731Thr	0.00113977%	Disease Causing	Possibly damaging (score 0.596)	Deleterious (score -3.827)	4	8	Pathogenic	Likely pathogenic
c.2229T>A	p.Asp743Glu	0.001139939%	Disease Causing	Probably damaging (score 0.912)	Deleterious (score -3.618)	4	7	Pathogenic	Likely pathogenic
c.2245G>T	p.Ala749Ser	0.011401079%	Disease Causing	Benign (score 0.201)	Neutral (score -1.829)	4	8	Pathogenic	Likely benign
c.2276C>T	p.Pro759Leu	0.00114537%	Disease Causing	Probably damaging (score 0.942)	Deleterious (score -8.333)	4	8	Pathogenic	Likely pathogenic
c.2382C>A	p.Phe794Leu	0.0011399%	Disease Causing	Possibly damaging (score 0.823)	Deleterious (score -3.602)	4	7	Pathogenic	Likely pathogenic
c.2400G>T	p.Glu800Asp	0.0011399%	Disease Causing	Possibly damaging (score 0.836)	Neutral (score -2.086)	4	7	Pathogenic	Unknown significance
c.2410T>A	p.Cys804Ser	0.001139965%	Disease Causing	Benign (score 0.223)	Deleterious (score -4.226)	4	7	Pathogenic	Likely pathogenic
c.2416G>A	p.Glu806Lys	0.001139965%	Disease Causing	Benign (score 0.273)	Neutral (score -1.272)	4	7	Pathogenic	Likely benign
c.2418G>T	p.Glu806Asp	0.001139978%	Disease Causing	Benign (score 0.261)	Neutral (score -0.973)	4	7	Pathogenic	Likely benign
c.2419C>A	p.Leu807Met	0.001139939%	Disease Causing	Possibly damaging (score 0.837)	Neutral (score -0.939)	4	7	Pathogenic	Unknown significance
c.2429G>A	p.Arg810Gln	0.001140043%	Disease Causing	Benign (score 0.190)	Neutral (score -0.883)	4	7	Pathogenic	Likely benign
c.2474T>C	p.Ile825Thr	0.001143654%	Disease Causing	Possibly damaging (score 0.833)	Deleterious (score -4.270)	3	6	Pathogenic	Likely pathogenic
c.2477C>G	p.Ser826Cys	0.00228467%	Disease Causing	Benign (score 0.111)	Deleterious (score -2.682)	4	6	Pathogenic	Likely pathogenic
c.2531G>A	p.Arg844Gln	0.001139692%	Disease Causing	Benign (score 0.393)	Neutral (score -0.487)	2	5	Unknown significance	Benign
c.2533G>C	p.Glu845Gln	0.001139705%	Disease Causing	Probably damaging (score 0.980)	Deleterious (score -2.663)	3	6	Pathogenic	Likely pathogenic
c.2551G>A	p.Glu851Lys	0.001139614%	Polymorphism	Benign (score 0.003)	Neutral (score -0.954)	1	3	Benign	Benign
c.2563G>A	p.Val855Ile	0.002279254%	Polymorphism	Benign (score 0.003)	Neutral (score 0.611)	1	3	Benign	Benign
c.2594C>A	p.Thr865Asn	0.001139432%	Disease Causing	Benign (score 0.063)	Neutral (score 0.385)	2	3	Unknown significance	Benign
c.2596A>G	p.Ser866Gly	0.001139445%	Disease Causing	Benign (score 0.029)	Neutral (score -1.822)	3	6	Pathogenic	Likely benign
c.2627T>A	p.Met876Lys	0.001139432%	Disease Causing	Benign (score 0.002)	Neutral (score 0.182)	2	3	Unknown significance	Benign
c.2627T>C	p.Met876Thr	0.002278865%	Polymorphism	Benign (score 0.007)	Neutral (score -0.453)	2	3	Unknown significance	Benign
c.2650C>T	p.Arg884Cys	0.001139419%	Disease Causing	Probably damaging (score 0.943)	Deleterious (score -4.910)	3	6	Pathogenic	Likely pathogenic
c.2656C>T	p.Arg886Cys	0.001139432%	Disease Causing	Benign (score 0.003)	Deleterious (score -4.110)	2	3	Pathogenic	Likely benign
c.2662A>G	p.Ile888Val	0.001139419%	Disease Causing	Benign (score 0.001)	Neutral (score 0.375)	3	5	Pathogenic	Benign
c.2680T>A	p.Phe894Ile	0.00797639%	Disease Causing	Probably damaging (score 0.989)	Deleterious (score -5.015)	3	6	Pathogenic	Likely pathogenic
c.2689G>T	p.Gly897Trp	0.001139775%	Polymorphism	Possibly damaging (score 0.781)	Deleterious (score -2.886)	2	4	Unknown significance	Likely benign
c.2695G>A	p.Glu899Lys	0.00227993%	Disease Causing	Benign (score 0.022)	Neutral (score -0.527)	2	3	Unknown significance	Benign

OCRL1 variants obtained from ExAC[236] that were used to investigate the effectiveness of *in silico* methods for variant analysis (Chapter 6). Nucleotide number is according to transcript ENST00000371113 and amino acid number is according to the full-length 901 amino acid protein (NCBI NP_00267; UniProt) as displayed on ExAC. *Reported vAFs were also obtained from ExAC[236]. Evolutionary conservation scores were based on the number of orthologs each WT residue was conserved in, the number of orthologs studied in each analysis is detailed in the column heading, as detailed in Chapter 6. Combined analysis 1 and 2 are based on the criteria detailed in Chapter 6.

Table 48. *In silico* analysis of *UMOD* variants obtained from ExAC

Nucleotide change	Amino acid change	*Reported vAFs	Prediction of functional effects			Evolutionary conservation		Combined analysis	
			MutationTaster	PolyPhen-2	Provean Protein	4 Orthologs	8 Orthologs	1	2
c.10C>A	p.Pro4Thr	0.000825573%	Polymorphism	Benign (score 0.005)	Neutral (score -0.630)	2	2	Unknown significance	Likely benign
c.13T>C	p.Ser5Pro	0.000825396%	Polymorphism	Benign (score 0.001)	Neutral (score -0.598)	0	0	Benign	Likely benign
c.22T>C	p.Trp8Arg	0.000825069%	Polymorphism	Benign (score 0.003)	Neutral (score -1.929)	3	4	Pathogenic	Likely benign
c.33G>T	p.Met11Ile	0.001650111%	Polymorphism	Benign (score 0.001)	Neutral (score -0.316)	1	1	Benign	Benign
c.37G>C	p.Val13Leu	0.000825137%	Polymorphism	Benign (score 0)	Neutral (score -0.217)	3	3	Pathogenic	Likely benign
c.46T>C	p.Ser16Pro	0.000825287%	Polymorphism	Benign (score 0.002)	Neutral (score -0.224)	3	5	Pathogenic	Likely benign
c.53T>C	p.Phe18Ser	0.000825287%	Polymorphism	Benign (score 0.001)	Neutral (score -0.897)	2	2	Unknown significance	Likely benign
c.56T>C	p.Ile19Thr	0.001650683%	Polymorphism	Benign (score 0.001)	Neutral (score 0.346)	2	3	Unknown significance	Benign
c.73G>A	p.Asp25Asn	0.005781684%	Polymorphism	Benign (score 0.004)	Neutral (score 0.347)	1	2	Benign	Benign
c.74A>G	p.Asp25Gly	0.00412841%	Polymorphism	Benign (score 0.004)	Neutral (score 0.043)	1	2	Benign	Benign
c.77C>G	p.Thr26Ser	0.002477251%	Polymorphism	Benign (score of 0)	Neutral (score 0.045)	2	3	Unknown significance	Benign
c.77C>T	p.Thr26Ile	0.0016515%	Polymorphism	Benign (score 0.001)	Neutral (score -0.891)	2	3	Unknown significance	Benign
c.96C>A	p.Cys32*	0.00089332%	Disease Causing	N/A	N/A	4	7	Pathogenic	Pathogenic
c.97T>C	p.Ser33Pro	0.001775663%	Polymorphism	Probably damaging (score 0.952)	Neutral (score -2.000)	4	7	Pathogenic	Likely benign
c.116C>T	p.Ala39Val	0.000861312%	Disease Causing	Probably damaging (score 0.998)	Neutral (score -1.767)	4	7	Pathogenic	Pathogenic
c.125C>T	p.Thr42Met	0.002562613%	Polymorphism	Benign (score 0.006)	Neutral (score -0.574)	3	3	Pathogenic	Benign
c.143C>A	p.Thr48Lys	0.000849098%	Polymorphism	Possibly damaging (score 0.642)	Neutral (score -1.291)	3	4	Pathogenic	Likely benign
c.143C>T	p.Thr48Met	0.000849098%	Polymorphism	Probably damaging (score 0.928)	Neutral (score -0.655)	3	4	Pathogenic	Likely benign
c.152C>A	p.Thr51Asn	0.002552757%	Polymorphism	Benign (score 0.139)	Neutral (score -1.160)	2	2	Unknown significance	Benign
c.172G>A	p.Gly58Ser	0.002588528%	Disease Causing	Probably damaging (score of 1.000)	Deleterious (score -2.858)	4	7	Pathogenic	Likely pathogenic
c.184A>C	p.Thr62Pro	0.037717313%	Polymorphism	Benign (score 0.212)	Neutral (score -1.491)	1	2	Benign	Benign
c.208G>A	p.Ala70Thr	0.000978684%	Polymorphism	Possibly damaging (score 0.508)	Neutral (score -1.405)	4	5	Pathogenic	Likely benign
c.209C>T	p.Ala70Val	0.00196742%	Polymorphism	Benign (score 0.046)	Neutral (score -1.392)	4	5	Pathogenic	Benign
c.226A>G	p.Asn76Asp	0.001190051%	Polymorphism	Benign (score 0.04)	Neutral (score -1.788)	3	5	Pathogenic	Benign
c.250G>A	p.Val84Ile	0.001710981%	Polymorphism	Benign (score 0.404)	Neutral (score -0.289)	4	6	Pathogenic	Likely benign
c.256A>T	p.Thr86Ser	0.001842842%	Polymorphism	Benign (score 0.028)	Neutral (score -1.425)	4	6	Pathogenic	Likely benign
c.257C>G	p.Thr86Arg	0.00374911%	Polymorphism	Possibly damaging (score 0.843)	Neutral (score -2.052)	4	6	Pathogenic	Likely benign
c.259C>G	p.Pro87Ala	0.001939789%	Polymorphism	Benign (score 0.138)	Neutral (score -0.498)	2	3	Unknown significance	Benign
c.289G>A	p.Gly97Ser	0.002918174%	Disease Causing	Probably damaging (score of 1.000	Neutral (score -2.235)	4	6	Pathogenic	Likely pathogenic
c.295C>T	p.Arg99Cys	0.003101352%	Disease Causing	Possibly damaging (score 0.832)	Neutral (score -1.969)	2	4	Unknown significance	Likely benign
c.313G>C	p.Gly105Arg	0.00727855%	Polymorphism	Probably damaging (score 0.984)	Neutral(score -1.264)	2	4	Unknown significance	Benign
c.317G>T	p.Cys106Phe	0.003703704%	Disease Causing	Probably damaging (score 0.999)	Deleterious (score -4.504)	4	6	Pathogenic	Likely pathogenic
c.319A>G	p.Thr107Ala	0.003713882%	Polymorphism	Benign (score 0.016)	Neutral (score -0.892)	2	2	Unknown significance	Benign
c.325G>T	p.Val109Leu	0.007590133%	Disease Causing	Possibly damaging (score 0.745)	Neutral (score -0.926)	3	4	Pathogenic	Likely benign
c.326T>A	p.Val109Glu	0.003827898%	Disease Causing	Probably damaging (score 0.982)	Neutral (score -2.3)	3	4	Pathogenic	Likely benign
c.343C>A	p.Pro115Thr	0.004030958%	Polymorphism	Possibly damaging (score 0.864)	Neutral (score -2343)	3	6	Pathogenic	Likely benign
c.361C>T	p.His121Tyr	0.004297379%	Polymorphism	Probably damaging (score 0.996)	Neutral (score -1.575)	4	7	Pathogenic	Likely benign
c.389T>C	p.Val130Ala	0.009918667%	Polymorphism	Benign (score 0.006)	Neutral (score -0.079)	2	2	Unknown significance	Benign
c.392G>A	p.Gly131Asp	0.015222245%	Disease Causing	Probably damaging (score 0.995)	Deleterious (score -3.159)	4	7	Pathogenic	Likely pathogenic

Nucleotide change	Amino acid change	*Reported vAFs	Prediction of functional effects			Evolutionary conservation		Combined analysis	
			MutationTaster	PolyPhen-2	Provean Protein	4 Orthologs	8 Orthologs	1	2
c.416C>T	p.Ala139Val	0.01734104%	Polymorphism	Benign (score 0.018)	Neutral (score -1.070)	2	3	Unknown significance	Benign
c.425G>A	p.Arg142Gln	1.962673089%	Polymorphism	Benign (score 0.014)	Neutral (score -0.148)	1	2	Benign	Benign
c.439C>T	p.His147Tyr	0.006292474%	Polymorphism	Benign (score 0.007)	Neutral (score -0.095)	2	2	Unknown significance	Benign
c.488C>T	p.Pro163Leu	0.006887052%	Disease Causing	Benign (score 0.076)	Neutral (score -2.066)	2	3	Unknown significance	Benign
c.502C>G	p.Leu168Val	0.006946374%	Polymorphism	Benign (score 0.05)	Neutral (score -0.51)	3	3	Pathogenic	Benign
c.505G>A	p.Val169Met	0.020847811%	Polymorphism	Benign (score 0.052)	Neutral (score -0.694)	3	4	Pathogenic	Benign
c.527C>A	p.Ala176Glu	0.007667536%	Polymorphism	Benign (score 0.001)	Neutral (score 0.541)	1	1	Benign	Benign
c.538C>G	p.Leu180Val	0.336854999%	Disease Causing	Probably damaging (score 0.973)	Neutral (score -1.934)	4	8	Pathogenic	Likely pathogenic
c.562G>A	p.Glu188Lys	0.007375719%	Polymorphism	Benign (score 0.229)	Neutral (score -1.612)	3	4	Pathogenic	Benign
c.590C>T	p.Thr197Met	0.006253909%	Polymorphism	Benign (score 0.075)	Neutral (score -1.3)	1	1	Benign	Benign
c.635G>T	p.Arg212Leu	0.004753755%	Polymorphism	Benign (score 0.307)	Deleterious (score -3.884)	4	7	Pathogenic	Likely benign
c.655C>G	p.Pro219Ala	0.003203485%	Polymorphism	Benign (score 0.243)	Deleterious (score -4.032)	4	7	Pathogenic	Likely benign
c.656C>T	p.Pro219Leu	0.003146237%	Disease Causing	Possibly damaging (score 0.858)	Deleterious (score -5.341)	4	7	Pathogenic	Likely pathogenic
c.685A>T	p.Met229Leu	0.011038015%	Polymorphism	Benign (score 0.003)	Neutral (score -1.019)	4	7	Pathogenic	Likely benign
c.713G>C	p.Ser238Thr	0.001792886%	Polymorphism	Benign (score 0.055)	Neutral (score -0.477)	3	6	Pathogenic	Likely benign
c.714C>G	p.Ser238Arg	0.007138778%	Polymorphism	Benign (score 0.008)	Neutral (score -1.131)	3	6	Pathogenic	Likely benign
c.734G>A	p.Arg245His	0.014098628%	Disease Causing	Benign (score 0.018)	Neutral (score -2.308)	4	6	Pathogenic	Likely benign
c.746C>T	p.Ala249Val	0.001418882%	Disease Causing	Probably damaging (score 0.998)	Deleterious (score -2.624)	4	8	Pathogenic	Likely pathogenic
c.758G>A	p.Gly253Asp	0.001316274%	Polymorphism	Benign (score 0.006)	Neutral (score -1.926)	3	6	Pathogenic	Likely benign
c.790G>A	p.Val264Met	0.001068536%	Disease Causing	Possibly damaging (score 0.854)	Neutral (score -1.996)	3	7	Pathogenic	Unknown significance
c.794A>T	p.Lys265Met	0.000977345%	Disease Causing	Probably damaging (score 0.998)	Deleterious (score -4.496)	4	8	Pathogenic	Pathogenic
c.796G>T	p.Ala266Ser	0.000969876%	Disease Causing	Probably damaging (score 0.980)	Neutral (score -1.874)	4	8	Pathogenic	Pathogenic
c.805G>A	p.Gly269Ser	0.000941957%	Disease Causing	Possibly damaging (score 0.630)	Deleterious (score -3.830)	4	8	Pathogenic	Pathogenic
c.808G>A	p.Gly270Ser	0.000930094%	Polymorphism	Probably damaging (score 0.964)	Deleterious (score -3.467)	4	7	Pathogenic	Pathogenic
c.816C>A	p.Tyr272*	0.00091696%	Disease Causing	N/A	N/A	3	7	Pathogenic	Pathogenic
c.821A>G	p.Tyr274Cys	0.000906964%	Disease Causing	Probably damaging (score 0.999)	Deleterious (score -6.576)	4	8	Pathogenic	Pathogenic
c.824A>G	p.Asn275Ser	0.001783994%	Polymorphism	Benign (score 0.2)	Neutral (score -1.131)	4	6	Pathogenic	Likely benign
c.842A>G	p.Glu281Gly	0.006042296%	Polymorphism	Benign (score 0.031)	Neutral (score -2.051)	3	5	Pathogenic	Benign
c.854C>T	p.Ala285Val	0.00084809%	Polymorphism	Possibly damaging (score 0.844)	Neutral (score -2.257)	4	7	Pathogenic	Likely pathogenic
c.875C>A	p.Ser292Tyr	0.001647528%	Disease Causing	Probably damaging (score 0.921)	Deleterious (score -2.938)	4	7	Pathogenic	Likely pathogenic
c.884G>C	p.Gly295Ala	0.000823696%	Disease Causing	Possibly damaging (score 0.622)	Neutral (score -1.592)	4	6	Pathogenic	Likely pathogenic
c.892G>A	p.Glu298Lys	0.001647392%	Polymorphism	Benign (score 0.059)	Neutral (score -1.240)	3	4	Pathogenic	Benign
c.894G>C	p.Glu298Asp	0.000823696%	Polymorphism	Benign (score 0.012)	Neutral (score -0.710)	3	4	Pathogenic	Likely benign
c.897G>T	p.Glu299Asp	0.000823683%	Polymorphism	Benign (score 0.015)	Neutral (score -0.555)	3	4	Pathogenic	Likely benign
c.910G>C	p.Glu304Gln	0.000823696%	Polymorphism	Probably damaging (score 0.995)	Neutral (score -2.275)	4	7	Pathogenic	Likely pathogenic
c.912G>C	p.Glu304Asp	0.000823683%	Polymorphism	Possibly damaging (score 0.620)	Neutral (score -2.191)	4	7	Pathogenic	Likely pathogenic
c.913G>A	p.Asp305Asn	0.000823683%	Polymorphism	Benign (score 0.439)	Neutral (score -2.084)	3	5	Pathogenic	Likely benign
c.919A>T	p.Lys307*	0.000823683%	Disease Causing	N/A	N/A	2	2	Pathogenic	Likely pathogenic
c.927T>G	p.Asn309Lys	0.000823683%	Polymorphism	Benign (score 0.012)	Neutral (score -0.081)	0	0	Benign	Likely benign
c.953A>G	p.Lys318Arg	0.001647446%	Polymorphism	Benign (score 0.052)	Neutral (score -0,218)	3	5	Pathogenic	Benign
c.955C>T	p.Gln319*	0.000823737%	Disease Causing	N/A	N/A	3	6	Pathogenic	Pathogenic

Nucleotide change	Amino acid change	*Reported vAFs	Prediction of functional effects			Evolutionary conservation		Combined analysis	
			MutationTaster	PolyPhen-2	Provean Protein	4 Orthologs	8 Orthologs	1	2
c.965A>G	p.Asn322Ser	0.000823818%	Polymorphism	Benign (score 0.057)	Neutral(score -2.309)	3	4	Pathogenic	Likely benign
c.966C>G	p.Asn322Lys	0.000823873%	Polymorphism	Possibly damaging (score 0.493)	Deleterious (score -2.872)	3	4	Pathogenic	Unknown significance
c.970A>G	p.Thr324Ala	0.002471781%	Polymorphism	Benign (score 0.059)	Neutral (score -1.352)	3	4	Pathogenic	Benign
c.986T>C	p.Leu329Pro	0.000825232%	Disease Causing	Probably damaging (score 0.997)	Deleterious (score -5.193)	4	7	Pathogenic	Pathogenic
c.988G>A	p.Glu330Lys	0.000825151%	Disease Causing	Benign (score (0.009)	Neutral (score -0.581)	3	5	Pathogenic	Likely benign
c.992A>T	p.His331Leu	0.002474635%	Polymorphism	Benign (score 0.045)	Neutral (score -1.705)	1	1	Benign	Benign
c.993C>G	p.His331Gln	0.001649757%	Polymorphism	Benign (score 0.045)	Neutral(score -0.164)	1	1	Benign	Benign
c.1001A>C	p.Glu334Ala	0.000824565%	Polymorphism	Benign (score 0.216)	Neutral (score -2.042)	3	4	Pathogenic	Likely benign
c.1009G>A	p.Ala337Thr	0.000824307%	Polymorphism	Benign (score 0.371)	Neutral (score -1.931)	2	5	Unknown significance	Likely benign
c.1028C>T	p.Ser343Leu	0.001648098%	Disease Causing	Possibly damaging (score 0.642)	Deleterious (score -3.943)	4	7	Pathogenic	Likely pathogenic
c.1042C>T	p.Gln348*	0.005768724%	Disease Causing	N/A	N/A	4	5	Pathogenic	Likely benign
c.1050G>T	p.Lys350Asn	0.000824117%	Polymorphism	Benign (score 0.06)	Neutral (score -0.832)	2	3	Unknown significance	Likely benign
c.1063G>A	p.Asp355Asn	0.000824158%	Polymorphism	Benign (score 0.027)	Neutral (score -0.573)	2	2	Unknown significance	Likely benign
c.1076T>G	p.Met359Arg	0.001648696%	Disease Causing	Possibly damaging (score 0.664)	Neutral (score -2.064)	3	4	Pathogenic	Likely benign
c.1077G>A	p.Met359Ile	0.000824362%	Polymorphism	Benign (score 0.229)	Neutral (score -0.327)	3	4	Pathogenic	Likely benign
c.1081C>A	p.Leu361Met	0.00247337%	Polymorphism	Probably damaging (score of 1.000)	Neutral (score -1.688)	4	7	Pathogenic	Likely benign
c.1091G>C	p.Ser364Thr	0.000824701%	Polymorphism	Benign (score 0.309)	Neutral (score -1.210)	3	4	Pathogenic	Likely benign
c.1093C>T	p.Arg365Trp	0.001649675%	Polymorphism	Possibly damaging (score 0.849)	Deleterious (score -2.600)	1	1	Unknown significance	Likely benign
c.1094G>A	p.Arg365Gln	0.001649757%	Polymorphism	Benign (score 0.007)	Neutral (score 0.422)	1	1	Benign	Benign
c.1100C>T	p.Ser367Leu	0.000825083%	Polymorphism	Benign (score 0.052)	Deleterious (score -3.066)	3	4	Pathogenic	Likely benign
c.1123C>T	p.Arg375Trp	0.001652893%	Polymorphism	Probably damaging (score 0.930)	Deleterious (score -3.497)	3	5	Pathogenic	Likely benign
c.1124G>A	p.Arg375Gln	0.076906538%	Polymorphism	Benign (score 0.036)	Neutral (score -0.346)	3	5	Pathogenic	Benign
c.1129T>A	p.Trp377Arg	0.000827212%	Disease Causing	Probably damaging (score 0.988)	Deleterious (score -7.317)	3	6	Pathogenic	Pathogenic
c.1131G>C	p.Trp377Cys	0.00082739%	Disease Causing	Probably damaging (score 0.994)	Deleterious (score -6.968)	3	6	Pathogenic	Pathogenic
c.1132G>C	p.Val378Leu	0.000827294%	Polymorphism	Benign (score 0.026)	Neutral (score -0.657)	1	3	Benign	Likely benign
c.1132G>T	p.Val378Leu	0.000827294%	Polymorphism	Benign (score 0.026)	Neutral (score -0.657)	1	3	Benign	Likely benign
c.1144A>G	p.Thr382Ala	0.000828226%	Disease Causing	Possibly damaging (score 0.688)	Neutral (score -1.455)	3	6	Pathogenic	Likely pathogenic
c.1148C>T	p.Pro383Leu	0.000828706%	Disease Causing	Probably damaging (score 0.954)	Deleterious (score -6.821)	3	7	Pathogenic	Pathogenic
c.1153C>G	p.Arg385Gly	0.000830068%	Polymorphism	Benign (score 0.112)	Deleterious (score -3.551)	3	5	Pathogenic	Likely benign
c.1153C>T	p.Arg385Trp	0.016601368%	Polymorphism	Possibly damaging (score 0.893)	Deleterious (score -3.822)	3	5	Pathogenic	Likely benign
c.1154G>A	p.Arg385Gln	0.004149998%	Polymorphism	Benign (score 0.01)	Neutral (score 0.04)	3	5	Pathogenic	Benign
c.1160G>A	p.Gly387Asp	0.000830648%	Disease Causing	Probably damaging (score 0.977)	Deleterious (score -3.922)	3	6	Pathogenic	Pathogenic
c.1162C>T	p.Pro388Ser	0.000830993%	Disease Causing	Possibly damaging (score 0.674)	Neutral (score -0.867)	3	5	Pathogenic	Unknown significance
c.1175T>G	p.Val392Gly	0.000832723%	Disease Causing	Possibly damaging (score 0.830)	Deleterious (score -4.040)	3	4	Pathogenic	Likely pathogenic
c.1181C>T	p.Thr394Met	0.00417411%	Polymorphism	Benign (score 0.028)	Neutral (score -0.744)	2	3	Unknown significance	Benign
c.1189G>T	p.Glu397*	0.000824307%	Disease Causing	N/A	N/A	3	5	Pathogenic	Likely pathogenic
c.1198G>T	p.Ala400Ser	0.000824144%	Disease Causing	Probably damaging (score 0.995)	Neutral (score -2.311)	4	7	Pathogenic	Pathogenic
c.1201A>G	p.Thr401Ala	0.001648152%	Disease Causing	Possibly damaging (score 0.777)	Neutral (score -1.417)	3	6	Pathogenic	Unknown significance
c.1208G>A	p.Ser403Asn	0.000823968%	Disease Causing	Possibly damaging (score 0.900)	Neutral (score -1.119)	3	6	Pathogenic	Likely pathogenic
c.1228G>T	p.Asp410Tyr	0.001647664%	Polymorphism	Probably damaging (score 0.934)	Deleterious (score -3.343)	2	3	Pathogenic	Likely benign
c.1237A>C	p.Ile413Leu	0.000823818%	Disease Causing	Possibly damaging (score 0.517)	Neutral (score -1.764)	4	6	Pathogenic	Likely pathogenic

Nucleotide change	Amino acid change	*Reported vAFs	Prediction of functional effects			Evolutionary conservation		Combined analysis	
			MutationTaster	PolyPhen-2	Provean Protein	4 Orthologs	8 Orthologs	1	2
c.1243C>T	p.Arg415Cys	0.0016476915	Disease Causing	Probably damaging (score 0.982)	Deleterious (score -6.749)	3	7	Pathogenic	Likely pathogenic
c.1244G>A	p.Arg415His	0.0016476645	Disease Causing	Probably damaging (score 0.982)	Deleterious (score -4.274)	3	7	Pathogenic	Likely pathogenic
c.1246G>A	p.Asp416Asn	0.006590546%	Disease Causing	Probably damaging (score 0.992)	Deleterious (score -3.511)	4	7	Pathogenic	Likely pathogenic
c.1265A>G	p.Asn422Ser	0.002471495%	Polymorphism	Probably damaging (score 0.973)	Deleterious (score -2.585)	3	6	Pathogenic	Likely pathogenic
c.1271C>T	p.Ala424Val	0.000823859%	Polymorphism	Benign (score 0.369)	Neutral (score -1.755)	2	3	Unknown significance	Likely benign
c.1283C>T	p.Pro428Leu	0.001647854%	Disease Causing	Probably damaging (score of 0.999)	Deleterious (score -8.355)	4	7	Pathogenic	Likely pathogenic
c.1288G>A	p.Asp430Asn	0.004119906%	Disease Causing	Probably damaging (score 0.980)	Deleterious (score -3.777)	4	7	Pathogenic	Likely pathogenic
c.1291A>G	p.Met431Val	0.000823981%	Disease Causing	Probably damaging (score 0.972)	Deleterious (score -2.900)	4	7	Pathogenic	Pathogenic
c.1297G>A	p.Val433Ile	0.000824008%	Disease Causing	Benign (score 0.181)	Neutral (score -0.408)	3	5	Pathogenic	Likely benign
c.1310C>G	p.Thr437Ser	0.003296577%	Polymorphism	Possibly damaging (score 0.626)	Neutral (score -2.317)	4	7	Pathogenic	Likely benign
c.1312G>A	p.Ala438Thr	0.001648478%	Polymorphism	Possibly damaging (score 0.487)	Deleterious (score -2.685)	1	4	Unknown significance	Likely benign
c.1312G>T	p.Ala438Ser	0.001648478%	Polymorphism	Benign (score 0.047)	Neutral (score -1.711)	1	4	Benign	Benign
c.1318C>G	p.Gln440Glu	0.001648506%	Disease Causing	Benign (score 0.403)	Neutral (score -1.681)	3	6	Pathogenic	Likely benign
c.1320G>T	p.Gln440His	0.000824266%	Disease Causing	Benign (score 0.071)	Neutral (score -2.324)	3	6	Pathogenic	Likely pathogenic
c.1332T>A	p.Ser444Arg	0.000824701%	Polymorphism	Probably damaging (score of 0.999)	Deleterious (score -4.605)	4	7	Pathogenic	Pathogenic
c.1336C>G	p.Leu446Val	0.000824538%	Polymorphism	Possibly damaging (score 0.874)	Neutral (score -1.336)	3	6	Pathogenic	Likely pathogenic
c.1354G>A	p.Gly452Arg	0.002472595%	Disease Causing	Probably damaging (score of 0.999)	Deleterious (score -6.551)	4	6	Pathogenic	Likely pathogenic
c.1360G>A	p.Gly454Ser	0.001648207%	Disease Causing	Probably damaging (score of 1.000	Deleterious (score -5.315)	4	7	Pathogenic	Likely pathogenic
c.1372G>A	p.Val458Met	0.001647962%	Disease Causing	Probably damaging (score of 0.999)	Neutral (score -2.92)	3	6	Pathogenic	Likely pathogenic
c.1372G>C	p.Val458Leu	0.006591849%	Disease Causing	Probably damaging (score 0.988)	Neutral (score -2.326)	3	6	Pathogenic	Likely pathogenic
c.1372G>T	p.Val458Leu	2.024521679%	Polymorphism	Probably damaging (score 0.988)	Neutral (score -2.326)	3	6	Benign	Likely benign
c.1375C>T	p.Arg459Trp	0.042023039%	Disease Causing	Probably damaging (score 0.969)	Deleterious (score -5.497)	3	5	Pathogenic	Likely benign
c.1376G>A	p.Arg459Gln	0.113711272%	Polymorphism	Benign (score 0.260)	Neutral (score -2.460)	3	5	Pathogenic	Benign
c.1381G>A	p.Ala461Thr	0.002471984%	Disease Causing	Probably damaging (score of 0.999)	Deleterious (score -3.156)	4	7	Pathogenic	Likely pathogenic
c.1382C>T	p.Ala461Val	0.003296848%	Disease Causing	Probably damaging (score of 0.999)	Deleterious (score -3.156)	4	7	Pathogenic	Likely pathogenic
c.1390C>T	p.Gln464*	0.001648044%	Disease Causing	N/A	N/A	3	4	Pathogenic	Likely benign
c.1403A>C	p.Tyr468Ser	0.000824063%	Disease Causing	Probably damaging (score 0.988)	Deleterious (score -8.380)	4	7	Pathogenic	Pathogenic
c.1406C>A	p.Thr469Lys	0.002472066%	Polymorphism	Probably damaging (score 0.998)	Deleterious (score -3.446)	3	7	Pathogenic	Likely pathogenic
c.1406C>T	p.Thr469Met	0.066745773%	Polymorphism	Probably damaging (score 0.998)	Deleterious (score -4.118)	3	7	Pathogenic	Likely pathogenic
c.1410G>C	p.Gln470His	0.00164818%	Polymorphism	Benign (score 0.063)	Neutral (score 0.057)	3	3	Pathogenic	Benign
c.1414T>C	p.Tyr472His	0.000824103%	Polymorphism	Benign (score 0.330)	Deleterious (score -4.464)	3	6	Pathogenic	Likely pathogenic
c.1424C>G	p.Ser475Cys	0.000823995%	Polymorphism	Probably damaging (score 0.950)	Deleterious (score -2.751)	2	5	Pathogenic	Likely pathogenic
c.1429G>A	p.Val477Met	0.003296359%	Disease Causing	Probably damaging (score 0.996)	Neutral (score -2.307)	3	5	Pathogenic	Likely benign
c.1436T>C	p.Leu479Pro	0.000824035%	Disease Causing	Probably damaging (score of 1.000	Deleterious (score -6.440)	4	7	Pathogenic	Pathogenic
c.1439C>A	p.Ser480Tyr	0.000824035%	Disease Causing	Probably damaging (score of 0.971)	Deleterious (score -3.040)	3	6	Pathogenic	Pathogenic
c.1444G>A	p.Glu482Lys	0.003296685%	Polymorphism	Possibly damaging (score 0.698)	Neutral (score -2.213)	3	6	Pathogenic	Likely benign
c.1447G>A	p.Ala483Thr	0.000824131%	Disease Causing	Benign (score 0.297)	Neutral (score -0.439)	3	6	Pathogenic	Likely pathogenic
c.1448C>T	p.Ala483Val	0.0107131675	Disease Causing	Possibly damaging (score 0.752)	Neutral (score -2.295)	3	6	Pathogenic	Unknown significance
c.1458C>A	p.Tyr486*	0.000824212%	Disease Causing	N/A	N/A	4	7	Pathogenic	Pathogenic
c.1459G>A	p.Val487Met	0.000824253%	Disease Causing	Probably damaging (score of 1.000	Deleterious (score -2.742)	3	6	Pathogenic	Pathogenic
c.1468A>C	p.Met490Leu	0.001648478%	Polymorphism	Benign (score 0.01)	Neutral (score -0.181)	3	4	Pathogenic	Benign

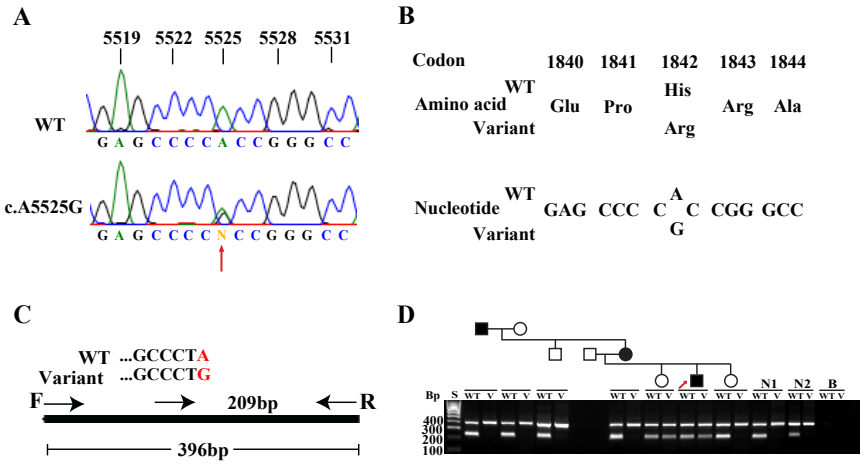
Nucleotide change	Amino acid change	*Reported vAFs	Prediction of functional effects			Evolutionary conservation		Combined analysis	
			MutationTaster	PolyPhen-2	Provean Protein	4 Orthologs	8 Orthologs	1	2
c.1469T>C	p.Met490Thr	0.000824226%	Polymorphism	Benign (score 0.216)	Neutral (score -2.348)	3	4	Pathogenic	Likely benign
c.1475A>G	p.Asp492Gly	0.002473044%	Disease Causing	Possibly damaging (score 0.719)	Deleterious (score -3.583)	4	5	Pathogenic	Likely benign
c.1476T>A	p.Asp492Glu	0.000824307%	Polymorphism	Benign (score of 0.040)	Neutral (score 0.390)	4	5	Pathogenic	Likely benign
c.1483G>A	p.Asp495Asn	0.000824538%	Disease Causing	Probably damaging (score 0.968)	Deleterious (score -4.637)	4	7	Pathogenic	Pathogenic
c.1492C>T	p.Arg498*	0.000824729%	Disease Causing	N/A	N/A	3	5	Pathogenic	Likely pathogenic
c.1493G>A	p.Arg498Gln	0.000824756%	Polymorphism	Benign (score of 0.053)	Neutral (score -0.727)	3	5	Pathogenic	Likely benign
c.1497T>A	p.Phe499Leu	0.001649539%	Disease Causing	Probably damaging (score of 0.999)	Deleterious (score -4.344)	4	7	Pathogenic	Likely pathogenic
c.1499C>T	p.Ala500Val	0.000824865%	Polymorphism	Benign (score of 0.006)	Neutral (score -0.862)	2	3	Unknown significance	Likely benign
c.1526C>T	p.Thr509Ile	0.001652183%	Disease Causing	Probably damaging (score of 1.000	Deleterious (score-5.804)	4	8	Pathogenic	Likely pathogenic
c.1534A>G	p.Ser512Gly	0.000827116%	Polymorphism	Benign (score of 0.001)	Neutral (score -1.926)	3	5	Pathogenic	Likely benign
c.1544C>G	p.Thr515Arg	0.000829573%	Disease Causing	Possibly damaging (score 0.895)	Deleterious (score -2.846)	3	6	Pathogenic	Pathogenic
c.1544C>T	p.Thr515Met	0.005807008%	Disease Causing	Benign (score 0.418)	Deleterious (score -3.442)	3	6	Pathogenic	Likely pathogenic
c.1546G>T	p.Asp516Tyr	0.000830813%	Disease Causing	Probably damaging (score of 0.999)	Deleterious (score -7.413)	4	7	Pathogenic	Pathogenic
c.1549C>T	p.Pro517Ser	0.000831781%	Disease Causing	Probably damaging (score 0.977)	Deleterious (score -5.317)	4	8	Pathogenic	Pathogenic
c.1560C>G	p.Tyr520*	0.00084011%	Disease Causing	N/A	N/A	4	7	Pathogenic	Pathogenic
c.1562T>C	p.Phe521Ser	0.002526018%	Disease Causing	Probably damaging (score 0.997)	Deleterious (score -5.755)	3	5	Pathogenic	Likely benign
c.1564A>G	p.Ile522Val	0.001688733%	Disease Causing	Possibly damaging (score 0.855)	Neutral (score -0.795)	4	8	Pathogenic	Unknown significance
c.1576A>G	p.Arg526Gly	0.000869218%	Disease Causing	Benign (score 0.023)	Neutral (score -1.145)	3	4	Pathogenic	Likely benign
c.1579T>C	p.Cys527Arg	0.000825696%	Disease Causing	Probably damaging (score of 1.000)	Deleterious (score -10.718)	4	7	Pathogenic	Pathogenic
c.1589C>T	p.Thr530Ile	0.000824974%	Polymorphism	Benign (score 0.023)	Neutral (score -1.765)	3	5	Pathogenic	Likely benign
c.1594G>T	p.Asp532Tyr	0.000824661%	Disease Causing	Probably damaging (score of 1.000)	Deleterious (score -7.830)	4	7	Pathogenic	Pathogenic
c.1603A>C	p.Ile535Leu	0.000824362%	Polymorphism	Possibly damaging (score of 0.589)	Neutral (score -1.792)	3	6	Pathogenic	Likely pathogenic
c.1622G>A	p.Gly541Glu	0.000824035%	Disease Causing	Probably damaging (score of 1.000)	Deleterious (score -7.016)	4	7	Pathogenic	Pathogenic
c.1624G>A	p.Glu542Lys	0.000824008%	Polymorphism	Benign (score 0.309)	Neutral (score -0.788)	3	4	Pathogenic	Likely benign
c.1636G>A	p.Gly546Ser	0.000823981%	Polymorphism	Benign (score 0.277)	Neutral (score -0.514)	2	5	Unknown significance	Likely benign
c.1639C>T	p.Arg547*	0.001647935%	Disease Causing	N/A	N/A	4	6	Pathogenic	Likely pathogenic
c.1640G>A	p.Arg547Gln	0.002471943%	Disease Causing	Possibly damaging (score 0.692)	Deleterious (score -2.873)	4	6	Pathogenic	Likely pathogenic
c.1645T>C	p.Ser549Pro	0.000823968%	Disease Causing	Probably damaging (score 0.998)	Deleterious (score -4.33)	4	7	Pathogenic	Pathogenic
c.1648G>A	p.Val550Ile	0.013183264%	Polymorphism	Benign (score 0.415)	Neutral (score -0.503)	3	5	Pathogenic	Benign
c.1660C>T	p.Arg554Trp	0.001647827%	Disease Causing	Probably damaging (score 0.47)	Deleterious (score -2.863)	3	5	Pathogenic	Likely benign
c.1661G>A	p.Arg554Gln	0.006591306%	Disease Causing	Possibly damaging (score 0.490)	Neutral (score -0.847)	3	5	Pathogenic	Likely benign
c.1680C>G	p.Asp560Glu	0.000824049%	Disease Causing	Probably damaging (score 0.994)	Deleterious (score -2.842)	3	6	Pathogenic	Pathogenic
c.1715A>G	p.Asp572Gly	0.000825232%	Disease Causing	Probably damaging (score 0.995)	Deleterious (score -5.505)	4	7	Pathogenic	Pathogenic
c.1717A>G	p.Thr573Ala	0.0008253%	Polymorphism	Benign (score 0.008)	Neutral (score -1.316)	2	4	Unknown significance	Likely benign
c.1741A>T	p.Thr581Ser	0.001655245%	Polymorphism	Benign (score 0.023)	Neutral (score -0.009)	4	6	Pathogenic	Likely benign
c.1742C>A	p.Thr581Asn	0.025647814%	Disease Causing	Possibly damaging (score 0.589)	Neutral (score -1.826)	4	6	Pathogenic	Unknown significance
c.1742C>T	p.Thr581Ile	0.000827349%	Disease Causing	Possibly damaging (score 0.507)	Deleterious (score -3.420)	4	6	Pathogenic	Pathogenic
c.1748C>T	p.Ser583Phe	0.00082605%	Polymorphism	Benign (score 0.363)	Deleterious (score -4.277)	3	6	Pathogenic	Likely pathogenic
c.1751G>T	p.Gly584Val	0.000825655%	Disease Causing	Possibly damaging (score 0.826)	Deleterious (score -4.470)	3	5	Pathogenic	Likely pathogenic
c.1754C>T	p.Thr585Ile	0.099862998%	Polymorphism	Benign (score 0.196)	Neutral (score -2.390)	3	5	Pathogenic	Benign
c.1760T>G	p.Phe587Cys	0.0008248925	Disease Causing	Possibly damaging (score 0.593)	Neutral (score 1.328)	3	4	Pathogenic	Unknown significance

Nucleotide change	Amino acid change	*Reported vAFs	Prediction of functional effects			Evolutionary conservation		Combined analysis	
			MutationTaster	PolyPhen-2	Provean Protein	4 Orthologs	8 Orthologs	1	2
c.1762C>T	p.Arg588*	0.000824729%	Disease Causing	N/A	N/A	3	5	Pathogenic	Likely pathogenic
c.1763G>A	p.Arg588Gln	0.005772244%	Disease Causing	Benign (score 0.206)	Neutral (score -2.449)	3	5	Pathogenic	Benign
c.1772G>T	p.Ser591Ile	0.000824212%	Polymorphism	Benign (score 0.028)	Neutral (score -0.836)	2	2	Unknown significance	Likely benign
c.1780G>A	p.Asp594Asn	0.001648207%	Disease Causing	Benign (score of 0.05)	Neutral (score -0.627)	3	4	Pathogenic	Benign
c.1789C>T	p.Arg597Cys	0.000824008%	Disease causing	Possibly damaging (score of 0.776)	Deleterious (score -3.823)	3	4	Pathogenic	Likely pathogenic
c.1790G>A	p.Arg597His	0.000823995%	Polymorphism	Benign (score of 0.009)	Neutral (score -0.839)	3	4	Pathogenic	Likely benign
c.1798A>T	p.Asn600Tyr	0.001647881%	Disease causing	Probably damaging (score of 0.947)	Deleterious (score -4.199)	3	5	Pathogenic	Likely benign
c.1800C>A	p.Asn600Lys	0.002471821%	Disease causing	Possibly damaging (score of 0.776)	Neutral (score -0.839)	3	5	Pathogenic	Likely benign
c.1814C>T	p.Thr605Ile	0.000823954%	Polymorphism	Possibly damaging (score of 0.613)	Deleterious (score -3.513)	3	5	Pathogenic	Unknown significance
c.1816C>T	p.Arg606Trp	0.001647908%	Polymorphism	Probably damaging (score of 0.998)	Deleterious (score -4.041)	4	6	Pathogenic	Likely pathogenic
c.1817G>A	p.Arg606Gln	0.000823968%	Polymorphism	Possibly damaging (score of 0.791)	Neutral (score -2.262)	4	6	Pathogenic	Likely pathogenic
c.1846G>C	p.Ala616Pro	0.000825641%	Polymorphism	Possibly damaging (score of 0.601)	Neutral (score -1.678)	3	5	Pathogenic	Likely benign
c.1873G>A	p.Val625Ile	0.001956564%	Polymorphism	Benign (score of 0.001)	Neutral (score -0.424)	2	2	Unknown significance	Benign
c.1895C>T	p.Ser632Leu	0.002776647%	Polymorphism	Benign (score of 0.001)	Neutral (score -1.872)	3	4	Pathogenic	Benign
c.1900A>T	p.Thr634Ser	0.000918476%	Polymorphism	Benign (score of 0.002)	Neutral (score -1.064)	3	4	Pathogenic	Likely benign
c.1901C>T	p.Thr634Ile	0.000918746%	Polymorphism	Benign (score of 0.001)	Neutral (score -0.25)	3	4	Pathogenic	Likely benign
c.1916T>C	p.Phe639Ser	0.07914159%	Polymorphism	Benign (score of 0)	Neutral (score -2.214)	1	1	Benign	Benign

UMOD variants obtained from ExAC[236] that were used to investigate the effectiveness of *in silico* methods for variant analysis (Chapter 6). Nucleotide number is according to transcript ENST00000570689 and amino acid number is according to the amino acid protein (UniProt P07911) as displayed on ExAC. *Reported vAFs were also obtained from ExAC[236]. Evolutionary conservation scores were based on the number of orthologs each WT residue was conserved in, the number of orthologs studied in each analysis is detailed in the column heading, as detailed in Chapter 6. Combined analysis 1 and 2 are based on the criteria detailed in Chapter 6. N/A, not applicable.

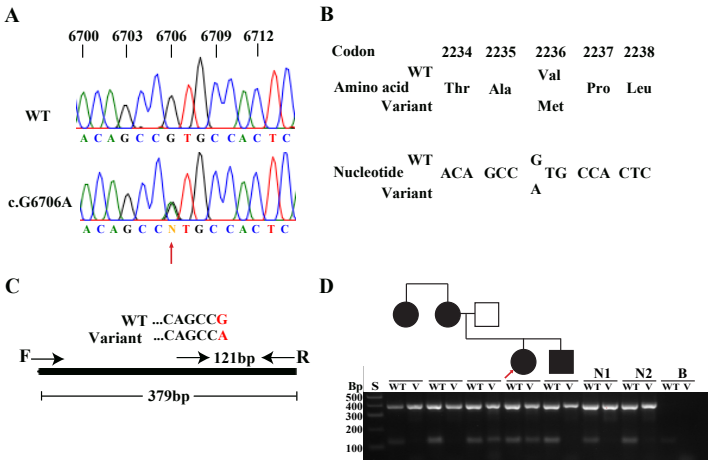
The results for the 19 variants in 11 genes that did not co-segregate with FJHN are displayed in Figure 82 to Figure 100.

Figure 82. Confirmation and segregration analysis of a His1842Arg variant in BSN in a family diagnosed with FJHN



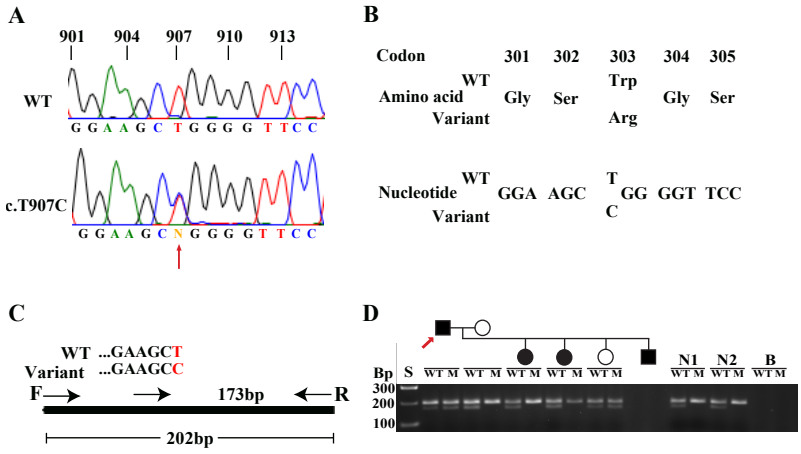
(A) A heterozygous A-to-G transition at nucleotide c.5525 was identified in proband III.2 of family 2 within the FJHN cohort. (B) This (CAC to CGC) is predicted to result in a missense amino acid change from histidine (His) to arginine (Arg) at codon 1842 of the bassoon presynaptic cytomatrix (BSN) protein. (C) ARMS PCR map showing the last 6bp of the WT and variant internal ARMS primers that would result in two products of 396bp and 209bp. The nucleotide highlighted in red is the terminal nucleotide for the primers and corresponds to the first nucleotide affected by the A-to-G transition. (D) ARMS PCR of *BSN* exon 5 demonstrating the heterozygous A-to-G transition in the proband (arrow) and an unaffected sister by the presence of two bands in both the WT and variant (V) reactions; and the lack of the A-to-G transition in the remaining family members and two normal controls (N1 and N2) shown by the presence of two bands in the WT reaction and one in the variant reaction. S= size marker, B= water blank.

Figure 83. Confirmation and segregration analysis of a Val2236Met variant in BSN in a family diagnosed with FJHN



(A) A heterozygous G-to-A transition at nucleotide c.6706 was identified in proband II.1 of family 7 within the FJHN cohort. (B) This (GTG to ATG) is predicted to result in a missense amino acid change from valine (Val) to methionine (Met) at codon 2236 of the BSN protein. (C) ARMS PCR map showing the last 6bp of the WT and variant internal ARMS primers that would result in two products of 379bp and 121bp. The nucleotide highlighted in red is the terminal nucleotide for the primers and corresponds to the first nucleotide affected by the G-to-A transition. (D) ARMS PCR of *BSN* exon 5 demonstrating the heterozygous G-to-A transition in the proband (highlighted by an arrow) and the unaffected father by the presence of two bands in both the WT and variant (V) reactions; and the lack of the G-to-A transition in the remaining family members and two normal controls (N1 and N2) shown by the presence of two bands in the WT reaction and one in the variant reaction. S= size marker, B= water blank.

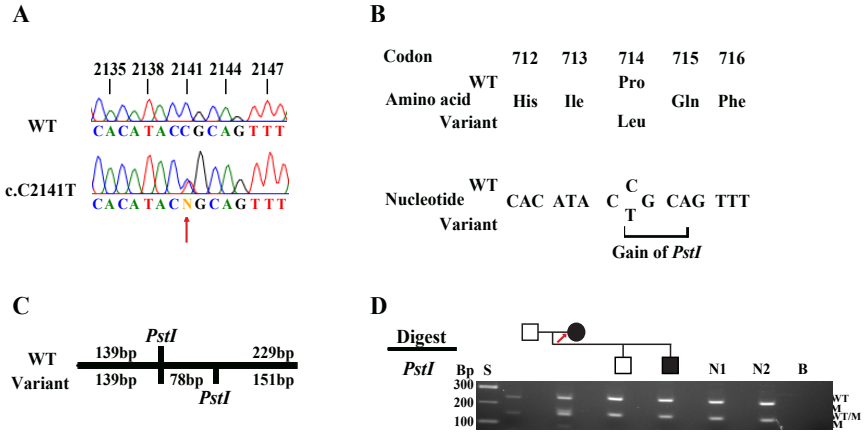
Figure 84. Confirmation and segregration analysis of a Trp303Arg variant in ClC-6 in a family diagnosed with FJHN



(A) A heterozygous T-to-C transition at nucleotide c.907 was identified in proband I.1 of family 3 within the FJHN cohort. (B) This (TGG to CGG) is predicted to result in a missense amino acid change from tryptophan (Trp) to arginine (Arg) at codon 303 of the chloride voltage-gated channel 6 (ClC-6) protein. (C) ARMS PCR map showing the last 6bp of the WT and variant 5' (F) ARMS primers that would result in two products of 202bp and 173bp. The nucleotide highlighted in red is the terminal nucleotide for the primers and corresponds to

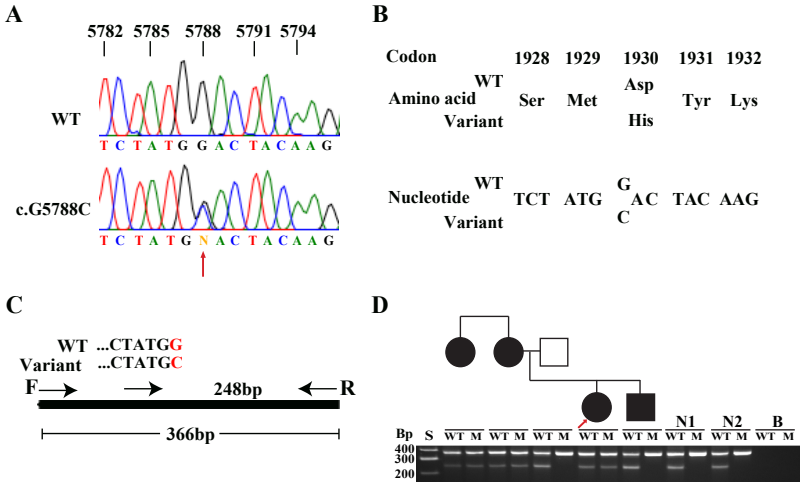
the first nucleotide affected by the T-to-C transition. (D) ARMS PCR of *CLCN6* exon 11 demonstrating the heterozygous T-to-C transition in the proband (highlighted by an arrow) and an unaffected daughter by the presence of two bands in both the WT and variant (V) reactions; and the lack of the T-to-C transition in the remaining family members and two normal controls (N1 and N2) shown by the presence of two bands in the WT reaction and one in the variant reaction. S= size marker, B= water blank.

Figure 85. Confirmation and segregration analysis of a Pro714Leu variant in Fat1 in a family diagnosed with FJHN



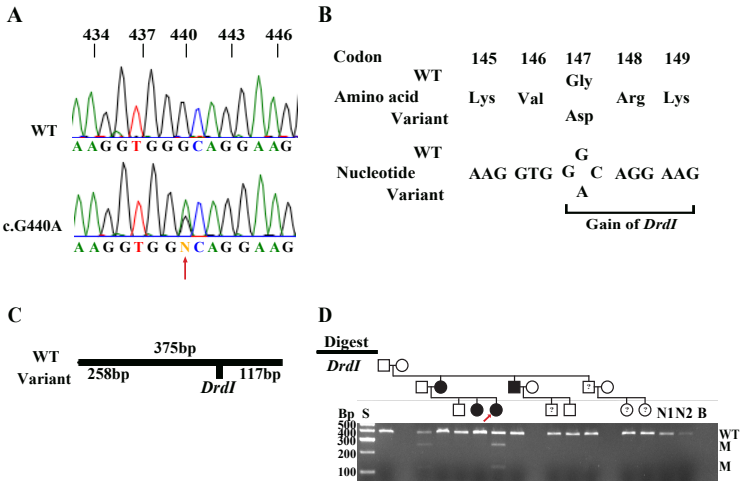
(A) A heterozygous C-to-T transition at nucleotide c.2141 was identified in proband I.2 of family 6 within the FJHN cohort. (B) This (CCG to CTG) is predicted to result in a missense amino acid change from proline (Pro) to leucine (Leu) at codon 714 of the FAT atypical cadherin 1 (Fat1) protein, which would also result in the gain of a *PstI* RE site. (C) Restriction map showing that *PstI* digestion would result in two products of 139bp and 229bp for the WT and three products of 139bp, 78bp and 151bp for the variant. (D) RED of *FAT1* exon 2 PCR products demonstrating the heterozygous C-to-T transition in the proband (highlighted by an arrow) by the presence of four bands, as well as the absence of the C-to-T transition in the remaining family members and two normal controls (N1 and N2) shown by the presence of two bands. S=size marker and B=water blank.

Figure 86. Confirmation and segregration analysis of an Asp1930His variant in Fat1 in a family diagnosed with FJHN



(A) A heterozygous G-to-C transversion at nucleotide c.5788 was identified in proband II.2 of family 7 within the FJHN cohort (N=9). (B) This (GAC to CAC) is predicted to result in a missense amino acid change from aspartic acid (Asp) to histidine (His) at codon 1930 of the Fat1 protein. (C) ARMS PCR map showing the last 6bp of the WT and variant internal ARMS primers that would result in two products of 366bp and 248bp. The nucleotide highlighted in red is the terminal nucleotide for the primers and corresponds to the first nucleotide affected by the G-to-C transversion. (D) ARMS PCR of *FAT1* exon 2 demonstrating the heterozygous G-to-C transversion in the proband (highlighted by an arrow), the affected mother and affected aunt by the presence of two bands in both the WT and variant (V) reactions; and the lack of the G-to-C transversion in the remaining family members and two normal controls (N1 and N2) shown by the presence of two bands in the WT reaction and one in the variant reaction. S= size marker, B= water blank.

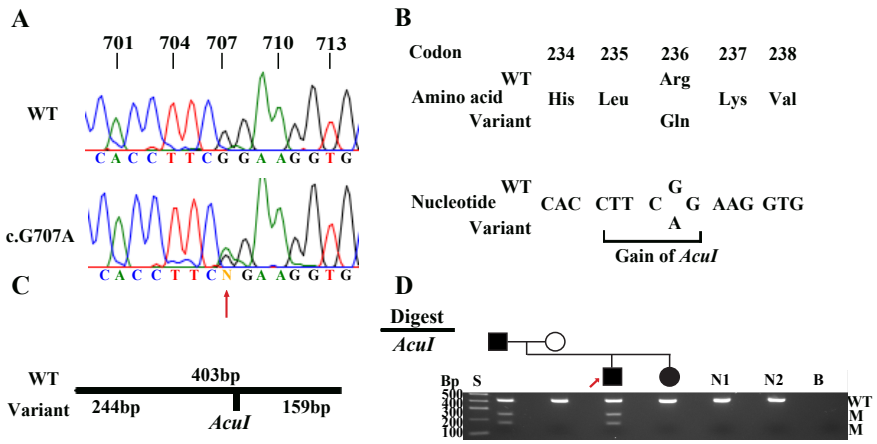
Figure 87. Confirmation and segregration analysis of a Gly147Asp variant in fibromodulin in a family diagnosed with FJHN



(A) A heterozygous G-to-A transition at nucleotide c.440 was identified in proband III.3 of family 1 within the FJHN cohort. (B) This (GGC to GAC) is predicted to result in a missense amino acid change from glycine (Gly) to aspartic acid (Asp) at codon 147 of the fibromodulin protein, which would also result in the gain of a *DrdI* RE site. (C) Restriction map showing that *DrdI* digestion would result in one product of 375bp for the WT and two products of 258bp

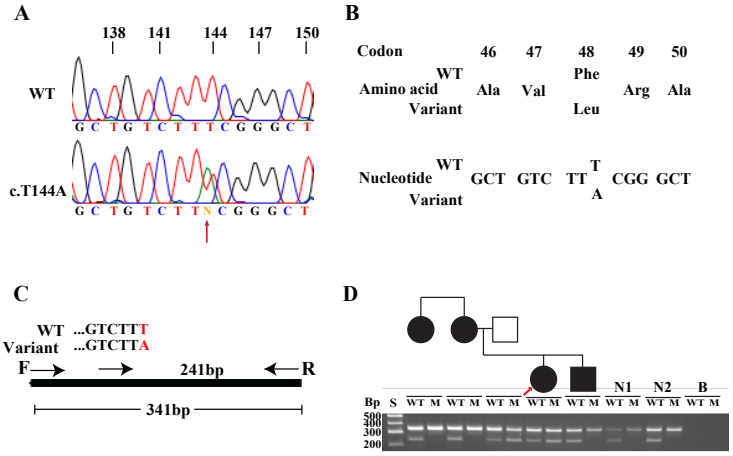
and 117bp for the variant. (D) RED of *FMOD* exon 2 PCR products demonstrating the heterozygous G-to-A transition in the proband (highlighted by an arrow) and unaffected father by the presence of three bands, as well as the absence of the G-to-A transition in the remaining family members and two normal controls (N1 and N2) shown by the presence of one band. S=size marker and B=water blank.

Figure 88. Confirmation and segregration analysis of an Arg236Gln variant in fibromodulin in a family diagnosed with FJHN



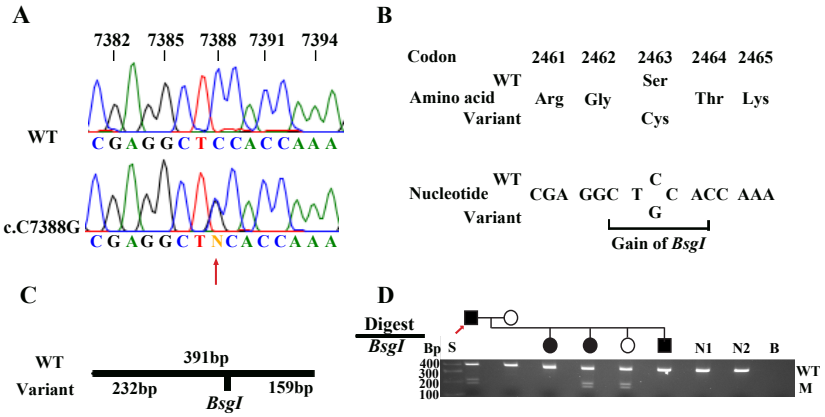
(A) A heterozygous G-to-A transition at nucleotide c.707 was identified in proband II.1 of family 5 within the FJHN cohort. (B) This (CGG to CAG) is predicted to result in a missense amino acid change from arginine (Arg) to glutamine (Gln) at codon 236 of the fibromodulin protein, which would also result in the gain of an *AcuI* RE site. (C) Restriction map showing that *AcuI* digestion would result in one product of 403bp for the WT and two products of 244bp and 159bp for the variant. (D) RED of *FMOD* exon 2 PCR products demonstrating the heterozygous G-to-A transition in the proband (highlighted by an arrow) and affected father by the presence of three bands, as well as the absence of the G-to-A transition in the remaining family members and two normal controls (N1 and N2) shown by the presence of one band. S=size marker and B=water blank.

Figure 89. Confirmation and segregration analysis of a Phe48Leu variant in Igfn1 in a family diagnosed with FJHN



(A) A heterozygous T-to-A transvesion at nucleotide c.144 was identified in proband II.1 of family 7 within the FJHN cohort.(B) This T-to-A transversion (TTT to TTA) is predicted to result in a missense amino acid change from phenylalanine (Phe) to Leucin (Leu) at codon 48 of the immunoglobulin-like and fibronectin type III domain containing 1 (Igfn1) protein. (C) ARMS PCR map showing the last 6bp of the WT and variant internal ARMS primers that would result in two products of 341bp and 241bp. The nucleotide highlighted in red is the terminal nucleotide for the primers and corresponds to the first nucleotide affected by the T-to-A transversion. (D) ARMS PCR of *IGFN1* exon 4 demonstrating the heterozygous T-to-A transversion in the proband (highlighted by an arrow) and the unaffected father by the presence of two bands in both the WT and variant (V) reactions; and the lack of the T-to-A transversion in the remaining family members and two normal controls (N1 and N2) shown by the presence of two bands in the WT reaction and one in the variant reaction. S= size marker, B= water blank.

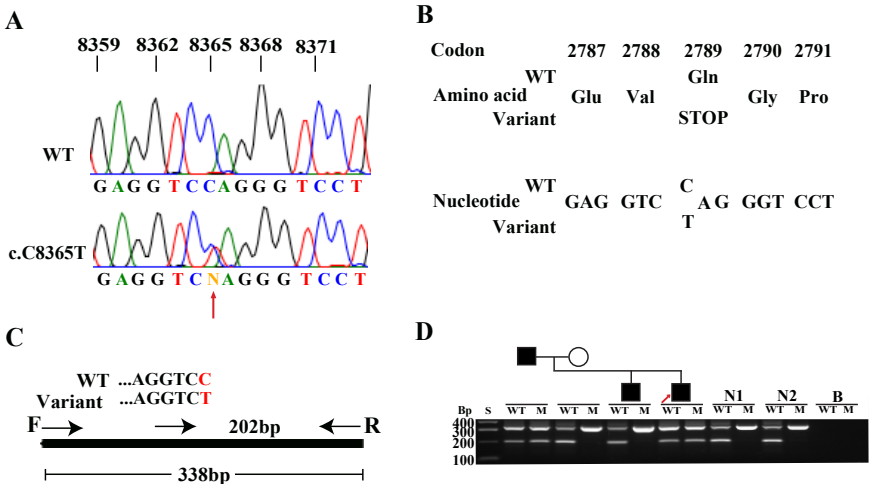
Figure 90. Confirmation and segregration analysis of a Ser2463Cys variant in Igfn1 in a family diagnosed with FJHN



(A) A heterozygous C-to-G transversion at nucleotide c.7388 was identified in proband I.1 of family 3 within the FJHN cohort. (B) This C-to-G transversion (TCC to TGC) is predicted to result in a missense amino acid change from serine (Ser) to cysteine (Cys) at codon 2463 of the Igfn1 protein, which would also result in the gain of a *BsgI* RE site. (C) Restriction map showing that *BsgI* digestion would result in one product of 391bp for the WT and two products of 232bp and 159bp for the variant. (D) RED of *IGFN1* exon 12 PCR products demonstrating the heterozygous C-to-G transversion in the proband (highlighted by an

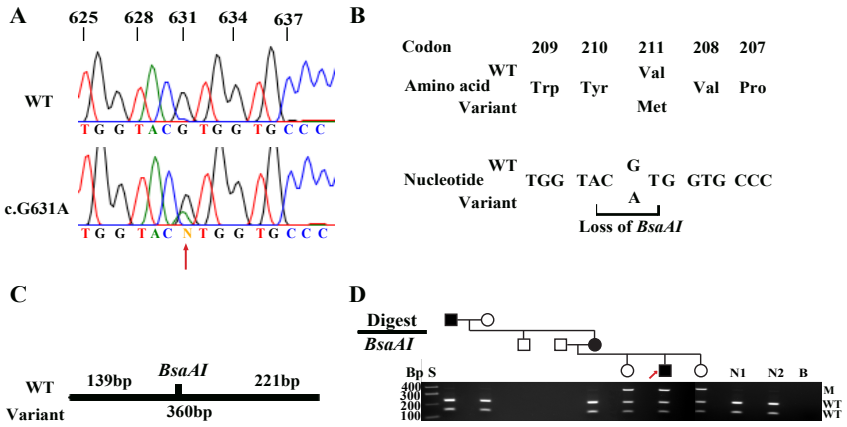
arrow), an affected daughter and the unaffected daughter by the presence of three bands, as well as the absence of the C-to-G transversion in the remaining family members and two normal controls (N1 and N2) shown by the presence of one band. S=size marker and B=water blank.

Figure 91. Confirmation and segregration analysis of a Gln2789* variant in Igfn1 in a family diagnosed with FJHN



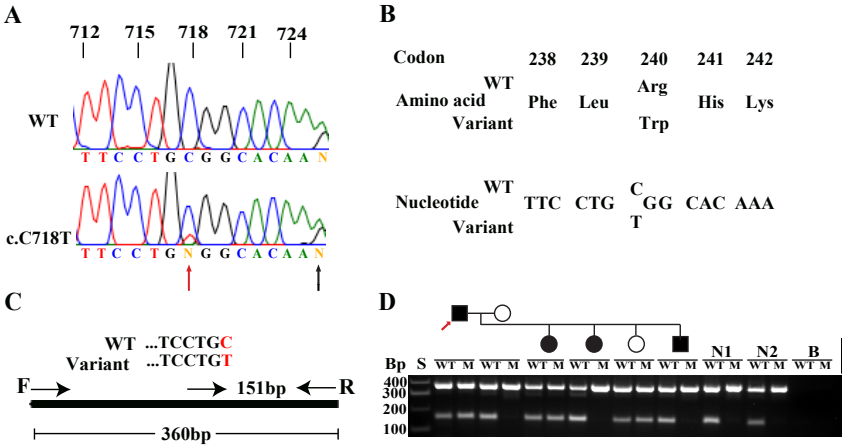
(A) A heterozygous C-to-T transition at nucleotide c.8365 was identified in proband II.2 of family 4 within the FJHN cohort. (B) This (CAG to TAG) is predicted to result in a nonsense amino acid change from glutamine (Gln) to a STOP codon at codon 2789 of the Igfn1 protein. (C) ARMS PCR map showing the last 6bp of the WT and variant internal ARMS primers that would result in two products of 338bp and 202bp. The nucleotide highlighted in red is the terminal nucleotide for the primers and corresponds to the first nucleotide affected by the C-to-T transition. Each ARMS reaction is specific for the WT or variant sequences, if the highlighted nucleotide differs from the sample sequence only one product of 338bp will result. (D) ARMS PCR of *IGFN1* exon 12 demonstrating the heterozygous C-to-T transition in the proband (highlighted by an arrow) and the affected father by the presence of two bands in both the WT and variant (V) reactions; and the lack of the C-to-T transition in the remaining family members and two normal controls (N1 and N2) shown by the presence of two bands in the WT reaction and one in the variant reaction. S= size marker, B= water blank.

Figure 92. Confirmation and segregration analysis of a Val211Met variant in KDM4E in a family diagnosed with FJHN



(A) A heterozygous G-to-A transition at nucleotide c.631 was identified in proband III.2 of family 2 within the FJHN cohort. (B) This (GTG to ATG) is predicted to result in a missense amino acid change from valine (Val) to methionine (Met) at codon 211 of the lysine demethylase 4E (KDM4E) protein, which would also result in the loss of a *BsaAI* RE site. (C) Restriction map showing that *BsaAI* digestion would result in two products of 139bp and 221bp for the WT and one product of 360bp for the variant. (D) RED of *KDM4E* exon 1 PCR products demonstrating the heterozygous G-to-A transition in the proband (highlighted by an arrow) and both unaffected sisters by the presence of three bands, as well as the absence of the G-to-A transition in the affected mother, affected grandfather, unaffected grandmother and two normal controls (N1 and N2) shown by the presence of two bands. S=size marker and B=water blank.

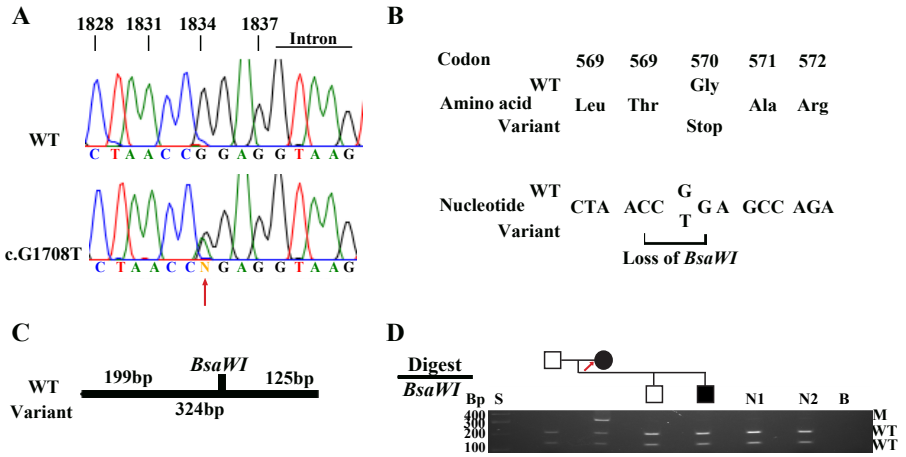
Figure 93. Confirmation and segregration analysis of an Arg240Trp variant in KDM4E in a family diagnosed with FJHN



(A) A heterozygous C-to-T transition at nucleotide c.718 (red arrow) was identified in proband I.1 of family 3 within the FJHN cohort. A synonymous heterozygous A-to-G transition at nucleotide c.726 was also identified in the proband and normal control (WT) (black arrow). (B) This C-to-T transition (CGG to TGG) is predicted to result in a missense amino acid change arginine (Arg) to tryptophan (Trp) at codon 4240 of the KDM4E protein. (C) ARMS map showing the last bp of the WT and variant internal ARMS primers that would result in two products of 360bp and 151bp. The nucleotide highlighted in red is the terminal nucleotide for the primers and corresponds to the first nucleotide affected by the C-to-T transition. (D) ARMS PCR of *KDM4E* exon 1 demonstrating the heterozygous C-to-T transition in the proband

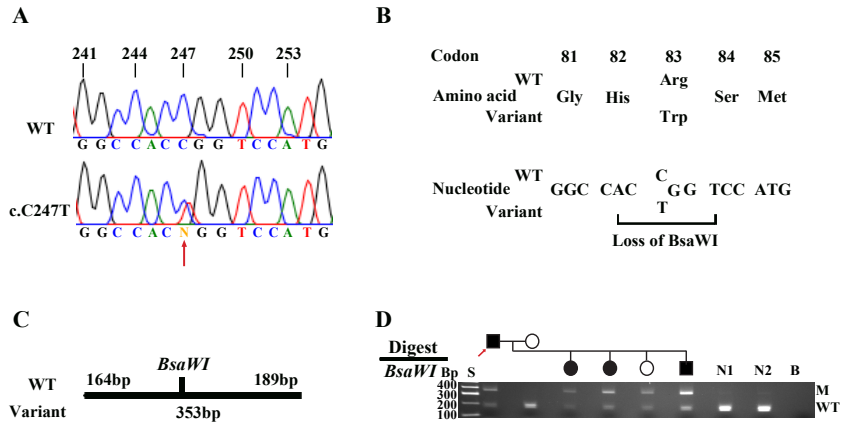
(highlighted by an arrow), an affected daughter and an unaffected daughter by the presence of two bands in both the WT and variant (V) reactions; and the lack of the C-to-T transition in the remaining family members and two normal controls (N1 and N2) shown by the presence of two bands in the WT reaction and one in the variant reaction. S= size marker, B= water blank.

Figure 94. Confirmation and segregration analysis of a Gly570* variant in myosin XVI in a family diagnosed with FJHN



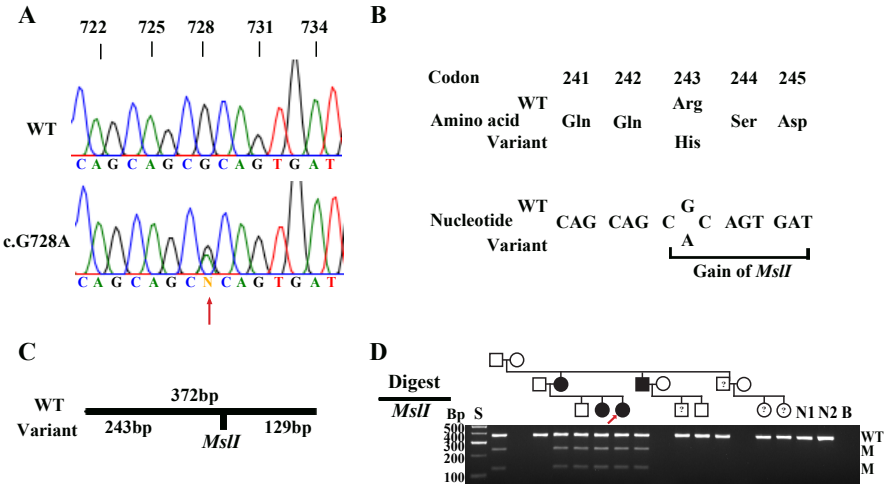
(A) A heterozygous G-to-T transversion at nucleotide c.1708 was identified in proband I.2 of family 6 within the FJHN cohort. (B) This G-to-T transversion (GGA to TGA) is predicted to result in a nonsense amino acid change from glycine (Gly) to a STOP codon at codon 570 of the myosin XVI protein, which would also result in the loss of a *BsaWI* RE site. (C) Restriction map showing that *BsaWI* digestion would result in two products of 199bp and 125bp for the WT and one product of 324bp for the variant. (D) RED of *MYO16* exon 15 PCR products demonstrating the heterozygous G-to-T transversion in the proband (highlighted by an arrow) by the presence of three bands, as well as the absence of the G-to-T transversion in the remaining family members and two normal controls (N1 and N2) shown by the presence of two bands. S=size marker and B=water blank.

Figure 95. Confirmation and segregration analysis of an Arg83Trp variant in neuraminidase 2 in a family diagnosed with FJHN



(A) A heterozygous C-to-T transition at nucleotide c.247 was identified in proband I.1 of family 3 within the FJHN cohort (N=9). (B) This (CGG to TGG) is predicted to result in a missense amino acid change from arginine (Arg) to tryptophan (Trp) at codon 83 of the neuraminidase 2 protein, which would also result in the loss of a *BsaWI* RE site. (C) Restriction map showing that *BsaWI* digestion would result in two products of 164bp and 189bp for the WT and one product of 353bp for the variant. (D) RED of *NEU2* exon 2 PCR products demonstrating the heterozygous C-to-T transition in the proband (highlighted by an arrow), all affected and unaffected daughters and the affected son by the presence of three bands, as well as the absence of the C-to-T transition in the unaffected wife and two normal controls (N1 and N2) shown by the presence of two bands. S=size marker and B=water blank.

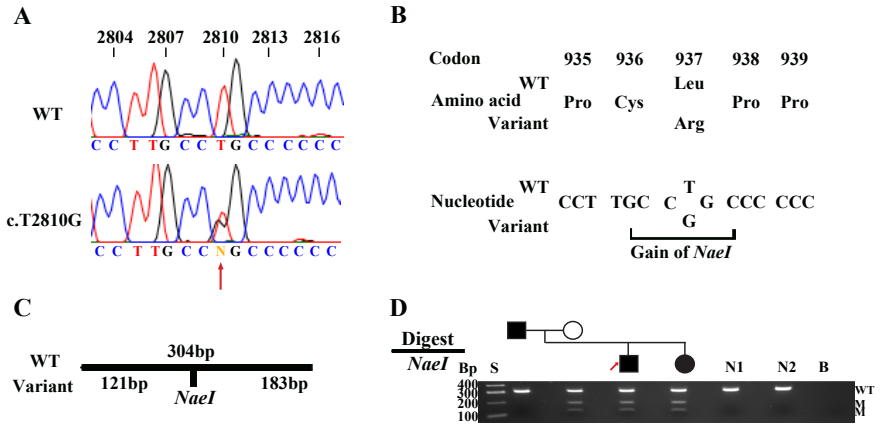
Figure 96. Confirmation and segregration analysis of an Arg243His variant in PPRC1 in a family diagnosed with FJHN



(A) A heterozygous G-to-A transition at nucleotide c.728 was identified in proband III.3 of family 1 within the FJHN cohort. (B) This (CGC to CAC) is predicted to result in a missense amino acid change from arginine (Arg) to histidine (His) at codon 243 of the peroxisome proliferator-activated receptor gamma, coactivator-related 1 (PPRC1) protein, which would also result in the gain of a *MslI* RE site. (C) Restriction map showing that *MslI* digestion would result in one product of 372bp for the WT and two products of 243bp and 129bp for the variant. (D) RED of *PPRC1* exon 5 PCR products demonstrating the heterozygous G-to-A transition in the proband (highlighted by an arrow), both siblings, affected mother and unaffected grandfather by the presence of three bands, as well as the absence of the G-to-A

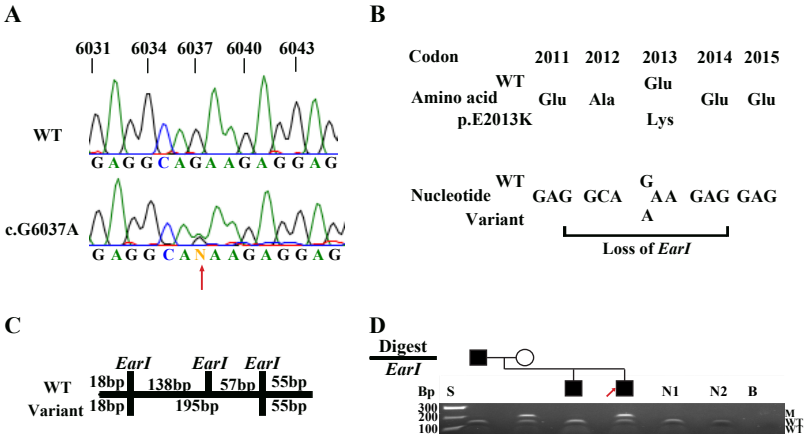
transition in the remaining family members and two normal controls (N1 and N2) shown by the presence of one band. S=size marker and B=water blank.

Figure 97. Confirmation and segregration analysis of a Leu937Arg variant in PPRC1 in a family diagnosed with FJHN



(A) A heterozygous T-to-G transversion at nucleotide c.2810 was identified in proband II.1 of family 5 within the FJHN cohort. (B) This (CTG to CGG) is predicted to result in a missense amino acid change from leucine (Leu) to arginine (Arg) at codon 937 of the PPRC1 protein, which would also result in the gain of a *NaeI* RE site. (C) Restriction map showing that *NaeI* digestion would result in one product of 304bp for the WT and two products of 121bp and 183bp for the variant. (D) RED of *PPRC1* exon 5 PCR products demonstrating the heterozygous T-to-G transversion in the proband (highlighted by an arrow), the affected sister and unaffected mother by the presence of three bands, as well as the absence of the T-to-G transversion in the affected father and two normal controls (N1 and N2) shown by the presence of one band. S=size marker and B=water blank.

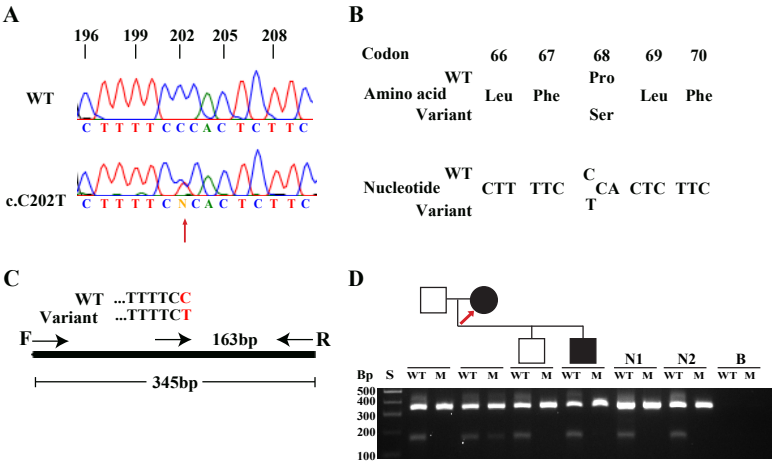
Figure 98. Confirmation and segregration analysis of a Glu2013Lys variant in RP1 like 1 in a family diagnosed with FJHN



(A) A heterozygous G-to-A transition at nucleotide c.6037 was identified in proband II.2 of family 4 within the FJHN cohort. (B) This (GAA to AAA) is predicted to result in a missense amino acid change from glutamic acid (Glu) to lysine (Lys) at codon 2013 of the RP1 like 1 protein, which would also result in the gain of an *EarI* RE site. (C) Restriction map showing that *EarI* digestion would result in four products of 18bp, 138bp, 57bp and 55bp for the WT and three products of 18bp, 195bp and 55bp for the variant. (D) RED of *RP1L1* exon 4 PCR products demonstrating the heterozygous G-to-A transition in the proband (highlighted by

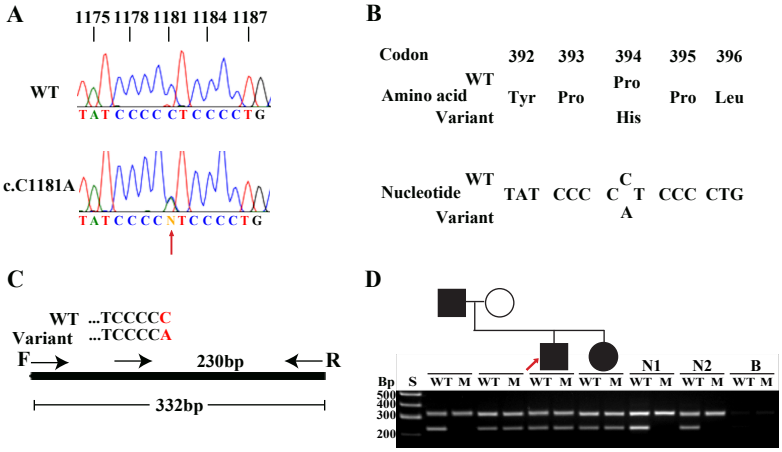
an arrow) and unaffected mother by the presence of a band at 195bp, as well as the absence of the G-to-A transition in the remaining family members and two normal controls (N1 and N2) shown by the absence of a band at 195bp. S=size marker and B=water blank.

Figure 99. Confirmation and segregration analysis of a Pro68Ser variant in NACT in a family diagnosed with FJHN



(A) A heterozygous C-to-T transition at nucleotide c.202 was identified in proband I.2 of family 6 within the FJHN cohort. (B) This (CCA to TCA) is predicted to result in a missense amino acid change from proline (Pro) to Serine (Ser) at codon 68 of the solute carrier family 13 member 5 (NACT) protein. (C) ARMS PCR map showing the last 6bp of the WT and variant internal ARMS primers that would result in two products of 345bp and 163bp. The nucleotide highlighted in red is the terminal nucleotide for the primers and corresponds to the first nucleotide affected by the C-to-T transition. (D) ARMS PCR of *SLC13A5* exon 2 demonstrating the heterozygous C-to-T transition in the proband (highlighted by an arrow) by the presence of two bands in both the WT and variant (V) reactions; and the lack of the C-to-T transition in the remaining family members and two normal controls (N1 and N2) shown by the presence of two bands in the WT reaction and one in the V reaction. S= size marker, B= water blank.

Figure 100. Confirmation and segregration analysis of a Pro394His variant in NACT in a family diagnosed with FJHN



(A) A heterozygous C-to-A transversion at nucleotide c.1181 was identified in proband II.1 of family 5 within the FJHN cohort. (B) This (CCT to CAT) is predicted to result in a missense amino acid change from proline (Pro) to histidine (His) at codon 394 of the NACT protein. (C) ARMS PCR map showing the last 6bp of the WT and variant internal ARMS primers that would result in two products of 332bp and 220bp. The nucleotide highlighted in red is the terminal nucleotide for the primers and corresponds to the first nucleotide affected by the C-to-A transversion. (D) ARMS PCR of *SLC13A5* exon 9 demonstrating the heterozygous C-to-A transversion in the proband (highlighted by an arrow), the affected sister and the unaffected mother by the presence of two bands in both the WT and variant (V) reactions; and the lack of the C-to-A transversion in the affected father and two normal controls (N1 and N2) shown by the presence of two bands in the WT reaction and one in the V reaction. S= size marker, B= water blank.

Table 49. Clinical and biochemical details of the FHH probands for whom TSCA sequencing of *KLOTHO* was performed

Patient ID	Serum					UCCR *>0.02	Family history
	Adjusted Ca^{2+} (mmol/L) *2.2-2.6	Pi (mmol/L) *0.7-1.4	Creatinine (µmol/L) *40-130	ALP (U/L) *30-130	PTH (pmol/L) *1-7		
6	Not known	Not known	Not known	Not known	Not known	Not Known	Not known
7	Mild, asymptomatic hypercalcaemia	Not known	Not known	Not known	Normal	Low/normal urinary Ca^{2+}excretion	Not known
8	Not known	Not known	Not known	Not known	Not known	Not known	Not known
9	Raised	Not known	Not known	Not known	Raised	Low, fractional urinary Ca^{2} excretion	Not known
10	Not known	Not known	Not known	Not known	Not known	Not Known	Not known
11	Not known	Not known	Not known	Not known	Not known	Not Known	Not known
12	Not known	Not known	Not known	Not known	Not known	Not Known	Not known
13	Not known	Not known	Not known	Not known	Not known	Not Known	Not known
14	Not known	Not known	Not known	Not known	Not known	Not Known	Not known
15	Raised	Not known	Not known	Not known	Raised	Decreased urinary Ca^{2} excretion	Not known
16	2.65	0.67	10.2	1.1	Not known	Borderline	Not known
17	2.62	0.86	67	97	10.2	0.006	Not known
18	Not known	Not known	Not known	Not known	Not known	Not Known	Not known
19	Not known	Not known	Not known	Not known	Not known	Not Known	Not known
20	Asymptomatic hypercalcaemia	Not known	Not known	Not known	Not known	Not known	Not known
21	Raised	Not known	Not known	Not known	Raised	Low/normal urinary Ca^{2} excretion	Not known
22	Hypercalcaemia	Not known	Not known	Not known	Raised	Hypocalciuria	Not known
23	Not known	Not known	Not known	Not known	Not known	Not Known	Not known
24	2.62	Not known	34	67	26.6	0.008	Not known
25	2.6	0.7	72	121	7.2	0.002	Not known
26	2.81	0.68	72	99	18	0.006	No
27	2.71	1.01	144	53	11.9	<0.01mmol/24hr (1.8L)	Not known
28	2.73	Not known	85	41	12.6	3.3mmol/24hr (vol N/A)	Not known
29	2.72	0.97	61	Not known	8.9	0.013	Not known
30	Not known	Not known	Not known	Not known	Not known	Not Known	Not known
31	2.95	1.11	75	113	8.4	0.002	Not known
32	Not known	Not known	Not known	Not known	Not known	Not Known	Not known
33	2.72	0.7	68	103	12.7	0.016	No
34	2.75	Not known	Not known	Not known	Not known	Low urinary calcium excretion	Not known
35	Raised	Not known	Not known	Not known	Normal	Equivocal fractional urinary Ca^{2} excretion	Not known
36	Not known	Not known	Not known	Not known	Not known	Not Known	Not known
37	Not known	Not known	Not known	Not known	Not known	Not Known	Not known
38	Not known	Not known	Not known	Not known	Not known	Not Known	Not known
39	Hypercalcaemia	Not known	Not known	Not known	Not known	Low urinary calcium excretion	Not known
40	Mild asymptomatic hypercalcaemia	Not known	Not knonw	Not known	Normal	Low/normal urinary Ca^{2} excretion	Not known
41	Not known	Not known	Not known	Not known	Not known	Not known	Not known
42	2.58	0.9	71	84	6.8	0.013	Not known
43	2.84	0.94	89	Not known	10.2	0.015	Not known
44	Not known	Not known	Not known	Not known	Not known	Not known	Not known
45	2.63	1.06	69	63	8.9	0.016	No
46	2.74	1.1	79	112	13.1	0.014	No

Patient ID	Serum					UCCR *>0.02	Family history
	Adjusted Ca^{2+} (mmol/L) *2.2-2.6	Pi (mmol/L) *0.7-1.4	Creatinine (µmol/L) *40-130	ALP (U/L) *30-130	PTH (pmol/L) *1-7		
47	Not known	Not known	Not known	Not known	Not known	Not known	Not known
48	Not known	Not known	Not known	Not known	Not known	Not known	Not known
49	3	0.9	77	86	5.5	0.013	Not known
50	2.6	0.93	90	57	7.7	0.011	Not known
51	2.55	1.58	15	250	17.1	0.016	Not known
52	Not known	Not known	Not known	Not known	Not known	Not known	Not known
53	2.66	1.08	93	76	6.9	0.017	Not known
54	2.73	0.89	59	79	20.1	0.01	No
55	Not known	Not known	Not known	Not known	Not known	Not known	Not known
56	2.95	1.06	87	Not known	8.6	0.016	No
57	Not known	Not known	Not known	Not known	Not known	Not known	Not known
58	Not known	Not known	Not known	Not known	Not known	Not known	Not known
59	Hypercalcaemia	Not known	Not known	Not knonw	Not known	Not known	Not known
60	Paroxysmal hypercalcaemia	Not knonw	Not known	Not known	Not known	Not known	Not known
61	2.83	0.9	71	153	17.7	1.58mmol/24hr	No
62	Not known	Not known	Not known	Not known	Not known	Not known	Not known
63	Not known	Not known	Not known	Not known	Not known	Not known	Not known
64	Not known	Not known	Not known	Not known	Not known	Not known	Not known
65	Not known	Not known	Not known	Not known	Not known	Not known	Not known
66	Asymptomatic hypercalcaemia	Not known	Not known	Not known	Not known	Not known	Not known
67	Hypercalcaemia	Not known	Not known	Not known	Not known	Not known	No
68	Hypercalcaemia	Not known	Not known	Not knonw	Undetectable	Raised	No
69	Persistant hypercalcaemia following parathryroidectomy	Not known	Not known	Not known	Not known	Not known	Not known
70	Not known	Not known	Not known	Not known	Not known	Not known	Not known
71	2.71	0.91	1.26	Not known	Not known	Not known	Not known
72	Not known	Not known	Not known	Not known	Not known	Not known	Not known
73	2.49	0.6	11.4	0.519	12.3	8.3	Not known
74	Not known	Not known	Not known	Not known	Not known	Not known	Not known
75	Raised	Not known	Not known	Not known	Raised	Low 24hr urinary Ca^{2} excretion	Not known
76	Hypercalcaemia	Not known	Not known	Not known	Not known	Low urinary Ca^{2} excretion	Not known
77	Not known	Not known	Not known	Not known	Not known	Not known	Not known
78	Not known	Not known	Not known	Not known	Not known	Not known	Not known
79	Not known	Not known	Not known	Not known	Not known	Not known	Not known

Clinical and biochemical details of the additional 74 FHH patients, lacking mutations in *CASR, GNA11* and *AP2S1* whose DNA was used for TSCA sequencing of *KLOTHO* in Chapter 9. Abbreviations: ALP, alkaline phosphatase activity; UCCR, urinary Ca^{2+}:creatinine ratio. *Denotes normal ranges: adjusted Ca^{2+} 2.2-2.6mmol/L[373]; Pi 0.7-1.4mmol/L[373]; creatinine 40-130µmol/L[373]; ALP 30-130U/L[373]; PTH 1-7pmol/L[373]; and UCCR >0.02[373].

12 Bibliography

1 Knepper, M. & Burg, M. Organization of nephron function. *Am J Physiol* **244**, F579-589,(1983).
2 Zhuo, J. L. & Li, X. C. Proximal nephron. *Compr Physiol* **3**, 1079-1123,(2013).
3 Pollak, M. R. *et al.* The glomerulus: the sphere of influence. *Clin J Am Soc Nephrol* **9**, 1461-1469,(2014).
4 Moor, M. B. & Bonny, O. Ways of calcium reabsorption in the kidney. *Am J Physiol Renal Physiol* **310**, F1337-1350,(2016).
5 Blaine, J. *et al.* Renal control of calcium, phosphate, and magnesium homeostasis. *Clin J Am Soc Nephrol* **10**, 1257-1272,(2015).
6 Curthoys, N. P. & Moe, O. W. Proximal tubule function and response to acidosis. *Clin J Am Soc Nephrol* **9**, 1627-1638,(2014).
7 Boron, W. F. Acid-base transport by the renal proximal tubule. *J Am Soc Nephrol* **17**, 2368-2382,(2006).
8 Klootwijk, E. D. *et al.* Renal Fanconi syndrome: taking a proximal look at the nephron. *Nephrol Dial Transplant* **30**, 1456-1460,(2015).
9 Igarashi, T. in *Pediatric Nephrology* (eds E. D. Avner, W. E. Harmon, P. Niaudet, & N. Yoshikawa) (Springer-Verlag, 2009).
10 Quamme, G. A. & Dirks, J. H. Magnesium transport in the nephron. *Am J Physiol* **239**, F393-401,(1980).
11 Rouse, D. & Suki, W. N. Renal control of extracellular calcium. *Kidney Int* **38**, 700-708,(1990).
12 Kim, W. Y. *et al.* Descending thin limb of the intermediate loop expresses both aquaporin 1 and urea transporter A2 in the mouse kidney. *Histochem Cell Biol* **146**, 1-12,(2016).
13 Mount, D. B. Thick ascending limb of the loop of Henle. *Clin J Am Soc Nephrol* **9**, 1974-1986,(2014).
14 Zacchia, M. *et al.* The importance of the thick ascending limb of Henle's loop in renal physiology and pathophysiology. *Int J Nephrol Renovasc Dis* **11**, 81-92,(2018).
15 Subramanya, A. R. & Ellison, D. H. Distal convoluted tubule. *Clin J Am Soc Nephrol* **9**, 2147-2163,(2014).
16 Houillier, P. Mechanisms and regulation of renal magnesium transport. *Annu Rev Physiol* **76**, 411-430,(2014).
17 Sebastian, A. *et al.* Disorders of distal nephron function. *Am J Med* **72**, 289-307,(1982).
18 Staruschenko, A. Regulation of transport in the connecting tubule and cortical collecting duct. *Compr Physiol* **2**, 1541-1584,(2012).
19 Meneton, P. *et al.* Sodium and potassium handling by the aldosterone-sensitive distal nephron: the pivotal role of the distal and connecting tubule. *Am J Physiol Renal Physiol* **287**, F593-601,(2004).
20 Kokko, J. P. The role of the collecting duct in urinary concentration. *Kidney Int* **31**, 606-610,(1987).
21 Roy, A. *et al.* Collecting duct intercalated cell function and regulation. *Clin J Am Soc Nephrol* **10**, 305-324,(2015).
22 Schuster, V. L. Function and regulation of collecting duct intercalated cells. *Annu Rev Physiol* **55**, 267-288,(1993).
23 Palmer, L. G. & Schnermann, J. Integrated control of Na transport along the nephron. *Clin J Am Soc Nephrol* **10**, 676-687,(2015).
24 Dantzler, W. H. Regulation of renal proximal and distal tubule transport: sodium, chloride and organic anions. *Comp Biochem Physiol A Mol Integr Physiol* **136**, 453-478,(2003).

25 Bobulescu, I. A. & Moe, O. W. Luminal Na(+)/H (+) exchange in the proximal tubule. *Pflugers Arch* **458**, 5-21,(2009).
26 Forster, I. C. *et al.* Proximal tubular handling of phosphate: A molecular perspective. *Kidney Int* **70**, 1548-1559,(2006).
27 Khundmiri, S. J. *et al.* PTH and Vitamin D. *Compr Physiol* **6**, 561-601,(2016).
28 Hilpert, J. *et al.* Megalin antagonizes activation of the parathyroid hormone receptor. *J Biol Chem* **274**, 5620-5625,(1999).
29 Bajwa, A. *et al.* Specific regulation of CYP27B1 and VDR in proximal versus distal renal cells. *Arch Biochem Biophys* **477**, 33-42,(2008).
30 Bacic, D. *et al.* The renal Na+/phosphate cotransporter NaPi-IIa is internalized via the receptor-mediated endocytic route in response to parathyroid hormone. *Kidney Int* **69**, 495-503,(2006).
31 Bacic, D. *et al.* Involvement of the MAPK-kinase pathway in the PTH-mediated regulation of the proximal tubule type IIa Na+/Pi cotransporter in mouse kidney. *Pflugers Arch* **446**, 52-60,(2003).
32 Picard, N. *et al.* Acute parathyroid hormone differentially regulates renal brush border membrane phosphate cotransporters. *Pflugers Arch* **460**, 677-687,(2010).
33 Brenza, H. L. *et al.* Parathyroid hormone activation of the 25-hydroxyvitamin D3-1alpha-hydroxylase gene promoter. *Proc Natl Acad Sci U S A* **95**, 1387-1391,(1998).
34 Urakawa, I. *et al.* Klotho converts canonical FGF receptor into a specific receptor for FGF23. *Nature* **444**, 770-774,(2006).
35 Kurosu, H. *et al.* Regulation of fibroblast growth factor-23 signaling by klotho. *J Biol Chem* **281**, 6120-6123,(2006).
36 Masuyama, R. *et al.* Vitamin D receptor in chondrocytes promotes osteoclastogenesis and regulates FGF23 production in osteoblasts. *J Clin Invest* **116**, 3150-3159,(2006).
37 Liu, S. *et al.* Pathogenic role of Fgf23 in Hyp mice. *Am J Physiol Endocrinol Metab* **291**, E38-49,(2006).
38 Ben-Dov, I. Z. *et al.* The parathyroid is a target organ for FGF23 in rats. *J Clin Invest* **117**, 4003-4008,(2007).
39 Krajisnik, T. *et al.* Fibroblast growth factor-23 regulates parathyroid hormone and 1alpha-hydroxylase expression in cultured bovine parathyroid cells. *J Endocrinol* **195**, 125-131,(2007).
40 Prie, D. *et al.* Latest findings in phosphate homeostasis. *Kidney Int* **75**, 882-889,(2009).
41 Zhao, W. *et al.* Bone resorption induced by parathyroid hormone is strikingly diminished in collagenase-resistant mutant mice. *J Clin Invest* **103**, 517-524,(1999).
42 Lavi-Moshayoff, V. *et al.* PTH increases FGF23 gene expression and mediates the high-FGF23 levels of experimental kidney failure: a bone parathyroid feedback loop. *Am J Physiol Renal Physiol* **299**, F882-889,(2010).
43 Meir, T. *et al.* Parathyroid hormone activates the orphan nuclear receptor Nurr1 to induce FGF23 transcription. *Kidney Int* **86**, 1106-1115,(2014).
44 Chanakul, A. *et al.* FGF-23 regulates CYP27B1 transcription in the kidney and in extra-renal tissues. *PLoS One* **8**, e72816,(2013).
45 Bai, X. Y. *et al.* The autosomal dominant hypophosphatemic rickets R176Q mutation in fibroblast growth factor 23 resists proteolytic cleavage and enhances in vivo biological potency. *J Biol Chem* **278**, 9843-9849,(2003).
46 Andrukhova, O. *et al.* FGF23 acts directly on renal proximal tubules to induce phosphaturia through activation of the ERK1/2-SGK1 signaling pathway. *Bone* **51**, 621-628,(2012).
47 Dusso, A. S. *et al.* Vitamin D. *Am J Physiol Renal Physiol* **289**, F8-28,(2005).

48 Fukumoto, S. Phosphate metabolism and vitamin D. *Bonekey Rep* **3**, 497,(2014).
49 Komaba, H. & Fukagawa, M. FGF23-parathyroid interaction: implications in chronic kidney disease. *Kidney Int* **77**, 292-298,(2010).
50 Trechsel, U. *et al.* Regulation of the metabolism of 25-hydroxyvitamin D3 in primary cultures of chick kidney cells. *J Clin Invest* **64**, 206-217,(1979).
51 Zhu, Y. *et al.* Ablation of the Stimulatory G Protein alpha-Subunit in Renal Proximal Tubules Leads to Parathyroid Hormone-Resistance With Increased Renal Cyp24a1 mRNA Abundance and Reduced Serum 1,25-Dihydroxyvitamin D. *Endocrinology* **157**, 497-507,(2016).
52 St-Arnaud, R. *et al.* The 25-hydroxyvitamin D 1-alpha-hydroxylase gene maps to the pseudovitamin D-deficiency rickets (PDDR) disease locus. *J Bone Miner Res* **12**, 1552-1559,(1997).
53 Takeyama, K. *et al.* 25-Hydroxyvitamin D3 1alpha-hydroxylase and vitamin D synthesis. *Science* **277**, 1827-1830,(1997).
54 Christakos, S. *et al.* Vitamin D: metabolism. *Endocrinol Metab Clin North Am* **39**, 243-253, table of contents,(2010).
55 Weinman, E. J. *et al.* Parathyroid hormone inhibits renal phosphate transport by phosphorylation of serine 77 of sodium-hydrogen exchanger regulatory factor-1. *J Clin Invest* **117**, 3412-3420,(2007).
56 Weinman, E. J. *et al.* Dynamics of PTH-induced disassembly of Npt2a/NHERF-1 complexes in living OK cells. *Am J Physiol Renal Physiol* **300**, F231-235,(2011).
57 Wang, B. *et al.* Ezrin-anchored protein kinase A coordinates phosphorylation-dependent disassembly of a NHERF1 ternary complex to regulate hormone-sensitive phosphate transport. *J Biol Chem* **287**, 24148-24163,(2012).
58 Chauvin, S. *et al.* Parathyroid hormone receptor recycling: role of receptor dephosphorylation and beta-arrestin. *Mol Endocrinol* **16**, 2720-2732,(2002).
59 Blind, E. *et al.* Phosphorylation of the cytoplasmic tail of the PTH/PTHrP receptor. *J Bone Miner Res* **11**, 578-586,(1996).
60 Qian, F. *et al.* Agonist-dependent phosphorylation of the parathyroid hormone/parathyroid hormone-related peptide receptor. *Biochemistry* **37**, 6240-6246,(1998).
61 Ferrari, S. L. *et al.* Endocytosis of ligand-human parathyroid hormone receptor 1 complexes is protein kinase C-dependent and involves beta-arrestin2. Real-time monitoring by fluorescence microscopy. *J Biol Chem* **274**, 29968-29975,(1999).
62 Bastepe, M. *et al.* Heterotrimeric G proteins in the control of parathyroid hormone actions. *J Mol Endocrinol* **58**, R203-R224,(2017).
63 Kawai, M. The FGF23/Klotho axis in the regulation of mineral and metabolic homeostasis. *Horm Mol Biol Clin Investig* **28**, 55-67,(2016).
64 Han, X. *et al.* Conditional Deletion of Fgfr1 in the Proximal and Distal Tubule Identifies Distinct Roles in Phosphate and Calcium Transport. *PLoS One* **11**, e0147845,(2016).
65 Saito, H. *et al.* Human fibroblast growth factor-23 mutants suppress Na+-dependent phosphate co-transport activity and 1alpha,25-dihydroxyvitamin D3 production. *J Biol Chem* **278**, 2206-2211,(2003).
66 Yu, X. *et al.* Analysis of the biochemical mechanisms for the endocrine actions of fibroblast growth factor-23. *Endocrinology* **146**, 4647-4656,(2005).
67 Shimada, T. *et al.* Targeted ablation of Fgf23 demonstrates an essential physiological role of FGF23 in phosphate and vitamin D metabolism. *J Clin Invest* **113**, 561-568,(2004).
68 Wolf, M. T. *et al.* Klotho up-regulates renal calcium channel transient receptor potential vanilloid 5 (TRPV5) by intra- and extracellular N-glycosylation-dependent mechanisms. *J Biol Chem* **289**, 35849-35857,(2014).

69 Chang, Q. *et al.* The beta-glucuronidase klotho hydrolyzes and activates the TRPV5 channel. *Science* **310**, 490-493,(2005).
70 Cha, S. K. *et al.* Removal of sialic acid involving Klotho causes cell-surface retention of TRPV5 channel via binding to galectin-1. *Proc Natl Acad Sci U S A* **105**, 9805-9810,(2008).
71 Yu, A. S. Claudins and the kidney. *J Am Soc Nephrol* **26**, 11-19,(2015).
72 Kirk, A. *et al.* Differential expression of claudin tight junction proteins in the human cortical nephron. *Nephrol Dial Transplant* **25**, 2107-2119,(2010).
73 Krug, S. M. *et al.* Claudin-17 forms tight junction channels with distinct anion selectivity. *Cell Mol Life Sci* **69**, 2765-2778,(2012).
74 Fromm, M. *et al.* Tight junctions of the proximal tubule and their channel proteins. *Pflugers Arch* **469**, 877-887,(2017).
75 Yu, A. S. *et al.* Molecular basis for cation selectivity in claudin-2-based paracellular pores: identification of an electrostatic interaction site. *J Gen Physiol* **133**, 111-127,(2009).
76 Muto, S. *et al.* Claudin-2-deficient mice are defective in the leaky and cation-selective paracellular permeability properties of renal proximal tubules. *Proc Natl Acad Sci U S A* **107**, 8011-8016,(2010).
77 Wright, F. S. Sites and mechanisms of potassium transport along the renal tubule. *Kidney Int* **11**, 415-432,(1977).
78 Palmer, B. F. Regulation of Potassium Homeostasis. *Clin J Am Soc Nephrol* **10**, 1050-1060,(2015).
79 Gunzel, D. & Yu, A. S. Claudins and the modulation of tight junction permeability. *Physiol Rev* **93**, 525-569,(2013).
80 Van Itallie, C. M. *et al.* Two splice variants of claudin-10 in the kidney create paracellular pores with different ion selectivities. *Am J Physiol Renal Physiol* **291**, F1288-1299,(2006).
81 Purkerson, J. M. & Schwartz, G. J. The role of carbonic anhydrases in renal physiology. *Kidney Int* **71**, 103-115,(2007).
82 Igarashi, T. *et al.* Mutations in SLC4A4 cause permanent isolated proximal renal tubular acidosis with ocular abnormalities. *Nat Genet* **23**, 264-266,(1999).
83 Venta, P. J. *et al.* Carbonic anhydrase II deficiency syndrome in a Belgian family is caused by a point mutation at an invariant histidine residue (107 His----Tyr): complete structure of the normal human CA II gene. *Am J Hum Genet* **49**, 1082-1090,(1991).
84 Hall, C. L. & Hardwicke, J. Low molecular weight proteinuria. *Annu Rev Med* **30**, 199-211,(1979).
85 Maack, T. *et al.* Renal filtration, transport, and metabolism of low-molecular-weight proteins: a review. *Kidney Int* **16**, 251-270,(1979).
86 Birn, H. & Christensen, E. I. Renal albumin absorption in physiology and pathology. *Kidney Int* **69**, 440-449,(2006).
87 Christensen, E. I. & Birn, H. Megalin and cubilin: multifunctional endocytic receptors. *Nat Rev Mol Cell Biol* **3**,(2002).
88 Pandey, K. N. Functional roles of short sequence motifs in the endocytosis of membrane receptors. *Front Biosci (Landmark Ed)* **14**, 5339-5360,(2009).
89 Chen, W. J. *et al.* NPXY, a sequence often found in cytoplasmic tails, is required for coated pit-mediated internalization of the low density lipoprotein receptor. *J Biol Chem* **265**, 3116-3123,(1990).
90 Jentsch, T. J. Chloride and the endosomal-lysosomal pathway: emerging roles of CLC chloride transporters. *J Physiol* **578**,(2007).
91 Tojo, A. & Kinugasa, S. Mechanisms of glomerular albumin filtration and tubular reabsorption. *Int J Nephrol* **2012**, 481520,(2012).

92 Zelikovic, I. & Chesney, R. W. Sodium-coupled amino acid transport in renal tubule. *Kidney Int* **36**, 351-359,(1989).
93 Verrey, F. *et al.* Kidney amino acid transport. *Pflugers Arch* **458**, 53-60,(2009).
94 Mather, A. & Pollock, C. Glucose handling by the kidney. *Kidney Int Suppl*, S1-6,(2011).
95 Kleta, R. *et al.* Renal glucosuria due to SGLT2 mutations. *Mol Genet Metab* **82**, 56-58,(2004).
96 Santer, R. *et al.* Mutations in GLUT2, the gene for the liver-type glucose transporter, in patients with Fanconi-Bickel syndrome. *Nat Genet* **17**, 324-326,(1997).
97 Bakris, G. L. *et al.* Renal sodium-glucose transport: role in diabetes mellitus and potential clinical implications. *Kidney Int* **75**, 1272-1277,(2009).
98 Devuyst, O. & Thakker, R. V. Dent's disease. *Orphanet Journal of Rare Diseases* **5**, 28,(2010).
99 Lloyd, S. E. *et al.* A common molecular basis for three inherited kidney stone diseases. *Nature* **379**,(1996).
100 Hoopes, R. R. *et al.* Dent Disease with mutations in OCRL1. *Am J Hum Genet* **76**,(2005).
101 Mansour-Hendili, L. *et al.* Mutation Update of the CLCN5 Gene Responsible for Dent Disease 1. *Hum Mutat* **36**, 743-752,(2015).
102 Claverie-Martin, F. *et al.* Dent's disease: clinical features and molecular basis. *Pediatr Nephrol* **26**, 693-704,(2011).
103 Bokenkamp, A. *et al.* Dent-2 disease: a mild variant of Lowe syndrome. *J Pediatr* **155**, 94-99,(2009).
104 Hoopes, R. R., Jr. *et al.* Evidence for genetic heterogeneity in Dent's disease. *Kidney Int* **65**, 1615-1620,(2004).
105 Zifarelli, G. A tale of two CLCs: biophysical insights toward understanding ClC-5 and ClC-7 function in endosomes and lysosomes. *J Physiol* **593**, 4139-4150,(2015).
106 Picollo, A. & Pusch, M. Chloride/proton antiporter activity of mammalian CLC proteins ClC-4 and ClC-5. *Nature* **436**, 420-423,(2005).
107 Gunther, W. *et al.* ClC-5, the chloride channel mutated in Dent's disease, colocalizes with the proton pump in endocytotically active kidney cells. *Proc Natl Acad Sci U S A* **95**, 8075-8080,(1998).
108 Lippiat, J. D. & Smith, A. J. The CLC-5 2Cl(-)/H(+) exchange transporter in endosomal function and Dent's disease. *Front Physiol* **3**, 449,(2012).
109 Gorvin, C. *et al.* in *Society for Endocrinology BES*
110 Sawyer, S. L. *et al.* Utility of whole-exome sequencing for those near the end of the diagnostic odyssey: time to address gaps in care. *Clin Genet* **89**, 275-284,(2016).
111 Hu, Y. B. *et al.* The endosomal-lysosomal system: from acidification and cargo sorting to neurodegeneration. *Transl Neurodegener* **4**, 18,(2015).
112 Huotari, J. & Helenius, A. Endosome maturation. *EMBO J* **30**, 3481-3500,(2011).
113 Devuyst, O. & Luciani, A. Chloride transporters and receptor-mediated endocytosis in the renal proximal tubule. *J Physiol* **593**, 4151-4164,(2015).
114 Gorvin, C. M. *et al.* Receptor-mediated endocytosis and endosomal acidification is impaired in proximal tubule epithelial cells of Dent disease patients. *Proc Natl Acad Sci U S A* **110**, 7014-7019,(2013).
115 Piwon, N. *et al.* ClC-5 Cl--channel disruption impairs endocytosis in a mouse model for Dent's disease. *Nature* **408**,(2000).
116 Fleet, J. C. & Schoch, R. D. Molecular mechanisms for regulation of intestinal calcium absorption by vitamin D and other factors. *Crit Rev Clin Lab Sci* **47**, 181-195,(2010).

117 Lee, S. M. *et al.* 1,25-Dihydroxyvitamin D3 Controls a Cohort of Vitamin D Receptor Target Genes in the Proximal Intestine That Is Enriched for Calcium-regulating Components. *J Biol Chem* **290**, 18199-18215,(2015).
118 Letavernier, E. & Daudon, M. Vitamin D, Hypercalciuria and Kidney Stones. *Nutrients* **10**,(2018).
119 Habbig, S. *et al.* Nephrocalcinosis and urolithiasis in children. *Kidney Int* **80**, 1278-1291,(2011).
120 Attree, O. *et al.* The Lowe's oculocerebrorenal syndrome gene encodes a protein highly homologous to inositol polyphosphate-5-phosphatase. *Nature* **358**, 239-242,(1992).
121 De Matteis, M. A. *et al.* The 5-phosphatase OCRL in Lowe syndrome and Dent disease 2. *Nat Rev Nephrol* **13**, 455-470,(2017).
122 Wu, F. *et al.* Mutational Analysis of CLC-5, Cofilin and CLC-4 in Patients with Dent's Disease. *Nephron Physiol* **112**,(2009).
123 Ludwig, M. & Utsch, B. Dent disease-like phenotype and the chloride channel ClC-4 (CLCN4) gene. *Am J Med Genet A* **128A**, 434-435,(2004).
124 Tosetto, E. *et al.* Locus heterogeneity of Dent's disease: OCRL1 and TMEM27 genes in patients with no CLCN5 mutations. *Pediatr Nephrol* **24**, 1967-1973,(2009).
125 Bankir, L. T. & Trinh-Trang-Tan, M. M. Renal urea transporters. Direct and indirect regulation by vasopressin. *Exp Physiol* **85 Spec No**, 243S-252S,(2000).
126 Nielsen, S. *et al.* Aquaporins in the kidney: from molecules to medicine. *Physiol Rev* **82**, 205-244,(2002).
127 Lei, T. *et al.* Role of thin descending limb urea transport in renal urea handling and the urine concentrating mechanism. *Am J Physiol Renal Physiol* **301**, F1251-1259,(2011).
128 Grunewald, R. W. *et al.* Characteristics of urea transport of cells derived from rabbit thick ascending limb of Henle's loop. *Kidney Int* **54**, 152-159,(1998).
129 Knepper, M. A. & Roch-Ramel, F. Pathways of urea transport in the mammalian kidney. *Kidney Int* **31**, 629-633,(1987).
130 Matsumura, Y. *et al.* Overt nephrogenic diabetes insipidus in mice lacking the CLC-K1 chloride channel. *Nat Genet* **21**, 95-98,(1999).
131 Estevez, R. *et al.* Barttin is a Cl- channel beta-subunit crucial for renal Cl- reabsorption and inner ear K+ secretion. *Nature* **414**, 558-561,(2001).
132 Fischer, M. *et al.* Barttin activates ClC-K channel function by modulating gating. *J Am Soc Nephrol* **21**, 1281-1289,(2010).
133 Kramer, B. K. *et al.* Mechanisms of Disease: the kidney-specific chloride channels ClCKA and ClCKB, the Barttin subunit, and their clinical relevance. *Nat Clin Pract Nephrol* **4**, 38-46,(2008).
134 Schlingmann, K. P. *et al.* Salt wasting and deafness resulting from mutations in two chloride channels. *N Engl J Med* **350**, 1314-1319,(2004).
135 Zaika, O. *et al.* New perspective of ClC-Kb/2 Cl- channel physiology in the distal renal tubule. *Am J Physiol Renal Physiol* **310**, F923-930,(2016).
136 Simon, D. B. *et al.* Paracellin-1, a renal tight junction protein required for paracellular Mg2+ resorption. *Science* **285**, 103-106,(1999).
137 Konrad, M. *et al.* Mutations in the tight-junction gene claudin 19 (CLDN19) are associated with renal magnesium wasting, renal failure, and severe ocular involvement. *Am J Hum Genet* **79**, 949-957,(2006).
138 Toka, H. R. *et al.* Deficiency of the calcium-sensing receptor in the kidney causes parathyroid hormone-independent hypocalciuria. *J Am Soc Nephrol* **23**, 1879-1890,(2012).

139 Gong, Y. *et al.* Claudin-14 regulates renal Ca(+)(+) transport in response to CaSR signalling via a novel microRNA pathway. *EMBO J* **31**, 1999-2012,(2012).
140 Turner, J. J. *et al.* UROMODULIN mutations cause familial juvenile hyperuricemic nephropathy. *J Clin Endocrinol Metab* **88**, 1398-1401,(2003).
141 *Seldin and Giebisch's The Kidney: Physiology & Pathophysiology 1-2*. 4 edn, 109-110 (Elsevier, 2007).
142 Kim, Y. H. *et al.* Expression of urea transporters in the developing rat kidney. *Am J Physiol Renal Physiol* **282**, F530-540,(2002).
143 Uchida, S. *et al.* Molecular cloning of a chloride channel that is regulated by dehydration and expressed predominantly in kidney medulla. *J Biol Chem* **268**, 3821-3824,(1993).
144 Pannabecker, T. L. Structure and function of the thin limbs of the loop of Henle. *Compr Physiol* **2**, 2063-2086,(2012).
145 Kondo, Y. Mechanism of sodium chloride reabsorption in the ascending thin limb of Henle's loop. *Clinical and Experimental Nephrology* **1**, 67-75,(1997).
146 Zivna, M. *et al.* Dominant renin gene mutations associated with early-onset hyperuricemia, anemia, and chronic kidney failure. *Am J Hum Genet* **85**, 204-213,(2009).
147 Piret, S. E. *et al.* Genome-wide study of familial juvenile hyperuricaemic (gouty) nephropathy (FJHN) indicates a new locus, FJHN3, linked to chromosome 2p22.1-p21. *Hum Genet* **129**, 51-58,(2011).
148 Bingham, C. *et al.* Atypical familial juvenile hyperuricemic nephropathy associated with a hepatocyte nuclear factor-1beta gene mutation. *Kidney Int* **63**, 1645-1651,(2003).
149 Kumar, S. & Muchmore, A. Tamm-Horsfall protein--uromodulin (1950-1990). *Kidney Int* **37**, 1395-1401,(1990).
150 Rampoldi, L. *et al.* The rediscovery of uromodulin (Tamm-Horsfall protein): from tubulointerstitial nephropathy to chronic kidney disease. *Kidney Int* **80**, 338-347,(2011).
151 Tokonami, N. *et al.* Uromodulin is expressed in the distal convoluted tubule, where it is critical for regulation of the sodium chloride cotransporter NCC. *Kidney Int* **94**, 701-715,(2018).
152 Serafini-Cessi, F. *et al.* Biosynthesis and oligosaccharide processing of human Tamm-Horsfall glycoprotein permanently expressed in HeLa cells. *Biochem Biophys Res Commun* **194**, 784-790,(1993).
153 Malagolini, N. *et al.* Intracellular transport, cell-surface exposure and release of recombinant Tamm-Horsfall glycoprotein. *Kidney Int* **52**, 1340-1350,(1997).
154 Cavallone, D. *et al.* Mechanism of release of urinary Tamm-Horsfall glycoprotein from the kidney GPI-anchored counterpart. *Biochem Biophys Res Commun* **280**, 110-114,(2001).
155 Williams, S. E. *et al.* Uromodulin mutations causing familial juvenile hyperuricaemic nephropathy lead to protein maturation defects and retention in the endoplasmic reticulum. *Hum Mol Genet* **18**, 2963-2974,(2009).
156 Vylet'al, P. *et al.* Alterations of uromodulin biology: a common denominator of the genetically heterogeneous FJHN/MCKD syndrome. *Kidney Int* **70**, 1155-1169,(2006).
157 Piret, S. E. *et al.* A mouse model for inherited renal fibrosis associated with endoplasmic reticulum stress. *Dis Model Mech* **10**, 773-786,(2017).
158 Gomez, R. A. & Sequeira-Lopez, M. L. S. Renin cells in homeostasis, regeneration and immune defence mechanisms. *Nat Rev Nephrol* **14**, 231-245,(2018).
159 Lopez, M. L. & Gomez, R. A. The renin phenotype: roles and regulation in the kidney. *Curr Opin Nephrol Hypertens* **19**, 366-371,(2010).

160 Sparks, M. A. *et al.* Classical Renin-Angiotensin system in kidney physiology. *Compr Physiol* **4**, 1201-1228,(2014).
161 Peach, M. J. Renin-angiotensin system: biochemistry and mechanisms of action. *Physiol Rev* **57**, 313-370,(1977).
162 Verhave, J. C. *et al.* Hepatocyte Nuclear Factor 1beta-Associated Kidney Disease: More than Renal Cysts and Diabetes. *J Am Soc Nephrol* **27**, 345-353,(2016).
163 Bingham, C. & Hattersley, A. T. Renal cysts and diabetes syndrome resulting from mutations in hepatocyte nuclear factor-1beta. *Nephrol Dial Transplant* **19**, 2703-2708,(2004).
164 Gresh, L. *et al.* A transcriptional network in polycystic kidney disease. *EMBO J* **23**, 1657-1668,(2004).
165 Mochizuki, T. *et al.* PKD2, a gene for polycystic kidney disease that encodes an integral membrane protein. *Science* **272**, 1339-1342,(1996).
166 Onuchic, L. F. *et al.* PKHD1, the polycystic kidney and hepatic disease 1 gene, encodes a novel large protein containing multiple immunoglobulin-like plexin-transcription-factor domains and parallel beta-helix 1 repeats. *Am J Hum Genet* **70**, 1305-1317,(2002).
167 Ward, C. J. *et al.* The gene mutated in autosomal recessive polycystic kidney disease encodes a large, receptor-like protein. *Nat Genet* **30**, 259-269,(2002).
168 Pearce, D. *et al.* Collecting duct principal cell transport processes and their regulation. *Clin J Am Soc Nephrol* **10**, 135-146,(2015).
169 Soundararajan, R. *et al.* The role of the ENaC-regulatory complex in aldosterone-mediated sodium transport. *Mol Cell Endocrinol* **350**, 242-247,(2012).
170 Walsh, S. B. & Unwin, R. J. Renal tubular disorders. *Clin Med (Lond)* **12**, 476-479,(2012).
171 Scott, J. H. & Dunn, R. J. in *StatPearls* (2018).
172 Yang, C. L. *et al.* WNK kinases regulate thiazide-sensitive Na-Cl cotransport. *J Clin Invest* **111**, 1039-1045,(2003).
173 Imai, M. & Nakamura, R. Function of distal convoluted and connecting tubules studied by isolated nephron fragments. *Kidney Int* **22**, 465-472,(1982).
174 Walder, R. Y. *et al.* Mutation of TRPM6 causes familial hypomagnesemia with secondary hypocalcemia. *Nat Genet* **31**, 171-174,(2002).
175 Schlingmann, K. P. *et al.* Hypomagnesemia with secondary hypocalcemia is caused by mutations in TRPM6, a new member of the TRPM gene family. *Nat Genet* **31**, 166-170,(2002).
176 Hoenderop, J. G. *et al.* Renal Ca2+ wasting, hyperabsorption, and reduced bone thickness in mice lacking TRPV5. *J Clin Invest* **112**, 1906-1914,(2003).
177 van der Hagen, E. A. *et al.* Coordinated regulation of TRPV5-mediated Ca(2)(+) transport in primary distal convolution cultures. *Pflugers Arch* **466**, 2077-2087,(2014).
178 Madsen, K. M. *et al.* Relationship between structure and function in distal tubule and collecting duct. *J Electron Microsc Tech* **9**, 187-208,(1988).
179 Madsen, K. M. *et al.* Structure and function of the inner medullary collecting duct. *Kidney Int* **34**, 441-454,(1988).
180 Sands, J. M. Mammalian urea transporters. *Annu Rev Physiol* **65**, 543-566,(2003).
181 Wang, W. H. & Giebisch, G. Regulation of potassium (K) handling in the renal collecting duct. *Pflugers Arch* **458**, 157-168,(2009).
182 Hannan, F. M. *et al.* Disorders of the calcium-sensing receptor and partner proteins: insights into the molecular basis of calcium homeostasis. *J Mol Endocrinol* **57**, R127-142,(2016).

183 Pollak, M. R. *et al.* Mutations in the human Ca(2+)-sensing receptor gene cause familial hypocalciuric hypercalcemia and neonatal severe hyperparathyroidism. *Cell* **75**, 1297-1303,(1993).
184 Nesbit, M. A. *et al.* Mutations affecting G-protein subunit alpha11 in hypercalcemia and hypocalcemia. *N Engl J Med* **368**, 2476-2486,(2013).
185 Nesbit, M. A. *et al.* Mutations in AP2S1 cause familial hypocalciuric hypercalcemia type 3. *Nat Genet* **45**, 93-97,(2013).
186 Hannan, F. M. & Thakker, R. V. Calcium-sensing receptor (CaSR) mutations and disorders of calcium, electrolyte and water metabolism. *Best Pract Res Clin Endocrinol Metab* **27**, 359-371,(2013).
187 Volpe, A. *et al.* Familial hypocalciuric hypercalcemia revealed by chondrocalcinosis. *Joint Bone Spine* **76**, 708-710,(2009).
188 Pearce, S. H. *et al.* Calcium-sensing receptor mutations in familial hypocalciuric hypercalcaemia with recurrent pancreatitis. *Clin Endocrinol (Oxf)* **45**, 675-680,(1996).
189 McMurtry, C. T. *et al.* Significant developmental elevation in serum parathyroid hormone levels in a large kindred with familial benign (hypocalciuric) hypercalcemia. *Am J Med* **93**, 247-258,(1992).
190 Pollak, M. R. *et al.* Autosomal dominant hypocalcaemia caused by a Ca(2+)-sensing receptor gene mutation. *Nat Genet* **8**, 303-307,(1994).
191 Magno, A. L. *et al.* The calcium-sensing receptor: a molecular perspective. *Endocr Rev* **32**, 3-30,(2011).
192 Hofer, A. M. & Brown, E. M. Extracellular calcium sensing and signalling. *Nat Rev Mol Cell Biol* **4**, 530-538,(2003).
193 Conigrave, A. D. & Ward, D. T. Calcium-sensing receptor (CaSR): pharmacological properties and signaling pathways. *Best Pract Res Clin Endocrinol Metab* **27**, 315-331,(2013).
194 Grant, M. P. *et al.* Agonist-driven maturation and plasma membrane insertion of calcium-sensing receptors dynamically control signal amplitude. *Sci Signal* **4**, ra78,(2011).
195 Collins, B. M. *et al.* Molecular architecture and functional model of the endocytic AP2 complex. *Cell* **109**, 523-535,(2002).
196 Kelly, B. T. *et al.* A structural explanation for the binding of endocytic dileucine motifs by the AP2 complex. *Nature* **456**, 976-979,(2008).
197 Riccardi, D. & Valenti, G. Localization and function of the renal calcium-sensing receptor. *Nat Rev Nephrol* **12**, 414-425,(2016).
198 Ba, J. *et al.* Calcium-sensing receptor regulation of PTH-inhibitable proximal tubule phosphate transport. *Am J Physiol Renal Physiol* **285**, F1233-1243,(2003).
199 Bland, R. *et al.* Constitutive expression of 25-hydroxyvitamin D3-1alpha-hydroxylase in a transformed human proximal tubule cell line: evidence for direct regulation of vitamin D metabolism by calcium. *Endocrinology* **140**, 2027-2034,(1999).
200 Riccardi, D. & Kemp, P. J. The calcium-sensing receptor beyond extracellular calcium homeostasis: conception, development, adult physiology, and disease. *Annu Rev Physiol* **74**, 271-297,(2012).
201 Riccardi, D. & Brown, E. M. Physiology and pathophysiology of the calcium-sensing receptor in the kidney. *Am J Physiol Renal Physiol* **298**, F485-499,(2010).
202 Topala, C. N. *et al.* Activation of the Ca2+-sensing receptor stimulates the activity of the epithelial Ca2+ channel TRPV5. *Cell Calcium* **45**, 331-339,(2009).
203 Blankenship, K. A. *et al.* The calcium-sensing receptor regulates calcium absorption in MDCK cells by inhibition of PMCA. *Am J Physiol Renal Physiol* **280**, F815-822,(2001).

204 Shimkets, R. A. *et al.* Liddle's syndrome: heritable human hypertension caused by mutations in the beta subunit of the epithelial sodium channel. *Cell* **79**, 407-414,(1994).
205 Strautnieks, S. S. *et al.* A novel splice-site mutation in the gamma subunit of the epithelial sodium channel gene in three pseudohypoaldosteronism type 1 families. *Nat Genet* **13**, 248-250,(1996).
206 Hansson, J. H. *et al.* Hypertension caused by a truncated epithelial sodium channel gamma subunit: genetic heterogeneity of Liddle syndrome. *Nat Genet* **11**, 76-82,(1995).
207 Salih, M. *et al.* A Missense Mutation in the Extracellular Domain of alphaENaC Causes Liddle Syndrome. *J Am Soc Nephrol* **28**, 3291-3299,(2017).
208 Deen, P. M. *et al.* Requirement of human renal water channel aquaporin-2 for vasopressin-dependent concentration of urine. *Science* **264**, 92-95,(1994).
209 Simon, D. B. *et al.* Genetic heterogeneity of Bartter's syndrome revealed by mutations in the K+ channel, ROMK. *Nat Genet* **14**, 152-156,(1996).
210 Newey, P. J. *et al.* in *Genetics of Bone Biology and Skeletal Disease* Ch. 1, (Academic Press, 2018).
211 Shendure, J. & Ji, H. Next-generation DNA sequencing. *Nat Biotechnol* **26**, 1135-1145,(2008).
212 Katsanis, S. H. & Katsanis, N. Molecular genetic testing and the future of clinical genomics. *Nat Rev Genet* **14**, 415-426,(2013).
213 Groopman, E. E. *et al.* Genomic medicine for kidney disease. *Nat Rev Nephrol* **14**, 83-104,(2018).
214 Schwarze, K. *et al.* Are whole-exome and whole-genome sequencing approaches cost-effective? A systematic review of the literature. *Genet Med*,(2018).
215 Sun, Y. *et al.* Next-generation diagnostics: gene panel, exome, or whole genome? *Hum Mutat* **36**, 648-655,(2015).
216 Boycott, K. M. *et al.* Rare-disease genetics in the era of next-generation sequencing: discovery to translation. *Nat Rev Genet* **14**, 681-691,(2013).
217 Lo, Y. F. *et al.* Recurrent deep intronic mutations in the SLC12A3 gene responsible for Gitelman's syndrome. *Clin J Am Soc Nephrol* **6**, 630-639,(2011).
218 de Bruin, C. & Dauber, A. Insights from exome sequencing for endocrine disorders. *Nat Rev Endocrinol* **11**, 455-464,(2015).
219 Cooper, G. M. & Shendure, J. Needles in stacks of needles: finding disease-causal variants in a wealth of genomic data. *Nat Rev Genet* **12**, 628-640,(2011).
220 Thouvenot, P. *et al.* Functional Assessment of Genetic Variants with Outcomes Adapted to Clinical Decision-Making. *PLoS Genet* **12**, e1006096,(2016).
221 MacArthur, D. G. & Tyler-Smith, C. Loss-of-function variants in the genomes of healthy humans. *Hum Mol Genet* **19**, R125-130,(2010).
222 Sambrook, J. *et al. Molecular cloning : a laboratory manual*. 3rd ed edn, (Cold Spring Harbor Laboratory Press, 2001).
223 Piret, S. E. *et al.* Identification of a G-Protein Subunit-alpha11 Gain-of-Function Mutation, Val340Met, in a Family With Autosomal Dominant Hypocalcemia Type 2 (ADH2). *J Bone Miner Res* **31**, 1207-1214,(2016).
224 Sun, S. *et al.* Cloning and characterization of the lipooligosaccharide galactosyltransferase II gene of Haemophilus ducreyi. *J Bacteriol* **182**, 2292-2298,(2000).
225 Choi, Y. *et al.* Predicting the functional effect of amino acid substitutions and indels. *PLoS One* **7**, e46688,(2012).
226 Newton, C. R. *et al.* Analysis of any point mutation in DNA. The amplification refractory mutation system (ARMS). *Nucleic Acids Research* **17**, 2503-2516,(1989).

227 Little, S. in *Current Protocols in Human Genetics* (John Wiley & Sons, Inc., 2001).
228 Gorvin, C. M. *et al.* N-ethyl-N-nitrosourea-Induced Adaptor Protein 2 Sigma Subunit 1 (Ap2s1) Mutations Establish Ap2s1 Loss-of-Function Mice. *JBMR Plus* **1**, 3-15,(2017).
229 Robinson, J. *et al.* Integrative genomics viewer. *Nature Biotechnology* **29**, 24-26,(2011).
230 Pegg, D. E. Principles of cryopreservation. *Methods Mol Biol* **368**, 39-57,(2007).
231 Chesnoy, S. & Huang, L. Structure and function of lipid-DNA complexes for gene delivery. *Annu Rev Biophys Biomol Struct* **29**, 27-47,(2000).
232 Hirko, A. *et al.* Cationic lipid vectors for plasmid DNA delivery. *Curr Med Chem* **10**, 1185-1193,(2003).
233 Gorvin, C. M. *et al.* Galpha11 mutation in mice causes hypocalcemia rectifiable by calcilytic therapy. *JCI Insight* **2**, e91103,(2017).
234 Lines, K. E. *et al.* Epigenetic pathway inhibitors represent potential drugs for treating pancreatic and bronchial neuroendocrine tumors. *Oncogenesis* **6**, e332,(2017).
235 Stenson, P. D. *et al.* The Human Gene Mutation Database: towards a comprehensive repository of inherited mutation data for medical research, genetic diagnosis and next-generation sequencing studies. *Human Genetics* **136**, 665-677,(2017).
236 Lek, M. *et al.* Analysis of protein-coding genetic variation in 60,706 humans. *Nature* **536**, 285-291,(2016).
237 Richards, S. *et al.* Standards and guidelines for the interpretation of sequence variants: a joint consensus recommendation of the American College of Medical Genetics and Genomics and the Association for Molecular Pathology. *Genet Med* **17**, 405-423,(2015).
238 Auton, A. *et al.* A global reference for human genetic variation. *Nature* **526**, 68-74,(2015).
239 Exome Variant Server. *NHLBI GO Exome Sequencing Project (ESP)*, <http://evs.gs.washington.edu/EVS/> (
240 Schwarz, J. M. *et al.* MutationTaster2: mutation prediction for the deep-sequencing age. *Nat Methods* **11**, 361-362,(2014).
241 Choi, Y. & Chan, A. P. PROVEAN web server: a tool to predict the functional effect of amino acid substitutions and indels. *Bioinformatics* **31**, 2745-2747,(2015).
242 Adzhubei, I. *et al.* A method and server for predicting damaging missense mutations. *Nature Methods* **7**, 248-249,(2010).
243 Sim, N. L. *et al.* SIFT web server: predicting effects of amino acid substitutions on proteins. *Nucleic Acids Res* **40**, W452-457,(2012).
244 Vaser, R. *et al.* SIFT missense predictions for genomes. *Nat Protoc* **11**, 1-9,(2016).
245 Ng, P. C. & Henikoff, S. Predicting deleterious amino acid substitutions. *Genome Res* **11**, 863-874,(2001).
246 Tang, H. & Thomas, P. D. Tools for Predicting the Functional Impact of Nonsynonymous Genetic Variation. *Genetics* **203**, 635-647,(2016).
247 Sievers, F. *et al.* Fast, scalable generation of high-quality protein multiple sequence alignments using Clustal Omega. *Molecular Systems Biology* **7**,(2011).
248 Wang, F. *et al.* A TBX5 3'UTR variant increases the risk of congenital heart disease in the Han Chinese population. *Cell Discov* **3**, 17026,(2017).
249 Moszynska, A. *et al.* SNPs in microRNA target sites and their potential role in human disease. *Open Biol* **7**,(2017).
250 Wong, N. & Wang, X. miRDB: an online resource for microRNA target prediction and functional annotations. *Nucleic Acids Res* **43**, D146-152,(2015).

251 Wang, X. Improving microRNA target prediction by modeling with unambiguously identified microRNA-target pairs from CLIP-ligation studies. *Bioinformatics* **32**, 1316-1322,(2016).
252 Bhattacharya, A. *et al.* PolymiRTS Database 3.0: linking polymorphisms in microRNAs and their target sites with human diseases and biological pathways. *Nucleic Acids Research* **42**, D86-D91,(2014).
253 Agarwal, V. *et al.* Predicting effective microRNA target sites in mammalian mRNAs. *eLife* **4**, e05005,(2015).
254 Barenboim, M. *et al.* MicroSNiPer: a web tool for prediction of SNP effects on putative microRNA targets. *Human Mutation* **31**, 1223-1232,(2010).
255 Vagin, O. *et al.* Role of N-glycosylation in trafficking of apical membrane proteins in epithelia. *Am J Physiol Renal Physiol* **296**, F459-469,(2009).
256 Gupta R *et al. Prediction of N-glycosylation sites in human proteins* (2004).
257 Schrodinger, LLC. *The PyMOL Molecular Graphics System, Version 1.8* (2015).
258 Park, E. *et al.* Structure of a CLC chloride ion channel by cryo-electron microscopy. *Nature* **541**, 500-505,(2017).
259 Markovic, S. & Dutzler, R. The structure of the cytoplasmic domain of the chloride channel ClC-Ka reveals a conserved interaction interface. *Structure* **15**, 715-725,(2007).
260 Chen, G. *et al.* alpha-Klotho is a non-enzymatic molecular scaffold for FGF23 hormone signalling. *Nature* **553**, 461-466,(2018).
261 Gorvin, C. M. *et al.* AP2? Mutations Impair Calcium-Sensing Receptor Trafficking and Signaling, and Show an Endosomal Pathway to Spatially Direct G-Protein Selectivity. *Cell Rep* **22**, 1054-1066,(2018).
262 Esapa, C. T. *et al.* A mouse with an N-Ethyl-N-nitrosourea (ENU) Induced Trp589Arg Galnt3 mutation represents a model for hyperphosphataemic familial tumoural calcinosis. *PLoS One* **7**, e43205,(2012).
263 Newey, P. J. *et al.* Utility of Population-Level DNA Sequence Data in the Diagnosis of Hereditary Endocrine Disease. *J Endocr Soc* **1**, 1507-1526,(2017).
264 Yohe, S. & Thyagarajan, B. Review of Clinical Next-Generation Sequencing. *Arch Pathol Lab Med* **141**, 1544-1557,(2017).
265 Green, E. D. *et al.* Charting a course for genomic medicine from base pairs to bedside. *Nature* **470**, 204-213,(2011).
266 Lohmann, K. & Klein, C. Next generation sequencing and the future of genetic diagnosis. *Neurotherapeutics* **11**, 699-707,(2014).
267 Di Resta, C. *et al.* Next-generation sequencing approach for the diagnosis of human diseases: open challenges and new opportunities. *EJIFCC* **29**, 4-14,(2018).
268 Vezzoli, G. *et al.* Autosomal dominant hypocalcemia with mild type 5 Bartter syndrome. *J Nephrol* **19**, 525-528,(2006).
269 Al Shibli, A. & Narchi, H. Bartter and Gitelman syndromes: Spectrum of clinical manifestations caused by different mutations. *World J Methodol* **5**, 55-61,(2015).
270 Simon, D. B. *et al.* Mutations in the chloride channel gene, CLCNKB, cause Bartter's syndrome type III. *Nat Genet* **17**, 171-178,(1997).
271 Nozu, K. *et al.* Molecular analysis of digenic inheritance in Bartter syndrome with sensorineural deafness. *J Med Genet* **45**, 182-186,(2008).
272 Devuyst, O. *et al.* Intra-renal and subcellular distribution of the human chloride channel, CLC-5, reveals a pathophysiological basis for Dent's disease. *Hum Mol Genet* **8**,(1999).
273 Kieferle, S. *et al.* Two highly homologous members of the ClC chloride channel family in both rat and human kidney. *Proceedings of the National Academy of Sciences* **91**, 6943-6947,(1994).

274 Toka, H. R. *et al.* Calcium Sensing in the Renal Tubule. *Physiology (Bethesda)* **30**, 317-326,(2015).
275 Riccardi, D. *et al.* Localization of the extracellular Ca(2+)-sensing receptor and PTH/PTHrP receptor in rat kidney. *Am J Physiol* **271**, F951-956,(1996).
276 Duzkale, H. *et al.* A systematic approach to assessing the clinical significance of genetic variants. *Clin Genet* **84**, 453-463,(2013).
277 Thusberg, J. *et al.* Performance of mutation pathogenicity prediction methods on missense variants. *Human Mutation* **32**, 358-368,(2011).
278 Goodwin, S. *et al.* Coming of age: ten years of next-generation sequencing technologies. *Nat Rev Genet* **17**, 333-351,(2016).
279 Green, R. C. *et al.* ACMG recommendations for reporting of incidental findings in clinical exome and genome sequencing. *Genet Med* **15**, 565-574,(2013).
280 Soden, S. E. *et al.* Effectiveness of exome and genome sequencing guided by acuity of illness for diagnosis of neurodevelopmental disorders. *Sci Transl Med* **6**, 265ra168,(2014).
281 Lee, H. *et al.* Clinical exome sequencing for genetic identification of rare Mendelian disorders. *JAMA* **312**, 1880-1887,(2014).
282 Yang, Y. *et al.* Clinical whole-exome sequencing for the diagnosis of mendelian disorders. *N Engl J Med* **369**, 1502-1511,(2013).
283 Yang, Y. *et al.* Molecular findings among patients referred for clinical whole-exome sequencing. *JAMA* **312**, 1870-1879,(2014).
284 Oetting, W. S. *et al.* Clinical Interpretation of Variants from Next-Generation Sequencing: The 2016 Scientific Meeting of the Human Genome Variation Society. *Hum Mutat* **37**, 1110-1113,(2016).
285 Saito-Ohara, F. *et al.* Assignment of the genes encoding the human chloride channels, CLCNKA and CLCNKB, to 1p36 and of CLCN3 to 4q32-q33 by in situ hybridization. *Genomics* **36**, 372-374,(1996).
286 Goda, N. *et al.* Polymorphism in microRNA-binding site in HNF1B influences the susceptibility of type 2 diabetes mellitus: a population based case–control study. *BMC Medical Genetics* **16**, 75,(2015).
287 van Mil, A. *et al.* MicroRNA-214 inhibits angiogenesis by targeting Quaking and reducing angiogenic growth factor release. *Cardiovascular Research* **93**, 655-665,(2012).
288 Zhang, M. *et al.* miR-214-5p Targets ROCK1 and Suppresses Proliferation and Invasion of Human Osteosarcoma Cells. *Oncology Research Featuring Preclinical and Clinical Cancer Therapeutics* **25**, 75-81,(2017).
289 Shih, T.-C. *et al.* MicroRNA-214 downregulation contributes to tumor angiogenesis by inducing secretion of the hepatoma-derived growth factor in human hepatoma. *Journal of Hepatology* **57**, 584-591,(2012).
290 Laurila, E. M. & Kallioniemi, A. The diverse role of miR-31 in regulating cancer associated phenotypes. *Genes, Chromosomes and Cancer* **52**, 1103-1113,(2013).
291 Pandey, P. *et al.* Microarray-based approach identifies microRNAs and their target functional patterns in polycystic kidney disease. *BMC Genomics* **9**, 624,(2008).
292 Sekine, T. *et al.* Japanese Dent disease has a wider clinical spectrum than Dent disease in Europe/USA: genetic and clinical studies of 86 unrelated patients with low-molecular-weight proteinuria. *Nephrol Dial Transplant* **29**, 376-384,(2014).
293 Ludwig, M. *et al.* Recent advances in understanding the clinical and genetic heterogeneity of Dent's disease. *Nephrol Dial Transplant* **21**, 2708-2717,(2006).
294 Yang, H. *et al.* MicroRNA expression profiling in human ovarian cancer: miR-214 induces cell survival and cisplatin resistance by targeting PTEN. *Cancer Res* **68**, 425-433,(2008).

295 Denby, L. *et al.* miR-21 and miR-214 Are Consistently Modulated during Renal Injury in Rodent Models. *The American Journal of Pathology* **179**, 661-672,(2011).
296 Denby, L. *et al.* MicroRNA-214 Antagonism Protects against Renal Fibrosis. *Journal of the American Society of Nephrology : JASN* **25**, 65-80,(2014).
297 Godwin, J. G. *et al.* Identification of a microRNA signature of renal ischemia reperfusion injury. *Proceedings of the National Academy of Sciences of the United States of America* **107**, 14339-14344,(2010).
298 .(!!! INVALID CITATION !!! 4).
299 Cappola, T. P. *et al.* Loss-of-function DNA sequence variant in the CLCNKA chloride channel implicates the cardio-renal axis in interindividual heart failure risk variation. *Proceedings of the National Academy of Sciences of the United States of America* **108**, 2456-2461,(2011).
300 Barlassina, C. *et al.* Common genetic variants and haplotypes in renal CLCNKA gene are associated to salt-sensitive hypertension. *Human Molecular Genetics* **16**, 1630-1638,(2007).
301 Tavira, B. *et al.* A CLCNKA polymorphism (rs10927887; p.Arg83Gly) previously linked to heart failure is associated with the estimated glomerular filtration rate in the RENASTUR cohort. *Gene* **527**, 670-672,(2013).
302 Shi, S. *et al.* Podocyte-selective deletion of dicer induces proteinuria and glomerulosclerosis. *J Am Soc Nephrol* **19**, 2159-2169,(2008).
303 Harvey, S. J. *et al.* Podocyte-specific deletion of dicer alters cytoskeletal dynamics and causes glomerular disease. *J Am Soc Nephrol* **19**, 2150-2158,(2008).
304 Uchida, S. *et al.* Localization and functional characterization of rat kidney-specific chloride channel, ClC-K1. *J Clin Invest* **95**, 104-113,(1995).
305 Jentsch, T. J. *et al.* The CLC chloride channel family. *Pflugers Arch* **437**, 783-795,(1999).
306 Waldegger, S. *et al.* Barttin increases surface expression and changes current properties of ClC-K channels. *Pflugers Arch* **444**, 411-418,(2002).
307 Janssen, A. G. *et al.* Disease-causing dysfunctions of barttin in Bartter syndrome type IV. *J Am Soc Nephrol* **20**, 145-153,(2009).
308 Scholl, U. *et al.* Barttin modulates trafficking and function of ClC-K channels. *Proc Natl Acad Sci U S A* **103**, 11411-11416,(2006).
309 Mindell, J. A. & Maduke, M. ClC chloride channels. *Genome Biol* **2**, REVIEWS3003,(2001).
310 Tajima, M. *et al.* Barttin binds to the outer lateral surface of the ClC-K2 chloride channel. *Biochem Biophys Res Commun* **362**, 858-864,(2007).
311 Addis, M. *et al.* An atypical Dent's disease phenotype caused by co-inheritance of mutations at CLCN5 and OCRL genes. *Eur J Hum Genet* **21**, 687-690,(2013).
312 Wilcox, W. D. Abnormal serum uric acid levels in children. *J Pediatr* **128**, 731-741,(1996).
313 McBride, M. B. *et al.* Presymptomatic detection of familial juvenile hyperuricaemic nephropathy in children. *Pediatr Nephrol* **12**, 357-364,(1998).
314 Gallagher, D. *et al.* Ankrd11 is a chromatin regulator involved in autism that is essential for neural development. *Dev Cell* **32**, 31-42,(2015).
315 Zhang, A. *et al.* Identification of a novel family of ankyrin repeats containing cofactors for p160 nuclear receptor coactivators. *J Biol Chem* **279**, 33799-33805,(2004).
316 Sirmaci, A. *et al.* Mutations in ANKRD11 cause KBG syndrome, characterized by intellectual disability, skeletal malformations, and macrodontia. *Am J Hum Genet* **89**, 289-294,(2011).

317 Barbaric, I. *et al.* An ENU-induced mutation in the Ankrd11 gene results in an osteopenia-like phenotype in the mouse mutant Yoda. *Physiol Genomics* **32**, 311-321,(2008).
318 Chu, A. Y. *et al.* Epigenome-wide association studies identify DNA methylation associated with kidney function. *Nat Commun* **8**, 1286,(2017).
319 Tsukita, S. *et al.* Multifunctional strands in tight junctions. *Nat Rev Mol Cell Biol* **2**, 285-293,(2001).
320 Lu, Z. *et al.* Claudins in intestines: Distribution and functional significance in health and diseases. *Tissue Barriers* **1**, e24978,(2013).
321 Rahner, C. *et al.* Heterogeneity in expression and subcellular localization of claudins 2, 3, 4, and 5 in the rat liver, pancreas, and gut. *Gastroenterology* **120**, 411-422,(2001).
322 Reyes, J. L. *et al.* The renal segmental distribution of claudins changes with development. *Kidney Int* **62**, 476-487,(2002).
323 Kiuchi-Saishin, Y. *et al.* Differential expression patterns of claudins, tight junction membrane proteins, in mouse nephron segments. *J Am Soc Nephrol* **13**, 875-886,(2002).
324 Weber, S. *et al.* Novel paracellin-1 mutations in 25 families with familial hypomagnesemia with hypercalciuria and nephrocalcinosis. *J Am Soc Nephrol* **12**, 1872-1881,(2001).
325 Ulmann, A. *et al.* Renal magnesium and phosphate wastage in a patient with hypercalciuria and nephrocalcinosis: effect of oral phosphorus and magnesium supplements. *Nephron* **40**, 83-87,(1985).
326 Praga, M. *et al.* Familial hypomagnesemia with hypercalciuria and nephrocalcinosis. *Kidney Int* **47**, 1419-1425,(1995).
327 Yoshimura, S. *et al.* Family-wide characterization of the DENN domain Rab GDP-GTP exchange factors. *J Cell Biol* **191**, 367-381,(2010).
328 Itzen, A. & Goody, R. S. GTPases involved in vesicular trafficking: structures and mechanisms. *Semin Cell Dev Biol* **22**, 48-56,(2011).
329 Goody, R. S. & Hofmann-Goody, W. Exchange factors, effectors, GAPs and motor proteins: common thermodynamic and kinetic principles for different functions. *Eur Biophys J* **31**, 268-274,(2002).
330 Sano, H. *et al.* Insulin-stimulated GLUT4 protein translocation in adipocytes requires the Rab10 guanine nucleotide exchange factor Dennd4C. *J Biol Chem* **286**, 16541-16545,(2011).
331 Babbey, C. M. *et al.* Rab10 regulates membrane transport through early endosomes of polarized Madin-Darby canine kidney cells. *Mol Biol Cell* **17**, 3156-3175,(2006).
332 Kalamajski, S. & Oldberg, A. Fibromodulin binds collagen type I via Glu-353 and Lys-355 in leucine-rich repeat 11. *J Biol Chem* **282**, 26740-26745,(2007).
333 Iozzo, R. V. The biology of the small leucine-rich proteoglycans. Functional network of interactive proteins. *J Biol Chem* **274**, 18843-18846,(1999).
334 Hedbom, E. & Heinegard, D. Interaction of a 59-kDa connective tissue matrix protein with collagen I and collagen II. *J Biol Chem* **264**, 6898-6905,(1989).
335 Gill, M. R. *et al.* Fibromodulin-null murine knee joints display increased incidences of osteoarthritis and alterations in tissue biochemistry. *Osteoarthritis Cartilage* **10**, 751-757,(2002).
336 Jian, J. *et al.* Fibromodulin promoted in vitro and in vivo angiogenesis. *Biochem Biophys Res Commun* **436**, 530-535,(2013).
337 Mondal, B. *et al.* Integrative functional genomic analysis identifies epigenetically regulated fibromodulin as an essential gene for glioma cell migration. *Oncogene* **36**, 71-83,(2017).

338 Mikaelsson, E. *et al.* Fibromodulin, an extracellular matrix protein: characterization of its unique gene and protein expression in B-cell chronic lymphocytic leukemia and mantle cell lymphoma. *Blood* **105**, 4828-4835,(2005).
339 Patel, K. G. *et al.* Myr 8, a novel unconventional myosin expressed during brain development associates with the protein phosphatase catalytic subunits 1alpha and 1gamma1. *J Neurosci* **21**, 7954-7968,(2001).
340 Kengyel, A. *et al.* Ankyrin domain of myosin 16 influences motor function and decreases protein phosphatase catalytic activity. *Eur Biophys J* **44**, 207-218,(2015).
341 Yokoyama, K. *et al.* NYAP: a phosphoprotein family that links PI3K to WAVE1 signalling in neurons. *EMBO J* **30**, 4739-4754,(2011).
342 Mack, T. G. & Eickholt, B. J. New WAVEs in neuronal PI3K signalling. *EMBO J* **30**, 4693-4695,(2011).
343 Liu, Y. F. *et al.* Autism and Intellectual Disability-Associated KIRREL3 Interacts with Neuronal Proteins MAP1B and MYO16 with Potential Roles in Neurodevelopment. *PLoS One* **10**, e0123106,(2015).
344 Terzic, J. *et al.* Expression of PAX2 gene during human development. *Int J Dev Biol* **42**, 701-707,(1998).
345 Dressler, G. R. *et al.* Pax2, a new murine paired-box-containing gene and its expression in the developing excretory system. *Development* **109**, 787-795,(1990).
346 Nornes, H. O. *et al.* Spatially and temporally restricted expression of Pax2 during murine neurogenesis. *Development* **109**, 797-809,(1990).
347 Sanyanusin, P. *et al.* Mutation of the PAX2 gene in a family with optic nerve colobomas, renal anomalies and vesicoureteral reflux. *Nat Genet* **9**, 358-364,(1995).
348 Weaver, R. G. *et al.* Optic nerve coloboma associated with renal disease. *Am J Med Genet* **29**, 597-605,(1988).
349 Bower, M. A. *et al.* in *GeneReviews((R))* (eds M. P. Adam *et al.*) (1993).
350 Bower, M. *et al.* Update of PAX2 mutations in renal coloboma syndrome and establishment of a locus-specific database. *Hum Mutat* **33**, 457-466,(2012).
351 Megaw, R. D. *et al.* Papillorenal syndrome in a family with unusual complications. *Br J Ophthalmol* **97**, 945-946,(2013).
352 Schimmenti, L. A. Renal coloboma syndrome. *Eur J Hum Genet* **19**, 1207-1212,(2011).
353 Devriendt, K. *et al.* Missense mutation and hexanucleotide duplication in the PAX2 gene in two unrelated families with renal-coloboma syndrome (MIM 120330). *Hum Genet* **103**, 149-153,(1998).
354 Uhlen, M. *et al.* Proteomics. Tissue-based map of the human proteome. *Science* **347**, 1260419,(2015).
355 *ANKRD11*, <https://www.proteinatlas.org/ENSG00000167522-ANKRD11/tissue> (
356 *FMOD*, <https://www.proteinatlas.org/ENSG00000122176-FMOD/tissue> (
357 *CLDN3*, <https://www.proteinatlas.org/ENSG00000165215-CLDN3/tissue> (
358 *DENND4C*, <https://www.proteinatlas.org/ENSG00000137145-DENND4C/tissue> (
359 *MYO16*, <https://www.proteinatlas.org/ENSG00000041515-MYO16/tissue> (
360 Angelow, S. & Yu, A. S. Claudins and paracellular transport: an update. *Curr Opin Nephrol Hypertens* **16**, 459-464,(2007).
361 Srinivasan, B. *et al.* TEER measurement techniques for in vitro barrier model systems. *J Lab Autom* **20**, 107-126,(2015).
362 Dukes, J. D. *et al.* The MDCK variety pack: choosing the right strain. *BMC Cell Biol* **12**, 43,(2011).

363 Grimley, E. *et al.* Inhibition of Pax2 Transcription Activation with a Small Molecule that Targets the DNA Binding Domain. *ACS Chem Biol* **12**, 724-734,(2017).
364 Cai, Y. *et al.* Groucho suppresses Pax2 transactivation by inhibition of JNK-mediated phosphorylation. *EMBO J* **22**, 5522-5529,(2003).
365 Alur, R. P. *et al.* Papillorenal syndrome-causing missense mutations in PAX2/Pax2 result in hypomorphic alleles in mouse and human. *PLoS Genet* **6**, e1000870,(2010).
366 Mutig, K. *et al.* Activation of the bumetanide-sensitive Na+,K+,2Cl- cotransporter (NKCC2) is facilitated by Tamm-Horsfall protein in a chloride-sensitive manner. *J Biol Chem* **286**, 30200-30210,(2011).
367 Renigunta, A. *et al.* Tamm-Horsfall glycoprotein interacts with renal outer medullary potassium channel ROMK2 and regulates its function. *J Biol Chem* **286**, 2224-2235,(2011).
368 Milatz, S. *et al.* Claudin-3 acts as a sealing component of the tight junction for ions of either charge and uncharged solutes. *Biochim Biophys Acta* **1798**, 2048-2057,(2010).
369 Sheller, R. A. *et al.* Comparison of transepithelial resistance measurement techniques: Chopsticks vs. Endohm. *Biol Proced Online* **19**, 4,(2017).
370 Sadacca, L. A. *et al.* Specialized sorting of GLUT4 and its recruitment to the cell surface are independently regulated by distinct Rabs. *Mol Biol Cell* **24**, 2544-2557,(2013).
371 Chua, C. E. L. & Tang, B. L. Rab 10-a traffic controller in multiple cellular pathways and locations. *J Cell Physiol* **233**, 6483-6494,(2018).
372 Hannan, F. M. *et al.* Identification of 70 calcium-sensing receptor mutations in hyper- and hypo-calcaemic patients: evidence for clustering of extracellular domain mutations at calcium-binding sites. *Hum Mol Genet* **21**, 2768-2778,(2012).
373 Gorvin, C. M. *et al.* A G-protein Subunit-alpha11 Loss-of-Function Mutation, Thr54Met, Causes Familial Hypocalciuric Hypercalcemia Type 2 (FHH2). *J Bone Miner Res* **31**, 1200-1206,(2016).
374 Kuro-o, M. *et al.* Mutation of the mouse klotho gene leads to a syndrome resembling ageing. *Nature* **390**, 45-51,(1997).
375 Li, S. A. *et al.* Immunohistochemical localization of Klotho protein in brain, kidney, and reproductive organs of mice. *Cell Struct Funct* **29**, 91-99,(2004).
376 Lim, K. *et al.* alpha-Klotho Expression in Human Tissues. *J Clin Endocrinol Metab* **100**, E1308-1318,(2015).
377 Ichikawa, S. *et al.* A homozygous missense mutation in human KLOTHO causes severe tumoral calcinosis. *J Musculoskelet Neuronal Interact* **7**, 318-319,(2007).
378 Yoshida, T. *et al.* Mediation of unusually high concentrations of 1,25-dihydroxyvitamin D in homozygous klotho mutant mice by increased expression of renal 1alpha-hydroxylase gene. *Endocrinology* **143**, 683-689,(2002).
379 Tsujikawa, H. *et al.* Klotho, a gene related to a syndrome resembling human premature aging, functions in a negative regulatory circuit of vitamin D endocrine system. *Mol Endocrinol* **17**, 2393-2403,(2003).
380 Olauson, H. *et al.* Targeted deletion of Klotho in kidney distal tubule disrupts mineral metabolism. *J Am Soc Nephrol* **23**, 1641-1651,(2012).
381 Esapa, C. *et al.* N-ethyl-N-Nitrosourea (ENU) Induced Mutations within the Klotho Gene Lead to Ectopic Calcification and Reduced Lifespan in Mouse Models. *Plos One* **10**,(2015).
382 Matsumura, Y. *et al.* Identification of the human klotho gene and its two transcripts encoding membrane and secreted klotho protein. *Biochem Biophys Res Commun* **242**, 626-630,(1998).

383 Chen, C. D. *et al.* Identification of cleavage sites leading to the shed form of the anti-aging protein klotho. *Biochemistry* **53**, 5579-5587,(2014).
384 Chen, C. D. *et al.* Insulin stimulates the cleavage and release of the extracellular domain of Klotho by ADAM10 and ADAM17. *Proc Natl Acad Sci U S A* **104**, 19796-19801,(2007).
385 Shiraki-Iida, T. *et al.* Structure of the mouse klotho gene and its two transcripts encoding membrane and secreted protein. *FEBS Lett* **424**, 6-10,(1998).
386 Hinnie, J. *et al.* The prevalence of familial hypocalciuric hypercalcemia. *Calcif Tissue Int* **68**, 216-218,(2001).
387 Diener, S. *et al.* Development of A Cell-Based Assay to Identify Small Molecule Inhibitors of FGF23 Signaling. *Assay Drug Dev Technol* **13**, 476-487,(2015).
388 Wortzel, I. & Seger, R. The ERK Cascade: Distinct Functions within Various Subcellular Organelles. *Genes Cancer* **2**, 195-209,(2011).
389 Gille, H. *et al.* ERK phosphorylation potentiates Elk-1-mediated ternary complex formation and transactivation. *EMBO J* **14**, 951-962,(1995).
390 Ornitz, D. M. & Itoh, N. The Fibroblast Growth Factor signaling pathway. *Wiley Interdiscip Rev Dev Biol* **4**, 215-266,(2015).
391 Brown, E. M. Role of the calcium-sensing receptor in extracellular calcium homeostasis. *Best Pract Res Clin Endocrinol Metab* **27**, 333-343,(2013).
392 Breitwieser, G. E. The calcium sensing receptor life cycle: trafficking, cell surface expression, and degradation. *Best Pract Res Clin Endocrinol Metab* **27**, 303-313,(2013).
393 Arking, D. E. *et al.* Association of human aging with a functional variant of klotho. *Proc Natl Acad Sci U S A* **99**, 856-861,(2002).
394 Arking, D. E. *et al.* KLOTHO allele status and the risk of early-onset occult coronary artery disease. *Am J Hum Genet* **72**, 1154-1161,(2003).
395 Low, A. F. *et al.* Aging syndrome genes and premature coronary artery disease. *BMC Med Genet* **6**, 38,(2005).
396 Holstein, D. M. *et al.* Calcium-sensing receptor-mediated ERK1/2 activation requires Galphai2 coupling and dynamin-independent receptor internalization. *J Biol Chem* **279**, 10060-10069,(2004).
397 Kifor, O. *et al.* Regulation of MAP kinase by calcium-sensing receptor in bovine parathyroid and CaR-transfected HEK293 cells. *Am J Physiol Renal Physiol* **280**, F291-302,(2001).
398 Thomsen, A. R. *et al.* Biased agonism of the calcium-sensing receptor. *Cell Calcium* **51**, 107-116,(2012).
399 Gorvin, C. M. *et al.* A calcium-sensing receptor mutation causing hypocalcemia disrupts a transmembrane salt bridge to activate beta-arrestin-biased signaling. *Sci Signal* **11**,(2018).
400 Olauson, H. *et al.* Parathyroid-specific deletion of Klotho unravels a novel calcineurin-dependent FGF23 signaling pathway that regulates PTH secretion. *PLoS Genet* **9**, e1003975,(2013).
401 Shalhoub, V. *et al.* FGF23 neutralization improves chronic kidney disease-associated hyperparathyroidism yet increases mortality. *J Clin Invest* **122**, 2543-2553,(2012).
402 Smith, E. R. *et al.* FGF23 activates injury-primed renal fibroblasts via FGFR4-dependent signalling and enhancement of TGF-beta autoinduction. *Int J Biochem Cell Biol* **92**, 63-78,(2017).
403 Faul, C. *et al.* FGF23 induces left ventricular hypertrophy. *J Clin Invest* **121**, 4393-4408,(2011).
404 Gregg, J. & Fraizer, G. Transcriptional Regulation of EGR1 by EGF and the ERK Signaling Pathway in Prostate Cancer Cells. *Genes Cancer* **2**, 900-909,(2011).

405 Devuyst, O. *et al.* Rare inherited kidney diseases: challenges, opportunities, and perspectives. *Lancet* **383**, 1844-1859,(2014).
406 Shashi, V. *et al.* The utility of the traditional medical genetics diagnostic evaluation in the context of next-generation sequencing for undiagnosed genetic disorders. *Genet Med* **16**, 176-182,(2014).
407 (ed Eurodis- Rare Diseases Europe) (2007).
408 Ziemba, J. B. & Matlaga, B. R. Epidemiology and economics of nephrolithiasis. *Investig Clin Urol* **58**, 299-306,(2017).
409 Yasukochi, Y. *et al.* Identification of nine novel loci related to hematological traits in a Japanese population. *Physiol Genomics* **50**, 758-769,(2018).
410 Gast, C. *et al.* Collagen (COL4A) mutations are the most frequent mutations underlying adult focal segmental glomerulosclerosis. *Nephrol Dial Transplant* **31**, 961-970,(2016).
411 Malone, A. F. *et al.* Rare hereditary COL4A3/COL4A4 variants may be mistaken for familial focal segmental glomerulosclerosis. *Kidney Int* **86**, 1253-1259,(2014).
412 Kashtan, C. E. in *GeneReviews((R))* (eds M. P. Adam *et al.*) (1993).
413 M'Rad, R. *et al.* Alport syndrome: a genetic study of 31 families. *Hum Genet* **90**, 420-426,(1992).
414 Lemmink, H. H. *et al.* Mutations in the type IV collagen alpha 3 (COL4A3) gene in autosomal recessive Alport syndrome. *Hum Mol Genet* **3**, 1269-1273,(1994).
415 Mochizuki, T. *et al.* Identification of mutations in the alpha 3(IV) and alpha 4(IV) collagen genes in autosomal recessive Alport syndrome. *Nat Genet* **8**, 77-81,(1994).
416 van der Loop, F. T. *et al.* Autosomal dominant Alport syndrome caused by a COL4A3 splice site mutation. *Kidney Int* **58**, 1870-1875,(2000).
417 Voskarides, K. *et al.* COL4A3/COL4A4 mutations producing focal segmental glomerulosclerosis and renal failure in thin basement membrane nephropathy. *J Am Soc Nephrol* **18**, 3004-3016,(2007).
418 Lemmink, H. H. *et al.* Benign familial hematuria due to mutation of the type IV collagen alpha4 gene. *J Clin Invest* **98**, 1114-1118,(1996).
419 Buzza, M. *et al.* COL4A4 mutation in thin basement membrane disease previously described in Alport syndrome. *Kidney Int* **60**, 480-483,(2001).
420 Tryggvason, K. & Patrakka, J. Thin basement membrane nephropathy. *J Am Soc Nephrol* **17**, 813-822,(2006).
421 Clissold, R. L. *et al.* HNF1B-associated renal and extra-renal disease-an expanding clinical spectrum. *Nat Rev Nephrol* **11**, 102-112,(2015).
422 de Andrade, S. C. *et al.* Novel mutation of the calcium sensing receptor gene in familial hypocalciuric hypercalcaemia and neonatal severe hyperparathyroidism. *Clin Endocrinol (Oxf)* **65**, 826-827,(2006).
423 Pidasheva, S. *et al.* Impaired cotranslational processing of the calcium-sensing receptor due to signal peptide missense mutations in familial hypocalciuric hypercalcemia. *Hum Mol Genet* **14**, 1679-1690,(2005).
424 Miyashiro, K. *et al.* Severe hypercalcemia in a 9-year-old Brazilian girl due to a novel inactivating mutation of the calcium-sensing receptor. *J Clin Endocrinol Metab* **89**, 5936-5941,(2004).
425 Nissen, P. H. *et al.* Identification of rare and frequent variants of the CASR gene by high-resolution melting. *Clin Chim Acta* **413**, 605-611,(2012).
426 Nissen, P. H. *et al.* Molecular genetic analysis of the calcium sensing receptor gene in patients clinically suspected to have familial hypocalciuric hypercalcemia: phenotypic variation and mutation spectrum in a Danish population. *J Clin Endocrinol Metab* **92**, 4373-4379,(2007).

427 Ward, B. K. *et al.* Novel mutations in the calcium-sensing receptor gene associated with biochemical and functional differences in familial hypocalciuric hypercalcaemia. *Clin Endocrinol (Oxf)* **64**, 580-587,(2006).
428 Chikatsu, N. *et al.* An adult patient with severe hypercalcaemia and hypocalciuria due to a novel homozygous inactivating mutation of calcium-sensing receptor. *Clin Endocrinol (Oxf)* **50**, 537-543,(1999).
429 Hu, J. *et al.* Autosomal dominant hypocalcemia in monozygotic twins caused by a de novo germline mutation near the amino-terminus of the human calcium receptor. *J Bone Miner Res* **19**, 578-586,(2004).
430 Aida, K. *et al.* Familial hypocalciuric hypercalcemia associated with mutation in the human Ca(2+)-sensing receptor gene. *J Clin Endocrinol Metab* **80**, 2594-2598,(1995).
431 Vargas-Poussou, R. *et al.* Functional characterization of a calcium-sensing receptor mutation in severe autosomal dominant hypocalcemia with a Bartter-like syndrome. *J Am Soc Nephrol* **13**, 2259-2266,(2002).
432 Cole, D. E. *et al.* Calcium-sensing receptor mutations and denaturing high performance liquid chromatography. *J Mol Endocrinol* **42**, 331-339,(2009).
433 Okazaki, R. *et al.* A novel activating mutation in calcium-sensing receptor gene associated with a family of autosomal dominant hypocalcemia. *J Clin Endocrinol Metab* **84**, 363-366,(1999).
434 Heath, H., 3rd *et al.* Clustered inactivating mutations and benign polymorphisms of the calcium receptor gene in familial benign hypocalciuric hypercalcemia suggest receptor functional domains. *J Clin Endocrinol Metab* **81**, 1312-1317,(1996).
435 Pearce, S. H. *et al.* Calcium-sensing receptor mutations in familial benign hypercalcemia and neonatal hyperparathyroidism. *J Clin Invest* **96**, 2683-2692,(1995).
436 Waller, S. *et al.* Neonatal severe hyperparathyroidism: genotype/phenotype correlation and the use of pamidronate as rescue therapy. *Eur J Pediatr* **163**, 589-594,(2004).
437 Chou, Y. H. *et al.* Mutations in the human Ca(2+)-sensing-receptor gene that cause familial hypocalciuric hypercalcemia. *Am J Hum Genet* **56**, 1075-1079,(1995).
438 Pidasheva, S. *et al.* Calcium-sensing receptor dimerizes in the endoplasmic reticulum: biochemical and biophysical characterization of CASR mutants retained intracellularly. *Hum Mol Genet* **15**, 2200-2209,(2006).
439 Wilhelm-Bals, A. *et al.* Successful use of bisphosphonate and calcimimetic in neonatal severe primary hyperparathyroidism. *Pediatrics* **129**, e812-816,(2012).
440 Ward, B. K. *et al.* Functional deletion of the calcium-sensing receptor in a case of neonatal severe hyperparathyroidism. *J Clin Endocrinol Metab* **89**, 3721-3730,(2004).
441 Warner, J. *et al.* Genetic testing in familial isolated hyperparathyroidism: unexpected results and their implications. *J Med Genet* **41**, 155-160,(2004).
442 Nakamura, A. *et al.* Loss-of-function and gain-of-function mutations of calcium-sensing receptor: functional analysis and the effect of allosteric modulators NPS R-568 and NPS 2143. *J Clin Endocrinol Metab* **98**, E1692-1701,(2013).
443 Baron, J. *et al.* Mutations in the Ca(2+)-sensing receptor gene cause autosomal dominant and sporadic hypoparathyroidism. *Hum Mol Genet* **5**, 601-606,(1996).
444 Pearce, S. H. *et al.* A familial syndrome of hypocalcemia with hypercalciuria due to mutations in the calcium-sensing receptor. *N Engl J Med* **335**, 1115-1122,(1996).
445 Hu, J. *et al.* Autosomal dominant hypocalcemia caused by a novel mutation in the loop 2 region of the human calcium receptor extracellular domain. *J Bone Miner Res* **17**, 1461-1469,(2002).

446 Hendy, G. N. *et al.* Mutations of the calcium-sensing receptor (CASR) in familial hypocalciuric hypercalcemia, neonatal severe hyperparathyroidism, and autosomal dominant hypocalcemia. *Hum Mutat* **16**, 281-296,(2000).
447 Lienhardt, A. *et al.* Activating mutations of the calcium-sensing receptor: management of hypocalcemia. *J Clin Endocrinol Metab* **86**, 5313-5323,(2001).
448 Hirai, H. *et al.* A novel activating mutation (C129S) in the calcium-sensing receptor gene in a Japanese family with autosomal dominant hypocalcemia. *J Hum Genet* **46**, 41-44,(2001).
449 Burren, C. P. *et al.* A family with autosomal dominant hypocalcaemia with hypercalciuria (ADHH): mutational analysis, phenotypic variability and treatment challenges. *J Pediatr Endocrinol Metab* **18**, 689-699,(2005).
450 Watanabe, S. *et al.* Association between activating mutations of calcium-sensing receptor and Bartter's syndrome. *Lancet* **360**, 692-694,(2002).
451 Suzuki, M. *et al.* A case of gain-of-function mutation in calcium-sensing receptor: supplemental hydration is required for renal protection. *Clin Nephrol* **63**, 481-486,(2005).
452 Gupta, S. *et al.* in *European Society for Paediatric Endocrinology.* 146 (Hormone Research in Paediatrics).
453 Soei, Y. L. *et al.* in *ASBMR/ISCD Joint Symposium on Bone Densitometry Y2K to Y3K.* 1631 (Journal of Bone and Mineral Research).
454 Letz, S. *et al.* Novel activating mutations of the calcium-sensing receptor: the calcilytic NPS-2143 mitigates excessive signal transduction of mutant receptors. *J Clin Endocrinol Metab* **95**, E229-233,(2010).
455 Lovlie, R. *et al.* The Ca(2+)-sensing receptor gene (PCAR1) mutation T151M in isolated autosomal dominant hypoparathyroidism. *Hum Genet* **98**, 129-133,(1996).
456 Simonds, W. F. *et al.* Familial isolated hyperparathyroidism: clinical and genetic characteristics of 36 kindreds. *Medicine (Baltimore)* **81**, 1-26,(2002).
457 Ho, J. *et al.* Kabuki syndrome and Crohn disease in a child with familial hypocalciuric hypercalcemia. *J Pediatr Endocrinol Metab* **23**, 975-979,(2010).
458 Hinnie, J. *et al.* Two novel mutations causing familial benign hypocalciuric hypercalcaemia in three Scottish families. *Scott Med J* **54**, 11-14,(2009).
459 Felderbauer, P. *et al.* A novel mutation of the calcium sensing receptor gene is associated with chronic pancreatitis in a family with heterozygous SPINK1 mutations. *BMC Gastroenterol* **3**, 34,(2003).
460 Ward, B. K. *et al.* A novel mutation (L174R) in the Ca2+-sensing receptor gene associated with familial hypocalciuric hypercalcemia. *Hum Mutat* **10**, 233-235,(1997).
461 Zajickova, K. *et al.* Identification and functional characterization of a novel mutation in the calcium-sensing receptor gene in familial hypocalciuric hypercalcemia: modulation of clinical severity by vitamin D status. *J Clin Endocrinol Metab* **92**, 2616-2623,(2007).
462 Kobayashi, M. *et al.* Two novel missense mutations in calcium-sensing receptor gene associated with neonatal severe hyperparathyroidism. *J Clin Endocrinol Metab* **82**, 2716-2719,(1997).
463 Nanjo, K. *et al.* Identification and functional analysis of novel calcium-sensing receptor gene mutation in familial hypocalciuric hypercalcemia. *Endocr J* **57**, 787-792,(2010).
464 Demedts, M. *et al.* A new missense mutation in the CASR gene in familial interstitial lung disease with hypocalciuric hypercalcemia and defective granulocyte function. *Am J Respir Crit Care Med* **177**, 558-559,(2008).

465 Marcocci, C. *et al.* Familial hypocalciuric hypercalcemia in a woman with metastatic breast cancer: a case report of mistaken identity. *J Clin Endocrinol Metab* **88**, 5132-5136,(2003).
466 Elamin, W. F. & de Buyl, O. A novel mutation in the calcium-sensing receptor gene in an Irish pedigree showing familial hypocalciuric hypercalcemia: a case report. *J Med Case Rep* **4**, 349,(2010).
467 Cetani, F. *et al.* Two Italian kindreds with familial hypocalciuric hypercalcaemia caused by loss-of-function mutations in the calcium-sensing receptor (CaR) gene: functional characterization of a novel CaR missense mutation. *Clin Endocrinol (Oxf)* **58**, 199-206,(2003).
468 D'Souza-Li, L. *et al.* Four novel calcium-sensing receptor mutations in familial hypocalciuric hypercalcemia and autosomal dominant hypocalcemia. *Bone*,(1998).
469 Conley, Y. P. *et al.* Three novel activating mutations in the calcium-sensing receptor responsible for autosomal dominant hypocalcemia. *Mol Genet Metab* **71**, 591-598,(2000).
470 Al-Khalaf, F. A. *et al.* Neonatal severe hyperparathyroidism: further clinical and molecular delineation. *Eur J Pediatr* **170**, 625-631,(2011).
471 Nakajima, K. *et al.* Novel gain of function mutations of the calcium-sensing receptor in two patients with PTH-deficient hypocalcemia. *Intern Med* **48**, 1951-1956,(2009).
472 Perry, Y. N. *et al.* (American Journal of Human Genetics, 1994).
473 Guarnieri, V. *et al.* Calcium-sensing receptor (CASR) mutations in hypercalcemic states: studies from a single endocrine clinic over three years. *J Clin Endocrinol Metab* **95**, 1819-1829,(2010).
474 Starker, L. F. *et al.* Frequent germ-line mutations of the MEN1, CASR, and HRPT2/CDC73 genes in young patients with clinically non-familial primary hyperparathyroidism. *Horm Cancer* **3**, 44-51,(2012).
475 Hannan, F. M. *et al.* A homozygous inactivating calcium-sensing receptor mutation, Pro339Thr, is associated with isolated primary hyperparathyroidism: correlation between location of mutations and severity of hypercalcaemia. *Clin Endocrinol (Oxf)* **73**, 715-722,(2010).
476 Vigouroux, C. *et al.* A new missense mutation in the calcium-sensing receptor in familial benign hypercalcaemia associated with partial lipoatrophy and insulin resistant diabetes. *Clin Endocrinol (Oxf)* **53**, 393-398,(2000).
477 Park, S. Y. *et al.* Identification and characterization of D410E, a novel mutation in the loop 3 domain of CASR, in autosomal dominant hypocalcemia and a therapeutic approach using a novel calcilytic, AXT914. *Clin Endocrinol (Oxf)* **78**, 687-693,(2013).
478 Lietman, S. A. *et al.* A novel loss-of-function mutation, Gln459Arg, of the calcium-sensing receptor gene associated with apparent autosomal recessive inheritance of familial hypocalciuric hypercalcemia. *J Clin Endocrinol Metab* **94**, 4372-4379,(2009).
479 Leech, C. *et al.* Identification of a novel inactivating R465Q mutation of the calcium-sensing receptor. *Biochem Biophys Res Commun* **342**, 996-1002,(2006).
480 Koltin, D. *et al.* Mild infantile hypercalcemia: diagnostic tests and outcomes. *J Pediatr* **159**, 215-221 e211,(2011).
481 Rodrigues, L. S. *et al.* New mutation in the CASR gene in a family with familial hypocalciuric hypercalcemia (FHH) and neonatal severe hyperparathyroidism (NSHPT). *Arq Bras Endocrinol Metabol* **55**, 67-71,(2011).
482 Rus, R. *et al.* Novel inactivating mutations of the calcium-sensing receptor: the calcimimetic NPS R-568 improves signal transduction of mutant receptors. *J Clin Endocrinol Metab* **93**, 4797-4803,(2008).

483 D'Souza-Li, L. *et al.* Identification and functional characterization of novel calcium-sensing receptor mutations in familial hypocalciuric hypercalcemia and autosomal dominant hypocalcemia. *J Clin Endocrinol Metab* **87**, 1309-1318,(2002).
484 Al-Salameh, A. *et al.* A novel mutation in the calcium-sensing receptor in a French family with familial hypocalciuric hypercalcaemia. *Eur J Endocrinol* **165**, 359-363,(2011).
485 Toke, J. *et al.* Neonatal severe hyperparathyroidism associated with a novel de novo heterozygous R551K inactivating mutation and a heterozygous A986S polymorphism of the calcium-sensing receptor gene. *Clin Endocrinol (Oxf)* **67**, 385-392,(2007).
486 Schwarz, P. *et al.* Familial hypocalciuric hypercalcemia and neonatal severe hyperparathyroidism associated with mutations in the human Ca2+-sensing receptor gene in three Danish families. *Scand J Clin Lab Invest* **60**, 221-227,(2000).
487 Tonyushkina, K. N. *et al.* A novel CaSR mutation presenting as a severe case of neonatal familial hypocalciuric hypercalcemia. *Int J Pediatr Endocrinol* **2012**, 13,(2012).
488 Livadariu, E. *et al.* Mutations of calcium-sensing receptor gene: two novel mutations and overview of impact on calcium homeostasis. *Eur J Endocrinol* **165**, 353-358,(2011).
489 Nakayama, T. *et al.* A novel mutation in Ca2+-sensing receptor gene in familial hypocalciuric hypercalcemia. *Endocrine* **15**, 277-282,(2001).
490 Burski, K. *et al.* Parathyroid adenoma in a subject with familial hypocalciuric hypercalcemia: coincidence or causality? *J Clin Endocrinol Metab* **87**, 1015-1016,(2002).
491 Nyweide, K. *et al.* Hypocalciuric hypercalcemia presenting as neonatal rib fractures: a newly described mutation of the calcium-sensing receptor gene. *Pediatr Emerg Care* **22**, 722-724,(2006).
492 Cetani, F. *et al.* Identification and functional characterization of loss-of-function mutations of the calcium-sensing receptor in four Italian kindreds with familial hypocalciuric hypercalcemia. *Eur J Endocrinol* **160**, 481-489,(2009).
493 Tan, Y. M. *et al.* Autosomal dominant hypocalcemia: a novel activating mutation (E604K) in the cysteine-rich domain of the calcium-sensing receptor. *J Clin Endocrinol Metab* **88**, 605-610,(2003).
494 Rasmussen, A. Q. *et al.* Clinical and biochemical outcomes of cinacalcet treatment of familial hypocalciuric hypercalcemia: a case series. *J Med Case Rep* **5**, 564,(2011).
495 Stock, J. L. *et al.* Autosomal dominant hypoparathyroidism associated with short stature and premature osteoarthritis. *J Clin Endocrinol Metab* **84**, 3036-3040,(1999).
496 Jap, T. S. *et al.* A novel mutation in the calcium-sensing receptor gene in a Chinese subject with persistent hypercalcemia and hypocalciuria. *J Clin Endocrinol Metab* **86**, 13-15,(2001).
497 Guarnieri, V. *et al.* CASR gene activating mutations in two families with autosomal dominant hypocalcemia. *Mol Genet Metab* **107**, 548-552,(2012).
498 Aparicio Lopez, C. *et al.* Familial hypocalciuric hypercalcemia: new mutation in the CASR gene converting valine 697 to methionine. *Eur J Pediatr* **171**, 147-150,(2012).
499 Mittelman, S. D. *et al.* A hypocalcemic child with a novel activating mutation of the calcium-sensing receptor gene: successful treatment with recombinant human parathyroid hormone. *J Clin Endocrinol Metab* **91**, 2474-2479,(2006).

500 Raue, F. *et al.* Activating mutations in the calcium-sensing receptor: genetic and clinical spectrum in 25 patients with autosomal dominant hypocalcaemia - a German survey. *Clin Endocrinol (Oxf)* **75**, 760-765,(2011).
501 Wong, W. C. *et al.* Persistent hypocalcaemia in a Chinese girl due to a novel de-novo activating mutation of the calcium-sensing receptor gene. *Hong Kong Med J* **17**, 157-160,(2011).
502 Dixit, S. & Penas, P. F. Sarcoidosis, hypercalcemia and calcium-sensing receptor mutation: a case report. *Acta Derm Venereol* **91**, 468,(2011).
503 Uckun-Kitapci, A. *et al.* A novel mutation (E767K) in the second extracellular loop of the calcium sensing receptor in a family with autosomal dominant hypocalcemia. *Am J Med Genet A* **132A**, 125-129,(2005).
504 De Luca, F. *et al.* Sporadic hypoparathyroidism caused by de Novo gain-of-function mutations of the Ca(2+)-sensing receptor. *J Clin Endocrinol Metab* **82**, 2710-2715,(1997).
505 Hendy, G. N. *et al.* Recurrent familial hypocalcemia due to germline mosaicism for an activating mutation of the calcium-sensing receptor gene. *J Clin Endocrinol Metab* **88**, 3674-3681,(2003).
506 Watanabe, T. *et al.* Familial hypoparathyroidism: identification of a novel gain of function mutation in transmembrane domain 5 of the calcium-sensing receptor. *J Clin Endocrinol Metab* **83**, 2497-2502,(1998).
507 Lam, C. W. *et al.* Novel missense mutation in the CASR gene in a Chinese family with familial hypocalciuric hypercalcemia. *Clin Chim Acta* **360**, 167-172,(2005).
508 Lia-Baldini, A. S. *et al.* Two novel mutations of the calcium-sensing receptor gene affecting the same amino acid position lead to opposite phenotypes and reveal the importance of p.N802 on receptor activity. *Eur J Endocrinol* **168**, K27-34,(2013).
509 Miyashiro, K. *et al.* Identification and functional analysis of a novel inactivating mutation (A804D) of the calcium-sensing receptor gene. *Clin Endocrinol (Oxf)* **61**, 780-782,(2004).
510 Timmers, H. J. *et al.* Normalization of serum calcium by cinacalcet in a patient with hypercalcaemia due to a de novo inactivating mutation of the calcium-sensing receptor. *J Intern Med* **260**, 177-182,(2006).
511 Schouten, B. J. *et al.* Four cases of autosomal dominant hypocalcaemia with hypercalciuria including two with novel mutations in the calcium-sensing receptor gene. *Ann Clin Biochem* **48**, 286-290,(2011).
512 Nagase, T. *et al.* A family of autosomal dominant hypocalcemia with a positive correlation between serum calcium and magnesium: identification of a novel gain of function mutation (Ser(820)Phe) in the calcium-sensing receptor. *J Clin Endocrinol Metab* **87**, 2681-2687,(2002).
513 Shiohara, M. *et al.* A novel gain-of-function mutation (F821L) in the transmembrane domain of calcium-sensing receptor is a cause of severe sporadic hypoparathyroidism. *Eur J Pediatr* **163**, 94-98,(2004).
514 Inoue, D. *et al.* in *Second Joint Meeting of The American Society for Bone and Mineral Research and The International Bone and Mineral Society.* 382 (Bone).
515 Hu, J. *et al.* A region in the seven-transmembrane domain of the human Ca2+ receptor critical for response to Ca2+. *J Biol Chem* **280**, 5113-5120,(2005).
516 Zhao, X. M. *et al.* A missense mutation in the seventh transmembrane domain constitutively activates the human Ca2+ receptor. *FEBS Lett* **448**, 180-184,(1999).
517 Carling, T. *et al.* Familial hypercalcemia and hypercalciuria caused by a novel mutation in the cytoplasmic tail of the calcium receptor. *J Clin Endocrinol Metab* **85**, 2042-2047,(2000).

518 Lazarus, S. *et al.* A novel mutation of the primary protein kinase C phosphorylation site in the calcium-sensing receptor causes autosomal dominant hypocalcemia. *Eur J Endocrinol* **164**, 429-435,(2011).
519 Morimoto, T. *et al.* Mutations in CLCN5 chloride channel in Japanese patients with low molecular weight proteinuria. *J Am Soc Nephrol* **9**, 811-818,(1998).
520 Hoopes, R. R., Jr. *et al.* CLCN5 chloride-channel mutations in six new North American families with X-linked nephrolithiasis. *Kidney Int* **54**, 698-705,(1998).
521 Lloyd, S. E. *et al.* Characterisation of renal chloride channel, CLCN5, mutations in hypercalciuric nephrolithiasis (kidney stones) disorders. *Hum Mol Genet* **6**, 1233-1239,(1997).
522 Tosetto, E. *et al.* Novel mutations of the CLCN5 gene including a complex allele and A 5' UTR mutation in Dent disease 1. *Clin Genet* **76**, 413-416,(2009).
523 Sethi, S. K. *et al.* Vitamin A responsive night blindness in Dent's disease. *Pediatr Nephrol* **24**,(2009).
524 Ludwig, M. *et al.* Hypercalciuria in patients with CLCN5 mutations. *Pediatr Nephrol* **21**,(2006).
525 Cho, H. Y. *et al.* Renal manifestations of Dent disease and Lowe syndrome. *Pediatr Nephrol* **23**, 243-249,(2008).
526 Frishberg, Y. *et al.* Dent's disease manifesting as focal glomerulosclerosis: Is it the tip of the iceberg? *Pediatr Nephrol* **24**,(2009).
527 Ramos-Trujillo, E. *et al.* A missense mutation in the chloride/proton ClC-5 antiporter gene results in increased expression of an alternative mRNA form that lacks exons 10 and 11. Identification of seven new CLCN5 mutations in patients with Dent's disease. *J Hum Genet* **52**, 255-261,(2007).
528 Grand, T. *et al.* Novel CLCN5 mutations in patients with Dent's disease result in altered ion currents or impaired exchanger processing. *Kidney Int* **76**, 999-1005,(2009).
529 Ramos-Trujillo, E. *et al.* Molecular analysis of the CLCN5 gene in Dent's disease: first mutation identified in a patient from South America. *Clin Nephrol* **68**, 367-372,(2007).
530 Tosetto, E. *et al.* Dent's disease and prevalence of renal stones in dialysis patients in Northeastern Italy. *J Hum Genet* **51**, 25-30,(2006).
531 Bogdanovic, R. *et al.* A novel CLCN5 mutation in a boy with Bartter-like syndrome and partial growth hormone deficiency. *Pediatr Nephrol* **25**, 2363-2368,(2010).
532 Igarashi, T. *et al.* Functional characterization of renal chloride channel, CLCN5, mutations associated with Dent'sJapan disease. *Kidney Int* **54**, 1850-1856,(1998).
533 Tosetto, E. *et al.* Phenotypic and genetic heterogeneity in Dent's disease--the results of an Italian collaborative study. *Nephrol Dial Transplant* **21**, 2452-2463,(2006).
534 Vaisbich, M. H. *et al.* The long-term use of enalapril and hydrochlorothiazide in two novel mutations patients with Dent's disease type 1. *J Bras Nefrol* **34**, 78-81,(2012).
535 Lloyd, S. E. *et al.* Idiopathic low molecular weight proteinuria associated with hypercalciuric nephrocalcinosis in Japanese children is due to mutations of the renal chloride channel (CLCN5). *J Clin Invest* **99**,(1997).
536 Ludwig, M. *et al.* Functional evaluation of Dent's disease-causing mutations: implications for ClC-5 channel trafficking and internalization. *Hum Genet* **117**, 228-237,(2005).
537 Tanuma, A. *et al.* Functional characterization of a novel missense CLCN5 mutation causing alterations in proximal tubular endocytic machinery in Dent's disease. *Nephron Physiol* **107**, p87-97,(2007).

538 Akuta, N. *et al.* Mutations of CLCN5 in Japanese children with idiopathic low molecular weight proteinuria, hypercalciuria and nephrocalcinosis. *Kidney Int* **52**, 911-916,(1997).
539 Carballo-Trujillo, I. *et al.* Novel truncating mutations in the ClC-5 chloride channel gene in patients with Dent's disease. *Nephrol Dial Transplant* **18**, 717-723,(2003).
540 Valina, M. R. *et al.* A novel CLCN5 mutation in a boy with asymptomatic proteinuria and focal global glomerulosclerosis. *Clin Nephrol* **80**, 377-384,(2013).
541 Zhu, B. Z. *et al.* [Clinical and genetic analysis of Dent' s disease in 6 Chinese children with low molecular weight proteinuria]. *Zhonghua Er Ke Za Zhi* **48**, 329-333,(2010).
542 Matsuyama, T. *et al.* Molecular and clinical studies of Dent's disease in Japan: biochemical examination and renal ultrasonography do not predict carrier state. *Clin Nephrol* **61**, 231-237,(2004).
543 Takemura, T. *et al.* Identification of two novel mutations in the CLCN5 gene in Japanese patients with familial idiopathic low molecular weight proteinuria (Japanese Dent's disease). *Am J Kidney Dis* **37**, 138-143,(2001).
544 Okamoto, T. *et al.* A patient with Dent disease and features of Bartter syndrome caused by a novel mutation of CLCN5. *Eur J Pediatr* **171**, 401-404,(2012).
545 Cheong, H. I. *et al.* Phenotype and genotype of Dent's disease in three Korean boys. *Pediatr Nephrol* **20**, 455-459,(2005).
546 Yamamoto, K. *et al.* Characterization of renal chloride channel (CLCN5) mutations in Dent's disease. *J Am Soc Nephrol* **11**, 1460-1468,(2000).
547 Yu, Y. *et al.* Identification and functional analysis of novel mutations of the CLCNKB gene in Chinese patients with classic Bartter syndrome. *Clin Genet* **77**, 155-162,(2010).
548 Bettinelli, A. *et al.* Simultaneous mutations in the CLCNKB and SLC12A3 genes in two siblings with phenotypic heterogeneity in classic Bartter syndrome. *Pediatr Res* **58**, 1269-1273,(2005).
549 Nozu, K. *et al.* The pharmacological characteristics of molecular-based inherited salt-losing tubulopathies. *J Clin Endocrinol Metab* **95**, E511-518,(2010).
550 Konrad, M. *et al.* Mutations in the chloride channel gene CLCNKB as a cause of classic Bartter syndrome. *J Am Soc Nephrol* **11**, 1449-1459,(2000).
551 Robitaille, P. *et al.* Bartter syndrome in two sisters with a novel mutation of the CLCNKB gene, one with deafness. *Eur J Pediatr* **170**, 1209-1211,(2011).
552 Keck, M. *et al.* Novel CLCNKB mutations causing Bartter syndrome affect channel surface expression. *Hum Mutat* **34**, 1269-1278,(2013).
553 Vargas-Poussou, R. *et al.* Spectrum of mutations in Gitelman syndrome. *J Am Soc Nephrol* **22**, 693-703,(2011).
554 Brochard, K. *et al.* Phenotype-genotype correlation in antenatal and neonatal variants of Bartter syndrome. *Nephrol Dial Transplant* **24**, 1455-1464,(2009).
555 Lee, B. H. *et al.* Genetic basis of Bartter syndrome in Korea. *Nephrol Dial Transplant* **27**, 1516-1521,(2012).
556 Bettinelli, A. *et al.* Patients with biallelic mutations in the chloride channel gene CLCNKB: long-term management and outcome. *Am J Kidney Dis* **49**, 91-98,(2007).
557 Urbanova, M. *et al.* DNA analysis of renal electrolyte transporter genes among patients suffering from Bartter and Gitelman syndromes: summary of mutation screening. *Folia Biol (Praha)* **57**, 65-73,(2011).
558 Chiang, W. F. *et al.* Hypokalemic paralysis in a middle-aged female with classic Bartter syndrome. *Clin Nephrol* **81**, 146-150,(2014).
559 Garcia Castano, A. *et al.* Genetics of type III Bartter syndrome in Spain, proposed diagnostic algorithm. *PLoS One* **8**, e74673,(2013).

560 Lin, C. M. *et al.* Chronic renal failure in a boy with classic Bartter's syndrome due to a novel mutation in CLCNKB coding for the chloride channel. *Eur J Pediatr* **168**, 1129-1133,(2009).
561 Martinez, G. Q. & Maduke, M. A cytoplasmic domain mutation in ClC-Kb affects long-distance communication across the membrane. *PLoS One* **3**, e2746,(2008).
562 Fukuyama, S. *et al.* Novel mutations of the chloride channel Kb gene in two Japanese patients clinically diagnosed as Bartter syndrome with hypocalciuria. *J Clin Endocrinol Metab* **89**, 5847-5850,(2004).
563 Shrimpton, A. E. *et al.* OCRL1 mutations in Dent 2 patients suggest a mechanism for phenotypic variability. *Nephron Physiol* **112**,(2009).
564 Pasternack, S. M. *et al.* A premature termination mutation in a patient with Lowe syndrome without congenital cataracts: dropping the "O" in OCRL. *Klin Padiatr* **225**, 29-33,(2013).
565 Bockenhauer, D. *et al.* Renal phenotype in Lowe Syndrome: a selective proximal tubular dysfunction. *Clin J Am Soc Nephrol* **3**, 1430-1436,(2008).
566 Hichri, H. *et al.* From Lowe syndrome to Dent disease: correlations between mutations of the OCRL1 gene and clinical and biochemical phenotypes. *Hum Mutat* **32**, 379-388,(2011).
567 Addis, M. *et al.* OCRL mutation analysis in Italian patients with Lowe syndrome. *Hum Mutat* **23**, 524-525,(2004).
568 Utsch, B. *et al.* Novel OCRL1 mutations in patients with the phenotype of Dent disease. *Am J Kidney Dis* **48**, 942 e941-914,(2006).
569 Chabaa, L. *et al.* [Oculo-cerebro-renal Lowe syndrome: clinical, biochemical and molecular studies in a Moroccan patient]. *Ann Biol Clin (Paris)* **64**, 53-59,(2006).
570 Sethi, S. K. *et al.* Mutations in OCRL1 gene in Indian children with Lowe syndrome. *Clin Exp Nephrol* **12**, 358-362,(2008).
571 Craigen, W. J. *et al.* Exome sequencing of a patient with suspected mitochondrial disease reveals a likely multigenic etiology. *BMC Med Genet* **14**, 83,(2013).
572 Ke, Y. H. *et al.* Identification of two novel mutations in the OCRL1 gene in two Chinese families with Lowe syndrome. *Nephrology (Carlton)* **17**, 20-25,(2012).
573 Lin, T. *et al.* Spectrum of mutations in the OCRL1 gene in the Lowe oculocerebrorenal syndrome. *Am J Hum Genet* **60**, 1384-1388,(1997).
574 Satre, V. *et al.* Characterization of a germline mosaicism in families with Lowe syndrome, and identification of seven novel mutations in the OCRL1 gene. *Am J Hum Genet* **65**, 68-76,(1999).
575 Monnier, N. *et al.* OCRL1 mutation analysis in French Lowe syndrome patients: implications for molecular diagnosis strategy and genetic counseling. *Hum Mutat* **16**, 157-165,(2000).
576 Lin, T. *et al.* Mutations are not uniformly distributed throughout the OCRL1 gene in Lowe syndrome patients. *Mol Genet Metab* **64**, 58-61,(1998).
577 Bockenhauer, D. *et al.* Novel OCRL mutations in patients with Dent-2 disease. *Journal of Pediatric Genetics* **1**, 15,(2012).
578 Kubota, T. *et al.* Identification of two novel mutations in the OCRL1 gene in Japanese families with Lowe syndrome. *Clin Genet* **54**, 199-202,(1998).
579 Chou, Y. Y. *et al.* Identification of OCRL1 mutations in two Taiwanese Lowe syndrome patients. *Acta Paediatr Taiwan* **46**, 226-229,(2005).
580 Tasic, V. *et al.* Clinical and laboratory features of Macedonian children with OCRL mutations. *Pediatr Nephrol* **26**, 557-562,(2011).
581 Kawano, T. *et al.* Oculocerebrorenal syndrome of Lowe: three mutations in the OCRL1 gene derived from three patients with different phenotypes. *Am J Med Genet* **77**, 348-355,(1998).

582 Simsek, E. *et al.* A novel pathogenic DNA variation in the OCRL1 gene in Lowe syndrome. *J Clin Res Pediatr Endocrinol* **3**, 29-31,(2011).
583 Roschinger, W. *et al.* Carrier assessment in families with lowe oculocerebrorenal syndrome: novel mutations in the OCRL1 gene and correlation of direct DNA diagnosis with ocular examination. *Mol Genet Metab* **69**, 213-222,(2000).
584 Kaneko, K. *et al.* Focal segmental glomerulosclerosis in a boy with Dent-2 disease. *Pediatr Nephrol* **25**, 781-782,(2010).
585 Yuksel, A. *et al.* Magnetic resonance imaging, magnetic resonance spectroscopy, and facial dysmorphism in a case of Lowe syndrome with novel OCRL1 gene mutation. *J Child Neurol* **24**, 93-96,(2009).
586 Topaloglu, R. *et al.* Selective proximal renal tubular involvement and dyslipidemia in two cousins with oculocerebrorenal syndrome of Lowe. *Turk J Pediatr* **55**, 331-334,(2013).
587 Leahey, A. M. *et al.* Nonsense mutations in the OCRL-1 gene in patients with the oculocerebrorenal syndrome of Lowe. *Hum Mol Genet* **2**,(1993).
588 Bollee, G. *et al.* Phenotype and outcome in hereditary tubulointerstitial nephritis secondary to UMOD mutations. *Clin J Am Soc Nephrol* **6**, 2429-2438,(2011).
589 Benetti, E. *et al.* Immature renal structures associated with a novel UMOD sequence variant. *Am J Kidney Dis* **53**, 327-331,(2009).
590 Kudo, E. *et al.* Familial juvenile hyperuricemic nephropathy: detection of mutations in the uromodulin gene in five Japanese families. *Kidney Int* **65**, 1589-1597,(2004).
591 Zaucke, F. *et al.* Uromodulin is expressed in renal primary cilia and UMOD mutations result in decreased ciliary uromodulin expression. *Hum Mol Genet* **19**, 1985-1997,(2010).
592 Dahan, K. *et al.* A cluster of mutations in the UMOD gene causes familial juvenile hyperuricemic nephropathy with abnormal expression of uromodulin. *J Am Soc Nephrol* **14**, 2883-2893,(2003).
593 Lee, M. N. *et al.* A novel UMOD mutation (c.187T>C) in a Korean family with juvenile hyperuricemic nephropathy. *Ann Lab Med* **33**, 293-296,(2013).
594 Wolf, M. T. *et al.* The Uromodulin C744G mutation causes MCKD2 and FJHN in children and adults and may be due to a possible founder effect. *Kidney Int* **71**, 574-581,(2007).
595 Hart, T. C. *et al.* Mutations of the UMOD gene are responsible for medullary cystic kidney disease 2 and familial juvenile hyperuricaemic nephropathy. *J Med Genet* **39**, 882-892,(2002).
596 Liu, M. *et al.* Novel UMOD mutations in familial juvenile hyperuricemic nephropathy lead to abnormal uromodulin intracellular trafficking. *Gene* **531**, 363-369,(2013).
597 Rampoldi, L. *et al.* Allelism of MCKD, FJHN and GCKD caused by impairment of uromodulin export dynamics. *Hum Mol Genet* **12**, 3369-3384,(2003).
598 Moskowitz, J. L. *et al.* Association between genotype and phenotype in uromodulin-associated kidney disease. *Clin J Am Soc Nephrol* **8**, 1349-1357,(2013).
599 Bleyer, A. J. *et al.* Mutations in the uromodulin gene decrease urinary excretion of Tamm-Horsfall protein. *Kidney Int* **66**, 974-977,(2004).
600 Lhotta, K. *et al.* Familial juvenile hyperuricemic nephropathy: report on a new mutation and a pregnancy. *Clin Nephrol* **71**, 80-83,(2009).
601 Schaeffer, C. *et al.* Urinary secretion and extracellular aggregation of mutant uromodulin isoforms. *Kidney Int* **81**, 769-778,(2012).
602 Bleyer, A. J. *et al.* Renal manifestations of a mutation in the uromodulin (Tamm Horsfall protein) gene. *Am J Kidney Dis* **42**, E20-26,(2003).

603 Wolf, M. T. *et al.* Mutations of the Uromodulin gene in MCKD type 2 patients cluster in exon 4, which encodes three EGF-like domains. *Kidney Int* **64**, 1580-1587,(2003).
604 Bernascone, I. *et al.* Defective intracellular trafficking of uromodulin mutant isoforms. *Traffic* **7**, 1567-1579,(2006).
605 Nasr, S. H. *et al.* Uromodulin storage disease. *Kidney Int* **73**, 971-976,(2008).
606 Bleyer, A. J. *et al.* Clinico-pathologic findings in medullary cystic kidney disease type 2. *Pediatr Nephrol* **20**, 824-827,(2005).
607 Calado, J. *et al.* A novel heterozygous missense mutation in the UMOD gene responsible for Familial Juvenile Hyperuricemic Nephropathy. *BMC Med Genet* **6**, 5,(2005).
608 Lens, X. M. *et al.* A novel pattern of mutation in uromodulin disorders: autosomal dominant medullary cystic kidney disease type 2, familial juvenile hyperuricemic nephropathy, and autosomal dominant glomerulocystic kidney disease. *Am J Kidney Dis* **46**, 52-57,(2005).
609 Tinschert, S. *et al.* Functional consequences of a novel uromodulin mutation in a family with familial juvenile hyperuricaemic nephropathy. *Nephrol Dial Transplant* **19**, 3150-3154,(2004).
610 Lee, D. H. *et al.* A case of familial juvenile hyperuricemic nephropathy with novel uromodulin gene mutation, a novel heterozygous missense mutation in Korea. *J Korean Med Sci* **25**, 1680-1682,(2010).
611 Wei, X. *et al.* Novel uromodulin mutation in familial juvenile hyperuricemic nephropathy. *Am J Nephrol* **36**, 114-120,(2012).